SEA ICE

An Introduction to its Physics, Chemistry, Biology and Geology

Edited by

David N. Thomas* and Gerhard S. Dieckmann†

** School of Ocean Sciences, University of Wales, Bangor, UK*
† Alfred Wegener Institute for Polar and Marine Research, Bremerhaven, Germany

Blackwell
Science

VISIT…

SEA ICE

An Introduction to its Physics, Chemistry, Biology and Geology

Edited by

David N. Thomas* and Gerhard S. Dieckmann†

** School of Ocean Sciences, University of Wales, Bangor, UK*
† Alfred Wegener Institute for Polar and Marine Research, Bremerhaven, Germany

Blackwell
Science

© 2003 by Blackwell Science Ltd,
a Blackwell Publishing Company
Editorial Offices:
9600 Garsington Road, Oxford OX4 2DQ, UK
Tel: +44 (0)1865 776868
Blackwell Publishing, Inc., 350 Main Street,
Malden, MA 02148-5020, USA
Tel: +1 781 388 8250
Iowa State Press, a Blackwell Publishing
Company, 2121 State Avenue, Ames, Iowa 50014-
8300, USA
Tel: +1 515 292 0140
Blackwell Publishing Asia Pty Ltd, 550 Swanston
Street, Carlton South, Victoria 3053, Australia
Tel: +61 (0)3 9347 0300
Blackwell Verlag, Kurfürstendamm 57, 10707
Berlin, Germany
Tel: +49 (0)30 32 79 060

The right of the Author to be identified as the
Author of this Work has been asserted in
accordance with the Copyright, Designs and
Patents Act 1988.

All rights reserved. No part of this publication may
be reproduced, stored in a retrieval system, or
transmitted, in any form or by any means,
electronic, mechanical, photocopying, recording or
otherwise, except as permitted by the UK
Copyright, Designs and Patents Act 1988, without
the prior permission of the publisher.

First published 2003 by Blackwell Science Ltd

Library of Congress
Cataloging-in-Publication Data
Sea ice: an introduction to its physics, chemistry,
biology, and geology/edited by David N.
Thomas and Gerhard S. Dieckmann.
p. cm.
Includes bibliographical references (p.).
ISBN 0-632-05808-0
1. Sea ice. I. Thomas, David N. (David
Neville), 1962– II. Dieckmann, Gerhard.

GB2403.2.S43 2003
551.34′3—dc21

2002038346

ISBN 0-632-05808-0

A catalogue record for this title is available from
the British Library

Set in 10/13pt Times
by DP Photosetting, Aylesbury, Bucks
Printed and bound in Great Britain by
MPG Books Ltd, Bodmin, Cornwall

For further information on
Blackwell Publishing, visit our website:
www.blackwellpublishing.com

Dedication

This book is dedicated to all the ships' crews, air support teams, field station/base crews and the myriad of other people associated with the logistic support that makes sea ice research possible. Beyond their help, however, our families and friends have had to come to terms with us being at the *ends of the earth*, often for long periods of time. In most cases they never get to experience, first hand, the wonders we have seen. It is only right that this book is dedicated to them.

And now there came both mist and snow,
And it grew wondrous cold:
And ice, mast-high, came floating by,
As green as emerald.

And through the drifts the snowy clifts
Did send a dismal sheen:
Nor shapes of men nor beasts we ken,
The ice was all between.

The ice was here, the ice was there,
The ice was all around:
It cracked and growled, and roared and howled,
Like noises in a swound!

Extracted from *The Rime of the Ancient Mariner*, Samuel Taylor Coleridge (1772–1834).

Contributors

David G. Ainley, H.T. Harvey & Associates, San Jose. USA

Leanne K. Armand, ACRC, University of Tasmania, Hobart. Australia

Kevin R. Arrigo, Department of Geophysics, Stanford University. USA

Josefino C. Comiso, NASA/Goddard Space Flight Center, Greenbelt. USA

Gerhard S. Dieckmann, Alfred Wegener Institute, Bremerhaven. Germany

Hajo Eicken, Geophysical Institute, University of Alaska, Fairbanks. USA

G.E. (Tony) Fogg, Emeritus, School of Ocean Sciences, University of Wales, Bangor. UK

Christian Haas, Alfred Wegener Institute, Bremerhaven. Germany

Hartmut H. Hellmer, Alfred Wegener Institute, Bremerhaven. Germany

Amy Leventer, Department of Geology, Colgate University, Hamilton. USA

Michael P. Lizotte, Bigelow Laboratory for Ocean Sciences, West Boothbay Harbor. USA

Stathis Papadimitriou, School of Ocean Sciences, University of Wales, Bangor. UK

Sigrid B. Schnack-Schiel, Alfred Wegener Institute, Bremerhaven. Germany

Ian Stirling, Canadian Wildlife Service, Edmonton. Canada

David N. Thomas, School of Ocean Sciences, University of Wales, Bangor. UK

Cynthia T. Tynan, Woods Hole Oceanographic Institution, Woods Hole. USA

Contents

Foreword by G.E. (Tony) Fogg		vii
Acknowledgements		xiv
Chapter 1	The Importance of Sea Ice: An Overview *Gerhard S. Dieckmann and Hartmut H. Hellmer*	1
Chapter 2	From the Microscopic, to the Macroscopic, to the Regional Scale: Growth, Microstructure and Properties of Sea Ice *Hajo Eicken*	22
Chapter 3	Dynamics versus Thermodynamics: The Sea Ice Thickness Distribution *Christian Haas*	82
Chapter 4	Large-scale Characteristics and Variability of the Global Sea Ice Cover *Josefino C. Comiso*	112
Chapter 5	Primary Production in Sea Ice *Kevin R. Arrigo*	143
Chapter 6	The Microbiology of Sea Ice *Michael P. Lizotte*	184
Chapter 7	The Macrobiology of Sea Ice *Sigrid B. Schnack-Schiel*	211
Chapter 8	Sea Ice: A Critical Habitat for Polar Marine Mammals and Birds *David G. Ainley, Cynthia T. Tynan and Ian Stirling*	240
Chapter 9	Biogeochemistry of Sea Ice *David N. Thomas and Stathis Papadimitriou*	267

Chapter 10 Particulate Flux From Sea Ice in Polar Waters 303
Amy Leventer

Chapter 11 Palaeo Sea Ice Distribution – Reconstruction and Palaeoclimatic Significance 333
Leanne K. Armand and Amy Leventer

Glossary 373

Index 385

The colour plates may be found throughout the book as follows:

Plates 1.1 after page 2
Plates 2.1-4 after page 66
Plates 3.1-2 after page 98
Plates 4.1-9 after page 130
Plates 6.1 after page 194
Plates 7.1-3 after page 226
Plates 8.1-3 after page 258
Plates 11.1-3 after page 354

Foreword

G.E. (Tony) Fogg

Almost everything discussed in this book stems from the unique nature of water. Whereas comparable compounds are gases at what we regard as normal temperatures, water is a liquid, with a greater heat capacity than almost all other substances and which, on solidifying, unlike most other fluids, becomes a solid lighter than itself. Laboratory scientists have explained these peculiarities, but the all-pervading complexities to which they give rise in the natural environment are still insufficiently investigated and understood. These complexities are especially evident in sea ice and their study is becoming increasingly important. Sea ice covers some 7% of our planet and knowledge of its distribution and behaviour is needed for the purely practical purposes of navigation but, beyond that, as we now begin to realize, sea ice acts as an extremely powerful heat engine, controlling global temperatures at levels which make life sustainable.

Sea ice also provides a habitat for living organisms which, in spite of apparently extreme conditions, play an important part in the ecosystems of the polar seas. In studying these things tremendous difficulties have to be faced in making observations under natural conditions and progress has been slow. However, problems are being overcome and knowledge advances. In the past, seafarers, although not altogether unmindful of the beauties of form and colour in sea ice, generally looked on it as exasperatingly unpredictable – Captain William Parry wrote in 1819 of its 'whimsicalities' – formidable in its destructive power, but unproductive and uninteresting in itself. Only a few thought it worth studying. James Cook, on his voyage in Antarctic waters in 1772–75, discussed the origin of sea ice with his naturalist J.R. Forster but, obviously, could not make detailed observations (Hoare, 1982). The most comprehensive account from around this time was that of the whaler William Scoresby in his paper on Greenland ice (1815). This dealt with kinds of ice, the differences between those of fresh and salt waters, their formation, distribution, movement and seasonal changes. The effects of ice movements on bird behaviour were noted, as were the relationships between ice, sea and atmosphere, and particularly the capacity of the ice as 'a powerful equaliser of temperature'. Scoresby entertained his crew by fashioning lenses from clear sea ice and using them to light pipes and ignite gun-powder. Robert Hooke in the early days of the Royal Society had already demonstrated the transparency of freshwater ice to radiant heat – an

important point – and Chinese conjurers had similarly used ice burning glasses some fourteen centuries before that (Needham, 1962).

However, of all people in Scoresby's time, the Inuit had the deepest understanding of sea ice. Since they migrated into the Canadian Arctic and Greenland some four thousand years before, they had travelled much on the ice and the 'little ice age' (*ca*. 1600–1850 AD) forced them to resort to hunting seals in the winter at breathing holes and leads, devising sophisticated techniques for pursuing their quarry at different seasons and under varying conditions of ice surface (Aporta, 2002). Obviously, such experience would have been invaluable in the polar explorations carried out in the 19th century but, for example, the British Royal Navy would have none of it and even Scoresby, being a whaler rather than a naval man, was not allowed to play a part.

During these times some advances were being made on the small-scale, mainly biological, level. Some of the early explorers in Antarctic waters, Bellingshausen in 1820 for example (Debenham, 1945), had commented on the discoloration of sea ice and surmised that dust from the land or droppings of seabirds were responsible. James Clark Ross, on his voyage south in 1839–43, was initially inclined to such a view but his assistant surgeon, Joseph Hooker, collected some of the material and found it to consist of the remains of microscopic organisms which the eminent German protozoologist C.G. Ehrenberg later identified as diatoms (Ross, 1847). The existence of microscopic plants in the open sea was unrecognized at that time but Hooker realized the abundance and importance of diatoms in ocean waters and thus provided the basis for biological oceanography. The significance of their presence in ice as well as in the ambient water was passed by. Fridthof Nansen (1897) seems to have been the first to make serious studies of micro-organisms in sea ice. The fact that the same species of diatoms, quite different from those elsewhere, were to be found in ice from the Bering Strait and from the east coast of Greenland was used by him in formulating his theory of Arctic Ocean currents. However, progress remained slow. An idea, now abandoned, that water molecule polymers concentrated around thawing ice are particularly favourable for living organisms was put forward to explain the abundance of algae in ice by V. Lebedev (1959). Identification of sea ice diatoms was carried out by various authors but *in situ* investigations of sea ice communities did not develop until the work of J.S. Bunt (1963), using scuba diving in the Antarctic, and R.A. Horner and V. Alexander (1972), investigating heterotrophy in sea ice communities in the Arctic.

The necessity of gaining a better knowledge of sea ice distribution and movements became acute, both for navigation and geographical purposes, at the beginning of the 20th century. Studies of the geophysics of sea ice had been initiated by Nansen in his crossing of the Arctic Ocean but advances were slow and uneven. With sea ice extending some 160° of longitude to the north of them and with the possibilities of a north-east passage, the Russians in particular were quick to employ recently developed ice-breaking ships for both survey and scientific purposes. A succession of research vessels being beset in Antarctic ice, culminating in the

crushing and sinking of Shackleton's ship *Endurance* in 1915, emphasized the need for much more information about the physical characteristics of sea ice. Following World War II, increased use of ice-breakers, the introduction of helicopters to place scientists and their equipment on ice, and an amazing proliferation of remote-sensing techniques have made it possible to get some of the information required.

Chapter 1 in this book, by Gerhard Dieckmann and Hartmut Hellmer, adds detail to this historical sketch. The chapter outlines a framework on which a coherent picture, basic and still with large gaps, of sea ice science may ultimately be built. The relationships between sea ice, ocean and atmosphere are clearly dominant but complicated in the extreme. There are different ice classes, thermodynamics which must allow for multiple layering, viscous-plastic rheology, snow cover, seawater flooding and the formation of superimposed ice, brine pockets and the biological activity they harbour, all coupled to circulation patterns of different degrees of complexity in both atmosphere and ocean. Then there are surprising differences, as well as similarities, between the sea ices of the Arctic and the Antarctic. Present information about these usually comes from spot localities, and extrapolation to large-scale processes can be problematic.

Sea ice phenomena extend over wide ranges of scale in time and space, and the question arises as to whether those at the microscopic end of the scale are of interest only to specialists or are of significance in the global context. This question is considered by Hajo Eicken in Chapter 2. Putting aside the hypothetical butterfly flapping its wings to annoy meteorologists, one can easily think of more likely possibilities in this complex system. The chance establishment of algal growth may, for example, cause considerable alterations in albedo over extensive ice surfaces. Eicken discusses the links between microstructure and behaviour of ice on the large scale, covering the growth, decay and heat budget of ice, simple models of sea ice growth, the physical chemistry of sea ice, solute segregation and ice microstructure, salinity evolution, thermal properties, dielectric and optical properties, and macroscopic ice strength (including advice on walking on thin ice). It becomes evident that small-scale processes do affect large-scale behaviour to a considerable extent.

The growth of sea ice is not a matter of thermodynamics alone. There is a mechanical aspect arising when winds and currents break up the initial cover and build up the fragments into pressure ridges. It is necessary to have a measure of ice thickness or, better, volume, as well as horizontal distribution in order to determine the effects of climate change. This matter is dealt with by Christian Haas in Chapter 3. Model, field, and remote-sensing studies are all required but have been rather limited. The satellite CryoSat, which employs a synthetic interferometric aperture radar altimeter, if ground validation proves it satisfactory, should provide a main source of information for the improvement of sea ice models. Approaching the problem from below, the British Autosub project has had some success in the Antarctic.

Sea ice as an insulator limits flow of heat between ocean and atmosphere and its high albedo results in reflection of solar radiation back into the atmosphere. Given

the vast extent and seasonal two-fold expansion in the Arctic and the reciprocal change of five-fold in the Antarctic, the geophysical impacts are enormous and fluctuating. Added to this, the formation and melting of ice bring about vertical redistribtion of salt, which is a potent factor in ocean circulation and productivity. Especially if we are to get an idea of the trend of global warming we need to have reliable data on the variations of sea ice. Josefino Comiso reviews the situation in Chapter 4. Satellite data obtained over two decades show large seasonal fluctuations in ice extent which are inversely correlated with those in sea temperature. Large-scale trends in ice cover point to decline in the Arctic but to increase over most of Antarctica. Results so far have some statistical uncertainty and cyclic patterns have to be taken into account.

Primary production in sea ice has been dismissed in the past as making only a negligible contribution to the global total. Recent research, as summarized by Kevin Arrigo (Chapter 5), is still hampered by logistic restraints and lack of adequate techniques for measuring primary production *in situ*, but such data as have been obtained point to it being greater per unit area than has been thought, and one must not forget that it is one of the most extensive ecosystems on earth. Microprobes capable of non-invasive sampling of the different microhabitats in sea ice are desirable and numerical models can perhaps be used to suggest where information is most lacking.

The smudges of colour noticed in sea ice by the early explorers and eventually recognized as responsible for this primary production have proved to be more than accidental and more varied, active and complicated in organization than could have been supposed. In Chapter 6 Michael Lizotte points out that sea ice microbiology is just one beneficiary of the tremendous advances made in aquatic microbiology generally in recent years. Biochemical analysis, isotopic tracers, specific metabolic inhibitors, genetic analysis, advanced microscopy and micromanipulation are employed as well as helicopters, drills, and diving equipment. Apart from the algae responsible for the photosynthesis there are small invertebrates, protozoa, fungi, bacteria, archeabacteria and viruses. Besides having to tolerate low temperatures these organisms are often cut off from the ambient environment, which may involve nutrient deficiency, and subject to abrupt osmotic stress. They may live in a rich organic soup in which the webs of transfer of metabolites and energy must be intertwined in a most complicated way. There is everything to be learned about the development and functioning of ecological relationships in the ice.

Small animals use sea ice for feeding, refuge and breeding, either as permanent residents or temporary visitors. Biogeography comes to the fore here, the difference between the Arctic, where rotifers and nematodes are most abundant, and the Antarctic, where copepods, euphausiids, and turbellarians are most prominent, being at the phylum rather than the species level. This is discussed by Sigrid Schnack-Schiel in Chapter 7. The life cycles of these animals are largely determined by the seasonal fluctuation of the ice, the behaviour of the Antarctic krill being of particular interest in relation to the food web of the Southern Ocean.

Ecophysiological investigations have not progressed far except that the survival mechanisms used by fish frequenting pack ice have been found to involve glycoproteins as antifreeze agents.

Large air-breathing animals, the epifauna, are not dependent directly on sea ice as a source of food but may use it as a solid platform on which they can live and breed, and from which they can launch foraging forays into the water. Others, which as David Ainley, Cynthia Tynan and Ian Stirling point out in Chapter 8 include the human species, find it merely a barrier to getting at food or, at another level, carrying out exploration. Seals in both polar regions have rather the same general behaviour habits on and under sea ice but differ in minor respects. Polar bears in the north and emperor penguins in the south have fascinating and completely different adaptations to the rigorous conditions on the upper surface of the ice. Seasonal changes in sea ice, both in bulk and distribution, have ecological consequences for both mammals and seabirds, maybe producing species-specific alterations in demography, range and population size. These must be studied not only for purposes of both economic exploitation and conservation but as potentially sensitive indicators of long-term changes in climate or marine pollution.

One might think that sea ice can play no great part in marine geochemistry. Indeed this was so until recently, but when it was realized that sea ice is the site of considerable microbiological activity the situation changed. However, as David Thomas and Stathis Papadimitriou emphasize in Chapter 9, it is necessary to have a background of the abiotic changes in chemistry which take place when sea water freezes, in order to assess the biological activities. This is no easy matter but the large-scale ice tank facilities, such as have become available in Hamburg, will help greatly. A comprehensive view of what is known and what might be known with the aid of new techniques of the chemistry of a wide variety of substances is given in this chapter. Among them the occurrence of dimethyl sulphide in sea ice is of particular interest since this product of marine algae is involved in the formation of aerosol particles, providing cloud condensation nuclei which become important factors in localized and global climate control.

Chapter 10, by Amy Leventer, deals with particulate flux, both living and nonliving, from sea ice. Downward transport of solid material plays an integral part in the cycling of carbon and silica in the oceans besides providing food for benthic organisms and contributing to the sedimentary record. Long-term monitoring with sediment traps could provide much information on the interannual variability of ecosystems. The release of living material by melting ice not only provides a source of food for pelagic grazers but potential inoculum for the seasonal growth of plankton. What happens at this stage, of course, will have a considerable impact on higher trophic levels. Another aspect is that particles from the atmosphere may be intercepted by sea ice, and it is an interesting possiblity that these may contain iron, an essential but scarce trace element in phytoplankton growth, and so contribute to blooms at the ice edge.

Finally, in Chapter 11, Leanne Armand and Amy Leventer discuss the past

distribution of sea ice, an important matter for reconstructing past oceanic and climatic conditions. The evidence comes from the records extending over the Quaternary period provided by microfossils and geochemical and sedimentary tracers, including ice-rafted debris. Dinoflagellate cysts have played an important part in Arctic studies whereas in the Antarctic dependence is mainly on diatom distributions. Such information has to be combined with modern physical interaction studies between ice, ocean and atmosphere, involving complex statistical treatments. Sea ice conditions can now be reasonably incorporated in general circulation models predicting future climates but palaeontologically determined conditions have not yet been used in models to simulate past climates.

The chapters in this book are of necessity specialized. At the one extreme the physicist, concerned with the thermodynamics or hydrodynamics of the ice itself, regards living organisms as of marginal importance. At the other extreme the biologist may study organisms in isolation. Nevertheless, sea ice functions as an integrated system. The physicist should remember that there is always a remote but real chance that the most elegant of mathematical models of ice movement can be put awry by seemingly trivial biological activity. A walrus, for example, may take it into its head to bash through 20 cm of ice at a critical spot. The biologist is more consciously aware that he needs information about the physical and chemical processes going on in the environment in which his organisms live but may not be sufficiently well informed.

However, in this book we have the different aspects linked together into a coherent picture. The incentives attracting 'pure' scientists to study sea ice are strong. For the physicist there is the challenge of overcoming technical problems, such as reconciling remote-sensing data with ground data and having the excitement of getting out into the field in order to do it, then constructing numerical models which can account elegantly for the 'whimsical' behaviour of sea ice. The biologist has the thrill of exploring a unique ecosystem which ranks in novelty with the astonishing communities found around hydrothermal vents in the deep ocean and in porous sandstone in the dry valleys of Antarctica.

Sea ice research also has its practical applications. These include the everyday tasks of charting sea ice for navigation and the management of fisheries. At present, though, the matter of global warming draws most attention, sea ice being a major component of the earth's heat engine, the understanding of which is a necessary part of predicting what may happen in the near future. Related to this is the tracing of variations in climate in the past. Studies of sea ice microbiology can be of help in counteracting the effects of oil spills in Arctic waters or in finding micro-organisms active at low temperatures which may be used to avoid the expense of providing elevated temperatures in industrial processes. In a wider field, investigation of sea ice microhabitats may indicate what is to be expected in looking for life elsewhere in the solar system and what techniques should be used in detecting it. 'There are more things in heaven and earth, Horatio, Than are dreamt of in your philosophy' (William Shakespeare, 1603, *Hamlet*).

References

Aporta, C. (2002) Life on the ice: understanding the codes of a changing environment. *Polar Record*, **38**, 341–354.

Bunt, J.F. (1963) Diatoms of Antarctic sea-ice as agents of primary production. *Nature*, **199**, 1255–1257.

Debenham, F. (Ed.) (1945) *The Voyage of Captain Bellingshausen to the Antarctic seas 1819–1821*. Hakluyt Society, London.

Hoare, M.E. (Ed.) (1982) *The Resolution Journal of Johann Reinhold Forster (1772–75)*. Hakluyt Society, London.

Horner, R. & Alexander, V. (1972) Algal populations in Arctic sea ice: an investigation of heterotrophy. *Limnology and Oceanography*, **17**, 454–455.

Lebedev, V. (1959) *Antarctica*. Foreign Languages Pulishing House, Moscow.

Nansen, F. (1897) *Furthest North*. Archibald Constable & Co., London.

Needham, J. (1962) *Science and Civilisation in China, Vol. 4, Part I Physics*. Cambridge University Press, Cambridge.

Ross, J.C. (1847) *A Voyage of Discovery and Research in the Southern and Antarctic Regions*. John Murray, London.

Scoresby, W., Jr (1815) On the Greenland or Polar Ice. *Memoirs of the Wernerian Society*, **2**, 328–336. Reprinted in 1980 by Caedmon of Whitby.

Acknowledgements

We wish to thank the National Aeronautics and Space Administration, USA; the Alfred Wegener Institute, Germany; the Antarctic Cooperative Research Centre, Australia; the Hanse Institute for Advance Study, Germany; and the Geophysical Institute, University of Fairbanks, USA, for supporting this work and enabling colour to be used for some of the illustrations.

We are very grateful to the Hanse Institute of Advanced Study, Delmenhorst, Germany, for the Fellowship awarded to David Thomas. Without this opportunity it is unlikely that this book would have been produced.

We also thank David Roberts and Brian Long from the University of Wales, Bangor, for their help in producing the final version of the manuscript, and to the copy editor Caroline Savage.

We are grateful to the following institutions, individuals and publishers for permission to reproduce images and figures for which they hold copyright:

American Geophysical Union – Figs 2.13, 2.14, 3.5, 3.10, 3.11, Plate 4.2 and Fig. 5.2; *American Meterological Society* – Figs 3.12 and 3.13; *American Association for the Advancement of Science* – Fig. 7.6; *Antarctic Science Ltd*, *published by Cambridge University Press* – Fig. 7.5; *Cold Regions Research & Engineering Laboratory* – Figs 2.4, 2.9, 2.16 and 2.18; *Elsevier Science* – Figs 2.5 and 7.4; *Kluwer Academic/Plenum Publishers* – Fig. 2.3; *NRC Research Press* – Fig. 7.7; *N. Wu* – Plates 7.1 and 7.2; *D.N. Nettleship* – Fig. 8.2; *C. Lydersen* – Plate 8.3; *J.C. George* – Fig. 8.3; *R. Dunbar, Standford University* – Figs 10.1 and 10.2; *P. Marschall (AWI)* – Plate 7.3; *C. Krembs and J. Deming, University of Washington* – Plate 6.1; *S. Grossmann (AWI)* – Plate 6.1; *K. Riska, Helsinki University of Technology* – Fig. 3.7; *J. Lieser* – Fig. 3.8; *J. Comiso (NASA)* – Plate 1.1; *A. Bartsch (AWI)* – Plate 1.1; *J. Weissenberger (AWI)* – Plate 1.1; *T.M. Hrudey, University of Alberta* – Fig. 2.17; *D.M. Cole* – Fig. 2.11; *J.P. Zarling, University of Alaska* – Fig. 2.12.

Chapter 1

The Importance of Sea Ice: An Overview

Gerhard S. Dieckmann and Hartmut H. Hellmer

1.1 Introduction

Following the initial freezing of sea water, sea ice is profoundly modified by the interaction of physical, biological and chemical processes to form an extremely heterogeneous semi-solid matrix. Oceanic, atmospheric and continental inputs all serve to influence the formation, consolidation and subsequent melt when the ice returns to water. Probably the most important property of sea ice is that, despite it being solid, it is less dense than sea water and therefore floats.

During the course of a year, tremendous areal expanses of sea water in the Arctic, the Southern Ocean, and also in the Baltic and other seas such as the Caspian and Okhotsk, undergo a cycle of freezing and melting. In winter, sea ice covers an area of up to 7% of the earth's surface, and as such is clearly one of the largest biomes on earth (Comiso, Chapter 4).

With the exception of the Inuit, who over several thousand years adapted to a life closely associated with Arctic sea ice, until the turn of the last century sea ice was simply a hostile environment and an obstruction to the navigation of sea routes and the hunting of birds and mammals (Fogg, 1992; Weeks, 1998). It is only during the past 200 years, and mostly within the past 100 years, that adventurous expeditions have visited the polar oceans and our understanding of the significance of sea ice in a global context has begun to develop.

Today we know that the annual cycle of sea ice formation and degradation not only plays a pivotal role in governing the world's climate, but also influences processes in the oceans down to the abyss. The life cycles of marine plants and animals ranging from micro-organisms to whales, and even man, are also influenced by the large-scale cycles of ice formation. Sea ice is recognized as a fundamental component of system earth, which cannot be ignored in the large-scale environmental discussions and the predictions of future climate conditions.

Recently, disturbing headlines from the high latitudes regarding the effects of ozone holes, collapsing ice sheets and rising temperatures seem to indicate that rapid climate change is underway. The seeming inevitability of shrinking ice on the

Arctic Ocean, for instance, would infer a threat to the indigenous way of life of local human communities, hard times ahead for Arctic birds and mammals including the polar bears, and an ice-free Northwest Passage (Kerr, 2002; Smith et al., 2002). In the Antarctic, significant changes in the extent and distribution of sea ice cover are attributed to global climate warming. These changes are closely related to obvious ecological changes in krill and whale feeding, and have severely affected local seabird populations (Croxall et al., 2002).

Sea ice research spans many modern scientific disciplines including, among others, geophysics, glaciology, geology, chemistry, biogeochemistry and numerous branches of biology. Sea ice research is important for climate researchers and oceanographers interested in processes pertinent for the localized polar regions and also for global-scale climate and ocean processes. Present-day sea ice research ranges from molecular studies into the composition and structure of the ice itself, to that of the elements and the microorganisms living within the ice, through to scales many orders of magnitude greater up to the monitoring of ice cover from space (Plate 1.1).

Modern ice-breakers, as well stations on the peripheries of Antarctica or the Arctic, greatly facilitate access to sea ice, even during seasons when in the past ice and weather conditions prohibited effective work. During the past 50 years these facilities have greatly enhanced the chances for regional meso-scale studies on the development and growth of sea ice and the dynamics of pack ice fields. These include investigations into the physicochemical interactions between the atmosphere, ice and underlying water, as well as into the fauna and flora living within or in close association with sea ice (Eicken, Chapter 2; Haas, Chapter 3; Schnack-Schiel, Chapter 7; Ainley et al., Chapter 8). Geologists use information gathered from sediment cores in areas beneath past and present sea ice cover, obtained by ice-breaker, to reconstruct the earth's history, particularly that of the sea ice extent (Leventer, Chapter 10; Armand & Leventer, Chapter 11).

On an even larger scale, airborne equipment used from helicopters or light airplanes provides information on heat exchange, floe distribution and sea ice thickness as well as on the distribution of birds and animals. Submarines and remotely operated, or autonomous, vehicles are the latest tools to be used for obtaining insight into the underside topography of sea ice fields, ice thickness and the behaviour of animals under the ice (Brierley & Thomas, 2002; Brierley et al., 2002). New technologies have been harnessed to investigate the fluxes of organic matter from sea ice to benthic communities on the sea floor, as well as investigating the seasonal dynamics and growth of these communities (Haas, Chapter 3; Schnack-Schiel, Chapter 7; Leventer, Chapter 10).

Constantly improving remote-sensing technology and new satellites (Haas, Chapter 3; Comiso, Chapter 4) enable high-resolution, large-scale monitoring of the ice cover, surface roughness, dynamics and thickness on a seasonal and interannual basis. This information is being compiled to drive models that reconstruct and forecast the behaviour and role of sea ice with regard to past and present climate

change, as well as enabling assessment of its large-scale ecological significance (Comiso, Chapter 4; Arrigo, Chapter 5). Satellite and global positioning technologies allow the tracking of birds and animals, including seals and polar bears, and their seasonal migrations associated with sea ice (Ainley et al., Chapter 8). Sophisticated suites of information such as diving depths, water temperature and salinity, and foraging behaviour can be transmitted daily over many months allowing a far greater understanding of animal behaviour in sea ice covered regions than has ever been possible before (Bornemann et al., 2000; Plötz et al., 2001).

This chapter provides a brief overview of the importance of sea ice. It spans the historical development of sea ice research and the expansion in research interests through to the current state-of-the-art issues and new perspectives that are receiving increasing attention.

1.2 Historical aspects of sea ice exploration

For obvious reasons the historical development of sea ice research differs greatly between the northern and southern hemispheres. A detailed chronological account is beyond the scope of this chapter and is more fully covered by Fogg (1992), Martin (1998) and Weeks (1998). Excerpts have been extracted from these works to compile the brief summary that follows.

In both hemispheres it was probably the biology associated with sea ice that led to man's interest, association and confrontation with this hostile environment. Around the Arctic, Baltic and Caspian Seas man has inhabited coastal areas for millennia, living off the animals closely associated with sea ice, and adapting their lifestyles and migrations to the seasonal fluctuations in sea ice cover. In the Antarctic it was the whalers and sealers of the 19th century who first encountered sea ice during the pursuit of their prey.

The first records of sea ice date back to reports in the Baltic, and near Greenland, when Irish monks crossed Mare Concretum during their voyages to Iceland. These journeys actually took place in approximately 795 AD (Weeks, 1998). In about 1070, Adam of Bremmen described both Iceland and Greenland as well as sea ice. Two hundred years later a book containing descriptions of sea ice was written by the priest Ivarr Bodde. There is a detailed report with a map showing the crossing of sea ice on the Baltic Sea prepared by Olaus Magnus Gothus in 1539, whilst expedition reports containing general descriptions of sea ice in the Arctic, such as those of Martin Frobisher, date back to 1576 (Weeks, 1998). Because of the general expansion of ocean trade routes during the later 18th century, interest increased in finding a route that offered faster passage between Europe and the Orient. One of the most notable expeditions during that time was the Great Northern Expedition started in 1733 under the command of Vitus Bering, who concluded in 1774 that the route was probably not navigable with the ships available at that time.

The 19th century began with a series of expeditions established mainly to clarify

the existence of a north-west or north-east passage. The best known are the expeditions of Ross (1818, 1829–33), William Edward Parry and Franklin in 1845. By 1870 the first scientific papers on the properties and variations in sea ice conditions had started to appear (Tomlinson, 1871; Petterson, 1883), as had reports on the first sea ice experiments (Buchanan, 1874). Ehrenberg (1841, 1853) was the first to describe diatoms from Arctic sea ice, after which many papers followed describing diatoms and organisms in sea ice (Dickie, 1880; Cleve, 1883; summarized by Horner, 1985). Probably the most epic voyage with a scientific background at the end of the 19th century was that of Nansen on the *Fram*. This voyage initiated the beginning of modern sea ice geophysics.

Sea ice research in the 20th century was governed by political, logistical, as well as scientific, enterprise interrupted by the two world wars. At the forefront of 20th century research was engineering and the development of metal ice-breaking ships. The first, the *Yermak* was actually built for Admiral Makarov in 1898 and used for the first sea ice research programme in the summer of 1901, with the additional intention of discovering the northern sea route. In 1927 Malmgren published his doctoral thesis on sea ice growth and property observations carried out during the drift of the *Maud* between 1918 and 1925. This probably made him the first true student of sea ice geophysics (Weeks, 1998).

The Russians were very active in sea ice research even prior to and during World War II. Particularly noteworthy is the book on Arctic ice by Zubov (1945). Other pioneering work on sea ice during this period was conducted by Tsurikov who developed the first geometric model for the variation in sea ice strength with changes in the gas and brine volumes. Usachev (1949) reviewed work that had been carried out on sea ice algae. Western scientists were evidently not active during the period up to 1945 although Ringer, a Dutch chemist, worked on phase relationships in sea water and brines in 1906, only publishing his work in German in 1926. Other scientists involved in sea ice research at that time were Whitman, Barnes, Smith, Crary and Ewing, the last later becoming the Chief Scientist for the US IGY (International Geophysical Year 1–1957) Program in the Antarctic (Weeks, 1998).

After World War II sea ice research increased markedly. Emphasis changed from that of finding appropriate sea routes and facing the challenges that sea ice posed to shipping to other priorities. These were in part directed by the then developing political 'cold war' with the consequences for the missile race, submarine strategy, Arctic offshore oil exploration, remote sensing, the role of sea ice in global climate and the transfer of pollutants via sea ice.

The first mention of the Antarctic continent is that of Aristotle in 322 BC who described, an as yet unknown, extreme southern region *Antarktikos.* The name was derived from 'opposite the Bear', *Arktos* being the Great Bear (or Big Dipper) constellation above the North Pole (Martin, 1996). Yet while the ancient Greeks only imagined the continent, the first human to actually encounter the Antarctic may well have been a 7th century Raratongan traveller, Ui-te-Rangiara, who according to Polynesian legend is said to have 'sailed south to a place of bitter cold

where white rock-like forms grew out of a frozen sea'. However, the actual recorded discovery and exploration of the Antarctic dates back just 200 years.

Voyages into sub-Antarctic waters began in the 16th and 17th centuries. The first recorded crossing of the Antarctic Circle and encounter with sea ice was in 1773 by British Captain James Cook who described that there must be 'a tract of land at the Pole that is the source of all the ice that is spread over this vast Southern Ocean'. Cook reached 71°S, a higher latitude than anyone before him. These voyages were followed by a period when American and British sealers travelled south encountering sea ice during their pursuit of seals (Fogg, 1992).

Scientific expeditions followed in the wake of the sealing parties. From the late 1830s onwards investigations into the earth's magnetic fields encouraged expeditions to set out to locate the South Magnetic Pole. The Frenchman Dumont d'Urville and the American Charles Wilkes searched for the South Magnetic Pole in 1840. The following year James Clark Ross of Great Britain sailed into the Ross Sea on HMS *Erebus* and HMS *Terror* on an unsuccessful expedition to determine the approximate position of the South Magnetic Pole. He was successful, however, in charting unknown territory and was probably the first to show a scientific interest in the sea ice. In fact, Joseph Hooker, the young naturalist on board HMS *Erebus*, investigated the discoloured sea ice they often encountered and which was first thought to contain volcanic ash. Hooker's examination of the melted ice samples showed this discoloration to be made by diatoms.

From then onwards, almost every expedition to the Antarctic resulted in scientific work being carried out, often including sea ice studies. Among the most significant were the descriptions of Antarctic sea ice by Drygalski (1904) which he recorded during the expedition of the *Gauss*. Wright and Priestley, who were members of Scott's last expedition, reported their interesting observations of sea ice both in the Journals and Reports of Scott's last expedition and in a classic book entitled *Glaciology* in 1922. A subsequent expedition, which provided new insight into the understanding of sea ice, was that of Shackleton between 1914 and 1917 published by Wordie (1921).

With the advent of new technology and scientific interest, the past 70 years has resulted in an almost exponential expansion in sea ice research, not only in the sense of reports and papers published, but also in the numbers of scientists participating in expeditions, workshops and dedicated sea ice symposia. Sea ice research is of great international importance, and present-day sea ice campaigns tend to bring scientists from many countries together in order to consolidate their efforts in a truely multi- and inter-disciplinary research focus.

1.3 Sea ice influence on ocean and atmosphere

Sea ice can be thought of as a thin blanket covering the ocean surface which controls, but is also controlled by, the fluxes of heat, moisture and momentum across

the ocean–atmosphere interface. Because it is relatively thin, sea ice is vulnerable to small perturbations within the ocean and/or the atmosphere, which significantly change the extent and thickness of the polar ice cover. Both, in turn, have a major influence on the state of the ocean and the atmosphere. Due to this complex interaction between key components of the earth's climate system sea ice has become one, if not the most important, component in the research of the past, present and future climate. The consequences of these interactions for the state of the sea ice itself are discussed separately.

Sea ice extent and thickness are controlled by the growth/decay and drift of the ice cover. They are therefore linked to thermodynamic and dynamic processes in the ocean and the atmosphere (and the sea ice). Cooling of the ocean surface below the freezing temperature, which ranges from 0°C for fresh water to −1.9°C for salty Antarctic shelf waters, initiates the formation of sea ice. The growth rate, and later the age, determines how much brine is expelled to the ocean (Eicken, Chapter 2), causing a densification of the surface waters.

For both hemispheres, these waters primarily correspond to shelf waters, indicating that on earth the continental shelves are the prime location for sea ice formation. In contrast to the Arctic where strongly diluted surface waters, due to river run off, buffer most of the salt input in autumn, brine rejection in the Southern Ocean causes deep convection, a cooling and salt enrichment of the whole shelf water column. At salinities greater than 34.46, these waters have the potential to initiate deep and bottom water formation during mixing with open ocean components at various locations of the Antarctic continental shelf break (Gill, 1973).

Especially in the Weddell and Ross Seas a most southerly located broad continental shelf results in surface waters being exposed to cold air, transported from high elevations of Antarctica's interior to the coast by strong katabatic winds. These winds, supported by tidal action, maintain narrow (hundreds of metres to a few kilometres) coastal polynyas along the ice shelf edges in which new ice forms at rates of up to 10 cm per day. In addition, coastal polynyas are very productive because the environmental conditions are such that sea ice formation occurs almost all year round. They are called *latent* heat polynyas because of the heat the surface water gains from the formation of ice crystals. This is the only heat available, but it is insufficient for melting sea ice because shelf convection transports only very limited, if any, heat from the depth to the surface (shelf waters are characterized by near-surface freezing temperatures). Therefore, it is the action of external forces (wind and tides) that mainly maintains low ice concentrations close to the Antarctic coast line.

The route high salinity shelf water takes on the shelf determines the mixing process and its contribution to the formation of new bottom water. Observations from the southern Weddell Sea are presented here, but the types of processes described are applicable to all broad continental shelves fringed by large ice shelves:

- A direct route towards the continental shelf break results in the mixing with different open ocean components forming Weddell Sea Bottom Water (WSBW) at the slope front (Foster & Carmack, 1976).
- A sloping shelf topography towards the south induces high salinity shelf water to flow into the ice shelf cavity participating in the sub-ice shelf circulation.
- Interaction with the deep ice shelf base initiates melting and possibly freezing, and the formation of a meltwater plume. This is less saline and, with temperatures below surface freezing, is defined as Ice Shelf Water (ISW). If bottom topography allows, ISW might reach the continental shelf break where mixing with deep waters of circumpolar origin again results in the formation of WSBW (Foldvik et al., 1985).

It has been speculated that the latter route might be sensitive to climate shifts, and related changes in the sea ice cover will have consequences for the ice shelf mass balance and the characteristics of the meltwater plume (Nicholls, 1997). The spreading of the new bottom water is confined to the Weddell Basin, but through mixing with overlying water masses it is able to escape as Weddell Sea Deep Water (WSDW) through gaps in the confining ridges. Outside the Weddell Sea this water mass is historically called Antarctic Bottom Water which has been observed in the Atlantic as far as 40°N.

The most famous *sensible* heat polynya is the Weddell polynya. Initiated by the heat of warm deep waters, at its maximum it has exposed nearly 250 000 km^2 of ice-free ocean to the winter atmosphere in the eastern Weddell Sea. It occurred most impressively during the mid-1970s. Thin ice and/or low ice concentration are common winter conditions in the vicinity of Maud Rise, a seamount at 65°S, 2.5°E which rises from the 5000 m deep abyssal plain to within 1600 m of the ocean surface. Interaction of ocean currents and tides with the steep bottom topography is assumed to trigger a complex regional circulation pattern which transports warm deep waters of circumpolar origin to the near surface. For a short period of time, the winter heat fluxes associated with this upwelling can be almost 200 $W m^{-2}$ with an areal average of 25 $W m^2$ (Muench et al., 2001). Under the perennial pack of the western Weddell Sea, however, heat fluxes are as low as 3 $W m^2$ (Lytle & Ackley, 1996) similar to the 2 $W m^{-2}$ in the central Arctic Ocean. Although ocean processes might initiate the polynya's onset, a persistent wind resulting from the interaction of the ice-free ocean with the atmosphere seems necessary to keep the area clean of ice, as indicated by results from a sea ice–mixed layer model coupled with a simple atmosphere (Timmermann et al., 1999). However, for the better understanding of the processes related to the onset, maintenance and decay of a polynya, further small-scale field studies accompanied by high-resolution numerical models combining atmosphere, sea ice and ocean processes are necessary.

As in the coastal polynya, sea ice formation and the resulting densification of the surface layer initiates open ocean convection which can affect a water column up to 4000 m thick (Gordon, 1978). As a result, most of the underlying deep water is

cooled with consequences for deep and bottom water formation and the characteristics of the world ocean abyss ventilated by these waters. For example, the cooling of the bottom layer of the Argentine Basin in the late 1980s can be related to the cooling of the deep Weddell Sea during the polynya years of the 1970s (Coles et al., 1996). Similar open ocean convection sites influenced by sea ice related processes exist in the northern hemisphere, namely the Greenland and Labrador Seas where the parent water masses of the North Atlantic Deep Water (NADW) are formed. NADW dominates the lower stratum of the Atlantic Ocean and has a global distribution by feeding the deep waters of the Antarctic Circumpolar Current.

A sensitivity of the formation process to changes in the Arctic sea ice cycle was assumed for the period of the Great Salinity Anomaly (Lazier, 1980). In the late 1960s a lens of fresh water caused by enhanced sea ice export through the Fram Strait, travelled south with the boundary current influencing both the Greenland and Labrador Seas. Nowadays, open ocean convection in the North Atlantic is supposed to be controlled by the atmospheric circulation, which might be influenced by anomalous sea ice conditions (Dickson et al., 1996).

In the central Arctic Ocean, convection is restricted to the upper 50–100 m due to the strong stratification of the water column. The deeper layers are renewed by advection of water masses of Atlantic origin entering through the Fram Strait and across the Barents Sea. Further modification occurs due to the admixture of cold and increased saline waters from the shallow continental shelf as the deep water flows anticlockwise with the gyre circulations which dominate the three Arctic basins (Rudels et al., 1994). Finally, these deep waters escape from the Arctic Ocean, again through the Fram Strait (sill depth $\sim$2500 m), into the Greenland and Norwegian Seas to contribute either there, or further downstream, to deep water formation. However, due to a sill depth of 600–800 m at the Greenland–Scotland Ridge only the upper deep waters of Arctic origin are able to continue towards the Labrador Sea.

The influence of sea ice on the atmosphere is manifold, covering a wide range of physical processes, and spatial and temporal scales. Primarily, sea ice, and the snow cover it can sustain, prevent the ocean from heating the lower atmosphere due to turbulent fluxes across the interface. A cooler atmosphere is also supported by a high surface albedo in summer and the emission of long-wave radiation in winter. The former reduces the absorption of short-wave solar radiation (absent in winter) that would otherwise warm (and melt) the ice or the ocean surface. The latter cools the snow and ice surfaces which in turn extract heat from the air blown across the interface. The winter cooling, however, can be mitigated by the existence of clouds, resulting from evaporation in ice-free areas, that effectively trap long-wave radiation. In summer, the warming of the atmosphere due to clouds might be less because a denser cloud cover reduces the incoming solar radition.

All of these factors illustrate a positive feedback mechanism, initiated by a climatic warming, that might lead to a reduced extent and thickness of the polar ice

cover. Sensitivity studies with a thermodynamic sea ice model reveal that the summer Arctic ice cover would completely disappear with a 3–5°C increase in air temperature or a 15–20% decrease in albedo (Maykut & Untersteiner, 1971). This model, however, did not include the relevant ice dynamics that might enhance an ice retreat because thinner ice is more compressible.

The influence of the sea ice on the dynamics of the atmosphere is concentrated on the atmospheric boundary layer. The exchange of momentum due to turbulent processes primarily controls the sea ice drift on time scales of 1 day and more; ocean currents dominate the sea ice motion on time scales of more than 1 month (Kottmeier & Sellmann, 1996). Among other things, polar field experiments are designed to determine drag coefficients used to parameterize the transfers of heat, moisture and momentum in atmosphere and sea ice models. The state-of-the-art sea ice models take numerous parameters into consideration including: different ice classes, thermodynamics based on a one-dimensional heat diffusion equation applied to multiple layers, a viscous-plastic rheology, a snow cover, sea water flooding due to the suppression of the ice–snow interface, and the formation of superimposed ice, the treatment of brine pockets, and biology. This information is all coupled to circulation models of different complexity for the atmosphere and the ocean.

The deep and bottom waters produced by the polar oceans form part of the global thermohaline circulation. Therefore, sea ice processes contribute to the driving of the global distribution of water mass characteristics, the ventilation of the deep world ocean, and the transport of natural and anthropogenic substances (tracers) from the ocean surface to the abyss where these can be stored for centuries. The latter is of climatic relevance in the view of increasing concentrations of greenhouse gases in the atmosphere, which are assumed to have caused the 0.5 K increase in global temperatures during the last century (Jones et al., 1999).

This warming, in turn, is thought to be responsible for the rapid reduction in summer extent of the Arctic ice cover during the past two decades (Comiso, Chapter 4). Since the warming predominately affects the perennial ice cover, it is not surprising that during the same period Arctic mean ice drafts also declined by 42% (Wadhams, 2001). Whether this trend continues or reverses due to, so far, unknown feedback mechanisms, and the consequences of an ice-free summer Arctic Ocean on the climate of the northern hemisphere and beyond, are still speculative. Further research is necessary to understand the complex climate system of which sea ice is one key component.

While in the Arctic, despite a large interannual variability, negative trends are becoming obvious. In contrast such changes are minor in the Antarctic where sea ice is more influenced by alternating anomalies propagating around Antarctica as part of the Antarctic Circumpolar Wave (ACW) (White & Peterson, 1996; Comiso, Chapter 4). The latter, however, seems to be linked to the El Niño Southern Oscillation (ENSO) cycle, indicating a control on the sea ice conditions far beyond the limits of the polar southern hemisphere.

1.4 Similarities and differences between Arctic and Antarctic sea ice

The most significant difference between the two polar regions, with regard to sea ice, is that the Arctic is a closed basin surrounded by land with only one deep passage through which water can be readily exchanged with the rest of the world's oceans. In contrast, the Antarctic Ocean is circumpolar and connected with the Indian, Atlantic and Pacific Oceans surrounding the continent.

Shelf seas in the Arctic take up about one-third of the ocean area with a depth below 100 m and the mean depth is 1800 m (Wadhams, 2000). In a broader sense, the Arctic encompasses estuaries, gulfs and bays such as Hudson Bay or smaller seas such as the Sea of Okhotsk and the White Sea. At the time of its maximum advance in February and March, sea ice covers the entire Arctic Ocean. By September it has reached its minimum (Comiso, Chapter 4). Sea ice in the Arctic extends from the North Pole to about latitude 44° in the Sea of Japan (Wadhams, 2000).

Antarctic annual sea ice has a much higher amplitude and year-to-year variability than in the Arctic (Table 1.1). Sea ice here occurs between about 55° and 75°S. In the Antarctic the continental shelves are very narrow, and so the Antarctic pack ice zone is largely over ocean basins between 4000 and 6500 m deep.

Ice growth and melting in both polar regions are governed by the same energy fluxes but several factors differ considerably between the hemispheres. The most notable is the oceanic heat flux. The heat flux in the Arctic is estimated to be about $2\,W\,m^{-2}$, whereas the average annual flux in many parts of the Southern Ocean may be as high as $30\,W\,m^{-2}$ (Lytle et al., 2000). More than half of the sea's ice in the Arctic is multi-year ice (Table 1.1) whereas in the Southern Ocean multi-year ice only constitutes a small fraction (Table 1.1; Eicken, Chapter 2; Haas, Chapter 3; Comiso, Chapter 4).

In the Arctic, sea ice is subjected to considerable terrestrial input, due to river run-off in the form of sediment and/or suspension freezing of bottom sediments. Pollution of sea ice in the Arctic can be considerable and is either aeolian or due to terrestrial and riverine runoff resulting from the proximity of industrial centres (Thomas & Papdimitriou, Chapter 9; Leventer, Chapter 10). In contrast, Antarctic sea ice can still be considered pristine, with terrestrial input playing an insignificant role and only found where sea ice occurs in the vicinity of exposed rocks or nunataks where strong winds may blow dust onto the sea ice. Aeolian pollution through industrial input is also of minor significance; however, signs of elevated PCB (polychlorinated biphenyls) have been found in birds and seals associated with sea ice.

Many other differences between Antarctic and Arctic sea ice exist, some of which are summarized in Table 1.1. They range from structural and textural differences, such as the composition of different ice textures, to differences in the salinity regime, heat flux and the biology.

One of the most significant differences is that in the Arctic man has been

Table 1.1 Examples of major differences between Arctic and Antarctic sea ice.

Feature	Arctic	Antarctic
Maximum extent	15.7×10^6 km^2 (February–March) (Comiso, Chapter 4)	18.8×10^6 km^2 (September) (Comiso, Chapter 4)
Minimum extent	9.3×10^6 km^2 (September) (Comiso, Chapter 4)	3.6×10^6 km^2 (February) (Comiso, Chapter 4)
Mean thickness	1996: 3 m 1976: 5 m (Wadhams, 2000)	0.5–0.6 m (Wadhams, 2000)
Annual ice cover (first-year ice)	7×10^6 km^2: < 50% (Comiso, Chapter 4)	15.5×10^6 km^2: > 80% (Comiso, Chapter 4)
Latitudinal range	90°N to 44°N	55°S to 75°S
Multi-year ice	9×10^6 km^2 (Gloersen et al. 1992) (Comiso, Chapter 4)	3.5×10^6 km^2 (Comiso, Chapter 4)
Extent of land-fast ice	Not known	5% (0.8×10^6 km^2) (Fedotov et al. 1998)
Annual average heat flux	2 W m^{-2} (Wadhams, 2000)	5–30 W m^{-2} (Lytle et al. 2000)
Platelet ice	Sporadic Fresh water under floes	Common under fast ice (Gow et al., 1998)
Polynyas	Coastal	Large, open ocean
Melt ponds	Significant feature	Insignificant feature
Superimposed ice	Present (Haas, Chapter 3)	Significant (Haas, Chapter 3)
Flooding	Not extensive	Extensive
Sea ice residence time	5–7 years	1–2 years
Drift velocity	2 km d^{-1} (Gow & Tucker, 1990)	> 20 km d^{-1} (Ackley, 1981)
Texture	5–20% frazil (Tucker et al., 1987)	50–60% frazil (Lange et al., 1989)
Salinity	Generally low	Higher
Pollution	Considerable riverine and aeolian	Insignificant aeolian
Sediment inclusion	Considerable	Insignificant
Top predators	Polar bear, polar fox	Leopard seal
Seals	Walrus; ringed, harp, bearded and hooded seal	Weddell seal, crabeater seal, Ross seal, fur seal
Flightless birds	None (except during moulting)	Emperor penguin, Adélie penguin
Fish associated with sea ice	Arctic cod (*Boreogadus saida*)	Broadhead fish (*Pagothenia borchgrevinki*)
Central crustaceans associated with sea ice	Amphipods	Krill (*Euphausia superba*)
Foraminifers	Planktonic foraminifera *Neogloboquadrina pachyderma*	Planktonic foraminifera *Neogloboquadrina pachyderma*
Nematodes	Several species, common	One record (Blome & Riemann, 1999)

associated with sea ice for millennia, whereas in the southern hemisphere man has only come into contact with sea ice very recently. The biology associated with sea ice has both similarities and large differences when Arctic and Antarctic ecologies are compared. In fact some species are cosmopolitan. Whales such as the minke whale frequent the pack ice of both the Arctic and the Antarctic, yet both hemispheres do not share the same seal species (Ainley et al., Chapter 8). While the polar bear is the top predator on Arctic sea ice, an equivalent predator is missing from Antarctic sea ice, although the leopard seal occupies a similar niche, living off penguins and other seals.

Many different seal species associated with sea ice occur in both polar regions where they have a very similar function in the food web (Ainley et al., Chapter 8). Many birds, both endemic and migratory, frequent the sea ice fields in both polar regions, the most significant difference being the flightless Adélie and emperor penguins in the Antarctic while the Arctic does not have flightless birds (Ainley et al., Chapter 8). Notable differences exist between the fish associated with the sea ice. The most important species in the Arctic is the arctic cod (*Boreogadus saida*) while in Antarctica it is the broadhead fish (*Pagothenia borchgrevinki*). These species occupy similar niches, often living amongst ice crystals, and have developed almost identical antifreeze proteins in response to similar environmental conditions although they are genetically unrelated.

Another major difference between Arctic and Antarctic sea ice associated organisms is found in the crustacea. In Antarctica, krill (*Euphausia superba*) is the pivotal crustacean, in terms of biomass, associated with sea ice. It is adapted to live off the micro-algae growing on the peripheries of ice floes as well as in the water column (Schnack-Schiel, Chapter 7). Although krill species occur in the Arctic, they do not reach the biomasses reported in Antarctic waters and *E. superba* is absent from the Arctic. Amphipods are not frequently found in Antarctic sea ice, whereas in the Arctic amphipods are the most dominant crustaceans associated with sea ice.

Smaller metazoans and protozoans such as copepods, ciliates, nematodes, turbellarians and foraminifers have been found in the sea ice of both hemispheres. An example is the planktonic foraminifer, *Neogloboquadrina pachyderma*, which has been found by many studies to be present in large numbers in Antarctic sea ice but has rarely been reported in Arctic sea ice. On the other hand, there is only one record of nematodes from sea ice in the Antarctic (Blome & Riemann, 1999), whereas they are commonly found in Arctic sea ice. The same applies to rotifers, often found in large numbers in Arctic sea ice, but which have not yet been recorded in Antarctic sea ice (Schnack-Schiel, Chapter 7).

There are well over 100 diatom species that are commonly found to live within the brine channel labyrinth of sea ice. Some of the important diatom species, such as *Fragilariopsis cylindrus* and *F. curta*, are bipolar and constitute important representatives in the sea ice of both polar oceans. Other species such as *Melosira arctica* have a central role in the sea ice ecosystem of the Arctic only.

Many of the similar, as well as different, features pertaining to sea ice relate to the

geological history of the poles. The bipolar occurrence of the same organisms in sea ice is often found in those that are able to migrate long distances, such as some birds and whales, or in the case of smaller planktonic organisms, those that are transported by ocean currents. However, some conundrums, such as the occurrence of the large numbers of krill in Antarctica and not in the Arctic, still need to be clarified.

1.5 Implications for astrobiology and future natural resource exploitation

Sea ice as a proxy for extraterrestrial systems

During the past 10 years sea ice has received increasing interest as a proxy for extraterrestrial systems and the search for life in other parts of our solar system. The fact that the earth's ice-covered poles appear to closely resemble those of other planets such as Mars or Jupiter's moons, Europa and Ganymede, makes ice, particularly sea ice, a possible proxy to assess and compare the suitability of extraterrestrial life (Chyba & Phillips, 2001). Based on the understanding of life processes on earth, some scientists argue that analogically life on another planet or moon might exist if four conditions are met (McKay, 2000):

- The presence of water or a similar solvent to enable biochemical activity.
- The availability of carbon, nitrogen, phosphorus and sulphur.
- Environmental stability.
- Energy to maintain biochemical processes.

Since sea ice appears to be an ideal terrestrial analogy, scientists are focusing on the psychrophilic environmental conditions and constraints for organisms living within. One theory is that life may have originated under just such conditions (Deming, 2002; Soare & Green, 2002). Because of its brine network, sea ice has the capacity to retain liquid pockets containing nutrients and organic resources down to -35°C. Metabolic activity, such as respiration and functional protein synthesizing machinery, has been detected at -20°C in sea ice. This, combined with the further evidence that bacteria have been observed to live at the interface between crystal and liquid (Junge et al., 2001), indicates that the eutectic interface between solid and liquid phases of water may well be a biochemical crucible for life (Deming, 2002). In particular, these ideas are enhanced by the findings that freezing improves and enhances important biomolecular reactions (Vajda, 1999).

Although these are possible analogues for the conditions that may have sustained primitive life on earth, countless questions concerning the origin of life and antecedent pre-biotic conditions remain unresolved (Levy & Miller, 1998). However, despite the tantalizing lure to compare the brown colourations observed on Europa's surface to diatom-coloured sea ice, these ice systems, tens to hundreds of

kilometres thick, are substantially different to the 1–10 m thick ice we know from polar oceans. Surface water or near surface water required for photosynthesis or sub-surface energetic conditions required for chemosynthesis have also not yet been discerned in this extraterrestrial system. With the intense radiation acting on the extraterrestrial ice, if life forms do exist, or have existed in the past, it seems that they will be quite unlike those that dominate sea ice found on earth today (Thomas & Dieckmann, 2002).

Use of ice organisms for novel biotechnologies

Because organisms, particularly bacteria and micro-algae living within the sea ice, have a high degree of biochemical and physiological adaptation to cold and changeable salinity conditions, they have a high potential for biotechnological applications (Russell, 1997; Cavicchioli et al., 2002; Thomas & Dieckmann, 2002; Thomas & Papadimitriou, Chapter 9). Adaptation to a permanently cold environment includes the optimization of basic cell processes necessary for growth and survival. These can be summarized into three categories: enzyme function, nutrient transport and cell membrane function. The adaptations of cellular processes in each of these areas represent potential biotechnology products for exploitation (Cavicchioli et al., 2002).

Two such examples are the production of polyunsaturated fatty acids (PUFAs) and the production of cold-active enzymes by bacteria and diatoms from Antarctic sea ice (Thomas & Dieckmann, 2002). A critical metabolic requirement at low temperatures is the maintenance of functional membranes. The fatty acid composition of membrane phospholipids regulates the degree of fluidity (Russell & Nichols, 1999). Therefore an increase in PUFAs is required to retain membrane fluidity at low temperatures. This approach may lead to new ways of manufacturing these fatty acids for the expanding market in these compounds as dietary supplements for humans, livestock and fish. To this day PUFAs have remained as a natural product due to the synthetic difficulty of reproducing the methylene interrupted double bond sequence by industrial chemistry. Their significance to animals and humans lies in their biological activity, as precursors for groups of nutritionally important compounds and as essential cellular components (Meyer et al., 1999). Interest in the production of PUFAs from alternative sources for use in aquaculture feeds and human health supplements has fuelled recent research into the molecular biology of PUFA production in sea ice organisms (Mock & Kroon, 2002a,b)

Cold-active or cold-adapted enzymes are produced by organisms existing in permanently cold habitats located in polar zones, at high altitudes or in the deep sea. These enzymes provide opportunities to study the adaptation of life to low temperature and also the potential for biotechnological exploitation (Morita et al., 1997; Deming, 2002; Thomas & Dieckmann, 2002). Applications exist in a range of industries for cold-active enzyme applications, e.g. cleaning agents, leather processing, degradation of xenobiotic compounds in cold climes, food processing

(fermentation, cheese manufacture, bakery, confectionery, meat tenderization) and molecular biology (Margesin & Schinner, 1999). Cold-active enzymes typically have maximal catalytic activity at temperatures below 40°C and usually display some degree of thermolability. Recent research has focused on determining the structural characteristics that confer cold adaptation in enzymes (Feller & Gerday, 1997). Individual enzyme types possess different structural strategies to gain overall increased flexibility, suggesting that protein folding has a critical role in conferring activity at low temperature. Preliminary data have been obtained for a variety of psychrophilic and psychrotolerant (cold-tolerant) enzymes from Antarctic bacterial isolates from sea ice indicating that they are good sources of cold-active enzymes (Nichols et al., 1999).

In addition to enzyme applications and PUFA production, cold-adapted archaea, bacteria and eukaryotes have wide-ranging biotechnological applications. These range from sources of cryoprotectants, bioremediation of oil spills, frost protection and low temperature waste treatment (Cavicchioli et al., 2002). The vastness of sea ice extent, and the diversity of abiotic regimes that are found within the sea ice zone, clearly promise tremendous potential for the discovery of novel low temperature extremophiles and their exploitation for future biotechnological applications.

1.6 Recent advances and perspectives

As we become increasingly aware of the tremendous influence sea ice has on global processes, particularly climate, it is not surprising that scientific interest is steadily growing and making rapid advances in all disciplines. Possibly one of the most crucial and pressing issues is whether the observed changes in sea ice cover, particularly in the Arctic, are part of some natural cycle or represent a climatic regime change in which the feedbacks associated with the presence of a sea ice cover play an important role. It is not yet really understood what the connections are between what is happening in the Arctic or Antarctic and other changes both inside and outside the polar regions. These questions will hopefully be answered with the advent of new remote-sensing technology and the development of improved models. Cryosat, for instance, is a 3-year radar altimetry mission, scheduled for launch in 2004, to determine variations in the thickness of the earth's continental ice sheets and marine ice cover. Its primary objective is to test the prediction of thinning Arctic ice due to global warming.

There are still fundamental problems with sea ice dynamical models that prevent their useful application in Global Circulation Models (GCMs). Parameter tuning is required because current sea ice models do not resolve physical processes below grid sizes of 100 km. Such tuning can, at best, provide a good fit to reality over limited periods of time. Accurate simulation over decadal and longer time-scales requires models with parameters that can be independently assessed. Ice thickness remains a largely uncertain parameter (Haas, Chapter 3).

The lack of sub-100 km scale model physics is compounded by the fact that, because ice floes are of typically 0.1–10 km^2, the continuity assumption of existing models breaks down below 100 km. Therefore the observed discontinuities in properties such as ice velocity, thickness and motion cannot be represented. Although these problems have been recognized for almost three decades, recent advances in numerical climate prediction make the study of the impact of improved sea ice physics especially relevant (Eicken, Chapter 2). There is a need to include comprehensive, elastic–viscous–plastic models of sea ice rheology. Further improvements to sea ice dynamical models require fundamental advances in understanding sub-grid scale physics down to the microstructure of sea ice. However, here too considerable advances are being made. Meso-scale ice thickness is being obtained with airborne EM (electromagnetic) instrumentation and upward looking sonars (ULS) either tethered to the sea floor or deployed in submarines (Haas, Chapter 3).

Recent improvements in analytical techniques, with the development of *in situ* earth-magnetic field NMR spectroscopy as a particularly interesting example, hold considerable promise in resolving some of the microstructural issues (Eicken, Chapter 2). Further down the scale, the eutectic interface between the solid and liquid phases of water in sea ice can be studied with sophisticated microscope technology being developed to examine micro-scale processes within sea ice (Junge et al., 2001; Deming, 2002).

The ecological significance of sea ice in the polar regions, whilst recognized as being considerable, is still difficult to assess because of logistical constraints and problems encountered in the methodology to investigate the heterogeneous and multiple ecological niches of the ice. Remote-sensing technology using ocean colour satellites such as the Sea-viewing Wide Field-of-view Sensor (SeaWiFS) and long time-series of sea ice concentration data from microwave sensors, available from the National Snow and Ice Data Center, one of eight NASA Distributed Active Archive Centers (DAACs), enable the examination of how variations in sea ice cover affect primary production associated with a retreating or advancing ice edge (Arrigo et al., 1999). Long-term records of environmental effects due to sea ice dynamics are scarce and incomplete. Yet these are essential to interpret correctly the observed fluctuations in krill, bird and animal populations (Croxall et al., 2002).

Large-scale under-ice surveys of organisms associated with the sea ice, particularly krill, using remotely operated or autonomous underwater vehicles, have improved our understanding of the relationship between krill and sea ice cover (Brierley et al., 2002). Biogeochemical processes, and the growth and survival of organisms within the ice or at the sea ice peripheries, are difficult to study without interfering or destroying the ice itself. The latest designs in microelectrodes and optodes are being successfully developed to avoid these problems and to measure parameters such as oxygen, nutrients and light in brine channels or the skeletal layer of sea ice (Mock et al., 2002; Thomas & Papadimitriou, Chapter 9). As mentioned

before, the psychrophilic sea ice organisms, particularly bacteria and diatoms, are being investigated and screened using molecular biological techniques to understand their adaptation and potential use in biotechnology.

The progress which has been made in obtaining physical, ecological and biogeochemical data on sea ice has benefited the first attempts to model and estimate primary production of sea ice, particularly in the Antarctic (Arrigo, Chapter 5). Yet despite these advances sea ice research is often comparable to the proverbial 'needle in a haystack'. If we consider the field experiments and measurements we come to the conclusion that only a very small proportion and area of the total sea ice cover has been investigated. The total number of cores extracted for physical and biological investigations probably does not even amount to more than a few hundred thousand, covering an area of only a few square kilometres. We use the data acquired in this manner to extrapolate, well knowing that sea ice samples taken only a few centimetres apart may differ tremendously in their fundamental properties.

We have a good knowledge of the fundamentals of chemistry and physics leading to the first crystals of ice (Eicken, Chapter 2). However, do we understand the chemical changes that take place from the point of freezing to the time of melting within the sea ice matrix, especially when there is extensive growth of biological assemblages which can be highly variable in composition (Lizotte, Chapter 6; Thomas & Papadimitriou, Chapter 9)?

Today more than ever, sea ice in the Arctic is receiving attention because of the search and quest for oil. The exploration and drilling for oil is known to be hazardous and often devastating to the environment. In the case of sea ice this is even more acute. The consequences of accidental oil spill in cold regions will clearly be far reaching. However, it is still unclear as to how oil will react with sea ice and how the sea ice biota and associated ecology will be affected. Preliminary studies have been conducted, but our understanding about the recovery of sea ice ecosystems following massive oil spill events still remains highly speculative. There is therefore a need to increase our awareness and to expand our research activities on sea ice in order to answer the many open questions. Increasingly we need to realize that with the expanding human population and the ever-widening quest for resources, sea ice will more than ever constitute a challenge to scientists and environmentalists alike.

Despite an overwhelming wealth of information which has been gathered over the past 200 years, sea ice still remains a largely unexplored realm. This is largely due to its inaccessibility, its complexity and extreme heterogeneity. Sea ice research remains a costly enterprise because of the specialized logistics essential for any fieldwork campaign. Most of our knowledge is derived from the summer months with very little direct information or data during the winter. More information is required on small- and large-scale processes. Longer time-series are required to understand seasonal and annual variations in the many processes that interact to make sea ice the complex, yet fascinating, substratum so important in a global context.

References

Arrigo, K.R., Robinson, D.H., Worthen, D.L., Dunbar, R.B., DiTullio, G.R, VanWoert, M. & Lizotte, M.P. (1999) Phytoplankton community structure and the drawdown of nutrients and CO_2 in the Southern Ocean. *Science,* **283**, 365–367.

Blome, D. & Riemann, F. (1999) Antarctic sea ice nematodes, with description of *Geomonhystera glaciei* sp. nov. (Monhysteridae). *Mitteilungen aus dem Hamburgischen Zoologischen Museum und Institut*, **96**, 15–20.

Bornemann, H., Kreyscher, M., Ramdohr, S., Martin, T., Carlini, A., Sellmann, L. & Plötz, J. (2000) Southern elephant seal movements and Antarctic sea ice. *Antarctic Science*, **12**, 3–15.

Brierley, A.S., Fernandes, P.G., Brandon, M.A., Armstrong, N.W., McPhail, S.D., Stevenson, P., Pebody, M., Perrett, J., Squires, M., Bone, D.G. & Griffiths, G. (2002) Antarctic krill under sea ice: elevated abundance in a narrow band just south of ice edge. *Science*, **295**, 1890–1892.

Brierley, A.S. & Thomas, D.N. (2002) On the ecology of Southern Ocean pack ice. *Advances in Marine Biology*, **43**, 173–278.

Buchanan, J.Y. (1874) Some observations on sea-water ice. *Proceedings of the Royal Society London*, **22**, 431–432.

Cavicchioli, R., Siddiqui, K.S., Andrews, D. & Sowers, K.R. (2002) Low-temperature extremophiles and their applications. *Current Opinion in Biotechnology*, **13**, 253–261.

Chyba, F.F. & Phillips, C.B. (2001) Possible ecosystems and the search for life on Europa. *Proceedings of the National Academy of Sciences*, **98**, 801–804.

Cleve, P.T. (1883) Diatoms collected during the expedition of the Vega. *Vega Expeditions*, Vetenskap Iakttagelsen, Stockholm, **3**, 455–542.

Coles, V.J., McCartney, M.S., Olson, D.B. & Smethie, W.M. Jr (1996) Changes in Antarctic Bottom Water properties in the western South Atlantic in the late 1980s. *Journal of Geophysical Research*, **101**, 8957–8970.

Croxall, J., Trathan, P.N. & Murphy, E.J. (2002) Environmental change and Antarctic seabird populations. *Science*, **297**, 1510–1514.

Deming, J.W. (2002) Psycrophiles and polar regions. *Current Opinion in Microbiology*, **5**, 301–309.

Dickie, G. (1880) On the algae found during the Arctic Expedition. *Botanical Journal of the Linnean Society, London*, **17**, 6–12.

Dickson, R., Lazier, J., Meincke, K., Rhines, P. & Swift, J. (1996) Long-term coordinated changes in the convective activity of the North Atlantic. *Progress in Oceanography*, **38**, 241–295.

Drygalski, E. (1904) *Zum Kontinent des eisigen Südens – Deutsche Südpolarexpedition – Fahrten und Forschungen des 'Gauß' 1901–1903*.Verlag Georg Reimer, Berlin.

Ehrenberg, C.G. (1841) Nachtrag zu dem Vortrage über Verbreitung und Einfluss des mikroskipischen Lebens in Süd- und Nordamerika. *Berichte über die zur Bekanntmachung geeigneten Verhandlung der Königlich-Preussischen Akademie der Wissenschaften zu. Berlin*, **1841**, 201–209.

Ehrenberg, C.G. (1853) Über neue Anschauungen des kleinstein nördlichen Polarlebens. *Berichte über die zur Bekanntmachung geeigneten Verhandlung der Königlich-Preussischen Akademie der Wissenschaften zu. Berlin*, **1853**, 522–529.

Fedotov, V.I., Cherepanov, N.V. & Tyshko, K.P. (1998) Some features of the growth, structure and metamorphism of East Antarctic landfast ice. In: *Antarctic Sea Ice: Physical Processes, Interactions and Variability*, (Ed. M.O. Jeffries), American Geophysical Union, Washington, D.C. *Antarctic Research Series*, **74**, 343–354.

Feller, G. & Gerday, C. (1997) Psychrophilic enzymes – molecular basis of cold adaptation. *Cellular and Molecular Life Sciences*, **53**, 830–841.

Fogg, G.E. (1992) *A History of Antarctic Science*. Studies in Polar Research, Cambridge University Press, Cambridge.

Foldvik, A., Gammelsrød, T. & Tørresen, T. (1985) Circulation and water masses on the southern Weddell Sea shelf. In: *Oceanology of the Antarctic Continental Shelf*, (Ed. S.S. Jacobs), American Geophysical Union, Washington, D.C. *Antarctic Research Series*, **43**, 5–20.

Foster, T.D. & Carmack, E.C. (1976) Frontal zone mixing and Antarctic bottom water formation in the southern Weddell Sea. *Deep-Sea Research*, **23**, 301–317.

Gill, A.E. (1973) Circulation and bottom water production in the Weddell Sea. *Deep-Sea Research*, **20**, 111–140.

Gloersen P., Campbell, W.J. Cavalieri, D.J., Comiso, J.C., Parkinson, C.L. & Zwally, H.J. (1992) *Arctic and Antarctic Sea Ice, 1978–1987: Satellite Passive Microwave Observations and Analysis*. NASA Special Publication, **511**, 289 pp. National Aeronautics and Space Administration, Washington, D.C.

Gordon, A.L. (1978) Deep Antarctic convection west of Maud Rise. *Journal of Physical Oceanography*, **8**, 600–612.

Gow, A.J., Ackley, S.F. & Govoni, J.W. (1998) Physical and structural properties of land-fast ice in McMurdo Sound, Antarctica. In: *Antarctic Sea Ice: Physical Processes, Interactions and Variability*, (Ed. M.O. Jeffries), American Geophysical Union, Washington, D.C. *Antarctic Research Series*, **74**, 355–374.

Horner, R.A. (Ed.) (1985) *Sea Ice Biota*. CRC Press, Boca Raton, Florida.

Jones, P.D., New, M., Parker, D.E., Martin, S. & Rigor, I.G. (1999) Surface air temperature and its changes over the past 150 years. *Reviews in Geophysics*, **37**, 173–199.

Junge, K., Krembs, C., Deming, J., Stierle, A. & Eicken, H. (2001) A microscopic approach to investigate bacteria under *in situ* conditions in sea ice samples. *Annals of Glaciology*, **33**, 304–310.

Kerr, R.A. (2002) A warmer Arctic means change for all. *Science*, **297**, 1490–1492.

Kottmeier, C. & Sellman, L. (1996) Atmospheric and oceanic forcing of the Weddell Sea ice motion. *Journal of Geophysical Research*, **101**, 20809–20824.

Lange M.A., Ackley, S.F., Wadhams, P., Dieckmann, G.S. & Eicken, H. (1989) Development of sea ice in the Weddell Sea, Antarctica. *Annals of Glaciology*, **12**, 92–96.

Lazier, J. (1980) Oceanographic conditions at ocean weather ship *Bravo*, 1964–1974. *Atmosphere and Ocean*, **18**, 227–238.

Levy, M. & Miller, S.L. (1998) The stability of the RNA bases: implications for the origin of life. *Proceedings of the National Academy of Sciences USA*, **95**, 7933–7938.

Lytle, V.I. & Ackley, S.F. (1996) Heat flux through sea ice in the western Weddell Sea: convective and conductive transfer processes. *Journal of Geophysical Research*, **101**, 8853–8868.

Lytle, V.I., Massom, R., Bindoff, A., Worby, A. & Allison, I. (2000) Winter-time heat flux to the underside of East Antarctic pack ice. *Journal of Geophysical Research*, **105**, 28759–28770.

McKay, C.P. (2000) The deep biosphere: lessons for planetary exploration. In: *Subsurface Microbiology and Biogeochemistry*, (Eds J.K. Fredrickson & M. Fletcher), pp. 315–328. John Wiley & Sons, New York.

Margesin, R. & Schinner, F. (1999) *Biotechnological Applications of Cold-Adapted Organisms*. Springer-Verlag, Berlin.

Martin, S. (1996) *A History of Antarctica*. State Library of New South Wales Press, Sydney.

Maykut, G.A. & Untersteiner, N. (1971) Some results from a time dependent thermodynamic model of sea ice. *Journal of Geophysical Research*, **76**, 1550–1575.

Meyer, B.J., Tsivis, E., Howe, P.R.C., Tapsell, L. & Calvert, G.D. (1999) Polyunsaturated fatty acid content of foods: differentiating between long and short chain omega-3 fatty acids. *Food Australia*, **51**, 82–95.

Mock, T., Dieckmann, G.S., Haas, C., Krell, A., Tison, J.-L., Belem, A.L., Papadimitriou, S. & Thomas, D.N. (2002) Micro-optodes in sea ice: a new approach to investigate oxygen dynamics during sea ice formation. *Aquatic Microbial Ecology*, **29**, 297–306.

Mock, T. & Kroon, B.M.A. (2002a) Photosynthetic energy conversion under extreme conditions. I. Important role of lipids as structural modulators and energy sink under N-limited growth in Antarctic sea ice diatoms. *Phytochemistry*, **61**, 41–51.

Mock, T. & Kroon, B.M.A. (2002b) Photosynthetic energy conversion under extreme conditions. II. The significance of lipids at low temperature and low irradiances in Antarctic sea ice diatoms. *Phytochemistry*, **61**, 53–60.

Morita, Y., Nakamura, T., Hasan, Q., Murakami, Y., Yokoyama, K. & Tamiya, E. (1997) Cold-active enzymes from cold-adapted bacteria. *Journal of the American Oil Chemists' Society*, **74**, 441–444.

Muench, R.D., Morison, J.M., Padman, L., Martinson, D., Schlosser, P., Huber, B. & Hohmann, R. (2001) Maud Rise revisited. *Journal of Geophysical Research*, **106**, 2423–2440.

Nicholls, K.W. (1997) Predicted reduction in basal melt rates of an Antarctic ice shelf in a warmer climate. *Nature*, **388**, 460–462.

Nichols, D.S., Sanderson, K., Bowman, J., Lewis, T., Mancuso, C.A., McMeekin, T.A. & Nichols, P.D. (1999) Developments with Antarctic microorganisms: PUFA, culture collections, bioactivity screening and cold adapted enzymes. *Current Opinions in Biotechnology*, **10**, 240–246.

Petterson, O. (1833) On the properties of water and ice. *Vega Expeditions*, Vetenskap Iakttagelsen, Stockholm, **3**, 249–323.

Plötz, J., Bornemann, H., Knust, R., Schröder, A. & Bester, M. (2001) Foraging behaviour of Weddell seals, and its ecological implications. *Polar Biology*, **24**, 901–909.

Rudels, B., Jones, E.P., Anderson, L.G. & Kattner, G. (1994) On the intermediate depth waters of the Arctic Ocean. In: *The Polar Oceans and Their Role in Shaping the Global Environment*, (Eds O.M. Johannessen, R.D. Muench & J.E. Overland), American Geophysical Union, Washington, D.C. *Geophysical Monograph*, **85**, 33–46.

Russell, N.J. (1997) Psychrophilic bacteria – molecular adaptations of membrane lipids. *Comparative Biochemistry and Physiology*, **118**, 489–493.

Russell, N.J. & Nichols, D.S. (1999) Polyunsaturated fatty acids in marine bacteria – a dogma rewritten. *Microbiology*, **145**, 767–779.

Smith, J., Stone, R. & Fahrenkamp-Uppenbrink, J. (2002) Trouble in Polar paradise. *Science*, **297**, 1489.

Soare, R.J. & Green, D.M. (2002) The habitability of Europa: a cautionary note. *EOS, Transactions of the American Geophysical Union*, **83**, 231.

Thomas, D.N. & Dieckmann, G.S. (2002) Antarctic sea ice – a habitat for extremophiles. *Science*, **295**, 641–644.

Timmermann, R., Lemke, P. & Kottmeier, C. (1999) Formation and maintenance of a polynya in the Weddell Sea. *Journal of Physical Oceanography*, **29**, 1251–1264.

Tomlinson, C. (1871) *Frozen Stream: Formation and Properties of Ice*. SPCK, London.

Tucker, W.B., Gow, A.J. & Weeks, W.F. (1987) Physical properties of summer sea ice in the Fram Strait. *Journal of Geophysical Research*, **92**, 6787–6803.

Usachev, P.I. (1949) The microflora of polar ice. *Transactions of the Institute Okeanology, Akademii Nauk SSSR*, **3**, 216 pp (in Russian).

Vajda, T. (1999) Cryo-bioorganic chemistry: molecular interactions at low temperature. *Cellular and Molecular Life Sciences*, **56**, 398–414.

Wadhams, P. (2000) *Ice in the Ocean*. Gordon and Breach Science Publishers, Amsterdam.

Wadhams, P. (2001) Sea ice: variations in extent and thickness. In: *Encyclopedia of Ocean Sciences*, (Eds J.H. Steele & K.K. Turekian), pp. 2582–2599. Academic Press, San Diego.

Weeks, W.F. (1998) On the history of research on sea ice. In: *Physics of Ice-covered Seas*, Vol. 1, (Ed. M. Leppäranta), pp. 1–24, University of Helsinki Press, Helsinki, Finland.

White, W.B. & Peterson, R.G. (1996) An Antarctic circumpolar wave in surface pressure, wind, temperature, and sea ice extent. *Nature*, **380**, 699–702.

Wordie, J.M. (1921) Shackleton Antarctic Expedition, 1914–1917: The natural history of pack ice as observed in the Weddell Sea. *Transactions of the Royal Society of Edinburgh*, **52**, 795–829.

Wright, I.P. & Priestley, R.E. (1922) *Glaciology. British (Terra Nova) Antarctic Expedition 1910–1913*. Harrison & Sons, London.

Zubov, N.N. (1945) *Arctic Ice*. US Navy Electronics Laboratory, San Diego, California (originally published in Russian by Izdatelstvo Glasevmorputi in 1943).

Chapter 2

From the Microscopic, to the Macroscopic, to the Regional Scale: Growth, Microstructure and Properties of Sea Ice

Hajo Eicken

2.1 Introduction

Motivation and context

The scope and individual chapters of this book provide an indication of the importance of sea ice over a wide range of scales in time and space. Considering the degree to which ice cover is intertwined with other phenomena and processes, this brief introduction and overview can only skim the surface and cover selected aspects but not do justice to the subject matter as a whole. For more complete and rigorous treatises of the growth, structure and properties of sea ice, readers are referred to the overview articles by Weeks & Ackley (1986), Weeks (1998) and Wettlaufer (1998) in the comprehensive monograph by Leppäranta (1998). The same monograph also includes a highly relevant chapter on the optical properties of sea ice by Perovich (1998). Aspects of sea ice characteristics relevant for microwave remote sensing are covered by Hallikainen & Winebrenner (1992) and Tucker et al. (1992) as well as the paper by Golden et al. (1998b) which introduces a series of studies of sea ice electromagnetic properties. While Maykut (1986) provides a thorough treatment of ice growth and properties in the context of the sea ice energy and mass balance, Steele & Flato (2000) extend this to include a detailed discussion of ice growth models. A useful summary and review of sea ice physical property data sets and measurements has been provided by Yen et al. (1991). Articles by Pfirman et al. (1990) and Reimnitz et al. (1992) provide further insight into the importance of sea ice as a geological agent.

This contribution is dedicated to the memory of Karoline Frey (1974–2002).

Approach

This chapter borrows from previous treatments of the topic, but attempts to splice these sometimes isolated and disparate approaches into a common thread that may help in appreciating the simplicity, as well as the complexity, of sea ice as one of the more interesting and influential (geo-) materials on our planet.

The importance of sea ice microstructure as both a result and a record of ice growth processes will be discussed in several sections below (for deformation processes see Haas, Chapter 3, and Weeks, 1998). The microstructure and texture of sea ice are a result of the meteorological and hydrographic boundary conditions prevailing during the growth of an ice layer (Fig. 2.1). Hence, the vertical stratigraphy of the ice cover, as revealed in thick or thin sections prepared from sea ice cores, contains an archive of ice growth conditions that can be interpreted in a similar manner to the climate records laid down in polar ice sheets. Due to the stark con-

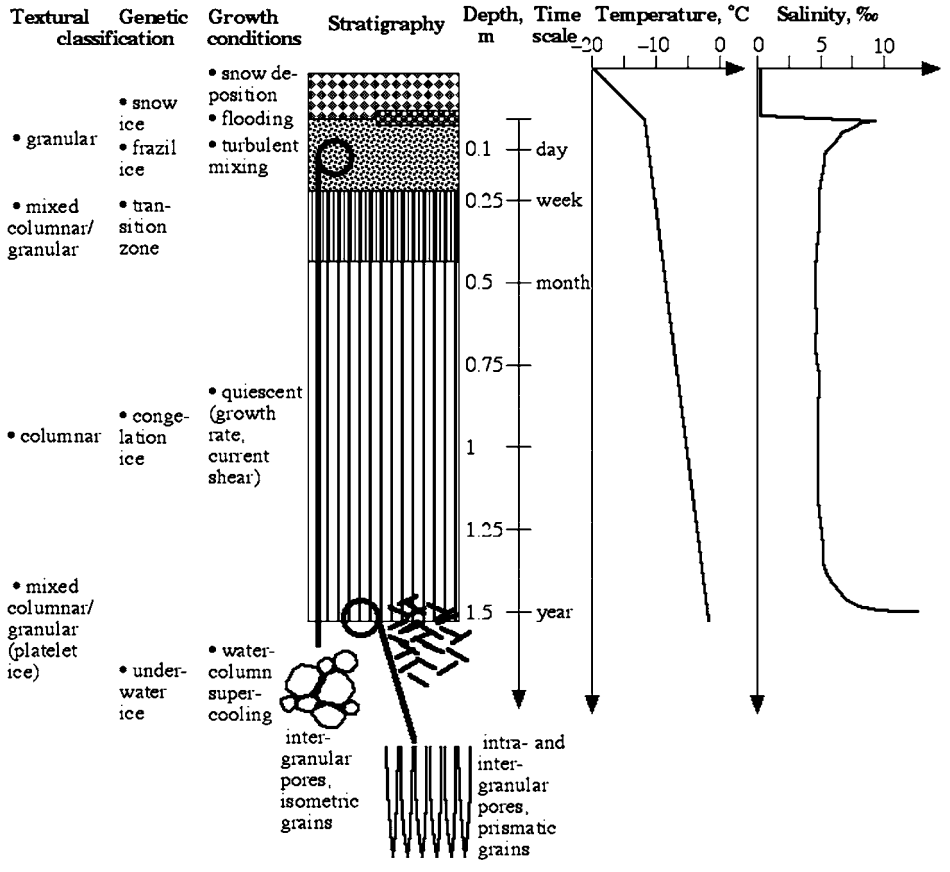

Fig. 2.1 Schematic summarizing the main ice textures, growth conditions and time scales, as well as typical winter temperature and salinity profiles for first-year sea ice.

trasts in the thermal, optical and mechanical properties of the component phases of sea ice (solid ice, brine and gas inclusions and, to a lesser extent, particulate inclusions) and strong anisotropy in the physical properties of these phases, as well as their spatial arrangement (i.e. microstructure and texture), the microstructure feeds back into the mode and rate of ice growth.

The central importance of sea ice microstructure requires that conceptual and mathematical models and representations of ice properties consider in detail the volume fraction, size, shape and spatial arrangement of brine, gas and particulate inclusions. For scalar quantities, such as ice density, only the volume fraction of inclusions is of concern (Cox & Weeks, 1988), whereas tensor properties such as the thermal conductivity or permeability require a more sophisticated approach. Simplification, such as the reduction of heat transport to a one-dimensional problem with temperature gradients restricted to the vertical direction of ice growth, can help reduce the complexity of such problems. Furthermore, for some processes such as heat transport, simple microstructural models (e.g. the Schwerdtfeger or Ono models with spherical or cylindrical brine inclusions, see Section 2.7) may already suffice. Ultimately, one hopes to integrate from the microscopic scale, that includes an explicit treatment of the microstructure of the material (as exemplified by the thin section photographs shown in Plate 2.1), to the macroscopic scale of bulk material properties (e.g. the individual stratigraphic layers or even the entire thickness of the ice cover shown in Fig. 2.1).

Much of the excitement and controversy in current sea ice research derives from the fact that modern methods of microstructural analysis are providing us with unprecedented detail of the three-dimensional microstructure. At the same time, large-scale models are only barely incorporating more complex or sophisticated representations (commonly referred to as parameterizations) of processes and properties on smaller scales (Steele & Flato, 2000). In the discussion below it is argued that some of this newly acquired knowledge may require us to revisit previous concepts of sea ice processes and phenomena and their dependence on events occurring at small scales. Some of it will undoubtedly only be of relevance for highly specialized approaches to the study of sea ice. Separating these domains, each important in its own right, may be a further challenge for sea ice researchers in the years to come.

Considering the limitations of the present contribution, the links between microstructure and ice properties cannot be discussed in the depth or detail they deserve. However, Section 2.4 illustrates the central role that both the bulk salinity and the *in situ* temperature of a given volume of ice play in determining key microstructural variables as well as ice properties. Furthermore, Section 2.5 outlines how microstructural evolution and chemical composition or salinity of sea ice are linked through processes confined to a bottom layer of a few centimetres thickness that govern much of what distinguishes sea ice from other types of ice.

Lake ice versus sea ice

As a way of illustrating how the aspects discussed above are intertwined in nature, and as an example of the manner in which ice growth, microstructure and properties manage to affect important processes up to regional scales, consider the following example.

The photographs in Plate 2.1 show the surface of a snow-free lake ice and sea ice cover in late spring near Barrow, Alaska. Despite comparable thickness and growth conditions, the lake ice, due to its high transparency, appears much darker than the sea ice. This is also expressed in a large difference in albedo (the fraction of the incident short-wave radiation reflected from a surface, Section 2.8), such that more than three-quarters of the incoming short-wave irradiative flux penetrates the lake ice surface and the underlying water, compared with less than half for the sea ice cover. This obviously has substantial consequences for the heat budget of the ice cover and the water beneath. The fact that the albedo of sea ice is typically higher than that of open water by a factor of up to ten gives rise to so-called ice-albedo feedback processes: a perturbation in the surface energy balance resulting in a decrease in ice extent due to warming may propagate and amplify since the reduction in ice extent in turn increases the amount of solar energy absorbed by the system (Curry et al., 1995). Under natural conditions, this contrast is affected by snow deposition in winter which increases albedo, at least prior to the onset of ice surface melt, and by the drainage of melt water from lake ice, potentially bringing up albedo later in the melt season. For low-albedo lake ice, this effect is less pronounced.

What is the cause underlying these contrasts? As the thin-section photographs in Plate 2.1 demonstrate, lake ice is nearly devoid of millimetre and sub-millimetre liquid inclusions, whereas sea ice can contain more than $10\,mm^{-3}$. Hence, while light passes through the clear lake ice with only minor attenuation along its path, much of the light entering sea ice is scattered back into the direction of the incoming rays. This explains both the high albedo and lack of transparency of thicker ice samples (Plate 2.1).

This contrast in ice properties and appearance is only in part explained by the mere difference in salinity between lake and sea water. Microscopically, i.e. at the scale of brine inclusions and below, lake ice grows differently from sea ice, with the interface between liquid and solid being planar rather than lamellar as is the case with sea ice. Hence, typically more than 99.9% of the impurities such as ions dissolved in lake water are expelled from the ice cover. In sea ice, brine is trapped between the lamellae at the bottom of the ice, allowing for a retention of between 10 and 40% of the ions in the ice (see Sections 2.5 and 2.6 for details).

These contrasts also highlight the differences between a macroscopic and a microscopic approach to the study of sea ice, as the former has to stop short at the larger scales exemplified by the surface photograph and the thin-section images shown in Plate 2.1. Here, the term ‘microscopic’ does not describe an absolute scale,

but rather the range of scales at which the different component phases can be clearly distinguished. By averaging over the individual, microscopic component phases one arrives at a macroscopic representation of the material where the specific properties of the microscopic component phases are subsumed in a single, bulk parameter. This approach requires a microstructural model of the medium.

While the differences in bulk ice properties such as albedo or optical extinction coefficient are immediately obvious from these images, the physical features and processes responsible for these differences only reveal themselves to the microscopic approach, as exemplified by the thin-section images depicting individual inclusions (Plate 2.1d, h). In the sections below, we will consider in more detail how microstructure and microphysics are linked to sea ice growth and evolution, and how both in turn determine the properties of the ice cover as a whole.

2.2 Growth, decay and the heat budget of sea ice

Freezing of sea water

Salinity of ocean water is measured in practical salinity units as defined by UNESCO (1978). The practical salinity scale (pss) assumes constant seawater composition (ideal salinity) and is based on conductivity ratios measured in the salinity interval from 1 to 42. Since bulk salinities of sea ice and brine are often well below or above these values, and given the varying chemical composition of ice and brine (Section 2.4), salinities of sea ice and brine will be quoted in ‰ as based on measurements of electrolyte conductivity of melted samples. Assuming standard seawater composition, for practical purposes concentrations in ‰ and psu (practical salinity units) can be assumed to coincide between 1 and 42‰.

The freezing point of sea water with a salinity of 34 is at -1.86°C due to the freezing-point depression by the dissolved inorganic salts (see Section 2.4). Pure sea water, lacking solid impurities that can act as nuclei for ice crystal formation, can be cooled substantially below the freezing point without ice formation (supercooling). However, maximum supercoolings observed in the oceans are typically less than 0.1 K due to the abundant presence of impurities upon which nucleation of ice crystals takes place (Fletcher, 1970).

In contrast to lake or brackish water, the temperature of the density maximum coincides with the freezing point of sea water. A body of sea water above the freezing point cooled from the surface will experience thermohaline convection (overturning of colder surface water which is in turn replaced by warmer water displaced at depth) until the entire upper water layer stirred by wind, waves and thermohaline mixing (mixed layer) is at the freezing point. In a lake of zero salinity, the water has its maximum density at 4°C, such that once the entire water column has cooled to this temperature, the surface waters stratify with ice forming as soon as

the very surface layer is at the freezing point, while denser, warmer water remains underneath.

The combination of thermohaline mixing and the action of wind stress at the ocean surface only rarely allows for quiescent initial formation of ice typical of lakes. Rather, ice crystals form throughout the upper water layers and are kept in suspension until a surface layer of ice slush builds up, reducing wind and thermohaline mixing. The ice crystals forming in the water take the shape of needles, spicules or platelets, often intertwined into aggregates and are known as frazil ice (Fig. 2.1, Plate 2.2). Individual crystals are typically a few to a few tens of millimetres across and less than a millimetre in thickness (Weeks & Ackley, 1986). Following further freezing and consolidation of this surface slush layer composed of frazil ice, the microstructure and texture of the ice changes as layer upon layer is added to the bottom of the ice sheet through quiescent growth of so-called congelation ice (Fig. 2.1). The stratigraphy of such a 'typical' ice cover, as revealed through analysis of vertical core sections, consists of a sequence of granular ice (a few tens of centimetres at most in the Arctic, but substantially more in other, more dynamic environments such as the Antarctic; crystals are isometric or prismatic (see detailed descriptions in Weeks & Ackley, 1986; Tyshko et al., 1997), followed by a transitional layer that is underlain by columnar ice, composed of vertically elongated prismatic crystals that can grow to several centimetres in diameter and tens of centimetres in length (Fig. 2.1, see Section 2.5 for details).

Formation of sea ice

In the Arctic Ocean, with its perennial ice cover and surrounding land masses, frazil ice forms mostly in the marginal seas and in leads or other openings in the ice pack, while most of the ice cover (between 60 and 80%) is composed of congelation ice. In the Antarctic, on the other hand, higher wind speeds, the effects of ocean swell penetrating from higher latitudes and the larger number of openings in the pack greatly favour the formation of frazil ice, which can constitute as much as 60–80% of the total ice thickness in some regions (Lange et al., 1989; Jeffries et al., 1994).

In the Southern Ocean, the ice edge advances northward from the continent by as much as 2500 km in austral autumn through spring (Comiso, Chapter 4). This dynamic ice-growth environment favours growth of frazil ice and leads to the predominance of so-called pancake ice (Plate 2.2). Pancake ice forms through accretion of frazil crystals into centimetre-sized flocs of ice which in turn accrete into decimetre-sized pans of ice. Under the action of wind and ocean swell penetrating deep into the sea ice zone, these pans bump and grind against one another, resulting in a semi-consolidated ice cover composed of ice discs that are from a few centimetres to more than 10 cm thick, with raised edges. Pancakes congeal into larger units, which may turn into 'meta pancakes' under the action of swell in the outermost pack ice zone (Wadhams et al., 1987). Once the ice cover has consolidated into a continuous, solid sheet or large floes, with snow accumulating on top, only characteristic surface

roughness features ('stony fields') betray its dynamic origins. However, stratigraphic analysis of ice cores clearly demonstrates that the ice cover is largely composed of individual pancakes, often tilted or stacked in multiplets on top of one another. The interstices between the individual pancakes eventually consolidate through a combination of frazil growth and freezing of congelation ice (Lange et al., 1989). Typically, these processes account for ice thicknesses of up to 0.5 m (Wadhams et al., 1987; Worby et al., 1998).

Surface energy balance and heat budget of sea ice

The fact that in the Southern Ocean, level, undeformed ice typically grows to less than 0.7 m thickness within a single year, compared to as much as 1.8 m in the Arctic (Haas, Chapter 3), leads us to the question as to what exactly controls the thickness that an ice floe can attain through freezing of sea water onto its bottom. The enthalpy of freezing, often referred to as latent heat of freezing, associated with the phase transition from water to ice is $334\,\mathrm{J\,g^{-1}}$ for pure ice and somewhat less for sea ice depending on salinity (Yen et al., 1991). Heat released from bottom freezing and cooling of the ice interior is then transferred to the upper surface of the ice cover and ultimately released to the atmosphere. The rate at which heat can be extracted is determined by the energy balance at the upper and lower surfaces of the ice sheet as well as the snow and ice thermal properties. For a surface that is in thermal equilibrium with the atmosphere, conservation of energy requires that the heat fluxes out of and into the ice be balanced:

$$(1-\alpha)F_\mathrm{r} - I_0 + F_\mathrm{L}\Downarrow - F_\mathrm{L}\Uparrow + F_\mathrm{s} + F_\mathrm{e} + F_\mathrm{c} + F_\mathrm{m} = 0 \qquad \text{(Equation 2.1)}$$

Here, the individual heat flux terms are: incoming solar short-wave flux, F_r (with ice albedo, α, indicating the ratio between incident and reflected short-wave energy for a given ice surface); the short-wave flux penetrating into the ice/water, I_0; the incoming long-wave flux, $F_\mathrm{L}\Downarrow$; the outgoing long-wave flux, $F_\mathrm{L}\Uparrow$; the turbulent sensible and latent heat fluxes F_s and F_e; the heat flux due to melting or freezing of ice at the surface, F_m (in the Arctic typically only relevant during the summer after the ice surface starts to melt); and the conductive heat flux, F_c. By convention, fluxes directed away from the surface are negative; details on the surface energy balance can be found in Maykut (1986) and Steele & Flato (2000).

While a detailed discussion of the magnitude of all these terms is given in Maykut (1986) or Persson et al. (2002), over Arctic multi-year ice the net radiation balance typically does not drop below $-50\,\mathrm{W\,m^{-2}}$ during winter and has its maximum in July at just over $100\,\mathrm{W\,m^{-2}}$. The other fluxes range between a few to a few tens of $\mathrm{W\,m^{-2}}$.

The conductive heat flux, F_c, indicates how much energy is transferred into a unit area of the surface ice layer per unit time (not only through heat conduction but also through convective or advective processes). It depends on the thermal conductivity, λ_si, of the ice and the local temperature gradient $\partial T/\partial z$ at depth z (for the simplified one-dimensional case, with $z = 0$ at the ice surface):

$$F_c(z) = -\lambda_{si}\left(\frac{\partial T}{\partial z}\right)_z \qquad \text{(Equation 2.2)}$$

For thin ice of thickness H, or slow variations in surface energy balance terms – with respect to the rate of conductive heat transfer, the temperature gradient can be approximated as linear, such that:

$$F_c = -\lambda_{si}\left(\frac{T_0 - T_f}{H}\right) \qquad \text{(Equation 2.2a)}$$

where T_f is the salinity-dependent freezing temperature at the ice bottom (typically constant at -1.86°C or 271.29 K) and T_0 is the surface temperature. Since most terms in the surface energy balance (Equation 2.1) depend on T_0 themselves, thermal equilibrium at the ice surface is the result of a number of physical processes that adjust T_0 such that all the terms in Equation 2.1 are balanced. Hence, the conductive heat flux can be thought of as a residual term that responds to changes in the other fluxes into and out of the surface layer by inducing variable rates of accretion (or melting) at the ice bottom.

The ice growth rate, in turn, is determined by the energy balance at the lower boundary, i.e. the ice bottom. Here, the conductive heat flux out of the interface, F_c (which is equal in magnitude to that into the upper surface for a linear temperature gradient), and the oceanic heat flux, F_w, out of the underlying water into the ice are balanced by the release or uptake of latent heat, L, during freezing or melting for a thickness change dH/dt for ice of density ρ_i:

$$F_c + F_w + \rho_i L \frac{dH}{dt} = 0 \qquad \text{(Equation 2.3)}$$

In the absence of an oceanic heat flux, the ice cover would thicken as long as the surface temperature of the ice were less than the freezing point of sea water at the lower interface (assuming no radiative transfer of energy into the ice). Typically, however, the ocean underlying the ice contains a reservoir of heat that is either remnant from solar heating of the mixed layer in summer (Maykut & McPhee, 1995) or due to transfer of heat from deeper water layers. In the Arctic, where the amount of heat transported into the polar basin and entrained into the surface mixed layer from below the halocline is comparatively small, F_w amounts to a few W m^{-2} at maximum in most regions (Steele & Flato, 2000). In the North American Arctic, where advection of heat is minimal, the seasonal cycle of F_w is almost exclusively controlled by the absorption of solar short-wave radiation in the upper ocean, which is transferred to the ice bottom later in the season (Maykut & McPhee, 1995).

In the Antarctic, ocean heat flow can be in the order of several tens of W m^{-2} (Martinson & Iannuzzi, 1998). As a result, even an ice cover that is cooled substantially from the atmosphere in winter, may only grow to a maximum thickness

that is determined by the balance of ocean and conductive heat flow, $F_c = F_w$. Measurements of ice thickness and surface hydrography indicate that this maximum (winter equilibrium) thickness is in the order of 0.5 to 0.7 m (Wadhams et al., 1987; Martinson & Iannuzzi, 1998). As shown in Section 2.3, such estimates can also be obtained from simple analytical modelling.

In areas where oceanic heat fluxes can episodically increase to several hundred $W\,m^{-2}$ due to convective exchange with a deeper ocean well above freezing (McPhee et al., 1996), an ice cover can thin significantly, or vanish entirely, by melting from below. Such extended areas where the ocean is ice free even in mid-winter are referred to as polynyas. The vast Weddell Sea polynya of the 1970s is the most prominent example of open water maintained through active melting and heating of the surface ocean (Dieckmann & Hellmer, Chapter 1; Comiso, Chapter 4). Alternatively, polynyas can also form dynamically, with strong, steady winds pushing ice away from a coastline or stretches of land-fast ice.

The role of the snow cover in sea ice growth

Though it typically accounts for less than 10% of the total mass of ice in the polar seas, the snow cover plays a major role in the heat budget of sea ice. First, snow albedos are consistently higher than those of bare sea ice (Section 2.9). More importantly, the insulating properties of the snow cover, with thermal conductivities between 0.1 and $0.4\,W\,m^{-1}\,K^{-1}$, as compared to roughly $2\,W\,m^{-1}\,K^{-1}$ for sea ice (Massom et al., 2001; Sturm et al., 2002), can impede ice growth by reducing the conductive heat flux, F_c (equation 2.2), by as much as 50%. At the same time, the sensitivity of the ice cover to changes in the oceanic heat flux increases (Equation 2.3). In the Antarctic, where snow depths on sea ice reach several tens of centimetres and more than a metre in some regions (Jeffries et al., 1994), model simulations show that snow deposition approximately halves the ice thickness in the Weddell Sea and east Antarctica. Another consequence of snow deposition on sea ice is a reduction in the amount of short-wave radiation entering into the ice and underlying water, and a temperature increase in the upper sea ice layers. Both have important ramifications for overall ice properties and the role of sea ice as a habitat for micro-organisms (Arrigo, Chapter 5).

In most cases snow-covered ice grows to be thinner than snow-free ice. However, once the load of a thicker snow cover is sufficient to depress the ice surface below the sea surface, sea water and brine may percolate either vertically or laterally through the ice cover (Maksym & Jeffries, 2000). Such seawater flooding shifts the locale of ice growth from the bottom of the ice cover to its top surface and the bottom of the snow pack. The ensuing increase in the conductive heat flux, F_c (Equation 2.2), allows more ice to grow per unit area and time than would be possible through freezing at the ice bottom.

In the Arctic, snow depths in relation to ice thickness are rarely high enough to allow for surface flooding and snow ice formation. In the Antarctic, however, an

overall thinner ice cover and higher snow accumulation rates result in widespread occurrence of this phenomenon, with more than 50% of the surface flooded in some areas (Eicken et al., 1994; Jeffries et al., 1994; Worby et al., 1998). This has important consequences for sea ice remote sensing as it substantially changes the dielectric properties of sea ice and hence its signature in active and passive microwave remote-sensing data sets (Section 2.8; Comiso, Chapter 4). Similarly, sea ice ecology is also strongly affected by this process (Lizotte, Chapter 6; see infiltration layer community in Plate 2.3b).

As the flooded snow refreezes, the microstructural traces of its meteoric origin are often obliterated and it becomes exceedingly difficult to distinguish such snow ice from similarly fine-grained consolidated frazil ice. Here, the stark contrast in the stable-isotope signatures of snow, which is greatly depleted in the heavy isotopes of oxygen (^{18}O) and hydrogen (D), and ice grown from sea water with its stable, undepleted composition, can help determine the total contribution of precipitation (often referred to as meteoric ice) to the total ice thickness (Eicken et al., 1994). Numerous studies in the Southern Ocean have established that snow ice (the frozen mixture of snow and sea water and/or brine) is exceedingly common, accounting for between a few per cent to more than 50% of the total ice thickness, with the actual meteoric ice fraction generally less than 20%. Both small- and large-scale model simulations (Eicken et al., 1995; Fichefet & Morales Maqueda, 1999; Maksym & Jeffries, 2000) indicate snow ice formation to be important also on the global scale.

Snow ice formation may also help prevent the complete removal of sea ice from areas with high oceanic heat fluxes, F_w. For example, in the eastern Weddell Sea bottom topography and local hydrography result in winter values of F_w in excess of $100\,W\,m^{-2}$ for extended periods of time (McPhee et al., 1996). In the mid-1970s this region was the site of a vast polynya that persisted for several years (Comiso, Chapter 4). Considering that such high heat fluxes would halt ice growth and induce bottom melt even in mid-winter, one wonders how an ice cover can survive at all in this region. Observations during the ANZFLUX study (McPhee et al., 1996) demonstrated that level ice of several tens of centimetre thickness does in fact melt at rates of several centimetres per day in the area during intervals of high oceanic heat flux. At the surface of the ice, buffered against the oceanic heat by the ice layers below, snow ice growth seems to be able to compensate for the intermittent substantial bottom ice losses.

Sea ice melt

As has been demonstrated above, ice melts at the bottom whenever the oceanic heat flux into the ice–water interface exceeds the conductive heat flux out of the interface. For sea water of constant salinity, the interface temperature is not subject to change but remains constant at the ice melting/freezing point of, for example, $-1.86^{\circ}C$ for a salinity of 34. At the upper surface of sea ice, temperatures are typically much lower in winter, such that the corresponding situation of a net heat

flux into the ice cover does not immediately result in melting, but first of all in a warming of the ice cover. As will become evident in Section 2.4, warming of sea ice is also associated with melting, but on a microscopic scale, not at the scale of the ice thickness. Typically, this warming is accompanied by a reduction in ice salinity, with the surface layer of sea ice approaching zero salinity as a result of surface warming and snow melt that flush salt downwards into the ice cover (Untersteiner, 1968).

While the linkage between surface salinity, ice temperature and microscopic melt is more complex and discussed in more detail in Section 2.7, warming eventually brings the temperature up to the bulk melting point of ice. Any further input of heat into the surface layer results in melting (i.e. the term $F_m > 0$ in Equation 2.1) and a reduction in ice thickness through surface ablation. In contrast with bottom melt, surface melt generates liquid water above sea level, and the subsequent fate of this melt water plays an important role in the energy and mass balance of the ice cover as a whole. Typically, in the Arctic a quarter of this water is retained in surface melt ponds (Eicken et al., 2002), resulting in a significant decrease in surface albedo (apparent in Plate 2.3a and discussed in more detail in Section 2.9). As much as half of it percolates downward into the ice, flushing out salt in the process, with the rest running off into the upper ocean.

While surface melting is the dominant ablation process in the Arctic, accounting for a loss of between 0.3 and 1 m of ice from the surface of the perennial ice in the central Arctic, recent studies indicate that bottom melt is increasing in importance: As much as 0.5 m of level ice melted off the bottom in a single season (McPhee et al., 1998; Perovich et al., in press). Only a minor fraction of bottom melt can be explained by transfer of heat from the deeper ocean into the surface layer, with most of it supplied by solar heating. Decreasing ice concentrations and ice extent over the Arctic Ocean in the 1990s (Serreze et al., 2000) have apparently resulted in an increase in the amount of solar short-wave energy stored in the upper ocean and released during the latter part of the summer melt season. In combination with atmospheric warming and shifts in ice circulation, these changes are believed to be underlying observations of a thinning of the Arctic ice pack (Rothrock et al., 1999) and, if continuing unabated, may result in significant shrinkage, if not complete disappearance, of the perennial Arctic sea ice.

Currently, and probably for the past hundreds of thousands of years (Armand & Leventer, Chapter 11), most of the Arctic sea ice cover survives summer melt, with subsequent surface melting and winter accretion resulting in a gradual thickening of the ice cover. The amount of winter ice growth at the bottom decreases with ice thickness (see Equation 2.2 and Section 2.3), whereas the amount of surface and bottom melt does not. Consequently, at some point perennial sea ice reaches a maximum equilibrium thickness for which the amount of summer melt is compensated by the amount of a winter's growth. While the concept of an equilibrium thickness is highly idealized, neglecting, among other things, interseasonal and interannual variability in atmospheric and oceanic forcing or ice properties, it is of substantial value in discussing the impacts of variability in the forcing.

Numerical simulations by Maykut and Untersteiner indicate that ice which has attained equilibrium thickness is between 2.5 and 3 m thick at the onset of summer melt (Maykut, 1986). These model results were obtained for atmospheric forcing data representative of the 1960s to the 1980s and recent observations indicate that equilibrium thickness may have substantially decreased (Perovich et al., in press; Haas, Chapter 4). Among other factors, such as the depth of the snow cover, the magnitude of the oceanic heat flux plays a prominent role in determining the equilibrium thickness. Maykut and Untersteiner's model results suggest that the perennial ice vanishes for $F_w > 7\,W\,m^{-2}$, with only seasonal ice remaining in the Arctic Ocean.

By contrast, the surface of Antarctic sea ice floes appears almost unchanged during the summer months (Plate 2.3b), as most of the melting takes place along their margins and bottom, due to heat transfer from the deeper ocean as well as absorption of solar radiation in surface waters. The lack of ice surface ablation and development of melt ponds, characteristic of the Arctic ice pack, is commonly explained by a combination of a colder, drier atmosphere in the Antarctic that effectively cools the ice surface even during summer (Andreas & Ackley, 1981) along with smaller concentrations of surface impurities in Antarctic snow and ice as compared with the Arctic. Nevertheless, recent observations of melt ponding, both on sea ice (Drinkwater & Xiang, 2000) as well as on the floating ice shelves of the Antarctic Peninsula, raise the question whether the Antarctic ice pack can also be subject to extensive surface melt and the associated drastic reductions in surface albedo under a variable or changing climate regime.

The importance of ice deformation

In discussing the impact of climate variability and change on the state of the polar sea ice covers, one needs to consider more than thickening or thinning of the ice cover through ice growth or melt. Deformation of the ice cover through rafting and ridging of floes (Plate 2.2) not only accounts for the thickest ice observed in the polar oceans, it also provides a mechanism for rapid thickening in cases where freezing rates at the ice bottom are approaching zero (see Section 2.3). The complex interplay of different deformation processes and their overall impact on the ice thickness distribution are the topic of Chapter 3 by Haas. Here it suffices to state that predicting the response of an ice cover to changes in the meteorological and oceanographic boundary conditions requires an assessment of both the static component of ice growth and melt, as well as the dynamic component of thickening through rafting or ridging. Deformation processes are particularly important in a warming climate, as they may be capable of compensating for some of the thinning due to lesser ice growth and increased ice melt.

2.3 Simple models of sea ice growth

A rigorous mathematical treatment of the problem of ice growth requires numerical techniques because the individual terms in the surface energy balance (Equation 2.1) depend either directly or indirectly on the surface temperature, which in turn determines the magnitude of the conductive heat flux and hence the ice growth rate (Steele & Flato, 2000). Thus, it is not possible to describe the surface ice temperature and the ensuing ice growth rate through a simple, closed (analytical) statement. Nevertheless, as demonstrated more than a century ago by Stefan (Leppäranta, 1993) through some simplifications it is actually possible to arrive at fairly accurate predictions of ice growth. Such simple, so-called degree-day models can also help us in understanding key aspects of the heat budget of sea ice and are therefore discussed in more detail below.

The principal aim of ice-growth modelling is to evaluate the growth rate $\mathrm{d}H/\mathrm{d}t$ of sea ice as a function of time. Assuming heat-transfer only in the vertical and a linear temperature profile (see Section 2.2), $\mathrm{d}H/\mathrm{d}t$ is given by

$$\frac{\mathrm{d}H}{\mathrm{d}t} = \frac{\lambda_\mathrm{i}}{H\rho_\mathrm{i}L}\left(T_0 - T_\mathrm{f}\right) \qquad \text{(Equation 2.4)}$$

with ice density ρ_i, latent heat of fusion L, ice thermal conductivity λ_i, surface temperature T_0 and bottom temperature T_f. During the polar winter, the short-wave fluxes can be ignored and one furthermore finds that net long-wave radiative fluxes can be described as a function of surface or air temperature. Likewise, the turbulent heat fluxes F_s and F_e depend on air and surface temperature. In his analysis of the problem, Stefan assumed that the ice surface temperature is equal to the air temperature, T_a. This is a reasonable simplification, in particular for large ice thicknesses, and as discussed above and in Section 2.2, air and surface temperature are in fact closely coupled. Substituting T_a for T_0 and integrating Equation 2.4 over time (i.e up to day t_e) yields

$$\frac{1}{2}H^2 = \frac{\lambda_\mathrm{i}}{\rho_\mathrm{i}L}\int_0^{t_\mathrm{e}}\left(T_\mathrm{f} - T_\mathrm{a}\right)\mathrm{d}t \qquad \text{(Equation 2.5)}$$

Commonly, the term

$$\theta = \int_0^{t_\mathrm{e}}\left(T_\mathrm{f} - T_\mathrm{a}\right)\mathrm{d}t \qquad \text{(Equation 2.5a)}$$

is computed for discrete time steps of $\Delta t = 1$ day; θ is then referred to as the number of freezing-degree days, a variable easily derived from standard meteorological observations.

Rather than solving Equation 2.5 for H, one can take into account differences in ice surface and air temperature (T_0 and T_a) by introducing a transfer coefficient, K_a, that describes the heat flux out of the upper surface as a result of the difference between T_a and T_0. For T_0 below freezing, this simplified flux balance is then given by

$$K_a(T_a - T_0) = \frac{\lambda_i}{H}(T_0 - T_f) \qquad \text{(Equation 2.6)}$$

which yields

$$\frac{dH}{dt} = -\frac{\lambda_i K_a}{(\lambda_i + K_a H)\rho_i L}(T_a - T_f) \qquad \text{(Equation 2.7)}$$

for the ice growth rate. Integrating, one obtains

$$H^2 + \frac{2\lambda_i H}{K_a} = \frac{2\lambda_i}{\rho_i L}\theta \qquad \text{(Equation 2.8)}$$

Whereas the thermal properties of the ice λ_i, L and its density ρ_i are known, the heat transfer coefficient K_a is likely to vary depending on the local boundary conditions. Reasonable accuracy can be achieved by deriving K_a empirically, typically from a time-series of ice thickness and air temperatures for a given location. One such empirical approach is that by Anderson (1961) with ice thickness given as

$$H^2 + 5.1H = 6.7\theta \qquad \text{(Equation 2.9)}$$

Figure 2.2 shows a comparison between the Anderson model and measurements. As indicated by the quadratic nature of Equation 2.8, ice growth slows as the ice cover thickens with time. As a consequence, differences in thickness between ice floes formed at different stages in winter tend to diminish with time. In the absence of ocean (or solar) heat fluxes into the ice, and without any summer melt, there would be no limiting thickness for sea ice growth. However, since the oceanic heat flux, F_w, is rarely 0, at some point the ice thickness reaches a limiting, maximum value for which the conductive heat flux out of the ice bottom equals that of the oceanic heat flux into it (Equation 2.3) and all ice growth stops. The magnitude of this limiting or equilibrium thickness, H_{eq}, is given by

$$H_{eq} = \frac{\lambda_i(T_f - T_0)}{F_w} \qquad \text{(Equation 2.10)}$$

For typical Antarctic conditions, with $T_f - T_0 = 5\,K$, $\lambda_i = 2.0\,W\,m^{-1}\,K^{-1}$ and $F_w = 20\,W\,m^{-2}$, the limiting thickness is 0.5 m, suggesting that the ocean does in fact limit growth of level ice. In the Arctic, owing to F_w typically being smaller by an order of

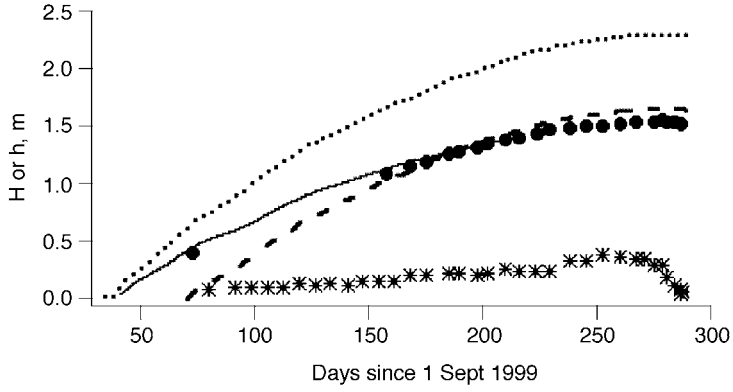

Fig. 2.2 Simulations and measurements of ice growth near Barrow, Alaska. The solid line corresponds to results from a numerical model (as described in Eicken, 1998), whereas the dotted (no snow cover) and dashed (0.1 m snow) lines show results from an analytical degree-day model based on Anderson (1961). Measurements of ice thickness (*H*) and snow depth (*h*) are represented by large dots and asterisks, respectively.

magnitude, the limiting thickness greatly exceeds what can be achieved within a single year of ice growth.

As discussed in Section 2.4, Equation 2.8 may be overly simplistic insofar as it ignores the impact of a snow cover on ice growth. This problem can be addressed, however, by deriving an effective ice thickness, H_{eff}, that follows from the balance of fluxes at the snow-ice interface and takes into account the additional impact of an insulating snow layer of thickness h and thermal conductivity λ_s:

$$H_{eff} = H + \frac{\lambda_i}{\lambda_s} h \qquad \text{(Equation 2.11)}$$

Substituting into Equation 2.7 and integrating yields

$$H^2 + \left(\frac{2\lambda_i}{\lambda_s} h + \frac{2\lambda_i}{K_a}\right) H = \frac{2\lambda_i}{\rho_i L}\theta \qquad \text{(Equation 2.12)}$$

Evaluating this equation with typical values as given by (Maykut, 1986), where $K_a = 209\,\mathrm{J\,cm^{-2}\ day^{-1}\ K^{-1}}$, $\lambda_i = 1758\,\mathrm{J\,cm^{-1}\ day^{-1}\ K^{-1}}$, $\rho_i L = 272\,\mathrm{J\,cm^{-3}}$, $\lambda_s = \lambda_i/6.5$, we obtain the following general expressions for H (in cm):

$$H^2 + 16.8H = 12.9\theta \qquad (h = 0) \qquad \text{(Equation 2.13a)}$$

and

$$H^2 + (13.1h + 16.8)H = 12.9\theta \qquad (h > 0) \qquad \text{(Equation 2.13b)}$$

As evident from Fig. 2.2, the impact of a snow cover on the ice thickness evolution is substantial. Comparing the measurements to results from the analytical model (which assumes a constant snow depth) and a more sophisticated numerical model, the discrepancies between the three growth curves are as much dependent on uncertainties in the amount and timing of snowfall as on uncertainties in the ice and snow thermal properties.

2.4 A brief overview of the physical chemistry of sea ice

Crystal structure of ice Ih

Ultimately, the characteristic properties of sea ice and its role in the environment, as exemplified by the stark contrasts in ice albedo between sea and lake ice (Plate 2.1), are governed by the crystal lattice structure of ice Ih. Depending on pressure and temperature, water ice can appear in more than a dozen different modifications. At the earth's surface, freezing of water under equilibrium conditions results in the formation of the modification ice Ih, with the 'h' indicating crystal symmetry in the hexagonal system. Throughout this chapter, the term 'ice' refers to ice Ih.

The water molecules (H_2O) in ice Ih are arranged tetrahedrally around each other, with a six-fold rotational symmetry apparent in the so-called basal plane (Fig. 2.3). The principal crystallographic axis (referred to either as the corresponding unit

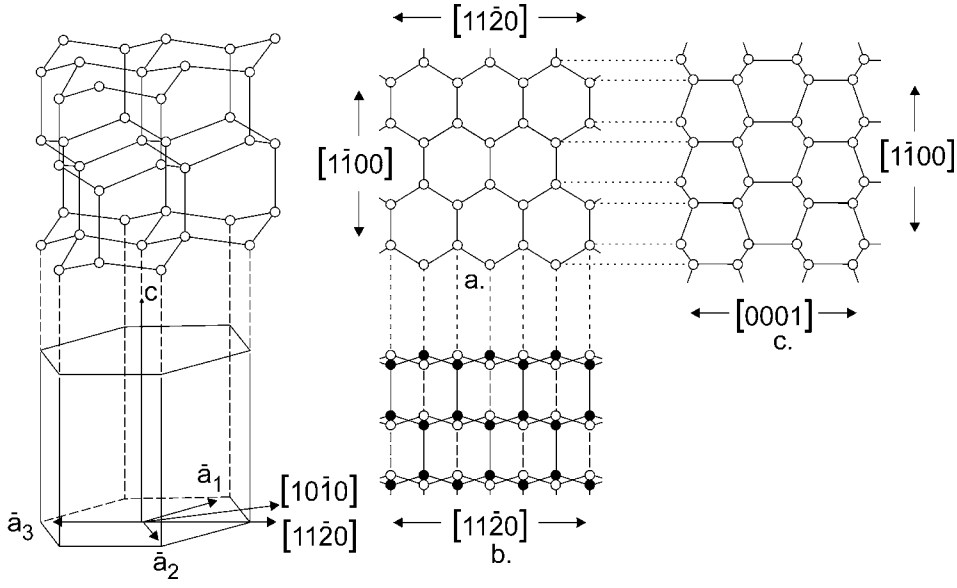

Fig. 2.3 Crystal structure of ice Ih. The c-axis is indicated at left and right, the centre panel corresponds to a view along (top) and normal (bottom) to the c-axis. From Weeks & Ackley (1986).

vector [0001] or simply as the c-axis) is normal to the basal plane and corresponds to the axis of maximum rotational symmetry (Fig. 2.3b). The basal plane defined by the crystal a-axes typically also coincides with the plane of fastest ice growth, resulting in, for example, individual frazil crystals having thickness–width aspect ratios in the order of 1:10 to 1:100 (Hobbs, 1974).

Another key aspect of the ice crystal structure is the fact that the packing density of water molecules in ice, and hence its material density, is lower than in the liquid. In the liquid state, water molecules are arranged into clusters with impurities such as sea salt ions surrounded by hydrate shells owing to the strong polarity of the water molecule. Accommodation of sea salt ions in the voids of the ice crystal lattice (Fig. 2.3) is greatly restricted, however. The constraints in size and electric charge imposed on ions or molecules substituting water molecules or individual atoms in the lattice or occupying voids within the crystal lattice are such that only very few ions or molecules actually qualify. Among them are fluorine and ammonium ions and some gases. The major ions present in sea water (Na^+, K^+, Ca^{2+}, Mg^{2+}, Cl^-, SO_4^{2-}, CO_3^{2-}), however, cannot be incorporated into the ice crystal lattice and are rejected by the advancing ice–water interface during crystal growth. This has very important consequences for the microstructure and properties of sea ice, as part of the salt is retained in liquid inclusions in the solid ice matrix, with a larger fraction rejected into the underlying water column. Both of these processes will be discussed next.

Phase relations in sea ice

Having established that sea salts and ice do not form a solid solution, in which the ions would be intermingled with the water molecules in a fashion similar to the way different proportions of zinc and copper can form a brass alloy, the question arises as to what exactly is the fate of ions in freezing sea water. In order to fully address this problem, one needs to consider the physicochemical phase relations of an idealized or somewhat simplified seawater system. Sodium and chloride ions (Na^+, Cl^-) account for roughly 85%, sulphate ions (SO_4^{2-}) for 8% and magnesium, calcium and potassium for another 6% of the mass of salts dissolved in sea water. While many aspects of sea ice properties and structure can hence already be observed in a simple sodium chloride solution, more sophisticated representations of sea water typically take into account H_2O, Na^+, K^+, Ca^{2+}, Mg^{2+}, Cl^-, SO_4^{2-}, CO_3^{2-}. In his classical study of the phase relations in sea ice, Assur (1960) also took this approach, assuming a constant 'standard' composition for sea ice. While such an approach is inadequate for geochemical studies (Marion & Grant 1997; Thomas & Papadimitriou, Chapter 9) and does present problems with ice that is strongly desalinated or grown in isolated basins, it is sufficient to predict the most important characteristics of sea ice behaviour upon cooling or warming.

Figure 2.4, taken from Assur's work, serves to illustrate the key aspects of the phase relations in sea ice. In a closed system (i.e. the mass fraction of all components

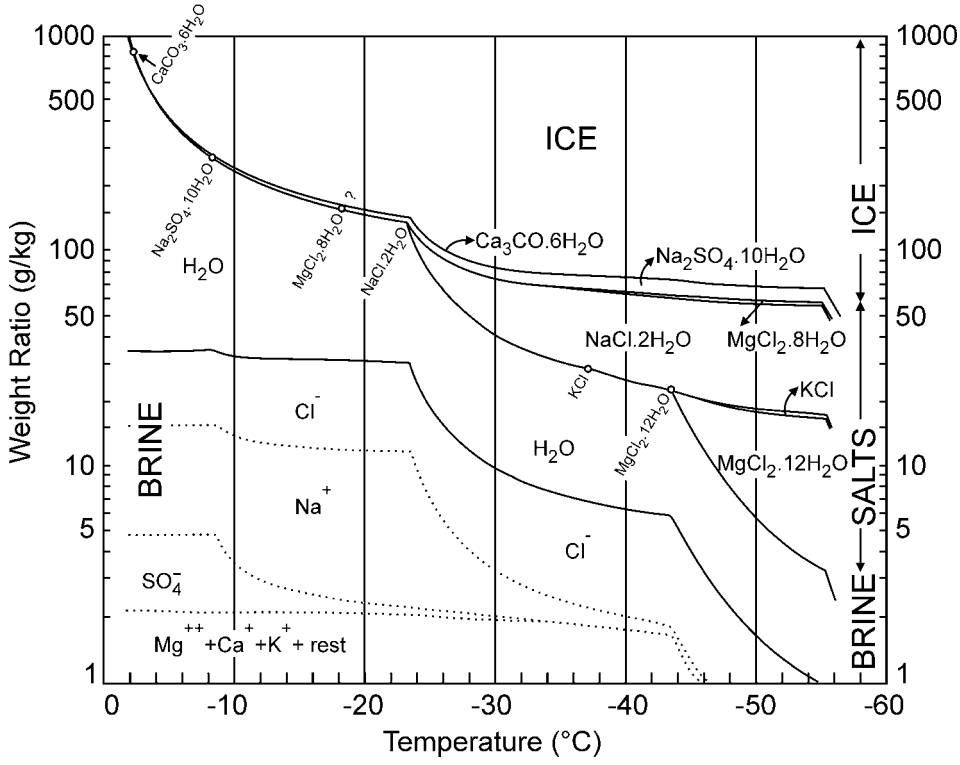

Fig. 2.4 Phase diagram of sea ice. The different curves indicate the mass fraction of solid ice (top), salts (middle) and liquid brine (bottom) present in a closed volume of ideal sea water at different temperatures. From Assur (1960).

is constant) of sea water of salinity 34, cooled below the freezing point at -1.86°C, one would observe a steady increase in the ice fraction as the temperature is lowered, assuming that the individual phases are in thermodynamic equilibrium at all times. As the salts dissolved in sea water are not incorporated into the ice crystal lattice (see above), their concentration in the remaining brine increases steadily. At the same time, the freezing point of the brine decreases, co-evolving with the increasing salinity of the liquid phase. At a temperature of -5°C, the ice mass fraction in the system amounts to 65% and the salinity of the brine in equilibrium with the ice has risen to 87. At -8.2°C, the concentration of salts has increased to the point that the solution is supersaturated with respect to sodium sulphate, a major component of sea water, resulting in the onset of mirabilite precipitation ($Na_2SO_4.10H_2O$, Fig. 2.4, Plate 2.4). If one were to continue lowering the temperature of the system, mirabilite would continue to precipitate in the amounts specified in Fig. 2.4. Other salts precipitating during the freezing of sea water include ikaite ($CaCO_3.6H_2O$), about whose distribution and mineralogy in sea ice little is known, as well as hydrohalite ($NaCl.2H_2O$). The latter is predicted to start

precipitating at $-22.9^{\circ}C$, with roughly 90% of the precipitable sodium chloride present as hydrohalite at $-30^{\circ}C$ (Fig. 2.4, Plate 2.4). While the mass fraction of brine drops below 8% at $-30^{\circ}C$, even at the lowest temperatures typically encountered in sea ice (around $-40^{\circ}C$), a small but non-negligible liquid fraction remains. The presence of unfrozen water even at these low temperatures has important consequences, in particular for the survival of micro-organisms overwintering in sea ice (Lizotte, Chapter 6).

Phase fractions and microstructural evolution

A phase diagram, such as that shown in Fig. 2.4, in itself contains no direct information on the (microscopic) configuration of individual phases within the system, i.e. its microstructure. In the case of natural sea ice, the latter depends on two principal factors, the growth environment and the boundary conditions at the advancing ice–water interface (Fig. 2.1), a topic discussed in detail in the following section, and the *in situ* temperature and chemical composition of the ice horizon under consideration. This second controlling factor is of prime importance for a wide range of ice properties considered individually in Sections 2.7–2.10. Owing to the stark contrast in physical properties between ice, brine, salts and gas inclusions, knowledge of their relative volume fraction can already provide us with a first-order estimate of the bulk (macroscopic) properties of sea ice of a given bulk salinity and temperature. For example, the mechanical strength of sea ice depends strongly on the relative brine and gas volume fraction, because these two phases effectively have no strength (see Section 2.10).

A specific example of the microstructural evolution of sea ice as a function of temperature is given in Fig. 2.5, which shows the relative volume fraction and microstructure of elongated pores (brine layers and brine channels, whose spacing and spatial orientation are determined mostly by the ice growth conditions, see Section 2.5) in a core sample of columnar sea ice. The data for these images were obtained using magnetic resonance imaging (MRI) of samples at the indicated temperature. This permitted the microstructural evolution of brine-filled pores to be followed without disturbing or destroying the sample. One particular challenge common to most studies of ice microstructure and properties is the strong dependence of the relative liquid pore volume on temperature. Commonly, samples are cooled to temperatures below $-20^{\circ}C$ immediately after sampling to avoid loss of brine from the sample, which would also strongly affect properties and microstructure. As evident in Figs 2.4 and 2.5, such temperature changes strongly affect the pore microstructure. Hence it requires either special sampling and sample preparation techniques or non-destructive methods, such as MRI, to actually obtain insight into the pore microstructure at the *in situ* temperature (Eicken et al., 2000).

As the sample is warmed from its *in situ* temperature, at which it was maintained for the entire period after sampling, the brine volume fraction increases as prescribed by the phase relations. At the same time, however, the size, morphology and

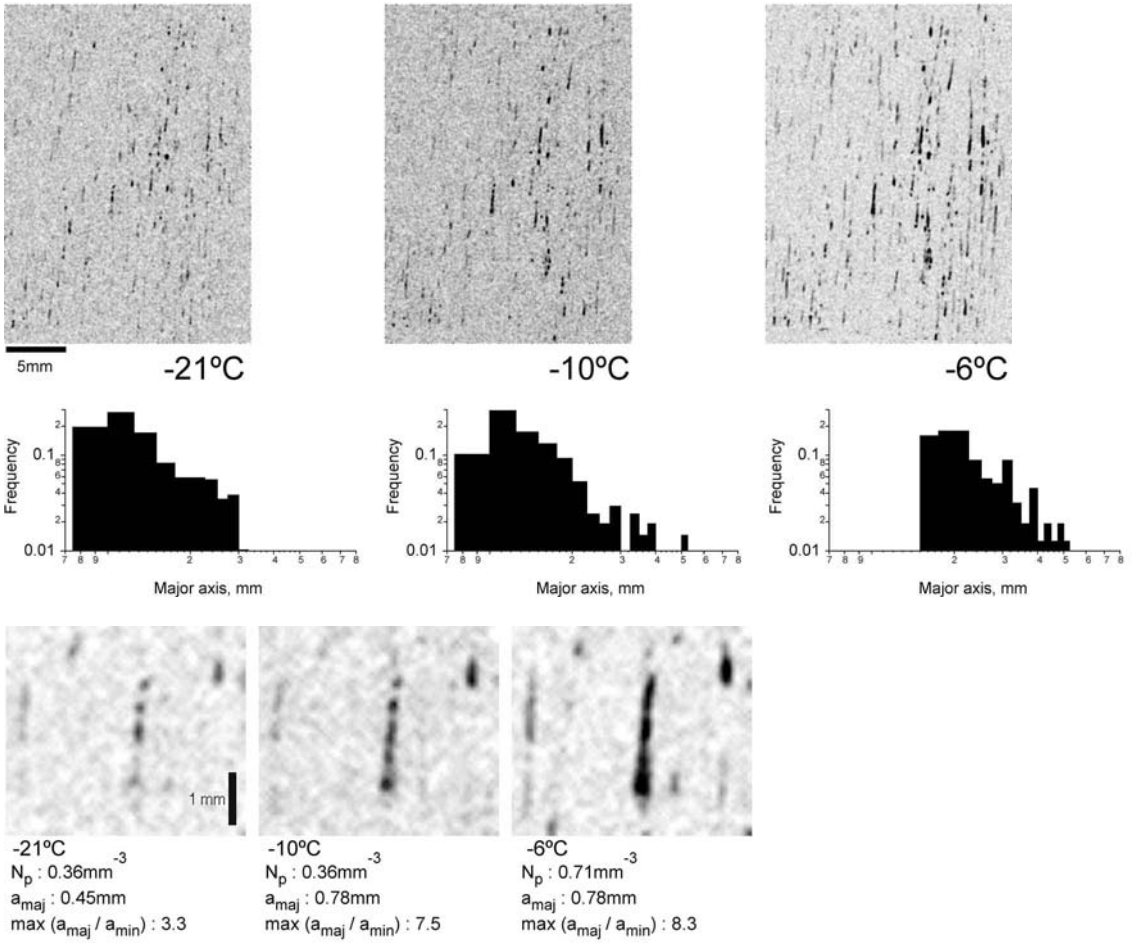

Fig. 2.5 Thermal evolution of fluid inclusions in first-year sea ice obtained near Barrow, Alaska (0.13–0.16 m depth, sample obtained in March 1999 and maintained at *in situ* temperatures after sampling up until the experiment as studied with magnetic resonance imaging (MRI) techniques. The upper three panels show a vertical cross-section through the sample as it is warmed, with pores appearing dark. The middle panels show the size distribution of the major pore axes a_{maj} (upper 10-percentile), indicating enlarging and merging of pores in the vertical. The change in pore size, morphology (as indicated by the maximum ratio between major and minor pore axis length max a_{maj}/a_{min}) and number density, N_p, is apparent in the lower panels, which show a smaller subset of pores at 0.15 m depth. From Eicken et al. (2000).

connectivity of pores evolve, with pores linking up at warmer temperatures ($-6°C$, Fig. 2.5). This process of interconnecting isolated pores as the temperature increases above a critical threshold (for a given salinity) is an important aspect of microstructural evolution and of great importance for sea ice transport properties, such as thermal conductivity or permeability. Indirect evidence from studies of physical properties and simple microstructural models suggests that for columnar sea ice such a critical transition (percolation threshold) with a strongly non-linear variation in the magnitude of transport properties occurs at a brine volume fraction of around 50‰ (Golden et al., 1998). However, both microscopic observations and measurements of bulk permeability provide evidence of a more complex microstructural evolution that requires further attention.

Temperature and salinity as state variables

From the phase relations (as summarized in Fig. 2.4), it follows that for an isothermal volume of sea ice in thermodynamic equilibrium at atmospheric pressure, the relative volume fraction of brine is fixed and depends solely on the ice temperature, T, and its bulk composition or rather, in the case of 'standard' sea ice, its bulk salinity, S_{si}. The salinity of the brine, S_b, contained within such an ice volume would similarly be prescribed by the phase relations (see also Fig. 2.5). Hence, temperature and salinity of the ice are the prime controlling or state variables governing not only the phase fractions but, as outlined below, a whole host of other physical properties. Here, use of the term 'state variable' occurs in a very loose sense, as formulation of a true equation of state for sea ice has been elusive to date. For deeper insight into the problem and recent progress, see Feistel & Hagen (1998).

The thermodynamic coupling between these different variables is a key aspect of sea ice as a geophysical material and a habitat, since any temperature change directly affects the porosity and pore microstructure of the ice as well as the salinity and chemical composition of the brine. Direct measurement of these properties in the field is difficult. Commonly, the *in situ* brine volume fraction and other properties are derived from the bulk salinity of an ice sample and its *in situ* temperature. The latter can be measured by inserting thermistors into freshly drilled holes in a core or measured from sensors frozen into the ice. The former is typically obtained by dividing an ice core into sections, melting these in the lab and then deriving the salinity from electrolytical conductivity measurements. Ideally, one would also measure the density of a sea ice sample, ρ_{si}, in order to estimate the pore volume fraction V_a/V, which in fresh ice is typically much smaller than the brine volume fraction, but can increase substantially in multi-year or deteriorated ice.

From the data compiled by Assur (1960) for the phase relations[1] and based on the

[1] The data assembled by Assur originate mostly from the first half of the 20th century but have been verified to some extent by nuclear magnetic resonance studies of the liquid volume fraction (Richardson, 1976). Nevertheless, some cautions apply (see Section 2.5).

continuity equations for a multi-phase sea ice mixture, Cox & Weeks (1983) derived a rather useful set of equations describing the brine volume fraction as a function of ice temperature and salinity. Thus, the brine volume fraction is derived as:

$$\frac{V_b}{V} = \left(1 - \frac{V_a}{V}\right) \frac{\rho_i S_{si}}{F_1(T) - \rho_i S_{si} F_2(T)} \qquad \text{(Equation 2.14)}$$

The density of pure ice is given as

$$\rho_i = 0.917 - 1.403 \times 10^{-4} T \qquad \text{(Equation 2.15)}$$

with ρ_i in g cm^{-3} and T in °C. $F_1(T)$ and $F_2(T)$ are empirical polynomial functions $F_i(T) = a_i + b_i\, T + c_i\, T^2 + d_i T^3$, based on the phase relations. The coefficients for different temperature intervals are listed in Table 2.1. The brine salinity and density can be approximated for temperatures above -23°C as

$$S_b = \left(1 - \frac{54.11}{T}\right)^{-1} \times 1000\,‰ \qquad \text{(Equation 2.16)}$$

$$\rho_b = 1 + 8 \times 10^{-4}\, S_b \qquad \text{(Equation 2.17)}$$

with T in °C. Equations 2.14 through to 2.17 thus provide us with a simple tool to derive key quantities of importance for a wide range of physical, biological and chemical studies of sea ice.

Table 2.1 Coefficients for functions $F_1(T)$ and $F_2(T)$ for different temperature intervals. From Cox & Weeks (1983), Leppäranta & Manninen (1988).

T, °C	a_1	b_1	c_1	d_1
$0 \geq T > -2$	-0.041221	-18.407	0.58402	0.21454
$-2 \geq T \geq -22.9$	-4.732	-22.45	-0.6397	-0.0174
$-22.9 > T \geq -30$	9899	1309	55.27	0.7160
T, °C	a_2	b_2	c_2	d_2
$0 \geq T > -2$	0.090312	-0.016111	1.2291×10^{-4}	1.3603×10^{-4}
$-2 \geq T \geq -22.9$	0.08903	-0.01763	-5.330×10^{-4}	-8.801×10^{-6}
$-22.9 > T \geq -30$	8.547	1.089	0.04518	5.819×10^{-4}

Caveats and limitations

In arguing the case for the overriding importance of temperature and salinity in determining ice properties, one needs to be aware of some important limitations and knowledge gaps that may, at least in some cases, invalidate the approach outlined above. Plate 2.4 can serve as a simple illustration of one such caveat. In contrast with

the assumption of the system under consideration being of constant chemical composition and attaining thermodynamic equilibrium with respect to its bulk composition, the microphotograph illustrates that chemical fractionation, of which there is also evidence in chemical data, cannot always be ignored. Here, the fraction of mirabilite in a particular brine pocket greatly exceeds the corresponding bulk concentration of Na^+ and SO_4^{2-} in sea water. Assuming that this particular pore is not connected to the remainder of the pore space, then its contents are not easily equilibrated with the rest of the pore matrix and both morphology and chemistry of the liquid inclusion can deviate substantially from the idealized, 'standard' case. Here, it could be possible to retain mirabilite precipitates in equilibrium at temperatures significantly above $-8.2^\circ C$, also affecting the macroscopic evolution of sea ice undergoing thermal changes. Such deviations from the evolution of a microscopically homogeneous system are potentially of great significance for biological processes within the ice cover. Recent improvements in analytical techniques, with development of *in situ* earth magnetic field NMR (nuclear magnetic resonance) spectroscopy as a particularly interesting example (Callaghan et al., 1999), as well as advances in geochemical modelling of aqueous solutions at low temperatures (Spencer et al., 1990; Marion & Grant, 1997) hold considerable promise in resolving some of these issues. Geochemical modelling is particularly useful, as it allows us to easily treat systems of different chemical composition, whereas the empirical approach outlined above is only valid for a single system of a given, standard composition.

2.5 Solute segregation and ice microstructure

Planar versus lamellar ice–water interface

After discussing how temperature controls the brine porosity and changes in pore microstructure of an ice volume with constant salinity, we will now consider the factors that control the bulk salinity and the initial pore microstructure of a given ice layer. Both of these are closely linked, as pointed out in Section 2.1 and evident from the contrasting appearance of lake and sea ice sections shown in Plate 2.1. The processes governing the contrasting evolution of such different ice types are confined to the bottom-most few centimetres of the ice (Figs 2.1, 2.6).

As ice grows and the ice–water interface advances downwards into the melt, salt ions are rejected from the ice (Section 2.4). The salt builds up ahead of the advancing interface, increasing the salinity of a thin layer of a few millimetres to a few centimetres in thickness. The resulting gradient in salt concentration leads to diffusion of salt away from and heat towards the interface. Thermodynamic equilibrium dictates that the interface itself is always at the respective melting/freezing point, such that an increase in salt concentration goes along with a drop in temperature relative to the underlying sea water. At the same time, the higher density

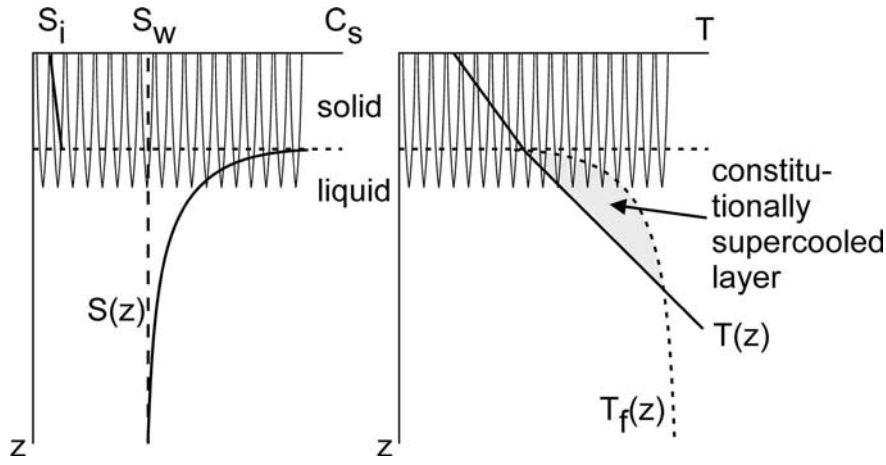

Fig. 2.6 Schematic depiction of the lamellar ice–water interface (skeletal layer) and the corresponding salinity (left) and temperature (right) gradients. The freezing temperature profile is shown as a dashed line on the right, with a constitutionally supercooled layer bounded by the actual temperature gradient and the salinity-dependent freezing-point curve.

(Equation 2.17) of the more saline brine in contact with the ice bottom can also lead to enhanced transport of brine through convective overturning (Niedrauer & Martin, 1979; Wettlaufer et al., 1997). While convective processes play an important role in the salinity evolution of the ice cover (see Sections 2.6 and 2.7), in a simplified approach the effects of convective transport and molecular diffusion can be subsumed in an 'effective' salt transport or diffusion coefficient. Heat transport through this boundary layer from the warmer ocean to the colder interface is faster (roughly by an order of magnitude) than the transport of salt away from the interface, since the former corresponds to a transfer of momentum whereas the latter constitutes an actual flux of ions. As a result, a thin layer is established ahead of the interface which is cooled as a result of upward heat transport, but which has not yet received the entirety of the corresponding influx of salt from above. This layer is said to be constitutionally supercooled, since salt concentration and temperature are at a mismatch with respect to the local freezing point (Figs 2.4, 2.6).

It is this constitutional supercooling that distinguishes the growth of lake ice from that of sea ice and helps explain their respective characteristic properties. Any small (sub-millimetre) perturbation of a planar ice–water interface that protrudes into the constitutionally supercooled zone finds itself at a growth advantage, since heat is not only conducted upward and away from the ice–water interface but the supercooled water layer also provides a non-negligible heat sink. Part of the heat flux sustaining this growth occurs at the 'cost' of adjacent portions of the ice surface set back against the growing protrusion. The salt rejected by such a protrusion contributes to a freezing-point reduction of the brine retained along the protrusion boundaries. Consequently, such perturbations can grow into ordered patterns of lamellar bulges

at the ice–water interface (for a full quantitative analysis of constitutional supercooling and its impact on ice microstructure see Weeks & Ackley (1986) and Wettlaufer (1998)). In its most pronounced manifestation, this process of localized, non-linear heat and salt dissipation leads to so-called dendritic growth, with a rough, complex interface typical of, for example, snowflakes. In the case of sea ice, the morphology of the interface is mostly reported to be lamellar or cellular (Figs 2.6, 2.7) rather than fully dendritic. For lake ice or brackish ice grown from water with low salinities (details given in Weeks & Ackley (1986)), a planar interface remains stable throughout the growth process, resulting in rejection of the bulk of the impurities and low porosities.

When fully developed, as in the case of ordinary columnar sea ice (see Section 2.2 and Fig. 2.1), the lamellar interface consists of sub-millimetre thick blades of ice, separated by narrow layers of brine. The transitional layer, demarcated by ice volume fractions tending towards zero at its lower end and with a transition to laterally interconnected ice lamellae at a porosity $\leq 30\%$ or so at its upper end, is commonly referred to as the skeletal layer. It is this thin, low- to zero-strength layer that determines much of the bulk salinity as well as the microstructure of the growing ice cover.

As evident from Fig. 2.6, the arrays of brine layers between ice blades extend all the way up into the ice sheet. If we were to consider the fate of the skeletal layer in a thickening ice cover with time, we would in essence be following a trajectory in the phase diagram shown in Fig. 2.4 (though for a smaller bulk salinity). As more ice is added underneath the layer under consideration, its temperature drops (as discussed on the scale of the entire ice thickness in Sections 2.2 and 2.3) and consequently the fraction of liquid decreases while ice is added onto the ice blades. Eventually, the ice layer is entrained into the floe interior and the ice lamellae join up and consolidate into lower-porosity sea ice. During this consolidation process, brine is being lost from the ice as discussed in more detail in Section 2.6. Though not an accurate quantitative or even qualitative representation of the process itself, one can visualize this process in principle as something in reverse of the warming sequence depicted in Fig. 2.5. In fact, the question of whether warming and cooling events in sea ice lead to changes in microstructure that are reversible or, instead, are associated with significant hysteresis effects, is of considerable interest in the context of ice transport properties.

During this transformation of individual ice horizons, the basic patterns of the grain and pore microstructure, such as the size and orientation of crystals and the spacing and arrangement of pores, remain essentially unchanged from what was laid down in the skeletal layer. This is illustrated in Fig. 2.7, which shows horizontal thin sections of two different varieties of columnar ice grown under the same boundary conditions save a difference in the under-ice current regime. Ice grown in the absence of externally imposed currents exhibits the typical lamellar sub-structure, with rows of brine layers within individual crystals, and remnants of the liquid separating individual blades of ice within the skeletal layer. Along grain boundaries, the size and shape of pores is more heterogeneous, with brine tubes and channels of

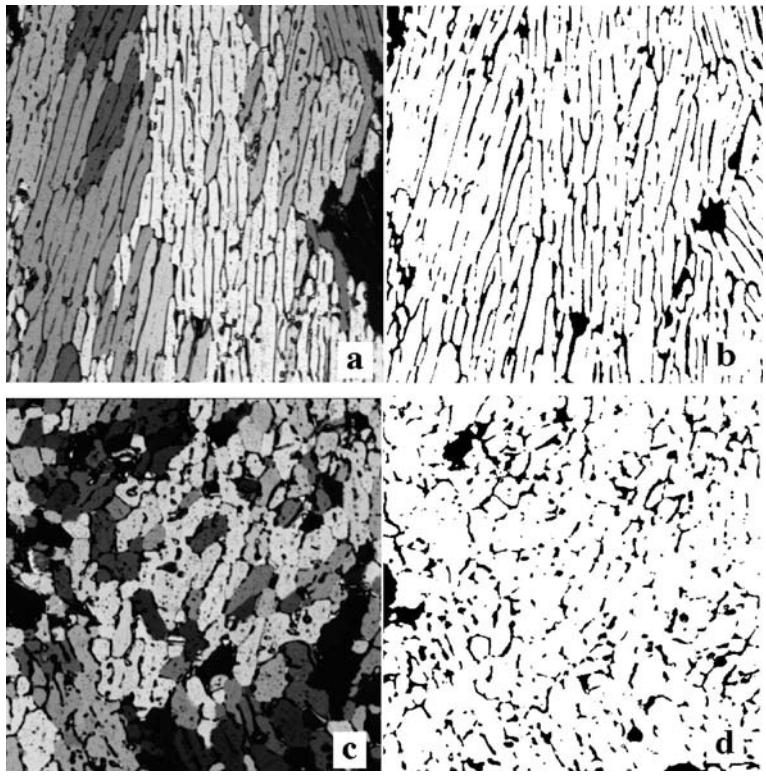

Fig. 2.7 Thin-section photographs of columnar sea ice grown in a large ice tank (Hamburg Environmental Test Basin, INTERICE experiments) in the absence of an under-ice current (a, b: porosity 154‰, mean pore area 0.096 mm^2) and with a current speed of 0.16 m s^{-1} (c, d: porosity 138‰, mean pore area 0.077 mm^2). Images a and c have been recorded between crossed polarizers (section is 20 mm wide) with grain boundaries apparent as transitions in grey shades due to different interference colours. Images b and d show the same section with pores indicated in black, based on processing of images recorded in incident light.

several millimetres in diameter apparent in the lower right of Fig. 2.7b. The ice grown in a current (0.16 m s^{-1} measured 0.5 m below the ice bottom) also exhibits a grain sub-structure delineated by pores, but the degree of parallel alignment of pores and the aspect ratios of individual inclusions are much different, as are the grain sizes (Fig. 2.7c,d). This is a result of the fact that the thickness and degree of supercooling of the constitutionally supercooled zone, as well as the thickness of the skeletal layer, depend on a variety of factors, such as the ice growth velocity, the salinity of the underlying water and, as illustrated here, the magnitude of currents enhancing transport away from the ice.

The impact of currents, though not all that well understood quantitatively, has been shown to have dramatic effects on the orientation of individual ice lamellae and hence the crystals they are constituting. Independent of under-ice currents, in a growing new ice sheet (Fig. 2.1) the number of grains with horizontal c-axes increases rapidly downward, such that the vast majority of crystals exhibit

horizontal c-axes and vertically oriented ice lamellae (see Section 2.4) within less than 20 cm below the top of the columnar ice layer (Weeks & Wettlaufer, 1996). This is interpreted to be the result of 'geometric selection' during the growth process, such that crystals with ice lamellae tilted more into the vertical (c-axis horizontal) are at a growth advantage, displacing lamellae of a more horizontal orientation during the thickening of an ice cover. A second process that results in strong parallel alignment of c-axes within the horizontal requires the presence of a unidirectional under-ice current (Weeks & Wettlaufer, 1996). It appears that salt transport away from the interface is enhanced for crystals with lamellae oriented perpendicular to the current, providing them with a growth advantage that eventually results in the dominance of current-parallel c-axes. Both of these processes result in a pronounced anisotropy of the ice cover.

A further, important aspect of the lamellar sub-structure is the observation that the width of ice lamellae, and hence the spacing of brine layers, exhibits an exponential dependence on growth velocity. Nakawo & Sinha (1984) demonstrated this for Arctic sea ice, where the down-core reduction in growth velocity (see Section 2.3) closely corresponded to an increase in the brine layer spacing a_0. Typically, a_0 is in the order of a few tenths of a millimetre. However, in what is probably the oldest sea ice sampled to date, grown at velocities of a few centimetres per year, Zotikov et al. (1980) found brine layer spacings in the order of several millimetres. As discussed in more detail in the following section, brine layer spacing and salt retention within the ice are closely coupled and deserve further study.

In spite of contributing only marginally to the total mass of sea ice, the skeletal layer is of importance since it is the origin of a significant salt flux into the underlying ocean. Moreover, this layer harbours one of the greatest concentrations of phytoplankton in the world's oceans by providing a habitat for diatoms and other micro-organisms and in turn grazers (Smith et al., 1990; Arrigo, Chapter 5; Lizotte, Chapter 6; Schnack-Schiel, Chapter 7). As algae depend not only on sunlight but also on nutrients for photosynthetic activity, in many areas the most active layer of ice organisms is found within the bottom few centimetres of the ice cover in the skeletal layer, where high porosities and permeabilities, and the proximity of the ocean reservoir, provide a sufficient influx of inorganic nutrients and gas exchange (Arrigo, Chapter 5; Thomas & Papadimitriou, Chapter 9). At the same time this layer offers some protection from the largest grazers (Schnack-Schiel, Chapter 7) and presents photosynthetic organisms with a foothold at the top of the water column where irradiative fluxes are highest (Eicken, 1992b).

Frazil and granular ice

Whereas congelation growth of sea ice with columnar texture typically dominates in the Arctic, frazil growth resulting in granular textures is also common, in particular in the Southern Ocean (Section 2.2). Growth of individual platelets and needles of frazil in a supercooled water column differs from growth of congelation ice insofar

as both heat and salt have to be transported away from the interface into the surrounding ocean water. Consequently, beyond a certain size, individual frazil crystals also develop rough, dendritic surfaces as a result of solute build-up. Frazil growing in the turbulent uppermost metres of the ocean has the tendency to aggregate into flocs of crystals that are capable of sweeping particulates and biota from the water column, carrying them to the surface as a layer of frazil or grease ice accumulates (Reimnitz et al., 1990; Smedsrud, 2001; Lizotte, Chapter 6). Despite its abundance, some aspects of frazil growth are not that well understood, including the inherent 'stickiness' attributed to its role in enhancing concentrations of biota in Antarctic sea ice or the conditions governing the growth of larger ice platelets at greater depths in water parcels supercooled through interaction with the melting Antarctic ice shelves (Bombosch, 1998). The latter process is capable of generating large volumes of crystals that contribute both to the mass balance of the ice shelves as well as the coastal sea ice, where one finds platelets as large as 10 cm across and a few millimetres thick floating towards the surface and accumulating in layers of several metres thickness.

Another aspect of frazil growth that is currently not well understood is the actual consolidation of loose masses of frazil crystals, with ice volume fractions between about 10 and 30% into solid granular sea ice. Evidence from oxygen stable-isotope and salinity measurements of individual crystals and layers of granular ice suggests that the consolidation process is a combination of downward freezing of voids among the mesh of frazil crystals and transformations in the size distribution and morphology of the crystals themselves. This is similar to what has been observed to occur in water-saturated snow slush (Eicken, 1998). Further studies are required to elucidate the specific processes and resultant heat and salt fluxes, since frazil ice growth is a key process in the interaction of ocean and atmosphere.

2.6 Salinity evolution of sea ice

Salinity profiles of growing and melting sea ice

In a pioneering study, Malmgren (1927)[2] studied the salinity evolution of Arctic first-year sea ice during the course of winter and into the summer melt season (Fig. 2.8). In this section, we will briefly consider the processes responsible for the

[2] Malmgren's work and fate may also serve to illustrate how scientific investigation, exploration and the incalculable were intertwined in the early 20th century (and arguably continue to be so to some extent). Finn Malmgren's thorough and ground-breaking study of sea ice properties was prompted by Harald Sverdrup who had suggested this work as a project to at least gain something out of the unplanned freezing in of Roald Amundsen's vessel *Maud* during the Northeast Passage expedition of 1922–25. Malmgren's experience and scientific prowess predestined him to be one of the key participants in Nobile's ill-fated airship expedition to the North Pole, where Malmgren perished in the ice pack on a trek to reach the Svalbard archipelago.

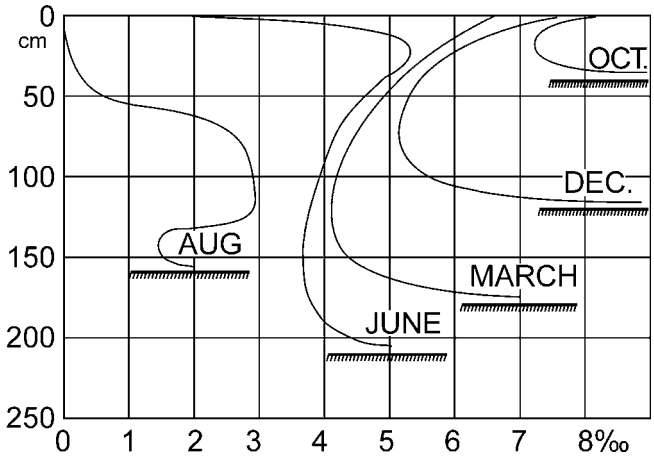

Fig. 2.8 Evolution of sea ice salinity profiles as determined by Malmgren (1927). Note the characteristic C-shape of the young and first-year ice salinity profile and the reduction in surface salinity due to meltwater flushing with the onset of summer melt.

characteristic C-shape of the salinity profile of young and first-year ice as well as the reduction in surface salinities during the first melt season in an ice floe's evolution. The importance of understanding the evolution of an ice cover's salinity profile is rooted in the central role temperature and salinity play with respect to ice porosity and pore microstructure (Section 2.4). The vast majority of large-scale sea ice models currently assume constant ice salinity, thus depriving the simulated ice cover of an important response mechanism to changes in the atmospheric or oceanic boundary conditions.

The importance of these processes is illustrated by comparing the first-year winter sea ice salinity profile in Fig. 2.8 with that of summer or multi-year sea ice. As dictated by the phase relationships (Fig. 2.4; Section 2.4), the transition from the former to the latter generally corresponds to a change in the direction of the conductive heat flux through an ice floe from being directed upward to being directed downward. It is the complex, and to this date not fully understood, response of the salinity profile that underlies this change, rather than simply the surface temperature forcing.

Segregation of salt during ice growth

In principle, at least for cold first-year sea ice, the single most important factor in controlling ice salinity is the segregation of sea salt ions at the ice–water interface, as discussed in Section 2.5. This initial distribution of salt between the ice and the underlying water is then further affected by a number of brine drainage processes that are considered in the next section. The salinity of a newly grown layer of ice at time $t = 0$, $S_{i,0}$, can be described in terms of an effective segregation coefficient, k_{eff},

and the salinity of the sea water, S_w, far away from the interface such that (Weeks & Ackley, 1986):

$$S_{i,0} = k_{eff} S_w \qquad \text{(Equation 2.18)}$$

For columnar ice grown from sea water (i.e. salinities around 34), the magnitude of k_{eff} is proportional to the ice-growth rate (Fig. 2.9). Based on an idealization of the salt entrainment comparable to solid solutions, and integrating results from laboratory experiments (Cox & Weeks, 1988) and field work (Nakawo & Sinha, 1981), Cox & Weeks derived the following dependence of k_{eff} on growth rate v_i:

$$\begin{aligned} k_{eff} &= \frac{0.26}{0.26 + 0.74\exp(-7243 v_i)}, \qquad v_i > 3.6 \times 10^{-5}\,\mathrm{cm\,s^{-1}} \\ k_{eff} &= 0.8925 + 0.0568 \ln v_i, \qquad 3.6 \times 10^{-5} \geq v_i \geq 2.0 \times 10^{-6}\,\mathrm{cm\,s^{-1}} \\ k_{eff} &= 0.12 \qquad v_i < 2.0 \times 10^{-6}\,\mathrm{cm\,s^{-1}} \end{aligned} \qquad \text{(Equation 2.19)}$$

Conceptually, these relationships are founded on the same principles underlying the process of constitutional supercooling as discussed in Section 2.5. The slower the ice growth, the less build-up of salt ahead of the ice–water interface with diffusive and convective transport capable of removing substantial amounts of salt before it is trapped between ice lamellae (Fig. 2.6). The limiting case for zero growth velocities is determined by an effective equilibrium segregation coefficient k_{eq}^{*} that has been determined as 0.12 (Equation 2.19), based on salinity measurements in Arctic fast

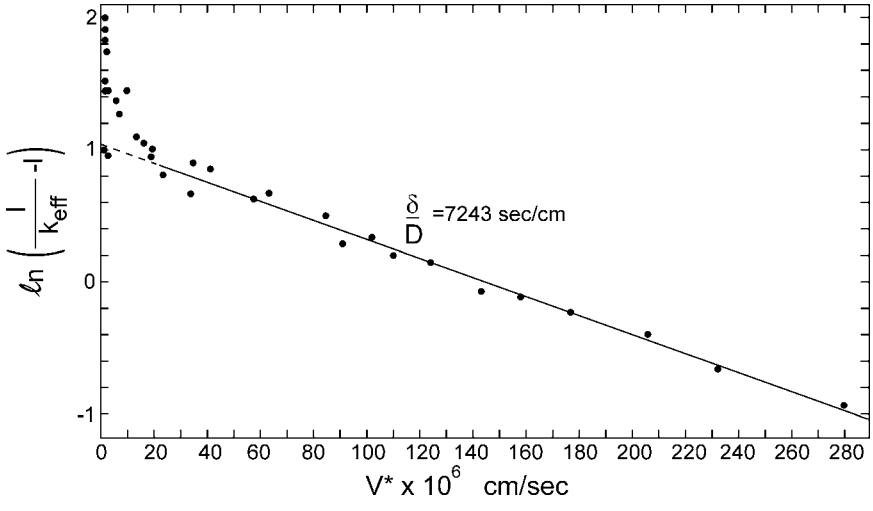

Fig. 2.9 Dependence of the effective salt segregation coefficient k_{eff} (shown here as $\ln(1/k_{eff} - 1)$) on ice growth rate v*. From Cox & Weeks (1975).

ice (Nakawo & Sinha, 1981) as well as a combination of salinity and oxygen stable-isotope tracer measurements in Antarctic sea ice (Eicken, 1998). The latter study, however, also identified limitations in the approach to deriving k_{eff}, which implicitly assumes a planar rather than a lamellar ice–water interface. While a simple microstructural model yielded a similar dependence of salinity at $t = 0$, further work is required to link our understanding of lamellar ice growth (Section 2.5; Wettlaufer, 1998) with that of impurity and oxygen stable-isotope segregation at the interface. Nevertheless, as it is based on experimental data, Equation 2.19 is still useful in estimating salt segregation. Thus, salinities of the slowest sea ice growth on earth correspond well with a k_{eff} of 0.12 (Eicken, 1998). Similarly, high salinities found in young sea ice, such as the example shown in Fig. 2.10 for experimental data with ice

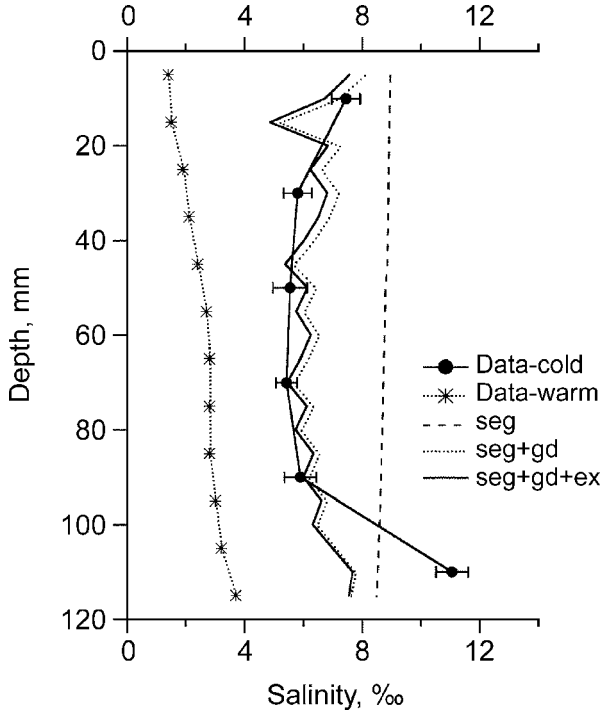

Fig. 2.10 Salinity profiles for young columnar sea ice grown in a large ice tank (Hamburg Environmental Test Basin, INTERICE experiments, see also Fig. 2.7a,b for microstructural photographs of the same ice) as compared to model simulations of salinity profile evolution. The solid dots represent measurements of the salinity of 'cold' ice (surface temperature -8 to -10°C) 5 days after the start of the experiment (standard deviation for measurements on four parallel samples indicated by horizontal bars). Salinity of 'warm' ice (surface temperature between -1 and -2°C) 2 weeks after the start of the experiment, following an 8-day melting period, is indicated by asterisks. The dashed line (seg) gives the salinity of newly grown ice layers ($t = 0$) following segregation of salts at the interface as predicted by a segregation model (Equations 2.18 and 2.19) based on measured growth rates. If only gravity drainage (Equation 2.20) were to occur, the profile would evolve into the dotted line (seg + gd). Brine expulsion accounts for another decrease in salinity corresponding to the solid line (seg + gd + ex).

growth velocities of several centimetres per day, are also quite similar to values predicted by salt segregation alone (Equation 2.19).

Sea ice desalination processes

The deviations apparent in Fig. 2.10 between a measured salinity profile and that predicted from the growth-rate/segregation relations (Equation 2.19) are mostly due to the loss of salt from the ice during the consolidation and ageing process. Essentially, there are two different types of desalination mechanisms:

- Those that are active in 'cold' ice during the ice-growth period, driven mostly by temperature gradients $(T_0 - T_f)/H < 0$ established in the ice cover and the cooling of individual ice layers (see Section 2.3).
- Those dominating desalination of 'warm' ice, requiring the presence of low-salinity melt water either at the surface or the bottom of the ice.

Among the first group of processes, gravity drainage and brine expulsion are of quantitative importance. The migration of individual brine pockets in a temperature gradient (see Weeks & Ackley, 1986) is significant on a microscopic level, and its impacts on these scales are still not well understood. However, it has been shown to be of no or little significance for the overall evolution of salinity profiles and will not be considered further here. The most effective desalination mechanism under 'cold' conditions is so-called gravity drainage. As growing sea ice is typically cooled from above, the density profile of the brine is inherently unstable and, boundary conditions permitting, likely to result in convective exchange: cold, saline brine within the ice is replaced by warmer, less saline sea water or brine from lower ice layers.

The processes and features associated with this gravitative transport mechanism will be discussed in more detail in the context of heat transport and ice thermal properties. Cox and Weeks (see summary in Weeks & Ackley, 1986) conducted a series of elegant experiments to derive empirical relationships that describe the desalination rate $\Delta S_i/\Delta t$ (in ‰ s^{-1}) as a function of the local temperature gradient $\Delta T/\Delta z$ (in K cm^{-1}):

$$\frac{\Delta S_i}{\Delta t} = 1.68 \times 10^{-5} \frac{\Delta T}{\Delta z} - 3.37 \times 10^{-7} \frac{V_b}{V} \frac{\Delta T}{\Delta z} \qquad \text{(Equation 2.20)}$$

where V_b/V (in ‰) is the brine volume fraction. As the pressure gradients associated with gravity drainage are quite small, this process depends strongly on the connectivity and size of pores, which is generally simplified to be proportional to the brine volume fraction. Evidence from the laboratory and the field suggests that below a critical threshold, $V_b/V \approx 50$ to 70‰, gravity drainage stops altogether (Weeks & Ackley, 1986; Golden et al., 1998b). However, the actual nature of this critical transition, as well as the dependence of desalination on the microstructure of

the ice, are currently not well known. The quantitative importance of gravity drainage is well established, on the other hand, as indicated by the contribution of this process to overall desalination in Fig. 2.10.

Brine expulsion, the other important desalination process in 'cold' ice, is driven by the change in volume as ice forms in brine pockets that are cooled in a thickening ice cover, and hence depends on the density difference between brine and ice. Though not as effective as gravity drainage, it is generally assumed that owing to the pressure build-up in isolated pores, brine expulsion is mostly independent of ice permeability or porosity, with brine ejected through micro-cracks (direct evidence of which we are lacking) or microscopic pore networks. Its overall impact on ice salinity profiles is indicated in Fig. 2.10 as well.

The combination of salt segregation, gravity drainage and brine expulsion explains the typical 'C' shape of first-year sea ice. Thus, the decrease in growth rate as the ice cover thickens (see also Fig. 2.2 and Section 2.3) is responsible for an overall drop in the segregation coefficient and hence the salinity of newly grown ice layers. As freshly accreted bottom layers in an ice floe have had less growth time and less of a cooling history than the interior and surface ice, their salinity is disproportionately higher. Cox & Weeks (1988) developed an ice-growth/salt-flux model that allows for detailed sensitivity studies. Refinement of the model and comparison with oxygen stable-isotope tracer data indicate that the salinity profile in individual floes depends strongly on the date of ice-growth onset, the ocean heat flux as well as snow accumulation and, in particular, surface flooding (Eicken, 1992a; Maksym & Jeffries, 2000).

The most effective desalination processes are confined to the summer melt season when ice porosity and permeability are generally high and zero- or low-salinity meltwater production at the surface and the bottom of the ice is capable of displacing higher salinity brine from within the ice. Untersteiner (1968) described (and coined the term) meltwater flushing as the origin of the extremely low bulk salinities of Arctic multi-year sea ice (typically around 2 to 3) and the characteristic linear increase in ice salinity from values close to zero at the surface to a few per mil in the lower ice layers (Figs 2.8, 2.10). The desalination is driven by the hydraulic head of snow and ice melt water produced at the top surface, percolating downwards into the ice cover, displacing the resident higher-salinity brine. Recent studies involving different tracers have demonstrated that the vertical and lateral transport of melt water varies with season as a function of ice permeability. As much as a quarter of the melt water produced annually at the surface of Arctic sea ice can be retained in pores within the ice cover (Eicken et al., 2002). At the same time diffusive, as well as convective exchange of brine displaced by fresh water underplating summer Arctic sea ice (a form of gravity drainage), is capable of reducing the salinity of thinner ice to values close to zero throughout. Given the importance of these processes for ice thermal properties and ablation, more work is needed to help develop a conceptual and, ultimately, a numerical model of meltwater transport through sea ice.

2.7 Sea ice thermal properties

Thermal conductivity

The thermal properties control the amount of heat transferred through the ice cover and determine its response to variations in surface or bottom forcing. As detailed in Section 2.2 (Equation 2.2), the conductive heat flux through an ice cover, F_c, is given by the product of sea ice thermal conductivity, λ_{si}, and the temperature gradient, dT/dz. The thermal conductivity of pure ice as a function of temperature is given by Yen et al. (1991) as:

$$\lambda_i = 1.16\left(1.91 - 8.66 \times 10^{-3}T + 2.97 \times 10^{-5}T^2\right) \qquad \text{(Equation 2.21)}$$

with T in °C. At 0°C λ_i is approximately 2.0 W m^{-1} K^{-1}. The thermal conductivity of brine, on the other hand, is lower by a factor of roughly four, and can be approximated by

$$\lambda_b = 0.4184\left(1.25 + 0.030T + 0.00014T^2\right) \qquad \text{(Equation 2.22)}$$

with T in °C (Yen et al., 1991). Thus, the volume fraction of brine as well as its microstructural arrangement exert a significant influence on the bulk (i.e. macroscopic) sea ice thermal conductivity. Schwerdtfeger (1963) and Ono (1968) developed a model for the thermal conductivity of sea ice based on the thermal properties of the pure end-members, ice and brine, and assumptions about the ice microstructure. For vertically oriented, parallel lamellar brine inclusions one arrives at the following dependence of λ_{si} on brine volume (no gas inclusions):

$$\lambda_{si} = \lambda_i - (\lambda_i - \lambda_b)\frac{S_i\rho_{si}}{m\rho_b T} \qquad \text{(Equation 2.23)}$$

with sea ice salinity S_i (in ‰), temperature T (in K) and m the slope of the phase boundary in the phase diagram (Fig. 2.4). Under the assumption of parallel, vertical brine layers, the magnitude of λ_{si} does not depend on the actual size of the inclusions (nor for that matter, on the shape of their horizontal cross-section) but only on their volume fraction V_b/V. The latter depends solely on the *in situ* temperature and salinity of the ice layer under consideration, with the liquid volume fraction dictated by the phase equilibrium (Section 2.4; Fig. 2.4; Equation 2.14). Ono and Schwerdtfeger also considered the impact of spherical gas inclusions on λ_{si}. These are typically of minor importance in first-year ice, as gas volume fractions are mostly an order of magnitude lower than those of brine.

Untersteiner introduced a simple parameterization as a function of ice temperature, T, and salinity, S_i, that has been employed in some ice-growth models (Maykut, 1986):

$$\lambda_{si} = \lambda_i + 0.13\frac{S_i}{T} \qquad \text{(Equation 2.24)}$$

As is evident from Figs 2.5 and 2.7, however, the idealized microstructure underlying the approaches outlined above may only apply to certain types of columnar ice, requiring further work to elucidate microstructural controls of λ_{si}. The few determinations of sea ice thermal conductivity based on actual measurements available today are also indicative of gaps in our understanding of how λ_{si} is linked to microstructure and of the role of convective, as compared to conductive (i.e. molecular-diffusive), heat-transfer mechanisms (Trodahl et al., 2000).

Convective heat transfer and brine drainage features

Derivations of thermal conductivity from time-series measurements of ice temperature profiles in Antarctic first-year sea ice revealed a dependence of the thermal conductivity on the temperature gradient, with values larger by up to 20% than explained by simple molecular-diffusive heat transfer alone (Trodahl et al., 2000). This is at least in part explained by desalination through gravity drainage (Section 2.6), associated with enhanced heat transfer due to convective exchange. Lytle & Ackley (1996) have observed such convective exchange processes during freezing of a highly porous, flooded slush layer at the surface of Antarctic sea ice. Wettlaufer, Worster and collaborators (see detailed discussion in Wettlaufer, 1998) have demonstrated that the onset of convection in porous crystal–solute mixtures (mushy layers) can be described by a critical Rayleigh number that relates the characteristic time scale of fluid exchange to buoyancy and viscous drag forces as well as the permeability k (which is described in terms of the brine porosity V_b/V) of the mushy zone. Experiments and theoretical work suggest that the onset of convection is associated with a substantial salt and heat flux which diminishes as the fluid density gradients and the permeability of the ice matrix respond to the perturbation of the convective overturning (Wettlaufer, 1998).

The permeability of the interior layers of fully consolidated, cold sea ice is mostly too low to allow for convection that penetrates the entire volume. However, fluid in vertically elongated systems of brine tubes or brine channels, less than a millimetre to several centimetres in diameter and up to a metre in vertical extent, has been shown to overturn, resulting in periodic discharge of cold brine that is replaced by warmer sea water (Niedrauer & Martin, 1979). For typical brine channel densities in the order of one larger channel per 10 cm^2 and common temperature gradients, the convective contribution to the total heat transfer through the ice column can amount to several $W\,m^{-2}$. Figure 2.11 shows an example of well-developed systems of larger brine channels in Arctic sea ice. The actual

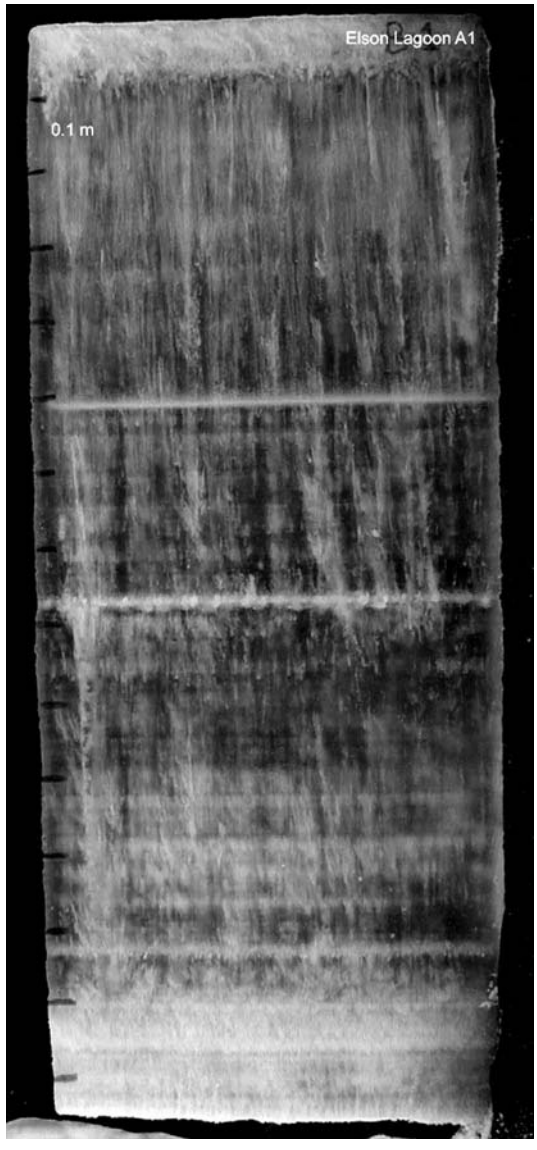

Fig. 2.11 Photograph of a slab of sea ice obtained from sea ice of approximately 1.4 m thickness near Barrow, Alaska. Note the distinct horizontal layering as well as the parallel rows of vertical brine channels (shown in horizontal cross-section in Plate 2.1e).

development and evolution of these large, secondary micro- and macro-structural features is currently not all that well understood. Evidence from experiments and numerical modelling suggests that it is a combination of hydrodynamic processes as well as microstructural controls that determines the density and morphology of individual channels.

Thermal conductivity of snow on sea ice

In areas with substantial snow accumulation, heat transfer through an ice floe may be controlled to a large extent by the overlying snow cover, as the thermal conductivity of snow is generally substantially lower (by roughly one order of magnitude) than that of sea ice (see Section 2.2). Sturm and co-workers indicate that the bulk thermal conductivity of snow typically ranges between 0.15 and 0.4 $W\,m^{-1}\,K^{-1}$ (Sturm et al., 2002). For low-conductivity snow, even a few centimetres' deposition on 0.5 m of sea ice can thus effectively double the effective 'thermal thickness' of an ice cover, as discussed in more detail in Sections 2.2 and 2.3 and shown in Fig. 2.2.

Latent heat of fusion and specific heat capacity of sea ice

Unlike freshwater ice, sea ice retains a significant fraction of liquid phase at temperatures below the freezing point of sea water (Fig. 2.4). Hence, the latent heat of fusion of sea ice, L_{si}, is smaller than that of pure freshwater ice (333.6 $J\,g^{-1}$), since a fraction of the mass of sea ice remains unfrozen even at sub-zero temperatures. Yen et al. (1991) provide an approximation of L_{si} as a function of temperature, T (in °C), and ice salinity, S_i, for temperatures above -8.2°C:

$$L_{si} = 4.187\left(79.68 - 0.505T - 0.0273S + 4.3115\frac{S_i}{T} + 0.0008S_iT - 0.009T^2\right) \quad \text{(Equation 2.25)}$$

Thus, the amount of latent heat released during growth of sea ice with a temperature of -2°C and a salinity of 10 amounts to a total of 246 $J\,g^{-1}$.

While this approximation provides a crude estimate of the latent heat of fusion and its dependence on ice salinity, a more rigorous approach to the amount of heat ΔQ released by cooling a mass of sea ice m_{si} by ΔT takes into account both the latent heat liberated during freezing of ice within brine pores as well as the amount of sensible heat lost by the entire volume of ice (and brine) of density ρ_{si}. For pure ice, the specific heat capacity, c_i, determines the magnitude of ΔQ for a mass of ice, m_i, according to

$$\Delta Q = m_i c_i \rho_i \Delta T \quad \text{(Equation 2.26)}$$

The magnitude of c_i also determines the rate of warming or cooling of a volume of ice, as derived from the heat transfer equation, describing the change in temperature with time dT/dt in terms of c_i, λ_i and ρ_i (in simplified form) as

$$\frac{dT}{dt} = \frac{\lambda_i}{c_i\rho_i}\frac{\partial^2 T}{\partial z^2} \quad \text{(Equation 2.27)}$$

Here, the term $(\lambda_i/c_i\rho_i)$ is commonly referred to as the ice thermal diffusivity.

In sea ice, a common approach is to include the latent heat term in an effective specific heat capacity, c_{si}, such that the magnitude of c_{si} is determined both by the specific heat capacity of pure ice and brine as well as by the latent heat associated with the phase change for a given temperature change. Untersteiner (see Maykut, 1986) provided a simple empirical approximation for c_{si}:

$$c_{si} = c_i + 17.2 \times 10^{-3} \frac{S_i}{T^2} \qquad \text{(Equation 2.28)}$$

with a c_i of 2.11 J g^{-1} K^{-1}, S_i the ice salinity and T the temperature in °C. As is evident from Equation 2.28 and from Fig. 2.12 showing measurements of c_{si} as a function of temperature, the specific heat capacity increases substantially above about −5°C. This increase implies that it takes substantially more energy to warm an ice cover by 1 K at a temperature close to the freezing point of sea water than at, say, −10°C, simply because the amount of heat that has to be supplied to increase the brine volume fraction from, e.g. 80‰ at a temperature of −3°C for ice of salinity 5 to 122‰ at −2°C amounts to 14 J g^{-1}. Ignoring the contribution of latent heat in raising or lowering the temperature of a sea ice volume has important ramifications, e.g. in large-scale sea ice or climate models, which would significantly overestimate the

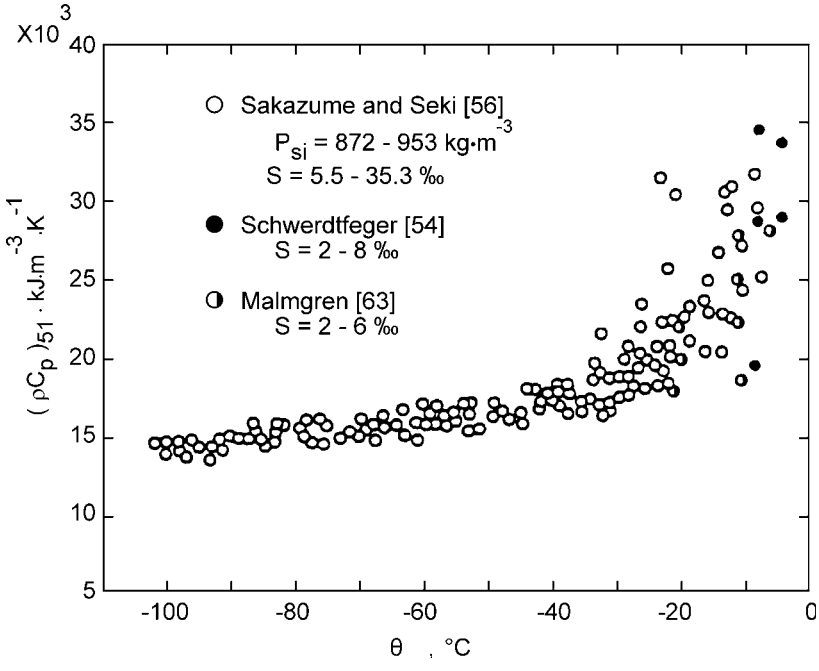

Fig. 2.12 Effective specific heat capacity of sea ice c_p (shown as product of c_p with ice density ρ) as a function of temperature θ in °C. From Yen et al. (1991).

amount of ice thinning or lateral melting, in cases where the ice cover may simply become more porous without the ensuing drastic reductions in surface albedo.

A further problem inherent in the approaches commonly taken in modelling the thermal properties of sea ice relates to the practical definition of the melting point of sea ice. The freezing point is typically defined as the highest temperature at which ice formation is observed (Section 2.2). A corresponding definition for the melting point as the lowest temperature at which melting is observed is problematic, however, since a liquid phase is present in sea ice down to temperatures as low as -55°C (Fig. 2.4). Thus, with a continuous increase in brine volume fractions as temperatures are increased from typical sea ice winter minima to summer values, sea ice is technically melting on a microscopic level at all times. Macroscopically, or on the scale of an individual ice floe, however, 'melting' is typically implied to include the complete melting of the entire ice volume. In a well-mixed water column, the latter would require the ice temperature to have reached the salinity-dependent freezing point of sea water. At the same time, the brine residing within the ice would be at seawater salinity. However, if the melt water in contact with the sea ice cover is of lower salinity, such as in the melt ponds shown in Plate 2.3 which typically have salinities of a few per mill, complete melting may require warming to temperatures well above -1°C. Minuscule though these temperature differences appear to be, the fact that they are associated with substantial amounts of heat that have to be provided in order to warm up the ice means they can have dramatic impacts on model performance and the heat budget of the polar regions. Currently, we are far from understanding these issues, either on microscopic, macroscopic or larger scales.

2.8 Dielectric properties of sea ice

The dielectric properties of sea ice govern the propagation and attenuation of electromagnetic waves which in turn determine both the optical properties of sea ice (Section 2.9) as well as sea ice signatures in remote-sensing data sets (Comiso, Chapter 4). For a detailed treatment of electromagnetic wave propagation in lossy dielectric media see Schanda (1986) and Hallikainen & Winebrenner (1992).

For an electromagnetic wave propagating in z-direction, at the time t, the electric field, E_x, in the x-direction is given by

$$E_x = E_0 \cos(\omega t - kz) \qquad \text{(Equation 2.29)}$$

where E_0 is the field at $z = 0$, k is the wave number and ω the angular frequency. Maxwell's equations yield the speed of wave propagation (v) in a medium with the relative electric permittivity, ε, and relative magnetic permeability, μ, as

$$v = \frac{c}{\sqrt{\varepsilon\mu}} \qquad \text{(Equation 2.30)}$$

with the speed of light in terms of the permittivity and permeability of free space

$$c = \frac{1}{\sqrt{\varepsilon_0 \mu_0}} \quad \text{(Equation 2.31)}$$

The relative (dimensionless) permittivity ε, also referred to as the dielectric constant, is a complex variable for a medium in which electromagnetic waves are absorbed (a so-called lossy medium), such that

$$\varepsilon = \varepsilon' - i\varepsilon'' = \varepsilon'(1 - i\tan\delta) \quad \text{(Equation 2.32)}$$

with i denoting the complex part of the permittivity and $i^2 = -1$; ε' describes the contrast with respect to free space ($\varepsilon'_{\text{air}} = 1$) and tan δ is the so-called loss tangent.

In a non-polar medium, ε' and ε'' are constant, whereas in substances such as water with the constituent molecules exhibiting a permanent dipole moment, resonance affects wave decay, resulting in a frequency dependence of ε' and ε''. Ionic impurities present in sea water and brine also affect the propagation of electromagnetic waves, such that ε'' depends on the conductivity σ

$$\varepsilon'' = \frac{\sigma}{\varepsilon_0 \omega} \quad \text{(Equation 2.33)}$$

(Fig. 2.13). Ignoring scattering and assuming a homogeneous medium, one can assess the penetration depth, δ_p, of electromagnetic radiation of a given frequency as:

$$\delta_p = \frac{1}{\kappa_a} = \frac{\sqrt{\varepsilon'}}{k_0 \varepsilon''} \ (\text{for } \varepsilon' \ll \varepsilon'') \quad \text{(Equation 2.34)}$$

Here, the attenuation of electromagnetic waves is described in simplified terms by an extinction coefficient κ, with separate contributions by absorption, κ_a, and scattering, κ_s:

$$\kappa = \kappa_a + \kappa_s \quad \text{(Equation 2.35)}$$

Despite its gross simplification of radiative transfer, the concept of a penetration depth can help in the interpretation of remote-sensing data, such as radar or passive microwave imagery (Comiso, Chapter 4). Thus, it is of particular relevance for remote sensing of the oceans and sea ice that the dielectric loss factor ε'' of water varies by more than one order of magnitude in the 1–100 GHz frequency range. Furthermore, at frequencies below 10 GHz, ε'' differs by as much as one order of magnitude for fresh water and sea water or brine, due to the impact of ionic impurities on wave decay. Hence, penetration depths at typical radar or passive-

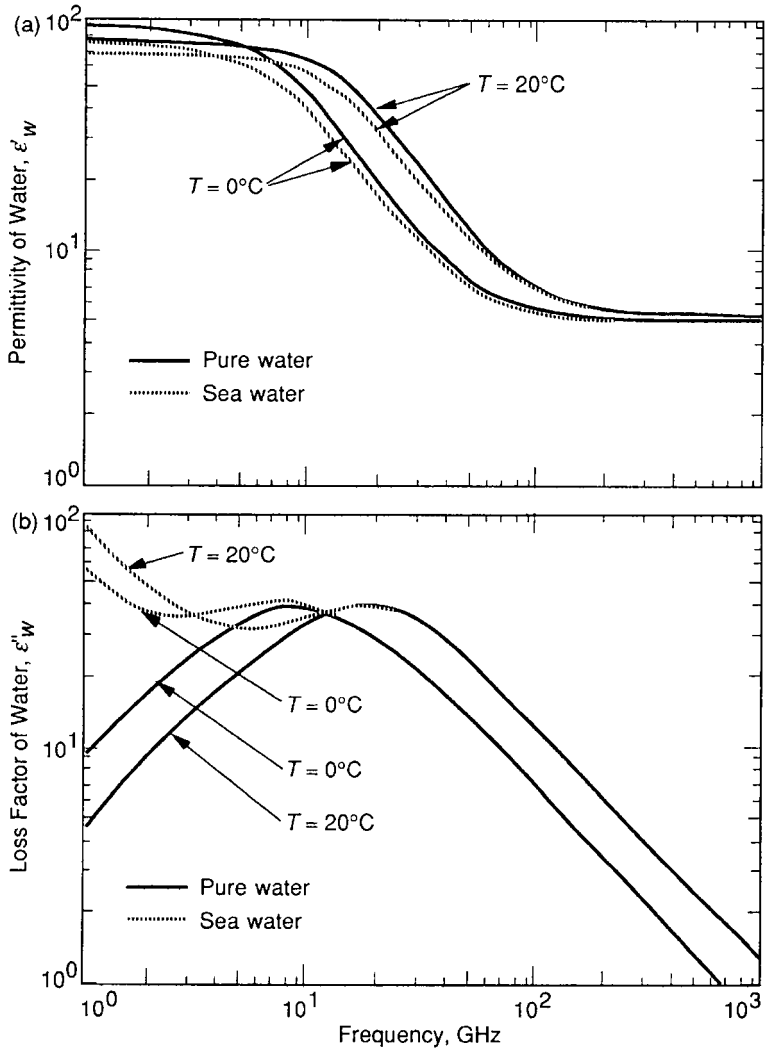

Fig. 2.13 Permittivity (a, top) and loss factor (b, bottom) for pure water and sea water at microwave frequencies. From Hallikainen & Winebrenner (1992).

microwave frequencies are in the order of millimetres to centimetres in sea water. For pure, cold ice, on the other hand, ε' is constant at 3.17 for frequencies between 10 MHz and 1000 GHz, whereas ε'' is up to several orders of magnitude smaller than that of water. Consequently, one can derive the dielectric properties of sea ice from the properties of its constituent phases based on an underlying microstructural model (Stogryn, 1987) specifying the shape, size and distribution of brine inclusions as well as their volume fraction. Rather than describing ice microstructure in highly idealized terms such as the Stogryn model (or other models discussed in Sections

2.4, 2.5 and 2.10), Lin et al. (1988) have derived the emissivity of sea ice at microwave frequencies based on a stochastic representation of sea ice microstructure. In this approach, the sub-parallel arrangement of brine layers within individual ice crystals (Figs 2.6, 2.7) is rendered in terms of the autocorrelation length of the two-dimensional autocorrelation function.

In simpler, empirical approaches, ε has been parameterized as a function of the fractional brine volume (Hallikainen & Winebrenner, 1992), which in turn is determined by the temperature and salinity of the ice (Section 2.4). The extent to which temperature and ice salinity dominate the penetration depth is illustrated in Fig. 2.14. At temperatures of around -5°C, radar waves can thus penetrate several tens of centimetres to more than a metre into low-salinity multi-year ice, whereas penetration depths in saline first-year ice are only in the order of a few centimetres at most. Under such conditions, the radar backscatter signatures of multi-year are dominated by volume scattering from gas bubbles and brine inclusions. In first-year and young sea ice, ice surface scattering predominates and radar backscatter coefficients are mostly determined by the surface roughness of the ice. This allows for discrimination of generally smooth first-year ice and multi-year sea ice in radar satellite imagery. Owing to the polarization and frequency dependence of the dielectric properties (Fig. 2.14), more sophisticated multi-frequency and multi-polarization instruments can be of considerable use in distinguishing between different ice types. The same principles apply to thermal emission at microwave fre-

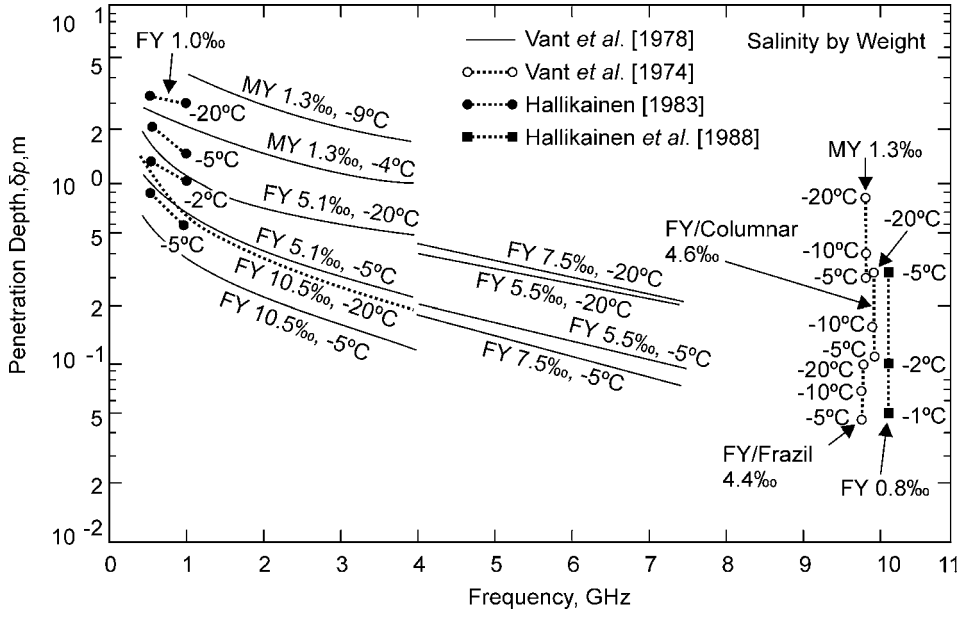

Fig. 2.14 Penetration depth at microwave frequencies for different types of first-year (FY) and multi-year (MY) sea ice. From Hallikainen &Winebrenner (1992).

quencies from different ice types and form the basis for commonly employed algorithms in discriminating between first- and multi-year sea ice in passive-microwave data (Comiso, Chapter 4).

2.9 Optical properties

Radiative transfer in sea ice

The thin section photographs in Plate 2.1, as well as the different ice types shown in Plate 2.2, provide some indication of the complexity of the topic of radiative transfer between atmosphere, ice and ocean. The amount of light scattered back from the ice cover (as measured in the albedo, α), the amount absorbed within the ice column and the fraction that ultimately penetrates into the ocean depend on the relative contribution of absorption and scattering or reflection along the path of individual photons (Perovich, 1998). In pure ice, free of gas or brine inclusions (some types of lake ice actually being acceptable approximations of such ice, Plate 2.1), the attenuation of light passing through the ice to a depth z can be described through Beer's or Bouguer–Lambert's law (essentially a simplification of the radiative transfer equation) (Perovich, 1998):

$$I(z, \lambda) = I(0, \lambda)\, e^{-\kappa_a z} \qquad \text{(Equation 2.36)}$$

where $I(z, \lambda)$ is the irradiative flux (i.e. light intensity averaged over all directions of the entire half space) of wavelength λ through ice with an absorption coefficient κ_a.

Owing to the ample presence of inclusions in sea ice, scattering is not to be ignored, however. The simplest approach to this problem is based on Beer's law of exponential decay, by simply replacing the absorption coefficient with an extinction coefficient that reflects the sum of absorption and scattering processes ($\kappa = \kappa_a + \kappa_s$), i.e. as introduced in more general terms in Equation 2.35 in Section 2.8. While not discussed explicitly here (see Equation 2.38), due to its wavelength dependence, the value of $\kappa(\lambda)$ is not constant with depth in the ice and furthermore depends on the spectral composition of the incoming solar radiation, which in turn strongly depends on cloudiness and other factors. This is commonly taken into account in models through suitable parameterizations of such processes (for details, see Perovich, 1998).

Qualitatively, the amount of scattering depends on the contrast in refractive indices between the host medium and inclusions, which in the case of sea ice explains the disproportionate importance of gas and salt inclusions for the scattering of light. This is apparent in Plate 2.4, in particular for the fine-grained hydrohalite conglomeration. While the Beer/Bouguer–Lambert approach is restricted to optically thick ice slabs, it does allow for reasonable estimates of short-wave attenuation in sea ice. Due to its computational simplicity it is still widely employed to derive the

extent of solar heating of individual ice layers (Perovich, 1998). Moreover, it may be more practical for applications with larger numbers of scatterers other than simple air or brine inclusions, such as in bio-optical models of sea ice (Arrigo & Sullivan, 1994; Arrigo, Chapter 5). More sophisticated approaches to the solution of the radiative transfer equation are those of Grenfell (1991), Jin et al. (1994) and those summarized in Perovich (1998). However, as apparent schematically in Fig. 2.15, such approaches also require a more sophisticated treatment of the ice microstructure, specifically those of brine, gas and salt inclusions. Such data are only now starting to become available (Light et al., in press) and it will require further efforts to develop a fully coupled optical/microstructural/heat-transfer model of sea ice.

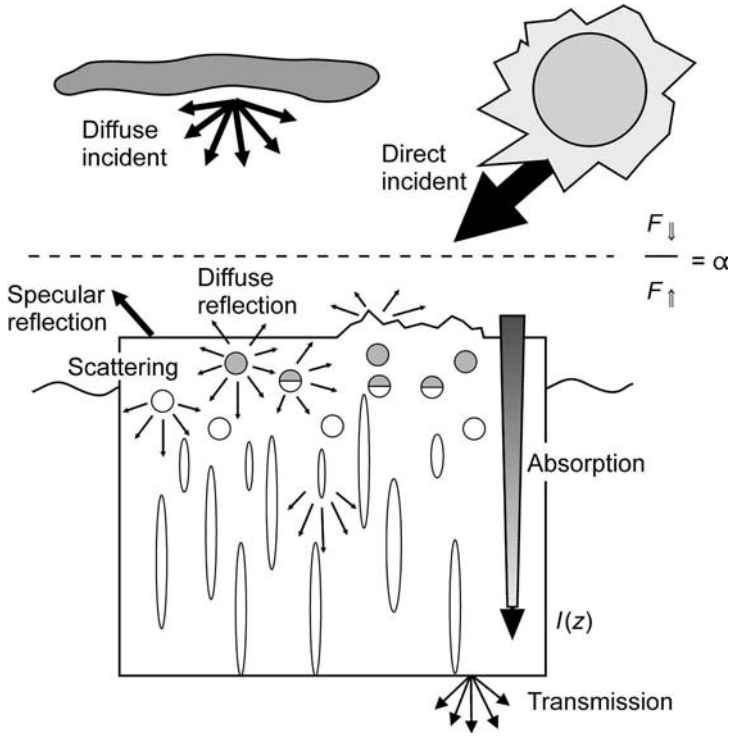

Fig. 2.15 Schematic depiction of sea ice radiative transfer processes.

Sea ice albedo

The spectral albedo of a sea ice cover is defined as the fraction of the incident irradiance that is reflected from the surface:

$$\alpha(\lambda) = \frac{F\Uparrow(0,\lambda)}{F\Downarrow(0,\lambda)} \qquad \text{(Equation 2.37)}$$

The total (all-wavelength) albedo, α_t, is then given by the integral over the entire range of the solar short-wave spectrum (commonly taken as 400–1500 nm; Perovich, 1998):

$$\alpha_t = \frac{\int \alpha(\lambda) F\Downarrow (0,\lambda)\, d\lambda}{\int F\Downarrow (0,\lambda)\, d\lambda} \qquad \text{(Equation 2.38)}$$

As shown schematically in Fig. 2.15, α is determined by the sum of specular reflection and scattering at the surface as well as scattering and absorption in the volume of the ice. Hence, the albedo depends strongly on the ice interior structure, which has been hinted at in Section 2.3 and is clearly apparent in Plate 2.1 in the contrast between lake ice with few inclusions and low albedo and snow-free sea ice with numerous brine inclusions and a significantly higher albedo. The number of brine inclusions acting as scatterers correlates with the thickness of the ice cover (Fig. 2.15), such that one typically observes a pronounced increase in ice albedo with an increase in ice thickness. This phenomenon is implicit in the nomenclature of thin ice types, identified as dark and light nilas, grey, grey-white and white ice (Plate 2.2, Fig. 2.16).

The range of albedos associated with the polar ice pack spans almost the entire range of albedo of different planetary surfaces (Fig. 2.16). Values increase during the course of the sea ice growth season as the ice cover thickens and snow accumulates. In summer, the trend in surface albedo is the opposite, with values dropping to about 0.65 for snow-free bare multi-year ice and decreasing to well below 0.5 for ponded multi-year ice (Plate 2.3). Whereas the stark contrast in albedo of the open versus the ice-covered ocean is an important driver of ice–albedo feedback processes (Sections 2.1 and 2.2), even the less drastic differences in albedo between different degrees of melt-pond coverage are of considerable importance. Model results suggest that Arctic sea ice is highly sensitive to changes in surface albedo. A difference in the degree of ponding, typically ranging between 10 and 50% areal coverage corresponding to albedos > 0.6 and < 0.5, would be critical for the stability and potential disappearance of the perennial ice pack (Steele & Flato, 2000).

Despite the importance of large-scale albedo variations, few if any models are currently able to fully predict the summer evolution of ice albedo. The key challenge that remains to be addressed is the ability to predict the changing pond fractions and depths, and their impact on the ice albedo. The vast majority of large-scale sea ice models and global circulation models (GCMs) is currently prescribing ice albedo through some type of parameterization scheme that links the surface albedo to the air or surface temperature or introduces a time-dependent albedo that varies during the course of the melt season. Some of the challenges of this problem and potential areas of improvement are discussed in more detail in Section 2.11.

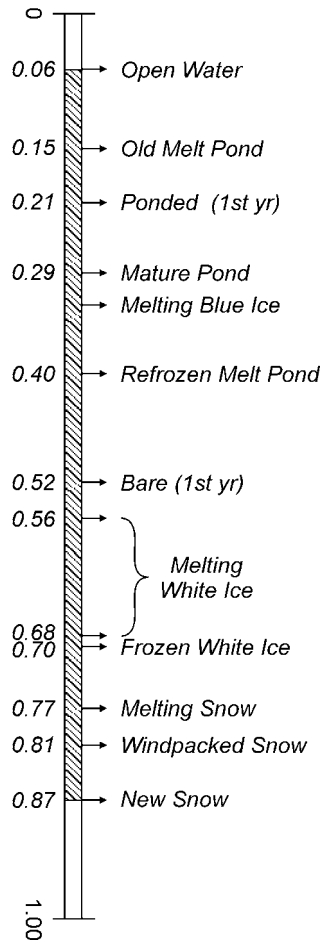

Fig. 2.16 Range of albedo of different ice pack surfaces. From Perovich (1998).

2.10 Macroscopic ice strength

Ice strength – at least on the macroscopic level as manifest, e.g. in a uniaxial compressive strength test commonly employed in studying the mechanical properties of sea ice (Richter-Menge, 1992) – is typically defined as the peak stress, σ_{max}, sustained by a sample when a load is applied. In simplified terms, σ corresponds to the magnitude of the force, F, applied per unit area, A

$$\sigma = \frac{F}{A} \qquad \text{(Equation 2.39)}$$

For an ideal elastic response, the strain ε resulting from a given stress σ is proportional to σ, with Young's modulus E as the proportionality constant:

$$\sigma = E\varepsilon \qquad \text{(Equation 2.40)}$$

Here, strain $\varepsilon = (l - l_0)/l_0$ is defined as the relative change in linear dimension that a body experiences as it is stretched or compressed from l_0 to l. For elastic deformation, the body fully recovers from a given strain in the way an ideal spring would (Fig. 2.17a). Upon reaching the yield stress σ_{max}, the sample fails catastrophically, i.e. by releasing the stored elastic energy mostly in the form of kinetic energy and sound. This process is referred to as brittle failure. The same mode of failure is experienced by a glass that shatters as it is dropped to the floor. Unlike glass, however, sea ice typically responds to a given stress not only through elastic but also through viscous (non-recoverable) deformation. For a Newtonian liquid, the latter is characterized by a linear relation between stress, σ, and strain rate, $d\varepsilon/dt$, with the viscosity of the medium η as the proportionality constant:

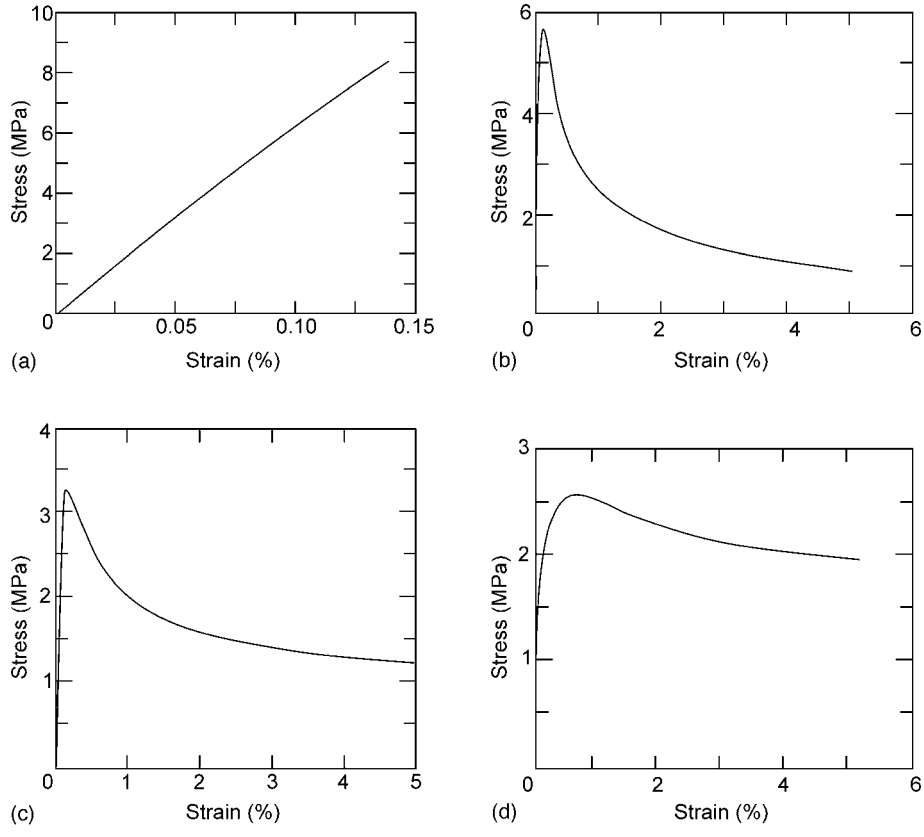

Fig. 2.17 Stress–strain curves for uniaxial compression tests of granular sea ice carried out at -10°C at different strain rates. (a) strain rate $10^{-2}\,s^{-1}$; (b) strain rate $10^{-3}\,s^{-1}$; (c) strain rate $10^{-4}\,s^{-1}$; (d) strain rate $10^{-5}\,s^{-1}$. For details see text. From Richter-Menge (1992).

$$\sigma = \eta \frac{d\varepsilon}{dt} \qquad \text{(Equation 2.41)}$$

Hence, deformation of natural sea ice is often best described by a model that takes into account both elastic and viscous strain components (Mellor, 1986). Equation 2.41 implies a connection between the magnitude of the stress and the strain rate. In fact, as evident from Fig. 2.17a–d, the deformation of natural sea ice samples at different strain rates conforms with such a visco-elastic model, with the peak stress σ_{max} reduced by a factor of three as the strain rate is dropped from $10^{-2}\,s^{-1}$ to $10^{-5}\,s^{-1}$. Also note that at smaller strain rates (Fig. 2.17b–d), the ice exhibits ductile failure and is still capable of supporting a load after attaining σ_{max}, in contrast with the brittle failure shown in Fig. 2.17a.

It requires a highly sophisticated approach to translate these results from laboratory experiments into the real world, in which the load could be applied by a person stepping on fairly thin, young ice, with the strain rate dictated by the speed at which the foot is set down on the ice surface. Nevertheless, based on this knowledge one could devise a strategy of how to best cross a very thin, young sea ice cover if one absolutely had to. First, one would not want to apply the full load fast enough to induce catastrophic brittle failure, as this would result in the person breaking through the ice without much of a warning (i.e. prior deflection of the ice sheet, see Fig. 2.17a). If strain rates were small enough to induce deformation in a ductile mode, then one would experience the ice giving way underneath after initially appearing quite strong (at least for strain rates corresponding to the transitional brittle–ductile regime characteristic of Fig. 2.17b) and, as long as the load would be reduced fast enough, the ice sheet would not fail (i.e. break).

Contrived though this example may appear, polar bears venturing out on nilas (≤ 10 cm thick) have been observed to make intuitive use of the physics underlying such different sea ice failure modes. Thus, in ambling across the thin ice, the bear sets down each foot just long enough for the peak stress to be surpassed (at the associated strain rates in the order of a few seconds at most) and then lifts it again to place it ahead on yet unstrained ice. This strategy (assuming it is strategy and not simply overinterpretation of a single observation by the author) allows for crossing of stretches of ice that would never support the weight of a bear if stationary for more than a few seconds at most. As the thin, warm ice flexes and is depressed below sea level, brine and sea water forced upwards through the ice onto the surface provide a visible indicator of the amount of accumulated strain.

The deformation process itself and the accommodation of strain on a microscopic level can be quite complex. Thus, the solid ice matrix experiences deformation of atomic bonds, slip along microcracks, movement of grain boundaries and other processes (Schulson, 1999). It is the combination of all of these individual, microscopic processes that determines the macroscopic response of the ice cover. Hence, the microstructure of the ice plays an important role in determining both ice strength and mode of failure (Schulson, 1999). The contrasting properties of lake

and sea ice have already been considered in Section 2.1 (see also Plate 2.1), and similar contrasts hold for ice deformation. Thus, for typical stresses and strain rates, the response of lake ice to an imposed loading is almost exclusively elastic, with failure occurring catastrophically in a brittle mode. This gives no advance warning to anybody who is about to break through the ice as the yield stress coincides with the complete failure of the material, similar to breaking glass. On the other hand, the lack of brine inclusions, which do not contribute to the overall strength of the material, is responsible for a somewhat higher strength of thin lake ice as compared to sea ice, which in the case of nilas can contain as much as 20% liquid-filled pores.

The actual macroscopic strength (i.e. the yield stress σ_{max}, see Fig. 2.17) of a sample or volume of sea ice is to a large extent controlled by the volume fraction of gas, V_a/V, and brine, V_b/V, both of which do not contribute to the mechanical strength of the material. As shown in an analysis by Assur (1960) (see summary in Weeks & Ackley, 1986) it is thus the ice cross-sectional area $(1 - \Psi)$ (with Ψ referred to as the 'plane porosity') that determines the magnitude of the *in situ* stress and hence the macroscopic yield stress, σ_{max}, such that

$$\sigma_f = (1 - \Psi)\sigma_0 \qquad \text{(Equation 2.42)}$$

where σ_0 would correspond to the strength of ice with all characteristics of sea ice but zero porosity. Based on Assur's (1960) pore model (Fig. 2.18), one can now derive the cross-sectional area of brine inclusions (assuming $V_a/V = 0$) in the vertical plane along which an ice sheet will typically fail under natural conditions. As shown in detail by Weeks & Ackley (1986), assuming the brine cell geometry outlined in Fig. 2.18, an expression can be derived for Ψ in terms of the platelet spacing, a_0, the minor and major radii of an ellipsoidal inclusion, r_a and r_b, spaced b_0 apart in the direction of the ice lamellae, and a vertical separation of inclusions of length g by g_0 such that Equation 2.42 can be evaluated as

$$\sigma_f = \left(1 - 2\sqrt{\frac{r_b}{r_a}\frac{g}{g_0}\frac{a_0}{b_0}\frac{V_b}{V}}\right)\sigma_0 \qquad \text{(Equation 2.43)}$$

A model of this form is commonly assumed to govern the porosity and pore-shape dependence of ice strength, although some recent work suggests more complex relationships. Apart from the stress-bearing, effective cross-sectional area, strength is also highly dependent on the nucleation and propagation of cracks that ultimately lead to failure. The latter depend strongly on other microstructural parameters, such as grain size or preferred alignment of crystals (Schulson, 1999).

On the scale of an individual ice floe, the bending of a sea ice sheet results in a vertical stress/strain distribution such that maximum tensile stress is found at the top of a flexing ice sheet, with σ decreasing to zero in the interior of the ice sheet and maximum compressive stress found at a point opposite the crest in the ice. As sea ice is stronger in compression than tension by a factor of 2 to 4, the ice typically fails by

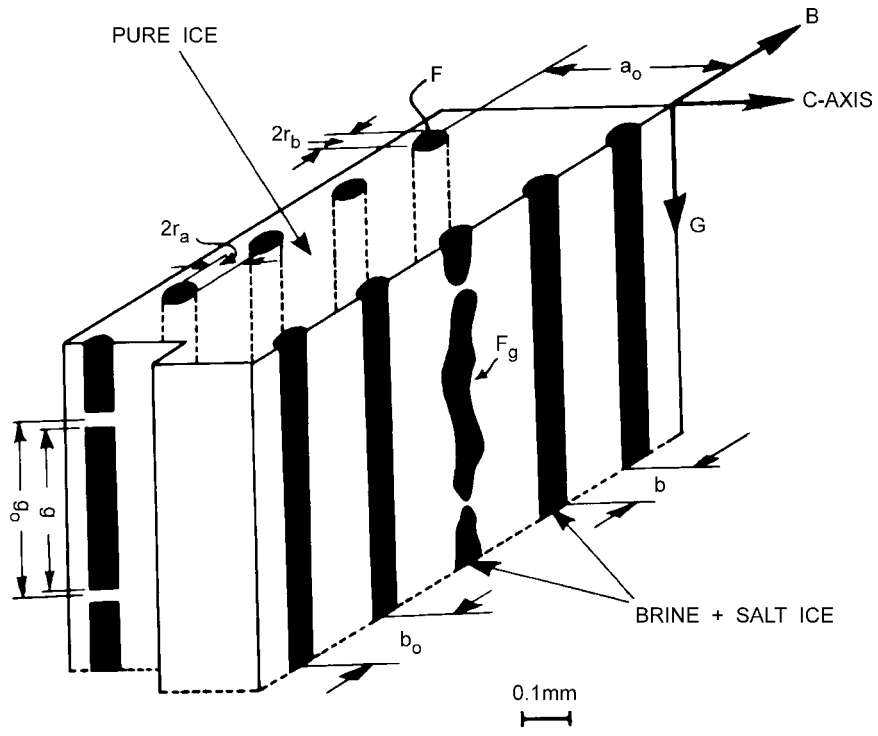

Fig. 2.18 Pore microstructural model from Assur (1960).

cracks developing at the outer surface that is in tension with the crack propagating into the interior of the ice sheet. At the same time, it is the colder, less porous and hence stronger layers that determine the overall strength of an ice sheet (Fig. 2.1). Ice strength is a property of sea ice that, probably unlike few others, is highly dependent on the scale at which it is being considered. Thus, at the scale of the ice pack, ice strength mostly is only in the order of tens to hundreds of kPa, whereas it is typically above 1 MPa in laboratory-scale experiments.

2.11 From the microscopic to the macroscopic: how the smallest can affect the largest of scales in sea ice

Much of this chapter has been concerned with features and processes occurring on sub-millimetre to at most metre scales. Sections 2.7 through 2.10 argued that an understanding of the magnitude and variability of sea ice macroscopic properties requires first of all thorough insight into the processes controlling the ice microstructural evolution, since it is the distribution of ice, brine, salts and gases that ultimately determines how energy and matter are transferred through a slab of ice.

Nevertheless, one may still wonder whether these small-scale processes and distinctions between different features at the microscopic level have any effect at all on the behaviour of sea ice on the largest of scales, such as those of concern in the context of global climate change (Haas, Chapter 3; Comiso, Chapter 4). One possible response to this question would be to point out that the interaction of light with sea ice, i.e. the processes that control ice albedo and ultimately the amount of solar energy absorbed by the polar oceans, strongly depends on the microscopic characteristics of brine and other inclusions in sea ice, because it is processes on the (sub)millimetre level that determine radiative transfer and in particular scattering of light in the medium. This is demonstrated by the differences in optical properties between lake and sea ice (Plate 2.1) as well as the impact of salt precipitation (Fig. 2.5).

However, the importance of small-scale processes extends far beyond the obvious, well-studied problems such as radiative transfer. Consider, for example, the fact that the albedo of bare Arctic multi-year sea ice is remarkably stable at values above 0.6, which has been established in numerous studies of the summer ice pack (Perovich et al., 2002). As illustrated in Plate 2.3a, this value is quite high, with completely bare sea ice taking on the appearance of being covered with snow. The magnitude of ice albedo and its constancy are controlled by the presence of a well-drained, decomposed layer developing in the uppermost 0.1–0.2 m of the ice cover (Perovich et al., 2002), i.e. on a scale comparable to the thin sections shown in Plate 2.1. If it were not for the increase in ice permeability associated with the absorption of short-wave radiation and surface warming, the brine could not drain from this surface layer, instead accumulating within pores and at the surface, rendering ice albedo significantly lower (< 0.5). Model results indicate that such low-albedo, undrained ice could not exist perennially in the Arctic Ocean (Curry et al., 1995). Hence, the microstructure and its control on the percolation of melt water and brine in the uppermost tens of centimetres of the ice cover arguably ensure the year-round presence of multi-year ice in the Arctic Ocean.

The impact of small-scale processes extends further than that, however, since microstructure and ice permeability also play a key role in locally reducing ice albedo through the formation of melt ponds with albedos as low as 0.3 (Perovich, 1998), such as those illustrated in Plate 2.3a. These ponds form as the result of pooling of melt water in depressions where the permeability of the underlying ice is not sufficiently high to allow complete drainage of the pond as driven by the local hydraulic head (Eicken et al., 2002). Recent field experiments have shown that the development of a thin impervious layer in the uppermost 0.1 m of the ice cover due to refreezing of melt water within the pore network sufficiently reduces the permeability to result in substantial pooling of melt water at the ice surface ($> 50\%$ area on first-year ice), while the absence of such a layer can reduce pond coverage to $< 20\%$. In all of these cases, it is processes occurring on sub-centimetre scales that ultimately decide the fate of the Arctic ice pack.

Currently, large-scale climate models are not capable of actually predicting the

albedo of summer sea ice based on first principles, and we need to further our understanding of the microstructural evolution of sea ice (and develop the appropriate conceptual and mathematical models) in order to progress beyond the limitations that currently hamper predictions of the vagaries of climate in the polar regions and their impact on lower latitudes.

2.12 Outlook

This chapter has highlighted the importance of small-scale and microscopic properties and processes in understanding, quantifying and predicting the role of sea ice in the polar regions and as part of the earth system. However, in discussing features at scales that are six to twelve orders of magnitude smaller than the earth, and in particular when considering the practical limitations of climate models, remote-sensing tools and field campaigns, one needs to consider whether a more detailed analysis of these microscopic scales only leads to mildly interesting work that is trailing off into the irrelevant. While this question definitely needs to be asked, the answer may vary considerably on a case-by-case basis. For example, based on recent work by Light et al. (in press) one could argue that sea ice radiative-transfer modelling is about to extend down to a microstructural scale beyond which further efforts may require substantial efforts but yield little in the way of model improvement. Thus, Light and co-workers have found that the number density of scatterers down to a scale of tens of micrometres (with number densities, N_p, of between 10 and 50 mm^{-3}) explains the bulk of the optical signal due to scattering (see also Fig. 2.15), while the contribution of smaller inclusions to the magnitude of optical properties is only of mostly negligible importance. In this context, recent measurements at higher magnifications of number densities of several tens to hundreds mm^{-3} are hence mostly irrelevant in an optical context. However, the role of such microscopic or sub-microscopic inclusions may nevertheless be of importance in controlling the shape and thermal evolution of larger pores (Eicken et al., 2000).

Another rapidly developing research field of microscopic and sub-microscopic processes that is potentially of great significance to the study of sea ice is that of surface pre-melting. As demonstrated and discussed in more detail by Wettlaufer (1999), dispersive intermolecular forces result in the presence of liquid films on ice phase boundaries at below-freezing temperatures. In pure water–ice systems, these films are typically mere fractions of a micrometre in thickness, such that they can play key roles in the transport of particulate impurities but rarely if at all dominate bulk heat fluxes through the system. However, in the presence of dissolved impurities, such as salts at seawater concentrations, film thicknesses can increase to several micrometres at small supercoolings with potentially significant impacts on the redistribution of particulate inclusions, such as sediment grains or algal cells, as well as desalination processes. Here, further work appears timely and potentially fruitful.

The smallest of scales also greatly impact biological and chemical processes in the sea ice and we are only beginning to understand the magnitude and importance of stationary and transient chemical gradients established at micrometre to millimetre scales. Thus, both the fine structure of algal communities, as well as the interaction of micro-organisms with ice and other surfaces at microscopic scales, are not well understood (Arrigo, Chapter 5; Lizotte, Chapter 6) and may hold surprises of more than just local relevance. Recent discoveries of the importance of surface catalytic processes in saline snow for trace gas production as well as the release of radiatively important compounds by sea ice biota are cases in point here (Thomas & Papadimitriou, Chapter 9).

One of the more interesting and pressing challenges at this point, however, is the development of a sea ice microstructural model that extends beyond the pioneering work of Assur and others (see Sections 2.4, 2.5 and 2.10). Presently, there is still something of a lack of comprehensive microstructural data sets, not least due to methodical problems, but recent efforts (Light et al., in press) as well as methodical developments (Callaghan et al., 1999) should result in more such data sets of high quality. Developing a microstructural model may nevertheless require further studies of the relevant processes underlying the establishment and transformation of primary and secondary grain and pore microstructure. Ultimately, such a model should be integrated into a fully coupled ice-growth/salt-flux/radiative transfer model (as far as the author is aware, the latter does not yet exist either). In developing such a model, one would furthermore want to revisit the concept of the 'standard', highly idealized sea ice chemical composition. Section 2.4 and Fig. 2.5 demonstrate that there are more things happening between -2 and -30°C than are dreamt of in the 'standard' sea ice philosophy. In spite of being computationally somewhat more intensive, state-of-the-art geochemical models such as those of Spencer et al. (1990) or Marion & Grant (1997) appear to be perfectly suitable for the study and prediction of phase equilibria in sea ice of variable composition at the macroscopic and microscopic level.

Here, one might again ask whether such a detailed approach is required only for specialized process studies or whether benefits extend into other fields of geophysical, biological or chemical research as well. Considering the case presented in Section 2.11, one could argue that only such a detailed model will ever allow for a full, independent prediction of the albedo of different sea ice types in various developmental stages. Admittedly, even simple albedo parameterization schemes are performing quite well in GCMs but, as hinted at above, the reason that these schemes work so well might well be considered worrisome rather than reassuring. If one accepts that the physics of the southern hemisphere is the same as that of the northern hemisphere (disregarding the difference in sign of the Coriolis vector), then the fact that global climate models employ different albedo parameterization schemes in the Antarctic as compared to the Arctic is a strong argument for closer scrutiny of the underlying microscopic and macroscopic processes.

Finally, in looking beyond the polar regions, sea ice may also serve as an

appropriate and useful physical model of other types of ice bodies in our solar system and of other geophysical and industrial materials at high homologous temperatures (i.e. relative to the freezing point of the melt). Sea ice is an ideal model substance, as it is a porous medium that is both simple – from a compositional point-of-view, with a three- to five-component aqueous system allowing fairly sophisticated simulations of the proper medium (Spencer et al., 1990; Marion & Grant, 1997) – and complex – from a microstructural point-of-view, with liquid phase fractions varying over more than four orders of magnitude under natural conditions, and with a complex microstructural evolution, as outlined in Sections 2.4 and 2.5. Consider, for example, the range of intrinsic permeabilities, as one of the most important measures of transport properties and processes, measured in different types of sea ice under natural conditions over a temperature range of approximately 15 K shown in Fig. 2.19. The more than six orders of magnitude in permeability depicted here represent more than half of the entire range of permeabilities found in other common geological media. Porosities vary almost over the same range of magnitudes, as do pore sizes (Section 2.4). Thus, the study of grain and pore microstructure of sea ice, and its effect on permeability, rivals that of an entire range

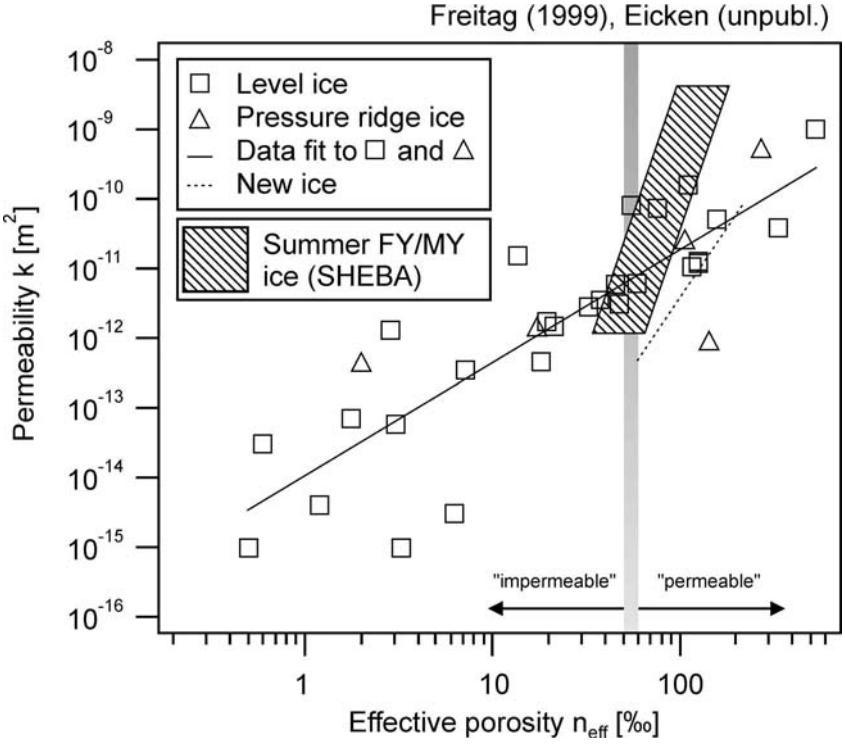

Fig. 2.19 Range of sea ice permeabilities measured in different ice types as a function of the effective (i.e. connected) porosity (Freitag, 1999; Eicken, unpublished).

of different geological and planetary materials over a wide range of homologous temperatures. This presents sea ice researchers with both a formidable challenge with respect to the representation of sea ice in large-scale climate models (see Section 2.11), as well as a tremendous opportunity with respect to the potential role of sea ice as an analogue of a wide variety of planetary materials. Recent advances in laboratory and field measurement technology, as well as remote sensing in combination with research on, for example, the ice crust of the Jovian moon Europa (Greeley et al., 1998), and studies of terrestrial geological systems, indicate a substantial potential for cross-disciplinary fertilization along with exciting opportunities and needs for future research.

Acknowledgements

As much as anything, this contribution is a summary of what I have learned from others, including my teachers, colleagues and the students who have been working with me. For this and other support that has been provided by numerous people and institutions I am more than grateful. While this article is also a manifestation of what I've failed to learn or properly grasp, these deficiencies are solely my responsibility. Support by the National Science Foundation and the Geophysical Institute at the University of Alaska is also gratefully acknowledged.

References

Anderson, D.L. (1961) Growth rate of sea ice. *Journal of Glaciology*, **3**, 1170–1172.

Andreas, E.L. & Ackley, S.F. (1981) On the differences in ablation seasons of the Arctic and Antarctic sea ice. *Journal of the Atmospheric Sciences*, **39**, 440–447.

Arrigo, K.R. & Sullivan, C.W. (1994) A high resolution bio-optical model of microalgal growth: tests using sea ice algal community time-series data. *Limnology and Oceanography*, **39**, 609–631.

Assur, A. (1960) Composition of sea ice and its tensile strength. *SIPRE Research Report*, **44**.

Bombosch, A. (1998) Interactions between floating ice platelets and ocean water in the southern Weddell Sea. In: *Ocean, Ice, and Atmosphere: Interactions at the Antarctic Continental Margin*, (Eds S.S. Jacobs & R. Weiss), American Geophysical Union, Washington, D.C. *Antarctic Research Series*, **75**, 257–266.

Callaghan, P.T., Dykstra, R., Eccles, C.D., Haskell, T.G. & Seymour, J.D. (1999) A nuclear magnetic resonance study of Antarctic sea ice brine diffusivity. *Cold Regions Science and Technology*, **29**, 153–171.

Cox, G.F.N. & Weeks, W.F. (1975) Brine drainage and initial salt entrapment in sodium chloride ice. *CRREL Research Reports*, **345**.

Cox, G.F.N. & Weeks, W.F. (1983) Equations for determining the gas and brine volumes in sea-ice samples. *Journal of Glaciology*, **29**, 306–316.

Cox, G.F.N. & Weeks, W.F. (1988) Numerical simulations of the profile properties of undeformed first-year sea ice during the growth season. *Journal of Geophysical Research*, **93**, 12449–12460.

Curry, J.A., Schramm, J.L. & Ebert, E.E. (1995) Sea ice-albedo climate feedback mechanism. *Journal of Climate*, **8**, 240–247.

Drinkwater, M.R. & Xiang, L. (2000) Seasonal to interannual variability in Antarctic sea-ice surface melt. *IEEE Transactions on Geoscience and Remote Sensing*, **38**, 1827–1842.

Eicken, H. (1992a) Salinity profiles of Antarctic sea ice: field data and model results. *Journal of Geophysical Research*, **97**, 15545–15557.

Eicken, H. (1992b) The role of sea ice in structuring Antarctic ecosystems. *Polar Biology*, **12**, 3–13.

Eicken, H. (1998) Factors determining microstructure, salinity and stable-isotope composition of Antarctic sea ice: deriving modes and rates of ice growth in the Weddell Sea. In: *Antarctic Sea Ice: Physical Processes, Interactions and Variability*, (Ed. M.O. Jeffries), American Geophysical Union, Washington, D.C. *Antarctic Research Series*, **74**, 89–122.

Eicken, H., Bock, C., Wittig, R., Miller, H. & Poertner, H.-O. (2000) Nuclear magnetic resonance imaging of sea ice pore fluids: methods and thermal evolution of pore microstructure. *Cold Regions Science and Technology*, **31**, 207–225.

Eicken, H., Fischer, H. & Lemke, P. (1995) Effects of the snow cover on Antarctic sea ice and potential modulation of its response to climate change. *Annals of Glaciology*, **21**, 369–376.

Eicken, H., Krouse, H.R., Kadko, D. & Perovich, D.K. (2002) Tracer studies of pathways and rates of meltwater transport through Arctic summer sea ice. *Journal of Geophysical Research*, **107** [DOI: 10.1029/2000JC000583].

Eicken, H., Lange, M.A., Hubberten, H.-W. & Wadhams, P. (1994) Characteristics and distribution patterns of snow and meteoric in the Weddell Sea and their contribution to the mass balance of sea ice. *Annales Geophysicae*, **12**, 80–93.

Feistel, R. & Hagen, E. (1998) A Gibbs thermodynamic potential for sea ice. *Cold Regions Science and Technology*, **28**, 83–142.

Fichefet, T. & Morales Maqueda, M.A. (1999) Modelling the influence of snow accumulation and snow-ice formation on the seasonal cycle of the Antarctic sea-ice cover. *Climate Dynamics*, **15**, 251–268.

Fletcher, N.H. (1970) *The Chemical Physics of Ice*. Cambridge University Press, Cambridge.

Freitag, J. (1999) The hydraulic properties of Arctic sea ice – implications for the small-scale particle transport. *Berichte zur Polarforschung*, **325**, 1–150 (in German).

Golden, K.M., Ackley, S.F. & Lytle, V.I. (1998a) The percolation phase transition in sea ice. *Science*, **282**, 2238–2241.

Golden, K.M., Cheney, M., Ding, K.-H., Fung, A.K., Grenfell, T.C., Isaacson, D., Kong, J.A., Nghiem, S.V., Sylvester, J. & Winebrenner, D.P. (1998b) Forward electromagnetic scattering models for sea ice. *IEEE Transactions on Geoscience and Remote Sensing*, **36**, 1655–1674.

Greeley, R., Sullivan, R., Coon, M.D., Geissler, P.E., Tufts, B.R., Head, J.W., III, Pappalardo, R.T. & Moore, J.M. (1998) Terrestrial sea ice morphology: considerations for Europa. *Icarus*, **135**, 25–40.

Grenfell, T.C. (1991) A radiative transfer model for sea ice with vertical structure variations. *Journal of Geophysical Research*, **96**, 16991–17001.

Hallikainen, M.T. (1983) New low-salinity sea-ice model for UHF radiometry. *Remote Sensing*, **4**, 655–681.

Hallikainen, M., Toilla, M.V.O., Hyyppä, J.M. & Guyenne, T.D. (1988) Microwave dielectric properties of low-salinity sea ice. IGARSS '88; remote sensing: moving towards the 21st

century, 12–16 September 1988, Edinburgh, UK. 1988 International Geoscience and Remote Sensing Symposium. ESTEC, ESA Publications Division, Noordwijk, 419–420.

Hallikainen, M. & Winebrenner, D.P. (1992) The physical basis for sea ice remote sensing. In: *Microwave Remote Sensing of Sea Ice*, (Ed. F.D. Carsey), American Geophysical Union, Washington, D.C. *Geophysical Monograph*, **68**, 29–46.

Hobbs, P.V. (1974) *Ice Physics*. Clarendon Press, Oxford.

Jeffries, M.O., Shaw, R.A., Morris, K., Veazey, A.L. & Krouse, H.R. (1994) Crystal structure, stable isotopes ($\partial^{18}O$), and development of sea ice in the Ross, Amundsen, and Bellingshausen seas, Antarctica. *Journal of Geophysical Research*, **99**, 985–995.

Jin, Z., Stamnes, K., Weeks, W.F. & Tsay, S.-C. (1994) The effect of sea ice on the solar energy budget in the atmosphere–sea ice ocean system: a model study. *Journal of Geophysical Research*, **99**, 25281–25294.

Lange, M.A., Ackley, S.F., Wadhams, P., Dieckmann, G.S. & Eicken, H. (1989) Development of sea ice in the Weddell Sea, Antarctica. *Annals of Glaciology*, **12**, 92–96.

Leppäranta, M. (1993) A review of analytical models of sea-ice growth. *Atmosphere-Ocean*, **31**, 123–138.

Leppäranta, M. (Ed.) (1998) *Physics of Ice-covered Seas* (2 vols). University of Helsinki Press, Helsinki, Finland.

Leppäranta, M. & Manninen, T. (1988) *The brine and gas content of sea ice with attention to low salinities and high temperatures*. Finnish Institute Marine Research Internal Report, 88–2, Helsinki.

Light, B., Maykut, G.A. & Grenfell, T.C. (in press) Effects of temperature on the microstructure of first-year sea ice. *Journal of Geophysical Research*.

Lin, F.C., Kong, J.A., Shin, R.T., Gow, A.J. & Arcone, S.A. (1988) Correlation function study for sea ice. *Journal of Geophysical Research*, **93**, 14055–14063.

Lytle, V.I. & Ackley, S.F. (1996) Heat flux through sea ice in the western Weddell Sea: convective and conductive transfer processes. *Journal of Geophysical Research*, **101**, 8853–8868.

McPhee, M.G., Ackley, S.F., Guest, P., Huber, B.A., Martinson, D.G., Morison, J.H., Muench, R.D., Padman, L. & Stanton, T.P. (1996) The Antarctic Zone Flux Experiment. *Bulletin of the American Meteorological Society*, **77**, 1221–1232.

McPhee, M.G., Stanton, T.P., Morison, J.H. & Martinson, D.G. (1998) Freshening of the upper ocean in the Arctic: is perennial sea ice disappearing? *Geophysics Research Letters*, **25**, 1729–1732.

Maksym, T. & Jeffries, M.O. (2000) A one-dimensional percolation model of flooding and snow ice formation on Antarctic sea ice. *Journal of Geophysical Research*, **105**, 26313–26331.

Malmgren, F. (1927) On the properties of sea-ice. *Norwegian North Pole Expedition 'Maud' 1918–1925*, **1**, 1–67.

Marion, G.M. & Grant, S.A. (1997) Physical chemistry of geochemical solutions at subzero temperatures. *CRREL Special Report*, **97–10**, 349–356.

Martinson, D.G. and Iannuzzi, R.A. (1998) Antarctic ocean-ice interaction: implications from ocean bulk property distributions in the Weddell Gyre. In: *Antarctic Sea Ice: Physical Processes, Interactions and Variability*, (Ed. M.O. Jeffries), American Geophysical Union, Washington., *Antarctic Research Series*, **74**, 243–271.

Massom, R.A., Eicken, H., Haas, C., Jeffries, M.O., Drinkwater, M.R., Sturm, M., Worby,

A.P., Wu, X.R., Lytle, V.I., Ushio, S., Morris, K., Reid, P.A., Warren, S. & Allison, I. (2001) Snow on Antarctic sea ice. *Reviews of Geophysics*, **39**, 413–445.

Maykut, G.A. (1986) The surface heat and mass balance. In: *The Geophysics of Sea Ice*, (Ed. N. Untersteiner), Plenum Press, New York. *NATO ASI Series B: Physics*, **146**, 395–463.

Maykut, G.A. & McPhee, M.G. (1995) Solar heating of the Arctic mixed layer. *Journal of Geophysical Research*, **100**, 24691–24703.

Mellor, M. (1986) Mechanical behavior of sea ice. In: *The Geophysics of Sea Ice*, (Ed. N. Untersteiner), *NATO ASI Series B: Physics*, **146**, 165–281.

Nakawo, M. & Sinha, N.K. (1981) Growth rate and salinity profile of first-year sea ice in the high Arctic. *Journal of Glaciology*, **27**, 315–330.

Nakawo, M. & Sinha, N.K. (1984) A note on brine layer spacing of first-year sea ice. *Atmosphere-Ocean*, **22**, 193–206.

Niedrauer, T.M. & Martin, S. (1979) An experimental study of brine drainage and convection in young sea ice. *Journal of Geophysical Research*, **84**, 1176–1186.

Ono, N. (1968) Thermal properties of sea ice: IV, Thermal constants of sea ice. *Low Temperature Science, Series A*, **26**, 329–349 (in Japanese).

Perovich, D.K. (1998) Optical properties of sea ice. In: *Physics of Ice-covered Seas*, Vol. 1, (Ed. M. Leppäranta), pp. 195–230, University of Helsinki Press, Helsinki, Finland.

Perovich, D.K., Grenfell, T.C., Light, B. & Hobbs, P.V. (2002) The seasonal evolution of Arctic sea ice albedo. *Journal of Geophysical Research*, **107**, DOI: 10.1029/2000JC000438.

Perovich, D.K., Grenfell, T.C., Richter-Menge, J.A., Light, B., Tucker, W.B., III & Eicken, H. (in press) Thin and thinner: ice mass balance measurements during SHEBA. *Journal of Geophysical Research*.

Persson, P.O.G., Fairall, C.W., Andreas, E.L. & Guest, P.S. (2002) Measurements near the Atmospheric Surface Flux Group tower at SHEBA. Near-surface conditions and surface energy budget. *Journal of Geophysical Research*, **107**, DOI: 10.1029/2000JC000705.

Pfirman, S., Lange, M.A., Wollenburg, I. & Schlosser, P. (1990) Sea ice characteristics and the role of sediment inclusions in deep-sea deposition: Arctic–Antarctic comparisons. In: *Geological History of the Polar Oceans: Arctic versus Antarctic*, (Eds U. Bleil & J. Thiede), NATO ASI Series C, Vol. 308, pp. 187–211. Kluwer Academic Publishers, Dordrecht.

Reimnitz, E., Kempema, E.W., Weber, W.S., Clayton, J.R. & Payne, J.R. (1990) Suspended-matter scavenging by rising frazil ice. *CRREL Monographs*, **90–1**, 97–100.

Reimnitz, E., Marincovich, L., McCormick, M. & Briggs, W.M. (1992) Suspension freezing of bottom sediment and biota in the Northwest Passage and implications for Arctic Ocean sedimentation. *Canadian Journal of Earth Science*, **29**, 693–703.

Richardson, C. (1976) Phase relationships in sea ice as a function of temperature. *Journal of Glaciology*, **17**, 507–519.

Richter-Menge, J.A. (1992) Compressive strength of frazil sea ice. *Proceedings of the IAHR Symposium on Ice, Banff, Alberta*, **2**, 1065–1074.

Rothrock, D.A., Yu, Y. & Maykut, G.A. (1999) Thinning of the Arctic sea-ice cover. *Geophysical Research Letters*, **26**, 3469–3472.

Sakazume, S. & Seki, N. (1978) On the thermal properties of ice and snow in a low temperature region. *Bulletin of the Japanese Society of Mechanical Engineering*, **44**, 2059–2069.

Schanda, E. (1986) *Physical Fundamentals of Remote Sensing*. Springer-Verlag, Berlin.

Schulson, E.M. (1999) The structure and mechanical behavior of ice. *JOM*, **51**, 21–27.

Schwerdtfeger, P. (1963) The thermal properties of sea ice. *Journal of Glaciology*, **4**, 789–807.

Serreze, M.C., Walsh, J., Chapin, F., Osterkamp, T., Dyurgerov, M., Romanovsky, V., Oechel, W., Morison, J., Zhang, T. & Barry, R. (2000) Observational evidence of recent change in the northern high-latitude environment. *Climatic Change*, **46**, 159–207.

Smedsrud, L.H. (2001) Frazil-ice entrainment of sediment: large-tank laboratory experiments. *Journal of Glaciology*, **47**, 461–471.

Smith, R.E.H., Harrison, W.G., Harris, L.R. & Herman, A.W. (1990) Vertical fine structure of particulate matter and nutrients in sea ice of the high Arctic. *Canadian Journal of Fisheries and Aquatic Science*, **47**, 1348–1355.

Spencer, R.J., Møller, N. & Weare, J.H. (1990) The prediction of mineral solubilities in natural waters: a chemical equilibrium model for the Na-K-Ca-Mg-Cl-SO_4-H_2O system at temperatures below 25°C. *Geochimica et Cosmochimica Acta*, **54**, 575–590.

Steele, M. & Flato, G.M. (2000) Sea ice growth, melt, and modeling: a survey. In: *The Freshwater Budget of the Arctic Ocean*, (Ed. E.L. Lewis), pp. 549–587, Kluwer Academic Publishers, Dordrecht.

Stogryn, A. (1987) An analysis of the tensor dielectric constant of sea ice at microwave frequencies. *IEEE Transactions on Geoscience and Remote Sensing*, **GE-25**, 147–158.

Sturm, M., Perovich, D.K. & Holmgren, J. (2002) Thermal conductivity and heat transfer through the snow on the ice of the Beaufort Sea. *Journal of Geophysical Research*, **107**, DOI: 10.1029/2000JC000409.

Trodahl, H.J., McGuinnes, M.J., Langhorne, P.J., Collins, K., Pantoja, A.E., Smith, I.J. & Haskell, T.G. (2000) Heat transport in McMurdo Sound first-year fast ice. *Journal of Geophysical Research*, **105**, 11347–11358.

Tucker, W.B., III, Perovich, D.K., Gow, A.J., Weeks, W.F. & Drinkwater, M.R. (1992) Physical properties of sea ice relevant to remote sensing. In: *Microwave Remote Sensing of Sea Ice*, (Ed. F.D. Carsey), American Geophysical Union, Washington, D.C. *Geophysical Monograph*, **68**, 9–28.

Tyshko, K.P., Fedotov, V.I. & Cherepanov, I.V. (1997) Spatio-temporal variability of the Arctic seas' ice cover structure. In: *Sea Ice*, (Eds I.E. Frolov & V.P. Gavrilo), pp. 191–213, Gidrometeoizdat, St. Petersburg.

UNESCO (1978) *Eighth report of the joint panel on oceanographic tables and standards*. Unesco Technical Papers in Marine Science 28. UNESCO, Paris.

Untersteiner, N. (1968) Natural desalination and equilibrium salinity profile of perennial sea ice. *Journal of Geophysical Research*, **73**, 1251–1257.

Vant, M.R., Gray, R.B., Ramseier, R.O. & Makios, V. (1974) Dielectric properties of fresh and sea ice at 10 and 35 GHz. *Journal of Applied Physics*, **45**, 4712–4717.

Vant, M.R., Ramseier, R.O. & Makios, V. (1978) Complex-dielectric constant of sea ice at frequencies in the range 0.1–40 GHz. *Journal of Applied Physics*, **49**, 1264–1280.

Wadhams, P., Lange, M.A. & Ackley, S.F. (1987) The ice thickness distribution across the Atlantic sector of the Antarctic ocean in midwinter. *Journal of Geophysical Research*, **92**, 14535–14552.

Weeks, W.F. (1998) Growth conditions and the structure and properties of sea ice. In: *Physics of Ice-covered Seas*, Vol. 1, (Ed. M. Leppäranta), pp. 25–104, University of Helsinki Press, Helsinki, Finland.

Weeks, W.F. & Ackley, S.F. (1986) The growth, structure and properties of sea ice. In: *The Geophysics of Sea Ice*, (Ed. N. Untersteiner), Plenum Press, New York. *NATO ASI Series B: Physics*, **146**, 9–164.

Weeks, W.F. & Wettlaufer, J.S. (1996) Crystal orientations in floating ice sheets. In: *The Johannes Weertman Symposium*, (Ed. R.J. Arsenault, D. Cole, T. Gross, G. Kostorz, P.K. Liaw, S. Parameswaran & H. Sizek), pp. 337–350, The Minerals, Metals & Materials Society, Warrendale, Pennsylvania.

Wettlaufer, J. (1998) Introduction to crystallization phenomena in natural and artificial sea ice. In: *Physics of Ice-covered Seas*, Vol. 1, (Ed. M. Leppäranta), pp. 105–194. University of Helsinki Press, Helsinki, Finland.

Wettlaufer, J.S. (1998) Impurity effects in the premelting of ice. *Physical Review Letters*, **82**, 2516–2519.

Wettlaufer, J.S., Worster, M.G. & Huppert, H.E. (1997) Natural convection during solidification of an alloy from above with application to the evolution of sea ice. *Journal of Fluid Mechanics*, **344**, 291–316.

Worby, A.P., Massom, R.A., Allison, I., Lytle, V.I. & Heil, P. (1998) East Antarctic sea ice: a review of its structure, properties and drift. In: *Antarctic Sea Ice: Physical Processes, Interactions and Variability*, (Ed. M.O. Jeffries), American Geophysical Union, Washington, D.C. *Antarctic Research Series*, **74**, 41–67.

Yen, Y.C., Cheng, K.C. & Fukusako, S. (1991) Review of intrinsic thermophysical properties of snow, ice, sea ice, and frost. In: *Proceedings 3rd International Symposium on Cold Regions Heat Transfer, Fairbanks, AK, June 11–14, 1991*, (Eds J.P. Zarling & S.L. Faussett), pp. 187–218, University of Alaska, Fairbanks, Alaska.

Zotikov, I.A., Zagorodnov, V.S. & Raikovsky, J.V. (1980) Core drilling through the Ross Ice Shelf (Antarctica) confirmed basal freezing. *Science*, **207**, 1463–1465.

Chapter 3

Dynamics versus Thermodynamics: The Sea Ice Thickness Distribution

Christian Haas

3.1 Introduction

Eicken (Chapter 2) has described how sea ice initially forms from open water and subsequently grows into an ice cover, or in other terms, how sea ice grows thermodynamically. One of the basic concepts is that the ice grows thicker the colder the air is due to the establishment of greater temperature gradients in the ice, and higher freezing rates. Vice versa, it would follow that as a consequence of climate warming, polar sea ice cover would become thinner. However, another process contributes to the sea ice thickness distribution: Due to its relative thinness – one to a few metres – sea ice floating over deep water is subject to winds and currents which steadily move the ice around, i.e. the ice cover drifts. As a result, it breaks up into floes interspersed by open water leads. With changing drift directions and speeds, the ice floes will be pushed together and collide with each other. If the resulting forces in the ice become too large, it will finally break. The resulting ice fragments and blocks will be pushed onto, and below, the edges of the floes forming so-called pressure ridges (Fig. 3.1).

Obviously, such dynamically formed ridges are much thicker than the adjacent, thermodynamically grown undeformed level ice. In terms of a statistical approach, this discussion shows that it is important to take into account different ice thickness classes (from thin to thick ice), and that a certain mean ice thickness can be attained by many different arrangements of thin and thick ice. As a consequence, it is quite difficult to interpret ice thickness data for indications of climate warming or cooling. This will be illustrated in later sections of this chapter.

The ultimate variable to assess the shrinking or growing of the global sea ice cover is ice volume, i.e the mathematical product of areal ice coverage and ice thickness. In contrast to ice thickness, sea ice coverage can be monitored reasonably well from space using satellites (Comiso, Chapter 4). However, from the discussion above it follows that as long as the ice thickness is unknown, the observed recent changes of

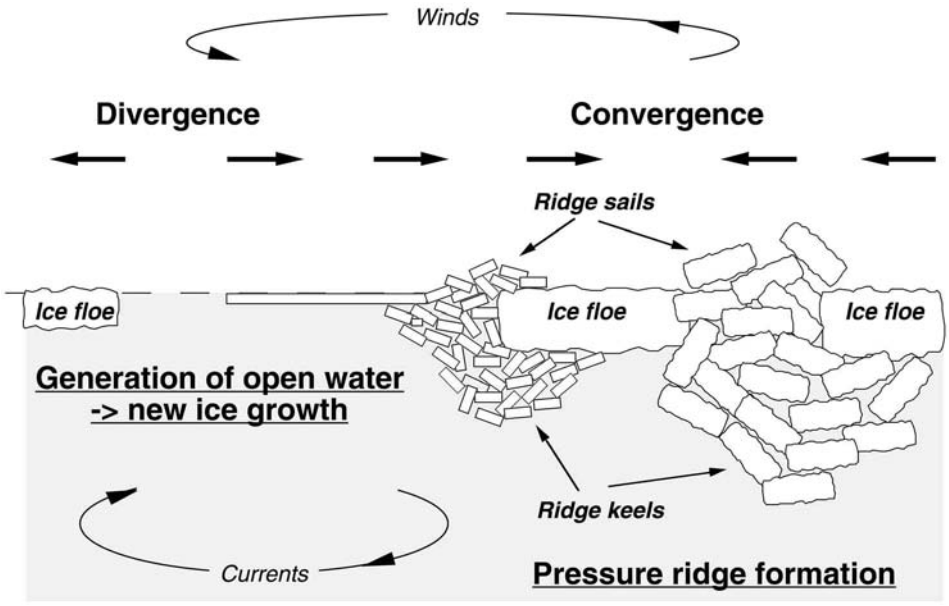

Fig. 3.1 Illustration of the processes that dynamically (i.e. by divergent or convergent ice motion) modify the ice thickness distribution.

ice coverage reported in that chapter are difficult to interpret in terms of overall ice volume and climate signals. These changes are mainly due to a retreat or advance of the ice edge in certain regions. It should be noted, however, that the location of the ice edge is a result of an equilibrium between ice drift, air temperature and ocean heat flux. Particularly, the latter is a function of the velocity and heat content of ocean currents, whose origin usually is in non-polar latitudes. Due to these complexities of the air–ice–ocean system, even the retreat of an ice edge is not necessarily linked to an overall decrease of ice volume.

This chapter presents the physical and statistical approaches used to understand and simulate the ice thickness distribution on a local and regional scale, as well as what is known about the global distribution of ice thicknesses. Different methods to determine ice thickness are presented, as well as some recent results of observations of the variability and trends of sea ice thickness in certain regions.

3.2 The sea ice thickness distribution

Statistical description

Figure 3.2 shows three thickness profiles of first- and second-year floes obtained by means of electromagnetic (EM) sounding (see Section 3.3). Figure 3.2a,b was obtained by ground-based profiling of single floes, whereas Fig. 3.2c is an airborne

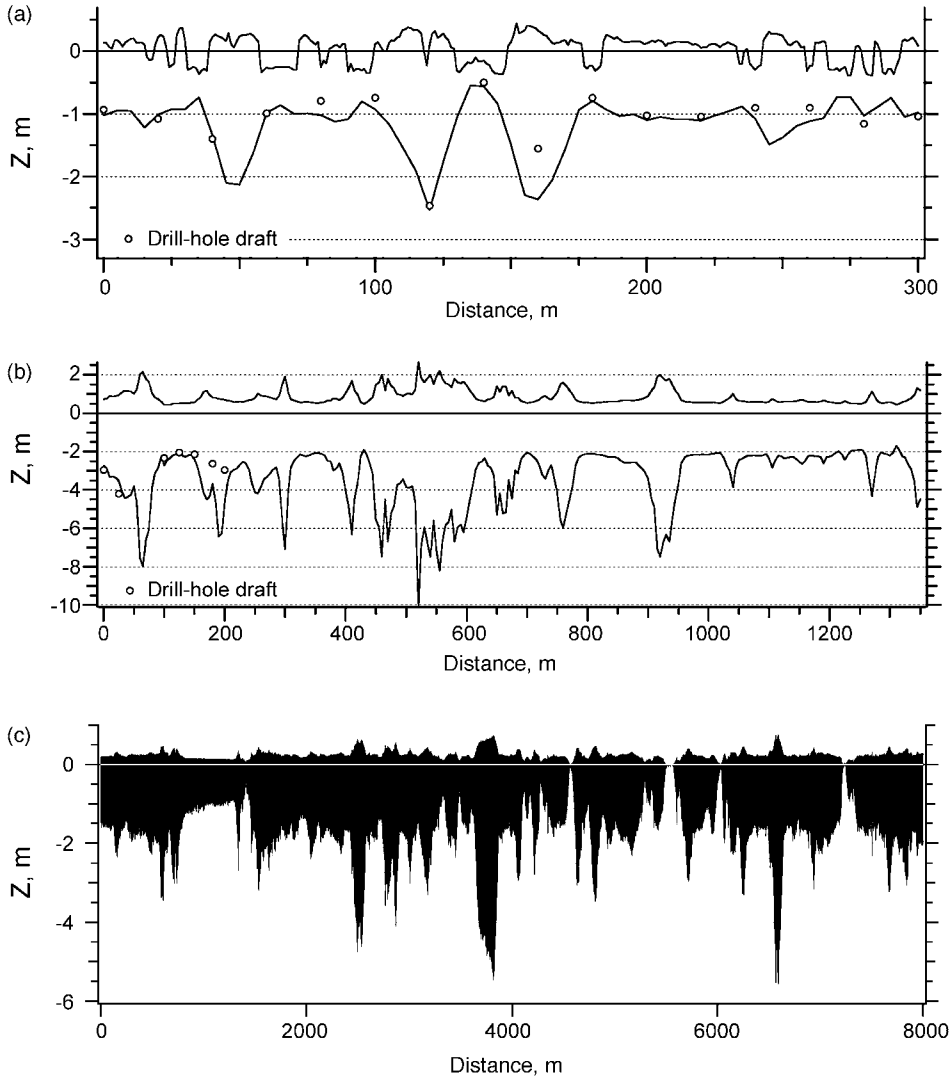

Fig. 3.2 Thickness profiles of first-year (a) and second-year (b, c) ice floes in the Transpolar Drift obtained from electromagnetic (EM) sounding. The water level is at $Z = 0$ m. (a) and (b) were obtained by ground measurements, while (c) is a typical helicopter EM profile. Circles in (a) and (b) show results from drill-hole measurements for comparison. In (a) the surface profile has been obtained from levelling and the draft was derived by subtracting ice thickness from surface elevation. Negative surface elevation occurred in locations where melt ponds had formed. In (b) and (c) surface elevation and draft were calculated from ice thickness assuming isostatic balance and an ice density obtained from drill-hole measurements.

profile extending over many floes and leads or cracks in between. The floes consist of alternating level areas and pressure ridges with thick ice. The thickness distribution is defined as a probability density function g(h) of the areal fraction of ice with a certain ice thickness (Thorndike et al., 1992). The probability density function (PDF) of ice thickness g(h) is given by

$$g(h)\,dh = dA(h, h + dh)/R$$

where $dA(h, h + dh)$ is the areal fraction of a region R covered with ice of thickness between h and $(h + dh)$. In practice, g(h) is derived by dividing a frequency histogram of ice thickness data by the bin-width (dh). Thus, its dimension is m^{-1}.

Figure 3.3 shows the ice thickness distributions derived from the profiles in Fig. 3.2, typical of ice thickness distributions in general. The distributions are dominated by a mode representing level ice thickness and by a long tail indicating the amount and thickness of pressure ridges. As a consequence, there is quite some difference between the mean and the typical ice thickness mode (Table 3.1), the latter being representative for level ice.

As the profiles in Fig. 3.2a,b have been measured on single ice floes, there is no thin ice or open water fraction present in the data. The presence of open water adds a peak or delta function at h = 0 m (Fig. 3.3b). In the airborne profile there is also another local maximum of 1.1 m, representative of first-year ice floes within the matrix of second-year floes. More thickness distributions, containing thin ice and open water as well will be shown in later figures.

Depending on the degree of deformation, pressure ridges can contribute as much as 30–80% to the total ice volume of a floe or ice field. Therefore, there have been extensive efforts to statistically describe the occurrence and thickness of ridges.

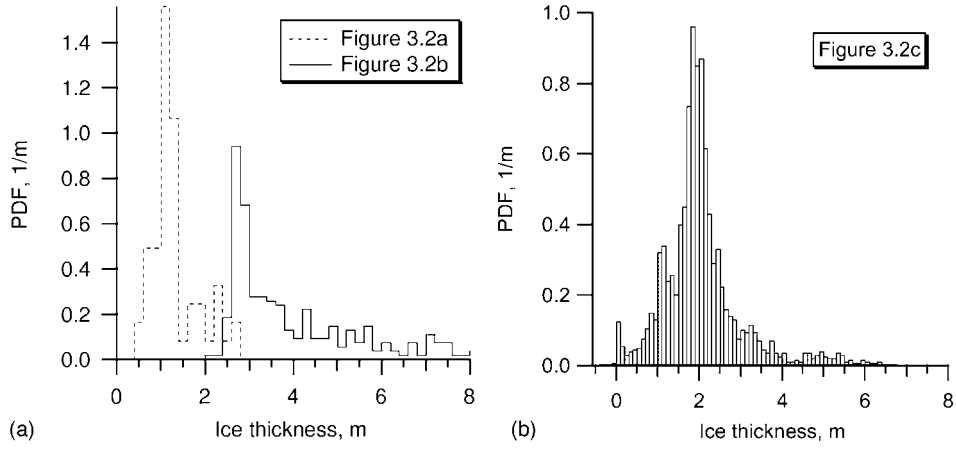

Fig. 3.3 Ice thickness distributions (given as probability density functions – PDFs) of the profiles in Fig. 3.2.

Table 3.1 Mean and modal ice thickness of profiles in Fig. 3.2.

	Mean ± SD	Mode
Fig. 3.2a	1.3 ± 0.5 m	1.1 m
Fig. 3.2b	4.3 ± 1.9 m	2.7 m
Fig. 3.2c	2.1 ± 0.9 m	1.9 m

After identifying ridges by means of certain criteria from a thickness profile, not only the thickness distributions, but also spacing distributions, can be calculated. Interestingly, the tails of both thickness and spacing distributions behave systematically, and can be well described by means of exponential or log-normal functions such as:

$$\mathrm{n}(h) = A \exp(-Bh)$$

where $\mathrm{n}(h)$ is the thickness or spacing distribution and A and B are coefficients derived from the mean thicknesses and spacings (e.g. Wadhams, 1994). However, it should be noted that there is some dispute as to which statistical function really fits best (Wadhams, 1994). Fortunately, this seems to be of little practical importance.

Modelling changes of the ice thickness distribution

As mentioned earlier, understanding and predicting the ice thickness distribution requires consideration of both thermodynamic as well as dynamic processes (Fig. 3.1). The temporal development of the ice thickness distribution $\partial g/\partial t$ can be written as

$$\partial g/\partial t = -\partial(fg)/\partial h + \mathrm{div}(\boldsymbol{v}g) + \Phi \qquad \text{(Equation 3.1)}$$

Three terms contribute to this equation (Fig. 3.4): $f(h,\boldsymbol{x},t) = \mathrm{d}h/\mathrm{d}t$ is the thermodynamic growth or melt rate of ice of thickness h at a location $\boldsymbol{x}$ and time t. $\boldsymbol{v}$ is the ice velocity vector, and Φ is the so-called redistribution function.

Thermodynamics

The thermodynamic growth term of Equation 3.1 has been described in detail in Chapter 2 by Eicken. It should be noted again, however, that it is dependent on ice thickness itself, i.e. that thin ice grows faster due to steeper temperature gradients. On the other hand, thermodynamic growth implies that thick ice exceeding a certain equilibrium thickness (e.g. pressure ridges) will melt, even in winter, if the oceanic heat flux exceeds the (generally low) heat flow through thick, insulating ice. The presence of snow, which by its low density has only about one third of the heat conductivity of ice, reduces ice growth and the equilibrium thickness.

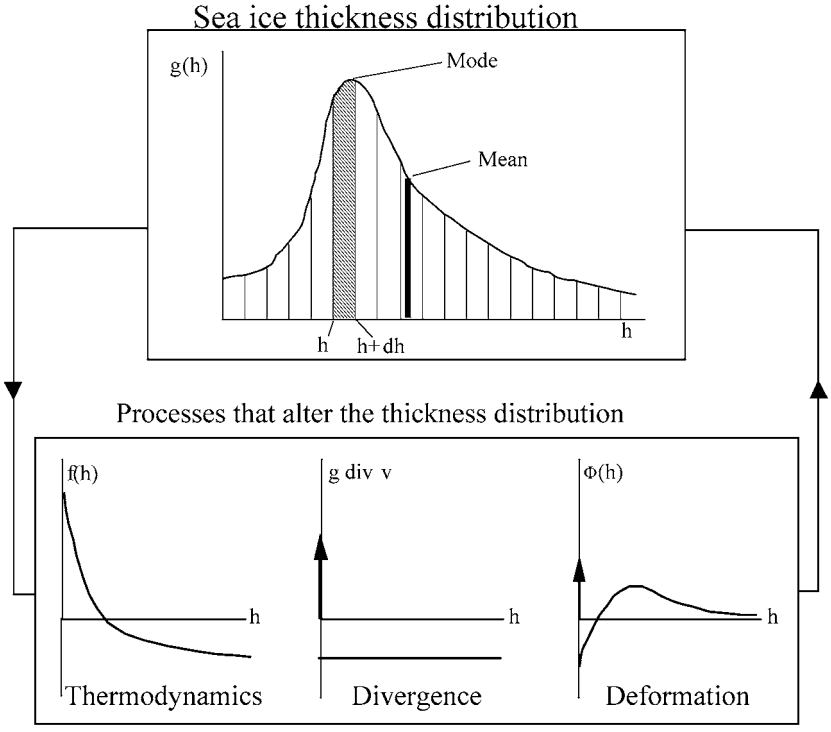

Fig. 3.4 Illustration of the contribution of the different terms and processes in Equation 3.1 to the ice thickness distribution.

Divergence and advection

The second term in Equation 3.1 represents ice divergence and advection due to ice motion. As mentioned earlier, the ice is subject to external forces, mainly due to wind and current action (see below for a quantitative description of the ice momentum balance). These forces cause the ice to drift. Away from the coast or other obstacles, the ice will drift freely, and drift direction and speed are closely related to the geostrophic wind. By comparing the motion of drifting buoys deployed on ice floes with geostrophic wind fields, it has been shown that ice in the Arctic drifts at 1% of the mean wind speed, and with an angle of 18° to the right (Colony & Thorndike, 1984; Serreze et al., 1989). For the Weddell Sea, these numbers are 1.6% and 10–15° to the left, respectively (Kottmeier et al., 1992).

Divergence within the ice generates cracks, leads, or polynyas with open water where new ice will form. Thus, for a certain location divergence removes ice of finite thickness and causes a delta signal at zero thickness (Fig. 3.4).

Deformation/convergence

The last term in Equation 3.1 is the redistribution function describing how thin ice is deformed and transformed into thicker ice classes in the case of ice convergence and deformation. It is the most critical term to realistically model the development of the thickness distribution. It is also the most unknown term, since it depends very much on fracture mechanics, and is very dependent on factors like small-scale ice properties, friction between ice blocks among each other as well as at the snow and ice interfaces, and deformation energy and lengths. A very promising approach to ridge formation modelling has been presented by Hopkins (1994) using a dynamic ridge growth model, where the fate of single ice blocks was computed as a function of external forces. However, generally thin ice will deform more easily than thick ice.

On a regional scale, the large-scale spatial thickness distribution is obtained by solving a momentum balance equation considering the main forces acting on a unit area of the sea ice cover:

$$M\,a = \tau_a + \tau_{\mathrm{w}} + F_{\mathrm{C}} + F_{\mathrm{i}} + F_{\mathrm{t}}, \qquad \text{(Equation 3.2)}$$

where the force of mass M times the acceleration a balances sum of the air and water drags τ_a and τ_w, the Coriolis force F_C, internal ice forces F_{i}, and of the force due to sea surface tilt F_{t}. Usually, the first two terms are most dominant by more than an order of magnitude. For every model grid cell, mean ice thickness is derived by solving Equation 3.2 for ice motion, and distributing the ice volume drifted into a cell equally over the cell area assuming mass conservation. Clearly, as with the redistribution term in Equation 3.1, ice strength and rheology are of great importance here. The first models involving plastic or viscous-plastic rheologies were developed by Hibler (1979) and Coon (1980). The rheology describes a viscous flow of an ice field, with plastic deformation once ice concentration and internal ice forces exceed a certain threshold. While these first models prescribed the atmospheric and oceanic forces acting on the ice, today complex coupled atmosphere–ice–ocean models exist (Gerdes & Koeberle, 1999; cf. Plate 3.1; Zhang et al., 2000; Timmermann et al., 2002).

Melting

Melting commences once the surface energy budget becomes positive. The excess energy is consumed by the latent heat of fusion needed for melting (Eicken, Chapter 2). Thus, the thermodynamic term in Equation 3.1 (thickness balance) just becomes negative.

A meteorological consequence is, for example, that even in summer, air temperatures hardly become positive over ice surfaces. At first sight, and on large scales, melting patterns correspond to the large-scale meteorological conditions and

to ocean heat flux regimes. However, even more than with freezing (see above), on small scales melt rates depend critically on the ice thickness distribution itself, and are different for different thickness classes and ice types. The heat flux through pressure ridges is lower than through level ice because of their greater thickness. Consequently they would melt faster. As their keels protrude far down into the water, they might even reach into warmer water. More importantly, ridge keels contribute to the roughness of the ice underside, thereby increasing upward turbulent fluxes of heat. The flanks of ridge sails are exposed more normally to the incident solar radiation than ridge crests, as solar elevation is low in polar regions. Therefore, melting can be expected to be higher on the flanks. Although the variations of melt rates might seem to be rather small, they can contribute to significantly different thickness changes in the course of the ablation season.

Much stronger differences in melt rates exist on small thickness classes, i.e. on level ice. Snow and ice melt water primarily accumulates at topographic low points to form melt ponds. Even small amounts of snow wetting, and the formation of melt ponds, significantly reduces surface albedo. Typical surface albedos are 0.8 for snow, 0.6 for bare ice and 0.15–0.3 for melt ponds. Thus, once formed, melt ponds absorb more energy than the neighbouring snow or bare ice, thereby increasing local melt rates. This positive feedback causes significant changes to the ice thickness distribution of level ice, and contributes to an increase in surface roughness. This is also demonstrated in the thickness profile shown in Fig. 3.2a, where the surface of melt ponds has fallen down to sea level, and the vertical pond walls reach deep into the floe.

The discussion in this section shows that many factors are responsible for shaping the ice thickness distribution. Thinning, for instance, can result from melting, but also from advection of thinner ice into a certain region. Therefore, any interpretation or forecast of changes of the ice thickness distribution in terms of climate change has to take into account both thermodynamic and dynamic processes. This will be highlighted later with the discussion of observations of interannual and decadal variations (Section 3.4).

Global sea ice thickness distributions

Plate 3.1 shows maps of mean ice drift and thickness in the Arctic and Southern Ocean, as derived from two coupled ice–ocean models operated at the Alfred Wegener Institute (North Atlantic Ocean Sea Ice Model [NAOSIM], Gerdes & Koeberle, 1999; and the Bremerhaven Regional Ice–Ocean Simulations [BRIOS], Timmermann et al., 2002). Both models have a three-dimensional multi-layer ocean model coupled to a dynamic–thermodynamic sea ice model with a viscous-plastic rheology (Hibler, 1979; see above).

It becomes immediately obvious that Arctic sea ice is generally thicker than its counterpart in the Southern Ocean. Whereas the bulk of Arctic ice is thicker than 2 m, hardly any ice grows as thick in the Southern Ocean. The hemispheric contrasts

are due to at least five main differences in the thermodynamic and dynamic conditions of ice growth:

(1) *Ocean heat flux:* One fundamental difference between the Arctic and Southern Oceans is the occurrence of a fresh mixed layer in the Arctic overlying a strong pycnocline. This layer is fed by the inflow of fresh water from large rivers, mainly from the Siberian continent. The fresh mixed layer is very stable and prohibits any significant heat fluxes from the much warmer Atlantic water underneath. An average value for the heat flux is $4\,W\,m^{-2}$. The 'Atlantic layer' at a depth of 200–300 m is 1–2°C warm. This heat would be sufficient to melt all ice during summer (Barry et al., 1993). In the Southern Ocean, no rivers enter the seas, so that the mixed layer is much saltier and not well stratified. Mean ocean heat fluxes amount to about $40\,W\,m^{-2}$.

(2) *Snow thickness:* With a thermal conductivity between 0.1 and $0.3\,W\,m^{-1}\,K^{-1}$ (Massom et al., 2001) snow is a strong thermal insulator. Therefore, ice with a thick snow cover grows slower than if the snow were thin. The Arctic Ocean is surrounded by large continents and mean snow thickness reaches only about 0.3 m in spring (Warren et al., 1999). In contrast, Antarctic sea ice is usually covered by thick snow. On perennial ice in the Pacific sector or in the western Weddell Sea mean snow thickness can be thicker than 0.5 m (Massom et al., 2001). This is due to the fact that the sea ice areas are completely surrounded by oceans, which provide a permanent moisture source. As a consequence of the thick snow and high ocean heat fluxes, Antarctic ice may melt at its underside even during winter, because the temperature gradients through the ice are only small.

(3) *Ice age:* Most ice in the Arctic Ocean drifts for 3–6 years (Colony & Thorndike, 1984) until it leaves the Basin through the Fram Strait where it melts further south. The older an ice field becomes, the more deformation events it will experience, where it thickens by the accumulation of pressure ridges. This dynamic thickening is accompanied by passing through several winters where the ice can also thicken by thermodynamic growth until it reaches an equilibrium thickness. In contrast, most Antarctic ice melts during summer. Thus, it seldom becomes older than 1 year.

(4) *Divergence versus convergence:* As mentioned above, the Arctic Ocean is surrounded by continents, and thus ice motion is confined by coasts where the ice converges and thickens by deformation. In contrast, ice drift around Antarctica is mostly divergent (Kottmeier et al., 1992) with a drift component towards the open seas. Divergence causes the opening of leads, and the addition of thin new ice to the thickness distribution.

(5) *Latitude:* Most of the ice in the Arctic is at latitudes north of 70°N, whereas in the southern hemisphere most ice extends into much lower latitudes, as far north as 60°S. Thus, air temperatures, total incoming solar radiation, and the length of the summer season, are generally lower in the Arctic than in the

Southern Ocean. However, the Antarctic ice sheet is a giant cold reservoir, and the sea ice region is well isolated from lower latitudes by the Circumantarctic Current so that warm and moist air advection are not as important as they are for the Arctic. There, despite its high latitude, strong surface melting occurs in summer even at the North Pole.

It should be noted that the order of these points is arbitrary and does not include any ranking between the most important and less important factors. The final ice thickness depends on the magnitude of, and interrelation between, these different aspects. Clearly, both dynamic and thermodynamic factors are responsible for the hemispheric differences. The importance of ice dynamics is highlighted by looking at the regional thickness differences of each hemisphere itself.

As 30–80% of the volume of an ice field is contained within pressure ridges, the mean thickness of a region is more dependent on the number and thickness of ridges than on the thickness of level ice. In other words, for the overall ice volume within a certain region, dynamics is more important than thermodynamics. Therefore, on a regional scale the average ice thickness distribution is determined by the prevailing atmospheric circulation regimes, which are responsible for mean ice motion and the dominant drift directions. Where the ice drifts against, or shears along a coast, there will be strong ice pressure, and the ice will become heavily deformed. As a result, the mean thickness in regions with mean drift convergence is larger than in regions with mean divergence, where thin new ice is permanently generated and exported.

The arrows in Plate 3.1 show the dominant drift patterns which develop as the result of the prevailing atmospheric circulation. Although the ice motion is presented only for winter in the plate, this is also representative for the average annual conditions. In the Arctic, mainly two drift systems exist. The Beaufort Gyre is an anticyclonic gyre in the Canada Basin north of the Canadian Archipelago and Alaska. It is caused by quasi-permanent high atmospheric pressure over the Beaufort Sea. The Beaufort Gyre can transport ice floes for a couple of years before they are exported into the Transpolar Drift. This is the other prominent drift system, which transports ice from the source regions on the Siberian Shelves within about 3 years across the North Pole into the Fram Strait and the East Greenland Current, where it finally melts. The Transpolar Drift is mainly driven by low pressure systems passing from the North Atlantic into the Barents and Kara Seas.

On average, these drift patterns push the ice against the coasts of northern Greenland and the Canadian Archipelago. Consequently, as a result of strong convergence and deformation, the thickest ice is found in these regions. Mean maximum thicknesses range between 6 and 8 m, mainly resulting from the large spatial density of ridges. Another region with predominantly convergent conditions can be in the East Siberian and Chukchi Seas. If the Beaufort Gyre is very strongly developed, ice is pushed against the coast of the New Siberian Islands.

The youngest and thinnest ice is found along the Siberian Shelf, from where it is permanently exported into the Transpolar Drift. Mean thicknesses in the Laptev

Sea range between 2 and 3 m in winter. The modelled Arctic Ocean thickness distribution is in good agreement with submarine sonar measurements collected over many years (Bourke & McLaren, 1992).

Plate 3.1 shows that the thickest ice in Antarctica occurs close to the continent, in accordance with the greatest age and latitude, and with the vicinity to the coast where it is sporadically compressed. The most prominent feature, however, is the thickest ice in the southern and western Weddell Sea. On the one hand, this is one of a few regions possessing perennial ice. On the other hand, it is a region where ice drift is directed towards the coast, and subsequently much deformation occurs. The so-called Weddell Gyre is caused by low average sea level pressure over the central Weddell Sea. It should be noted that both the Beaufort Gyre and the Weddell Gyre rotate clockwise. However, due to the Coriolis force on the northern hemisphere this results in ice convergence within the gyre centre, whereas in the south clockwise circulation results in net divergence inside the gyre. The great thickness in the western Weddell Sea is therefore caused by ice motion away from the divergent gyre centre, with the Antarctic Peninsula acting as an obstacle for the ice drift.

In contrast to the Arctic, regional ice thickness distributions in the Antarctic are less well known, because only few systematic measurements have been performed. The use of military nuclear submarines is prohibited by the Antarctic Treaty. Therefore, the accuracy of the model results in the map of Plate 3.1 is not really known. There is some evidence that at least in some years ice thicknesses in the Bellingshausen and Amundsen Seas, as well as in the Weddell Sea, can be much higher than shown on the map (Haas, 1998; Strass & Fahrbach, 1998).

It should be noted that the drift systems and thickness distributions shown in Plate 3.1 represent long-term average conditions. There is large seasonal, interannual and decadal variability superimposed on these mean patterns, which will be highlighted later in Section 3.4. For example, during June, July and August, the circulation is often reversed in the central Arctic. This is due to the development of an intensive low sea-level pressure area in this region during summer.

3.3 Measurement techniques

While extent and concentration of sea ice can be measured with sufficient accuracy by satellites from space, determining its thickness is much more involved, even from aircraft or while standing on the ice. This is due to its relative thinness, which is a challenge for any geophysical measurement technique. Therefore, most methods are indirect measurements, which derive thickness from a related variable which is actually measured instead.

The traditional direct method of ice thickness measurement is drilling a hole into the ice by a gas-driven motor. The thickness is measured with a ruler lowered into the hole. Although drilling is tedious, and only limited data can be gathered in a short time, most thickness information about the relatively thin Antarctic sea ice

still comes from drill-hole measurements (Lange & Eicken, 1991; Worby et al., 1996). Only recently have moored upward looking sonars (ULS) and electromagnetic (EM) methods (see below) been applied in Antarctica.

There are also a number of studies involving video recording of ice floes broken by an ice-breaker. The broken ice fragments are often moved side-up against the ship's hull, revealing their cross profile. From the video footage the thickness can then be manually retrieved. Some studies have shown reasonable agreement of level ice thickness estimates compared with data derived from other methods (Lensu & Haas, 1998). Similarly, ice thickness can be determined just visually while ice breaking.

Other direct thickness measurements would be pulse radar or ultrasonic sounding where the travel time of a signal through the ice is measured. For sufficient resolution and accuracy, the small thickness requires short wavelengths of only some decimetres of the respective signals. However, these high frequency signals suffer from the heterogenity of sea ice due to salt inclusions, fractures and rafted ice blocks. These lead to strong signal scatter on the one hand, and to highly variable signal propagation velocities which must be known to calculate thickness from travel time.

Submarine and moored upward looking sonars

So far, most thickness data have been acquired by means of upward looking sonars (ULSs) mounted either on military nuclear submarines or on oceanographic moorings. These instruments measure the travel time, t, of a sonar pulse transmitted by the ULS and reflected back from the ice bottom (Fig. 3.5). Additionally, the depth of the sonar beneath the water level, z, and the sound velocity, v, in the water must be known. Then, ice draft, d, is calculated according to

$$d = z - v * t/2$$

The depth of the ULS is derived from pressure sensors, whose signals are also dependent on air pressure. The sound velocity profile is either assumed constant with a certain sound speed, or taken from a mixed layer model (Strass & Fahrbach, 1998). This can become quite complicated in the case of strong water stratification or when the measurements are performed close to ocean frontal zones. A plausibility test for the depth measurement or the sound velocity profile can be performed when profiling open leads with ice thickness zero. Then, the measured sonar distance must equal the ULS depth.

Ice thickness, h, is calculated from draft, d, by assuming isostatic equilibrium, a certain snow depth, z_s, and water, ice and snow densities ρ_w, ρ_i and ρ_s:

$$h = (\rho_w d - \rho_s z_s)/\rho_i \qquad \text{(Equation 3.3)}$$

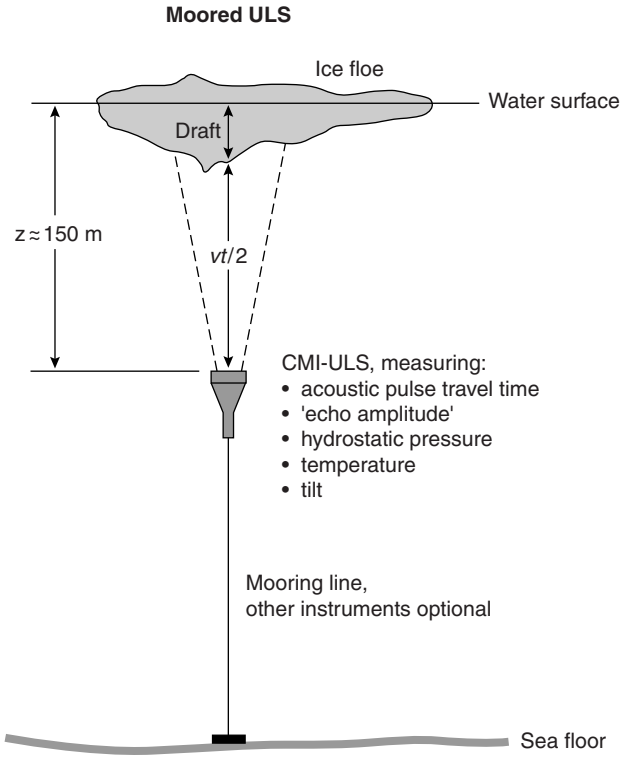

Fig. 3.5 Illustration of upward looking sonar (ULS) ice thickness measurements from an oceanographic mooring. Adapted from Strass & Fahrbach (1998).

The values for ice and snow density, as well as snow depth, are reasonably well known so that only small errors arise for h.

Due to the problems of assuming the correct sound velocity profiles and ULS depth, the accuracy of absolute level ice thickness measurements could be rather poor and might not be better than 0.5 m. However, an ULS is very sensitive to pressure ridge keels, and their depth relative to the level ice bottom can be reasonably well determined.

Submarines allow for long-range, basin-scale transects for determining the ice thickness profile. However, so far, submarine surveys have only been performed in conjunction with military cruises. This means they provide only snapshots of the ice thickness distribution, because the transects are not performed in a systematic manner. As a consequence, measurements often have to be corrected for seasonal variability before they can be compared with each other. Some improvement was achieved in the 1990s with the SCICEX missions, the Scientific Ice Expeditions of the US navy. These cruises were dedicated to meeting scientific goals, and a small number of scientists were allowed onboard the submarines. Meanwhile, Autonomous Underwater Vehicles (AUVs) are being developed, and they may provide an

alternative for the use of submarines in the near future. They can also be used in Antarctica, where the operation of military, nuclear submarines is prohibited by the Antarctic Treaty.

ULSs mounted on oceanographic moorings provide long time-series of ice thickness in a single location. These allow the temporal development of the ice thickness distribution to be studied, e.g. in the course of the growing season (Melling & Riedel, 1995). Transects can be achieved with several moorings across a certain region, e.g. the Fram Strait (Vinje et al., 1997) or the Weddell Sea (Strass & Fahrbach, 1998; Harms et al., 2001). The thickness distribution between single moorings can then be interpolated. Combined with ice drift velocity data retrieved from satellite imagery or buoys, mooring data allow for the calculation of ice volume fluxes, Q, according to

$$Q = v\,h$$

where v is ice velocity and h ice thickness.

While moored ULS can provide very valuable continuous data, the operation of the instruments at water depths of 50–150 m for periods of one, or more, years is still a technological challenge. Similarly, the recovery of the instruments is often difficult. As a result, the success rate of moored ULS measurements is only about 70%. Moorings cannot be deployed in shallow waters, where they might be destroyed by ridge keels or icebergs.

Electromagnetic induction sounding

In contrast to high-frequency electromagnetic (EM) techniques employing radar frequencies, low-frequency, frequency-domain electromagnetic induction (EMI) sounding has become a widely applied method. Typical operating frequencies are between 10 and 100 kHz. The technique is usually employed in geophysical problems related to the mapping of ore or groundwater deposits on land. With EM sounding, the mean or apparent electrical underground conductivity is determined. Sea ice is almost an electrical insulator with low electrical conductivities between 0 and 50 mS m^{-1} (milli-siemens per metre). In contrast, cold sea water with a salinity of 32 has a conductivity of 2500 mS m^{-1}. Consequently, the apparent conductivity of the underground decreases with increasing ice thickness, i.e. the more ice occupies the half-space underneath the EM instrument.

The sub-surface apparent conductivity is measured by means of two coils, one transmitter and one receiver coil (Fig. 3.6). The transmitter generates a primary EM field which induces eddy currents in the underground. As induction is dependent on the conductivity of the layer, the eddy currents are mainly induced in the sea water just below the ice bottom. These eddy currents in turn generate a secondary EM field, whose strength and phase is measured with the receiver coil. The secondary field strength and phase are dependent on the underground conductivity, or, in

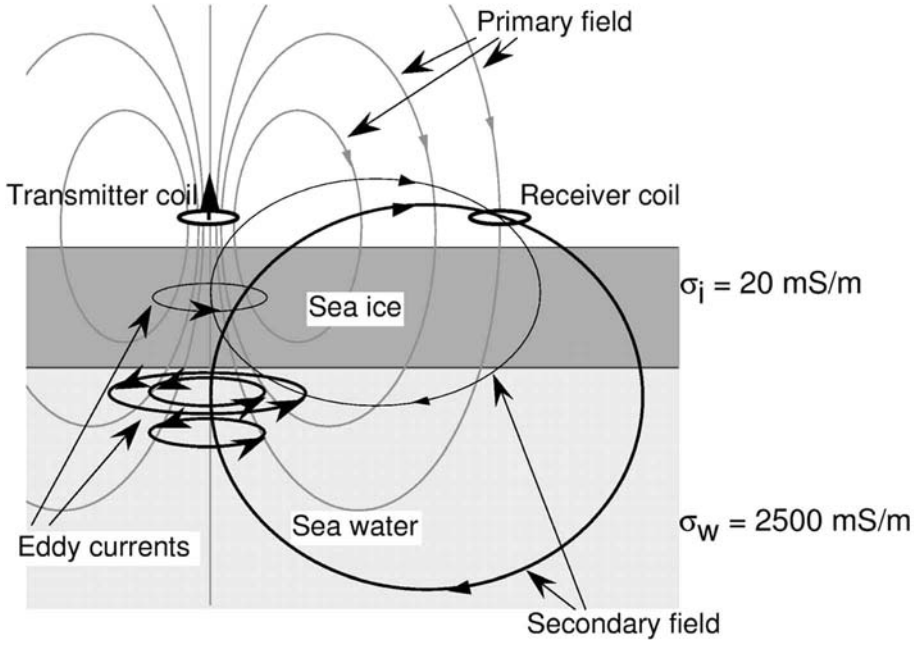

Fig. 3.6 Principle of electromagnetic (EM) ice thickness sounding, showing the generation of a primary field by a transmitter coil and induction of a secondary field, whose strength and phase are measured by a receiver coil.

other words, on the distance between the eddy currents at the water surface and the coils. This distance is equivalent to ice thickness, if the instrument is lying on the ice. Apparent conductivity is calculated from the imaginary part of the secondary field. Comparison with drill-hole measurements yielded the empirical equation

$$h = 7.81 - 1.09 \ln(\sigma_a - 62.5) \qquad \text{(Equation 3.4)}$$

for the calculation of ice thickness h from apparent conductivity σ_a using a Geonics EM-31 (Haas et al., 1997). This instrument is most widely used for sea ice thickness measurements and has a coil spacing of 3.66 m with an operating frequency of 9.8 kHz. For instruments with other frequencies and coil spacings, different equations would have to be developed. The equations can also be derived by numerical EM forward modelling, computing the EM response to a layered half-space. More involved equations can be calculated from two- or three-dimensional EM models, which can also represent pressure ridges.

Figure 3.2a,b has already shown two examples of ground-based EM profiles obtained by pulling a sledge with an EM instrument installed on it over the ice. Comparison with drill-hole measurements reveals a good agreement within $\pm$ 0.1 m over level ice. As the induced eddy currents possess a finite lateral extent, ice thickness is averaged over a certain area, called the 'footprint'. As a rule of thumb,

the footprint diameter approximately equals the distance between the EM sensor and the water surface. Consequently, EM measurements underestimate the maximum thickness of deformed ice such as ridge keels, because the signal is also affected by the occurrence of eddy currents induced in the water next to laterally confined deformed ice structures. Over pressure ridges, the accuracy of EM sounding can be rather bad, and thickness estimates might be too low by up to 30%.

EM measurements are hardly affected by seasonally varying ice properties, because these do not affect ice conductivity very much (Haas et al., 1997). However, in Antarctica, seawater saturated and saline gap layers can occur close to the surface, leading to underestimates of ice thickness by EM sounding if they are not detected (Haas, 1998).

An advantage of the EM technique is that it can be applied also from above the ice without any ground contact. As the EM measurement is essentially equivalent to determining the distance between the EM sensor and the water surface or ice underside, ice thickness is obtained by subtracting from it the instrument height above the ice surface. As an application of combined EM and laser measurements, EM sounding has been used continuously from onboard ice-breakers while steaming through the ice (Haas, 1998), yielding regional ice thickness distributions. Figure 3.7 shows a result of continuous ship-based measurements obtained in the Kara Sea during May 1998 using a Geonics EM-31 and a laser altimeter (Haas et al., 1999b). The characteristics of different ice regimes like thin new ice, deformed first-year ice or level fast ice, can be clearly distinguished with those data. These are:

- Coastal flaw leads along the Taimyr Peninsula with almost no or very thin ice (A).
- Convergent young ice fields off the Yenisey mouth, with modal thicknesses of about 0.8 m and a long tail of thicker deformed ice (B).
- Fast ice of Ob' Bay, uniformly distributed around thicknesses of 2 m (C).
- First-year pack ice fields in the southern Kara Sea with typical thicknesses ranging from 1 to 1.5 m (D).
- Thick, deformed ice in Kara Gate, with modal thicknesses of around 1.5 m (E).

Obviously, ship-based measurements are limited by the ice itself since ships cannot penetrate the thickest ice. More important, most ships follow the route of least resistance, which is the one with the thinnest or absent ice. Therefore, representative information on regional ice thickness distributions can only be obtained on dedicated, scientific cruises.

The ultimate goal of EM sounding is to perform systematic, large-scale surveys using aircraft. Airborne sensors have been deployed from helicopters or fixed wing aircrafts in the past (Kovacs & Holladay, 1990; Prinsenberg & Holladay, 1993; Multala et al., 1996). However, none of these systems was available for large-scale, systematic research studies. Recently, a modern, two-frequency, fully digital helicopter EM (HEM) bird was deployed from the research ice-breaker *RV Polarstern*

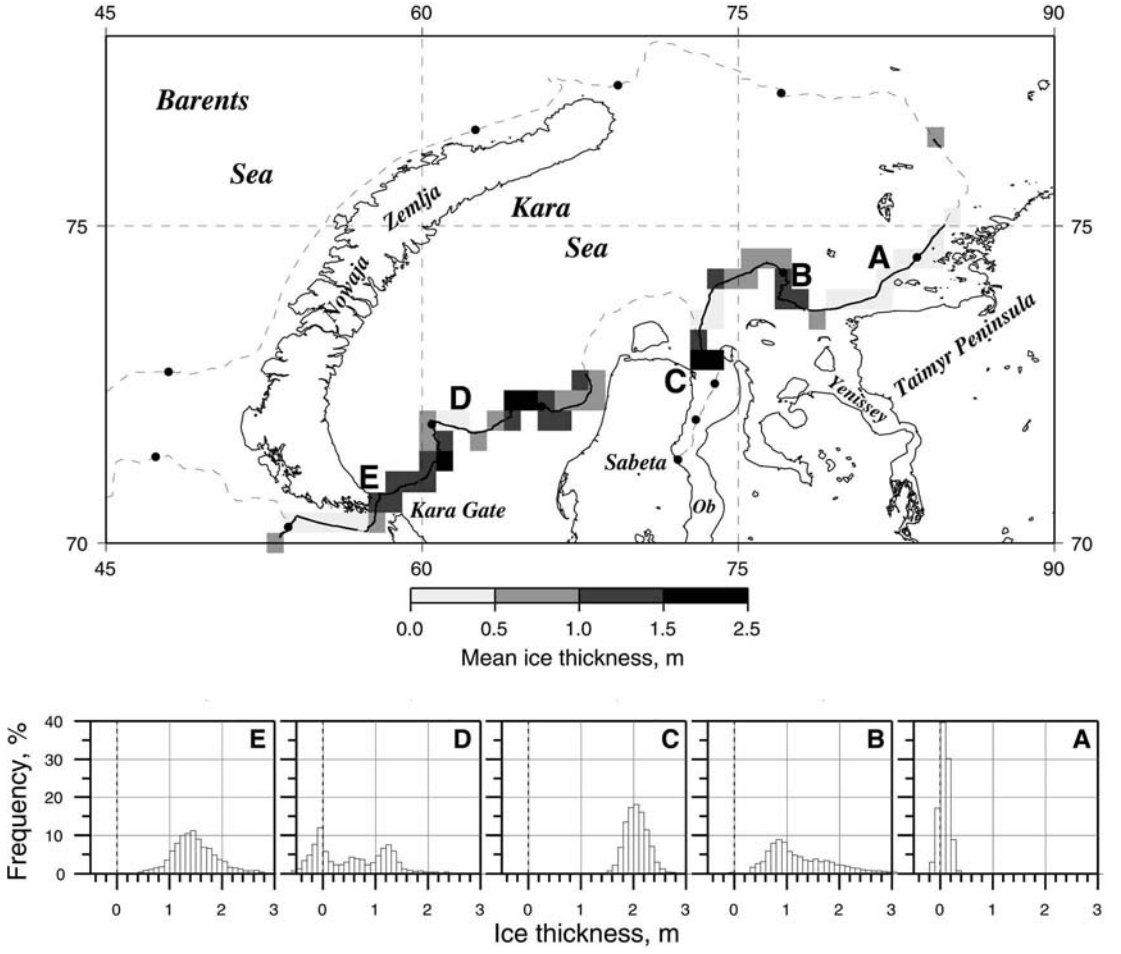

Fig. 3.7 Example of ship-based electromagnetic (EM) thickness measurements in the Kara Sea. The track of the ice-breaker is indicated by the wiggly dashed line. Circles indicate the position at 0 GMT every day. Superimposed on the track are the sections where ship-based ice thickness measurements have been performed (solid line) as well as mean ice thicknesses. Letters A–E indicate locations of typical ice conditions, for which thickness histograms are presented at the bottom. From Haas et al. (1999b).

in the Arctic. The bird was towed under a helicopter with a 20 m cable. It operates at frequencies of 3.6 and 112 kHz, and has a maximum coil spacing of 2.7 m with an overall length of 3.4 m (Fig. 3.8). Compared with common airborne systems, this is very small, but was designed to be deployed from small helicopter decks off ice-breakers. As a final step, such a small system could also be flown as a towed bird by fixed-wing aircraft.

Fig. 3.8 Photograph of Alfred Wegener Institute's fully digital helicopter electromagnetic (HEM) bird in operation in the Arctic.

As can be seen from Equation 3.4, the EM response decreases exponentially with increasing instrument height. This means that the EM response to small thickness changes along a profile decreases with height. Therefore, airborne systems must fly low and have to have very good signal-to-noise ratios to be able to resolve even small signal changes. This is particularly challenging for a system as small as the HEM bird.

In Fig. 3.2c an 8 km long section of a typical thickness profile obtained with the HEM bird was shown. The bird was flown at an altitude of 15 m above the ice surface. For plotting the profile, isostatic equilibrium and an ice thickness of

880 kg m^{-3} was assumed. Several ice floes with thicknesses of about 2 m can be clearly distinguished, with pressure ridges up to 6 m thick. The data have a very good signal-to-noise ratio, allowing even details of the thickness profile to be observed. With these measurements, it is possible to obtain representative thickness data along extended, linear profiles, also including open water, thin ice and rubble fields.

As a by-product of ship-based and airborne measurements, the surface profile of the ice is obtained from the laser data. This provides information on surface roughness and the calculation of pressure ridge statistics. The laser measurements could thus partially compensate for the lack of accuracy of EM data over pressure ridges, if relationships between the height of ridges and their overall thickness are known. At the very least, ice regimes can be described by their distinct level ice thickness and the amount of ridged ice.

If the system height above the water level is known with sufficient accuracy, ice freeboard, i.e. the height of the ice surface above the water level, could be estimated from the ice data. Freeboard itself is related to ice thickness by the same assumptions of isostatic equilibrium as with the submarine measurements of ice draft (similar to Equation 3.3). However, as freeboard is just 10–20% of total ice thickness, high accuracy in the freeboard estimate is required. This can be achieved if the aircraft height is determined by differential GPS or inertial platforms. Independent estimates of ice freeboard will become quite important with respect to the validation of future satellite radar altimeter missions (see below).

Satellite remote sensing

As mentioned above, there is so far no real operational space-borne sensor which is capable of measuring ice thickness. Most satellite sensors are imaging instruments, which provide areal information about specific surface properties rather than any information from inside the ice or its underside. Direct freeboard or thickness information is only obtainable from radar altimeters.

Among the imaging sensors are active and passive microwave sensors such as radiometers or radar scatterometers (Comiso, Chapter 4). Their signals are sensitive to the microwave emissivity, absorption and scattering properties of the ice surface. These properties are mainly dependent on the ice and snow salinity and small-scale surface roughness. As shown by Eicken in Chapter 2, large changes of surface salinity occur in first-year ice once it experiences its first melting season. The salt drains into deeper layers or is flushed by melt water. The pores widen considerably and brine is replaced by air. Therefore, second- and multi-year ice are characterized by lower microwave emissivities and higher radar backscatter coefficients than first-year ice. Consequently, mapping of regions with low brightness temperatures or high radar backscatter can provide estimates on the relative amount of thick multi-year and thin first-year ice. However, this technique is not sufficiently developed to yield quantitative thickness information or thickness distributions.

New possibilities have arisen with the advent of imaging Synthetic Aperture

Radars (SAR), flown aboard the European satellites ERS-1&2 and ENVISAT, and on the Canadian RADARSAT. These SAR antennas point to the earth's surface with viewing angles of 20–40°. These sensors provide a horizontal resolution of 12–50 m, sufficient to resolve leads and partially identify ridges or ridge zones. These features have different backscattering properties than the surrounding ice. Leads are covered by open water or thin new ice, which is rapidly thickening. Leads may be recognizable by their linear extended shape, and the salty ice is easily distinguished by its lower backscatter compared with the surrounding older ice. If there are frost flowers covering it, leads would be much brighter that the surrounding ice. Kwok et al. (1999) have developed a processing scheme allowing for tracking leads in successive SAR images and computing their thickness distribution by means of a thermodynamic model. The processor can also compute the thickening of the new ice by deformation if leads close under convergent drift conditions. The overall thickness distribution, including thick floes, is difficult to obtain though.

Ridge sails consist of piled ice blocks with arbitrarily tilted side walls. These provide a number of interfaces pointing normally to the incident radar signal. Thus, backscatter is higher than from the surrounding level ice. Ridge backscatter can also be increased by increased volume scattering, as aged ridge blocks become very weathered and porous. Therefore, single large ridges can be seen in SAR images. However, smaller ridges also contribute to the mean backscatter of a certain image pixel. By looking at the backscatter distribution of certain areas, the amounts of ridges can therefore be retrieved (Haas et al., 1999a). The number of ridges and the degree of deformation are relative measures for ice thickness.

Radar altimeters measure the height of the satellite above the earth's surface. As satellite orbital heights can be considered constant, the difference between measurements over ice and over water provides information about ice freeboard (Fig. 3.9). According to Equation 3.3, this can be transformed into ice thickness. Radar altimeters provide only regionally averaged thickness information. The typical footprint size is between 1 and 6 km, depending on surface roughness. However, this resolution is sufficient to resolve different ice regimes. As the freeboard is derived by comparing measurements over ice with measurements over water, particular problems result from the fact that the open water areas inside the closed pack are mostly smaller than the footprint size. Therefore, it is difficult to obtain clear water signals from inside the ice-covered regions.

A completely new approach is therefore the design of a Synthetic Interferometric Aperture Radar Altimeter (SIRAL) for the CryoSat-Mission. CryoSat is a European satellite dedicated to sea ice thickness and ice sheet topography measurements. Its goal is the observation of ice thickness trends with respect to climatic changes. With the SAR processing, echoes are coherently processed along-track to form very narrow across-track strips, which reduces the footprint size to 250 m (Fig. 3.9). This allows for much better differentiation between ice and water measurements. Consequently, freeboard retrievals from inside the pack ice areas will be significantly improved.

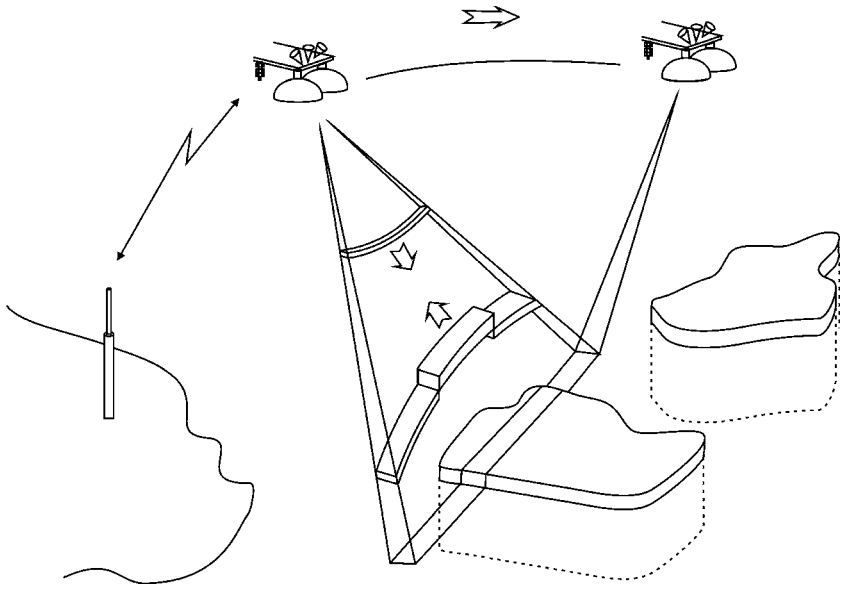

Fig. 3.9 The CryoSat 'SAR' measurement configuration.

Similarly, NASAs IceSat-Mission is equipped with a laser altimeter, which is capable of measuring ice freeboard, too, and with much higher spatial resolution (70 m) than CryoSat. However, the usage of the laser altimeter is impossible if a cloud cover exists, which is a very limiting condition for polar applications.

3.4 Ice thickness variability

Decadal thickness variability in the Arctic

As outlined above, the thickness distributions shown in Plate 3.1 represent 9-year average fields. Although average conditions over even longer time periods look similar (Bourke & McLaren, 1992), on time scales of years and decades the thickness distribution shows large interannual and decadal variability, and longer-term trends. Most spectacular observations of changes of the Arctic ice cover have been published by Rothrock et al. (1999). They compared submarine sonar data obtained in 28 regions of the Arctic Ocean during the period 1958–76 with those gathered in the same regions between 1993 and 1997. In all regions a decrease in the mean draft was observed (Fig. 3.10). On average, there was a 1.3 m decrease from a mean draft of 3.1 m in the earlier period to a mean draft of 1.8 m in the 1990s, equivalent to a reduction of 42% of ice thickness. The thinning was most pronounced in the Siberian Arctic and Nansen Basin, where the average decrease of draft was 1.8 m. Although their results indicated a continued thinning in some regions during the

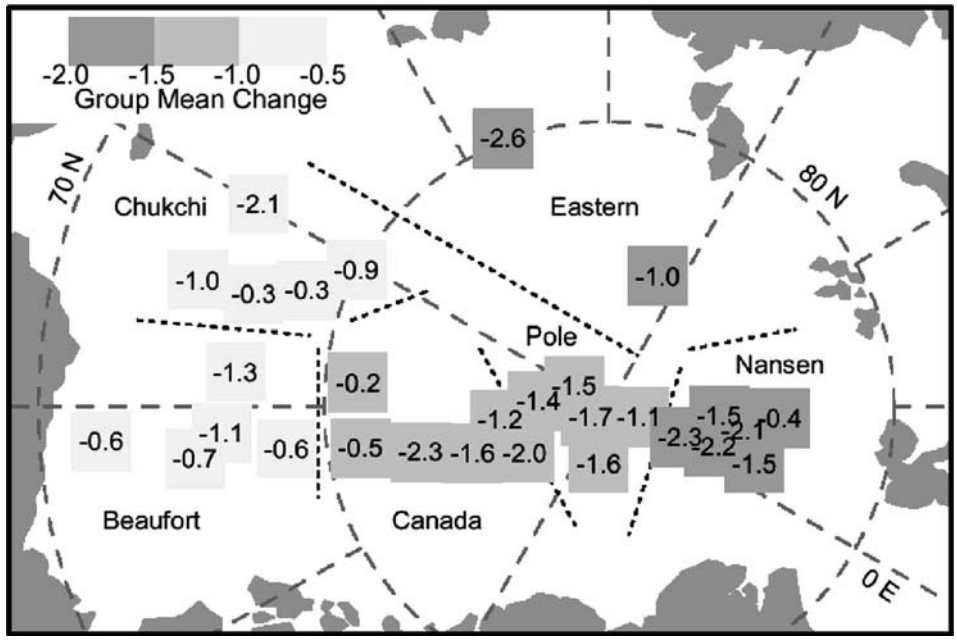

Fig. 3.10 Map of the Arctic showing the regions of coincident submarine tracks in 1958–76 and 1993–97. Numbers indicate the ice thickness difference between the two periods. From Rothrock et al. (1999).

1990s, the study essentially only compared two distinct periods (1958–76 and 1993–97) with each other. Therefore it is unclear if the results are an indication of a trend or just represent two arbitrary samples of a varying parameter.

Figure 3.11 shows the mean annual ice volume in the Arctic from 1951 to 1999 as retrieved from a dynamic–thermodynamic sea ice model (Hilmer & Lemke, 2000). The figure clearly shows that there are large decadal ice volume fluctuations of as much as $4 \times 10^3\,\mathrm{km}^3$ around a mean volume of $30.2 \times 10^3\,\mathrm{km}^3$. The data in fact show a marked thinning of about 20% between the 1960s and the 1990s, i.e. the period covered by Rothrock et al. (1999). However, for the complete model period, only a small decrease of ice volume of -4% per decade was computed. The model results indicate that this decrease is unevenly distributed over different regions of the Arctic. The largest decrease was obtained from the East Siberian Sea and central Arctic, whereas the regions north off the Canadian Archipelago showed slightly increasing ice thicknesses.

Tucker et al. (2001) compared complementary submarine draft measurements performed between off Alaska and the North Pole between 1985 and 1988 with data from the same transects obtained in 1992–94. During this short period mean ice drafts decreased by 1.5 m. Again, it remains unclear if this represents just some variability or an actual trend. The data are in agreement with the ice volume time-series presented in Fig. 3.11. However, Tucker et al. (2001) took a step further in

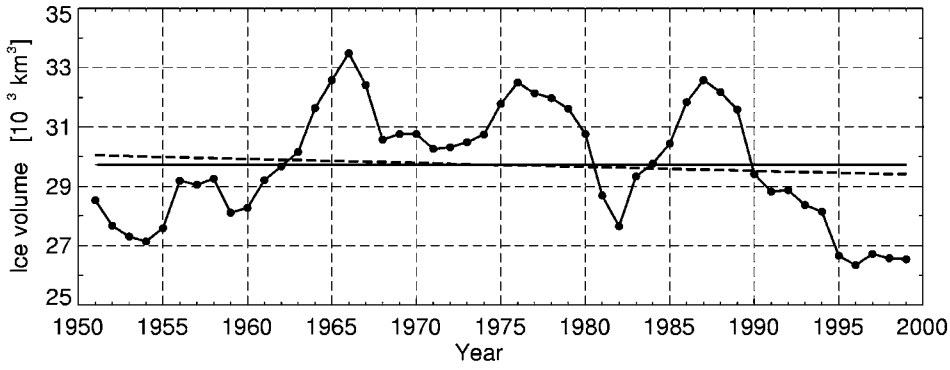

Fig. 3.11 Temporal change of Arctic ice volume 1951–99. The straight solid line indicates the mean volume of 30.2×10^3 km^3, whereas the dashed line shows a least square regression, corresponding to a decrease of -4% per decade. Updated from Hilmer & Lemke (2000).

relating their results to changes in the ice drift regime. While the Beaufort Gyre was well developed in the 1980s, it weakened considerably in the 1990s. This leads to stronger ice divergence and to less production of thick, deformed ice. The different circulation regimes also result in shorter residence times of the ice in the Canadian Basin, and therefore less time to accumulate deformed ice.

The relationship between ice thickness changes and different circulation regimes is thoroughly demonstrated by a coupled dynamic–thermodynamic ice–ocean model of Zhang et al. (2000) for the period 1979–96. This period was characterized by two distinct circulation regimes during 1979–88 and 1989–96, respectively. These different circulation regimes are characterized by high and low North Atlantic Oscillation (NAO) and Arctic Oscillation (AO) indices, parameters derived from the difference and variability of sea level pressure in the Arctic and at lower latitudes (Hurrel, 1995; Thompson & Wallace, 1998). The period 1979–88 was characterized by low NAO and AO indices, and therefore high sea level pressure over the central Arctic while the period 1989–96 was characterized by high NAO and AO indices and low sea level pressure. Figure 3.12a,b shows the mean sea level pressure contours and modelled ice velocity fields for both periods. Figure 3.12c,d shows the anomalies of ice velocity fields based on the differences between the 1979–88 and 1989–96 fields and the mean field of 1979–96, respectively. The latter period (1989–96) was characterized by smaller pressure gradients and a weaker Beaufort Gyre, which had also retreated more towards the Canadian Coast. Essentially, the anomaly fields show reversed conditions, with an anticyclonic circulation anomaly in 1979–88 and a cyclonic anomaly in 1989–96. Figure 3.13 shows the corresponding thickness anomalies, derived from the difference of the thickness fields in 1979–88 and in 1989–96. There was strong thinning in the East Siberian Sea (up to -2.5 m) and the central Arctic, whereas ice thickness increased in the Beaufort Sea and off the Canadian and Alaskan coasts. Ice volume decreased

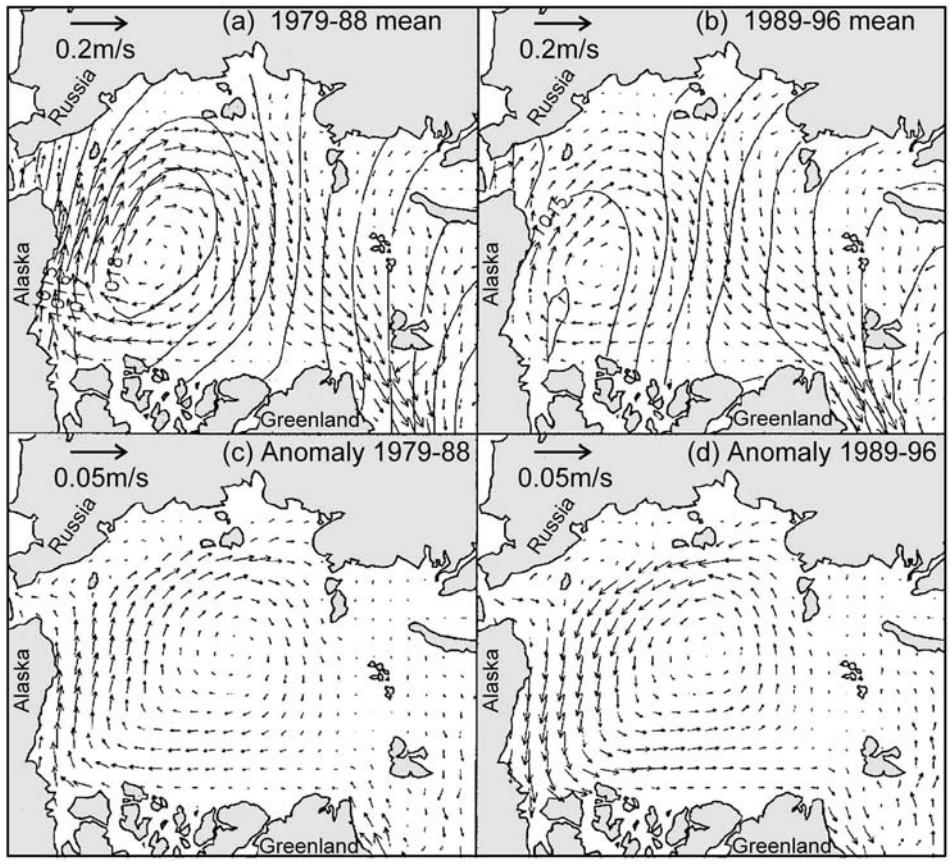

Fig. 3.12 Simulated mean ice velocity fields and annual mean sea level pressure contours for (a) 1979–88 and (b) 1989–96. Anomaly fields of ice velocity based on the differences (c) between the 1979–88 mean and the 1979–96 mean and (d) between the 1989–96 mean and the 1979–96 mean. From Zhang et al. (2000).

by 28% in the eastern Arctic and simultaneously increased by 16% in the western Arctic. Overall, in the whole Arctic it decreased by only 6% between 1979–88 and 1989–96. Note that the thickness measurements reported by Rothrock et al. (1999) and Tucker et al. (2001) were mostly in the regions of modelled thickness decrease and were consistent with the model results.

Although mean air temperatures were higher by about 1°C during 1989–96 compared with 1979–88, thermodynamic ice growth was hardly affected. Zhang et al. (2000) show that the ice volume difference to model runs using a constant thermal forcing is negligible. Thus, the ice thickness changes can almost exclusively be attributed to changes in the circulation regimes. This is mainly attributed to different amounts of ice exported from the western into the eastern Arctic. The study therefore shows that dynamics are far more

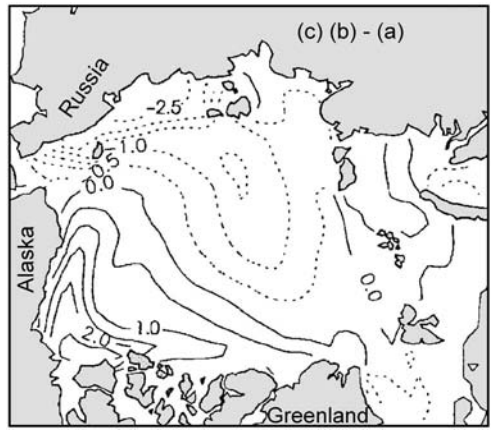

Fig. 3.13 Difference between the simulated ice thickness fields for 1979–88 and 1989–96. From Zhang et al. (2000).

important than thermodynamics in shaping the overall thickness distribution in the Arctic.

However, Zhang et al. (2000) also clearly demonstrate that thermodynamics play an important role in modifying the dynamically caused differences, both through negative and positive feedback mechanisms. The different circulation regimes also caused differences in the ice concentration fields. Between 1979–88 and 1989–96 there was a decrease of mean ice concentration in the eastern Arctic and an increase in the western Arctic, which were most pronounced during summer. The positive feedback was the higher absorption of incident solar radiation in the mixed layer due to an overall decrease of surface albedo caused by larger areas of open water. This led to enhanced lateral and bottom melting and to a later onset of freezing, consequently enhancing the thinning. However, due to the thinner ice and more open water, freezing rates during winter were also higher, and therefore ice growth increased. The net ice production remained almost constant under the different circulation regimes.

Cyclonic and anticyclonic circulation regimes were shown to follow each other with periods of 7–15 years (Proshutinsky & Johnson, 1997). Therefore it is quite likely that these also cause simultaneous long-term ice volume changes such as those shown in Fig. 3.11. This high level of dynamically caused variability makes the detection of temperature-induced climate changes very complicated.

Interannual thickness variability

Superimposed on the decadal thickness variations are large seasonal and interannual thickness variations. Only a few studies have had the opportunity to make repeated surveys in the same region over a couple of years. Among those are

moored ULS measurements, e.g. in the Weddell Sea (Strass & Fahrbach, 1998), the Beaufort Sea (Melling & Riedel, 1995) and the Fram Strait (Vinje et al., 1997). The last study showed that the ice volume flux through the Fram Strait is well explained by changes of the NAO, and thus possesses a pronounced interannual variability.

With ground-based EM thickness measurements in August and September of 1993, 1995 and 1996, Haas & Eicken (2001) demonstrated that there is large interannual variability in the Siberian and central Arctic, too. These are well explained by different atmospheric circulation regimes.

Plate 3.2 shows the location of the profiled floes for each of the three years, and the mean ice concentration during the study periods. In 1993, the western Laptev Sea was covered by much ice, whereas the ice edge of the eastern Laptev Sea had retreated far to the north. In 1995, the ice edge was the furthest north to be recorded since ice coverage has been monitored by satellites. In contrast, in 1996 almost the complete Laptev Sea remained ice covered. From the distribution of sea level pressure it can be seen that the coverage over the three years can be explained by the strength and location of the typical summer low pressure region and resulting geostrophic winds. In 1993, the low was north of the East Siberian Islands. The western Laptev Sea was dominated by northerly winds advecting ice southward, whereas over the East Siberian Sea southerly winds moved the ice edge north. In 1995, the low over the central Arctic was missing. Consequently, the annual mean drift conditions remained with a well-developed Transpolar Drift. This led to the record ice reduction in the Laptev Sea. In contrast, in 1996 a strong low pressure cell developed over the North Pole with resulting strong cyclonic circulation. This led to divergent ice drift from the central Arctic into the marginal seas including the Laptev Sea.

The thickness distributions obtained in the three summers are shown in Fig. 3.14. Buoy and satellite scatterometer data indicate that all floes were first-year ice. The thinnest ice, with a modal thickness of 1.25 m (mean 1.8 m), was observed in 1995. The ice was extensively covered with melt ponds. Figure 3.2a shows a typical profile surveyed in that year. In contrast, one year later (1996) the modal ice thickness was 1.85 m (mean 2.0 m). No melt ponds were observed on the ice, and instead an intact snow cover with a mean thickness of 0.14 m survived the summer. In 1993 ice thickness was intermediate, with a modal thickness of 1.75 m (mean 1.85 m).

The different thicknesses can be explained by the different circulation regimes. The pressure-induced ice drift caused more thick ice, grown further to the north, to be advected southward in 1993 and 1996. In contrast, the thinner ice from the south was advected northward in 1995, resulting in thinner ice at the same geographical regions like in 1993 and 1996. However, as demonstrated by the differences in melt pond and snow coverage, the different sea level pressure distributions also modified the advection of warm air and moisture into the Laptev Sea. This lead to differences in the energy balance and to a much stronger ice melt in 1995. It should be noted that the strong southward ice advection in 1996 lead to thicker ice in the Laptev Sea.

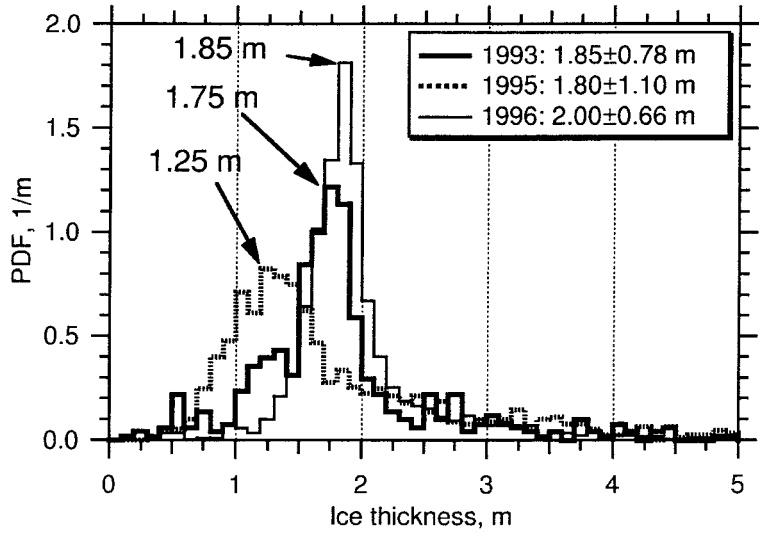

Fig. 3.14 Thickness distributions (given as probability density functions – PDF) of first-year ice in the Laptev Sea, in August/September 1993, 1995 and 1996 obtained by electromagnetic (EM) sounding (see Plate 3.2 for locations of profiled floes). The legend shows mean thicknesses and their standard deviation. From Haas & Eicken (2001).

However, although the ice floes were probably thicker than in other years in the central Arctic due to the absence of surface melting, the overall ice volume was probably quite reduced. This can be assumed from the occurrence of large polynyas north of 85°N, which are also visible in the ice concentration plots of Plate 3.2.

As large areas of the Laptev Sea were ice free in 1995, autumn freeze-up commenced about 3 weeks later than the average. Nevertheless the ice was thickest in the subsequent year. The open question is whether or not this was due to stronger than normal ice growth, or just to the absence of summer melt. This discussion shows another problem of interpreting end-of-summer level ice thicknesses, since it remains unclear if reduced (increased) thicknesses are due to reduced (increased) winter growth or increased (decreased) summer melt.

3.5 Conclusion and outlook

This chapter has shown that the sea ice thickness distribution is a result of complex thermodynamic and dynamic processes. There are many feedbacks involved in changes of ice thickness, and therefore the reasons for observed changes are not always clear at first sight. This is particularly true with respect to interpretations of recent observations of Arctic ice thinning in the context of climate change. Ice thickness research requires multi-disciplinary approaches including model, field and remote-sensing studies.

Field studies are always limited by their restricted spatial and temporal coverage. Completely new insights will therefore be possible with the launch of CryoSat, which is aimed to provide monthly fields of Arctic-wide mean sea ice thickness. Therefore, thickening or thinning due to advection of thick or thin ice into other regions will be well observable. For the first time, also, Arctic-wide time-series of seasonal thickness changes will become available. CryoSat will also provide the first data on regional thickness distributions and their seasonal and interannual variability in the Antarctic.

However, as with every satellite, CryoSat is not perfect, and extensive ground validation of its thickness retrievals will be required. This is a particular challenge for the observationalists, as CryoSat's anticipated accuracy is much better than that of any field technique. However, CryoSat's accuracy will only be achieved over large spatial (10^4 km^2) and temporal (1 month) scales, and these scales should also be covered by validation measurements. As the use of submarines is restricted by military constraints and will not be flexible enough to be synchronized with CryoSat, airborne EM methods will become particularly important. However, they also depend on ships or land stations as bases, and larger regions will not easily be surveyable within short time periods. Therefore, the technique has finally to be applied from fixed wing aircraft, which is not unrealistic with the use of an EM bird. Improvements will also be achieved by means of ULS mounted onto AUVs. Within the British Autosub project the first successful operations have been carried out under sea ice in the Antarctic. A thorough comparison of these different ULS and EM techniques is lacking and has to be performed to better judge the advantages and disadvantages of these methods.

Once better thickness data become available, e.g. from CryoSat, it will become obvious that better ice rheologies have to be developed and included in sea ice models. Thickness-class models will become more important in this respect. A key question here is the description of the transformation of thin into thick thickness classes during deformation events. Also this work will require better thickness data than are currently available. Again, EM or AUV measurements could provide this kind of data, as they yield high-resolution profiles and could be repeated over the same ice fields many times to document temporal changes.

References

Barry, R.G., Serreze, M.C., Maslanik, J.A. & Preller, R.H. (1993) The Arctic sea ice climate system: observations and modeling. *Reviews of Geophysics*, **31**, 397–422.

Bourke, R.H. & McLaren, A.S. (1992) Contour mapping of Arctic Basin ice draft and roughness parameters. *Journal of Geophysical Research*, **97**, 17715–17728.

Colony, R. & Thorndike, A.S. (1984) An estimate of the mean field of Arctic sea ice motion. *Journal of Geophysical Research*, **89**, 10623–10629.

Coon, M.D. (1980) A review of AIDJEX modelling. In: *Sea Ice Processes and Models*, (Ed. R.S. Pritchard), pp. 12–27, University of Washington Press, Seattle, Washington.

Gerdes, R. & Koeberle, C. (1999) Numerical simulation of salinity anomaly propagation in the Nordic seas and the Arctic Ocean. *Polar Research*, **18**, 159–166.

Haas, C. (1998) Evaluation of ship-based electromagnetic-inductive thickness measurements of summer sea-ice in the Bellingshausen and Amundsen Sea. *Cold Regions Science and Technology*, **27**, 1–16.

Haas, C. & Eicken, H. (2001) Interannual variability of summer sea ice thickness in the Siberian and Central Arctic under different atmospheric circulation regimes. *Journal of Geophysical Research*, **106**, 4449–4462.

Haas, C., Gerland, S., Eicken, H. & Miller, H. (1997) Comparison of sea-ice thickness measurements under summer and winter conditions in the Arctic using a small electromagnetic induction device. *Geophysics*, **62**, 749–757.

Haas, C., Liu, Q. & Martin, T. (1999a) Retrieval of Antarctic sea-ice pressure ridge frequencies from ERS SAR imagery by means of in-situ laser profiling and usage of a neural network. *International Journal of Remote Sensing*, **2**, 3111–3123.

Haas, C., Rupp, K.-H. & Uuskallio, A. (1999b) Comparison of along track EM ice thickness profiles with ship performance data. In: *Proceedings of the 15th International Conference on Port and Ocean Engineering Under Arctic Conditions (POAC 99), Espoo, Finland, August 23–27*, (Eds J. Tuhkuri & K. Riska), Vol. 1, pp. 343–353. Helsinki University of Technology, Ship Laboratory, Helsinki, Finland.

Harms, S., Farhbach, E. & Strass, V.H. (2001) Sea ice transports in the Weddell Sea. *Journal of Geophysical Research*, **106**, 9057–9073.

Hibler, W.D., III (1979) A dynamic thermodynamic sea ice model. *Journal of Physical Oceanography*, **7**, 987–1015.

Hilmer, M. & Lemke, P. (2000) On the decrease of Arctic sea ice volume. *Geophysical Research Letters*, **27**, 3751–3754.

Hopkins, M.A. (1994) On the ridging of intact lead ice. *Journal of Geophysical Research*, **99**, 16351–16360.

Hurrel, J.W. (1995) Decadal trends in the North Atlantic Oscillation: regional temperatures and precipitation. *Science*, **269**, 676–679.

Kottmeier, C., Olf, J., Frieden, W. & Roth, R. (1992) Wind forcing and ice motion in the Weddell Sea region. *Journal of Geophysical Research*, **97**, 20373–20382.

Kovacs, A. & Holladay, J.S. (1990) Sea-ice thickness measurements using a small airborne electromagnetic sounding system. *Geophysics*, **55**, 1327–1337.

Kwok, R., Cunningham, G.F. & Yueh, S. (1999) Area balance of the Arctic Ocean perennial ice zone: October 1996–April 1997. *Journal of Geophysical Research*, **104**, 25747–25759.

Lange, M.A. & Eicken, H. (1991) The sea ice thickness distribution in the northwestern Weddell Sea. *Journal of Geophysical Research*, **96**, 4821–4837.

Lensu, M. & Haas, C. (1998) Comparison of ice thickness from ship based video and field data. In: *Ice in Surface Waters*, (Ed. H.T. Shen), pp. 225–230. Proceedings of the 14th International Symposium on Ice, Potsdam, New York. Balkema, Rotterdam.

Massom, R.A., Eicken, H., Haas, C., Jeffries, M.O., Drinkwater, M.R., Sturm, M., Worby, A.P., Wu, X.R., Lytle, V.I., Ushio, S., Morris, K., Reid, P.A., Warren, S. & Allison, I. (2001) Snow on Antarctic Sea Ice. *Reviews of Geophysics*, **39**, 413–445.

Melling, H. & Riedel, D.A. (1995) The underside topography of sea ice over the continental shelf of the Beaufort Sea in the winter of 1990. *Journal of Geophysical Research*, **100**, 13641–13653.

Multala, J., Hautaniemi, H., Oksama, M., Leppäranta, M., Haapala, J., Herlevi, A., Riska, K. & Lensu, M. (1996) An airborne electromagnetic system on a fixed wing aircraft for sea ice thickness mapping. *Cold Regions Science and Technology*, **24**, 355–373.

Prinsenberg, S.J. & Holladay, J.S. (1993) Using air-borne electromagnetic ice thickness sensor to validate remotely sensed marginal ice zone properties. In: *Proceedings of the 12th International Conference on Port and Ocean Engineering under Arctic Conditions (POAC 93), Hamburg, 1993*, (Eds J. Schwarz & K.V. Evers), Vol. 2, pp. 936–948. Hamburgische Schiffbau-Versuchsanstalt, Hamburg.

Proshutinsky, A.Y. & Johnson, M.A. (1997) Two circulation regimes of the wind-driven Arctic Ocean. *Journal of Geophysical Research*, **102**, 12493–12514.

Rothrock, D.A., Yu, Y. & Maykut, G.A. (1999) Thinning of the Arctic sea-ice cover. *Geophysical Research Letters*, **26**, 3469–3472.

Serreze, M.C., McLaren, A.S. & Barry, R.G. (1989) Seasonal variations of sea ice motion in the Transpolar Drift Stream. *Geophysical Research Letters*, **16**, 811–814.

Strass V.H. & Fahrbach, E. (1998) Temporal and regional variation of sea ice draft and coverage in the Weddell Sea obtained from Upward Looking Sonars. In: *Antarctic Sea Ice: Physical Processes, Interactions and Variability*, (Ed. M.O. Jeffries), American Geophysical Union, Washington, D.C. *Antarctic Research Series*, **74**, 123–140.

Thompson, D.W.J. & Wallace, J.M. (1998) The Arctic Oscillation signature in the wintertime geopotential height and temperature fields. *Geophysical Research Letters*, **25**, 1297–1300.

Thorndike, A.S., Parkinson, C. & Rothrock, D.A. (Eds) (1992) *Report of the sea ice thickness workshop, 19–21 November 1991, New Carrollton, Maryland*. Polar Science Center, Applied Physics Laboratory, University of Washington, Seattle.

Timmermann, R., Beckmann, A. & Hellmer, H.H. (2002) Simulations of ice-ocean dynamics in the Weddell Sea. I: Model configuration and validation. *Journal of Geophysical Research*, **107**, 3024, DOI: 10.1029/2000JC000741.

Tucker, W.B., III, Weatherly, J.W., Eppler, D.T., Farmer, L.D. & Bentley, D.L. (2001) Evidence for rapid thinning of sea ice in the western Arctic Ocean at the end of the 1980s. *Geophysical Research Letters*, **28**, 2851–2854.

Vinje, T., Nordlund, N. & Kvambekk, A. (1997) Monitoring ice thickness in Fram Strait. *Journal of Geophysical Research*, **103**, 10437–10450.

Wadhams, P. (1994) Sea ice thickness changes and their relation to climate. In: *The Polar Oceans and Their Role in Shaping the Global Environment*, (Eds O.M. Johannessen, R.D. Muench & J.E. Overland), *Geophysical Monograph*, **85**, 337–362. American Geophysical Union, Washington, D.C.

Warren, S.G., Rigor, I.G., Untersteiner, N., Radionov, V.F., Bryazgin, N.N., Aleksandrov, Y.I. & Colony, R. (1999) Snow depth on Arctic sea ice. *Journal of Climate*, **12**, 1814–1829.

Worby, A.P., Jeffries, M.O., Weeks, W.F., Morris, K. & Jaña, R. (1996) The thickness distribution of sea ice and snow cover during late winter in the Bellingshausen and Amundsen Seas, Antarctica. *Journal of Geophysical Research*, **101**, 28441–28455.

Zhang, J., Rothrock, D. & Steele, M. (2000) Recent changes in Arctic sea ice: the interplay between ice dynamics and thermodynamics. *Journal of Climate*, **13**, 3099–3114.

Chapter 4

Large-scale Characteristics and Variability of the Global Sea Ice Cover

Josefino C. Comiso

4.1 Introduction

At high latitudes, the global oceans are covered by vast blankets of sea ice which range in extent at any one time between 17.5×10^6 to $28.5 \times 10^6\,km^2$. This corresponds to a significant fraction (3–6%) of the total surface area of the earth. In the Arctic region, the ice cover doubles its size from summer to winter, while in the Antarctic the corresponding value is five-fold (Zwally et al., 1983a; Parkinson et al., 1987; Gloersen et al., 1992). The sea ice cover is thus one of the most expansive and most seasonal geophysical parameters on the earth's surface, second only to the more variable and less predictable snow cover. The presence or absence of sea ice affects the atmosphere and the ocean, and therefore the climate, in many ways. For example, as an insulating material, it limits the flow of heat between the ocean and atmosphere. On account of its high albedo, a high fraction of solar radiation is kept from being directly absorbed by the surface and is instead reflected back to the atmosphere. It is because of such feedback effects between surface and atmosphere that climate change signals are expected to be amplified in polar regions (Budyko, 1966).

The impact of the sea ice cover on the ocean is equally significant. For example, the process of growth and decay of sea ice causes vertical and/or horizontal redistribution of salt in the ocean. During ice formation, brine rejection causes enhanced salinity of the underlying ocean and this process can initiate vertical convection and/or the formation of bottom water. Conversely, during ice retreat, low salinity melt water is introduced and causes the upper layer of the ocean to be stratified and vertically stable. The latter is conducive for phytoplankton growth and thereby increases the productivity of the region (Smith et al., 1988; Comiso et al., 1992; Arrigo, Chapter 5). Large polynyas within the pack and ice features, such as the Odden ice tongue, have been discovered and associated with deep ocean convection (Gordon & Comiso, 1988; Comiso et al., 2001). Latent heat polynyas, which are

usually near coastal regions and caused primarily by strong katabatic winds, have also been observed (Zwally et al., 1985; Comiso & Gordon, 1998; Markus et al., 1998; Massom et al., 1999), and have been postulated as the key source of the high salinity bottom water that is involved in global thermohaline circulation.

In-depth studies of the variability of sea ice cover is thus important, especially in light of recent reports of the declining extent (Johannessen et al., 1995; Cavalieri et al., 1997; Jacobs & Comiso, 1997) and thickness (Rothrock et al., 1999; Wadhams & Davis, 2000) of the Arctic ice cover. Large-scale variability in the sea ice cover has been quantified previously using satellite passive microwave data (Zwally et al., 1983a; Parkinson et al., 1987; Gloersen et al., 1992; Bjørgo et al., 1997; Stammerjohn & Smith, 1997; Parkinson et al., 1999; Zwally et al., 2002). Large changes in the ice cover were also reported in the 1990s, especially in the Arctic (Haas, Chapter 3), but more detailed studies are needed to better understand the climate system in the region.

In this chapter, the current state and variability of the sea ice cover is evaluated using the most up-to-date satellite data available. Analysis of an updated data set is useful because of large interannual variability and the rapidly changing state of the ice cover. There have also been some inconsistencies in previous reports. For example, a report by Kukla & Gavin (1981) of a rapidly declining Antarctic ice cover was associated with greenhouse warming, although a subsequent and more comprehensive study by Zwally et al. (1983a) showed inconclusive trends. More recent reports that made use of data with twice the record length used previously have shown trends going in the opposite direction (Cavalieri et al., 1997; Zwally et al., 2002). The discrepancies are mainly due to statistical errors due to different record lengths. In addition, different results are usually obtained when different techniques are used to derive geophysical products from the same set of satellite data (Comiso et al., 1997; Stammerjohn & Smith, 1997; Comiso & Steffen, 2001).

In this study, the variability in the sea ice cover in both hemispheres is evaluated for the 1978–2000 period using sea ice concentration data derived using the Bootstrap Algorithm. The merits of this data set and how it differs from others were discussed in detail by Comiso & Steffen (2001). The objectives of this chapter are:

(1) To provide a general overview of the large-scale characteristics of sea ice cover.
(2) To improve our understanding about the variability of sea ice cover.
(3) To provide a quantitative assessment of the current state of global sea ice using the still relatively short but spatially comprehensive record, and compare results with previous observations.
(4) To gain insights into the mechanisms of change and possible future of the ice cover.

A key parameter that is relevant and directly associated with the variability of the sea ice cover is surface temperature. Co-registered and concurrent satellite, as well

as longer-term station surface temperature data, are used to understand the last of these four objectives.

4.2 Satellite observations

Detailed studies of the global sea ice cover have been made possible by the advent of satellite data that provide comprehensive areal coverage at a relatively high temporal resolution. The use of satellite data for sea ice studies has been discussed in numerous publications (Shuchman & Onstott, 1990; Massom, 1991; Carsey, 1992). Satellite data can be divided into visible, infrared and microwave data, which are sometimes used in concert to obtain as complete an understanding of the properties of the ice cover as possible. Sometimes the data are used independently for certain applications.

When the weather and conditions are right, high-resolution visible data, such as Landsat, provide good, and spatially detailed, characterization of the ice cover. An excellent example of the utility of such data are the pair of Landsat TM (Thematic Mapper) images shown in Plate 4.1 that depict the small-scale and large-scale physical changes in the ice cover from one season to another at a resolution of 30 m. Plate 4.1a shows typical conditions during early stages of ice growth in the Antarctic, which in this case is located near the Cosmonaut Sea and Cape Ann (around 50°E). During this time period (27 March 1989) small platelets and needles, called frazil ice, are formed in supercooled water and, through wave action and wind, the ice particles accumulate to form grease ice, shuga and small pancakes (Eicken, Chapter 2). The spatial pattern of the ice cover shows a highly dynamic region with the apparent thermodynamic ice growth modified by wind, waves, tides and icebergs, resulting in the complex distribution of all forms of new ice. The image in Plate 4.1b was taken in spring, approximately 8 months later, in the same general area. During this latter period (24 November 1989), a much thicker ice cover is apparent, large ice floes are well defined and are shown to be composed of a complex conglomerate of various ice types. A spring polynya along the coast is also apparent and may be initiated mainly by ice break-up due to upwelling of warm water and/or advection due to wind. In evaluating interannual changes, it is thus important to know how and where the ice is changing, and such seasonality in physical characteristics of the ice cover should be taken into consideration.

The general large-scale distribution of the sea ice cover during both growth and decay periods is illustrated in Plate 4.2a,b, respectively, using observations from a visible channel of AVHRR (Advanced Very High Resolution Radiometer) during the last complete week of March and November 1989. Each of the images represents a weekly average derived from AVHRR Global Area Coverage (GAC) data and mapped onto a 6.25×6.25 km grid, as described by Comiso (2000). Polynyas, especially near the coastal regions, are shown in the AVHRR images as relatively darker than the thicker ice cover even when they are already covered by new ice. At

the marginal ice zones, the ice cover is also shown to be greyish and sometimes difficult to discriminate from open water. Overall, cloud-free visible-channel images provide good information about regions of high consolidation and areas of divergence or active ice formation. AVHRR data also have infrared channels that are useful for surface temperature studies as will be discussed in a later section. Visible data provide detailed information during daytime while infrared data are useful for both day and night conditions but both data sets are limited to cloud-free conditions only.

Passive and active microwave systems have been the more popular techniques for monitoring sea ice because of day/night almost all-weather capabilities and global coverage at a relatively high temporal resolution. For large-scale variability and trend studies, passive microwave data have been the primary tool because of a relatively long, comprehensive and consistent historical record. An apparent weakness of passive microwave data is the coarse spatial resolution (about 25×25 km) which makes such data difficult to use for detecting small spatial features in the ice cover, such as leads, ridges and ice bands. To partly overcome this weakness, the percentage of ice (called ice concentration) within each satellite grid element is calculated using a mixing algorithm, as discussed earlier, that takes advantage of the high contrast of the emissivity of ice and open water.

The colour-coded images in Plate 4.2c,d correspond to sea ice concentrations derived using the Bootstrap Algorithm (Comiso et al., 1997) for the periods corresponding to those of Plate 4.2a,b, respectively. Overall, there is a good coherence in the images, with the grey areas in the AVHRR satellite image corresponding to the relatively low concentration ice areas depicted in the passive microwave data. The spatial changes in signature look similar in both visible and passive microwave data for the two periods and reflect primarily changes in the physical properties of the ice cover. During the growth period in autumn, large areas covered by new ice look grey in the AVHRR image because of the relatively low reflectivity of the latter (Allison, 1981; Massom, 1991). The same surfaces also have low brightness temperatures and hence relatively low concentration (Plate 4.2c) because of low microwave emissivity for new ice compared to that of thick ice (Comiso et al., 1992; Grenfell et al., 1994). Conversely, during the break-up period, the grey (low reflectivity) areas (Plate 4.2b) correspond proportionately to relatively more open water and therefore lower ice concentration as depicted by the corresponding passive microwave data (Plate 4.2d). Thus, intermediate ice concentration values in the microwave data usually reflect the presence of newly formed ice (as in leads and polynyas) in autumn and winter, and the presence of mixtures of ice and open water in spring and summer. Since open water in leads and polynyas is covered by ice of some form within hours of formation in autumn and winter, this is also a more useful way of quantifying the ice cover compared to a strict ice and no ice discrimination that would show near 100% ice cover in practically all regions during growth stages.

For studies that require high spatial resolution irrespective of weather and time,

Synthetic Aperture Radar (SAR) data which has a resolution of about 35 m can be very useful. Ice floes and ridges are recognizable within the ice pack at this resolution but in some areas, especially near the ice edge, the interpretation of the data is sometimes ambiguous. However, with the use of time-series of images, some of these ambiguities can be resolved and the drift of sea ice and the thickness of seasonal ice can be inferred (Kwok et al. 1998). A problem in terms of global studies is the paucity of data and the lack of sufficient spatial and temporal coverage.

The other active microwave systems available that provide less resolution but more comprehensive coverage are the scatterometer (e.g. QuickSCAT) as described by Drinkwater & Lytle (1997), and the radar altimeter, as described by Fetterer et al. (1992). The data coverage and resolution are similar to those from passive microwave but more research is needed to accurately interpret the data, and algorithms have to be developed to retrieve geophysical parameters.

4.3 Spatial and temporal variations of the sea ice cover

The physical characteristics and spatial distribution of the global sea ice cover have been discussed extensively in the literature (Weeks & Ackley, 1986; Eicken et al., 1991; Tucker et al., 1992; Eicken, Chapter 2). The large-scale distribution of sea ice is vividly illustrated in the images shown in Plate 4.3. The images correspond to the ice cover in both hemispheres during maximum and minimum extent and were derived from Special Sensor Microwave/Imager (SSM/I) data in 2000. It is apparent that geographical considerations play an important role in the distribution of sea ice. In the northern hemisphere, a large fraction of the sea ice cover is surrounded by land with the latter providing an outer limit in the extent of the ice cover. During maximum extent in winter, the ice cover is shown to be fragmented with the largest fraction in the Arctic region, including the North Pole, and the rest in the Canadian Archipelago and as far south as 40°N in the peripheral seas and bays (Plate 4.3a). In the summer, the ice cover is basically contiguous and confined mainly to the Arctic Basin (Plate 4.3b). On the other hand, sea ice cover surrounds the Antarctic continent in the southern hemisphere with the highest latitude being about 80°N but no apparent limit at lower latitudes. The sea ice cover is shown as a contiguous ring surrounding Antarctica in winter (Plate 4.3c) and covering a significant part of the Indian, Pacific and Atlantic Oceans. During minimum extent at the end of the summer (Plate 4.3d), the ice cover is fragmented and located mainly in the western Weddell Sea, the Bellingshausen Sea, the Amundsen Sea and parts of the Ross Sea and the Indian Ocean.

A location map for both hemispheres is provided in Plate 4.4. This plate also shows difference maps of monthly climatologies in February and September to illustrate the large seasonality of the ice cover. In the northern hemisphere, the seasonal ice cover is shown in dark blue while in the southern hemisphere, it is shown in dark red. The perennial ice regions, depicted mainly by white, are shown to

be much more extensive in the northern than in the southern hemisphere. It is apparent that the ice cover is very seasonal and has very different spatial distributions in the two hemispheres.

The growth and decay of sea ice is primarily a response of the surface ocean to environmental changes from one season to another. For the two hemispheres, the growth periods are expected to be out of phase by exactly 6 months to correspond to the well-defined period between summer and winter. Climatological monthly averages of ice extent and area derived from 22 years of passive microwave data are shown in Fig. 4.1 and it is clear that the seasonal distributions for the two regions are different. In the northern hemisphere, the ice cover distribution is symmetrical in that the growth period takes approximately as long as the decay period. In the southern hemisphere, however, the growth season takes about 7 months while the decay season takes only 5 months. The difference can be partly explained in terms of the difference in geographical and environmental conditions as discussed earlier. For example, the retreat of sea ice in the Antarctic is accelerated by direct intrusions of warm water from lower latitudes and ice break-ups cause by large ocean waves. In the Arctic, the presence of surrounding land boundaries minimizes such effects. On the other hand, the presence of land that cools fast during autumn and winter leads to a cold environment during this time period and may in part cause the ice extent in the Arctic to reach its maximum value at a relatively faster rate. Meanwhile the relatively warm ocean that surrounds the ice cover in the Antarctic acts to moderate the growth of sea ice while the presence of the cold Antarctic continent may partly influence the lengthening of the growth season in the region.

In the northern hemisphere, the mean monthly extent, represented by a solid line in Fig. 4.1a is shown to vary from a minimum of $7.5 \times 10^6\,\mathrm{km}^2$ in the late summer (September) to about $15.5\,\mathrm{km}^2$ in the winter (March). The corresponding values in the southern hemisphere (Fig. 4.1b, solid line) are $3.8 \times 10^6\,\mathrm{km}^2$ (in February) and $19 \times 10^6\,\mathrm{km}^2$ (in September), respectively. Note that although the minimum values for sea ice in the northern hemisphere are greater than that in the southern hemisphere, the effective polar albedo in the latter is much greater than that of the former because of the presence of the snow-covered Antarctic continent which has a total area of about $14 \times 10^6\,\mathrm{km}^2$. Except for glaciers and Greenland, much of the snow-covered areas over land in the northern hemisphere are gone by summer. Thus, interannual changes in the sea ice cover in the northern hemisphere during summer, when the solar insolation is high, are likely to be more critical in terms of albedo feedback effects than in the southern hemisphere.

In the northern hemisphere, the monthly values during the year when the winter ice extent is most extensive (i.e. in 1979) during the 22-year period are represented by data points connected by dashed lines in Fig. 4.1a. It is apparent that the rate of decay during the year when ice is most extensive is less than average and the summer values are also above average. Conversely, the monthly values for the year when the ice is least extensive in winter (i.e. 1996) are shown by the dotted line and

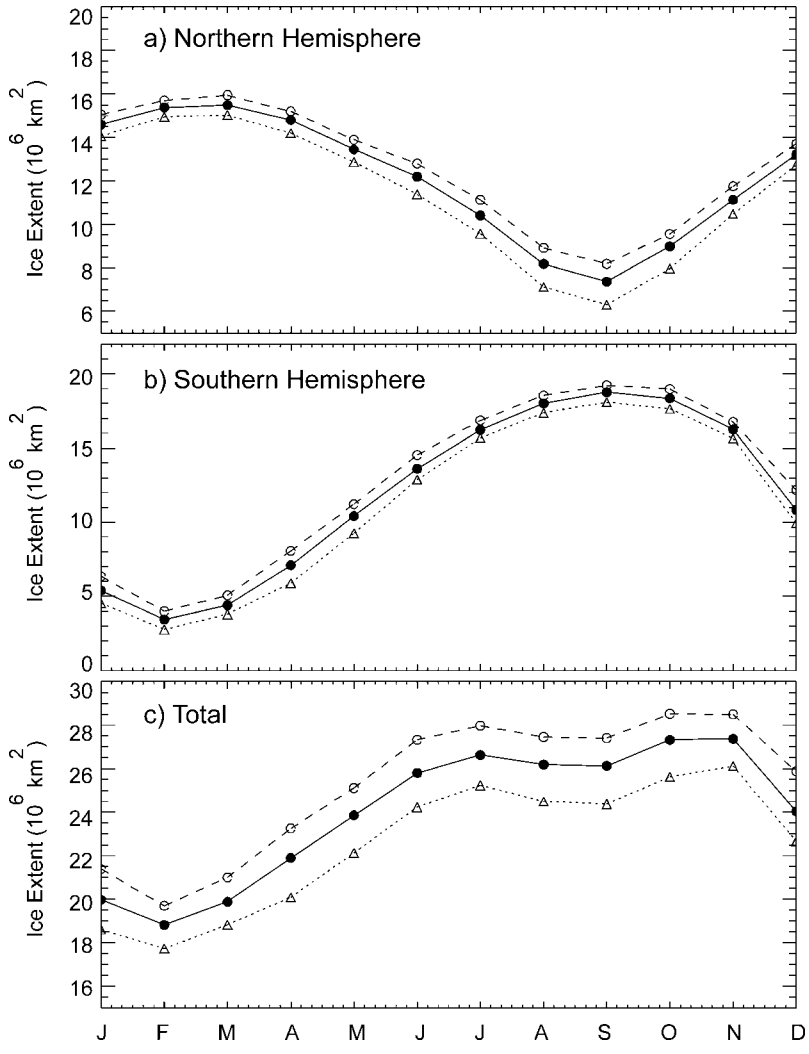

Fig. 4.1 Climatological seasonal variations derived from the monthly means from 1979 through 2000 in (a) the northern hemisphere, (b) the southern hemisphere. The solid line represents the climatological mean while dashed lines correspond to monthly values during the winter when ice extent is most extensive (1979 in the northern hemisphere and 1980 in the southern hemisphere) and dotted lines are for monthly values during the winter when ice extent is least extensive (1996 in the northern hemisphere and 1986 in the Southern hemisphere). (c) Sum of the monthly averages in the northern and southern hemispheres.

it is evident that the rate of decay is higher than average and with ice extent in summer is considerably less than average. Thus, extensive ice cover (icy) in winter is usually followed by extensive ice cover in summer and vice versa.

In the southern hemisphere, the monthly ice extents during the year when the winter was most expansive (1980) or least expansive (1986) are also shown in dashed and dotted lines in Fig. 4.1b, respectively. It is apparent from the plots that in this

hemisphere, the growth and decay patterns are similar to those of the average and are not significantly influenced by the extent of ice during the winter period. Regionally, however, effects opposite to that in the Arctic have been observed. For example, in the Weddell Sea, anomalously extensive ice cover in winter is usually followed by anomalously low ice cover area in the summer (Comiso & Gordon, 1998; Zwally et al., 1983b).

For completeness, the climatological global sea ice cover, which is basically the sum of data in Figs. 4.1a and 4.1b, is presented in Fig. 4.1c. The plot shows that at any one time, the average total ice cover ranges from 19.0 to $27.5 \times 10^6\,km^2$ but the extents can be as low as $17.5 \times 10^6\,km^2$ and as high as $28.5 \times 10^6\,km^2$. The low values occur in February, which is the peak of summer and winter in the Antarctic and the Arctic, respectively, while high values apparently occur in November which is spring and autumn for the Antarctic and Arctic, respectively. The latter date reflects the effect of the seasonal asymmetry in the Antarctic ice cover. It is also interesting to note that despite large hemispherical differences in the ice cover, the total area is almost constant from June through November.

The large seasonal variability in the extent (Fig. 4.1) makes it difficult to assess interannual changes or trends from the time-series of monthly data. Such interannual changes may be evaluated using seasonal averages such as those presented in Fig. 4.2 for the 1979–2000 period. In the northern hemisphere, significant interannual variability is apparent during summer (diamonds) and autumn (triangles), but during winter and spring only small changes are apparent, especially during the 1990–2000 period (Fig. 4.2a). The summer averages have higher values than the autumn averages because the latter includes September which is the month of minimum extent. In the southern hemisphere, the interannual changes appear minimal for all seasons except for 1980, 1982 and 1997 during summer and autumn. The plots for ice area in both hemispheres (not shown) are similar in characteristics to those for ice extents but the values are significantly lower. In this case, the summer values are lower than the values during autumn because of relatively lower concentrations during the period.

The dashed lines in the plots in Fig. 4.2 represent the trends in the ice cover for the different seasons as derived from linear regression of all the data points. The trends are all negative in the northern hemisphere and all slightly positive in the southern hemisphere, as has been reported previously (Parkinson et al., 1999; Zwally et al., 2002), but with slightly different values. This phenomenon suggests that the climates of the two hemispheres are not closely coupled. The results, however, are consistent with predictions from some Global Circulation Models (GCMs) (Manabe et al., 1992).

The Arctic region

The basic data used for studying the seasonal and the interannual variability in the ice cover are daily averages of ice concentrations mapped onto a polar stereographic

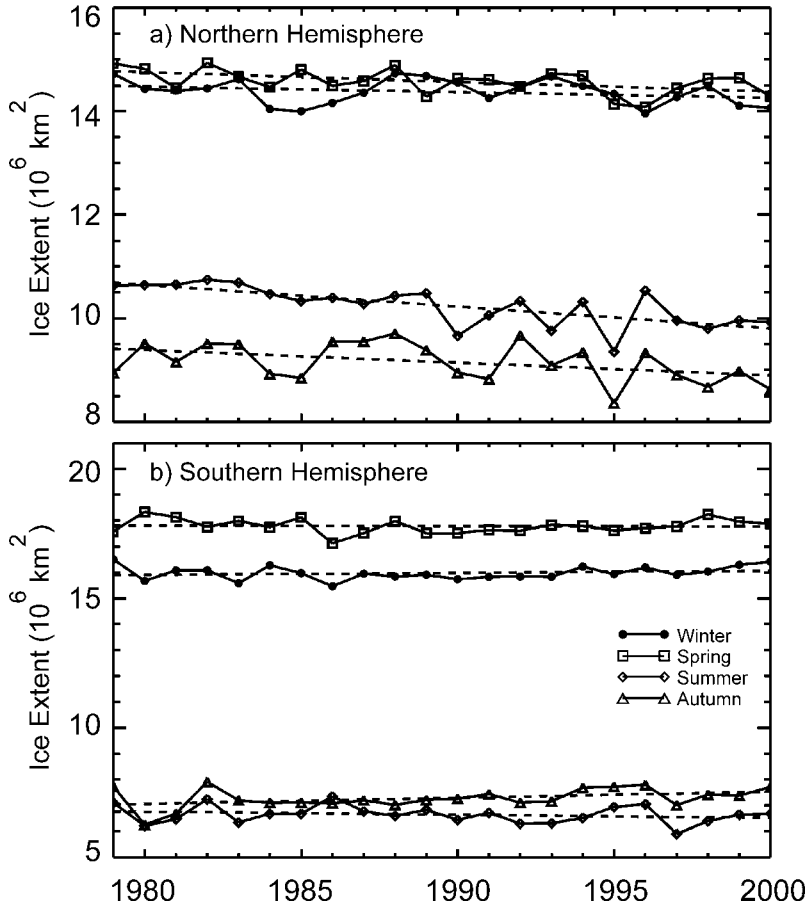

Fig. 4.2 Ice extent averages during the winter, spring, summer and autumn in (a) the northern hemisphere and (b) the southern hemisphere. Dashed lines show trends in each season.

grid with a 25 × 25 km resolution. The data provide good temporal resolution and are used for calculating the averages of ice extent, ice area and ice concentration for each month from 1979 to 2000, as presented in Figs 4.3a,b,c, respectively. The distributions for both ice extent and actual ice area are coherent and show similar patterns. The peak values are also shown to have much less interannual variability than the minimum values, especially in the 1990s. Relatively low values in the minimum ice extent (Fig. 4.3a) are apparent in 1990, 1991, 1993, 1995, 1998, 1999 and 2000. In the ice area plot (Fig. 4.3b), the minimum values during these years appear even relatively lower. This is partly because of relatively lower average concentrations (Fig. 4.3c) which in turn may be partly due to more divergence during these later years. The latter is consistent with more storms that may be associated with a declining surface level pressure as reported by Walsh et al. (1996).

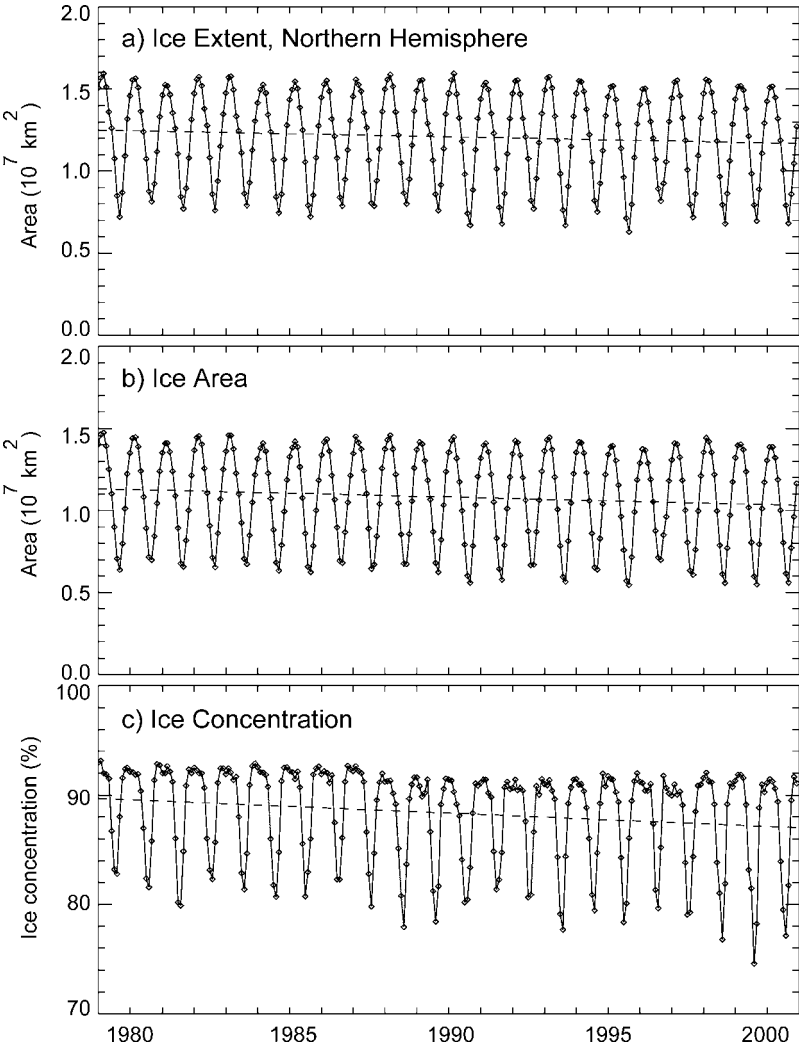

Fig. 4.3 Monthly (a) ice extent, (b) actual ice area and (c) average ice concentration in the northern hemisphere from January 1979 through December 2000.

The colour-coded yearly anomaly maps, presented in Plate 4.5, provide the means to assess large-scale and regional changes in the ice cover on a year-to-year basis. For uniformity in both hemispheres, yearly averages are calculated such that they represent averages for entire sea ice seasons. More specifically, in the northern hemisphere, the yearly averages are from August of one year to July the following year, while in the southern hemisphere, the averages are from January to December of the same year. This ensures that the averaging corresponds to the development of the same ice cover as it evolves from its growth stages through its maximum values in winter, and through to the melting stages in spring and summer. Each map in

Plate 4.5 thus represents the yearly anomalies for each ice season instead of for each calendar year. Positive anomalies in the ice cover are shown in the colour-coded maps as greys, greens or blues while negative anomalies are in oranges, purples and reds. The yearly climatology used for deriving the yearly anomalies is presented in the last image of Plate 4.5 and can be used as an aid in the interpretation of the latter.

It is apparent that the yearly anomalies are usually significant in the peripheral seas and bays. Among the most active areas are the Okhotsk Sea and the Bering Sea in the Pacific Ocean region. Some teleconnections between these two seas have been observed previously (Cavalieri & Parkinson, 1987) with negative anomalies in one sea occurring concurrently with positive anomalies in the other (e.g. 1984–85 and 1990–91). Such a pattern is apparently not consistent for the 1979–2000 period since the anomalies can be both negative in these regions, as in 1979–80, or both positives, as in 1995–96. In other years, the patterns are not so clear with a mixture of positives and negatives even in the same seas. In the Atlantic Ocean side, similar effects are also evident between the Kara and Barents Seas, and the Baffin and Hudson Bays. It is interesting to note that there was no year in which the anomalies were either all positive or all negative in the peripheral seas.

To quantitatively evaluate interannual changes, anomaly plots for the entire hemisphere and various sectors in the Arctic region (following previous analysis by Gloersen et al., 1992; Parkinson et al., 1999) are presented in Fig. 4.4 for the 1979–2000 period. Each data point in the anomaly plots is the difference of the value for each month and that of the monthly climatology. The monthly anomaly plots provide a means to assess interannual variability since the large seasonality is subtracted. Statistically, they also provide better accuracy for trend analysis than yearly averages. The anomalies in ice extent and ice area again show coherence and reflect very similar characteristics. It is also apparent that the abnormally low and high values stand out better in these plots than in the raw monthly plots shown in Fig. 4.3. It is interesting to note that an abnormally low value in 1995 is followed by an abnormally high value in 1996 (Plate 4.5). This is an indication that dramatic changes can occur from one year to another.

In the Arctic sector (Fig. 4.4b), the anomalies are significantly different from zero only during spring, summer and autumn, since during winter the entire Arctic basin is covered by ice. Note that the anomalies are generally positive in the 1980s and mainly negative in the 1990s, the exceptions being 1992, 1994 and 1996. This suggests that the ice cover in the region has been retreating. The anomalies in the Greenland Sea sector (Fig. 4.4c) show more variability through the 22-year period. A cyclical pattern is apparent in the distribution for this sector mainly as a result of a similar variability in the extent of the Odden, as described by Comiso et al. (2001). In the Kara and Barents Seas the ice variability (Fig. 4.4d) is similar to that of the Greenland Sea, although a cyclical pattern is not as apparent. In this sector, significant decreases are apparent in 1983, 1985, 1992, 1995 and 2000 whereas increases occurred in most other years. The sea ice anomalies in the Bering and Okhotsk Seas

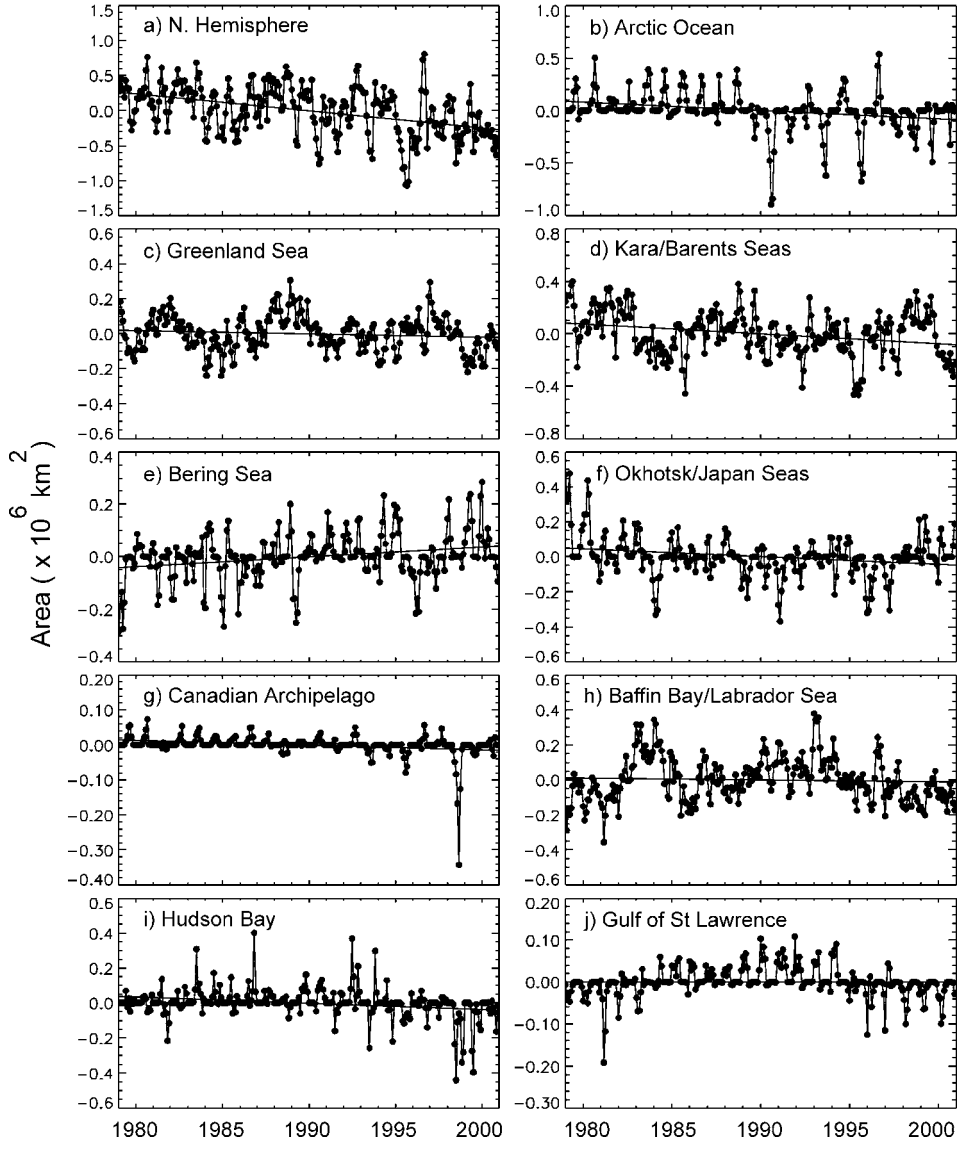

Fig. 4.4 Anomalies in the monthly ice extent from January 1979 through December 2000 in various regions.

(Figs 4.4e and 4.4f) have similar variability but with opposite trends, the former having negative anomalies in the 1980s and mainly positive anomalies in the 1990s. In the Okhotsk Sea, the anomalies were on the average positive in the 1980s, except in 1984, and negative in the 1990s, except for the last few years. The recovery in the last few years ended what was previously reported as a rapidly declining sea ice cover in the region (Parkinson et al., 1999).

In the Canadian Archipelago, the anomalies in extent were generally small except for the one big drop in extent in 1998. This was the same year that the Beaufort Sea had the largest open water area during the satellite era. In the Baffin Bay/Labrador Sea region, periodic fluctuations in the anomalies (Fig. 4.4h) are apparent in the 1980s, but in the 1990s, except for the recoveries in 1993 and 1996, the extent was generally declining. In the Hudson Bay (Fig. 4.4c), there was not much variability except for positive anomalies in 1983, 1986 and 1992 and negative anomalies in 1993, 1994, 1998 and 1999. In the Gulf of St Lawrence (Fig. 4.4j), there is a suggestion of periodicity with the anomalies being all negative up to 1983 followed by practically all positive anomalies up to 1993 and then almost all negative anomalies up to the present time.

The plots in Fig. 4.4 provide a quantitative means for assessing the changes in the anomaly patterns as depicted in Plate 4.5. It is apparent that there is a lack of coherence in the variability of the anomaly distributions at the different sectors. The peaks and the dips generally do not occur at the same time in the different regions, and periodicities, where they occur, are usually out of phase from each other. The lack of coherence is partly the result of a complex atmospheric system in the Arctic that produces different ice distributions in the different regions during different periods. The effect of surface-temperature anomalies will be discussed in a later section. Overall, negative trends of varying degree of significance are observed in all sectors, except for the Bering Sea sector in which the ice cover has been increasing at the rate of 11.9% per decade.

The Antarctic region

Monthly ice extents, ice area and ice concentration in the southern hemisphere for the period from 1979 through 2000 are presented in Fig. 4.5, and it is apparent that there are differences in the distributions compared to those in the northern hemisphere (Fig. 4.3). In the southern hemisphere the amplitude of each ice season is obviously larger while the yearly distributions are more regular than those in the northern hemisphere. The average ice concentration is almost constant at about 83% in winter, compared to about 92% in the Arctic, while the average ice concentration in the summer ranges from 59 to 69%, compared to 72 to 81% in the Arctic. Note that as expected the distributions for ice extents are again coherent with those of ice area, with the latter being lower in value.

Colour-coded anomaly maps for each year from 1979 through 2000, as shown in Plate 4.6, illustrate the large year-to-year variability in the ice cover in the region. The images show patterns of alternate negative and positive anomalies at the periphery of the sea ice cover around the continent. From one year to another these patterns tend to move around, propagating like a wave that has been referred to as the Antarctic Circumpolar Wave (ACW) (White & Peterson, 1996). The period of propagation has been estimated to be about 8 years with a revisit time of 4 years at every point, the wave number being mode 2. It is interesting to note that the pattern

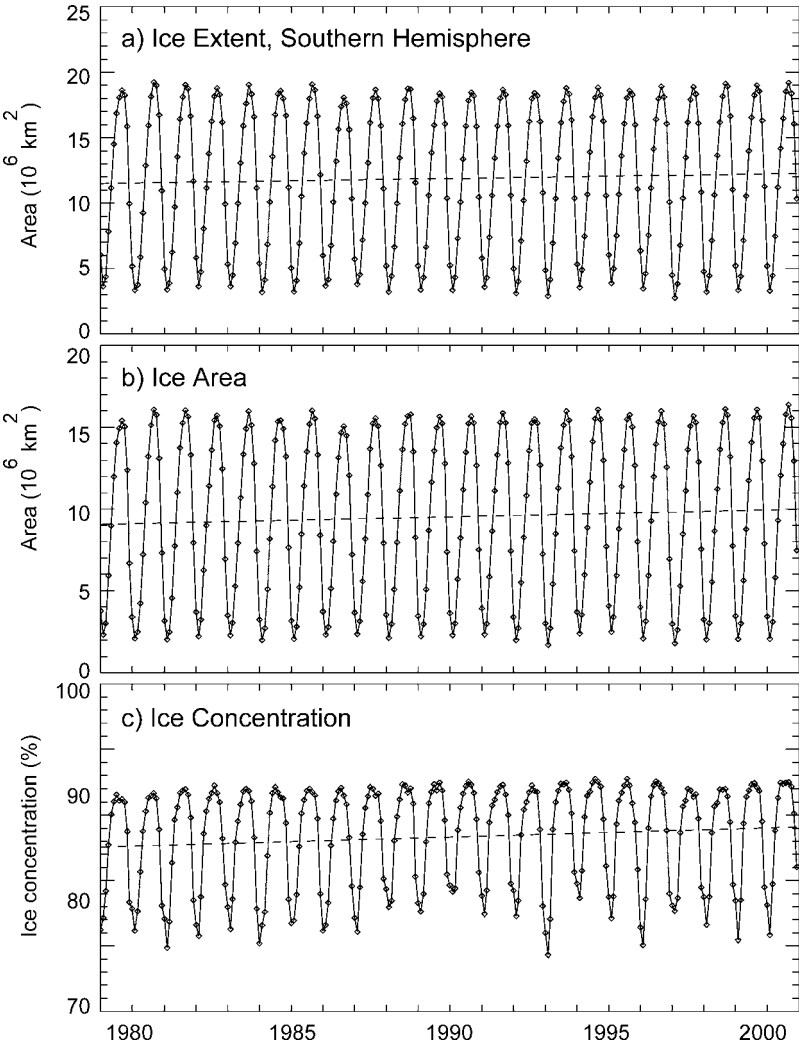

Fig. 4.5 Monthly (a) ice extent, (b) actual ice area and (c) average ice concentration in the southern hemisphere from January 1979 through December 2000.

of anomalies in 1980 is almost duplicated in 1992. Also, the anomaly pattern in 1999 is almost identical to that of 1980 but with opposite sign. The repetition of the patterns in some places suggests that there are local geographical or oceanographic factors that cause similar features to be reproduced in different years. White & Peterson (1996) described the ACW as an ice edge phenomenon. The anomaly patterns in Plate 4.6 indicate that the effect is not just an ice edge phenomenom since the patterns go all the way into the pack. The wave number is also not just mode 2 but sometimes mode 3 as illustrated in winter anomaly data by Comiso (2000) and in a less distinct way in 1980 and 1992 in Plate 4.6.

The time-series monthly ice extent anomalies for the entire hemisphere, as well as in various sectors (cf. Gloersen et al., 1992; Zwally et al., 2002), are indicative of a very variable and dynamic region (Fig. 4.6). The anomalies for the entire hemisphere (Fig. 4.6a) apparently had higher amplitudes in the 1980s than in the 1990s but this may be largely due to phase difference between sectors since the same phenomenon is not evident in the various sectors. The peaks and dips in the anomaly plots are again shown to occur in different years in the various sectors. This is partly because of the propagating wave (ACW), as described earlier, that causes the anomalies to circle around the continent. It is interesting to note that in the Weddell Sea sector (Fig. 4.6b), there is a significant negative anomaly in 1999 that appears to be associated with similar anomalies in the other sectors such as the 1998 negative anomaly in the Bellingshausen/Amundsen Seas, the 1997 anomaly in the Ross Sea and the 1996 anomaly in the Indian Ocean.

The lag from one region to another is consistent with the effect of the ACW. In the Indian Ocean sector (Fig. 4.6c), there are also negative anomalies in 1986, 1987 and 1988 which were followed by positive anomalies in 1989 and 1990. In the Western Pacific Ocean sector (Fig. 4.6d), the key events were the positive anomalies in 1982 and 1983, and the negative anomaly in 1989. In the Ross Sea (Fig. 4.6e), a large negative anomaly in the early 1980s was followed by positive anomalies, except for slight drops in 1986, 1991 and 1997. In the Bellingshausen/Amundsen Seas sector (Fig. 4.6f), the El Niño Southern Oscillation (ENSO) years of 1983, 1988, 1992 and 1998 are shown to coincide with negative anomalies, confirming observed relationships of ENSO with the ice cover and ACW as described by Peterson & White (1998) and Kwok & Comiso (2002). Note that the dips at the Ross Sea sector (i.e. 1980, 1986, 1992, 1995 and 1997), which is also regarded as a region affected by ENSO (Ledley & Huang, 1997), are not coincident with those of the Bellingshausen/Amundsen Seas sector. The patterns are relatively irregular at times because the atmospheric circulation in the region is complex and driven by many factors, some of which are regional in origin. For example, in the Weddell Sea a large positive anomaly in 1981 was followed by a negative anomaly in the subsequent summer, while a negative anomaly in 1991 was followed by two years of positive anomalies. Other anomalous patterns have also been cited in the literature (Hanna, 2001 and others).

4.4 Global and regional trends

Global climate change is expected to be amplified in polar regions because of feedback effects associated with the high albedo of ice and snow as indicated earlier. A global warming of 0.5 K was observed during the last century (Jones et al., 1999), and it would be of interest to know how such a trend is reflected in the Arctic and the Antarctic regions. Linear regression analyses have been applied on the monthly sea ice anomalies for the period from 1979 through 2000, and the results are shown

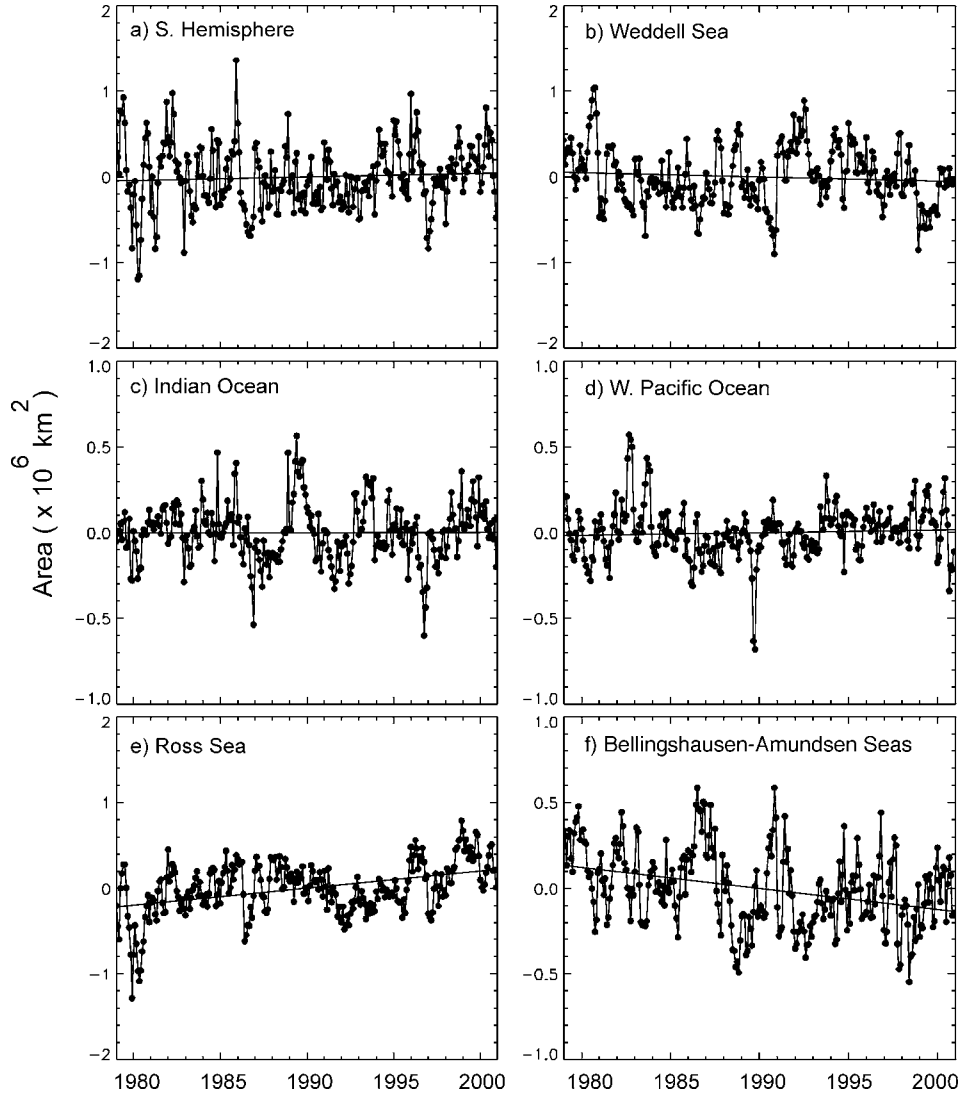

Fig. 4.6 Anomalies in the monthly ice extent from January 1979 through December 2000 in various regions.

as solid lines in Figs 4.4 and 4.6. The trend values are also tabulated in Tables 4.1 and 4.2 for the northern and southern hemispheres, respectively.

The trend in ice extent in the northern hemisphere, as inferred from monthly anomaly data from January 1979 through December 2000, is $-2.0 \pm 0.3\%$ per decade. This is less than the rate of about -3% per decade inferred previously from slightly different data sets and for the November 1978 to December 1996 period (Bjørgo et al., 1997; Parkinson et al., 1999). It is thus important to note that the

Table 4.1 Trends in extent and area (given in units of km^2/decade and in parentheses %/decade) in the northern hemisphere.

Sector/season	Trend in extent km^2/yr (%/dec)	Error in extent km^2/yr (%/dec)	Trend in area km^2/yr (%/dec)	Error in area km^2/yr (%/dec)
Northern hemisphere	−24 100 (−2.0)	3100 (0.3)	−35 080 (−3.1)	2800 (0.3)
Arctic Ocean	−7910 (−1.2)	1650 (0.2)	−11 570 (−1.8)	1780 (0.3)
Greenland Sea	−1950 (−2.7)	973 (1.3)	−2380 (−4.4)	770 (1.4)
Kara/Barents Sea	−7510 (−5.5)	1600 (1.2)	−8340 (−7.2)	1470 (1.3)
Bering Sea	3760 (11.9)	815 (2.6)	2560 (10.9)	697 (3.0)
Okhotsk/Japan Seas	−4410 (−11.0)	1080 (2.7)	−5200 (−17.1)	1020 (3.3)
Canadian Archipelago	−1360 (−1.9)	284 (0.4)	−2540 (−4.0)	352 (0.5)
Baffin Bay/Labrador Sea	−1070 (−1.3)	1220 (1.4)	−1670 (−2.4)	1060 (1.5)
Hudson Bay	−3570 (−4.3)	820 (1.0)	−3850 (−5.3)	695 (1.0)
Gulf of St Lawrence	−32.4 (−0.5)	338 (5.0)	−91.6 (−2.0)	256 (5.6)
Winter	−10 800 (−0.8)	7940 (0.5)	−20 700 (−1.6)	6820 (0.5)
Spring	−18 270 (−1.2)	6990 (0.5)	−27 840 (−2.1)	6530 (0.5)
Summer	−42 200 (−4.1)	9200 (0.9)	−51 350 (−6.0)	9290 (1.1)
Autumn	−24 630 (−2.7)	11 700 (1.3)	−32 220 (−3.9)	10 220 (1.2)
Maximum	−21 010 (−1.3)	9220 (0.6)	−26 870 (−1.9)	8370 (0.6)
Minimum	−45 890 (−6.4)	15 290 (2.1)	−50 820 (−8.5)	11 850 (2.0)

addition of a few years may cause a significant change in the trend, especially if the latest values are very different from the previous ones. The issue of accuracy associated with record lengths of data is addressed in the next section.

In the central Arctic Ocean region, the trend is $-1.2 \pm 0.2\%$ per decade, which is a less negative rate than that for the entire northern hemisphere. The slower rate is not unexpected since many of the anomalies are in the peripheral seas as discussed

Table 4.2 Trends in extent and area (given in units of km^2/decade and in parentheses %/decade) in the southern hemisphere.

Sector/season	Trend in extent km^2/yr (%/dec)	Error in extent km^2/yr (%/dec)	Trend in area km^2/yr (%/dec)	Error in area km^2/yr (%/dec)
Southern hemisphere	4420 (0.4)	3690 (0.3)	15 750 (1.7)	3240 (0.3)
Weddell Sea	−5100 (−1.2)	3320 (0.8)	−2760 (−0.8)	2800 (0.8)
Indian Ocean	280 (0.1)	1660 (0.9)	1020 (0.7)	1450 (1.0)
Western Pacific Ocean	1540 (1.2)	14 900 (1.2)	4450 (5.0)	1170 (1.3)
Ross Sea	20 000 (7.0)	2750 (1.0)	20 550 (8.7)	2320 (1.0)
Bellingshausen/Amundsen Seas	−12 400 (−8.1)	2080 (1.4)	−7510 (−6.3)	1760 (1.5)
Winter	8300 (0.52)	8890 (0.56)	19 740 (1.47)	8330 (0.62)
Spring	−1380 (−0.08)	9510 (0.54)	11 390 (0.78)	9680 (0.66)
Summer	−11 800 (−1.78)	11 750 (1.77)	924 (0.21)	8740 (1.95)
Autumn	23 340 (3.20)	12 360 (1.70)	30 720 (5.46)	12 220 (1.99)
Maximum	5260 (0.28)	10 320 (0.54)	19 150 (1.20)	9380 (0.59)
Minimum	−11 400 (−3.58)	8994 (2.82)	−7532 (−3.76)	6350 (3.17)

in the previous sections. The plot in Fig. 4.4b indicates spikes associated with changes in the spring and summer periods which are shown to be mainly positive in the 1980s and negative (except for 1992, 1994 and 1996) in the 1990s. The negative trend appears to be primarily influenced by unusually low ice extent events of 1990, 1993 and 1995.

The trends in other sectors are varied with the only positive trend occurring in the Bering Sea at $11.9 \pm 2.6\%$ per decade. This positive trend reflects increases in the winter ice cover in the region despite decreases in the ice cover in the adjacent (Arctic) region. Also, towards the south-west of this region at the Okhotsk Sea, the ice cover is changing at about the same magnitude but opposite sign with the trend being $-11.0 \pm 2.7\%$ per decade. In the latter, the trend would have been significantly more negative were it not for the relatively strong recovery during the last two years of the data. Other regions with significant negative trends are the Kara/Barents Seas and Hudson Bay with trends of $-5.5 \pm 1.2\%$ per decade and $-4.3 \pm 1.0\%$ per decade, respectively. The trend at the Canadian Archipelago is also significant at $-1.9 \pm 0.4\%$ per decade but this is mainly due to a big drop in the ice cover in the region in 1998. Trends are also negative in the Greenland Sea and Baffin Bay/Labrador Sea sectors at -2.7 ± 1.3 and $-1.3 \pm 1.4\%$ per decade, respectively. However, changes in these regions may be partly influenced by periodic patterns as mentioned previously. A negative but insignificant trend in the ice cover is inferred at the Gulf of St. Lawrence sector ($-0.5 \pm 5.0\%$ per decade) where a periodic pattern is also observed.

While the trend of ice cover in the entire northern hemisphere is basically controlled by trends in the peripheral seas, the most important trend of interest is actually that associated with the central Arctic. The northern hemisphere has smaller seasonal amplitude than the southern hemisphere because of the presence of extensive and thick multi-year ice cover in the central Arctic. Ice that survives the summer is often referred to as the perennial ice cover, which consists mainly of multi-year ice. The extent and area of the perennial ice cover can be inferred by finding the minimum value for each year from the time-series of daily data. The yearly record of the minimum extents of the ice cover for each year from 1979 to 2000 is shown together with that of maximum extent in Fig. 4.7. The trends in maximum ice values for both extent and ice area are -1.3 ± 0.6 and $-1.9 \pm 0.6\%$ per decade, respectively, and are basically consistent with those of the entire hemisphere (Fig. 4.7a). The trends in minimum ice cover, however, are $-6.4 \pm 2.1\%$ per decade and $-8.5 \pm 2.0\%$ per decade for ice extent and ice area, respectively (Fig. 4.7b). Such large negative trends (about four times higher than maximum trends) indicate that the perennial ice cover is shrinking at a relatively high rate as reported in Comiso (2002). A trend for the multi-year ice cover of a similar magnitude (7%) has also been reported by Johannessen et al. (1999) using multi-year ice fraction data derived during the winter period from passive microwave data. However, such data are known to have large uncertainties (Kwok et al., 1996) partly

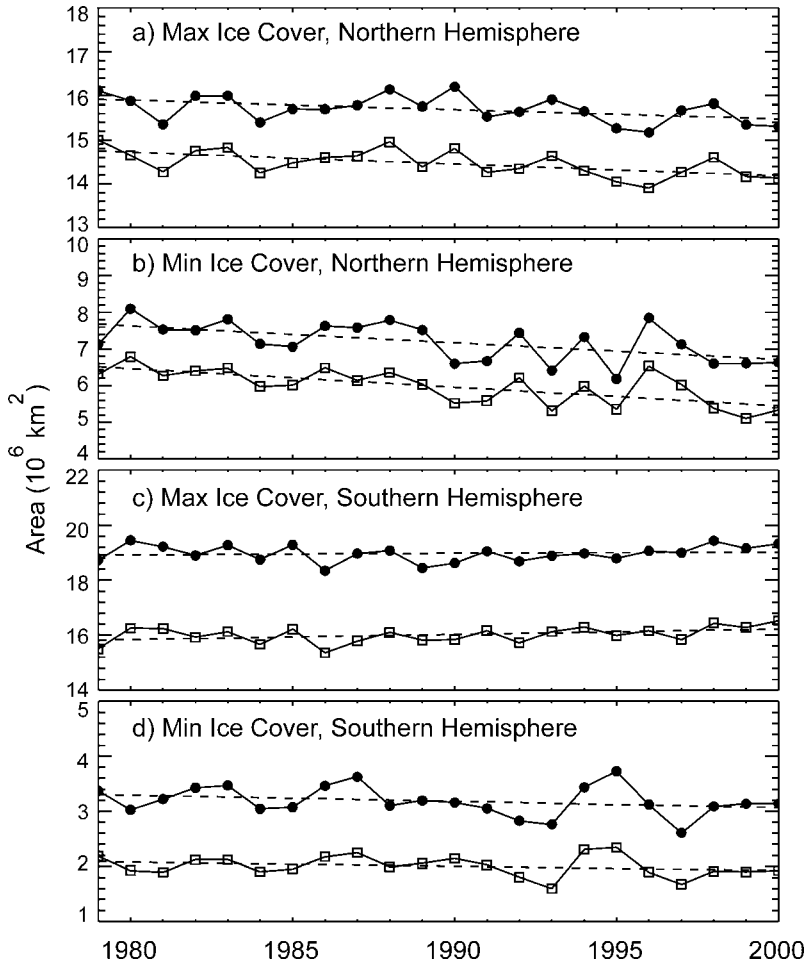

Fig. 4.7 Yearly (a) maximum and (b) minimum of ice extent and ice area in the northern hemisphere and yearly (c) maximum and (d) minimum of ice extent and ice area in the southern hemisphere.

because the emissivity of multi-year ice is highly variable and not constant as assumed in the algorithm that calculates the multi-year ice fraction.

It is of special interest to note that the ice minimums in the 1990s are highly variable compared to those in the 1980s (Fig. 4.7b). As reported in Comiso (2002) such variability suggests an increasing fraction of second-year ice cover in the 1990s, compared to the 1980s, which in effect means a thinning of the Arctic sea ice cover (that includes the second-year ice cover). This is consistent with reports by Rothrock et al. (1999) and Wadhams & Davis (2000) that the average ice thickness in the 1990s is significantly less than averages collected in the previous decades. A thinning through this mechanism would not necessarily mean a thinning in the older

and thicker ice floes. The issues associated with ice thickness and its variability are addressed by Haas in Chapter 3.

The variations of the ice cover on a season-by-season basis, have been discussed previously, and illustrated in Fig. 4.2 in which fitted lines are also shown to indicate interannual trends. The numerical values of the seasonal trends are given in Tables 4.1 and 4.2. In the northern hemisphere it is apparent that the trends are all negative with those for winter and spring being only slightly negative at $-0.8 \pm 0.5\%$ per decade and $-1.2 \pm 0.5\%$ per decade, respectively. In the autumn, the trend is more negative at $-2.7 \pm 1.3\%$ per decade but the highest rate of decrease occurs in the summer at $-4.1 \pm 0.9\%$ per decade. The latter is consistent with the large rate of decrease for the perennial ice cover. An even higher rate of decrease is observed when ice area data are used with the rate of decrease during the summer being as low as $-6.0 \pm 1.1\%$ per decade. This is consistent with the large decline observed for the perennial ice cover.

The trend results in the southern hemisphere (Fig. 4.6) are not as indicative of a changing ice cover as those of the northern hemisphere. The result of analysis of data from the 22-year period shows an insignificant trend of $0.4 \pm 0.3\%$ per decade for the entire southern hemisphere (Table 4.2). This is slightly less than the $1.0 \pm 0.4\%$ per decade reported by Zwally et al. (2002) for the 1979–1998 period. The trends are similarly insignificant at -1.2 ± 0.8, 0.1 ± 0.9 and $1.2 \pm 1.2\%$ per decade at the Weddell Sea, Indian Ocean, and Western Pacific Ocean sectors, respectively. In two other sectors, however, the trends are quite substantial with opposite signs of $7.0 \pm 1.0\%$ per decade and $-8.1 \pm 1.4\%$ per decade at the Ross Sea and Bellingshausen/Amundsen Seas sectors, respectively. Since the two sectors are adjacent to each other, it appears that the opposite trends in the two sectors are partly caused by advection of ice from one sector to the other. However, the Antarctic Peninsula that is adjacent to the Bellingshausen/Amundsen Seas sector has been an area of climate anomaly described by King (1994) and Jacobs & Comiso (1997). Also, the Ross Sea region has been associated with influences of ENSO (Ledley & Huang, 1997) and the continental area adjacent to it has been experiencing some cooling during the last two decades (Comiso, 2000). The positive trend in the Ross Sea, which is the site of a major coastal polynya, suggests increased ice production and a more important role of the region in bottom water formation.

The trends of maximum ice values for each year in the southern hemisphere are again similar to that inferred from the monthly time-series, being $0.3 \pm 0.5\%$ per decade and $1.20 \pm 0.6\%$ per decade for ice extent and ice area, respectively. It is, however, surprising that the trends of minimum values for each year are negative at -3.6 ± 2.8 and $-3.8 \pm 3.2\%$ per decade for ice extent and ice area, respectively. It appears that the summer ice cover has been declining as in the Arctic but errors are larger because of a much lower extent of ice in the summer. The negative trend is due in part to the retreating perennial ice cover in the Bellingshausen Sea as reported by Jacobs & Comiso (1997).

In the southern hemisphere the trends for extent in each season (Fig. 4.2b) are

basically insignificant except for in autumn. Quantitatively, the trends in winter, spring and summer are 0.5 ± 0.6, -0.1 ± 0.5 and $-1.8 \pm 1.8\%$ per decade, respectively, while in autumn, a positive and significant trend of $3.2 \pm 1.7\%$ per decade is inferred. Again, the trends for ice area are higher than those for ice extent, with that for autumn being $5.5 \pm 2.0\%$ per decade with those for winter, spring and summer being 1.5 ± 0.6, 0.8 ± 0.7 and $0.2 \pm 2.0\%$ per decade, respectively. These results show that the net positive trend overall for the entire hemisphere is due mainly to the positive trend in autumn. This in turn suggests that the onset of ice growth is now occurring earlier than normal. The negative trends in spring and summer indicate earlier ice break-up in later years but the values are not significant.

4.5 Surface temperature effects, temperature trends and cyclical patterns

To gain insights into the observed variability and trend in the ice cover, anomalies in the surface temperatures in conjunction with anomalies in ice concentration have been examined. Surface temperatures are used because they are known to be negatively correlated with ice extent and area (Jacobs & Comiso, 1997). Changes in surface level pressure, wind and other parameters are also important to consider (Walsh et al., 1996; White & Peterson, 1996), but the associated effects are too complex and are not within the scope of this chapter. Following similar analysis in Comiso (2000), the anomalies in yearly surface temperatures, as derived from AVHRR data for the northern and southern hemispheres, are shown in Plates 4.7 and 4.8, respectively. The last image in each figure is the climatological yearly average data that is used in generating the anomaly maps.

It is remarkable that the temperature anomaly maps in the northern hemisphere show generally negative anomalies (greens and blues) in the 1980s and positive anomalies (yellows and oranges) in the 1990s. This alone is indicative of warming in the region during the last two decades. The phenomenon is also consistent with a declining sea ice cover in the Arctic as shown previously. It should be noted, however, that there are areas of positive anomalies in the first decade of data as in the Greenland/Baffin Seas in 1981–82 and the Kara/Barents Seas in 1983–84. Conversely, there are also negative anomalies in the second decade such as in the Canadian Archipelago and Beaufort Sea in 1990–91, the Kara/Barents Seas in 1997–99 and the Bering Sea in 1997–2000. Thus, while warming is observed in most parts of the northern hemisphere, there is evidence of cooling in some areas.

The areas of positive anomalies in surface temperature are shown to be precisely where negative anomalies in the sea ice cover (Plate 4.5) are usually observed, and vice versa. The good coherence of ice cover with temperature is an indication that these two variables are strongly linked with each other. The temperature anomaly maps also show that the scope of warming and cooling goes beyond the boundaries of the sea ice cover indicating considerable atmospheric influence. Feedback effects

may accelerate the decline rate. For example, as the perennial sea ice cover declines and open water area increases in the Arctic Basin in spring and summer, more solar energy and heat are absorbed by the Arctic Ocean. This in turn warms up the latter and causes a further decline in the ice cover. Some evidence that the temperature of the Arctic Ocean has been increasing has in fact been reported (Gunn & Muench, 2001).

The yearly temperature anomaly maps in the southern hemisphere (Plate 4.8) do not exhibit the same warming trend observed in the northern hemisphere. What is of great interest, however, is the presence of alternating negative and positive temperature anomalies around the continent, especially at the ice edges. Such anomalies are again coherent with the sea ice cover anomalies shown in Plate 4.6. Note that the temperature anomalies beyond the sea ice covered regions (i.e. those of the open ocean and the continent) are also coherent with those observed over sea ice (Plate 4.6). As in the ice anomaly maps, the temperature anomaly maps also show that the influence of the ACW is not just an ice edge phenomenon as previously thought (White & Peterson, 1996). The anomaly patterns also indicate that atmospheric effects play an important role in the variability of the sea ice cover.

Trends in surface temperature are depicted in Plate 4.9a,b for the northern and southern hemispheres, respectively, using results from regression analysis (on a pixel-by-pixel basis) of the monthly anomaly data from 1981 to 2000. The monthly anomaly maps were derived by subtracting monthly climatology from the monthly temperatures in each data element. The trends were also calculated using yearly averages and the results (not shown) are consistent with those from monthly anomalies.

It is interesting to note that if the entire Arctic region ($> 60^{\circ}$N) is divided into two parts by a line along the 180°E meridian, the trends below this line are shown to be distinctly different from those above the line. The trends below the line are generally highly positive (except in Greenland) while those above this line are either slightly positive or negative. The high positive values are located primarily in northern Canada and the Beaufort Sea while negative values are located in either the Bering Sea or Russia. This spatial distribution of the trends is coherent with observed changes in the sea ice cover in the northern hemisphere. Regionally, negative trends in the Bering Sea are consistent with positive trends in the ice cover in the same region while positive trends in areas that include the Chukchi Sea, the Beaufort Sea, the Canadian Archipelago and northern Canada are correlated with an observed decline of the sea ice cover in the same general location. It is also apparent that the warming trend extends further to the south of the periphery of the western Arctic Ocean region indicating a general warming over a much more extensive region than the sea ice covered area.

In the Antarctic, the spatial distribution of trends (Plate 4.9b) is quite different from that of the Arctic in that although there is a predominance of positive values over sea ice covered regions, relatively large negative values are apparent in a large part of the continent, especially at the higher elevations in east Antarctica. Similar

trends were reported in Comiso (2000) and Doran et al. (2002). It is apparent that the highest positive trends are located in the Bellingshausen/Amundsen Seas where the sea ice cover has been retreating at a relatively high rate. As indicated earlier, the region, together with the western part of the Antarctic Peninsula, has been referred to as a region of climate anomaly (King, 1994; Jacobs & Comiso, 1997). The same region has been shown to be highly correlated with ENSO indices, suggesting strong connection of the trend with the large ENSO event in 1998. It is interesting to note that negative anomalies are mainly in high elevation areas of both hemispheres. This phenomenon may be associated with the observed cooling in the troposphere as reported by Spencer & Christy (1990).

Because of the high correlation of the sea ice cover with surface temperature, we can make use of long historical data from meteorological stations (Jones et al., 1999) to better understand the trends observed from satellite record which is currently limited to 22 years. While limited in spatial coverage, these data are useful in evaluating temporal variability of the variable over much longer time scales. Monthly anomalies in surface temperatures from meteorological stations in the northern and southern hemispheres are presented in Figs 4.8a and 4.9a. It is apparent that the anomalies are highly variable and that the length of a data record can make a big difference when trend analysis is being conducted. Three record lengths of the same surface-temperature data set from stations located $> 60^{\circ}$N were analysed and the results of trend analysis for the data yielded 0.048 ± 0.004, 0.032 ± 0.09 and 0.545 ± 0.019 K per decade, for the 95- (dotted line), 50- (dashed line), and 20-year (long dashed line) time records, respectively (Fig. 4.8a). The much higher rate for the shorter time period suggests that warming may be accelerating. To gain insight into the issue of record length, a more complete sensitivity analysis was conducted following Comiso (2000). The plot in Fig. 4.8b shows the variation of trend with record length and indicates that the trend tends to fluctuate greatly at the beginning and up to about 15 years. The trend then becomes relatively stable and declines exponentially from around 1985 through the 1930s. In the 1930s the trend becomes negative but slowly increases to positive values again. The plot shows that at least 15–20 years of data are needed for a meaningful trend analysis. The use of 20 or more years of satellite data for trend analysis is thus justified. However, the negative trends for record lengths between 65 and 70 years which are associated with the high surface-temperature anomalies in the 1930s can be viewed as a serious complication. The trend from a longer-term satellite data of about 65 to 70 years may actually be opposite in sign to that from a record length of 100 years or more, which is usually what is used in the analysis of station data. This raises the issue of possible effects of cyclical patterns and the ability to do trend analysis effectively even for a relatively long satellite record.

The result of a spectral analysis on the long-term surface-temperature data is presented in Fig. 4.8c. Cyclical patterns similar in period to the second peak (12 years) in the plot have been detected in the region using sea level pressure data, e.g. the North Atlantic Oscillation (Mysak, 1999) and the Arctic Oscillation (Thompson & Wallace, 1998; Polyakov et al., 1999). The vertical line corresponds to the 95%

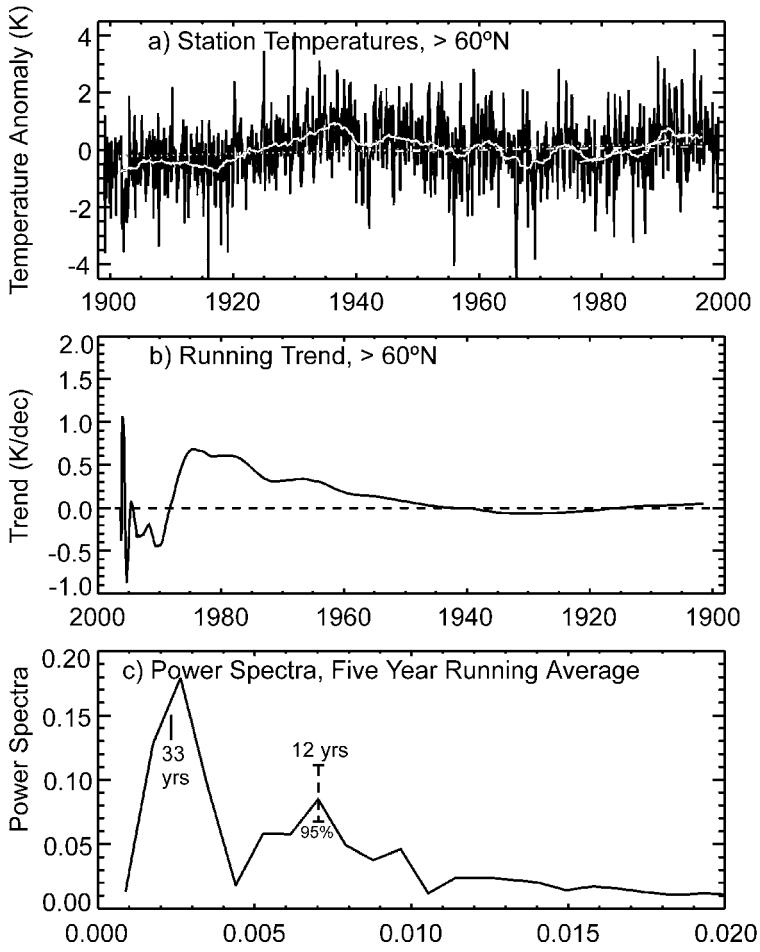

Fig. 4.8 (a) Monthly surface air temperature anomalies in the northern hemisphere for stations located at latitudes > 60°N with trend lines for 1900–98 (dotted line), 1948–98 (dashed line) and 1978–98 (long dashed line) periods; (b) trends versus record length starting with the year 1998; (c) power spectra using five-year running average data.

confidence limit. Periodic changes in pressure fields causes the atmospheric circulation in the Arctic to change from cyclonic to anticyclonic mode, and vice versa (Proshutinsky & Johnson, 1997). It is interesting to note that a peak at 33 years comes out predominantly in the spectral analysis. It is possible that the observed negative trends for record lengths of about 65–70 years, as shown in Fig. 4.8b, are associated with this cycle. In interpreting trend results, the existence of these periodic cycles has to be taken into consideration.

In the southern hemisphere, the temperature anomaly distribution is quite different from that of the Arctic. The trend results are also different for the three periods, being -0.017 ± 0.003, -0.025 ± 0.004 and -0.031 ± 0.009 K per decade for the 95-, 50- and 20-year record lengths, respectively (Fig. 4.9a). The negative

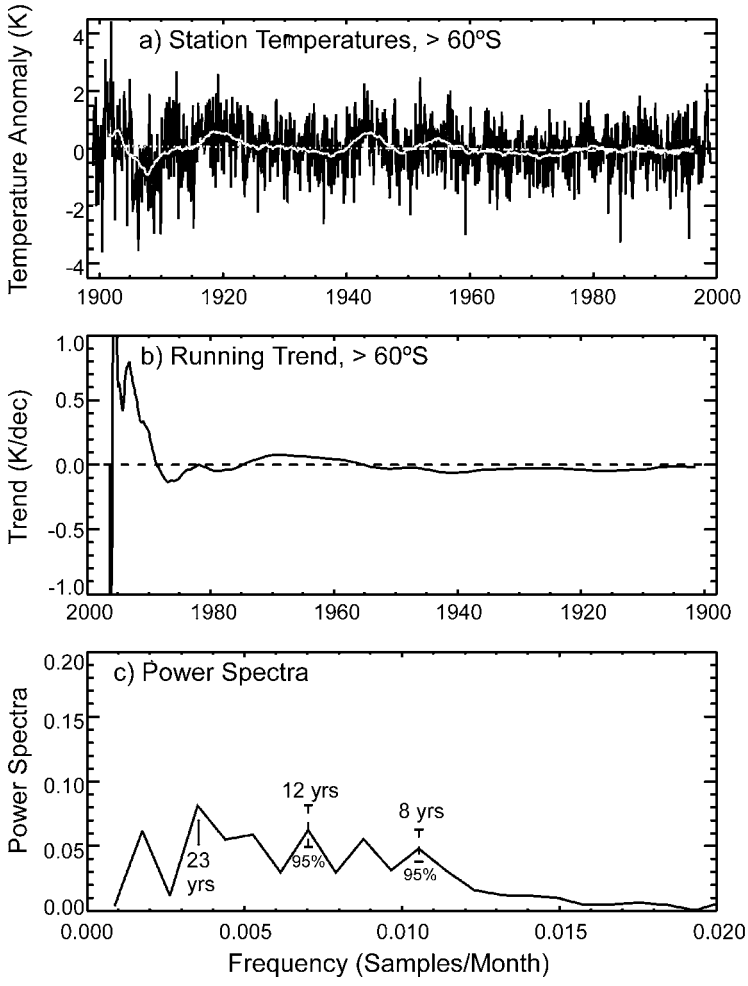

Fig. 4.9 (a) Monthly surface air temperatures anomalies in the southern hemisphere for stations located at latitudes > 60°N with trend lines for 1900–98 (dotted line), 1948–98 (dashed line) and 1978–98 (long dashed line); (b) trends versus record length starting with the year 1998; (c) power spectra using five-year running average data.

values for these three intervals is consistent with an expanding ice cover. A running trend plot similar to that for the Arctic is shown in Fig. 4.9b and indicates that after 15–20 years, the trend values stabilize, although fluctuate slowly from negative to positive and back to negative again. The estimated negative trend for a 20-year record is consistent with the results from satellite temperature and ice data. From 1950 to around 1970 (corresponding to record lengths of about 25–45 years), the trend is estimated to be positive. Such a positive trend is consistent with the observed decline in the ice cover from the 1950s and 1960s to the present as inferred from ship and whaling data sets by De la Mare (1998). While analysis of whaling data has its

problems, including the possible inconsistency in the identification of the ice edge, the correlation of the reported trend in ice edge location with surface-temperature trend is intriguing. The result of spectral analysis on the Antarctic temperature data, shown in Fig. 4.9c, indicates a more complex scenario in the Antarctic region than in the Arctic but a peak at 8 years, consistent with the periodicity of the ACW, is revealed. Further research is needed to better understand the cyclic patterns.

4.6 Summary

More than two decades of satellite data are now available for detailed study of the large-scale characteristics and changing state of the sea ice cover in both northern and southern hemispheres. Satellite passive microwave data provide, day and night, almost continuous observation of the global sea ice cover thereby enabling quantitative variability studies at various time and spatial scales. Despite relatively coarse sensor resolution, spatial detail is provided through the use of sea ice concentrations which are derived using an algorithm that determines the fraction of ice and open water within each satellite footprint. Satellite infrared data provide day/night coverage as well but are limited to only cloud-free conditions. However, the sampling statistics for this data are high and the results provide the only spatially detailed distributions of surface temperatures in the polar regions that have good enough accuracies to detect interannual changes in all regions. High-resolution satellite data are also shown to be useful in studies of small-scale characteristics and seasonal changes in the physical properties of the ice cover.

Large seasonal fluctuations in the ice extent and area are apparent, with those of the southern hemisphere having larger amplitudes but a less symmetrical seasonal distribution than those of the northern hemisphere. The large-scale interannual variability of the ice cover has been evaluated globally as well as regionally, and in the northern hemisphere, the yearly anomaly maps show large interannual variability and a predominance of positive values in the 1980s and negative values in the 1990s. Yearly anomaly maps of surface temperatures show similar anomalies but with opposite sign indicating a strong link between the ice cover and surface temperatures. In the Antarctic, large year-to-year anomalies in the ice cover are also observed but they follow a pattern of alternating positive and negative anomalies around the continent. Similar patterns are observed in the yearly surface ice temperature anomaly maps that, together with the ice data, show consistency with a propagating ACW that circles the oceans around Antarctica.

Globally, the sea ice cover is shown to be on a decline in the northern hemisphere while only minimal changes are observed in the southern hemisphere. Regression analysis shows that the ice extent and ice area in the northern hemisphere are declining at the rate of $-2.0 \pm 0.3\%$ and $-3.1 \pm 0.3\%$ per decade, respectively, but there are regions like the Bering Sea with positive trends. The rate of decline in extent is strongest in the summer at $-4.1 \pm 0.9\%$ per decade and weakest in the winter at $-0.8 \pm 0.5\%$ per decade.

The most remarkable result, however, is the rapidly declining state of the Arctic perennial sea ice cover, the rate of decline being -6.4 ± 2.1 and $-8.5 \pm 2.0\%$ per decade for ice extent and ice area, respectively. Such results are important in that the perennial ice cover consists mainly of the thick multi-year ice cover that basically controls the thickness distribution and limits the retreat of the ice during the summer. A sustained decline at this rate could mean the disappearance of the perennial ice in this century and profound changes in the Arctic Ocean and its environment. It should be noted as well that in consolidated ice regions, the average temperature during the summer has been increasing at about 1.2 ± 0.6 K per decade indicating a longer melt season and therefore decreasing ice volume (Hakkinen & Mellor, 1990).

In the southern hemisphere, the sea ice cover is highly variable but the predictability depends on how well the processes in the region are understood. Alternating negative and positive anomalies occur around the periphery of the ice-covered region, and year-to-year changes confirm the presence of an ACW that propagates in a clockwise direction around the continent. Both ice and temperature anomalies are highly correlated indicating that these two parameters are indeed closely linked with each other. The year-to-year changes in the anomaly patterns are, however, not always in line with that expected from the ACW, indicating that the ice cover is not so predictable on a year-by-year basis.

With the observed negative trends in ice cover in the Arctic, the trends in the Antarctic regions are surprisingly positive at $0.5 \pm 0.4\%$ per decade. While counter intuitive, a negative trend for the Antarctic during a scenario of global warming has actually been predicted (Manabe et al., 1992). The yearly surface temperature anomaly maps in the region, however, show interesting patterns while the trend map shows cooling in the continent. Trend results in the Bellingshausen/Amundsen Seas sector, however, show a strong negative decline at $-8.1 \pm 1.4\%$ per decade confirming previous suggestions that the climate of the region, including that of the Antarctic Peninsula, is different from that of the rest of the Antarctic region. The big rate of decline is compensated for by a big rate of increase ($7.0 \pm 1.0\%$ per decade) in the adjacent Ross Sea sector. The good correlation of ENSO indices with climate anomalies in these regions, as observed by Kwok & Comiso (2002), suggests that the sea ice anomalies may be in part influenced by recent ENSO episodes. The positive trend in the Ross Sea ice cover also suggests a more important role of the Ross Sea region as a source of global bottom water.

The relatively long data records of surface temperatures from meteorological stations are used as a proxy to gain insights into the variability and observed trends in the ice cover. Trend results are shown to vary with record lengths and although they become stable after about 15–20 years they can change sign even for relatively long records such as those observed for 65–70 years of record in the Arctic. Interpretation of trends should thus be done in the context of observed cyclic patterns, which could affect our ability to accurately predict future behaviour of the sea ice cover. Future challenges include a better understanding of these cyclical patterns and how they can be accounted for in trend studies.

Acknowledgments

The author is grateful to Rob Gersten and Larry Stocks for excellent programming support. This work was supported by NASA's Cryospheric Process Program and the Earth Science Enterprise. He is also indebted to GSFC collegues including J. Zwally, P. Gloersen, C. Parkinson and D. Cavalieri who initiated the compilation of satellite polar climate data sets and to NSIDC of the University of Colorado for continuing the effort and providing up-to-date data sets.

References

Allison, I. (1981) Antarctic sea ice growth and oceanic heat flux. *IAHS Publication*, **131**, 161–170. International Association of Hydrological Sciences, Guildfold, UK.

Bjørgo, E., Johannessen, O.M. & Miles, M.W. (1997) Analysis of merged SSMR-SSMI time series of Arctic and Antarctic sea ice parameters 1978–1995. *Geophysical Research Letters*, **24**, 413–416.

Budyko, M.I. (1966) Polar ice and climate. In: *Proceedings of the Symposium on the Arctic Heat Budget and Atmospheric Circulation*, (Ed. J.O. Fletcher), pp. 3–32. RM 5233-NSF. Rand Corporation, Santa Monica, California.

Carsey, F.D. (Ed.) (1992) *Microwave Remote Sensing of Sea Ice*. American Geophysical Union, Washington, D.C. *Geophysical Monograph*, **68**.

Cavalieri, D.J. & Parkinson, C.L. (1987) On the relationship between atmospheric circulation and the fluctuations in the sea ice extents of the Bering and Okhotsk seas. *Journal of Geophysical Review*, **92**, 7141–7162.

Cavalieri, D.J., Gloersen, P., Parkinson, C., Comiso, J.C. & Zwally, H.J. (1997) Observed hemispheric asymmetry in global sea ice changes. *Science*, **278**, 1104–1106.

Comiso, J.C. (2000) Variability and trends in Antarctic surface temperatures from in situ and satellite infrared measurements. *Journal of Climate*, **13**, 1674–1696.

Comiso, J.C. (2002) A rapidly declining perennial sea ice cover in the Arctic. *Geophysical Research Letters*, **29**, DOI: 1029/2002GL015650.

Comiso, J.C., Cavalieri, D.J., Parkinson, C.L. & Gloersen, P. (1997) Passive microwave algorithms for sea ice concentrations. *Remote Sensing of the Environment*, **60**, 357–384.

Comiso, J.C. & Gordon, A.L (1998) Interannual variabilities of summer ice minimum, coastal polynyas, and bottom water formation in the Weddell Sea. In: *Antarctic Sea Ice: Physical Properties and Processes*, (Ed. M.O. Jeffries), American Geophysical Union, Washington, D.C. *Antarctic Research Series*, **74**, 293–315.

Comiso, J.C., Grenfell, T.C., Lange, M., Lohanick, A., Moore, R. & Wadhams, P. (1992) Microwave remote sensing of the Southern Ocean ice cover. In: *Microwave Remote Sensing of Sea Ice*, (Ed. F.D. Carsey), American Geophysical Union, Washington, D.C. *Geophysical Monograph*, **68**, 243–259.

Comiso, J.C. & Steffen, K. (2001) Studies of Antarctic sea ice concentrations from satellite data and their applications. *Journal of Geophysical Research*, **106**, 31362–31385.

Comiso, J.C., Wadhams, P., Pedersen, L.T. & Gersten, R. (2001) The seasonal and interannual variability of the Odden and a study of environmental effects. *Journal of Geophysical Research*, **106**, 9093–9116.

De la Mare, W.K. (1997) Abrupt mid-twentieth-century decline in Antarctic sea ice extent from whaling records. *Nature*, **389**, 57–60.

Doran, P.T., Priscu, J.C., Lyons, W.B., Walsh, J.E., Fountain, A.G., McKnight, D.M., Moorhead, D.L., Virginia, R.A., Wall, D.H., Clow, G.D., Fritsen, C.H., McKay, C.P. & Parsons, A.N. (2002) Antarctic temperature cooling and terrestrial ecosystem response. *Nature*, **415**, 517–520.

Drinkwater, M.R. & Lytle, V.I. (1997) ERS 1 radar and field-observed characteristics of autumn freeze-up in the Weddell Sea. *Journal of Geophysical Research*, **102**, 12593–12608.

Eicken, H., Lange, M.A. & Dieckmann, G.S. (1991) Spatial variability of sea-ice properties in the Northwestern Weddell Sea. *Journal of Geophysical Research*, **96**, 10603–10615.

Fetterer, F.M., Drinkwater, M.R., Jezek, K.C., Laxon, S.W.C., Onstoot, R.G. & Ulander, L.M.H. (1992) Sea ice altimetry. In: *Microwave Remote Sensing of Sea Ice*, (Ed. F.D. Carsey), American Geophysical Union, Washington, D.C. *Geophysical Monograph*, **68**, 111–135.

Gloersen P., Campbell, W.J., Cavalieri, D.J., Comiso, J.C., Parkinson, C.L. & Zwally, H.J. (1992) *Arctic and Antarctic Sea Ice, 1978–1987: Satellite Passive Microwave Observations and Analysis*. NASA Special Publication, **511**, 289 pp. National Aeronautics and Space Administration, Washington, D.C.

Gordon, A.L. & Comiso, J.C. (1988) Polynyas in the Southern Ocean. *Scientific American*, **256**, 90–97.

Grenfell, T.C., Comiso, J.C., Lange, M.A., Eicken, H. & Wenshahan, M.R. (1994) Passive microwave observations of the Weddell Sea during austral winter and early spring. *Journal of Geophysical Research*, **99**, 9995–10010.

Gunn, J.T. & Muench, R.D. (2001) Observed changes in Arctic Ocean temperature structure over the past half decade. *Geophysical Research Letters*, **28**, 1035–1038.

Hakkinen, S. & Mellor, G.L. (1990) One hundred years of Arctic ice cover variations as simulated by a one-dimentional, ice–ocean model. *Journal of Geophysical Research*, **95**, 15959–15969.

Hanna, E. (2001) Anomalous peak in Antarctic sea-ice area, winter 1998. *Geophysical Research Letters*, **28**, 1595–1598.

Jacobs, S.S. & Comiso, J.C. (1997) A climate anomaly in the Amundsen and Bellingshausen Seas. *Journal of Climate*, **10**, 697–709.

Johannessen, O.M., Shalina, E.V. & Miles, M.W. (1999) Satellite evidence for an Arctic sea ice cover in transformation. *Science*, **286**, 1937–1939.

Jones, P.D., New, M., Parker, D.E., Martin, S. & Rigor, I.G. (1999) Surface air temperature and its changes over the past 150 years. *Reviews in Geophysics*, **37**, 173–199.

King, J.C. (1994) Recent climate variability in the vicinity of the Antarctic peninsula. *International Journal of Climatology*, **14**, 357–369.

Kukla, G.J. & Gavin, J. (1981) Summer ice and carbon dioxide. *Science*, **214**, 497–503.

Kwok, R. & Comiso, J.C. (2002) Southern ocean climate and sea ice anomalies associated with the Southern Oscillation. *Journal of Climate*, **15**, 487–501.

Kwok, R., Comiso, J.C. & Cunningham, G. (1996) Seasonal characteristics of the perennial ice cover of the Beaufort Sea. *Journal of Geophysical Research*, **101**, 28417–28439.

Kwok, R., Schweiger, A., Rothrock, D.A., Pang, S. & Kottmeier, C. (1998) Sea ice motion from satellite passive microwave imagery assessed with ERS SAR and buoy motions. *Journal of Geophysical Research*, **103**, 8191–8214.

Ledley, T.S. & Huang, Z. (1997) A possible ENSO signal in the Ross Sea. *Geophysical Research Letters*, **24**, 3253–3256.

Manabe, S., Spelman, M.J. & Stouffer, R.J. (1992) Transient responses of a coupled ocean–atmosphere model to gradual changes of atmospheric CO_2. Part II, Seasonal response. *Journal of Climate*, **5**, 105–126.

Markus, T., Kottmeier, C. & Fahrback, E. (1998) Ice formation in coastal polynyas in the Weddell Sea and their impact on oceanic salinity. In: *Antarctic Sea Ice: Physical Processes, Interactions and Variability*, (Ed. M.O. Jeffries), American Geophysical Union, Washington, D.C. *Antarctic Research Series*, **74**, 273–291.

Massom, R.A., (1991) *Satellite Remote Sensing of Polar Regions*. Belhaven Press, London.

Massom, R.A., Comiso, J.C., Worby, A.P., Lytle, V. & Stock, L. (1999) Satellite and *in situ* observations of regional classes of sea ice cover in the East Antarctic pack in winter. *Remote Sensing of the Environment*, **68**, 61–76.

Mysak, L.A. (1999) 1. Interdecadal variability at northern high latitutes. In: *Beyond El Niño: Decadal and Interdecadal Climate Variability*, (Ed. A. Navarra), pp. 1–24. Springer-Verlag, New York.

Parkinson, C.L., Cavalieri, D.J., Gloersen, P., Zwally, H.J. & Comiso, J.C. (1999) Arctic Sea ice extents, areas, and trends, 1978–1996. *Journal of Geophysical Research*, **104**, 20837–20856.

Parkinson, C.L., Comiso, J.C., Zwally, H.J., Cavalieri, D.J., Gloersen, P. & Campbell, W.J. (1987) *Arctic Sea Ice 1973–1976 from Satellite Passive Microwave Observations*. NASA Special Publication **489**, 296 pp. National Aeronautics and Space Administration, Washington, D.C.

Petersen, R.G. & White, W.B. (1998) Slow oceanic teleconnections linking the Antarctic Circumpolar Wave with tropical El-Niño–Southern Oscillation. *Journal of Geophysical Research*, **103**, 24573–24583.

Polyakov, I.V., Proshutinsky, A.Y. & Jackson, M.A. (1999) Seasonal cycles in two regimes of Arctic climate. *Journal of Geophysical Research*, **104**, 25761–25788.

Proshutinsky, A.Y. & Johnson, M.A. (1997) Two circulation regimes of the wind-driven Arctic Ocean. *Journal of Geophysical Research*, **102**, 12493–12514.

Rothrock, D.A., Yu, Y. & Maykut, G.A. (1999) Thinning of the Arctic sea-ice cover. *Geophysical Research Letters*, **26**, 3469–3472.

Shuchman, R.A. & Onstott, R.G. (1990) Remote sensing of the polar oceans. In: *Polar Oceanography: Part A Physical Science*, (Ed. W.O. Smith, Jr), pp. 123–169. Academic Press, San Diego, California.

Smith, W.O., Keene, N.K. & Comiso, J.C. (1988) Potential interannual variability in primary productivity of the Antarctic Marginal Ice Zone. In: *Antarctic Ocean and Resources Variability*, (Ed. D. Sahrhage), pp 131–139. Springer, New York.

Spencer, R.W. & Christy, J.R. (1990) Precise monitoring of global temperature trends from satellites. *Science*, **247**, 1558–1562.

Stammerjohn, S. & Smith, R. (1997) Opposing southern ocean climate patterns as revealed by trends in regional sea ice coverage. *Climatic Change*, **37**, 617–639.

Thompson, D.W.J. & Wallace, J.M. (1998) The Arctic oscillation signature in the wintertime: geopotential height and temperature fields. *Geophysical Research Letters*, **25**, 1297–1300.

Tucker, W.B., III, Perovich, D.K., Gow, A.J., Weeks, W.F. & Drinkwater, M.R. (1992) Physical properties of sea ice relevant to remote sensing. In: *Microwave Remote Sensing of*

Sea Ice, (Ed. F. Carsey), American Geophysical Union, Washington, D.C. *Geophysical Monograph*, **68**, 9–28.

Wadhams, P. & Davis, N.R. (2000) Further evidence of ice thinning in the Arctic Ocean. *Geophysical Research Letters*, **27**, 3973–3975.

Walsh, J.E., Chapman, W.L. & Shy, T.L. (1996) Recent decrease of sea level pressure in the Central Arctic. *Journal of Climate*, **9**, 480–486.

Weeks, W.F. & Ackley, S.F. (1986) The growth, structure, and properties of sea ice. In: *The Geophysics of Sea Ice*, (Ed. N. Unterstiener), Plenum Press, New York. *NATO ASI Series B: Physics*, **146**, 9–164.

White, W.B. & Peterson, R.G. (1996) An Antarctic circumpolar wave in surface pressure, wind, temperature, and sea ice extent. *Nature*, **380**, 699–702.

Zwally, H.J., Comiso, J.C. & Gordon, A.L. (1985) Antarctic offshore leads and polynyas and oceanographic effects. In: *Oceanology of the Antarctic Continental Shelf*, (Ed. S.S. Jacobs), American Geophysical Union, Washington, D.C. *Antarctic Research Series*, **43**, 203–226.

Zwally, H.J., Comiso, J.C., Parkinson, C.L., Campbell, W.J., Carsey, F.D. & Gloersen, P. (1983a) *Antarctic Sea Ice 1973–1976 from Satellite Passive Microwave Observations*. NASA Special Publication, **459**. National Aeronautics and Space Administration, Washington, D.C.

Zwally, H.J., Comiso, J.C., Parkinson, C.L., Cavalieri, D.J. & Gloersen, P. (2002) Variability of the Antarctic sea ice cover. *Journal of Geophysical Research*, **107**, 1029–1047.

Zwally, H.J., Parkinson, C.L. & Comiso, J.C. (1983b) Variability of Antarctic sea ice and changes in carbon dioxide. *Science*, **220**, 1005–1012.

Chapter 5

Primary Production in Sea Ice

Kevin R. Arrigo

5.1 Introduction

The extensive pack and fast ice that forms in both Antarctic and Arctic regions provides a unique habitat for polar microbial assemblages (Lizotte, 2001; Lizotte, Chapter 6). Algal communities, in particular, are known to flourish within the distinct microhabitats that are created when sea ice forms and ages. The primary advantage afforded by sea ice is that it provides a platform from which sea ice algae can remain suspended in the upper ocean where light is sufficient for net growth. These autotrophic organisms have a critical role to play in polar marine ecology in both the Arctic and the Antarctic. For example, although rates of primary production (photosynthetic carbon assimilation) by sea ice algae are generally low compared to their phytoplankton counterparts, they are often virtually the sole source of fixed carbon for higher trophic levels in ice-covered waters. Furthermore, sea ice algae have been shown to sustain a wide variety of organisms (Schnack-Schiel, Chapter 7), including krill, through the winter months when other sources of food are lacking. Finally, because of the unique isotopic and biochemical characteristics of sea ice algae (Rau et al., 1991), understanding primary production in sea ice has proven to be important to paleontological studies of global climate over the last glacial cycle (Leventer, Chapter 10; Armand & Leventer, Chapter 11).

Primary production via photosynthesis (as distinct from chemosynthesis) is a complex suite of processes that includes light harvesting, electron transport and carbon fixation. Each part of the process has different sensitivities to environmental conditions and cellular controls. The environmental conditions that have been studied thus far include light intensity and spectral quality, temperature, salinity and nutrient depletion.

Photosynthesis–irradiance (PE) response curves have been the most popular method of studying photoacclimation in sea ice algae. The approach is to measure carbon fixation at a range of light intensities in order to describe the change in rates from light-limited to light-saturated and even light-inhibited conditions. Derived parameters include the light-limited slope (α^*, where photosynthesis is limited primarily by light-harvesting mechanisms), the maximal rate (P^*_m, where enzymatic processes of carbon fixation limit photosynthesis), the photoadaptation parameter

(E_k, the quotient P^*_m/α^*, which tends to respond directly to major irradiance changes), and the slope of light inhibition (β, the negative slope for decreased rates at high irradiance).

These parameters have been compared amongst algae from different systems. Sea ice algae near the surface or within thin ice cover usually have photosynthetic characteristics similar to nearby surface phytoplankton populations. For thicker ice, particularly for high-latitude land-fast ice regions, sea ice algae have been reported to have some of the most extreme low-light adaptations ever recorded, including low E_k, low P^*_m, and high β. These algae flourish beneath several metres of ice and snow, receiving less than 1% of the surface solar irradiance. They show severe photoinhibition at modest light levels and high photosynthetic efficiency at extremely low irradiance. E_k values of $< 10\,\mu$mol photons $m^{-2}\,s^{-1}$ have been reported for bottom ice algae (compared to a typical phytoplankton E_k value of *ca.* 150 μmol photons $m^{-2}\,s^{-1}$). In acclimated algae, the E_k value closely matches average irradiance levels, which is the case for even the low-light sea ice communities.

The extreme low light adaptation is accomplished by an increase in light-harvesting efficiency (a^*) along with an even larger reduction in the maximal photosynthetic rate (P^*_m). Under nutrient-sufficient conditions, these diatom communities can approach theoretical maximum light absorption efficiencies and quantum efficiencies for photosynthesis (0.1 mol C fixed per mol photons absorbed). Thus, light harvesting and electron transport are peaked (maximizing α^*), and P^*_m is reduced to a level that will utilize the energy supplied by light harvesting at typical irradiances.

Under extreme low-light conditions, the photosynthetic apparatus of sea ice algae shows strong signs of acclimation. Accessory photosynthetic pigments (e.g. fucoxanthin and chlorophyll *c* for diatoms) are increased relative to the main photosynthetic pigment, chlorophyll *a* (Chl *a*). This adaptation allows the cell to enhance light harvesting at the wavelengths of light penetrating the ice and snow (green light that Chl *a* is less efficient at absorbing). Accessory pigments that serve a photoprotective role (e.g. β-carotene) are less important in this environment, and concentrations are low relative to Chl *a*. With decreasing light intensity, sea ice diatoms have been observed to increase carbon allocation to glycolipids, which are a component of thylakoid membranes in chloroplasts. Sea ice diatoms also acclimate to low irradiance by increasing the number of photosynthetic units per cell and the concentration of components of the photosynthetic electron transport chain (e.g. plastiquinone).

Carboxylating enzyme activity also varies with light intensity. The primary enzyme for carbon fixation, ribulose bisphosphate carboxylase/oxygenase (RUBISCO), is correlated with P^*_m, and increases per unit biomass as light intensity increases in spring. Alternative carbon fixing pathways are β-carboxylation reactions mediated by phosphoenolpyruvate carboxykinase (PEPCKase) and phosphoenolpyruvate carboxylase (PEPCase). Under light-limited conditions, carbon

fixation by PEPCase and/or PEPCKase can become a significant portion of total carbon fixation by sea ice algae. High β-carboxylation in sea ice algae can be significant for several reasons. The products of β-carboxylation are different from the products of RUBISCO, and they are particularly proficient at providing precursors to lipid synthesis. This capacity may be critical for acclimating membranes to temperature changes or determining carbon storage (lipid or carbohydrate) in nutrient-stressed diatoms. At the peak of blooms, neutral lipids (triglycerides) have been seen to accumulate, presumably as storage compounds accumulating as cell division rates decline. The substrate for β-carboxylation is bicarbonate rather than carbon dioxide; since the former has a higher ^{13}C:^{12}C composition, algae conducting significant β-carboxylation would be expected to have heavier carbon isotopic composition. Sea ice algae have been shown to have a heavier carbon isotopic composition than polar phytoplankton (see Thomas & Papadimitriou, Chapter 9). This isotopic tracer for sea ice algae has been useful in estimating contributions to food webs and export to the benthos.

The spectral quality of light can be greatly altered in an ice column (Eicken, Chapter 2). In the visible wavelength range (400–700 nm, referred to as photosynthetically available radiation, or PAR), spectral narrowing occurs with depth due to higher attenuation of blue and red regions of the solar spectrum by ice and snow. Layers of pigmented algae further narrow the spectrum, primarily due to blue and red peaks in chlorophyll absorbance. Detritus and sediments in the ice tend to shift the spectrum further by attenuating shorter wavelengths. The response of sea ice diatoms to this spectral narrowing (which is usually accompanied by low PAR) is to increase absorption of green light by increasing photosynthetic accessory pigments (fucoxanthin and chlorophyll *c*) and decreasing photoprotective pigments (β-carotene and diatoxanthin).

Ultraviolet (UV) light (280–400 nm) reaching the sea ice surface is attenuated strongly by ice and detritus, and by algal cells containing mycosporine-like amino acid (MAA) sunscreens. The responses of sea ice diatoms to enhanced UV light include increased concentrations of photoprotective pigments, as well as MAAs, though regulation of the latter is not well understood. Fluorescence-based studies also show that UV light, particularly UV-B (280–320 nm), inhibits photosynthesis in sea ice diatoms by diminishing Photosystem II performance, presumably via direct impacts on its binding protein or the primary electron acceptor. During high UV events such as the spring development of the Antarctic ozone hole, increased DNA damage has also been detected, which could also impact recovery of the photosynthetic apparatus.

In this chapter, the relationship between rates of primary production by sea ice micro-algae and the physical structure of the sea ice habitat will be explored. Examples from both the Arctic and the Antarctic regions will be included, noting, where appropriate, key differences and similarities between the two regions. Sea ice is an extremely difficult habitat to sample non-invasively and to obtain reliable *in situ* estimates of primary production. Therefore, particular attention will be paid to

the various ways that researchers have devised to sample and characterize primary production in this unique marine habitat.

5.2 Sea ice as a habitat

In the early stages of pack ice formation in both the Arctic and the Antarctic, dense concentrations of frazil ice can develop rapidly under turbulent conditions as large quantities of heat are extracted from the near-surface ocean during strong wind events (for more detail see Eicken, Chapter 2; Haas, Chapter 3). As winds diminish and the sea surface calms, ice crystals float to the sea surface where they coalesce into semi-consolidated grease ice, and eventually, into thicker nilas and pancake ice (Ackley & Sullivan, 1994; Eicken, Chapter 2). Additional freezing and horizontal movement fuses ice pancakes together to form a continuous ice pack. Frazil ice is more common in the Antarctic than in the Arctic, due primarily to the fact that more first-year ice forms in the southern hemisphere. In summer, the Arctic is covered by approximately $9 \times 10^6\,km^2$ of persistent multi-year ice, compared to only $3.5 \times 10^6\,km^2$ of multi-year ice in the Antarctic (Comiso, Chapter 4). During the winter, the Arctic adds $7 \times 10^6\,km^2$ of annual ice, bringing the total sea ice extent to $16 \times 10^6\,km^2$. The Antarctic, in contrast, produces more than twice as much first-year ice as the Arctic, averaging $15.5 \times 10^6\,km^2$ of new ice per year, and has a greater total sea ice extent of $19 \times 10^6\,km^2$ (Gloersen et al., 1992).

The initial stage of sea ice formation generally begins in the autumn when there are still substantial microbial populations left over in surface waters from the preceding spring blooms. As a result, during frazil ice formation, particles such as micro-algae, heterotrophic protists and bacteria are often scavenged from the water column as the newly formed frazil ice crystals rise to the surface (Garrison et al., 1989). In some cases, particle concentrations in very young frazil ice have been found to be over fifty times greater than in the underlying sea water, with the incorporation of large diatoms being observed most commonly.

Subsequent ice growth beyond the consolidated pancake stage proceeds vertically as heat is extracted from the sea ice surface by the cold atmosphere. This is also true for land-fast ice which does not have an initial frazil ice stage. Columnar ice crystals extend from the lower ice margin into the water column (Fig. 5.1). The lower margin of the growing columnar ice, referred to as the skeletal layer, is highly porous and has a temperature that is just below the freezing point of sea water. Rafting of ice floes as sea ice is moved by the wind and tides causes breakage and occasionally forces parts of the floe below freeboard, flooding the ice surface with sea water. Similarly, heavy snow cover can also force the ice floe below freeboard, resulting in surface flooding.

It is in those regions of the ice floe that are most tightly coupled to the underlying sea water that sea ice micro-algae flourish. This is because one of the primary factors controlling the growth of algae in sea ice is access to nutrients (Thomas &

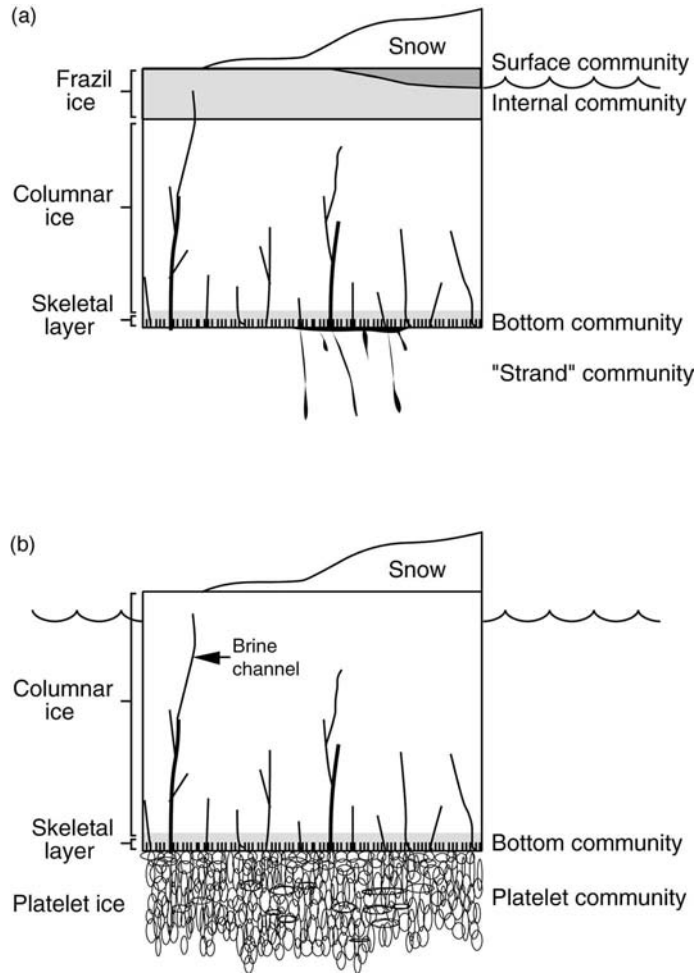

Fig. 5.1 Highly idealized schematic illustration of (a) pack ice and (b) land-fast ice ecosystems in the Arctic and the Antarctic showing the location of the major ice algal communities. Obviously, whether a given community is found in a particular location is highly variable and dependent on the sea ice structure and the formation history.

Papadimitriou, Chapter 9). Except for those areas where snow cover is extremely thick, light is usually sufficient for net photosynthesis during the polar spring and summer (Grossi et al., 1987). Sea ice habitats are often characterized by steep gradients in temperature, salinity, light and nutrient concentration. The greatest fraction of sea ice micro-algae often reside in the bottom 0.2 m of the ice sheet where environmental conditions are generally stable and more favourable for growth. Bottom ice communities form in the skeletal layer and extend upwards as far as 0.2 m, their upward distribution generally being limited by nutrient availability and

the high brine salinity characteristic of the sea ice interior when temperatures are low (Arrigo & Sullivan, 1992).

Under certain conditions, micro-algae may also be found in internal layers, where they are often subjected to large environmental fluctuations (Lizotte & Sullivan, 1991). For example, brines with salinities as high as 173 and temperatures as low as $-16^{\circ}C$ have been collected from the upper 1.0–1.5 m of the sea ice in McMurdo Sound, high enough to prevent detectable metabolic activity in most sea ice algae (Arrigo & Sullivan, 1992). In addition, increasing temperatures in the late spring may result in flushing of relatively fresh melt water through the ice sheet, exposing micro-algae to a low salinity environment. Internal communities are generally associated with a frazil ice layer or can be found at the freeboard level where sea water can infiltrate the ice floe. These communities are seeded by the particles scavenged during frazil ice formation and are especially dependent upon nutrient availability and salinity. They are more common in the Antarctic than the Arctic.

Sea ice micro-algae growing with the microhabitats of pack and land-fast ice are subject to growth limitation by the available light and nutrients. In land-fast ice, the growth of sea ice micro-algae in the skeletal layer is determined primarily by salinity (Arrigo & Sullivan, 1992) and by the thickness of the overlaying snow cover through its effect on vertical light attenuation (Arrigo et al., 1991). In contrast, pack ice algae frequently grow at or near the sea ice surface where light levels are generally high. Under these conditions, pack ice micro-algae were found to have high photosynthetic capacities, comparable to phytoplankton from the same region (Lizotte & Sullivan, 1992). These pack ice photosynthetic capacities are approximately an order of magnitude greater than values reported for land-fast algae (Palmisano et al., 1987; Arrigo et al., 1993b).

Although the surface and near-surface communities often have adequate light levels for growth, the availability of nutrients for these communities is often restricted. Measurements of salinity in the cavity of the freeboard layer indicate that this layer is infiltrated by sea water which provides the nutrients required by the algal community. However, this supply of nutrients depends on the porosity of the surrounding ice. For the algal communities growing at the snow–ice interface, surface flooding, caused by snow loading and submersion of the ice pack, is an important source of nutrients. Such surface flooding occurs over 15–30% of the ice pack in Antarctica (Wadhams et al., 1987). Although snow cover has the negative effect of reducing the amount of light available for algal growth, it is also responsible for providing nutrients to the surface community. This surface community is responsible for the majority of sea ice productivity in Antarctic sea ice (Legendre et al., 1992).

Less common sea ice assemblages include those that grow (1) at the sea ice surface, (2) in a 'strand' layer just beneath the sea ice, and (3) within a sub-ice platelet layer. Surface communities form in regions of the pack that become flooded with sea water, either as a result of rafting or snow loading (Fig. 5.1). These are more common in the Arctic where rafted multi-year ice is more common. Mat and strand

communities, where algae are loosely attached to the underside of the sea ice but extend well into the water column, are found mainly in Arctic regions (Melnikov & Bonderchuk, 1987; Johnsen & Hegseth, 1991). Conversely, platelet ice layers, a semi-consolidated layer of ice ranging from a few centimetres to several metres in thickness, are commonly observed beneath sea ice in regions adjacent to floating ice shelves in the Antarctic where 45% of the continental margin is associated with an ice shelf (Bindschadler, 1990; Kipfstuhl, 1991). Platelet ice is the most porous of all sea ice types, being composed of approximately 20% ice and 80% sea water by volume, and harbours some of the largest concentrations of algae found anywhere on earth.

5.3 Methods for estimating primary production in sea ice

Standard techniques: Algal biomass accumulation

Early estimates of primary production in sea ice were based on the accumulation of algal biomass, generally either Chl *a* or particulate organic carbon, during the growing season. To derive an estimate of production in this way, a station would be sampled repeatedly over time. Because obviously a single core cannot be sampled more than once, multiple cores would be taken from a small area of interest at each point in time. In this way, the spatial variation in a particular location could be quantified, allowing better characterization of changes in algal biomass over time. This technique is well suited to the sea ice habitat because sea ice micro-algae are anchored to the sea ice substrate and, therefore, there is no question that the same population is being sampled repeatedly. In other marine systems, such as the open ocean, advection continually moves algal populations around, making repeated sampling of the same population difficult.

However, this technique is not without its drawbacks. Primary production derived from changes in standing crop are by definition net primary production values, which are necessarily smaller than gross primary production. This is because losses of material due to respiration and exudation are not accounted for by this method. Neither is grazing, which also can result in the loss of newly fixed carbon. Where these losses are important, biomass accumulation may severely underestimate gross primary production. Estimating production via changes in algal biomass accumulation is still of value, however, because it is a simple, straightforward measurement that does not require invasive techniques and because it yields a reliable minimum estimate for primary production, a quantity that itself is of value. Furthermore, it is a direct *in situ* measurement that does not suffer from the problems inherent in many of the more complex, laboratory-based techniques that require removal of the algae from their habitat before productivity can be measured.

Standard techniques: Photosynthesis versus irradiance (PE) determinations

One of the most widely used methods for estimating primary production in sea ice is to collect ice algae from the field, bring them into the laboratory and measure, via ^{14}C-uptake, the maximum photosynthetic rate (or assimilation rate, P^*_m) and the photosynthetic efficiency (α^*) as a function of light intensity. When these photosynthetic parameters are combined with light measurements from the field, estimates of primary production at depth z can be obtained using the equation:

$$P_z = Chl_z\, P^*_m \left[1 - \exp\left(\frac{-\alpha^* E_z}{P^*_m}\right)\right] \qquad \text{(Equation 5.1)}$$

Generally, sea ice micro-algae and the associated microbial community are collected from the ice by removing a core using an ice auger. Because algae in sea ice are often acclimated to low light levels, it is critical that all work done subsequent to bringing the core to the ice surface is carried out in as near darkness as possible. Commonly, core sections are immediately placed into darkened polyethylene sample bottles to which an appropriate quantity of 0.2 μm filtered sea water is added to reduce osmotic shock. Samples must be kept cold until PE determinations take place.

Ice cores are then either allowed to melt, or, to reduce the time between sample collection and PE determination, the algal layer can be removed from the core, often by scraping, so that it can be separated from the ice matrix more quickly. Once this step is complete, algal samples are thoroughly but gently mixed, and a sub-sample is removed and spiked with ^{14}C bicarbonate. After mixing the sub-sample to distribute the radio-labelled bicarbonate evenly, a number of aliquots of algal suspension are removed and placed into separate incubation vessels, often glass or polycarbonate scintillation vials. These are to be the treatment sub-samples which are all incubated at different irradiance levels. Additional aliquots of algal suspension are used for time zero controls and for dark corrections. All samples (consisting of treatment sub-samples, dark uptake samples and time zero controls) are placed in the appropriate chamber of a darkened, pre-cooled (-2°C) photosynthetron and allowed to pre-incubate for 10 minutes. Time zero controls are then removed and any biological activity stopped by the addition of acid. The treatment sub-samples are illuminated and allowed to incubate for an appropriate period of time, usually a few hours.

After liquid scintillation counting and conversion of counts to primary productivity units (often mg C mg^{-1} Chl *a* h^{-1}), the data are plotted against PAR and fitted to an appropriate PE curve (e.g. Monod, hyperbolic tangent, etc.) to yield the photosynthetic parameters P^*_m, α^* and E_k. Once these parameters are known, they can be used in Equation 5.1 to estimate primary productivity at any depth, z, within the sea ice, assuming that the light levels and Chl *a* concentration within the ice at

that depth are known. Integration of Equation 5.1 over depth will then yield an estimate of the total sea ice primary production ($mg\,C\,m^{-2}$).

A significant problem with estimating primary productivity in sea ice using this approach is that the spectral quality of the light source used to estimate P^*_m and α^* is often very different from that within the sea ice. Incubation light sources are usually weighted towards the red end of the visible spectrum, while *in situ* radiation is dominated by blue or green wavelengths. Even though the amount of PAR measured under both circumstances may be equal, photosynthetic pigments produced by the algae are much more efficient at absorbing blue light than red light. As a result, the value derived for α^* (P^*_m is insensitive to spectral quality) is often underestimated during PE determinations.

One way to compensate for this effect is to apply a spectral filter to the light source used during the incubations so that it mimics the *in situ* light field the algae would be exposed to. Although this correction is simple to implement, it cannot completely account for the fact that the spectral light distribution changes with depth within the ice. Above the algal layer, it is dominated by the blue wavelengths that are readily absorbed by algal pigments. Further down, however, selective absorption of the blue wavelengths by algae results in a spectral light distribution that is dominated by green light. In this case, the value of α^* derived during PE determinations will be greater than that actually expressed by algae *in situ* and productivity will be overestimated accordingly. This correction works best under conditions where algal biomass is low and hence the spectral distribution of the incident light is not changing rapidly with depth within the algal layer. In this case, the α^* will be more appropriate to all depths within the algal layer, and not just those near the surface.

A better, albeit more difficult, approach to correct this problem is to apply a spectral correction to the PE-derived estimate of α^* so that it better represents *in situ* values (Arrigo & Sullivan, 1992). To do so, the fact that α^* is a function of the quantum yield of photosynthesis (ϕ_p) and the algal absorption coefficient (a^*) can be exploited. This correction requires, however, that both the spectral output of the incubator light source and the *in situ* spectral irradiance distribution, as well as the absorption spectrum of the algae, are reasonably well known. Assuming that ϕ_p remains constant, then the *in situ* value for α^* is calculated as

$$\alpha^*_{\text{in situ}} = \alpha^*_{\text{incubator}} \frac{a^*_{\text{in situ}}}{a^*_{\text{incubator}}} \qquad \text{(Equation 5.2)}$$

All that is needed then is to calculate $a^*_{\text{incubator}}$ and $a^*_{\text{in situ}}$ according to the relationship

$$a^* = \frac{\int_{400}^{700} a(\lambda)\, E(\lambda)\, d\lambda}{\int_{400}^{700} E(\lambda)\, d\lambda} \qquad \text{(Equation 5.3)}$$

where $a^*(\lambda)$ is the algal absorption spectrum and $E(\lambda)$ is either the spectral output of the incubator (when a^* will be $a^*_{\text{incubator}}$) or the spectral light distribution within the sea ice (when a^* will be $a^*_{\text{in situ}}$).

Although this may seem to be overly complicated, it is the only way to accurately estimate *in situ* α^* and derive a reasonable estimate of sea ice primary production. Plus, the measurements required to make this correction are becoming increasingly common. Determination of algal absorption spectra is almost routine and measurements of spectral irradiance associated with sea ice are more readily available. Even if measurements of spectral irradiance within the ice are not obtained directly, simple radiative transfer models exist which allow these quantities to be estimated with sufficient accuracy for the purposes of determining primary production (Perovich, 1990; Arrigo et al., 1991).

Unfortunately, despite the widespread knowledge that photosynthetic parameters measured in the laboratory do not always accurately reflect *in situ* values, parameter values in the literature are seldom spectrally corrected. This makes comparison across studies problematic and renders the data difficult to use for estimating rates of primary production. At a minimum, studies reporting photosynthetic parameters should give the type of incubation light source used. It would be even better if the spectral output of the light source were provided, along with a measurement of spectral absorption by the algae being studied.

Minimally invasive techniques: Oxygen microelectrodes

The ideal approach, but one that does not currently exist, would be to directly measure primary productivity *in situ*, without disrupting the algae or their sea ice habitat. New developments are coming closer to this ideal, although it has not yet been attained. Recently, oxygen (O_2) microelectrodes have been used to measure the photosynthetic rates of Antarctic fast ice algae in virtually intact cores, without having to seriously disrupt the algal community (McMinn & Ashworth, 1998; Rysgaard et al., 2001). With this approach, the bottom 0.2 m of the core is placed in a temperature-controlled water bath into which 0.2 μm filtered sea water is added. Ice cores are placed bottom-up in the water bath and illuminated from below so that O_2 concentrations can be easily measured across the diffusive boundary layer. After turning off the seawater circulation system of the tank, an O_2 microprobe, a temperature mini-sensor and a light electrode mounted on a slide track are slowly lowered vertically through the diffusive boundary layer until they reach the ice sample. Data are recorded on a computer and the resulting O_2 profile is used to estimate the O_2 flux from the sea ice using Fick's first law of diffusion:

$$J = D_0 \frac{\partial C}{\partial X} \qquad \text{(Equation 5.4)}$$

where D_0 is the molecular diffusion coefficient (1.14×10^{-5} cm^{-2} s^{-1} at -1°C), ∂C is the change in O_2 concentration across the diffusive boundary layer and ∂X is the effective thickness of the diffusive boundary layer, as deduced from the vertical O_2 profile. By repeating the experiments at a variety of light intensities, and by using dark controls to correct for respiration, PE relationships can be evaluated just as they are using the ^{14}C approach.

There are a number of shortcomings to this method, however. First, algae in the sea ice are distributed heterogeneously and it is assumed that the O_2 profile generated by this method averages over this variability, although this has not yet been demonstrated. Second, the act of inserting the sampling apparatus through the diffusive boundary layer reduces by 25–45% the thickness of that layer, altering the actual O_2 flux. Fortunately, this effect is minimized where O_2 gradients are small and when there is no fluid flow around the tip of the O_2 probe. Trenerry et al. (2002) have shown that variations in the method for estimating the thickness of the diffusive boundary layer did not significantly affect the measurements of O_2 flux using this technique. Given these caveats, this method is likely to be accurate to within $\pm$ 20%. Finally, this method is only effective at measuring productivity in bottom ice communities. Internal, surface and platelet ice communities have diffusion paths that are too long to evaluate O_2 diffusion reliably in this manner. However, considering the majority of algal biomass in both the Arctic and the Antarctic is found in the bottom layers of the congelation ice, this method is likely to prove valuable in the future. Early results using this technique were at the lower end of productivity estimates for fast ice and suggest that conventional ^{14}C techniques may overestimate sea ice algal productivity.

Minimally invasive techniques: In situ ^{14}C *incorporation*

A new, truly *in situ*, incubation technique has been developed to measure primary production in a wider variety of sea ice habitats than had been possible previously (Mock & Gradinger, 1999). The concept behind this method is that an ice core can be extracted from either fast or pack ice, sectioned into appropriate segments and placed into individual petri dishes for inoculation with ^{14}C bicarbonate. These petri dishes are then stacked in the order they were collected, placed in an acrylic-glass barrel, and returned to their original position in the ice floe where they are incubated. This method provides fine-scale (1 cm) resolution of primary productivity throughout the ice column without severe disruption of sea ice morphology and ambient light field. Rapid deployment is required, however, to minimize brine drainage and associated nutrient loss.

The primary advantage of this approach is that the algae are incubated under as natural a light field as possible, eliminating the need to correct for spectral quality as is required by the more widely used PE method. In addition, because the algae are incubated *in situ*, they are exposed to the same vertical gradients in temperature and brine salinity as undisturbed populations, resulting in more realistic productivity

estimates. Under conditions where nutrient concentrations are not limiting, this method is likely to yield estimates of primary production that are superior to most other methods.

The major drawback to this technique is the disruption of the ambient nutrient field. Brine tubes and channels can act as conduits in intact sea ice, providing nutrients to the upper layers of the sea ice that are not in intimate contact with underlying sea water. Severing these conduits by sectioning the core could alter the nutrient field and result in unrealistic rates of primary production. Furthermore, sectioning the core to add the radio-labelled bicarbonate could allow any residual nutrients to drain from the core, further depleting nutrient concentrations.

Numerical modelling: One-dimensional models

One of the more complex methods for determining, and understanding, primary production in sea ice is through numerical modelling of the sea ice system. This technique requires a thorough knowledge of both the physics and biology of the sea ice system and, to date, has been applied to very few sea ice habitats, being limited thus far to the fast ice of McMurdo Sound (Antarctica) and the pack ice of the Weddell Sea (Antarctica). Using such numerical models, the complete annual cycle of primary production can be simulated as a function of temperature, salinity, nutrient and light availability to gain a better understanding of the processes controlling algal distributions in sea ice as well rates of primary production.

The most sophisticated model of this type was developed for the combined congelation ice/platelet ice system of McMurdo Sound, Antarctica, using field data collected over a period of more than ten years for calibration and validation (Arrigo et al., 1993a; Arrigo & Sullivan 1994; and references therein). This fully prognostic model simulates the dynamics of algae as a function of predicted changes in the physicochemical characteristics of the sea ice environment.

Physical dynamics

The sea ice in McMurdo Sound is dominated by congelation ice 1–2 m in thickness, often with a layer of platelet ice below. The model simulates the seasonal growth dynamics of congelation ice by solving the appropriate heat balance equations once the congelation ice thickness on September 1 is specified. Because platelet layer growth is not well understood, it is not calculated by the model. Instead, seasonal variation in platelet layer thickness is specified for each run. If a platelet layer is not desired, the thickness of this layer is set to zero.

Congelation ice growth

In the model, the rate of congelation ice growth controls sea ice thickness (H), initial brine entrapment and convection within the skeletal layer. The growth rate is

determined by the conductive removal of latent heat (F_c) from the ice sheet and the vertical transfer of sensible heat from the relatively warm sea water to the bottom of the ice sheet (F_w)

$$\frac{dH}{dt} = \frac{1}{-\rho_i L}(F_c + F_w) \qquad \text{(Equation 5.5)}$$

where L is the latent heat of melting and ρ_i is the depth-averaged sea ice density. Sea ice thickness increases when the extraction of latent heat from the ice sheet exceeds the input of sensible heat from the water column; when, $F_c + F_w > 0$, ice thickness decreases.

Geophysical properties

Many of the chemical, thermal and optical characteristics of sea ice are influenced by its temperature (T_i), salinity (S_i), density (ρ_i), brine density (ρ_b), brine salinity (S_b), and brine volume (V_b), all of which are computed in the model. Some of these properties are also important in determining the physiological responses of micro-algae which inhabit the ice.

Nutrient flux

As brines flow out of the sea ice via gravity drainage, they are replaced by sea water flowing into the ice to replace them, providing a source of new nutrients for the algal populations. Unfortunately, there are still insufficient data to develop a functional relationship between the physical properties of sea ice (e.g. growth rate) and the brine flux from brine channels. Therefore, a constant mean flux volume rate from brine tubes due to gravity drainage, F_{vb}, of 10^{-6} cm s^{-1} has been used in the model. F_{vb} is used to calculate the depth-dependent transport T_b (mmol m^{-3} s^{-1}) of nutrient N (mmol m^{-3}) for those layers within the congelation ice that are influenced by brine tube convection:

$$T_b = 0.0001 f_b F_{vb} z_b \frac{\partial^2 N}{\partial x^2} \qquad \text{(Equation 5.6)}$$

where 0.0001 converts units from centimetres squared to metres squared, f_b is the fraction of the ice under-surface covered by brine tubes (0.05), z_b is the vertical distance over which sea ice is influenced by brine tube convection (depths where $V_b > 70‰$), and x is the vertical dimension of layer z.

Convection also occurs in the skeletal layer of an actively growing ice sheet as cold dense brine flows out from between the skeletal layer plates and is replaced by sea water. Assuming that the outflow of brine is replaced by an equivalent amount of sea water, the rate of convective exchange has been used to infer the degree of

nutrient replenishment within the skeletal layer. The flux volume of brine from the skeletal layer, F_{vs} (cm s^{-1}), is dependent upon the temperature gradient according to the relationship:

$$F_{vs} = 9.677 \times 10^{-9} + 4.49 \times 10^{-6} \frac{dH}{dt} - 1.39 \times 10^{-7} \left(\frac{dH}{dt}\right)^2 \qquad \text{(Equation 5.7)}$$

F_{vs} is used to calculate nutrient transport in the skeletal layer using the equation

$$T_s = 0.0001 f_s F_{vs} z_s \frac{\partial^2 N}{\partial x^2} \qquad \text{(Equation 5.8)}$$

where f_s is the fraction of the skeletal layer surface which is open to convection (0.5) and z_s is the vertical depth of the skeletal layer (20 mm).

Within the porous platelet layer, the rate of nutrient transport at depth z, T_p, is calculated as

$$T_p = T_m \frac{\partial^2 N}{\partial x^2} \qquad \text{(Equation 5.9)}$$

where the bulk transport coefficient, T_m, is 0.37 m^2 s^{-1}.

Radiative transfer

Spectral downwelling irradiance just beneath the ice (or snow if present) surface, E_{0-}, is determined as the sum of the direct, E_{sun}, and diffuse, E_{sky}, components after accounting for specular reflection (R_{sun} and R_{sky}):

$$E_{0-} = (1 - R_{sun})E_{sun} + (1 - R_{sky})E_{sky} \qquad \text{(Equation 5.10)}$$

where $R_{sky} = 0.05$ and R_{sun} is a function of the sun's angle. E is attenuated by snow or ice according to the Beer–Lambert law:

$$E = E_{0-} \exp(-Kz) \qquad \text{(Equation 5.11)}$$

where K is the spectral downwelling attenuation coefficient. For snow, K is determined by the attenuation coefficient of snow alone, K_s; for sea ice, K is determined from the optical properties of the ice (K_i) and any particles (K_p) present, such that

$$K = K_i + K_p \qquad \text{(Equation 5.12)}$$

K_i is determined by the brine volume of the ice sheet, and K_p is calculated as

$$K_p = \frac{a_m + a_d}{\mu} \qquad \text{(Equation 5.13)}$$

where a_m and a_d are the absorption coefficients for micro-algae and detritus, respectively (backscattering has been ignored), and μ is the mean cosine of the angular irradiance distribution (0.656). Micro-algal absorption is determined by the Chl *a*-specific absorption coefficient, a^* ($m^2\,mg^{-1}$ Chl *a*) and the concentration of Chl *a* ($mg\,m^{-3}$) such that

$$a_m = a^* \,\mathrm{Chl}\, a \qquad \text{(Equation 5.14)}$$

Micro-algal dynamics

The rate of change of micro-algae M ($mg\,C\,m^{-3}$) at all depths was calculated as

$$\frac{dM}{dt} = (g - G)M \qquad \text{(Equation 5.15)}$$

where g is the net specific micro-algal growth rate (d^{-1}) and G is the grazing rate (d^{-1}). Because of our poor understanding of grazing within sea ice ecosystems, the magnitude of G is assumed to be a constant fraction of any positive net production. Primary productivity (P, $mg\,C\,m^{-3}\,d^{-1}$) of sea ice micro-algae is simply calculated as

$$P = gM \qquad \text{(Equation 5.16)}$$

When considered together, the effects of temperature, salinity and resource limitation on micro-algal growth rate act multiplicatively. Therefore, algal growth is defined as

$$g = g_{max}\, r_{lim}\, S_g \qquad \text{(Equation 5.17)}$$

where g_{max} (d^{-1}) is the maximum temperature specific micro-algal net growth rate, r_{lim} is a dimensionless term which quantifies resource limitation (light or nutrients), and S_g (dimensionless) describes the dependence of algal growth on salinity. The non-limited temperature-dependent growth rate, g_{max}, is computed from

$$g_{max} = g_0 \exp(r_G T) \qquad \text{(Equation 5.18)}$$

where g_0 (d^{-1}) is the specific growth rate at 0°C (0.059) and r_G ($^\circ C^{-1}$) is a rate constant which determines the sensitivity of g_{max} to changes in temperature (0.06).

The rate of algal growth is determined in part by the availability of a single most limiting resource. Therefore, the maximum specific growth rate is reduced by the resource limitation term, r_{lim}, which is determined by the amount of either light or nutrients at a given depth, whichever is most limiting

$$r_{lim} = \mathrm{MIN}(N_{lim}, \rho) \qquad \text{(Equation 5.19)}$$

where r_{lim} is equivalent to the smaller of the nutrient limitation term, N_{lim}, and the light limitation term, ρ.

The Monod formulation commonly is modified to quantify the limitation imposed by the available concentration of each nutrient (in this case either nitrate or silicate) such that

$$\frac{g}{g_{\max}} = \frac{N}{K_s + N} \qquad \text{(Equation 5.20)}$$

where $(g/g_{\max})$ describes the fraction of the maximum temperature-dependent growth rate allowed by nutrient N and K_s is the half-saturation constant for nutrient N (K_s is 20 for silicate and 0.5 for nitrate) defined as the concentration where $g = 0.5g_{\max}$. Determination of $N_{\lim}$ is made by evaluating Equation 5.20 for each nutrient such that

$$N_{\lim} = \mathrm{MIN}\left(\frac{g}{g_{\max}}\right) \qquad \text{(Equation 5.21)}$$

Light limitation is calculated as

$$\rho = 1 - \exp\left(-\frac{PUR}{E_k'}\right). \qquad \text{(Equation 5.22)}$$

where PUR is the amount of photosynthetically usable radiation and E_k' is the spectral photoadaptation parameter.

Finally, the effects of sub- and supra-optimal salinity on sea ice algal growth are also included. At thermal equilibrium, the salinity of sea ice brine (S_b) is determined directly by temperature; thus colder temperatures at the upper sea ice surface result in higher S_b values. Salinity can have a substantial impact on rates of algal photosynthesis and growth, and appears to act independently of both temperature and resource limitation (Arrigo & Sullivan, 1992). The salinity-dependent growth coefficient, S_g, at a given depth was determined by the least-squares polynomial fit to the data

$$S_g = \alpha_0 + \alpha_1 S_b + \alpha_2 S_b^2 + \alpha_3 S_b^3 \qquad \text{(Equation 5.23)}$$

where S_b is the brine salinity, $\alpha_0 = -1.2073$, $\alpha_1 = 0.07097$, $\alpha_2 = -1.33 \times 10^{-3}$, and $\alpha_3 = 6.342 \times 10^{-6}$.

Most physical and biological rate processes in the model are simulated in 1-day time steps, although some are done more frequently. This temporal resolution is chosen based upon observed doubling times for sea ice micro-algae at temperatures of -1.5°C which are typically in the order of 3–7 days. A vertical resolution of 10 mm is used so that the steepness of physicochemical and biological gradients within the ice sheet can be resolved. Vertical profiles of salinity, Chl *a* and micro-heterotroph abundance are used to initialize each simulation.

Fritsen et al. (1998) modified the above model to simulate algal growth in the

pack ice of the Weddell Sea. The biological component and much of the physics were essentially the same as those developed for McMurdo Sound fast ice. The major modification concerned simulation of the flood–freeze cycles characteristic of some pack ice environments and the effects of this cycle on the physicochemical properties of the ice, including nutrient exchange.

Occasionally, heavy snow cover will force the surface of the ice pack below freeboard, potentially resulting in flooding of the surface snow and ice with sea water. The draft of the sea ice (H_d) is calculated as

$$H_d = \frac{H\rho_i + h_s\rho_s}{\rho_w} \qquad \text{(Equation 5.24)}$$

where ρ_i, ρ_s and ρ_w are the density of sea ice, snow (0.4–0.6 g cm^{-3}, depending on temperature) and sea water (1.028 g cm^{-3}), respectively, and h_s is the snow thickness. When H_d becomes negative, flooding occurs and nutrients are introduced into the ice floe as given in Equation 5.6. This continues as long as the flooded ice and snow remain unfrozen. Soon after flooding, however, freezing begins at the air–snow interface and a freezing front propagates downward at a rate determined by the extraction of heat from the floe. The rate of change in the depth of the freezing front (H_{ff}) within the ice is given as:

$$\frac{dH_{ff}}{dt} = \frac{1}{-\pi\rho_t L}\,(F_c + F_w) \qquad \text{(Equation 5.25)}$$

where π is the porosity of snow/ice at depth H_{ff}. Once this front propagates past a given layer of flooded snow or ice, nutrient exchange within that layer and all layers above ceases. All flooded and frozen snow is now considered to be ice and its thickness is added to H. When the freezing front reaches the bottom of the ice, the ice is no longer considered to be flooded and further sea ice growth is modelled using Equation 5.5. This mechanism has been shown to be an important factor in facilitating the blooms of surface algae in the pack ice of the Weddell Sea.

Numerical modelling: Quasi three-dimensional models

While our understanding of sea ice micro-algal physiology and the sea ice ecosystem continues to increase, little is presently known about either the large-scale horizontal distribution of sea ice algae or their contribution to total regional productivity due to the difficulty inherent in sampling ice-covered regions. Therefore, the physics of the one-dimensional (1-D) models described above were simplified to produce a quasi three-dimensional (3-D) model (no interaction between adjacent grid cells) to investigate the temporal and large-scale horizontal variation in standing crop and rates of primary production of ice algae in the Southern Ocean (Arrigo et al., 1997; 1998b, and references therein).

The spatial domain of this model is based on the Special Sensor Microwave/ Imager (SSM/I) grid. Using daily maps of sea ice concentration, algal productivity and biomass were calculated for any SSM/I pixel with an ice concentration exceeding 50%. Productivity was allowed in either an interfacial (0.02 m thick) layer at the ice–snow interface or within an internal freeboard (0.10 m thick) layer. A uniform (0.10 m thick) ice layer separated the interfacial and freeboard layer. The thickness of each of these layers was held constant for the length of the simulation. Algal growth within interior (other than freeboard) layers and the bottom ice layer was neglected because at the time these communities were thought to represent only a small fraction of pack ice production. It is now known, however, that bottom ice communities in pack ice are more widespread than was thought previously. The model was run with 1-hour time steps at a vertical resolution of 5 mm in the infiltration layer, 10 mm in the freeboard layer, and with a horizontal resolution of 25 km.

The thickness of ice below the freeboard layer was varied spatially in order to represent both relatively thin first-year ice and relatively thick multi-year ice in the model. The initial spatial distribution and thickness of multi-year ice were derived from the SSM/I sea ice distribution at the day of minimum ice extent of February 1989.

First-year ice was given a total thickness of 0.75 m, and multi-year ice was defined as having a total thickness between 0.75 and 1.50 m, depending on age. Daily maps of snow distribution and thickness required by the model were generated every other day using passive microwave imagery from the SSM/I. Both multi-year and first-year ice were initialized on October 1 with a uniform Chl *a* concentration of $1\,\mathrm{mg\,m^{-3}}$, consistent with ice-core observations. During the integration period, any pixel containing freshly formed ice, even if that pixel previously contained multi-year ice, was declared first-year ice with a thickness of 0.75 m and an initial Chl *a* concentration of $1\,\mathrm{mg\,m^{-3}}$.

In the infiltration layer, nutrients were assumed to be equivalent to seawater concentrations when the snow density and snow thickness were sufficient to force the sea ice below sea level (the ice surface became flooded). The amount of snow needed to submerge the ice sheet (hs_{crit}) was calculated as:

$$hs_{\mathrm{crit}} = (h_{\mathrm{s}} - H)\,\frac{\rho_{\mathrm{i}} - \rho_{\mathrm{w}}}{\rho_{\mathrm{s}}} \qquad \text{(Equation 5.26)}$$

When the daily air temperature was above freezing, the density of wet snow ($0.6\,\mathrm{g\,cm^{-3}}$) was used; for dry snow, a density of $0.4\,\mathrm{g\,cm^{-3}}$ was used. The density of sea ice was calculated daily from the brine salinity and brine density. In the freeboard layer, when either the surface flooded or the brine volume exceeded 70‰ nutrients were scaled to the seawater concentrations according to

$$N_{\mathrm{i}} = N_{\mathrm{w}}\frac{S_{\mathrm{b}}}{S_{\mathrm{w}}} \qquad \text{(Equation 5.27)}$$

where N_i and N_w are the nutrient concentrations in the ice and sea water, respectively, and S_w is the sea water salinity. Spatial variation in nutrient concentrations within sea water, which supplies the sea ice, were obtained from annual climatologies. Monthly climatological seawater salinity was interpolated daily.

If the individual criteria for the interfacial and freeboard layer were not met, ice algae within these layers were forced to survive on residual nutrients until the surface flooded or the ice became permeable again. During this time, changes in nutrient concentration were calculated solely as a function of algal uptake, such that

$$\frac{dN}{dt} = gM\frac{N}{C} \qquad \text{(Equation 5.28)}$$

where N is the nutrient concentration (either nitrate, silicic acid or phosphate), g is the algal growth rate (d^{-1}), M (mg C m^{-3} hr^{-1}) is the algal standing crop, and N/C is the Redfield ratio of cellular nutrient to carbon (g:g).

5.4 Measured algal biomass and production rates

In situ *measurements of biomass accumulation*

As can be seen from Table 5.1, sea ice algal biomass accumulation is extremely variable, particularly in the Antarctic where peak Chl *a* abundance ranges over four orders of magnitude. Even in a given sea ice habitat, Chl *a* accumulation can vary markedly depending upon the environmental conditions that prevailed during the growth phase. Despite this high degree of variability, Table 5.1 suggests that some important generalizations can be made concerning the productivity and amount of algal material that accumulates within different sea ice habitats.

First, Antarctic sea ice apparently supports higher algal biomass than Arctic ice. The highest algal biomass reported for Arctic sea ice was 300 mg Chl *a* m^{-2} in the congelation ice of Resolute Passage, with a spring–summer average for all studies of 87.5 mg Chl *a* m^{-2}. In contrast, in Antarctic sea ice Chl *a* accumulation in excess of 400 mg m^{-2} was observed in a number of habitats including the pack ice of the Weddell Sea, the bottom ice community of Adélie Land, and the platelet ice of McMurdo Sound where accumulations in excess of 1000 mg Chl *a* m^{-2} were reported in two different studies. The mean algal biomass in the Antarctic for all studies was 133 mg Chl *a* m^{-2}, 52% greater than in the Arctic. It should be noted, however, that the higher level of accumulation in the Antarctic is due entirely to the contribution of additional biomass by platelet ice. Removing platelet ice from the above analysis reduces the mean accumulated algal biomass in Antarctic sea ice to 88.1 mg Chl *a* m^{-2}, within 1% of the estimate for the Arctic.

Second, the most productive sea ice habitat in either the Arctic or the Antarctic is the platelet ice, a habitat exclusive to Antarctic regions (it is associated with floating ice shelves which are relatively rare in the Arctic). This porous, isothermal envir-

Table 5.1 Algal standing stock and production rates for various sea ice habitats in the Arctic and Antarctic. Standing stocks given are maximum observed values.

	Units/value		Reference	Comment
Antarctic				
Chlorophyll *a* (max value)	$mg\,m^{-3}$	$mg\,m^{-2}$		
	26.8	4	Garrison et al., 1983	New, Weddell Sea, summer
	5	—	Lizotte & Sullivan, 1991	New, Weddell Sea, autumn
	670	97	Meguro, 1962	Surface, Lutzow-Holm Bay
	407	117	Burkholder & Mandelli, 1965	Surface, Palmer Peninsula
	—	244	Whitaker, 1977	Surface, S. Orkneys
	43	—	Clarke & Ackley, 1984	Surface, Weddell Sea, late winter
	54	—	Garrison, unpub. obs.	Surface, Weddell Sea, spring
	—	80	Kottmeier & Sullivan, 1990	Surface, Weddell Sea, spring
	4.5	1.4	Ackley et al., 1979	Internal, Weddell Sea, summer
	9.8	9.6	Garrison & Buck, 1982	Internal, Weddell Sea, summer
	77	51	Garrison, unpub. obs.	Internal, Weddell Sea, spring
	3.8	0.6	Clarke & Ackley, 1984	Internal, Weddell Sea, late winter
	—	10	Stoecker et al., 2000	Internal, McMurdo, summer
	33	—	Lizotte & Sullivan, 1991	Internal, Weddell Sea, autumn
	—	170	Palmisano et al., 1988	Bottom, McMurdo, spring
	—	8.5	Grossi et al., 1987	Bottom, McMurdo, spring
	—	252	Palmisano et al., 1985	Bottom, McMurdo, spring
	—	170	Sullivan et al., 1985	Bottom, McMurdo, spring
	> 1000	—	Arrigo et al., 1995	Bottom, McMurdo, spring
	656	309	Palmisano & Sullivan, 1983	Bottom, McMurdo, spring
	9–24	0.8 to > 500	Riaux Gobin et al., 2000	Bottom, Adélie Land, spring
	> 829	—	Hoshiai, 1977	Bottom, Syowa, autumn
	> 1000	—	Hoshiai, 1977	Bottom, Syowa, spring
	944	65	Hoshiai, 1981	Bottom, Syowa, autumn
	5320	35	Hoshiai, 1981	Bottom, Syowa, spring
	—	15	McConville et al., 1985	Bottom, Davis
	—	294	Sullivan et al., 1982	Bottom, McMurdo, spring
	540	—	Lizotte & Sullivan, 1991	Bottom, Weddell Sea, autumn
	—	2–9	Dieckmann et al., 1990	Bottom, Weddell Sea

	—	110	McMinn & Ashworth, 1998	Congelation, Davis, spring
	36	20	Smetacek et al., 1992	Platelet, Weddell Sea, early spring
	—	76	Grossi et al., 1987	Platelet, McMurdo, spring
	132	164	Bunt & Lee, 1969	Platelet, McMurdo
	—	1076	Bunt & Lee, 1970	Platelet, McMurdo
	250	125	Bunt 1963, 1968	Platelet, McMurdo
	—	1090	Arrigo et al., 1993a	Platelet, McMurdo, spring
	> 6000	—	Arrigo et al., 1995	Platelet, McMurdo, spring
	400	60	Thomas et al., 1998	Pack, Amundsen, summer
	—	30	Fritsen et al., 1994	Pack, Weddell Sea, autumn
	23	29	Garrison & Close, 1993	Pack, Weddell Sea, winter
	19	53	Quetin & Ross, 1988	Pack, Weddell Sea, winter
	15	16	Schnack-Schiel, 1987	Pack Weddell Sea, winter
	—	23	Kottmeier et al., 1987	Pack, Weddell Sea, late winter
	14	18	Augstein et al., 1991	Pack, Weddell Sea, late winter
	27	35	Schnack-Schiel, 1987	Pack, Weddell Sea, spring
	15	18	Hempel, 1989	Pack, Weddell Sea, spring
	23	47	Ainley & Sullivan, 1984	Pack, Weddell Sea, spring
	202	453	Hempel, 1985	Pack, Weddell Sea, summer
	59	99	Miller & Grobe, 1996	Pack, Weddell Sea, summer
	43	77	Bathmann et al., 1992	Pack, Weddell Sea, summer
	37	32	Spindler et al., 1993	Pack, Weddell Sea, autumn
	10	11	Garrison & Buck, 1982	Pack, Weddell Sea, autumn
	16	19	Lemke, 1994	Pack, Weddell Sea, autumn–winter
	16	18	Arrigo et al., 2003	Pack, Ross Sea, spring
Photosynthetic rate	mg C mg^{-1}Chl *a* h^{-1}			
		0.55–2.46	Lizotte & Sullivan, 1991	New, Weddell Sea, autumn
		3.94 ± 1.48	Palmisano & Sullivan, 1985	Surface, McMurdo, spring
		1.2	Lizotte & Sullivan, 1991	Internal, Weddell Sea, autumn
		0.04–0.38	Cota & Sullivan, 1990	Bottom, McMurdo, spring
		0.3–2.5	Kottmeier & Sullivan, 1988	Bottom, spring
		0.11–0.58	Palmisano et al., 1987	Bottom, McMurdo, spring
		0.17–1.95	Grossi et al., 1987	Bottom, McMurdo, spring

Contd

Table 5.1 *Contd*

	Units/value	Reference	Comment
	0.05–0.25	Palmisano et al., 1985	Bottom, McMurdo, spring
	0.12 ± 0.005	Palmisano & Sullivan, 1985	Bottom, McMurdo, spring
	0.06–0.32	Palmisano & Sullivan, 1985	Bottom, McMurdo, spring
	0.1	Arrigo & Sullivan, 1992	Bottom, McMurdo, spring
	0.57–0.76	Lizotte & Sullivan, 1991	Bottom, Weddell Sea, autumn
	0.02–0.05	McMinn et al., 1999	Bottom, Cape Evans, spring
	> 0.005–0.045	McMinn & Ashworth, 1998	Congelation, Davis, spring
	0.05–0.2	Arrigo et al., 1993a	Platelet, McMurdo, spring
	0.152	Palmisano & Sullivan, 1985	Platelet, McMurdo, spring
	0.1–0.76	Grossi et al., 1987	Platelet, McMurdo, spring
	0.26–4.7	Lizotte & Sullivan, 1992	Pack, Weddell Sea, autumn
	0.11–8.6	Lizotte & Sullivan, 1992	Pack, Bransfield, autumn
	0.04–8.6	Lizotte & Sullivan, 1992	Pack, Weddell-Scotia, autumn
	0.41–0.81	Arrigo et al., 2003	Pack, Ross Sea, spring
Primary production	mg C m^{-2} d^{-1}		
	0.5–12	Stoecker et al., 2000	Internal, McMurdo, summer
	43	McMinn et al., 1999	Bottom, Cape Evans, spring (h * 24)
	0.5–85	Grossi et al., 1987	Bottom, McMurdo, spring
	2–1249	Grossi et al., 1987	Platelet ice, McMurdo, spring
	200–1200	Arrigo et al., 1995	Platelet ice, McMurdo, spring
	35.0 ± 11.7	Kottmeier et al., 1987	Pack ice, Weddell Sea, winter
Primary production	g C m^{-2} yr^{-1}		
	3.8–38.0	Grossi et al., 1987	Platelet ice, McMurdo
	0.34–3.4	Grossi et al., 1987	Congelation, McMurdo
	1–6	Burkholder & Mandelli, 1965	Congelation, McMurdo
	1–6	Bunt & Lee, 1970	Congelation, McMurdo
Primary production	Tg C yr^{-1}		
	36	Arrigo et al., 1997	Surface + interior, Antarctic, annual
	30	Mathot et al., 1996	Antarctic, annual
	70	Legendre et al., 1992	Antarctic, annual
	63–70	Lizotte et al., 2001	Antarctic, annual

Arctic				
Chlorophyll *a* (max value)	mg m^{-3}	mg m^{-2}		
	—	70	Niebauer et al., 1981	Surface, Bering Sea
	—	170	Welch et al., 1991	Hudson Bay, spring
	—	300	Welch & Bergmann, 1989	Congelation, Resolute, spring
	—	260	Smith et al., 1988	Congelation, Resolute, spring
	—	119	Robineau et al., 1997	Bottom, Japan
	—	30	Kudoh, 1997	Bottom, Japan, winter
	—	89	Suzuki et al., 1997	Bottom, Resolute, spring
	—	160	Michel et al., 1996	Bottom, Resolute, spring
	704	—	Cota et al., 1990	Bottom, Resolute, spring
	15	—	Rysgaard et al., 2001	Bottom, Greenland, summer
	2.5	—	Gosselin et al., 1985	Bottom, Manitounuk Sound, spring
	—	16	Apollonio 1961	Bottom, Jones Sound
	—	11	Apollonio 1965	Bottom, Jones Sound
	427	24	Meguro et al., 1967	Bottom, Barrow
	—	30	Alexander, 1974	Bottom, Beaufort Sea
	—	31	Horner, 1976	Bottom, Barrow
	—	8–26	Horner & Schrader, 1982	Bottom
	—	19–130	Smith et al., 1987, 1989	Bottom
	—	5	Grainger, 1977	Bottom, Frobisher Bay
	—	12	Dunbar & Acreman, 1980	Bottom, Barrow
	—	8	Hsiao, 1980	Bottom, Frobisher Bay
	—	64	Alexander & Chapman, 1981	Bottom, Barrow
	—	20	Tremblay et al., 1989	Bottom
	—	15	Gosselin et al., 1997	Pack ice, central Arctic, summer
	—	191	Irwin, 1990	Pack ice, Labrador Shelf, spring
Photosynthetic rate	mg C mg^{-1} Chl *a* h^{-1}			
		1.43–3.11	Irwin, 1990	Pack ice, Labrador Shelf, spring
		0.6–1.17	Smith et al., 1988	Congelation, Resolute, spring
		0.16–0.24	Johnsen & Hegseth, 1991	Bottom, Barents, spring
		0.1–1.2	Gosselin et al., 1985	Bottom, Manitounuk Sound, spring
		0.03–0.09	Johnsen & Hegseth, 1991	Strand, Barents, summer

Contd

Table 5.1 *Contd*

	Units/value	Reference	Comment
Primary production	mg C m^{-2} d^{-1}		
	0.2	Rysgaard et al., 2001	Congelation, Greenland, summer
	0.5–310	Gosselin et al., 1997	Pack ice, central Arctic, summer
	0.1–0.2	Anderson, 1977	Davis Strait
	0.03–2.4	Booth, 1984	Davis Strait
	2.2–4.8	McRoy & Goering, 1974	Bering Sea
	58	Irwin, 1990	Pack ice, Labrador Shelf, spring
	0.8–9.7	Mock & Gradinger, 1999	
Primary production	g C m^{-2} yr^{-1}		
	5.3	Hegseth, 1998	Congelation, Barents Sea, summer
	15	Gosselin et al., 1997	Pack ice, central Arctic, summer
	5	Bergmann et al., 1991	Canadian Archipelago
Primary production	Tg C yr^{-1}		
	9–73	Legendre et al., 1992	Arctic, annual
	6	Subba Rao & Platt, 1984	Arctic, annual

onment has a salinity similar to sea water, and provided sufficient light is available, is an ideal habitat for algal growth. Reported peak Chl *a* accumulation in these habitats (> 1000 mg Chl *a* m^{-2}) is more than two-fold greater than that reported for any other habitat, either in the Arctic or the Antarctic. The uniqueness of platelet ice to Antarctic regions is the primary reason why sea ice in the southern hemisphere is on average more productive than its northern counterpart.

Third, land-fast ice accumulates more algal biomass than pack ice. In both Arctic and Antarctic regions, accumulation of algal biomass in land-fast ice was substantially greater than in the pack. This is especially clear in the Antarctic, where, with the exception of a single study, peak biomass accumulation was consistently less than 100 mg Chl *a* m^{-2}. In contrast, accumulation of Chl *a* in fast ice exceeded 200 mg Chl *a* m^{-2} in five studies, with a maximum accumulation of > 500 mg Chl *a* m^{-2}. Similarly, in the Arctic, three of the four highest Chl *a* accumulations were reported in land-fast congelation ice.

Fourth, bottom ice communities in the Antarctic are more productive than surface communities, which are themselves more productive than internal communities. The same may be true for the Arctic as well, but the data are more sparse for that region and differences between the communities are not as obvious. In the Antarctic, bottom ice communities exhibited the highest algal biomass accumulation of any sea ice habitat, with the exception of the platelet ice. The highest measured total Chl *a* in bottom ice was more than a factor of two greater than in surface communities, amounting to 244 and > 500 mg Chl *a* m^{-2}, respectively. This difference is largely due to the proximity of the bottom ice to the upper water column and its increased access to nutrients. Surface communities are dependent upon physical processes, such as high snow loading or rafting of adjacent ice floes, both of which result in flooding of the sea ice surface, to maintain access to nutrients. Algal biomass within internal communities is the lowest of all, likely reflecting the reduced access to nutrients, as well as the low temperature and high salinity often characteristic of this habitat. Because algal Chl *a* accumulation is an underestimate of production due to unaccounted for losses of algal biomass, and because losses from the bottom ice are probably greater than in the surface or the interior (due to increased access to grazers and the potential for sinking), the disparity between these two habitats is probably even larger than that implied by biomass accumulation.

Direct and indirect estimates of algal production

Owing to the difficulty of the measurement, estimates of primary production in sea ice, even indirect ones, are relatively rare. More common are estimates of photosynthetic rate, which when combined with measured light distributions in the ice, can be used to calculate sea ice primary production. Unfortunately, photosynthetic measurements are rarely used in this way because the data on light distributions in sea ice that are needed for the calculation are even less common than the

photosynthetic measurements. Measurements of photosynthetic rate, in particular P^*_m, do exhibit some interesting patterns, however, that, when combined with biomass accumulation patterns, can provide some insight into the factors responsible for regulating primary production in sea ice.

Unlike the hemispheric pattern exhibited by Chl *a* accumulation in sea ice, whereby values in the Antarctic are substantially higher than in the Arctic, data on P^*_m displayed no such bias, although the data set available for evaluation is somewhat small, particularly in the Arctic. While these two observations may seem initially to be inconsistent, they can be explained in part by the different habitats that dominate each region. A major reason for the difference in biomass accumulation between the two poles was that platelet ice, which contains so much more algal biomass than any other habitat, is restricted to the Antarctic. Ignoring the contribution by platelet ice brings algal biomass accumulation in the two hemispheres more closely in line.

An obvious pattern in P^*_m that does emerge from the data is the consistently higher values measured in pack ice relative to land-fast ice in both the Antarctic and the Arctic. Values of P^*_m for the fast ice are consistently < 2 mg C mg^{-1} Chl *a* h^{-1} and often much lower. In contrast, estimates of P^*_m for the pack ice can be as high as > 8 mg C mg^{-1} Chl *a* h^{-1}. The differences in P^*_m between these two habitats can probably be attributed to variation in sea ice thickness. Pack ice tends to be much thinner than land-fast ice in both polar regions and as a result, light levels are substantially higher. Because the P^*_m of algae is highly dependent upon previous light history, fast ice, with its reduced irradiance, exhibits lower values for P^*_m than that of the pack.

The fact that photosynthetic rates are greater in the pack ice is in apparent conflict, however, with the observation that land-fast ice accumulates more algal biomass than pack ice. These observations can be reconciled only if losses of algal biomass from the pack ice are greater than from land-fast ice. This provides strong, albeit indirect, evidence that grazing by zooplankton on sea ice algae is greater in pack ice than in the land-fast ice. Although quantitative data with which to compare relative grazing effort in pack and land-fast ice are lacking, structural characteristics of the two habitats support a higher grazing rate within pack ice. Pack ice tends to be composed of a mixture of congelation and frazil ice whereas land-fast ice is predominantly congelation ice. As a result, pack ice tends to be more porous, and therefore, more susceptible to grazers. Consistent with this notion, there have been numerous reports of herbivores such as copepods, amphipods, protists, etc., actively grazing within pack ice in both the Arctic and the Antarctic (Schnack-Schiel, Chapter 7). These organisms appear to be less common in the more consolidated congelation ice type characteristic of land-fast ice until much later in the season when the ice begins to melt and the brine volume increases dramatically (Stoecker et al., 2000). Losses due to sinking of algal material must also be considered, but because pack ice has a higher fraction of surface and internal communities which should be resistant to sinking, differences in sinking are unlikely to be important. In

addition, fast ice, at least in the Antarctic, is often associated with an under-ice platelet layer which would tend to further minimize losses from the ice due to sinking and grazing.

Therefore, pack ice may represent the more important sea ice habitat in terms of providing a food source for upper trophic level organisms. Having production rates as much as four-fold higher than land-fast ice and accumulating only half the algal biomass (with little expected difference in sinking losses) implies that a much larger fraction of the primary production in pack ice is being consumed by higher trophic levels. The importance of these differences in food web structure is further magnified by the fact that pack is so much more prevalent than fast ice in both the Arctic and the Antarctic.

Interestingly, two of the most recently developed, minimally invasive *in situ* techniques came to very different conclusions concerning the accuracy of standard ^{14}C incubation techniques used most often for estimating primary production in sea ice. Estimates of photosynthetic carbon fixation made using microelectrodes to measure diffusion of oxygen through the boundary layer were very low, with P^*_m values ranging only from 0.02 to 0.05 mg C mg^{-1} Chl *a* h^{-1} and hourly production rates of 0–1.78 mg C m^{-2} h^{-1}. As can be seen from Table 5.1, these estimates are on the low side for Antarctic sea ice, particularly in the spring when rates are generally the highest. Because this technique is the least invasive of all known methods for estimating sea ice primary production, the low values obtained by this technique have led the developers to speculate that previous estimates of sea ice production may be too high. In contrast, the *in situ* ^{14}C technique (whereby core sections are placed into individual petri dishes that are inoculated with ^{14}C bicarbonate, placed in an acrylic-glass barrel, and returned to their original position in the ice floe for incubation) showed that production within the sea ice interior was much higher than previously reported and that estimates of primary production based on bottom ice communities were likely to severely underestimate production in both the Antarctic and the Arctic. Clearly, additional data need to be collected to evaluate the relative ability of these two approaches to estimate sea ice primary productivity. Using both approaches in the same study would provide valuable insights in this regard.

Estimates of annual sea ice primary production from direct ^{14}C uptake rate measurements are uncommon. The few studies that have been conducted indicate annual production in the Arctic and the Antarctic is similar in magnitude, ranging from 5 to 15 g C m^{-2} yr^{-1} and from 0.3 to 34 g C m^{-2} yr^{-1}, respectively. These values are consistent with biomass accumulation data from the two regions which represent a minimum estimate of annual production. For example, assuming a carbon:Chl *a* ratio for sea ice diatoms of 40, then annual production estimated from maximum spring/summer Chl *a* abundance ranges from 0.2 to 12 g C m^{-2} yr^{-1} for the Arctic and from 0.04 to 44 g C m^{-2} yr^{-1} for the Antarctic. Ignoring production in the platelet ice reduces the range for the Antarctic to 0.04–20 g C m^{-2} yr^{-1}. Despite the small sample sizes, it is still probably fair to conclude that even in the most productive sea ice

habitats, annual production is below 50 g C m^{-2} yr^{-1}, an amount similar in magnitude to the oligotrophic central gyres of the open oceans.

Even rarer still are estimates of total primary production integrated over both the entire Arctic and Antarctic regions. Because of the paucity of data used to make such estimates, they are necessarily crude and provide little or no information about either regional patterns of production or its annual cycle. Nevertheless, these estimates can be a useful tool when evaluating the contribution of the sea ice habitat to total regional (ice + water column) production, and that has generally been the context in which they have been made.

Measurements made in near-shore sea ice led to early estimates of 1–6 g C m^{-2} yr^{-1}, suggesting that sea ice production was several orders of magnitude lower than that being reported for phytoplankton. As a result, the contribution of primary production in sea ice was dismissed as insignificant. More recent estimates of basin-wide production in both the Arctic and Antarctic regions are both much higher and very similar, with approximately 70 Tg C estimated to be fixed annually. This is approximately equivalent to 10% of total phytoplankton production in the same regions. Although crude, these estimates provide a useful baseline with which to evaluate more sophisticated studies of large-scale variation in sea ice primary productivity conducted using numerical modelling techniques.

Large-scale modelling of sea ice primary production

One of the advantages of using numerical models to assess large-scale changes in primary production is that it allows investigation of temporal as well as regional variability. Unfortunately, to date, only one such model has been developed and only for Antarctic sea ice during 1989–90 (Arrigo et al., 1997, 1998b). Regardless, this model has provided insights that are likely to be applicable to both polar regions.

Temporal variability

The annual rate of primary production within Antarctic sea ice was calculated by this model to be approximately 36 Tg C (Table 5.2), consistent with recent estimates which range from 30 to 70 Tg C. This estimate of total primary production in sea ice is a function of both the extent of the sea ice and the rate of carbon fixation per unit area. Although sea ice in the Antarctic is most extensive in October, because of low productivity, spatially integrated production at that time is only 3 Tg C $month^{-1}$ (Table 5.2). Spatially integrated primary production in Antarctic sea ice peaks in November at 12 Tg C $month^{-1}$ as photosynthetic rates increase by a factor of four and sea ice coverage remains high. Over 90% of this biogenic carbon is fixed within first-year sea ice. Spatially integrated production declines between December and April due to a large decrease in first-year sea ice coverage, despite the fact that the rate of production per unit area peaks in January in both first-year (2.2 g C m^{-2}

Table 5.2 Sea ice extent (10^6 km^2) and primary productivity (Tg C month^{-1}) in first-year ice and multi-year ice in the geographic sectors of the Antarctic ice pack defined in Fig. 5.2.

	Sea ice extent			Production		
Ice Type	First-year	Multi-year	All ice	First-year	Multi-year	All ice
Weddell Sea						
October	4.89	0.95	5.85	1.16	0.03	1.19
November	4.17	0.92	5.09	4.26	0.34	4.60
December	2.06	0.90	2.96	3.49	0.78	4.27
January	0.66	0.84	1.51	1.90	0.94	2.84
February	0.40	0.76	1.16	0.82	0.73	1.55
March	0.63	0.73	1.35	0.49	0.49	0.98
April	1.36	0.72	2.08	0.21	0.16	0.37
Annual production (Tg C)				12.3	3.47	15.8
Bellingshausen/Amundsen Seas						
October	1.37	0.47	1.85	0.15	0.01	0.16
November	1.19	0.46	1.65	0.93	0.12	1.05
December	0.52	0.44	0.96	0.58	0.33	0.91
January	0.25	0.40	0.64	0.27	0.36	0.63
February	0.12	0.30	0.42	0.09	0.26	0.35
March	0.20	0.24	0.44	0.04	0.23	0.27
April	0.44	0.23	0.67	0.03	0.16	0.19
Annual production (Tg C)				2.09	1.47	3.56
Ross Sea						
October	3.06	0.87	3.94	0.74	0.10	0.84
November	2.34	0.86	3.20	2.23	0.27	2.49
December	1.45	0.71	2.16	2.01	0.67	2.68
January	0.37	0.37	0.74	0.52	0.39	0.91
February	0.11	0.27	0.37	0.05	0.26	0.31
March	0.75	0.22	0.97	0.08	0.18	0.26
April	1.95	0.22	2.17	0.11	0.13	0.24
Annual production (Tg C)				5.74	2.00	7.74
Western South Pacific Ocean						
October	0.60	0.41	1.01	0.07	0.04	0.11
November	0.55	0.37	0.91	0.35	0.24	0.59
December	0.23	0.26	0.49	0.15	0.27	0.42
January	0.14	0.20	0.34	0.11	0.22	0.33
February	0.08	0.14	0.22	0.04	0.15	0.19
March	0.22	0.10	0.32	0.05	0.11	0.16
April	0.59	0.09	0.68	0.07	0.06	0.13
Annual production (Tg C)				0.84	1.09	1.93
Southern Indian Ocean						
October	3.45	0.25	3.70	0.65	0.05	0.70
November	2.55	0.24	2.79	2.56	0.21	2.77
December	0.94	0.19	1.13	1.31	0.21	1.52
January	0.33	0.15	0.48	0.74	0.18	0.92
February	0.16	0.11	0.26	0.29	0.13	0.42
March	0.16	0.07	0.23	0.10	0.09	0.19
April	0.57	0.05	0.62	0.07	0.06	0.13
Annual production (Tg C)				5.72	0.93	6.65

Contd

Table 5.2 *Contd*

	Sea ice extent			Production		
Ice Type	First-year	Multi-year	All ice	First-year	Multi-year	All ice
Southern Ocean						
October	13.4	2.96	16.3	2.78	0.23	3.01
November	10.8	2.84	13.6	10.3	1.17	11.5
December	5.19	2.50	7.69	7.55	2.26	9.81
January	1.75	1.96	3.71	3.54	2.10	5.64
February	0.87	1.57	2.43	1.29	1.52	2.81
March	1.97	1.35	3.31	0.76	1.09	1.85
April	4.90	1.32	6.22	0.49	0.57	1.06
Annual production (Tg C)				26.7	8.94	35.7

month^{-1}) and multi-year sea ice (1.1 g C m^{-2} month^{-1}). In February, spatially averaged rates of production in first-year sea ice exceed those in multi-year ice; however, due to the continued melting of first-year sea ice, the bulk of the biogenic carbon is produced in multi-year ice. While first-year sea ice increases in coverage again during March and April, the low productivity rates in this newly formed sea ice resulted in a lower amount of production than in the established multi-year ice.

A production rate of 36 Tg C yr^{-1} for Antarctic sea ice is equivalent to approximately 1% of the annual biogenic carbon production in Southern Ocean waters south of 50°S (Arrigo et al. 1998a). However, sea ice primary production is a much larger fraction (10–28%) of total production in ice-covered regions (141–383 Tg C yr^{-1}), including the highly productive marginal ice zones. Furthermore, because of the simplifying assumptions made when constructing the model, the value of 36 Tg C yr^{-1} may underestimate total production in the ice within the Southern Ocean by as much as a factor of two. For example, the model assumes that the ice pack consists of a single continuous sheet. However, the pack contains numerous leads which would increase both the surface area for algal colonization and the transmission of light through the snow and ice. This would result in higher growth rates than those predicted by the model. Similarly, the model does not account for complex features such as pressure ridges and rafted ice which increase the ice thickness and facilitate snow accumulation, both of which would increase surface flooding. In addition, because the distributions of land-fast ice and/or underlying platelet ice are largely unknown, they were ignored. However, rates of productivity within these habitats can be more than an order of magnitude higher than in pack ice and including them could increase estimates of productivity by up to 20%. Third, the model neglects the important bottom ice community which at the time was thought to be rare in pack ice. Finally, processes that drive nutrient exchange between the interior of the ice and the underlying water column (e.g. infiltration and freeze–thaw convection), and which may enhance production within internal bands, were omitted.

Spatial variability

Despite the fact that current versions of large-scale sea ice ecosystem models underestimate primary production, they can still provide valuable information regarding relative rates of production in different regions as well as their annual cycle. This in turn should help to elucidate the way in which regional differences in sea ice physics and external forcing control local rates of sea ice primary production.

Weddell Sea (60°W to 20°E)

The Weddell Sea (Fig. 5.2) had a more extensive ice cover than in any other sector of the Antarctic ice pack, in terms of both first-year and multi-year sea ice. First-year sea ice area in the Weddell Sea usually peaks in October at $4.9 \times 10^6\,km^2$ (Table 5.2) and can extend as far north as 60°S. By February, when ice coverage is at its lowest, less than 10% of the first-year sea ice remains. Coverage by multi-year ice is much less extensive but also less seasonally variable, ranging from $0.95 \times 10^6\,km^2$ in October to $0.72 \times 10^6\,km^2$ in April. Multi-year ice is concentrated in the western margin of the Weddell Sea near the Antarctic Peninsula. The snow thickness in the Weddell Sea averages about 0.15 m, 20% greater than that of the other Antarctic sectors. While this difference may appear small, the Weddell Sea has two- to seven-fold more area with snow thickness > 0.2 m (the approximate thickness above which surface flooding becomes substantial at the sea ice thicknesses used in the model) than other Antarctic sectors.

As a result, rates of sea ice primary production in the Weddell Sea are greater than those of all other sectors, frequently exceeding $> 100\,mg\,C\,m^{-2}\,d^{-1}$. The most productive region of the Weddell Sea, and indeed of the entire Antarctic ice pack, is located within the first-year ice where snow remains relatively deep for the duration of the simulation. Although the deep snow also reduces light availability, this effect was insufficient to seriously inhibit the algal growth, except in the thicker multi-year ice.

Almost 50% of annual Antarctic sea ice primary production was generated in the Weddell Sea due to its extensive ice coverage and high rate of carbon fixation. The peak areal rate of production in the Weddell Sea ($2.9\,g\,C\,m^{-2}\,month^{-1}$ in first-year ice in January) was more than twice that of the Ross Sea. Annually, first-year ice accounts for 75% of the sea ice production in the Weddell Sea; during the month of November this value grows to greater than 93%.

Bellingshausen/Amundsen Seas (130°W to 60°W)

Although total sea ice coverage in the Bellingshausen/Amundsen Seas in 1989–90 was only 30% of that in the Weddell Sea, a substantially larger fraction of total ice cover consisted of multi-year ice (25% in October to 71% in February). Mean snow thickness in the Bellingshausen/Amundsen Seas was 0.14 m, with the deepest snow

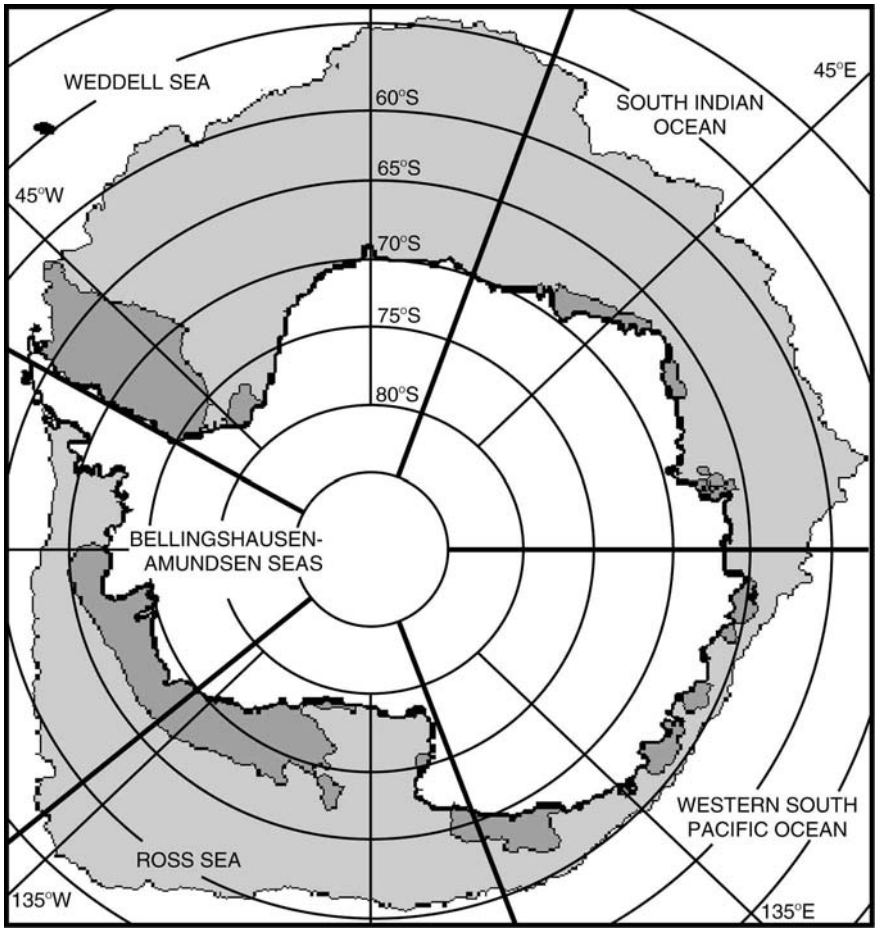

Fig 5.2 Map of the Southern Ocean showing the minimum (dark grey) and maximum (light grey) sea ice extent during the simulation (1989–90) as well as the boundaries of the five geographical sectors referred to in the text. Modified from Arrigo et al. (1998b).

(> 0.25 m) located near the Antarctic Peninsula in October and November. This peak in snow cover was short lived, however, and snow thickness declined markedly by December. From October through April, snow cover was thicker on ice near the coast than offshore, probably because of the prevalence of multi-year ice near-shore and the opportunity for long-term accumulation.

The thin snow cover over first-year ice in the Bellingshausen/Amundsen Seas resulted in infrequent flooding. The reduced nutrient supply in first-year ice and thick snow cover over multi-year ice resulted in generally low rates of primary production. Only the South Pacific Ocean sector had lower spatially averaged rates of production. Productivity in first-year ice was greatest in December and January ($1.0\,\mathrm{g\,C\,m^{-2}\ month^{-1}}$), but amounted to less than 50% of the rate in Weddell Sea

first-year ice. Of the 3.6 Tg C yr^{-1} produced annually in the sea ice of the Bellingshausen/Amundsen Seas, 59%, was associated with first-year ice.

Ross Sea (160°E to 130°W)

Sea ice extent in the Ross Sea ranges from a maximum of 3.1×10^6 km^2 in October to a minimum of 0.37×10^6 km^2 in February. Unlike other Antarctic sectors, the decay of the ice pack in the Ross Sea begins over coastal waters with the formation of the Ross Sea polynya beginning in late November and December. A large concentration of multi-year ice (0.22×10^6 km^2) persists in the eastern Ross Sea adjacent to the Bellingshausen/Amundsen Seas. Snow cover throughout the Ross Sea is relatively uniform, particularly in the west where snow thicknesses ranged from 0.08 to 0.16 m. Only over the multi-year ice in the east did the snow cover exceed 0.20 m in thickness over a sizable area. Thick snow cover was also located offshore during November in the first-year ice near 140°W.

The Ross Sea is the second most productive sector of the Antarctic ice pack (Table 5.2), contributing 7.7 Tg C annually due to its extensive sea ice cover. Algal biomass in the Ross Sea is most abundant in the offshore sea ice between October and December, where light levels are highest. Near-shore algal biomass is about 50% of the levels offshore during this time. Algal production was greatest in November (2.5 Tg C) and December (2.7 Tg C), most (74%) taking place in first-year ice (Table 5.2). In January, onshore-offshore differences in algal biomass disappeared due to the melting of vast amounts of first-year sea ice as sea ice extent diminished to approximately 10% of the maximum coverage in October. As a result, production dropped by 67% despite a peak in the areal rate of algal production (1.2 g C m^{-2} $month^{-1}$). Some multi-year ice at 160°E persisted to the end of the simulation and harboured the greatest algal standing crop in the Ross Sea, with levels in January occasionally exceeding 60 mg Chl *a* m^{-2}.

Western South Pacific Ocean (90°E to 160°E)

This sector is the least productive, contributing only 5% of total Antarctic sea ice production (Table 5.2) and, as such, it provides an interesting contrast to the highly productive Weddell Sea. Productivity in the western South Pacific Ocean was low in part because of the limited sea ice area, providing a much smaller habitat for algal growth. Even during maximal ice coverage (1.01×10^6 km^2), sea ice area in this sector was only 17% of that in the Weddell Sea.

Productivity also was low because of the reduced areal rates of production (maximum of 0.95 g C m^{-2} $month^{-1}$ in January), which were less than 50% of the rates in the Weddell Sea. These rates were depressed because of the high proportion of multi-year sea ice and a relatively thin snow cover over first-year ice. Between October and February, multi-year ice accounted for 40–64% of total sea ice cover, more than any other Antarctic sector. Snow depth in this sector was the thinnest of

the entire Antarctic ice pack, averaging only 0.14 m. Consequently, a large fraction of the first-year ice in this sector remained above freeboard and had limited access to nutrients, resulting in widespread nutrient limitation.

Southern Indian Ocean (20°E to 90°E)

Sea ice coverage in this sector was extensive (3.5×10^6 km^2 in October), similar to that in the Ross Sea (Table 5.2) but with a somewhat higher proportion of multi-year ice. One striking difference between this sector and the Ross Sea was the rapid decline in sea ice in December. Within the span of 1 month, ice cover in the southern Indian Ocean was reduced to less than 50% of that in the Ross Sea. Snow thickness was also similar to that in the Ross Sea, averaging 0.10 to 0.16 m. Because of the greatly diminished sea ice coverage in the southern Indian Ocean (Table 5.2), annual production was approximately 14% less than in the Ross Sea, amounting to 6.7 Tg C. In contrast, the rate of production per unit area was greater in the southern Indian Ocean than in the Ross Sea due to the high proportion of first-year ice.

The results from the first large-scale application of a sea ice primary production model to the Southern Ocean have been fruitful in a number of ways. First, model results demonstrate that the thickness of the snow cover in combination with the proportion of first-year ice in a given region are fundamental in controlling primary production within sea ice over large scales. This finding is likely to be applicable to Arctic regions as well. Second, the formulation and successful use of this sea ice productivity model provides a consistent framework for making comparisons with results from a similarly formulated model for Southern Ocean phytoplankton. Finally, because surface algal blooms will affect the quantity and quality of light reaching internal or bottom ice algal communities, as well as the water column below, the results from this model will be useful as input to models designed to estimate the productivity of algae deeper in the ice and in the water column.

5.5 Conclusions

Despite the fact that sea ice biota has been studied for over 40 years, basic information concerning variability at virtually all temporal and spatial scales is still mostly lacking, particularly in the Arctic. Although ice algal dynamics in a few areas and habitats have been rather well characterized, there is still no clear understanding of the magnitude and variability of ice algal primary production over most of the Arctic and the Antarctic. The most urgent need therefore is for more sampling.

Even though sea ice represents one of the largest ecosystems on earth, due to logistic constraints, it remains one of the most poorly sampled. This lack of sampling stems mainly from the perception that sea ice plays, at most, a minor role in providing nutrition for upper trophic levels and in regulating other biogeochemical

processes and, therefore, intense scrutiny is unwarranted. However, as ever more information becomes available, the relevance of the sea ice biota appears only to increase in importance. The recent discovery that productivity by sea ice algae in the central Arctic is an order of magnitude greater than previously estimated is a case in point.

New techniques for measuring primary production *in situ* must also be developed. In particular, emphasis must be placed upon reducing artifacts which plague most existing techniques. Recently developed methods which employ high resolution *in situ* incubations and measurements of O_2 diffusion through the sea ice boundary layer are an excellent start, but more is needed. More sophisticated microprobes should be developed to facilitate non-invasive sampling of a wider variety of sea ice properties.

Until the *in situ* data needed to describe the large-scale variability in sea ice algal production become available, numerical models must be further developed and utilized. This is particularly true for Arctic regions for which no models at any level (1-D or 3-D) currently exist. These models can provide a framework for testing our understanding of how these ecosystems operate and can also be used as a predictive tool for estimating the role of ice algae in regions where data are currently lacking. Existing models are still too oversimplified, however, and effort needs to be made to add those mechanisms that are known to be important but that are currently absent from existing models. Computer computational power is now much greater than was available when even the latest models were first developed and inclusion of much more mechanistic detail is now possible. This should be a major focus of future work in sea ice ecosystems in both polar regions.

References

Ackley, S.F., Buck, K.R. & Taguchi, S. (1979) Standing crop of algae in the sea ice of the Weddell Sea region. *Deep-Sea Research*, **26**, 269–281.

Ackley, S.F. & Sullivan, C.W. (1994) Physical controls on the development and characteristics of Antarctic sea ice biological communities – a review and synthesis. *Deep-Sea Research*, **41**, 1583–1604.

Ainley, D. & Sullivan, C.W. (1984) AMIEREZ 1983: a summary of activities on board the R/V Mellville and USCGC Westwind. *Antarctic Journal of the United States*, **19**, 177–179.

Alexander, V. (1974) Primary productivity regimes of the nearshore Beaufort Sea, with reference to potential roles of ice biota. In: *The Coast and Shelf of the Beaufort Sea*, (Eds J.C. Reed & J.E. Sater), pp. 609–632. Arctic Institute of North America, Arlington, Virginia.

Alexander, V. & Chapman, T. (1981) The role of epontic algal communities in Bering Sea ice. In: *The Eastern Bering Sea Shelf: Oceanography and Resources*, Vol. 2 (Eds D.W. Hood & J.A. Calder), pp. 773–780. University of Washington Press, Seattle.

Anderson, O.G.N. (1977) Primary production associated with sea ice at Godhavn, Dicko, West Greenland. *Ophelia*, **16**, 205–220.

Apollonio, S. (1961) The chlorophyll content of Arctic sea-ice. *Arctic*, **14**, 197–200.

Apollonio, S. (1965) Chlorophyll in Arctic sea ice. *Arctic*, **18**, 118–122.

Arrigo, K.R., Dieckmann, G., Gosselin, M., Robinson, D.H., Fritsen, C.H. & Sullivan, C.W. (1995) High resolution study of the platelet ice ecosystem in McMurdo Sound, Antarctica – biomass, nutrient and production profiles within a dense microalgal bloom. *Marine Ecology Progress Series*, **127**, 255–268.

Arrigo, K.R., Kremer, J.N. & Sullivan, C.W. (1993a) A simulated Antarctic fast-ice ecosystem. *Journal of Geophysical Research*, **98**, 6929–6946.

Arrigo, K.R., Lizotte, M.P., Worthen, D.L., Dixon, P. & Dieckmann, G.S. (1997) Primary production in Antarctic sea ice. *Science*, **276**, 394–397.

Arrigo, K.R., Robinson, D.H., Dunbar, R.B., Leventer, A.R. & Lizotte, M.P. (2003) Physical control of chlorophyll *a*, POC, and PON distributions in the pack ice of the Ross Sea, Antarctica. *Journal of Geophysical Research* (in press).

Arrigo, K.R., Robinson, D.H. & Sullivan, C.W. (1993b) A high resolution study of the platelet ice ecosystem in McMurdo Sound, Antarctica: photosynthetic and bio-optical characteristics of a dense microalgal bloom. *Marine Ecology Progress Series*, **98**, 173–185.

Arrigo, K.R. & Sullivan, C.W. (1992) The influence of salinity and temperature covariation on the photophysiological characteristics of Antarctic sea ice microalgae. *Journal of Phycology*, **28**, 746–756.

Arrigo, K.R. & Sullivan, C.W. (1994) A high resolution bio-optical model of microalgal growth: tests using sea-ice algal community time-series data. *Limnology and Oceanography*, **39**, 609–631.

Arrigo, K.R., Sullivan, C.W. & Kremer, J.N. (1991) A bio-optical model of Antarctic sea ice. *Journal of Geophysical Research*, **96**, 10581–10592.

Arrigo, K.R., Worthen, D.L., Dixon, P. & Lizotte, M.P. (1998a) Primary productivity of near surface communities within Antarctic pack ice. In: *Antarctic Sea Ice Biological Processes, Interactions, and Variability* (Eds M.P. Lizotte & K.R. Arrigo), American Geophysical Union, Washington, D.C. *Antarctic Research Series*, **72**, 23–43.

Arrigo, K.R., Worthen, D.L., Schnell, A. & Lizotte, M.P. (1998b) Primary production in Southern Ocean waters. *Journal of Geophysical Research*, **103**, 15587–15600.

Augstein, E., Bagriantsev, N. & Schenke, H.-W. (1991) Die expedition Antarktis VIII/1-2, 1989 mit der Winter Weddell Gyre study der Forschungsschiffe Polarstern and Akademik Federov. *Berichte zur Polarforschung*, **84**, 134 pp.

Bathmann, U., Schulz-Baldes, M., Farbach, E., Smetacek, V. & Hubberten, H.-W. (1992) Die expedition Antarktis IX/1-4 des Forschungsschiffes Polarstern. *Berichte zur Polarforschung*, **100**, 403 pp.

Bergmann, M.A., Welch, H.E., Butler-Walker, J.E. & Silfred, T.D. (1991) Ice algal photosynthesis at Resolute and Saqvaqjuac in the Canadian Arctic. *Journal of Marine Systems*, **2**, 43–52.

Bindschadler, R. (1990). SeaRISE: a multidisciplinary research initiative to predict rapid changes in global sea level caused by collapse of marine ice sheets. *NASA Conference Publication 3075*. National Aeronautics and Space Administration, Washington, D.C.

Booth, J.A. (1984) The epontic algal community of the ice edge zone and its significance to the Davis Strait ecosystem. *Arctic*, **37**, 234–243.

Bunt, J.S. (1963) Diatoms of Antarctic sea ice as agents of primary production. *Nature*, **199**, 1254–1257.

Bunt, J.S. (1968) Some characteristics of microalgae isolated from Antarctic sea ice. *Antarctic Research Series*, **11**, 1–14.

Bunt, J.S. & Lee, C.C. (1969) Observations within and beneath Antarctic sea ice in McMurdo Sound and the Weddell Sea, methods and data. *Institute of Marine Science Technical Report*, **69–1**, 32 pp.

Bunt, J.S. & Lee, C.C. (1970) Seasonal primary production in Antarctic sea ice at McMurdo Sound in 1967. *Journal of Marine Research*, **28**, 304–320.

Burkholder, P.R. & Mandelli, E.F. (1965) Productivity of microalgae in Antarctic sea ice. *Science*, **149**, 872–874.

Clarke, D.B. & Ackley, S.F. (1984) Sea ice structure and biological activity in the Antarctic marginal ice zone. *Journal of Geophysical Research*, **89**, 2087–2095.

Cota, G.F., Anning, J.L., Harris, L.R., Harrison, W.G. & Smith, R.E.H. (1990) Impact of ice algae on inorganic nutrients in seawater and sea ice in Barrow Strait, NWT, Canada, during spring, *Canadian Journal of Fisheries and Aquatic Sciences*, **47**, 1402–1415.

Cota, G.F. & Sullivan, C.W. (1990) Photoadaptation, growth and production of bottom ice algae in the Antarctic. *Journal of Phycology*, **26**, 399–411.

Dieckmann, G.S., Sullivan, C.W. & Garrison, D. (1990) Seasonal standing crop of ice algae in pack ice of the Weddell Sea, Antarctica. *EOS, Transactions of the American Geophysical Union*, **71**, 79.

Dunbar, M.J. & Acreman, J.C. (1980) Standing crops and species composition of diatoms in sea ice from Robeson Channel to the Gulf of St. Lawrence. *Ophelia*, **19**, 61–72.

Fritsen, C.H., Ackley, S.F., Kremer, J.N. & Sullivan, C.W. (1998) Flood–freeze cycles and microalgal dynamics in Antarctic pack ice. In: *Antarctic Sea Ice Biological Processes, Interactions, and Variability*, (Eds M.P. Lizotte & K.R. Arrigo), American Geophysical Union, Washington, D.C. *Antarctic Research Series*, **73**, 1–21.

Fritsen, C.H., Lytle, V.I., Ackley, S.F. & Sullivan, C.W. (1994) Autumn bloom of Antarctic pack-ice algae. *Science*, **266**, 782–784.

Garrison, D.L., Ackley, S.F. & Buck, K.R. (1983) A physical mechanism for establishing algal populations in frazil ice. *Nature*, **306**, 363–365.

Garrison, D.L. & Buck, K.R. (1982) Sea-ice algae in the Weddell Sea. I. Biomass distribution and the physical environment. *EOS, Transactions of the American Geophysical Union*, **63**, 47.

Garrison, D.L. & Close, A.R. (1993) Winter ecology of the sea-ice biota in Weddell Sea pack ice. *Marine Ecology Progress Series*, **96**, 17–31.

Garrison, D.L., Close, A.R. & Reimnitz, E. (1989) Algae concentrated by frazil ice: evidence from laboratory experiments and field measurements. *Antarctic Science*, **1**, 313–316.

Gloersen, P., Campbell, W.J., Cavalieri, D.J., Comiso, J.C., Parkinson, C.L. & Zwally, H.J. (1992) *Arctic and Antarctic Sea Ice, 1978–1987: Satellite Passive Microwave Observations and Analysis*. NASA Special Publication, **511**, 289 pp. National Aeronautics and Space Administration, Washington, D.C.

Gosselin, M., Legendre, L., Demers, S. & Ingram, R.G. (1985) Responses of sea-ice microalgae to climatic and fortnightly tidal energy inputs (Manitounuk Sound, Hudson Bay). *Canadian Journal of Fisheries and Aquatic Sciences*, **42**, 999–1006.

Gosselin, M., Levasseur, M., Wheeler, P.A., Horner, R.A. & Booth, B.C. (1997) New measurements of phytoplankton and ice algal production in the Arctic Ocean. *Deep-Sea Research, Part II*, **44**, 1623–44.

Grainger, E.H. (1977) The annual nutrient cycle in sea ice. In: *Polar Oceans* (Ed. M.J. Dunbar), pp. 285–299. Arctic Institute of North America, Calgary, Canada.

Grossi, S.M., Kottmeier, S.T., Moe, R.L., Taylor, G.T. & Sullivan, C.W. (1987) Sea ice microbial communities. VI. Growth and primary production in bottom ice under graded snow cover. *Marine Ecology Progress Series*, **35**, 153–164.

Hegseth, E.N. (1998) Primary production of the northern Barents Sea. *Polar Research*, **17**, 113–123.

Hempel, G. (1985) Die expedition Antarktis III/3 mit F.S. Polarstern 1984/85. *Berichte zur Polarforschung*, **25**, 1–222.

Hempel, I. (1989) The expedition Antarctic VII/1 and 2 (EPOS 1) of RV Polarstern in 1988/89. *Berichte zur Polarforschung*, **62**, 1–184.

Horner, R.A. (1976) Sea ice organisms. *Oceanography and Marine Biology, An Annual Review*, **14**, 167–182.

Horner, R.A. & Schrader, G.C. (1982) Relative contributions of ice algae, phytoplankton, and benthic microalgae to primary production in nearshore regions of the Beaufort Sea. *Arctic*, **35**, 485–503.

Hoshiai, T. (1977) Seasonal change of ice communities in the sea ice near Syowa Station, Antarctica. In: *Polar Oceans*, (Ed. M.J. Dunbar), pp. 307–317. Arctic Institute of North America, Calgary, Canada.

Hoshiai, T. (1981) Proliferation of ice algae in the Syowa Station area, Antarctica. *Memoirs of the National Institute of Polar Research, Series E*, **34**, 1–12.

Hsiao, S.I.C. (1980) Quantitative composition, distribution, community structure and standing stock of sea ice microalgae in the Canadian Arctic. *Arctic*, **33**, 768–793.

Irwin, B.D. (1990) Primary production of ice algae on a seasonally-ice-covered, continental shelf. *Polar Biology*, **10**, 247–254.

Johnsen, J. & Hegseth, E.N. (1991) Photoadaptation of sea ice microalgae in the Barents Sea. *Polar Biology*, **11**, 179–184.

Kipfstuhl, J. (1991). On the formation of underwater ice and the growth and energy budget of the sea ice in Atka Bay, Antarctica. *Berichte zur Polarforschung*, **85**, 1–89.

Kottmeier, S.T., Grossi, S.M. & Sullivan, C.W. (1987) Late winter primary production and bacterial production in the sea ice and seawater west of the Antarctic Peninsula. *Marine Ecology Progress Series*, **36**, 287–298.

Kottmeier, S.T. & Sullivan, C.W. (1988) Sea ice microbial communities. IX. Effects of temperature and salinity on metabolism and growth of autotrophs and heterotrophs. *Polar Biology*, **8**, 293–304.

Kottmeier, S.T. & Sullivan, C.W. (1990) Bacterial biomass and bacterial production in pack ice of Antarctic marginal ice edge zones. *Deep-Sea Research*, **37**, 1311–1330.

Kudoh, S., Robineau, B., Suzuki, Y., Fujiyoshi, Y. & Takahashi, M. (1997) Photosynthetic acclimation and the estimation of temperate ice algal primary production in Saroma-ko Lagoon, Japan. *Journal of Marine Systems*, **11**, 93–109.

Legendre, L., Ackley, S.F., Dieckmann, G.S., Gulliksen, B., Horner, R., Hoshiai, T., Melnikov, I.A., Reeburgh, W.S., Spindler, M. & Sullivan, C.W. (1992) Ecology of sea ice biota: 2. Global significance. *Polar Biology*, **12**, 429–444.

Lemke, P. (1994) Die expedition Antarktis X/4 mit F.S. Polarstern 1992. *Berichte zur Polarforschung*, **140**, 1–90.

Lizotte, M.P. (2001) The contributions of sea ice algae to Antarctic marine primary production. *American Zoologist*, **41**, 57–73.

Lizotte, M.P. & Sullivan, C.W. (1991) Photosynthesis-irradiance relationships in microalgae associated with Antarctic pack ice: evidence for *in situ* activity. *Marine Ecology Progress Series*, **71**, 175–184.

Lizotte, M.P. & Sullivan, C.W. (1992) Photosynthetic capacity in microalgae associated with Antarctic pack ice. *Polar Biology*, **12**, 497–502.

McConville, M.J., Mitchell, C. & Wetherbee, R. (1985) Patterns of carbon assimilation in a microalgal community from annual sea ice, East Antarctica. *Polar Biology*, **4**, 135–141.

McMinn, A. & Ashworth, C. (1998) The use of oxygen microelectrodes to determine the net production by an Antarctic sea ice algal community. *Antarctic Science*, **10**, 39–44.

McMinn A., Ashworth, C. & Ryan, K. (1999) Growth and productivity of Antarctic Sea ice algae under PAR and UV irradiances. *Botanica Marina*, **42**, 401–407.

McRoy, C.P. & Goering, J.J. (1974) The influence of ice on the primary productivity of the Bering Sea. In: *Oceanography of the Bering Sea with Emphasis on Renewable Resources*, (Eds D.W. Hood & E.J. Kelley), pp. 403–421. Institute of Marine Science, University of Alaska, Fairbanks, Alaska.

Mathot, S., Garrison, D.L. & Lancelot, C. (1996) Pelagic and ice based primary production in the Southern Ocean. *EOS, Transactions of the American Geophysical Union*, **76**, 143.

Meguro, H. (1962) Plankton ice in the Antarctic Ocean. *Antarctic Record*, **14**, 1192–1199.

Meguro, H., Ito, K. & Fukushima, H. (1967) Ice flora (bottom type): a mechanism of primary production in polar seas and the growth of diatoms in sea ice. *Arctic*, **20**, 114–133.

Melnikov, I.A. & Bonderchuk, L.L. (1987) To the ecology of the mass aggregations of colonial diatom algae under the Arctic drifting sea ice. *Okeanology*, **27**, 317–321.

Michel, C., Legendre, L., Ingram, R.G., Gosselin, M. & Levasseur, M. (1996) Carbon budget of sea-ice algae in spring: evidence of a significant transfer to zooplankton grazers. *Journal of Geophysical Research*, **101**, 18345–18360.

Miller, H. & Grobe, H. (1996) Die expedition Antarktis X1/3 mit F.S. Polarstern 1994. *Berichte zur Polarforschung*, **188**, 1–155.

Mock, T. & Gradinger, R. (1999) Determination of Arctic ice algal production with a new *in situ* incubation technique. *Marine Ecology Progress Series*, **177**, 15–26.

Niebauer, H.J., Roberts, J. & Royer, T.C. (1981) Shelf break circulation in the northern Gulf of Alaska. *Journal of Geophysical Research*, **86**, 4231–4242.

Palmisano, A.C., Lizotte, M.P., Smith, G.A., Nichols, P.D., White, D.C. & Sullivan, C.W. (1988) Changes in photosynthetic carbon assimilation in Antarctic sea-ice diatoms during spring bloom: variation in synthesis of lipid classes. *Journal of Experimental Marine Biology and Ecology*, **116**, 1–13.

Palmisano, A.C., SooHoo, J.B. & Sullivan, C.W. (1985) Photosynthesis–irradiance relationships in sea ice microalgae from McMurdo Sound, Antarctica. *Journal of Phycology*, **21**, 341–346.

Palmisano, A.C., SooHoo, J.B. & Sullivan, C.W. (1987) Effects of four environmental variables on photosynthesis–irradiance relationships in Antarctic sea-ice microalgae. *Marine Biology*, **94**, 299–306.

Palmisano, A.C. & Sullivan, C.W. (1983) Sea ice microbial communities (SIMCO). I. Distribution, abundance, and primary production of ice microalgae in McMurdo Sound, Antarctica in 1980. *Polar Biology*, **2**, 171–177.

Palmisano, A.C. & Sullivan, C.W. (1985) Pathways of photosynthetic carbon assimilation in sea-ice microalgae from McMurdo Sound, Antarctica. *Limnology and Oceanography*, **30**, 674–678.

Perovich, D.K. (1990) Theoretical estimates of light-reflection and transmission by spatially varying sea ice covers. *Journal of Geophysical Research*, **95**, 9557–9567.

Quetin, L. & Ross, R. (1988) Summary of WINCRUISE II to the Antarctic Peninsula during June and July, 1987. *Antarctic Journal of the United States*, **23**, 149–151.

Rau, G.H., Sullivan, C.W. & Gordon, L.I. (1991) $\delta^{13}C$ and $\delta^{15}N$ variations in Weddell Sea particulate organic matter. *Marine Chemistry*, **35**, 355–369.

Riaux Gobin, C., Treguer, P., Poulin, M. & Vetion, G. (2000) Nutrients, algal biomass and communities in land-fast ice and seawater off Adelie Land (Antarctica). *Antarctic Science*, **12**, 160–171.

Robineau, B., Legendre, L., Kishino, M. & Kudoh, S. (1997) Horizontal heterogeneity of microalgal biomass in the first-year sea ice of Saroma-ko Lagoon (Hokkaido, Japan). *Journal of Marine Systems*, **11**, 81–91.

Rysgaard, S., Kühl, M., Glud, R.N. & Hansen, J.W. (2001) Biomass, production and horizontal patchiness of sea ice algae in a high-Arctic fjord (Young Sound; NE Greenland). *Marine Ecology Progress Series*, **223**, 15–26.

Schnack-Schiel, S.B. (1987) The winter expedition of *RV Polarstern* to the Antarctic (ANT V/1–3). *Berichte zur Polarforschung*, **39**, 1–258.

Smetacek, V., Scharek, R., Gordon, L.I., Eicken, H., Fuhrbach, E., Rohardt, G. & Moore, S. (1992) Early spring phytoplankton blooms in ice platelet layers of the southern Weddell Sea, Antarctica. *Deep-Sea Research*, **39**, 153–168.

Smith, R.E.H., Anning, J., Clement, P. & Cota, G. (1988) Abundance and production of ice algae in Resolute Passage, Canadian Arctic. *Marine Ecology Progress Series*, **48**, 251–263.

Smith, R.E.H., Clement, P. & Cota, G. (1989) Population dynamics of bacteria in Arctic sea ice. *Microbial Ecology*, **17**, 63–76.

Smith, R.E.H., Clement, P., Cota, G. & Li, W.K.W. (1987) Intracellular photosynthate allocation and the control of Arctic marine ice algal production. *Journal of Phycology*, **23**, 124–132.

Spindler, M., Dieckmann, G. & Thomas, D.N. (1993) Die expedition Antarktis X/3 mit F.S. Polarstern. *Berichte zur Polarforschung*, **121**, 1–122.

Stoecker, D.K., Gustafson, D.E., Baier, C.T. & Black, M.M.D. (2000) Primary production in the upper sea ice. *Aquatic Microbial Ecology*, **21**, 275–287.

Subba Rao, D.V. & Platt, T. (1984) Primary productivity of Arctic waters. *Polar Biology*, **3**, 191–201.

Sullivan, C.W., Palmisano, A.C., Kottmeier, S.T., Grossi, S.M. & Moe, R. (1985) The influence of light on growth and development of the sea-ice microbial community of McMurdo Sound. In: *Antarctic Nutrient Cycles and Food Webs*, (Eds W.R. Siegfried, P.R. Condy & R.M. Laws), pp. 78–83. Springer-Verlag, Berlin.

Sullivan, C.W., Palmisano, A.C., Kottmeier, S.T. & Moe, R. (1982) Development of the sea ice microbial community in McMurdo Sound. *Antarctic Journal of the United States*, **17**, 155–157.

Suzuki, Y., Kudoh, S. & Takahashi, M. (1997) Photosynthetic and respiratory characteristics of an Arctic ice algal community living in low light and low temperature conditions. *Journal of Marine Systems*, **11**, 111–121.

Thomas, D.N., Lara, R.J., Haas, C., Schnack-Schiel, S.B., Dieckmann, G.S., Kattner, G., Nöthig, E.-M. & Mizdalski, E. (1998) Biological soup within decaying summer sea ice in the Amundsen Sea, Antarctica. In: *Antarctic Sea Ice Biological Processes, Interactions, and*

Variability (Eds. M.P. Lizotte & K.R. Arrigo), American Geophysical Union, Washington, D.C. *Antarctic Research Series*, **73**, 161–171.

Tremblay, C., Runge, J.A. & Legendre, L. (1989) Grazing and sedimentation of ice algae during and immediately after a bloom at the ice–water interface. *Marine Ecology Progress Series*, **56**, 291–300.

Trenerry, L.J., McMinn, A. & Ryan, K.G. (2002) *In situ* oxygen microelectrode measurements of bottom-ice algal production in McMurdo Sound, Antarctica. *Polar Biology*, **25**, 72–80.

Wadhams, P., Lange, M. & Ackley, S.F. (1987) The ice thickness distribution across the Atlantic sector of the Antarctic Ocean in midwinter. *Journal of Geophysical Research*, **92**, 14535–14552.

Welch, H.E. & Bergmann, M.A. (1989) Seasonal development of ice algae and its prediction from environmental factors near Resolute, NWT, Canada. *Canadian Journal of Fisheries and Aquatic Sciences*, **46**, 1793–1804.

Welch, H.E., Bergmann, M.A., Siferd, T.D. & Amarualik, P.S. (1991) Seasonal development of ice algae near Chesterfield inlet, NWT, Canada. *Canadian Journal of Fisheries and Aquatic Sciences*, **48**, 2395–2402.

Whitaker, T.M. (1977) Sea ice habitats of Signy Island (South Orkneys) and their primary productivity. In: *Adaptations within Antarctic Ecosystems*, (Ed. G.A. Llano), pp. 75–82. Gulf Publications, Houston.

Chapter 6

The Microbiology of Sea Ice

Michael P. Lizotte

6.1 Introduction

From the earliest observations of sea ice to the present, one of the most remarkable features that has been routinely noted by all that have ventured into sea ice covered regions is the presence of ice discoloration. While sediment and mineral inclusions can discolour ice, the most common cause is the growth of pigmented algae. These algae are the most conspicuous members of diverse microbial communities inhabiting a wide range of microhabitats provided by sea ice.

Scientific studies of sea ice microorganisms date back to the 1840s in both hemispheres. In the tradition of natural history, the material collected during these early scientific and exploration voyages was used to build taxonomic lists. These observations established that the dominant group of organisms in sea ice is the diatoms. Other algal groups and non-photosynthetic protists were not reported until 1906, cyanobacteria in the 1930s, non-photosynthetic bacteria in the 1960s, archaea and viruses in the 1990s, and photosynthetic purple bacteria after 2000 (Horner, 1985; Maranger et al., 1994; Bowman et al., 1997; Petri & Imhoff, 2001). Because the sea ice environment encompasses interfaces with surface sea water, it is reasonable to expect that sea ice microbial diversity is comparable to that found in the underlying waters. In addition, sea ice might harbour endemic species, and provide habitats amenable to bottom-dwelling microbes (a solid substrate) or terrestrial microbes (snow and summer melt ponds). Modern microbiological studies of sea ice have sought to understand adaptation to extreme environments and the ecology of sea ice.

6.2 Diversity and abundance

The known diversity of sea ice microbes is highly dependent on the history of scientific interests, the limitations of research tools, and a lack of descriptions for novel or rare taxa. The higher-level diversity for the major groups of microorganisms can be described (Table 6.1), but lists at the genus or species level are better developed for some groups than for others. The desire to pro-

Table 6.1 Microbiota reported from sea ice*. In deference to varied naming conventions and taxonomic schemes under revision, major groups are listed by common names within formally recognized kingdoms. Viruses have also been observed in sea ice.

Eukaryota
Diatoms
Dinoflagellates
Chrysophytes
Prasinophytes
Silicoflagellates
Prymnesiophytes (including coccolithophorids)
Cryptophytes
Chlorophytes
Euglenophytes
Kinetoplastids
Choanoflagellates
Ciliates
Heliozoans
Foraminiferans
Amoebae
Chytrids
incertae sedis (unknown affinity)
Bacteria
Proteobacter group (alpha, beta and gamma subgroups)
Flexibacter–Bacteroides–Cytophaga group
Gram-positive Bacteria (High GC and Low GC groups)
Cyanobacteria
Archaea
Crenarchaeota
Euryarchaeota

* Based on detailed lists in Horner, 1985; Garrison, 1991; Maranger et al., 1994; Bowman et al., 1997; Ikävalko & Gradinger, 1997; Ikävalko & Thomsen, 1997; Staley & Gosink, 1999.

duce a list of taxa is not solely for understanding biodiversity or systematics. Often, we do not attempt to measure biological processes without evidence that key *actors* are present. For example, the conspicuous abundance of photosynthetic algae in sea ice has strongly influenced the research conducted in sea ice biology (Palmisano & Garrison, 1993). Another caveat regarding the sea ice biota is the difficulty in distinguishing between organisms that are merely caught in the sea ice and the organisms that survive, thrive, or depend, on sea ice for habitat. High abundance (relative to nearby waters) and biological activity (i.e. metabolism and growth) are the most common clues we have for defining sea ice microbial associations as functional (an ecological community) rather than circumstantial (an assemblage). Thus, it is useful to review microbial diversity and abundance with respect to both taxonomy and ecological roles.

Taxonomy

Overall, the research on sea ice microbial diversity is heavily weighted towards protists, particularly diatoms. Diatoms are successful competitors in most sunlit aquatic ecosystems, but their dominance of sea ice blooms is extreme (Plate 6.1; see also Palmisano & Garrison (1993) and Ikävalko & Thomsen (1997) for photo galleries of sea ice microbes). Thus it is not surprising that this group has received most of the research attention. Diatoms are distinctive amongst algae primarily due to their large requirement for silica, which they use to construct a cell wall. The production of ornate silica cell walls, called frustules, makes them particularly amenable to study. First, a rich taxonomy of diatoms has been based on detailed descriptions of frustules, which are studied by approachable and affordable microscopy techniques. Second, frustules are easily preserved (compared to soft cells and tissues). Diatom samples are easily collected (not a trivial issue given the logistics of polar research) and stored as reference samples or slides. Diatom frustules are also preserved in marine sediments, providing detailed records of past microbiological communities (Leventer, Chapter 10; Armand & Leventer, Chapter 11).

Most of the known species diversity in sea ice protistans (single-celled eukaryotes) has been described for the diatoms (Medlin & Priddle, 1990; Palmisano & Garrison, 1993; Ikävalko & Thomsen, 1997; Melnikov, 1997; Tuschling et al., 2000). In the Arctic, close to 200 species of diatoms are recorded from sea ice. The Antarctic appears to have less diatom diversity (*ca.* 100 species reported). In contrast, species lists often include only a few members of the other protistan groups. However, protists are typically identified through microscopy; groups lacking a robust cell wall (diatoms), lorica (choanoflagellates), or shell (foraminiferans), were poorly represented in early surveys because samples of ice were melted rapidly, decreasing salinity and producing an osmotic stress that could lyse fragile cells. Over the past 20 years, live observations and improved sampling and preservation techniques have greatly improved our accounting of protistan diversity.

Protistan members of sea ice communities include a broad range of flagellates, ciliates and amoebae, in addition to the algal groups and their close relatives (Garrison, 1991; Ikävalko & Gradinger, 1997). Ciliates appear to be the most diverse group of non-algal sea ice protists, but species diversity has not been studied in great detail for most groups. Small heterotrophic flagellates are probably the least well known. The large shell-building foraminiferans include ice-specific species that have been useful tracers of ice extent (based on the presence of their shells in marine sediments).

The known diversity of prokaryotic organisms, archea and eubacteria, in sea ice expanded rapidly during the last decade due to the introduction of molecular phylogeny methods (DeLong et al., 1994; Bowman et al., 1997; Staley & Gosink, 1999; Petri & Imhoff, 2001; Junge et al., 2002). Prokaryotic diversity represents more than 20 genera including many novel groups. For example, the archaea

reported from sea ice include groups previously only reported from hyperthermal environments. Observations of cyanobacteria associated with sea ice are mostly for freshwater species colonizing surface melt ponds.

In sea ice, most studies on prokaryotic diversity have focused on cultivated organisms (Staley & Gosink, 1999). Most of the isolated organisms are from the γ-Proteobacter and Flexibacter–Bacteroides–Cytophaga groups. Diversity measured from cloned rRNA genes of sea ice prokaryotes showed significant overlap between groups represented in the clone libraries and the sequences from cultivated species (Brown & Bowman, 2001). Such overlap has not been observed in many environments studied to date, with planktonic systems having great disparities between low diversity in culturable strains and high genetic diversity in water samples. The higher rate of cultivation for sea ice bacteria compared to plankton, along with observations that sea ice bacteria are not substrate limited (Pomeroy & Wiebe, 2001), suggest that the dominant bacteria strains might be adapted to high substrate levels that accumulate in sea ice (Thomas & Papadimitriou, Chapter 9).

Ecological roles

A common division of ecological roles is based on modes of feeding. Autotrophic organisms are those capable of providing their own 'food' through energy-capturing processes. The most common mode is photoautotrophy, based on capturing light energy by the process of photosynthesis. Less common at the surface of the earth is chemoautotrophy, based on capturing chemical energy, which may be a capability of the archaea and bacteria found in sea ice (e.g. based on observations of ammonia oxidation). Heterotrophic organisms must acquire energy primarily through consumption of other organisms or organic materials derived from living organisms. Finally, mixotrophic organisms are those who carry out both autotrophic and heterotrophic processes.

For sea ice communities (Table 6.1), the dominant autotrophs are photosynthetic protists, including diatoms, dinoflagellates, prymnesiophytes, prasinophytes, chrysophytes, cryptophytes, chlorophytes, euglenophytes, and a photosynthetic ciliate, *Mesodinium* (= *Myrionecta*) *rubrum*. Cyanobacteria and purple sulphur bacteria can also contribute as photosynthetic autotrophs. The most common blooms are those dominated by diatoms, particularly pennate species. Comparably high biomass accumulation is occasionally observed for surface blooms of prymnesiophytes (e.g. *Phaeocystis*) or dinoflagellates, and ice, snow and melt ponds dominated by terrestrial freshwater species of cyanobacteria and chlorophytes.

Of the protistan groups with autotrophic species, some include members that are heterotrophic and possibly mixotrophic. Heterotrophic species of dinoflagellates, chrysophytes, cryptophytes and euglenophytes have been reported in sea ice. Of particular note are the heterotrophic dinoflagellates, which are often the dominant grazers of photosynthetic sea ice algae. In addition to engulfing smaller organisms (bacteria, small protists), some species of sea ice dinoflagellates can use an external

feeding veil to enclose and digest larger prey (e.g. large diatoms). Other microflagellates and ciliates are the dominant phagotrophs (particle consumers) in other sea ice systems (Sime-Ngando et al., 1997). Mixotrophy that includes engulfing particles is also common in these groups, though not well established for sea ice species. A broader definition of mixotrophy would include heterotrophic uptake of dissolved organic matter. The uptake of sugars and amino acids has been demonstrated for the sea ice diatoms, and might extend to most if not all the photosynthetic autotrophs. From an ecological perspective, the main issue is whether the degree of heterotrophic uptake is significant for acquiring carbon or a limiting nutrient, such as nitrogen from amino acids. Heterotrophic uptake of dissolved organic matter by photosynthetic autotrophs appears to be minor, though it could be important for overwinter survival in sea ice.

Heterotrophic micro-organisms in sea ice also include other protists, fungi, bacteria and archaea. In addition to the heterotrophic protists listed above, sea ice communities have included ciliates, kinetoplastids, choanoflagellates, amoebae, heliozoans, foraminiferans and some protists that belong to no known group. Bacteria are the most abundant sea ice heterotrophs, while fungi (chytrids) have only been reported as parasites on protists. Virus particles have also been observed in only very few sea ice investigations (reviewed by Brierley & Thomas, 2002), but little is known about which hosts are affected. It is notable that no virus has ever been observed to interact with a diatom, in any aquatic ecosystem. However, viruses are expected to be most important in regulating populations of other algae, protists and prokaryotes.

Bacterial heterotrophy includes direct consumption of dissolved substrates, and extracellular decomposition (via exoenzymes) of dissolved and particulate matter followed by uptake. The most common species of bacteria in sea ice are from the γ-Proteobacter and Flexibacter–Bacteroides–Cytophaga groups, which are psychrophilic, aerobic chemoheterotrophs able to degrade a broad spectrum of substrates. Bacteria might also be parasitic on eukaryotes and other bacteria. Some of the bacteria found in sea ice could also originate as gut flora of animals. Sea ice bacteria are often attached to algae (epiphytic), particularly to diatoms. In other aquatic systems, attached and free-living bacteria belong to different phylogenetic groups (DeLong et al., 1993). In sea ice, bacterial epiphytes occur on some diatom species but rarely on others. The fraction of attached bacteria in these communities is *ca*. 30% of the population (Sullivan & Palmisano, 1984; Smith et al., 1989), which is considerably higher than the 10–15% reported in most marine waters (Fenchel et al., 1998). It is not known whether the ecological relationship between epiphytic prokaryotes and algal host is trophic (e.g. infection; symbiosis), physical (a means to avoid loss by flushing of the sea ice) or cryptic (to avoid small grazers).

Abundance

The abundance of sea ice micro-organisms can be quantified as the concentration of

cells or biomass (Table 6.2; see also Arrigo, Chapter 5). Microbe concentrations in sea ice cover up to six orders of magnitude, ranging from low values typical of oceanic waters to some of the highest values recorded for any aquatic environment. Low abundance is more typical of newly formed ice or the upper ice column where environmental conditions are extreme. The highest concentrations are found at ice–seawater interfaces, ice-enclosed pockets of sea water (e.g. platelet layers, brash ice and crack pools) and surface ponds.

Quantitative sampling of sea ice is difficult due to the heterogeneous distribution of organisms among the liquid and solid matrices. The first challenge is to capture a representative volume. The most common tool used to sample sea ice is a vertical coring device. Corers function best on thicker ice (capable of supporting the human operator) when the ice is young and cold (minimal drainage channels). Because the corer is pulled up through the surface of the ice and is not leak-proof, liquids can drain from the core. This makes it difficult to capture a representative sea ice sample from ice that is porous, has liquid-filled voids or drainage features, is loosely consolidated, is melting, or has organisms loosely attached at the ice–seawater interface. Difficult-to-core environments have been sampled from below by scuba divers, reticulated arms, or undersea robotics. Since the microbial communities often flourish at ice–water interfaces and under spring–summer–autumn (warmer) conditions, quantitative sampling of sea ice communities will usually require a mix of methods.

The second challenge in quantitative sampling is to produce a liquid sample containing the sea ice organisms. This is straightforward when the sampling technique extracts liquids from the sea ice. Larger volumes of liquids enclosed by sea ice, within internal or platelet layers, can be sampled directly by pumping. Brine can be removed from a sea ice core sample by gravity drainage or centrifugation. These samples retain the chemical and temperature conditions experienced by sea ice

Table 6.2 Ranges for abundance and biomass of sea ice microbiota*.

Cell count (10^6 cells l^{-1})	
Algae	< 0.1 to 2800
Bacteria	1 to 20 000
Heterotrophic protists	< 0.01 to 250
Biomass (μg carbon l^{-1})	
Algae	2 to 1 200 000
Bacteria	< 1 to 2400
Heterotrophic protists	< 1 to 1800
Autotroph biomass (μg chlorophyll-*a* l^{-1})	
Algae	< 0.1 to 60 000

* Extreme values can be found in: Horner, 1985; Garrison & Buck, 1989; Smith et al., 1989; Kottmeier & Sullivan, 1990; Smith et al., 1990; Garrison & Close, 1993; Palmisano & Garrison, 1993; Gleitz et al., 1996; Gradinger & Zhang, 1997; Sime-Ngando et al., 1997; Dieckmann et al., 1998.

organisms, which are critical for physiological studies. However, liquid sampling is not a comprehensive sampling method because attached or larger sea ice organisms remain with the ice matrix. To recover a complete microbial sample, the ice must be melted. Organisms in a melting sea ice sample will experience a shift in salinity from marine or hypersaline (> 34) to brackish (as low as 3), which will produce an osmotic shock that can cause cells to expand and lyse. An extreme salinity shift could kill sea ice microbes and leave little trace of fragile cells. To avoid these osmotic losses, the ice can be melted into sufficient sea water to keep salinity near marine levels. The sea water is pre-filtered (usually 0.2 μm) to remove planktonic organisms, thus the organisms in the melt water can be attributed to the sea ice sample. While this approach produces a highly disturbed chemical environment and involves temperatures above freezing, it produces samples that can be analysed for microbial abundance and biomass using routine methods developed for marine plankton.

Microbial cell counting is most commonly accomplished by microscopy. Light microscopy was the first analytical technique applied in sea ice biology, when diatoms were first described in the 1840s. Specific stains have been used to make cells more visible and to distinguish cells from detritus. The development of epifluorescent microscopy (Plate 6.1) has been an important development because it makes it possible to distinguish algae with fluorescing pigments (e.g. the red fluorescence of chlorophyll *a*) and to stain small cells. Under light microscopy, very small cells stained with coloured compounds can be difficult to see because a small cell diameter provides only a short pathlength for light absorption (altering the colour of the light leaving the cell). In contrast, a fluorescing compound within a small cell will 'light up' the cell. Fluorescent stains specific to nucleic acids have been critical for quantifying small, non-pigmented cells such as bacteria. Electron microscopy has also been instrumental in elucidating fine structures on microbial cells. Details such as scales, cell wall features and cell–cell attachment have been studied by electron microscopy. Flow cytometry (which can include microscopy in addition to other optical detection methods) has not been widely applied in sea ice studies to date, but holds promise for rapid quantification of smaller cells, particularly with the development of species or group-specific fluorescent molecular probes. Finally, methods have recently been developed for microscopy on cells while still enclosed in sea ice (Plate 6.1; Deming, 2002; Junge et al., 2002), which will be particularly useful for observing *in situ* spatial organization of microbial communities.

The biomass of microbes can be derived from microscopic observations and from chemical analyses. Biomass can be defined as the mass of living organisms, but in ecology is often defined more specifically as the mass of organic material (i.e. not including inorganic structures or water, which have little or no nutritional value). This organic material is often quantified in units of carbon, the defining element for organic compounds. Microscopic observations can be extended from cell counting to include quantification of cell dimensions, which can then be combined to determine the biovolume (volume of cells) for a given group. Biovolume can be

converted to carbon using simple multipliers, making it possible to derive concentrations of living cells in units of carbon. Different biovolume-to-carbon conversion factors are needed for different organism types depending on their biochemical composition, inorganic structures (e.g. diatom frustules), vacuoles and extracellular organic matrices. The total carbon estimated from biovolume can be compared with a measurement of particulate organic carbon (POC). POC samples are collected on filters and measured by gas chromatography techniques. POC should exceed the total biovolume-derived carbon due to non-living detritus. If detritus content is low, POC provides a convenient check on biovolume-derived carbon estimates. If detritus content is high (which should be apparent in microscopy samples), the carbon content of detritus can be estimated by difference.

The most widely applied chemical method for biomass estimation is algal pigment concentration. Chlorophyll *a* is present in all the common photosynthetic organisms in sea ice. For a chemical marker to be a useful estimator of biomass, it must be present in living organisms at a fairly constant ratio to carbon. While the ratio of chlorophyll *a* to carbon can vary amongst species and in response to changes in light (cells become enriched in chlorophyll *a* to increase their ability to harvest light), it serves as a first-order estimate of biomass for photosynthetic organisms. Carbon-to-chlorophyll *a* ratios (*ca.* 20 to 40 for sea ice algae) have been used to estimate algal carbon based on chlorophyll concentrations. For pigment analysis, cells are collected on filters, then the pigments are extracted with solvents and quantified by various optical techniques. The most common is to measure the red fluorescence of chlorophyll *a* when exposed to blue light. Methods are also available based on light absorbance at specific wavelengths via spectrophotometry. Because photosynthetic organisms contain a suite of photosynthetic pigments, these methods are subject to some interference from other pigments that fluoresce and absorb light. Separation of pigments by high-performance liquid chromatography (HPLC), followed by fluorescence and/or absorbance detection, is becoming a routine procedure. While this overcomes the interference problem of a pigment mixture, it also provides new information since different taxonomic groups (at the level shown in Table 6.1) have specific marker pigments or signatures. Thus HPLC pigment analysis allows us to measure a sample pigment signature that can be used to estimate the contributions of major algal groups to the total chlorophyll *a* biomass (Lizotte et al., 1998).

Molecular methods for determining biomass of different groups have only recently been developed, almost exclusively for prokaryotic microbes. The most promising molecular methods exploit the 16S ribosomal RNA (rRNA) gene sequences used to study the diversity of sea ice prokaryotes (Brown & Bowman, 2001; Junge et al., 2002). Application of rRNA-targeted probes with fluorescent *in situ* hybridization (FISH) techniques will allow for specific labelling of cells, which can then be quantified by epifluorescent microscopy (Deming, 2002). Another potential measure of taxa-specific biomass is the number of copies of a gene, based on quantitative polymerase chain reaction (PCR) techniques for rRNA genes

(Suzuki et al., 2000), providing that gene copies can be correlated with cell number or biomass.

6.3 Physiology and biochemistry

A great deal of the work conducted on sea ice in recent decades has been from the perspective of understanding adaptation of sea ice microbes to extreme environmental conditions. Extremes of temperature, salinity, light and chemical concentrations (oxygen, nutrients, organic materials) can develop in sea ice microenvironments (Thomas & Dieckmann, 2002; Eicken, Chapter 2). The ability to survive or thrive under these conditions depends on physiological acclimation and tolerances. Physiological responses can be rapid or transient, but often produce a biochemical signature. An understanding of the relationships among biochemical signatures, physiological responses and environmental stressors, can also be used to gauge current and past conditions that are not directly measurable. Thus, the response of sea ice microbes to their extreme environments provides additional tools (beyond population data) for studying ecology, biogeochemistry and paleoceanography.

The major emphasis in microbiological observations of aquatic habitats has been in understanding algal physiology. Part of this bias is based on the central role of algae as primary producers through the process of photosynthesis. Another factor has been the development of methods to support algal studies, including: measuring key rates (e.g. $^{14}CO_2$ as a tracer for photosynthesis), estimating biomass (e.g. chlorophyll), monitoring physiology (chlorophyll fluorescence) and separation of algal cells (size filtration). Algal photosynthesis is described elsewhere in this text with respect to light conditions (Arrigo, Chapter 5) and biogeochemistry (Thomas & Papadimitriou, Chapter 9). Therefore, this chapter will focus on other aspects of physiology and biochemistry, particularly those providing insights into the microbial loop (nutrition and remineralization) and survival (adaptations to extreme conditions in temperature and salinity).

Nutrition and remineralization

The availability and accumulation of chemical constituents in sea ice habitats is reviewed elsewhere (Thomas & Papadimitriou, Chapter 9), thus the focus in this chapter will be on microbial response and their roles in transforming materials. Sea ice algae utilize inorganic nutrients and carbon dioxide, and the materials produced can be remineralized by the activity of grazers and decomposers. Growth of sea ice algae requires acquisition of relatively large amounts of C, N, P and, for diatoms, Si. The main forms available are the inorganic forms of carbon dioxide, nitrate, phosphate and silicic acid. This leads to accumulations of particulate organic matter (POM) quantified as C, N and P, along with biogenic Si (diatom cell walls, as

distinguished from lithogenic Si). Dissolved organic matter (DOM) quantified as C, N and P also accumulates if released from the algal cells via excretion, cell lysis (e.g. after viral infection) or grazing. POM can be utilized by bacteria, fungi and protists. Bacterial exudation of extracellular enzymes can catalyse the conversion of POM into DOM, as well as converting DOM into more usable forms (e.g. breaking down a protein into amino acids). Protists contribute as consumers of both POM and DOM. Waste products of degradation range from recalcitrant materials (slowly remineralized, often complex organic molecules) to partly remineralized forms to fully remineralized compounds (e.g. carbon dioxide, nitrate, phosphate).

One important recalcitrant material in POM is the biogenic silicate with associated organic matrix. There is little evidence for remineralization of Si in sea ice. The other major elements (C, N, P) are remineralized in sea ice. There is evidence that Si is the nutrient most likely to limit diatom growth in advanced stages of a bloom (e.g. Gosselin et al., 1990), particularly after a diverse microbial community (capable of recycling C, N and P) has formed. Observations also support occasional limitation of sea ice algae by insufficient nitrogen (Lizotte & Sullivan, 1992; Smith et al., 1997).

Chemistry and biological activity are also affected by changes in pH and oxygen levels (Thomas & Papadimitriou, Chapter 9). Photosynthetic depletion of inorganic carbon can shift carbonate buffering in the system, producing increases in pH. Direct effects of high pH on sea ice microbes are not known, but changes in the chemical environment are likely to influence ionic composition of substrates. For example, more ammonium dissociates to ammonia at higher pH, with the latter being more amenable to diffusion into microbial cells. Photosynthetic activity can lead to high dissolved oxygen concentrations, which can be detrimental to microbes if there is an increased production of harmful oxygen radicals and peroxides. Some remineralization processes depend on the activity of oxygen-sensitive bacteria (e.g. denitrification, dissimilatory iron reduction), which might be limited by high dissolved oxygen levels until photosynthetic rates diminish and respiratory processes exceed oxygen production. A decrease in photosynthetic oxygen production might follow a decrease in light availability during the seasonal transition to winter, or more rapidly following snow accumulation. A rapid shift from net autotrophy (oxygen production) to net heterotrophy (oxygen consumption) can also be caused by events leading to rapid die-off in sea ice communities, particularly when a large biomass has accumulated. A common cause of mass die-off could be the accumulation of low-salinity melt water within or beneath sea ice.

The changes described above are most evident in relatively 'closed' microenvironments, such as the internal communities of sea ice. Silicic acid and nitrate depletion are measurable once algal biomass accumulates through growth. High rates of nitrogen remineralization are evidenced by accumulation of ammonia and nitrite to concentrations orders of magnitude above those found in sea water. Active denitrification by bacteria has been observed with high nitrite concentrations in sea ice (Kaartokallio, 2001). Ammonium uptake is a common substrate for sea ice algae

and bacteria, including ammonium oxidizers (Palmisano & Garrison, 1993). Phosphorus concentrations are more variable, since they can be depleted due to uptake by photosynthetic and heterotrophic microbes, or enhanced by remineralization. Dissolved organic carbon (DOC) concentrations can also be much higher than observed in sea water due to high rates of algal production and decomposition (Thomas & Papadimitriou, Chapter 9). An alternative explanation for simultaneous occurrence of high ammonia, phosphate, DOC and oxygen is the direct release of algal cell contents due to lysis or breakage during grazing.

In sea ice micro-environments with significant seawater exchange (bottom ice or flooded surfaces), the depletion and accumulation signals are diluted. Flushing by sea water replaces nutrient-depleted interstitial waters to alleviate limitation of microbial growth and removes accumulated waste products. For heterotrophs requiring particular intermediates (e.g. nitrite) or preferring particular forms of DOM, rapid flushing might reduce growth by removing substrates. Flushing is also likely to produce changes in the biota, specifically the loss of small, unattached microbes, which will alter biogeochemical cycling in these micro-environments. Larger open spaces in sea ice (platelet layers, freeboard chambers) can also harbour substantial populations of small grazing metazoans that will increase decomposition of POM.

Nitrogen uptake and assimilation by sea ice diatoms has been studied in some detail (Priscu & Sullivan, 1998). Nitrate uptake shows much higher affinity (low half-saturation coefficients), in the μM range, compared to mM range for intracellular nitrate reductase enzyme affinity. The latter matches measurements of mM nitrate intracellular concentrations. This indicates that uptake and assimilation of nitrate are uncoupled, and that incorporation of this nitrogen source into cellular components is limited by transport into the cell. Nitrate reductase in sea ice diatoms has also shown weak inhibition (*ca.* 20% decrease) at environmental ammonium concentrations of *ca.* 1 μM, which could lead to a shift from nitrate to ammonium as a nitrogen source as ammonium accumulates in older sea ice. However, high nitrate utilization has been observed in sea ice with much higher ammonium concentrations, implying that some sea ice diatoms are even less susceptible to suppression of nitrate reductase by ammonium. High (mM) intracellular concentrations of ammonium and phosphate relative to low environmental concentrations (μM) suggest that uptake and assimilation might be uncoupled for these nutrients as well.

The production and utilization of DOM includes contributions from all members of the sea ice microbial community (Thomas & Papadimitriou, Chapter 9). Photosynthesizing algae excrete a portion of their photosynthate as DOM. The proportion excreted increases under high light stress due to photorespiration, in which high intracellular oxygen favours RUBISCO (ribulose bisphosphate carboxylase/oxygenase) oxidation (rather than carboxylation) of carbon-cycle intermediates. Products of photorespiration include low molecular weight compounds such as glycolate. Sea ice diatoms can also take up DOM (sugars, amino acids) in light and dark (Palmisano & Garrison, 1993). Algal heterotrophic uptake would be

most advantageous under conditions of light-limitation for photosynthesis or overwinter survival. Heterotrophic protists assist the production of DOM primarily through excretion after digestion of consumed particles. Protists might also release algal cell DOM by damaging or killing cells (e.g. chytrid fungi infestation of diatoms) or entering dead diatom cells to feed. Digestion by protists is likely to include 'leakage' from the cells, as observed for the algae. Bacterial interactions with DOM pools are primarily as consumers, but they also excrete organic waste products. Some bacteria excrete extracellular enzymes to decompose POM and DOM. Recovery of the excreted enzymes and their products is not 100% efficient, thus contributing to DOM pools. Finally, DOM is released when viruses and parasitic bacteria lyse their host cells. Overall, the rate of DOM production in sea ice communities appears to be high as a fraction of primary production (Gosselin et al., 1997).

Adaptations to extreme conditions

Low temperature adaptation

Sea ice environments are dominated by psychrophilic organisms. Psychrophiles are defined by growth temperatures with minima $< 0^{\circ}$C, optima $< 15^{\circ}$C, and maxima near 20°C. Some strains of sea ice bacteria have the lowest maxima known, $< 10^{\circ}$C (Staley & Gosink, 1999). The adaptations to low temperature have been studied primarily from three aspects: growth and physiological rates, enzyme activity and membrane fluidity (Gerday et al., 1999; Gounot & Russell, 1999; Thomas & Dieckmann, 2002).

Growth and physiological rate responses to temperature include definition of range (minimum, optimum, maximum) and Q_{10} (the change for every 10°C change in temperature). For comparision, most biological growth rates and specific enzyme reaction rates show Q_{10} values of *ca.* 2 (Stapleford & Smith, 1996). At near zero temperatures, Q_{10} values above 10 have been reported in sea ice diatoms, for carbon fixation, nitrate uptake and ammonium uptake (Priscu et al., 1989). This implies that a small change in temperature (e.g. from -4°C to -2°C) can have greater impacts on physiological rates than would occur for an equivalent temperature change (e.g. from 10°C to 12°C) in a temperate microbial ecosystem. In general, substrate uptake (organic and inorganic) has been shown to be temperature-limited in polar microbes (Nedwell, 1999; Pomeroy & Weibe, 2001).

In sea ice bacteria, short-term growth rates might be highest at temperatures exceeding environmental conditions, but the highest levels of viable cells at stationary growth are observed near the environmental temperatures of -2 to 4°C (Gounot & Russell, 1999). This implies that 'optimal' growth rates based on short-term measurements are biased to higher temperatures, and are not a good measure of optimal physiological state or potential for population growth. For this reason, several polar bacteria that have temperature optima exceeding the definition for

psychrophiles, based on short-term growth rates, have been re-defined as psychrophiles because they show higher production of extracellular enzymes (a response to environmental stimuli) at near-zero temperatures.

Enzyme activity has been studied primarily with respect to Q_{10} and structural stability (Gerday et al., 1999). As with the overall growth and physiology rates (which are often set by a rate-limiting enzymatic step), enzyme Q_{10} values often exceed 3 at low temperatures. The most common mechanism leading to this high Q_{10} value is reduced interaction between the enzyme and its substrate. Another factor thought to be important at low temperature is avoiding structural rigidity in the catalytic region (which might also contribute to a lower melting temperature and set the maximum temperature). In general, eukaryotes can respond to lower temperatures by expressing isotypes of an enzyme with higher efficiency at low temperature. This requires multiple genes, which are less common in prokaryotes. An alternate strategy is to increase the concentration of an enzyme at lower temperature, which comes at a high energetic and material cost. For marine polar organisms that are constantly exposed to low temperatures, the most commonly evolved strategy has been the selection for enzyme forms efficient at low temperatures.

Studies of enzymes from polar organisms have been primarily from bacteria and fish, and can be compared to those of organisms from higher temperature environments (Gerday et al., 1999; Deming, 2002). Although not directly isolated from sea ice, the bacteria studied might offer some insights into the adaptations likely to occur in sea ice microbes. All the enzymes studied show low thermostability, which implies flexibility at low temperatures. For the extracellular enzymes studied (α-amylase, lipase, protease, subtilisin, β-lactamase, xylanase), higher specific activity is observed at low temperature. For intracellular enzymes studied (alkaline phosphatase, triosphosphate isomerase, citrate synthase, phosphoglycerate kinase and β-galactosidase), high affinity was only noted in one enzyme. One interpretation is that adaptation for the extracellular enzymes is more likely since these enzymes are only induced when substrate concentrations are high (i.e. when the cell encounters a food source). Alternatively, the intracellular enzymes might not show the same degree of low-temperature adaptation because their catalytic efficiency is adequate for cellular metabolism rates. For example, the enzymes studied might not be those limiting growth rate or survival, thus natural selection pressures are weak.

Stress-induced proteins are also associated with viability at low temperature (Gounot & Russell, 1999). Cold-shock proteins are induced rapidly after a temperature decrease. These proteins are thought to play roles in translation, transcription and DNA replication. While most of the research on cold-shock proteins has been done in temperate bacteria, analogies have been identified in polar bacteria. In psychrophiles, some proteins (including cold-shock protein analogues) are permanently induced at low temperature, and are referred to as cold-acclimation proteins.

Membrane fluidity is critical to the functioning of membrane-bound proteins (Gounot & Russell, 1999). Temperature affects membrane fluidity because mem-

branes are composed of lipids, which become a gel as temperatures decrease and melt at higher temperatures. The temperature dependence depends primarily on the proportions of saturated and unsaturated fatty acids; other factors increasing fluidity include methyl branching and shorter chains. Saturated fatty acids are straight chains more easily ordered for solidification; unsaturation bends the chain at each double bond, making it less likely to align with a neighbouring fatty acid, increasing fluidity. In general, the membrane phospholipids of psychrophiles have a higher proportion of unsaturated fatty acids. Sea ice bacteria have polyunsaturated fatty acids (PUFAs) that are regulated by temperature, depending on modification by a desaturase enzyme (which has been identified as a cold-shock protein in a temperate bacterium). Sea ice bacteria also express novel enzymes, polyketide synthases, that allow for efficient production of PUFAs at low temperatures. Fatty acid desaturation is also thought to be critical in maintaining electron transport in the thylakoid membranes of chloroplasts in sea ice diatoms.

A final aspect of low-temperature survival is cellular production of molecules that improve freezing tolerance of cells. Ice-active substances that modify the shape of growing ice crystals have been observed in sea ice microbial communities, and are correlated to diatom populations (Raymond, 2000). These macromolecules appear to be glycoproteins that preferentially bind to ice. Dimethylsulphoxide (DMSO), a molecule widely used to enable cryostorage of cells, is produced by sea ice diatoms (Lee et al., 2001). However, intracellular concentrations are considered too low for significant freezing point depression of sea water, unless DMSO is concentrated at sub-cellular sites (e.g. associated with membranes or enzymes). For a small cell taking up nearly all the available space in a sea ice brine pocket, the need for antifreeze protection diminishes as the ordering behaviour, surface charge and polarity of water molecules dictate conditions that keep water in a liquid state (Mindock et al., 2001; Deming, 2002).

Salinity acclimation

Melting a sea ice sample directly will result in a solution with a salinity of *ca.* 1–6, which would lyse or significantly stress marine organisms, particularly if the sea ice microbes are residing in hypersaline brines. Conversely, decreasing ice temperatures result in more saline brine solutions, to >200 psu at the lowest sea ice temperatures (Eicken, Chapter 2). Natural variations in sea ice salinity are extreme, with only estuarine organisms experiencing salinity changes of this magnitude (though only for salinities less than sea water). The most common method for releasing organisms from sea ice has been to melt the sea ice into a large volume of sea water that has been pre-filtered to remove particles and plankton. Thus, most studies of sea ice microbes have been carried out at salinities at or below that of sea water (*ca.* 28–35).

Experiments to test salinity effects have been conducted from 3 to 110 (reviewed by Brierley & Thomas, 2002), a range covering ice melt to brines experienced during

the growth season. In general, increasing or decreasing salinity from those typical of sea water leads to decreasing photosynthetic rates. However, sea ice algae have been observed to have optimal activity at lower salinity during the ice melt, or at higher brine salinities during colder seasons. These differences have been attributed to acclimation and to species-specific differences, implying that changes in sea ice salinity influence microbial succession. Lower salinity levels (15–30) are also more common in northern hemisphere sea ice regions due to greater melt pond accumulations on the sea ice and riverine input to shallow coastal seas (Melnikov, 1997). Snow or freshwater species found on sea ice would be expected to have growth optima at lower salinity.

Specific adaptations to salinity stress in sea ice bacteria include changes in membrane fatty acid composition, production of salt-tolerant enzymes and regulation of osmolyte concentrations (reviewed by Thomas & Dieckmann, 2002). Osmolytes include inorganic ions and organic solutes within cells. As inorganic ion concentrations change as salinity changes, organic solutes become more critical for regulating osmotic pressure within the cell. Thus the cell can accumulate or synthesize organic solutes as salinity increases, and decompose or release organic solutes as salinity decreases. Many organic osmolytes have been identified, and most are simple sugars and polyols.

Dimethylsulphoniopropionate (DMSP) can also serve as an osmolyte; DMSP has been observed at relatively high concentrations in sea ice (DiTullio et al., 1998; Lee et al., 2001; Thomas & Papadimitriou, Chapter 9). DMSP decomposes into dimethyl sulphide (DMS) which is oxidized to sulphuric acid in the atmosphere providing a major source of sulphate aerosols and cloud condensation nuclei. Thus high rates of production of DMSP and release by sea ice microbes in response to their variable salinity environment, could potentially impact the earth's climate system. However, there are more specific implications of DMSP and DMS production for the sea ice microbial network (reviewed by Brierley & Thomas, 2002; Thomas & Papadimitriou, Chapter 9). DMSP is broken down to DMS and acrylic acid (acrylate). Bacteria can metabolize DMSP, DMS and acrylic acid, although at high levels of the last bacterial growth is inhibited. Considering the high levels of DMSP that have been detected in sea water, the potential for such inhibitory acrylic acid concentrations seems quite high. Acrylic acid may also deter protozoan and metazoan herbivores.

6.4 Ecology

Incorporation and colonization

The incorporation of microorganisms from the water column into sea ice occurs due to enclosure, active concentration and by colonization. Enclosure of water can occur as ice consolidates (from frazil ice) or as ice crystals growing on the sea ice surfaces conjoin (for congelation ice or platelet ice). Active concentration mechanisms are

best known for initial stages of ice formation from frazil ice, which are generally referred to as scavenging. A third mechanism for incorporation is the lifting of benthic material attached to anchor ice; this occurs only in the shallowest, coldest regions of polar seas.

Scavenging mechanisms usually concentrate algal cells and biomass by four- to ten-fold in new ice compared to the source waters (Ackley & Sullivan, 1994). One mode of scavenging is adherence of cells to ice crystals moving through the water column. Another scavenging mode occurs at the surface of the ocean as frazil ice collects to form a grease ice layer. Wave action causes a pumping of water through the grease ice layer which acts as a filter collecting particles. Both means of scavenging are selective for larger particles, but not strongly selective for smaller types of particle (e.g. cells versus detritus) or species. This implies that these scavenging mechanisms follow principles of particle aggregation (encounter rates) similar to those producing marine snow, rather than depending on cell attributes (e.g. cell surface properties). In later stages of sea ice structural development, 'filtering' of particles from sea water can occur in several ways. Sea water can infiltrate the surface ice and snow via wave action or by isostatic depression of the surface below sea level (due to snow accumulation). Sea water can also be exchanged with surface ponds, freeboard infiltration layers, or liquid pockets of platelet ice. Horizontal flow across sea ice surfaces can produce a vertical pulsing that will flush brine channels and cracks with sea water. In these cases, cells entering with sea water might settle or attach to the ice or snow and so remain associated with sea ice.

Since the initial incorporation of algal cells into new sea ice reflects the cells available in the water column during freezing, subsequent changes in species composition reflect selection, succession and later colonization. None of these processes has been explicitly studied in sea ice algal communities, to the extent that the changes in populations could be attributed to immigration, emigration, growth or death (natural, grazed or disease-related). Most interpretations of observed populations, e.g. in ice of different stages of development, have been attributed to selection against most species (slow growth, no growth or loss) and rapid growth in a few dominant species.

Colonization of ice microenvironments occurs after ice formation, with the source of cells being either older ice or the water column. A simple case is for new ice formed in autumn and winter, which grows in thickness during winter when phytoplankton cells are rare. If the ice that incorporated cells remains at the top of the ice column, those cells would need to migrate (actively or passively) to colonize the centimetres to metres of underlying ice that can grow in one winter. Algae from the surface could move down the ice column via brine drainage channels. This brine drainage also increases the rate of seawater exchange in the brine channels open to the sea, thus increasing the potential to import cells. Given the relatively better light environment in the sea ice compared to the deeply mixed, under-ice water column, it could be advantageous for algae to colonize the ice

substrate at the sea surface. The algae dominating sea ice blooms are often large cells or colonies (e.g. chain-forming diatoms), implying that size might be important in retention during these flushing events. Sub-ice attached communities are another macroscopic form taken by sea ice microbial communities. They form attached to the underside of the ice (extending centimetres to metres) supported on mucous structures produced by tube-dwelling and chain-forming diatoms (Melnikov, 1997).

For active sea ice regions where deformation, ridging, break-up and consolidation are common, there may be other means for redistributing cells within an ice column. Based solely on ice dynamics, algae incorporated near the surface of a floe could end up as an internal horizontal band (rafted floes), a near vertical band (ridge) or bottom ice (overturned floe). Ground up floes can be reconstituted with new frazil ice to randomly distribute microbial communities within an ice column. The same processes could also redistribute microbial communities from multi-year ice into newly forming ice. Given the numerous physical mechanisms for distributing and redistributing micro-organisms in sea ice, it is not surprising that pack ice regions show great variety in the shape of vertical profiles of microbial biomass (Ackley & Sullivan, 1994; Gradinger & Zhang, 1997; Lizotte et al., 1998).

Even if sea ice algal blooms were to originate primarily from stock incorporated via physical scavenging mechanisms, colonization from the water column could be important for heterotrophic organisms. The dense concentration of algal cells during blooms, their waste products and breakdown products, could be attractants to grazers (e.g. protists) and decomposers (e.g. bacteria) from the water column. As noted by Deming (2002), there has been little study of microbial chemotaxis in cold habitats.

Due to their small size, most marine bacteria in polar seas are not concentrated by ice scavenging mechanisms (Grossmann & Gleitz, 1993; Gradinger & Ikävalko, 1998). Exceptions are the largest cells (*ca.* 1 μm^3) and those attached to larger particles and cells. Bacterial incorporation relates primarily to the algal species being incorporated, presumably due to differences in the bacteria (ability to adhere) or algae (discouraging or encouraging epiphytic attachment). Some polar marine bacteria show high ice-nucleation activity (Sullivan, 1985), in which cells initiate ice crystal formation; these crystals and cells could become incorporated directly into a forming or growing sea ice cover.

Gas vacuolate bacteria from several groups listed in Table 6.1 have also been reported in sea ice (Staley & Gosink, 1999), though not from other marine habitats. Gas vacuoles increase buoyancy, allowing these bacteria to rise in the water column and come into contact with sea ice. Those encountered in the sea ice during the spring diatom bloom do not form gas vacuoles. These bacteria are also present in surface waters during ice melt, but not in deeper waters. Thus the field observations support the hypothesis that gas-vacuole production is related to remaining near the sea surface to increase potential for incorporation into sea ice.

Microbial food webs

Sea ice, like most marine habitats, is dominated by microbes and microbial processes. The dominance of microbes is enhanced in sea ice microhabitats due to the small spaces and extreme physical and chemical conditions that exclude large marine organisms (Krembs et al., 2000). This simplifies the ecosystem, lowering the diversity of ecological relationships. Thus a sea ice food web, along with its role in material cycling and energy transfer, should be fairly simple to describe. The limitations on our ability to quantify the sea ice microbial food web come primarily from: (1) the variety of sea ice microhabitats; (2) sampling difficulties; (3) the ephemeral nature of the sea ice habitat in most regions; and (4) the fact that sea ice is a thin, open system with major input and output to the sea.

Given these limitations, sea ice microbial food webs have been described primarily by conceptual models based on the presence/absence of organisms capable of carrying out certain processes, constrained by observations of accumulated biomass (Fig. 6.1). Feeding relationships amongst organisms are based primarily on size, making it important to recognize several size categories of heterotrophic protists. The photosynthetic algae and mixotrophs cover a size range over several orders of magnitude (10^{-6} to 10^{-4} m), with larger forms available primarily to the largest grazers. Sea ice microhabitats can also include invertebrate grazers for additional trophic levels (Schnack-Schiel, Chapter 7). In classical food chain terms, only the

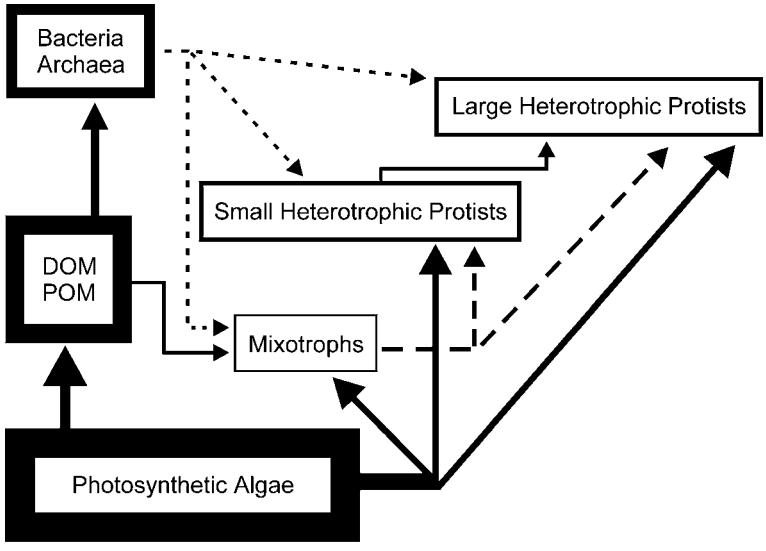

Fig. 6.1 Conceptual model of the main feeding relationships in sea ice microbial food webs. The loop returning dissolved organic matter (DOM) and particulate organic matter (POM) from all organismal reservoirs is not shown. The wall thickness for each reservoir represents relative biomass for typical summer conditions. Each of these reservoirs has been observed to dominate sea ice microbial biomass at some time and place.

strict autotrophic algae can be assigned to a trophic level (as primary producers, level 1), as the potential for feeding at several trophic levels exists for members of the sea ice grazing community. For example, a heterotrophic dinoflagellate would be a primary consumer (level 2) when feeding on a diatom, a secondary consumer (level 3) when feeding on a small flagellate that grazed on diatoms, or a tertiary consumer (level 4) when feeding on a small ciliate that had consumed a small flagellate that had consumed a diatom. If one knew the diet of this heterotrophic dinoflagellate along with the diets of its prey, an intermediate designation could be made (e.g. level 2.6). Such detailed trophic analyses are necessary to understand most aquatic food chains, though they have been attempted for only a few systems and macroscopic organisms (e.g. fisheries).

Our current understanding of sea ice microbial food webs is limited by the lack of process rate measurements beyond photosynthetic production (Arrigo, Chapter 5) and bacterial production (Table 6.3). The base of most sea ice food webs is *in situ* production by photosynthetic organisms. However, in some regions and at early stages of sea ice development, the food web can be based primarily on particles scavenged from the water column. These POM inputs can include terrestrial material from rivers, resuspended benthic materials in coastal regions, or planktonic organisms that did not survive ice formation. During autumn and winter, sea ice systems often have bacterial production equalling or surpassing algal production, and heterotrophic biomass (bacteria plus protists) exceeding autotrophic biomass. One explanation is autumn blooms of sea ice algae that have since degraded. Alternatively, the relatively high heterotrophic activity could be based at least partly on decomposition of imported materials during autumn/winter ice formation. When lacking significant primary production, sea ice microbial ecosystems form a decomposition-dominated food web.

A sea ice food web supported by algal primary production often develops with rapid growth of the algal population. At one extreme are systems with short sea ice seasons (e.g. low latitudes), in which the development of a food web might not progress beyond a primary production dominated stage. The sea ice melts before a

Table 6.3 Ranges for bacterial productivity: daily rates and as a ratio with photosynthetic production in sea ice.

Production rate (mg C m^{-3} d^{-1})	Bacterial production: photosynthetic production	Reference
0.0004–6.0	0.0001–0.09	Kottmeier et al., 1987
—	0.004–14	Kottmeier & Sullivan, 1987
—	5–6	Rivkin et al., 1989
4–1100	0.02–2.2	Kottmeier & Sullivan, 1990
0.2–10	0.1–2.0	Grossmann & Dieckmann, 1994
4.8–290	—	Grossmann et al., 1996
0.7–3600	0.2–19	Gleitz et al., 1996
2.9–5.6	—	Mock et al., 1997

significant heterotrophic community develops. The accumulated algal production is released to the water column before significant decomposition or recycling of materials can occur. At the other extreme, high latitude systems (particularly in the Arctic Basin) can have a short growing season but sea ice communities can develop for many years in multi-year pack ice. This can allow a diverse community to develop based on a short burst of primary production followed by a long season of decomposition and remineralization. This could constitute a microbial loop, in which organic materials are produced by algae and recycled by heterotrophs, including the consumption of bacteria and small protists by larger protists.

In most sea ice regions, the ice lasts 0.3–2 years, with time for multiple algal blooms. There is usually a spring bloom at the base of the ice column, where temperatures are moderated by the sea. Later blooms can occur near the surface of the ice when air temperatures rise and the sea ice warms. Surface flooding with sea water, due to isostatic depression by accumulated snow, can speed up this warming and deliver nutrients and organisms. Sea ice algal blooms are often low in algal diversity, approaching monospecific in many cases. One factor is the elimination of potential competitors due to the extreme environmental conditions experienced during ice formation or overwintering. Alternatively, it could be argued that some sea ice environments present few constraints (low grazing pressure, abundant resources), allowing competitive exclusion to occur as the most fit species outgrows competitors. The rapid algal growth of a spring bloom can end due to nutrient limitation, detrimental effects of accumulation (e.g. self-shading or accumulation of toxic waste products), or a loss of microhabitat (e.g. melting at ice–water interfaces). In cases where the sea ice community is not lost to ice melt, algal population growth could be decreasing as the growth of heterotrophic populations increases by utilizing the accumulated algal products. Decomposition of accumulated algal products can lead to conditions that reinvigorate algal growth by regenerating nutrient stocks, degenerating toxic waste products, or increasing light by decomposing pigments.

With continued primary production through summer and autumn, the sea ice ecosystem can develop a significant microbial loop. Additional factors could limit primary production, including supply rates for regenerated nutrients or loss to grazers. The diversity of the microbial community would be expected to increase as the number of controlling factors increases to include grazers, pathogens, and more diverse nutrient and food sources. However, it has been proposed that sea ice can be an environment where the development of a microbial loop is often thwarted, leading to accumulation of POM and DOM. The reasons include extreme environmental conditions and size restrictions that limit colonization, survival and success of key or complementary microbial loop species. Biological explanations include the possibility that algal secondary products, such as dimethylsuphide or acrylic acid (breakdown products of biologically produced DMSP), might limit activity of bacteria and grazers.

Succession

Community structure in sea ice changes over time, a process known as succession. Few time-series observations have been made for sea ice communities. Some researchers have attempted to reconstruct successional patterns by comparing communities from ice of different 'age' (e.g. new, first-year, multi-year). Algal diversity has been observed to decrease with time or 'age' (a common phenomenon in algal blooms), becoming more diatom dominated (Lizotte & Arrigo, 1998). Bacteria/archaea diversity may decrease, becoming more dominated by psychrophiles, with salinity tolerance and response to substrate availability implicated in selection (Pomeroy & Wiebe, 2001). Junge et al. (2002) offer several explanations for why sea ice prokaryotic communities are less diverse than other marine environments. One follows ecological theories stating that stressful environments favour a few species best adapted to survive rather than diverse species with many interactions. However, sea ice with well-developed autotrophic production has been observed to support a much higher diversity in prokaryotes (Bowman et al., 1997) and heterotrophic protists (Sime-Ngando et al., 1997), implying that food supply is one of the stresses limiting heterotrophic community succession.

An important aspect of any successional sequence is the continuous modification of the environment by organisms. Sea ice microbes modify their microenvironments chemically and physically. The inorganic chemical composition is altered for compounds that serve as nutrients, but there is little evidence for other inorganic chemical changes (e.g. precipitation of calcite due to pH change and carbon dioxide drawdown). Chemical modification is most obvious in the production and alteration of organic compounds, with DOM concentrations reaching orders of magnitude higher than the source sea water (Thomas & Papadimitriou, Chapter 9). The potential roles of this DOM in succession are poorly understood. DOM provides substrates for a wide array of microbes. DOM includes secondary products that might be used in signalling, deterring competitors or predators, or altering the physical environment. Polymeric substances in DOM could alter physical conditions by setting a gel, which could change flushing rates, diffusion or mobility. High concentrations of transparent exopolymer particles have been observed in sea ice during diatom blooms (Krembs & Engel, 2001). The ice-active substances produced by diatoms (Raymond, 2000) could also influence ice crystal formation, and thus might influence the geometry of ice surfaces. The organisms and their particulate remains also add physical structure to the environment, which might be colonized by other microbes.

These observations imply that sea ice microbial communities probably fit many of the theoretical definitions of successional stages and sequences, such as pioneer community, climax community, primary succession and secondary succession.

A pioneer community is clearly represented by the species observed growing in recently formed ice, which is only a subset of the organisms found in underlying waters. Pennate diatom species are the most common pioneer species, though other

algae have been observed to accumulate rapidly in sea ice. Bacteria (and possibly archaea) may play critical roles in a pioneer community, particularly those cells intimately associated with pioneer algal species. It is possible to consider sea ice communities solely as pioneer communities, particular for the majority of systems in which sea ice is an ephemeral, seasonal occurrence. Sea ice is an ecotone in the ocean, and ecotones are often dominated by opportunistic species such as pioneers.

For sea ice cover formed anew each year and lasting for many months, it is possible that a type of primary succession occurs. A primary succession beyond the pioneer stage is feasible within only a few months because that is enough time for tens of generations in microbial populations, providing a chance for major shifts in community structure. The most common primary succession would begin with a pioneer stage during autumn or winter ice formation. Early successional species are usually noted by small size, wide dispersal and high growth rates. Many of the dominant algae and bacteria reported from sea ice fit this description, including a common occurrence in the sea water from which sea ice is formed. Late successional species are usually less adept at dispersal and colonization, grow more slowly, and have more specific requirements (e.g. food sources). This definition fits many species of heterotrophic protists, which appear to be far more variable in composition between sites. The changes in community structure over time are primarily defined by the species present (a function of colonization and dispersal) and secondarily by the response to disturbance events (e.g. overwinter chilling, blooms, brine drainage). This primary succession can end within the year due to the loss of the habitat at ice melt.

In multi-year ice, it is debatable whether primary succession continues or a secondary succession ensues. If a microbial community survives intact in multi-year ice, in approximately the same physical relationship to air and seawater interfaces (i.e. the same position in an ice sheet), then primary succession could continue. In the second and ensuing years, a heterotrophic community might be significant from the start of the algal growth season, which could lead to less dramatic algal accumulation due to top-down grazer control. Nutrient regeneration rates might also be higher if a microbial loop remains intact.

Secondary succession is a sequence in which the succession occurs on a disturbed site previously occupied by organisms; thus it follows a mass die-off or removal of organisms. Examples of sea ice phenomena that could decimate microbial populations include: fresh water (low salinity drainage from melted snow cover, surface ponds or accumulation beneath ice cover); overwinter freezing (low temperature and high salinity near the air–sea surface); anaerobic conditions (oxygen depletion in organic rich layers after photosynthesis stops); or melting at ice–seawater interfaces during summer (e.g. due to radiation absorption by pigmented algae). For older ice incorporated into a growing ice cover, or re-worked in a multi-year ice pack in polar seas, a particular piece of sea ice might experience several major disturbances each year, leading to multiple secondary succession sequences.

Ecologists have also coined a term for the community structure at the end of a

successional sequence – the climax community. Climax communities are difficult to define and require an understanding of both biodiversity and functional diversity in the ecosystem. However, it is probable that climax communities are rarely, if ever, achieved in sea ice. Environmental disturbances are so common, extreme and frequent in the months to years that sea ice microbial communities exist, that succession might not proceed for more than a few months.

6.5 Conclusions and recommendations for future work

Sea ice microbiology has benefitted greatly from the ongoing revolution in aquatic microbiology. An increasing array of tools is available for biochemical analysis, radiotracer experiments, metabolic inhibition, genetic analysis, microscopy and micromanipulation. However, the major limitations in sea ice microbiology are associated with quantitative sampling and the lack of *in situ* or undisturbed observations. The sweep of new technologies in aquatic microbiology may even be exacerbating the problem by making the latter problems easier to avoid, i.e. scientific breakthroughs are possible with new analyses using traditional sampling methods. Thus, knowledge has improved greatly in biodiversity, bulk chemical properties and physiological potential, but remains limited for the microscale distribution of microbes, chemicals and ice surfaces, or for *in situ* rates of physiological processes or ecological interactions. The 'potential' rates, relationships and interactions will remain suspect until they can be confirmed by *in situ* measurements or experiments that adequately simulate sea ice environmental conditions.

The description of sea ice microbial diversity will change considerably as future studies extend to the use of genetic approaches to exploring all the microbial diversity (prokaryotic and eukaryotic). The rate of discovery in bacteria and archaea in the past decade is a good indicator of the potential for discovering new species and sorting out controversial identifications. These new technologies may also be easier to standardize than past microscopy-based methods, which will allow us to determine whether community composition is as wildly variable as reported to date.

Physiological and biochemical studies of sea ice microbes have the potential to combine well-described extremophile systems with modern molecular techniques to look at regulation, feedback and genetic control. Temperature response is particularly well-suited for this approach, specifically to explore the regulation of synthesis and turnover of enzymes and membrane lipids. This work would provide quantitative explanations for survival and growth in sea ice microbes, as well as having potential biotechnology applications. Ecological understanding would greatly increase if rates were measured routinely for more processes than photosynthetic production and bacterial growth, to provide a more complete picture of materials cycling and food web energetics.

The paucity of time-series information for sea ice microbial communities is a

major weakness for understanding how ecological relationships develop. Time-series have been limited by logistics to ice that can support people and vehicles, mostly lasting for one season at a near-shore site. Thus we know little about the key events at the beginning or end of the sea ice lifespan, and the transitions of organisms to and from the sea. For example, the concept of 'seeding' of phytoplankton blooms by sea ice algae has been discussed for decades based solely on circumstantial evidence (co-occurrence of species in the ice and water column). The converse, 'seeding' from water to ice, has received even less attention. Thus time-series studies are needed for representative sea ice regions in order to understand the incorporation, succession and demise of sea ice microbial communities. If key species populations can be monitored over time, then it may be possible to quantify colonization, selection pressures and the role of released organisms in developing planktonic populations.

References

Ackley, S.F. & Sullivan, C.W. (1994) Physical controls on the development and characteristics of Antarctic sea ice biological communities – a review and synthesis. *Deep-Sea Research*, **41**, 1583–1604.

Bowman, J.P., McCammon, S.A., Brown, M.V., Nichols, D.S. & McMeekin, T. (1997) Diversity and association of psychrophilic bacteria in Antarctic sea ice. *Applied and Environmental Microbiology*, **63**, 3068–3078.

Brierley, A.S. & Thomas, D.N. (2002) On the ecology of Southern Ocean pack ice. *Advances in Marine Biology*, **43**, 171–278.

Brown, M.V. & Bowman, J.P. (2001) A molecular phylogenetic survey of sea-ice microbial communities (SIMCO). *FEMS Microbiology Ecology*, **35**, 267–275.

DeLong, E. F., Franks, D.G. & Alldredge, A.L. (1993) Phylogenetic diversity of aggregate-attached versus free-living marine bacterial assemblages. *Limnology and Oceanography*, **38**, 924–934.

DeLong, E.F., Wu, K.Y., Prezelin, B.B. & Jovine, R.V.M. (1994) High abundance of Archaea in Antarctic marine picoplankton. *Nature*, **371**, 695–697.

Deming, J.W. (2002) Psychrophiles and polar regions. *Current Opinion in Microbiology*, **5**, 301–309.

Dieckmann, G.S., Eicken, H., Haas, C., Garrison, D.L., Gleitz, M., Lange, M., Nöthig, E.-M., Spindler, M., Sullivan, C.W., Thomas, D.N. & Weissenberger, J. (1998) A compilation of data on sea ice algal standing crop from the Bellingshausen, Amundsen and Weddell Seas from 1983 to 1994. In: *Antarctic Sea Ice: Biological Processes, Interactions and Variability*, (Eds M.P. Lizotte & K.R. Arrigo), American Geophysical Union, Washington, D.C. *Antarctic Research Series*, **73**, 85–92.

DiTullio, G.R., Garrison, D.L. & Mathot, S. (1998) Dimethylsulfoniopropionate in sea ice algae from the Ross Sea polynya. In: *Antarctic Sea Ice: Biological Processes, Interactions and Variability*, (Eds M.P. Lizotte & K.R. Arrigo), American Geophysical Union, Washington, D.C. *Antarctic Research Series*, **73**, 139–146.

Fenchel, T., King, G.M. & Blackburn, T.H. (1998) *Bacterial Biogeochemistry*, 2nd edn. Academic Press, San Diego.

Garrison, D.L. (1991) Antarctic sea ice biota. *American Zoologist*, **31**, 17–33.

Garrison, D.L. & Buck, K.R. (1989) The biota of Antarctic pack ice in the Weddell Sea and Antarctic Peninsula regions. *Polar Biology*, **10**, 211–219.

Garrison, D.L. & Close, A.R. (1993) Winter ecology of the sea ice biota in Weddell Sea pack ice. *Marine Ecology Progress Series*, **96**, 17–31.

Gerday, C., Aittaleb, M., Arpigny, J.L., Baise, E., Chessa, J.P., Francois, J.M., Garsoux, G., Petrescu, I. & Feller, G. (1999) Cold enzymes: a hot topic. In: *Cold-Adapted Organisms: Ecology, Physiology, Enzymology and Molecular Biology*, (Eds R. Margesin & F. Schinner), pp. 257–275. Springer-Verlag, Berlin.

Gleitz, M., Grossmann, S., Scharek, R. & Smetacek, V. (1996) Ecology of diatom and bacterial assemblages in water associated with melting summer ice in the Weddell Sea, Antarctica. *Antarctic Science*, **8**, 135–146.

Gosselin, M., Legendre, L., Therriault, J.-C. & Demers, S. (1990) Light and nutrient limitation of sea-ice microalgae (Hudson Bay, Canadian Arctic). *Journal of Phycology*, **26**, 220–232.

Gosselin, M., Levasseur, M., Wheeler, P.A., Horner, R.A. & Booth, B.C. (1997) New measurements of phytoplankton and ice algal production in the Arctic Ocean. *Deep-Sea Research*, **44**, 1623–1644.

Gounot, A.M. & Russell, N.J. (1999) Physiology of cold-adapted microorganisms. In: *Cold-Adapted Organisms: Ecology, Physiology, Enzymology and Molecular Biology*, (Eds R. Margesin & F. Schinner), pp. 33–55. Springer-Verlag, Berlin.

Gradinger, R. & Ikävalko, J. (1998) Organism incorporation into newly forming Arctic sea ice in the Greenland Sea. *Journal of Plankton Research*, **20**, 871–886.

Gradinger, R. & Zhang, Q. (1997) Vertical distribution of bacteria in Arctic sea ice from the Barents and Laptev Seas. *Polar Biology*, **17**, 448–454.

Grossmann, S. & Dieckmann, G.S. (1994) Bacterial standing stock, activity, and carbon production during formation and growth of sea ice in the Weddell Sea, Antarctica. *Applied and Environmental Microbiology*, **60**, 2746–2753.

Grossmann, S. & Gleitz, M. (1993) Microbial responses to experimental sea-ice formation: implications for the establishment of Antarctic sea-ice communities. *Journal of Experimental Marine Biology and Ecology*, **173**, 273–289.

Grossmann, S., Lochte, K. & Scharek, R. (1996) Algal and bacterial processes in platelet ice during late austral summer. *Polar Biology*, **16**, 623–633.

Horner, R.A. (Ed.) (1985) *Sea Ice Biota*. CRC Press, Boca Raton, Florida.

Ikävalko, J. & Gradinger, R. (1997) Flagellates and heliozoans in the Greenland Sea ice studied alive using light microscopy. *Polar Biology*, **17**, 473–481.

Ikävalko, J. & Thomsen, H.A. (1997) The Baltic Sea ice biota (March 1994): a study of the protistan community. *European Journal of Protistology*, **33**, 229–243.

Junge, K., Imhoff, F., Staley, T. & Deming, W. (2002) Phylogenetic diversity of numerically important Arctic sea-ice bacteria cultured at subzero temperature. *Microbial Ecology*, **43**, 315–328.

Kaartokallio, H. (2001) Evidence for active microbial nitrogen transformations in sea ice (Gulf of Bothnia, Baltic Sea) in midwinter. *Polar Biology*, **24**, 21–28.

Kottmeier, S.T., Grossi, S.M. & Sullivan, C.W. (1987) Sea ice microbial communities. VIII. Bacterial production in annual sea ice of McMurdo Sound, Antarctica. *Marine Ecology Progress Series*, **35**, 175–186.

Kottmeier, S.T. & Sullivan, C.W. (1987) Late winter primary production and bacterial production in sea ice and seawater west of the Antarctic Peninsula. *Marine Ecology Progress Series*, **36**, 287–298.

Kottmeier, S.T. & Sullivan, C.W. (1990) Bacterial biomass and production in pack ice of Antarctic marginal ice edge zones. *Deep-Sea Research*, **37**, 1311–1330.

Krembs, C. & Engel, A. (2001) Abundance and variability of microorganisms and transparent exopolymer particles across the ice–water interface of melting first-year ice in the Laptev Sea (Arctic). *Marine Biology*, **138**, 173–185.

Krembs, C., Gradinger, R. & Spindler, M. (2000) Implications of brine channel geometry and surface area for the interaction of sympagic organisms in Arctic sea ice. *Journal of Experimental Marine Biology and Ecology*, **243**, 55–80.

Lee, P.A., de Mora, S.J., Gosselin, M., Levasseur, M., Bouillon, R.-C., Nozais, C. & Michel, C. (2001) Particulate dimethylsulfoxide in Arctic sea-ice algal communities: the cryoprotectant hypothesis revisited. *Journal of Phycology*, **37**, 488–499.

Lizotte, M.P. & Arrigo, K.R. (Eds) (1998) *Antarctic Sea Ice: Biological Processes, Interactions and Variability.* American Geophysical Union, Washington, D.C. *Antarctic Research Series*, **73**, 1–198.

Lizotte, M.P., Robinson, D.H. & Sullivan, C.W. (1998) Algal pigment signatures in Antarctic sea ice. In: *Antarctic Sea Ice: Biological Processes, Interactions and Variability*, (Eds M.P. Lizotte & K.R. Arrigo), American Geophysical Union, Washington, D.C. *Antarctic Research Series*, **73**, 93–106.

Lizotte, M.P. & Sullivan, C.W. (1992) Biochemical composition and photosynthate distribution in sea ice algae of McMurdo Sound: evidence for nutrient deficiencies during the bloom. *Antarctic Science,* **4**, 23-30.

Maranger, R., Bird, D.F., & Juniper, S.K. (1994) Viral and bacterial dynamics in Arctic sea ice during the spring algal bloom near Resolute, NWT, Canada. *Marine Ecology Progress Series*, **111**, 121–127.

Medlin, L.K. & Priddle, J. (1990) *Polar Marine Diatoms*. British Antarctic Survey, Cambridge.

Melnikov, I.A. (1997) *The Arctic Sea Ice Ecosystem*. Gordon and Breach Science Publishers, Amsterdam.

Mindock, C.A., Petrova, M.A. & Hollingsworth, R.I. (2001) Re-evaluation of osmotic effects as a general adaptive strategy for bacteria in sub-freezing conditions. *Biophysical Chemistry*, **89**, 13–24.

Mock, T., Meiners, K.M. & Giesenhagen, H.C. (1997) Bacteria in sea ice and underlying brackish water at 54°26′50″N (Baltic Sea, Kiel Bight). *Marine Ecology Progress Series*, **158**, 23–40.

Nedwell, D.B. (1999) Effect of low temperature on microbial growth: lowered affinity for substrates limits growth at low temperature. *FEMS Microbiology Ecology*, **30**, 101–111.

Palmisano, A.C. & Garrison, D.L. (1993) Microorganisms in Antarctic sea ice. In: *Antarctic Microbiology*, (Ed. E.I. Friedmann), pp. 167–218. Wiley-Liss, New York.

Petri, R. & Imhoff, J.F. (2001) Genetic analysis of sea-ice bacterial communities of the Western Baltic Sea using an improved double gradient method. *Polar Biology*, **24**, 252–257.

Pomeroy, L.R. & Wiebe, W.J. (2001) Temperature and substrates as interactive limiting factors for marine heterotrophic bacteria. *Aquatic Microbial Ecology*, **23**, 187–204.

Priscu, J.C., Palmisano, A.C., Priscu, L.R. & Sullivan, C.W. (1989) Temperature dependence

of inorganic nitrogen uptake and assimilation in Antarctic sea-ice microalgae. *Polar Biology*, **9**, 443–446.

Priscu, J.C. & Sullivan, C.W. (1998) Nitrogen metabolism in Antarctic fast-ice microalgal assemblages. In: *Antarctic Sea Ice: Biological Processes, Interactions and Variability* (Eds. M.P. Lizotte & K.R. Arrigo), American Geophysical Union, Washington, D.C. *Antarctic Research Series*, **73**, 147–160.

Raymond, J. (2000) Distribution and partial characterization of ice-active molecules associated with sea-ice diatoms. *Polar Biology*, **23**, 721–729.

Rivkin, R.B., Putt, M., Alexander, S.P., Meritt, D. & Gaudet, L. (1989) Biomass and production in polar planktonic and sea ice microbial communities: a comparative study. *Marine Biology*, **101**, 273–283.

Sime-Ngando, T., Gosselin, M., Juniper, S.K. & Levasseur, M. (1997) Changes in sea-ice phagotrophic microprotists (20–200 μm) during the spring algal bloom, Canadian Arctic Archipelago. *Journal of Marine Systems*, **11**, 163–172.

Smith, R.E.H., Clement, P. & Cota, G.F. (1989) Population dynamics of bacteria in Arctic sea ice. *Microbial Ecology*, **17**, 63–76.

Smith, R.E.H., Gosselin, M. & Taguchi, S. (1997) The influence of major inorganic nutrients on the growth and physiology of high Arctic ice algae. *Journal of Marine Systems*, **11**, 63–70.

Smith, R.E.H., Harrison, W.G., Harris, L.R. & Herman, A.W. (1990) Vertical fine structure of particulate matter and nutrients in sea ice of the high Arctic. *Canadian Journal of Fisheries and Aquatic Sciences*, **47**, 1348–1355.

Staley, J.T. & Gosink, J.J. (1999) Poles apart: biodiversity and biogeography of sea ice bacteria. *Annual Review of Microbiology*, **53**, 189–215.

Stapleford, L.S. & Smith, R.E.H. (1996) The interactive effects of temperature and silicon limitation on the psychrophilic ice diatom *Pseudonitzschia seriata*. *Polar Biology*, **16**, 589–594.

Sullivan, C.W. (1985) Sea ice bacteria: reciprocal interactions of the organisms and their environment. In: *Sea Ice Biota*, (Ed. R.A. Horner), pp. 159–171. CRC Press, Boca Raton, Florida.

Sullivan, C.W. & Palmisano, A.C. (1984) Sea ice microbial communities: distribution, abundance, and diversity of ice bacteria in McMurdo Sound, Antarctica in 1980. *Applied and Environmental Microbiology*, **47**, 788–795.

Suzuki, M.T., Taylor, L.T. & DeLong, E.F. (2000) Quantitative analysis of small-subunit rRNA genes in mixed microbial populations via 5′-nuclease assays. *Applied and Environmental Microbiology*, **66**, 4605–4614.

Thomas, D.N. & Dieckmann, G.S. (2002) Antarctic sea ice – a habitat for extremophiles. *Science*, **295**, 641–644.

Tuschling, K., von Juterzenka, K., Okolodkov, Y. & Anoshkin, A. (2000) Composition and distribution of the pelagic and sympagic algal assemblages in the Laptev Sea during autumn freeze-up. *Journal of Plankton Research*, **22**, 843–864.

Chapter 7

The Macrobiology of Sea Ice

Sigrid B. Schnack-Schiel

7.1 Introduction

Apart from harbouring a diverse group of autotrophs, bacteria and protozoans (Garrison, 1991; Lizotte, Chapter 6), sea ice is also a feeding ground, refuge and breeding or nursery ground for a number of metazoans. These are adapted to live within the sea ice or at the ice–water interface, either permanently (autochthonous) or only temporarily (allochthonous). While some metazoans (mainly copepods, turbellarians, nematodes and rotifers) live within the sea ice, others – particularly larger animals such as euphausiids and amphipods – are often found in close association with the under-ice habitat, feeding on ice algae on the underside of the sea ice floes (Brierley & Thomas, 2002). In turn, the metazoans form a key component of the diet of many 'top trophics' (Ainley et al., Chapter 8), and are fundamental in the mediation of particulate fluxes from sea ice (Leventer, Chapter 10) and processes associated with bentho-pelagic coupling, especially in shallow shelf regions.

Compared to the species richness in the water column and the interstitial sediment faunas, the number of ice-inhabiting metazoan species is low, suggesting a highly specialized fauna (Friedrich, 1997; Schnack-Schiel et al., 1998). Those organisms inhabiting parts of the sea ice that are isolated from sea water have to be able to tolerate temperatures below -10°C and salinities three- or four-fold that of sea water. Hence, only a few species dominate the sympagic fauna (Table 7.1).

The major contrasting characteristics of Arctic and Antarctic sea ice (Dieckmann & Hellmer, Chapter 1) have resulted in differences in the role of sea ice for the ecology, life history strategies and seasonal dynamics of metazoans in both polar oceans. Most of the sea ice in the Antarctic is annual, whereas a significant portion of the Arctic Ocean is permanently frozen. Hence, sympagic metazoans in the Antarctic have to be adapted to the seasonal melt and growth of the ice cover. There have, therefore, been less pressing opportunities for the evolution of autochthonous metazoan species in the Antarctic sea ice compared to the Arctic.

Table 7.1 Dominant metazoan species found within sea ice*.

Nematodes	
Arctic	*Theristus melnikovii, Cryonema tenue*
Rotifers	
Arctic	*Synchaeta hyperborea, S. tamara*
Harpacticoid copepods	
Arctic	*Halectinosoma* sp., *Harpacticus* sp., *Tisbe furcata*
Antarctic	*Drescheriella glacialis*
Calanoid copepods	
Antarctic	*Paralabidocera antarctica, Stephos longipes*
Cyclopoid copepods	
Arctic	*Cyclopina gracilis, C. schneideri*

* Primary references: Grainger & Hsiao, 1990; Grainger, 1991; Carey, 1992; Riemann & Sime-Ngando, 1997; Friedrich, 1997; Schnack-Schiel et al., 1998; Blome & Riemann, 1999; Swadling et al., 2001.

7.2 Sea ice metazoan communities

The sea ice community

Both pelagic (such as calanoid copepods and rotifers) and benthic (such as turbellarians, nematodes and most harpacticoid copepods) metazoan species have been found in sea ice, and there is a significant difference between the main metazoan composition of Arctic and Antarctic sea ice assemblages (Fig. 7.1; Gradinger, 1999; Schnack-Schiel et al., 2001a). Copepods and acoel turbellarians dominate the metazoan fauna in Antarctic sea ice. Although these taxa are also present in Arctic sea ice, the most dominant groups in this ice are rotifers and nematodes.

Rotifers have only been reported from Arctic sea ice (Gradinger, 1999), and nematodes, which are numerous in Arctic sea ice samples, have only been recorded from Antarctic sea ice once (Blome & Riemann, 1999). All nematodes found in sea ice belong to the Monhysteroidea and are probably confined to the ice habitat, since they have not been described from the sediment (Riemann & Sime-Ngando, 1997; Blome & Riemann, 1999). Six rotifer species have been identified in sea ice in the Barents, Laptev and Greenland Seas, with *Synchaeta hyperborea* being the most abundant followed by *S. tamara* (Friedrich, 1997).

Within the copepods, three species clearly dominate the Antarctic sea ice metazoan fauna: the harpacticoid *Drescheriella glacialis* and the calanoids *Paralabidocera antarctica* and *Stephos longipes* (Table 7.1). The calanoid *Ctenocalanus citer*, the poecilostomacoid *Oncaea curvata*, the cyclopoid *Oithona similis* as well as several other harpacticoid species have been only occasionally reported from Antarctic sea ice cores. The reported densities of these other taxa are at least two orders of magnitude lower than those of the three abundant species (Swadling et al., 1997; Schnack-Schiel et al., 1998; Swadling et al., 2001).

In the Arctic the cyclopoid copepods *Cyclopina gracilis* and *C. schneideri*, as well

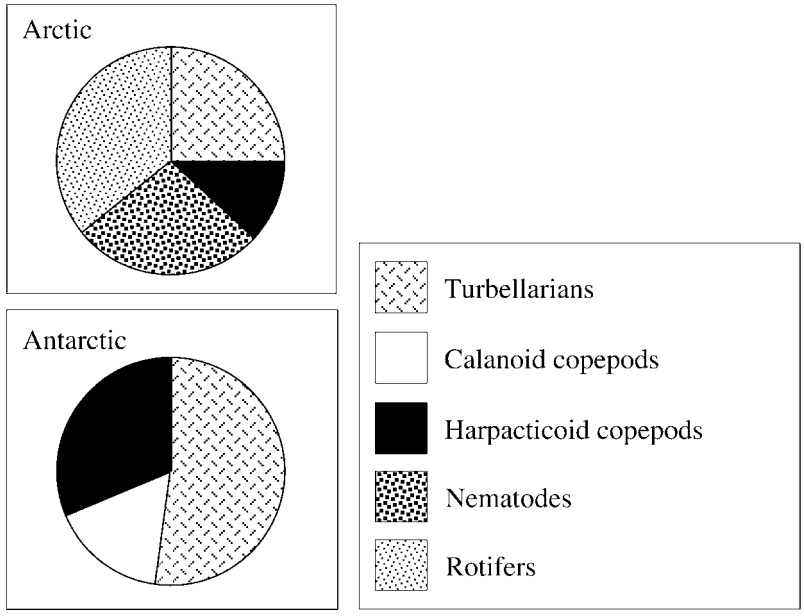

Fig. 7.1 Relative contribution of ice metazoans to mean abundance and biomass. Modified from Gradinger (1999) and Schnack-Schiel et al. (2001a).

as the harpacticoids *Harpacticus* spp., *Halectinosoma* sp. and *Tisbe furcata*, have often been found in sea ice samples. Commonly found calanoid species from the water column, such as *Acartia longiremis*, *Pseudocalanus* sp., *Calanus glacialis* and the cyclopoid *Oithona similis*, are only rarely reported from Arctic sea ice samples.

Larvae of benthic organisms such as polychaets and gastropods have been found in sea ice but their distribution is usually closely related to shallow water depths and is highly seasonal. They have been reported in high numbers in coastal fast ice in the Arctic (Carey, 1992), and to a lesser degree in Antarctic sea ice over the relatively deep shelf (Andriashev, 1968).

Spatial variability

The distribution and abundance of sea ice metazoans are very patchy and vary considerably within and between ice floes. This variability does not seem to be attributed to seasonal changes in sea ice physical conditions (Swadling et al., 1997; Gradinger, 1999; Schnack-Schiel et al., 2001a). The overriding factor governing the distribution of metazoans within the sea ice matrix is the space in the ice that is available for colonization. Sympagic metazoans differ greatly in their morphology: small elongated, 'plastic' animals, such as turbellarians and rotifers, are able to enter and traverse narrow brine channels, whereas larger animals such as the copepods and amphipods are restricted by their size. Krembs et al. (2000), using capillary

tubes of different sizes, showed experimentally that rotifers and turbellarians penetrate channels significantly smaller than their body dimension (57% and 60% of their normal body diameter, respectively), which they achieve by stretching and flexing their body. Turbellarians, which can tolerate salinities up to 75 (Gradinger & Schnack-Schiel, 1998), apparently change their body dimensions in response to salinity changes. In contrast, nematodes, although slender, only rarely penetrate the smallest brine channels. Harpacticoid copepods only entered the tubes of diameters similar to their body diameters. Amphipods avoid narrow passages (Krembs et al., 2000), and are only found in pockets and larger brine channels in the bottom layer of the ice (Cross, 1982). Hence, the patchiness can be partly explained by the highly heterogeneous size and spatial arrangement of pores and brine channels within the ice.

The highest numbers of sympagic metazoans are found in the lowermost regions of ice floes in the bottom ice layers (Tanimura et al., 1996; Schnack-Schiel et al., 2001a; Swadling et al., 2001) where an exchange of water with the surrounding sea water is possible. The temperature and salinity in the skeletal layers and brine channels at the ice–water interface are most similar to those of the underlying water (Fig. 7.2a), and therefore do not require the organisms to undergo any energetically costly physiological or metabolic acclimation. These high concentrations of metazoans at the periphery of ice floes often coincide with a high biomass of ice algae on which the metazoans feed (Hoshiai et al., 1987; Schnack-Schiel et al., 1995; Janssen & Gradinger, 1999; Fig. 7.2a). Additionally, due to the warmer temperatures towards the bottom of the ice, brine channels are larger and permit the colonization by the larger species. Higher in the ice, at colder temperatures, the narrower brine channels restrict, and/or possibly crush, trapped organisms. This is especially true in late autumn and winter when the brine channels in cold ice are narrow and small in diameter. Metazoans are rarely found in newly formed ice sheets (Schnack-Schiel et al., 1995, 2001b).

In the porous and rotten multi-year sea ice during late summer and autumn, ice sympagic metazoans can easily migrate to virtually all levels in the ice floes, and high concentrations are also encountered in upper and middle layers (Fig. 7.2b). Peak abundances in rotten slush layers are closely associated with high salinity and nutrient replete conditions and, hence, dense algal concentrations, which are attributed to secondary flooding with sea water (Schnack-Schiel et al., 1998; Thomas et al., 1998; Scnack-Schiel et al., 2001b; Thomas & Papadimitriou, Chapter 9).

The sub-ice community

The morphology of the ice underside is an important factor for colonization, and the variety of under-ice structures provides a wide range of different microhabitats (Krembs et al., 2001). These small-scale refuges are highly dependent on the prevailing water current direction and speed, and because of this are rather changeable in nature. Therefore, as in the sea ice itself, the animals in the sub-ice layer are

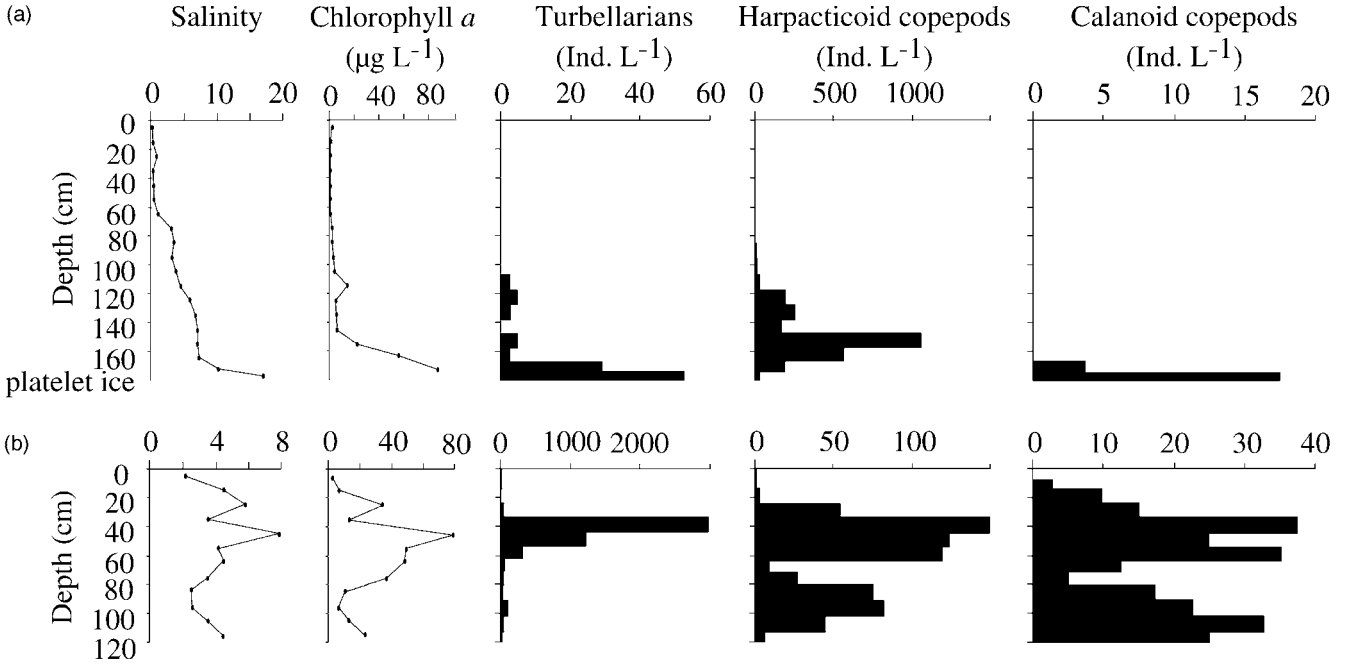

Fig. 7.2 Vertical distribution of salinity, chlorophyll *a* and abundances of turbellarians, harpacticoid and calanoid copepods: (a) in an ice core with an underlying platelet ice layer and (b) in an ice core.

patchily distributed and their abundance can vary greatly between sampling sites, even on the scales of centimetres to metres (Daly & Macaulay, 1988). The ice–water interface, which includes a huge complex surface of nooks and crannies, and where the mobility of the animals is largely unconstrained, is frequented by larger grazers. The most conspicuous of these are the euphausiids and gammeriid amphipods, which are seldom found within the ice itself, but largely exploit surfaces at the periphery of ice floes (Gulliksen & Lønne, 1991).

Of the euphausiid species *Euphausia crystallorophias*, but mainly *Euphausia superba*, are important members of the Antarctic sub-ice community (O'Brien, 1987). Euphausiids are only rarely found in the Arctic sea ice–water interface, and gammeriid amphipods are the most dominant members underneath Arctic sea ice (Carey, 1985, 1992; Poltermann, 1997). The biology, ecology and fisheries issues of krill, including those species found in polar waters are comprehensively reviewed by Everson (2000). Gammeriid amphipods have been found locally in high concentration also in Antarctic ice under-surfaces, although generally only in relatively shallow waters (Andriashev, 1968; Gulliksen & Lønne, 1991; Günther et al., 1999; Plate 7.1).

In the Arctic, *Gammarus wilkitzkii* and *Apherusa glacialis* are abundant in sea ice samples from the Barents and Greenland Seas as well as the Canadian High Arctic (Cross, 1982; Carey, 1985; Poltermann, 1997; Werner, 1997). Both species seem to have an autochthonous life history (Gulliksen & Lønne, 1989), and require multi-year ice to complete their life histories (Siferd et al., 1997). Hyperiid amphipods have only rarely been found beneath sea ice. The one exception to this rule is *Parathemisto libellula*, which is probably not a true sympagic species, but has been reported as being present in low numbers on the undersides of Arctic ice (Gulliksen & Lønne, 1991).

Copepods are found to be highly concentrated directly under the ice (Conover et al., 1986; Schnack-Schiel et al., 1995; Tanimura et al., 1996; Schnack-Schiel et al., 1998). *Stephos longipes*, *Paralabidocera antarctica* and *Drescheriella glacialis*, which are dominant within Antarctic sea ice (Table 7.1), are also abundant members of the sub-ice fauna in the Antarctic (Table 7.2; Schnack-Schiel et al., 1998; Swadling et al., 2001). Other copepod species, such as the calanoid *Ctenocalanus citer*, the cyclopoids *Oithona similis* and *Pseudocyclopina belgicae* and the poecilostomatoid, *Oncaea curvata*, as well as several harpacticoid species, are occasionally captured near the sea ice–water interface (Menshenina & Melnikov, 1995; Günther et al., 1999; Swadling et al., 2001).

In the Arctic, the calanoids *Pseudocalanus* sp., *Calanus glacialis* and nauplii of *C. hyperboreus* have been collected in high concentrations in the water directly adjacent to the ice under-surface. The small copepods *Acartia longiremis* (calanoid) and *Oithona similis* (cyclopoid) only occur in low numbers although regularly at the ice–water interface (Runge & Ingram, 1988; Conover et al., 1990).

At times, siphonophores, appendicularians, chaetognaths, mysids and the pelagic polychaete *Tomopteris carpenteri* have also been reported to be present in

Table 7.2 Dominant metazoan species found in the ice–water interface*.

Calanoid copepods	
Antarctic	*Stephos longipes, Paralabidocera antarctica*
Arctic	*Pseudocalanus* sp., *Calanus glacialis*
Euphausiids	
Antarctic	*Euphausia superba, E. crystallorophias*
Gammeriid amphipods	
Antarctic	*Paramoera walkeri, Cheirimedon fougneri, Pontogeneia antarctica, Eusirus antarcticus, Orchomene plebs*
Arctic	*Apherusa glacialis, Gammarus wilkitzkii, Onismus nanseni, O. glacialis, O. litoralis, Ischyrocerus anguipes, Weyprechtia pinguis*
Fishes	
Antarctic	*Pagothenia* (= *Trematomus*) *borchgrevinki*
Arctic	*Boreogadus saida, Arctogadus glacialis*

* Primary references: Richardson & Whitaker, 1979; Carey & Montagna, 1982; Cross, 1982; Conover et al., 1986; O'Brien, 1987; Runge & Ingram, 1988; Gulliksen & Lønne, 1989; Grainger & Hsiao, 1990; Gulliksen & Lønne, 1991; Carey, 1992; Menshenina & Melnikov, 1995; Schnack-Schiel et al., 1995; Tanimura et al., 1996; Poltermann, 1997; Siferd et al., 1997.

significant numbers in the sea ice–water boundary layer (Gulliksen & Lønne, 1989; Menshenina & Melnikov, 1995). High numbers of benthic invertebrate larvae, such as cirripede nauplii, can seasonally inhabit the underside of sea ice in shallow areas in the Arctic (Conover et al., 1990).

In the Arctic, the arctic cod (*Boreogadus saida*) and the glacial cod (*Arctogadus glacialis*) have been found to live in close association with the ice underside (Carey, 1985). For example, young fish specimens live in cavities within melting summer ice (Carey, 1985; Plate 7.2), whereas older specimens of *B. saida* are only rarely found just beneath the ice (Gulliksen & Lønne, 1989). In the Antarctic, swarms of young and adult broadhead fish, *Pagothenia borchgrevinki*, are reported to live just under the ice, as are young specimens of the giantfish *Dissostichus mawsoni* (Andriashev, 1968).

Platelet ice

Platelet ice layers are a unique ice habitat that is found mainly along the Antarctic coast underlying fast ice adjacent to ice shelves, and only seldom found underlying pack ice. These layers consist of accumulations of disc-shaped plates of ice that can be several metres thick. The surfaces of the platelets provide extensive surfaces for bacteria and algal growth (Dieckmann et al., 1986), and dense ice algal blooms can occur within these layers (Dieckmann et al., 1992). In turn platelet layers become an important habitat for grazing metazoans. Günther et al. (1999) found a diverse community in the platelet layers of Drescher Inlet in the eastern Weddell Sea, with many of the species found being new to science. Crustaceans, mainly copepods, were the most numerous and diverse group, with 16 species being identified.

Harpacticoids made up 76% of all the copepod species, although the most dominant species, in terms of abundance, were the same species that are commonly found in the sea ice cores from the Weddell Sea, *Drescheriella glacialis* and *Stephos longipes*.

The presence of high numbers of metazoans and their excretion in the platelet layers may partly account for the high ammonium values reported from this ice habitat, although, as discussed by Thomas & Papadimitriou (Chapter 9), this is only one of the potential sources of inorganic nitrogen inputs in such habitats. High concentrations of ammonium have been measured in numerous sea ice types (Dieckmann et al., 1992; Thomas & Papadimitriou, Chapter 9), including closed interior assemblages (Thomas et al., 1998). The role of metazoan excretion is probably an important pathway in the biogeochemical cycling of nitrogen within these habitats, although quantitative studies are yet to be conducted.

Sampling the sea ice community

A wide range of sea ice types and structures, depending on different growth processes, occur in the course of the year. This, combined with the fact that there is a great variety of different animals inhabiting the ice, makes standard sampling procedures difficult. Patchiness can be extreme even in replicate cores from one sampling site (reviewed by Brierley & Thomas, 2002). Adequate sampling is a major limitation, and a high coring frequency and spatial resolution are necessary to study such high levels of spatial heterogeneity. Coupled with this is the need for year-round studies for our understanding the full implication of seasonal changes in sea ice for the life cycle strategies of sympagic heterotrophs.

Fast ice and coastal pack ice can be sampled from land bases. Offshore pack ice is, however, difficult to access and requires an ice-going research vessel and/or air support. Sampling of the sea ice organisms, which can be scattered between ice crystals throughout the ice or concentrated in brine channels, cracks and cavities, is carried out using standard ice-coring techniques (Horner et al., 1992). Inadequate sampling can occur when coring porous and rotten ice with large brine channels or pockets, and care has to be taken to avoid brine drainage and contamination with sea water. Close attention also has to be paid to the careful sampling of gaps/voids that can occur within the ice mainly at or just below the water level. These freeboard layers can contain considerable metazoan biomass, and can only be sampled by carefully coring the overlying ice and sampling the gap water by immersing sampling devices into the gap layer.

Another major problem is to retain brine and interstitial organisms associated with the bottom layer of the ice during extraction of the core to the ice surface. Coring and sampling by divers from beneath the sea ice is by far the best way to reduce such problems (Horner et al., 1992). The boundary layer between the sea ice and the underlying water gets disturbed during coring; nevertheless, the core holes are the only access to sample quantitatively the sub-ice community. Metazoans in this habitat can be sampled by using pumps and small gear such as the NIPR-I

sampler in which water is sucked into the sampler by a current caused by a rotating propeller and collected by the net attached to the sampler (Tanimura et al., 1996). Besides scuba divers, remotely operated vehicles (ROV) and autonomous underwater vehicles (AUVs) are increasingly useful tools for the direct oberservations of the under-ice environment (Brierley & Thomas, 2002).

7.3 Biochemical adaptations

Ectothermic invertebrates and most fish have body temperatures corresponding to the ambient temperature. If the ambient temperature drops below the melting point of the body fluids, the animals face the problem of internal ice formation. Therefore freezing resistance is a prerequisite for sympagic organisms to survive in sea ice. However, organisms associated with sea ice not only have to survive below freezing temperatures, but are also exposed to seasonal changes in their physical environment as the sea ice melts and freezes. They therefore have to cope physiologically with highly variable conditions of both temperature and salinity. Many invertebrates avoid freezing by supercooling, where the body fluids are cooled below the equilibrium freezing point without freezing, or they have the potential to actually tolerate ice formation.

The Arctic gammeriid amphipods *Gammarus wilkitzkii* and *Onismus glacialis*, as well as the Antarctic *Eusirus antarcticus*, do not tolerate being frozen into solid sea ice. In contrast, the Arctic amphipod *G. oceanicus*, as well as juveniles of the Antarctic krill *Euphausia superba*, can actually survive being frozen into the solid ice (Aarset & Torres, 1989; Aarset, 1991). The Arctic sympagic crustaceans studied to date show relatively high supercooling points, whereas those from Antarctic species exhibit relatively low values, an indication that in general the Antarctic species have a greater supercooling capacity than those from the Arctic (Aarset, 1991).

As an adaptation to thrive in polar seas, large lipid depots are accumulated by many metazoans which help to buffer the strong seasonal variability in food supply. For example, in a recent study of krill in the Lazarev Sea at the onset of winter, juvenile and adult krill had very high lipid contents of 36 and 44% of their dry mass, respectively (Atkinson et al., 2002). According to Sargent et al. (1981) different lipid classes may indicate deviating feeding behaviours. Wax esters are stored as long-term energy reserves, and such wax ester storage is known for many polar animals which cease feeding in autumn and overwinter in a resting stage. These include the herbivorous Arctic copepods *Calanus hyperboreus* and *C. glacialis*, and the Antarctic *Calanoides acutus* (Kattner & Hagen, 1995; Schnack-Schiel & Hagen, 1995). In contrast, species which store triacylglycerols instead of wax esters, do not stop feeding during the dark season but seek alternative food sources. In fact, ice-associated animals that have a more opportunistic feeding behaviour and stay trophically active throughout the year, are primarily triacylglycerol-storing: the copepods *Stephos longipes* (Schnack-Schiel et al., 1995), *Paralabidocera antarctica*

(Swadling et al. 2000), the euphausiid *Euphausia superba* (Falk-Petersen et al., 2000), and the notothenioid fish *Pagothenia borchgrevinki* (Clarke et al., 1984) in the Antarctic, and the gammeriid amphipods *Apherusa glacialis*, *Gammarus wilkitzkii*, *Onismus nanseni* (Scott et al., 1999) and the gadiform fish *Boreogadus saida* in the Arctic (Scott et al., 1999).

One of the most critical requirements at low temperatures is maintenance of functional lipid membranes. The fatty acid composition of membrane phospholipids regulates the degree of membrane fluidity, and so an increase in the proportion of unsaturated fatty acids, a decrease in average chain length and an increase in polyunsaturated fatty acids (PUFAs) is important for retaining membrane fluidity at low temperatures. The amount of PUFAs in ice diatoms increases with decreasing temperature and light intensity but increasing nutrient concentrations (Mock & Kroon, 2002a,b). In winter, PUFA production is enhanced in ice diatoms, so that a very different quality of food is released into the food web than in other seasons when PUFA synthesis is lower. Hence, in winter when phytoplankton is scarce in the water column but rich in the sea ice, metazoans grazing on the ice algae not only encounter a highly concentrated food source, but one that is enriched in components that are needed to overcome temperature stress associated with winter conditions. The PUFAs are not only essential to the ice algae themselves, but are also an important component in the diet of grazing metazoans and their predators.

Low-temperature adaptation also seems to promote the expression of greater tolerance to changing external salinity. The Arctic sympagic amphipods *Gammarus wilkitzkii* and *Onismus glacialis* are hyperosmotic regulators at low salinity values (3–4) both regulating extracellular concentrations of sodium and chloride in the haemolymph. At higher salinities they respond by being osmoconformers over the tolerated salinity range (34–60, Aarset & Aunaas, 1987; Aarset, 1991). The Antarctic sympagic amphipod *Eusirus antarcticus* and juveniles of the Antarctic krill, *Euphausia superba*, are also osmoconformers with a low salinity tolerance (26–40 and 25–45, respectively, Aarset & Torres, 1989). These indicate that these species are less euryhaline than the Arctic species mentioned above. However, in summer adult krill have been observed moving from the water column, through rotten ice, into low salinity surface ponds (salinities below 15) to graze on strands of algae (Schnack-Schiel et al., 2001b; D.N. Thomas, pers. comm.).

Survival in a supercooled state can also result from 'thermal hysteresis agents' being present in the body fluids. In a range of crustaceans from both poles no such thermal hysteresis agents have been found (Aarset, 1991). However, they were adapted to living in the vicinity of ice by lowered melting points of their body fluids which in turn prevented internal ice formation at low temperatures (Aarset & Aunaas, 1987; Aarset & Torres, 1989; Aarset, 1991).

Almost all teleost fish are hyposmotic to sea water and, hence, the freezing point of the blood of polar species is about 1°C higher than that of the surrounding sea water. Various classes of macromolecular antifreezes have been found in polar fish. All of these macromolecular antifreezes are proteins (AFPs) or glycoproteins that

also have carbohydrate moieties (AFGPs) (DeVries, 1971, 1997). All macromolecular antifreezes lower the freezing point of the solution as efficiently as NaCl, i.e. solutions containing these macromolecular antifreezes exhibit thermal hysteresis and, hence, the blood serums of many polar fish freeze at approximately $-2^{\circ}C$. The content of antifreeze molecules varies greatly between species and depends upon the habitat of the fish. Species living in waters close to sea ice possess the highest amounts.

Notothenioid species in the Antarctic, such as the cryopelagic species *Pagothenia borchgrevinki* and *Dissostichus mawsoni*, possess glycoprotein macromolecules (AFGP) which are built up of repeating tripeptide units. In many Antarctic non-notothenioid fish, as well as in most Arctic fish, freezing is inhibited by AFPs. The Arctic cryopelagic gadiforms *Boreogadus saida* and *Arctogadus glacialis* have, however, glycoproteins similar in structure to the Antarctic ones, posing interesting questions on molecular evolution of such compounds. In Antarctic fish antifreeze glycopeptides are synthesized year-round, whereas in Arctic fish, where isolation is much less stringent, the synthesis of antifreeze molecules often occurs only during winter (Cheng & DeVries, 1991; DeVries, 1997; Wöhrmann, 1997).

7.4 Sea ice as a feeding ground

The sea ice fauna is important to the food web of the ice-covered oceans (Ainley et al., Chapter 8). The clearest interactions between ice biota and metazoan grazers take place mainly during autumn, winter and early spring when phytoplankton in the water column is scarce. The high algal, bacterial and protozoan biomass, within the sea ice as well as at the ice–water interface, clearly serves as food for the larger metazoan grazers and is a key food source for winter survival. The sub-ice metazoan fauna, on the other hand, functions as food for larger animals such as fish, seabirds and marine mammals (Fig. 7.3; Ainley et al., Chapter 8).

Euphausiids, amphipods and calanoid copepods are the conspicuous consumers of the ice microbial assemblages. The calanoids *Pseudocalanus* sp. and *Calanus glacialis* (Arctic), *Paralabidocera antarctica* and *Stephos longipes* (Antarctic) are known to graze heavily on ice algae, the latter two species being found within ice floes, as well as underneath the ice (Conover et al., 1986; Hoshiai et al., 1987; Runge & Ingram, 1988; Schnack-Schiel et al., 1995). The two euphausiid species found beneath sea ice, *Euphausia superba* and *E. crystallorophias*, seem to exploit different food items and do not compete directly for the same food source under the ice. They also differ in the major depot lipids they produce: *E. superba* stores triacylglycerols while *E. crystallorophias* stores wax esters (Falk-Petersen et al., 2000). During summer, the main food resources of *E. superba* are phytoplankton while it switches to a more omnivorous/carnivorous feeding mode in winter, and has been observed to feed directly on algae growing on the under-surface of the sea ice (O'Brien, 1987; Marschall, 1988). In contrast, *E. crystallorophias* has never been

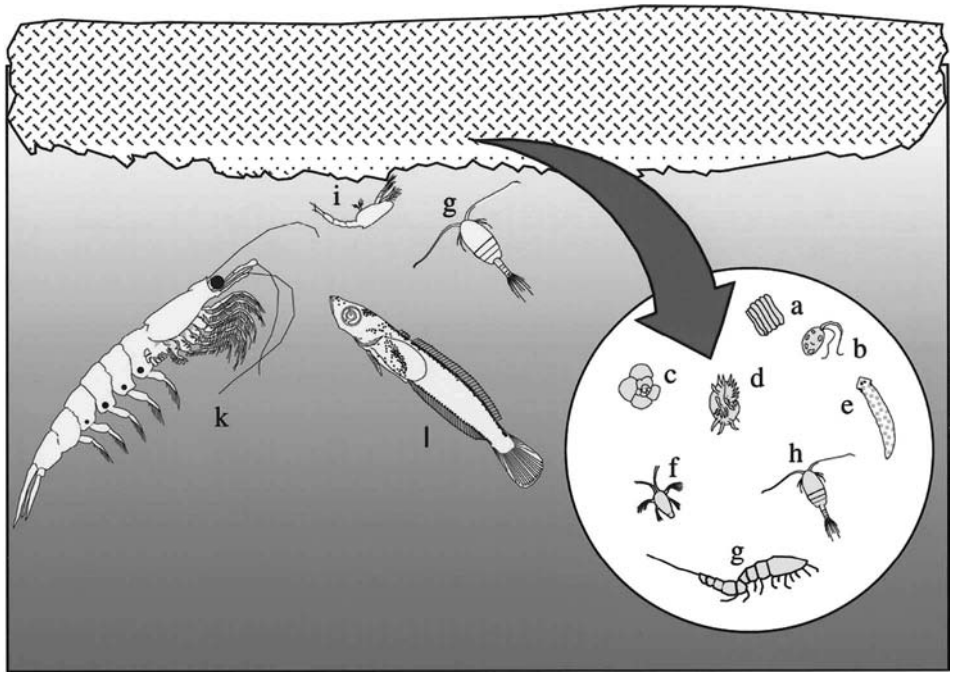

Fig. 7.3 Food web in the Antarctic pack ice. (a) Pennate diatoms; (b) autotrophic flagellates; (c) foraminiferas; (d) ciliates; (e) turbellarians; (f) copepod nauplii; (g) harpacticoid copepods; (h) calanoid copepods; (i) euphausiid larvae; (k) Antarctic krill; and (l) young notothenoid fish *Pagothenia borchgrevinki*.

observed scraping algae from the underside of the sea ice. It feeds on much finer organic matter and small zooplankton. Detrital material derived from ice algae and sinking faecal pellets from other sympagic animals are probably a major food source for this species (O'Brien, 1987; Falk-Petersen et al., 2000).

The ice-associated gammeriid amphipods at both poles feed on ice algae at the ice underside but differ in their feeding habits. The Antarctic *Pontogeneia antarctica* and the Arctic *Apherusa glacialis* are predominately herbivorous, feeding mainly on ice algae (Richardson & Whitaker, 1979; Werner, 1997). In contrast, detritus–algae aggregates which develop at the ice underside, together with animal remains, are probably the major food source for the Arctic *Onismus nanseni* and *O. glacialis* (Poltermann, 1997; Werner, 1997). Although ice algae have been found in the guts of the Antarctic *Paramoera walkeri* and the Arctic *Gammarus wilkitzkii,* these species clearly exhibit a predatory behaviour. Under fast ice, *P. walkeri* was observed to actively predate on the newly hatched young of *Pontogeneia antarctica*. Gut content studies of *G. wilkitzkii* also revealed strong preference for animal food, mainly for crustaceans (Gulliksen & Lønne, 1989). In *G. wilkitzkii* even cannibalism has been shown to take place (Poltermann, 1997).

Sea ice can attract different fish species as they migrate from deeper water to feed

on zooplankton living underneath the ice. In the Arctic, *Boreogadus saida* and *Arctogadus glacialis* live in the sub-ice environment and the former species is an opportunistic feeder, eating a wide range of food items. Under first-year ice, it feeds on copepods and the hyperiid amphipod *Parathemisto libellula* if present. Under multi-year ice, it feeds extensively on a range of gammeriid amphipod species except *Gammarus wilkitzkii.* This species is probably avoided because of its large size coupled with a characteristic spiny morphology (Gulliksen & Lønne, 1989).

The circumantarctic notothenoid fish, *Pagothenia borchgrevinki*, plays an important ecological role in the Antarctic ice-covered regions. *P. borchgrevinki* occurs in the sub-ice layer and also in dense platelet-ice layers, clearly utilizing this habitat as a feeding ground and as a refuge from predators (Gulliksen & Lønne, 1991). *Pagothenia borchgrevinki* is probably amongst the most important carnivores to feed on the metazoans of the accessible ice assemblages. The diet of *P. borchgrevinki* becomes more diverse with increasing size (Table 7.3).

Table 7.3 Relation of body size of *Pagothenia borchgrevinki* and its food items*.

Length	Food item
< 5 cm	Small copepods
5–10 cm	Copepods, small amphipods, ostracods
10–15 cm	Calanoid copepods, amphipods, euphausiids
> 15 cm	Amphipods, euphausiids, gastropods and smaller fish

* Primary references: Andriashev, 1968; Gulliksen & Lønne, 1991.

7.5 Importance of sea ice for life history cycles

There are several mechanisms by which metazoans may be incorporated into the sea ice:

- Planktonic organisms may be trapped during frazil ice formation in the upper metres of the water column (Garrison et al., 1983).
- Ice platelets formed at great water depth, often in large quantities, potentially act as vectors for lifting organisms from the depths to overlying waters (Dieckmann et al., 1986).
- Benthic species may be lifted up with anchor ice formed on the sea bottom as found in shallow waters in McMurdo Sound (Dayton et al., 1969).
- Sea ice turbellarians and nematodes could attach to free-swimming migrating invertebrates such as crustaceans and use these animals as vectors to arrive at or leave the ice habitat (Riemann & Sime-Ngando, 1997; Janssen & Gradinger, 1999).
- Metazoans may enter the ice at a later stage, simply by moving into large brine channels.

When the sea ice melts in summer, organisms are released into the water column. The organisms therefore must tolerate rapidly changing environmental conditions and undergo a pelagic period during their life cycle. However, although nematode and turbellarian species are able to swim, no real genuine planktonic life stages for many of these species have been found in polar seas, and how they survive the ice-free periods is unknown. Whereas the mechanisms outlined above are plausible means for the colonization of ice in shallow waters, it remains a mystery as to how ice overlying water several thousand metres deep is colonized by metazoans with relatively poor swimming abilities (Brierley & Thomas, 2002).

Due to the major differences in sea ice formation, age and structure, the number of animals with an autochthonous life history is greater in the Arctic compared to the Antarctic. Both sexes and all developmental stages of the Arctic gammeriid species *Gammarus wilkitzkii*, *Apherusa glacialis, Onismus* spp. as well as the mysid *Mysis polaris* occur within sea ice. Evidently they require multi-year ice for all stages of their life histories and are supposed to have an autochthonous life cycle (Gulliksen & Lønne, 1991; Poltermann, 1997; Werner, 1997). In contrast, the ice-associated metazoans in the Antarctic are probably allochthonous. Their life cycles are correlated to the seasonal dynamics in sea ice cover, particularly from autumn to spring, as has been shown for many Antarctic species such as copepods, euphausiids and amphipods. For instance, when the sea freezes, the Antarctic amphipods *Paramoera walkeri* and *Pontogeneia antarctica* migrate from the sea bed, their summer habitat, to the sea ice under-surface. Here, hatchlings are released and the next generation is protected in the bottom skeletal ice layers of floes (Rakusa-Suszczewski, 1972; Richardson & Whitaker, 1979).

Life cycles of ice-associated copepods

The life cycles of the three dominant ice-associated Antarctic copepod species (*Stephos longipes, Paralabidocera antarctica* and *Drescheriella glacialis*) show clearly that the survival strategies greatly depend on ice formation and persistence. However, the links between survival and/or life history strategy, and the seasonal sea ice cycle, are very different for these three species (Figs 7.4, 7.5).

Stephos longipes is a small neritic calanoid copepod. It has a generally circum-antarctic distribution with higher numbers found in the Weddell, Bellingshausen and Amundsen Seas compared to the Indian Ocean sector (Schnack-Schiel et al., 1995, 1998; Swadling et al., 2001). Its one-year life cycle is strongly associated with the seasonal fluctuation of the sea ice cover (Fig. 7.4). In winter and spring when sea ice predominates, *S. longipes* inhabits mainly the lowermost regions of ice floes and the ice–water interface, where it reaches abundances up to five orders of magnitude greater than those in the underlying water column (Schnack-Schiel et al., 1995). Adults dominate in the water column and in the under-ice water layer while the sea ice contains mainly nauplii.

This distribution pattern suggests that breeding takes place in the uppermost

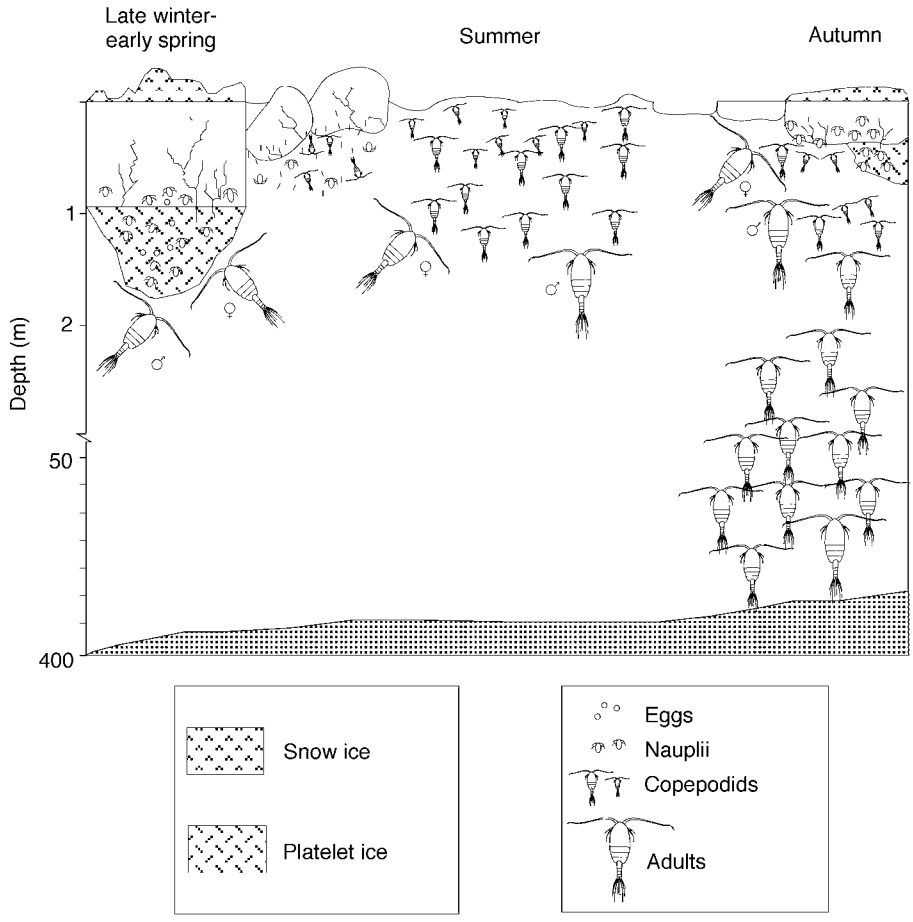

Fig. 7.4 Schematic diagram of the life cycle of *Stephos longipes*. From Schnack-Schiel et al. (1995).

layers of the water column and that the eggs or nauplii are transported or incorporated into the ice, or that *S. longipes* females attach their sticky eggs directly onto frazil ice crystals or ice platelets (Kurbjeweit et al., 1993). The nauplii develop within the ice to copepodids. In summer, even though *S. longipes* remain in rotten sea ice, it is most abundant in the upper water layers of the water column, where copepodite stages rapidly develop (Schnack-Schiel et al., 1995). With new ice formation in autumn, *S. longipes* begins to accumulate in the sea ice and at the ice–water interface where it attains abundances comparable to those observed in spring, and again, nauplii and the first copepodite stage dominate in the ice. In the water column, in contrast, late copepodite stages are numerous in mid-water layers.

Hence, *S. longipes* seems to have two alternative strategies for overwintering – a young population (nauplii–first copepodite stage) overwinters in the first-year sea ice, while an older population migrates deep into the water column and may even

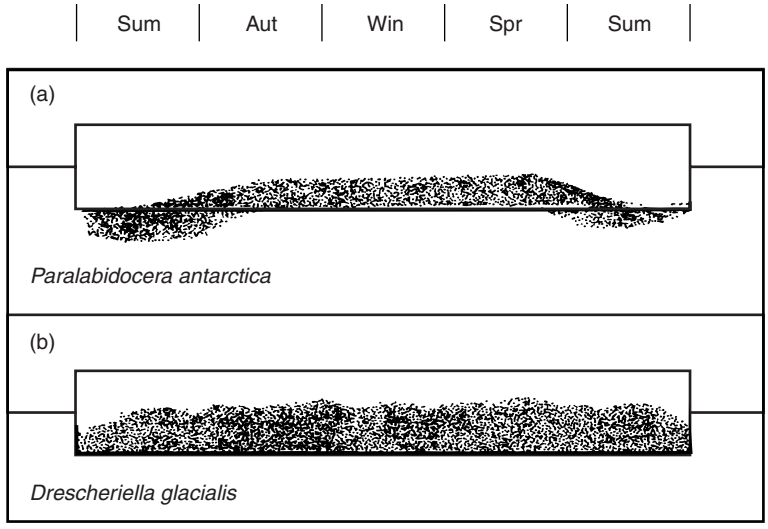

Fig. 7.5 Schematic comparison of the relations with sea ice among the Antarctic ice-associated copepods *Paralabidocera antarctica* (a) and *Drescheriella glacialis* (b). Strippled area indicates the main habitat throughout the life cycle in each copepod. Modified from Tanimura et al. (1996).

reach the sea bed. It is possible that at least a portion of the *S. longipes* population can also have a benthic phase in winter, living in or on top of the sediment. Nauplii in sea ice cores in winter have food in their guts, but whether or not the older copepodite stages overwintering near the sediment continue to feed is unknown. However, since *S. longipes* stores triglycerols as energy resources it is likely that it feeds year round.

The small calanoid species *Paralabidocera antarctica* is a dominant member of sea ice communities particularly in the east Antarctic (Tanimura et al., 1996; Swadling et al., 2001). This species occurs in the sea ice for most of the year except summer when the population concentrates just beneath the ice (Fig. 7.5a). In early summer, maturation and mating occur in the ice–water interface, and in late summer eggs are spawned. With the onset of ice formation, the nauplii enter the bottom part of the sea ice where they stay throughout the winter with slow development. In early spring the nauplii develop rapidly to early copepodids. The population then gradually shifts its habitat again from the sea ice to the underlying water. *Paralabidocera antarctica* utilizes ice algae throughout its life. The entire life cycle of *P. antarctica* is one year with prolonged naupliar life stages in the sea ice in winter and shortened copepodite life stages in spring.

In most Antarctic ice floes, independent of the geographical region, the harpacticoid *Drescheriella glacialis* is the dominant copepod species (Schnack-Schiel et al., 1998, 2001b; Swadling et al., 2001). All instars of *D. glacialis* are found in the ice suggesting that this species reproduces and develops within the ice matrix. This

species seems to spend most of its life in coastal ice where fast ice is often a perennial feature (Fig. 7.5b), although it has also been found in annual pack ice offshore in the northern Weddell Sea (Dahms et al., 1990). Recolonization from the benthos overlying deep waters is unlikely. Nauplii of *D. glacialis* are not able to swim but adults and copepodids seem to be good swimmers, and are capable of spending some time in the open water which is necessary to survive in the water column after annual melting of sea ice (Dahms et al., 1990).

Two Arctic copepod species, the cyclopoid *Cyclopina schneideri* and the harpacticoid *Tisbe furcata*, found in the annual ice-covered coast of Baffin Island in the Canadian Arctic, seem to have adopted a similar life cycle strategy to that of *S. longipes* in the Antarctic. Both Arctic species occur in the sea ice during winter. However, after the ice melts only small numbers of the copepods appear in the water column; instead they descend to near the bottom of the water column and live close to the sea bed during summer (Grainger, 1991).

Interaction between sea ice and the Antarctic krill, Euphausia superba

The distribution of *Euphausia superba* is primarily restricted to the region covered by ice in winter, and there is a close correspondence between the life cycle of krill with the oscillation of the sea ice cover (Brierley & Thomas, 2002). Krill has developed specific behaviour for foraging and predator-avoidance associated with pack ice, both important for overwintering survival (Meyer et al., 2002).

The distribution of both adults and larvae of *Euphausia superba* is linked with sea ice. Larvae, juveniles and adult krill have all been observed directly beneath sea ice (O'Brien, 1987; Daly & Macaulay, 1988; Marschall, 1988; Quetin et al., 1996; Brierley et al., 2002). However, the degree of association with the sea ice differs between developmental stages. Adults seem not to be tightly coupled to the underside of the sea ice in winter, but are detected in the water column in ice-covered regions with higher concentrations near the ice edge (Daly & Macaulay, 1991; Ross et al., 1996). However, in spring and summer aggregations of adults under the surface of sea ice have been observed (O'Brien, 1987; Marschall, 1988; Quetin & Ross, 1991). Acoustic survey data, gathered with the autonomous underwater vehicle Autosub-2, showed a significantly higher krill density under sea ice than in open water in the northern Weddell Sea in summer (Brierley et al., 2002). Krill were concentrated within a narrow band under the ice, and the abundance increased southward from the point where ice concentration was more than 40%, and extended from 1 to 13 km south of the ice edge, after which the abundance rapidly decreased (Fig. 7.6).

Foraging and predation behaviour can explain swarm distribution underneath the ice. Adult krill swarms found in regions of smooth or first-year ice are not directly underneath the ice but in deeper and darker waters. In contrast, under thicker and rafted multi-year ice, krill have been observed to concentrate in the vicinity of the keels of pressure ridges and in ice interstices. Under annual and/or smooth ice it is

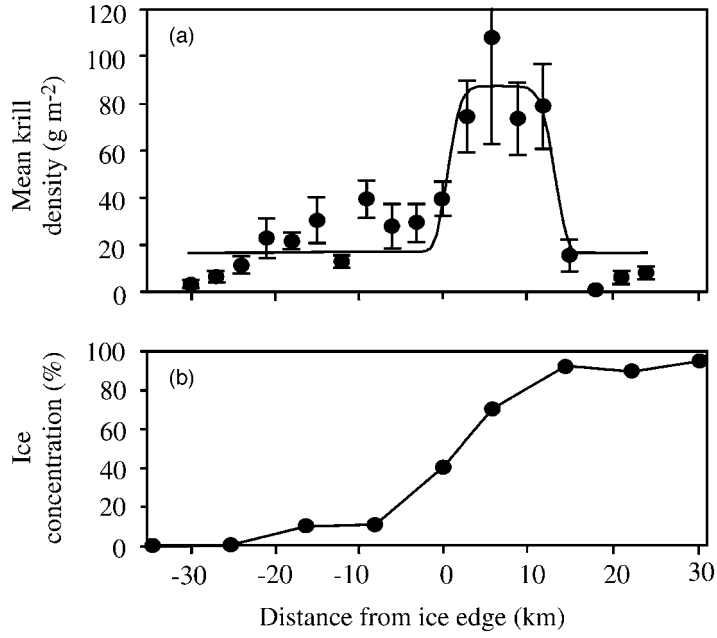

Fig. 7.6 Krill distribution relative to the sea ice edge and ice concentration. (a) Krill density by distance (in 3 km bins, positive is under sea ice) from the local sea ice edge. The line is a highly significant regression function, error bars are $\pm$ 1 SEM. (b) Sea ice concentration. From Brierley et al. (2002).

possible that there are not enough ice algae for an energetic advantage, and/or enough ice structure to serve as a refuge from predation. The krill swarms evidently adjust their depth to remain shallow enough to exploit algal standing stocks, but sufficiently deep to avoid visual predators (Quetin & Ross, 1991; Brierley & Watkins, 2000).

Euphausia superba adults have several different strategies for overwintering. They do not depend directly on sea ice algae for winter survival (Quetin et al., 1996; Atkinson et al., 2002), and mostly seem not to move beneath the ice before late winter when sea ice has begun to disintegrate. They can feed on ice organisms by scraping off ice algae growing on ice surfaces (Plate 7.3; Marschall, 1988). When ice finally melts they take advantage of the tremendous concentrations of ice algae released from the ice (Huntley et al., 1994). Adults are also capable of surviving long periods of starvation (211 days) through utilization of body reserves and shrinkage. However, it is uncertain how frequently krill really encounter food shortages sufficient to induce shrinkage in nature (Nicol, 2000). Other overwintering mechanisms include metabolic reduction and lipid depletion (Quetin & Ross, 1991), switching to carnivorous feeding on lipid-rich metazoans such as copepods (Huntley et al., 1994; Atkinson et al., 1999; Atkinson et al., 2002), and migration downwards to the seabed (Quetin et al., 1996). Atkinson et al. (2002) report a variety of strategies for changes in krill feeding stratagies in the autumn including a transition to a non-feeding

mode. However, some of the population they studied may have maintained a high feeding effort with the remainder not feeding. According to Quetin & Ross (1991) lowered metabolic rate ('hibernation') is by far the most important strategy of the adult krill for successfully surviving winter.

The distribution of larvae and juveniles is, in contrast to adults, closely coupled to sea ice, where they occur in large aggregations. Krill larvae shift their habitat from the water column to the sea ice to take advantage of ice algae both in winter and spring (Daly & Macaulay, 1988; Quetin & Ross, 1991). During periods of low food supply in the water column, larvae have to exploit the ice biota to fulfil their metabolic demands (Meyer et al., 2002). Probably the small size of larvae compared to adults may give them a refuge from predation and allow them to occupy even the smooth ice surfaces during winter without predation pressure. However, larvae and juveniles, as are the adults, are more often concentrated in areas around pressure ridge keels, and rafted and/or eroded ice surfaces which all provide better refuge from predators (Daly & Macaulay, 1988; Melnikov & Spiridonov, 1996; Frazer et al., 1997).

Krill larvae do not accumulate sufficient lipid stores during the short summer periods, and therefore can subsequently starve for only short periods in autumn and winter (Quetin et al., 1996). Ice algal assemblages are therefore a vital nutrient resource for larval krill (Daly, 1990; Hofman & Lascara, 2000). By feeding on ice algae, the larvae can ingest between 2 and 44% of their body carbon per day, covering the metabolic requirements for growth and development (Daly, 1990). Quetin et al. (1996) argued that in winters with a greater pack ice cover, larval and juvenile krill will be in better physiological condition, have higher growth and development rates, and a higher survival, than in winters of low ice cover (Quetin et al., 1996). The different distribution pattern of adults and larvae during the winter is a result of both the differences in starvation tolerance coupled with the need to avoid predation, since predation pressure is much higher on adults compared to larvae.

Interannual changes in krill abundances have been linked to oscillations in sea ice extent (Loeb et al., 1997). Abundance and duration of food availability is evidently greater after winters with a long sea ice cover covering a large spatial extent, compared to conditions following winters of low ice cover. Food availability is not only a factor in the timing of reproduction, but also important is the proportion of the population that reproduces and the number of broods per female. A combination of ice biota, ice-edge blooms and open water phytoplankton blooms seem to be necessary to meet the spring and summer food requirements of reproducing female krill (Quetin et al., 1996; Siegel, 2000). Larvae that hatch early in summer show a higher rate of survival during the feeding and growth season, and are well conditioned before their first winter. A second winter of extensive sea ice further ensures survival of larvae spawned the previous year as well as promoting early spawning. Protection from predation in winter with greater ice cover extents may be another reason for a higher survival rate, and may affect krill recruitment and stock size (Loeb et al., 1997; Siegel, 2000).

7.6 Sea ice and global climate change

Sea ice plays a vital role in the ecosystems of both polar oceans. Therefore, changes in ice extent and duration will strongly influence their survival, and hence have an impact on higher trophic levels. Our understanding of the response of sympagic metazoans to changes in sea ice extent is still very limited. As an example, the potential effect that climate changes may have on life cycle and survival rates will be described for *Euphausia superba*.

Krill stocks appear to have decreased in the Antarctic Peninsula region within the last two decades (Siegel & Loeb, 1995; Loeb et al., 1997). Reductions in krill densities have major consequences. Krill is the primary food source for a large number of 'higher trophic' species (Ainley et al., Chapter 8), and many workers consider it to be a *keystone species* in the Southern Ocean ecosystem (Quetin et al., 1996). Any decrease in krill abundance will have a subsequent effect on the predators. Many potential links are obvious between sea ice, krill and breeding success of krill predators (Brierley & Thomas, 2002). However, krill stocks display large interannual fluctuation in abundance and it remains to be proven whether or not the observed changes in krill demography are simply representative of a high degree of interannual variability or the beginning of a downward trend (Siegel, 2000).

Loeb et al. (1997) and Siegel (2000) provided data on a close relationship between krill, the pelagic tunicate *Salpa thompsoni* and sea ice extent and duration. Following winters with reduced sea ice cover, during which the successful recruitment of krill is not favoured, extensive blooms of salps tend to form. Salps are opportunistic feeders competing with krill for food and the salps exploit the spring phytoplankton bloom undergoing rapid population growth. Hence, salp blooms can severely affect the reproduction and survival of krill larvae (Fig. 7.7). On the other hand, after long periods of extensive sea ice cover that favours krill recruitment, and also induces a delayed seasonal spring phytoplankton bloom, krill out-compete the salps, and krill tend to dominate in the open waters.

Due to the uneven distribution of krill under sea ice, the reduction in length of winter sea ice cover does not necessarily lead directly to reductions in krill stocks. Krill reductions, instead, are thought to be proportional to the reduction of ice edge length (Brierley et al., 2002). The suggested decline of 25% of the area covered by sea ice (De la Mare, 1997) equates to only a 9% decline in ice edge length. Therefore, the reduction of sea ice cover may be less responsible for the reduction of krill than previously thought (Brierley et al., 2002).

Another possible factor for the decline in krill populations might be the increased ultraviolet-B (UV-B) irradiation due to seasonal depletions in atmospheric ozone. Krill have a relatively high concentration of absorbing mycosporine-like amino acids (MAAs) which may act as a natural ultraviolet (UV) filter system (Karentz et al., 1991). In contrast krill have the lowest percentage of guanine–cytosine base pairs (GC = 32%) of total DNA known for any metazoan (Jarman et al., 1999). The

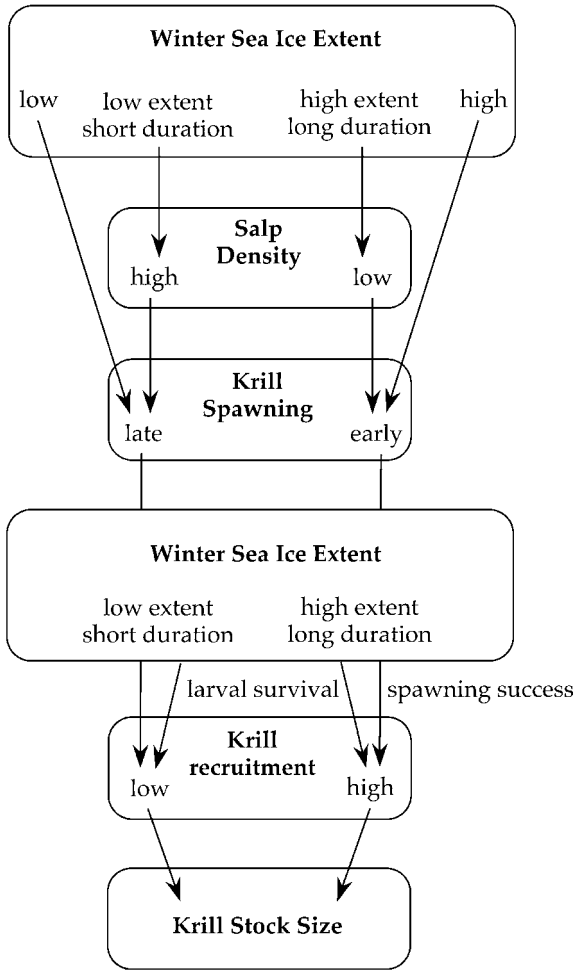

Fig. 7.7 Hypothesis on the relationship between krill recruitment success and sea ice condition and biological factors (salp abundance, spawning time). Modified from Siegel (2000).

consequence of this is a higher frequency of (T)n arrays. UV-B irradiation damages DNA primarily by converting (T)n arrays, and hence, krill seem to be susceptible to damage from increased UV-B radiation levels, especially near-surface stocks (Jarman et al., 1999). Ozone depletion could also have other indirect effects as increases to UV-B exposure are likely to also cause changes in phytoplankton, bacterioplankton and protozoan species composition as more tolerant species replace sensitive ones (Brierley & Thomas, 2002). Hence, the ability of krill to exploit a wider range of food sources than competitive organisms will be very important for maintaining the dominant role of krill in the Southern Ocean ecosystem.

7.7 Concluding remarks

Antarctic sympagic metazoans are dominated by turbellarians, copepods and euphausiids (Antarctic krill) while the Arctic is characterized by rotifers, nematodes and gammeriid amphipods. Sea ice is an extremely heterogeneous environment, and ice-associated organisms have to cope with strong seasonal changes in the physicochemical conditions. This is one of the main reasons for the high degree of spatial variability of sympagic organisms within sea ice and below at the ice–water interface.

Although sea ice is generally characterized by low temperatures and high salinities, the greatest restriction for metazoans is space. Peak abundances of metazoans often coincide with highly porous ice and, hence, more easily accessible ice. Only rotifers and turbellarians seem to be able to traverse 'channels' significantly smaller than their body diameter, while larger animals avoid narrow passages. Hence, in small pores and channels bacteria, pennate diatoms, flagellates and small protozoans benefit from very much reduced grazing pressure from larger heterotrophs (Krembs et al., 2000). However, there is little information on the feeding behaviour of sympagic heterotrophs (Hoshiai et al., 1987) and their grazing impact on ice algae (Gradinger, 1999). Further investigations into such aspects of sea ice metazoan ecology are highly pertinent. Future studies using both carbon and nitrogen stable isotopes will give valuable information as to the food web relationships of cryopelagic organisms and their role within the trophic transfer.

The life cycles of sympagic metazoans are strongly associated with the seasonal fluctuation of sea ice cover. Due to variability in sea ice formation patterns, the number of animals with an autochthonous life history is greater in the Arctic compared to the Antarctic. The distinct seasonality in polar environments is probably the most important factor influencing life cycles and adaptation. However, due to the lack of winter data, we do not have a clear understanding of the seasonal cycles, and how the sympagic metazoans survive the polar winter is still largely a matter for speculation.

The Antarctic sympagic calanoid copepod *Paralabidocera antarctica* changes its habitat from sea ice dwelling to a pelagic phase which occurs as a trade-off between phototactic and thigmotactic traits. These traits developed through evolutionary processes with the development of swimming ability. Young developmental stages seem to be poor swimmers and are characterized by strong thigmotactic behaviour (Tanimura et al., 2002). The authors hypothesize that with the development of greater swimming ability in older copepodite stages, the older stages actively leave the sea ice in a phototactic reponse. Whether or not such behavioural traits are also true for other sympagic metazoans with poor swimming ability, such as the harpacticoid *Drescheriella glacialis*, turbellarians and nematodes, is uncertain. This should be the focus of future studies as well as the hitherto unanswered conundrum as to how poor swimmers become incorporated into sea ice in non-coastal waters. These mechanisms remain largely a mystery for many metazoans.

The ice inhabitants have to be physiologically and metabolically adapted to the extreme conditions within the vicinity of sea ice. However, ecophysiological investigations on sympagic metazoans are still rare. Techniques such as nuclear magnetic resonance (NMR) imaging should be incorporated into future sea ice research to gain new insight into physiological responses to stress and supercooling (osmoregulation, enzyme kinetics, viscosity, oxygen concentration, blood flow). These studies, of course, need to be combined with new molecular analytical techniques to investigate the genetic control and evolution of cold adaptation in metazoans.

A fundamental step towards our understanding of the survival mechanisms of fish in ice-laden waters was the detection of glycoproteins as antifreeze agents in Antarctic notothenioid fish blood serum (DeVries, 1982). More recent research has shown that most polar fish synthesize antifreeze molecules which are highly varied in structure and amino acid composition (DeVries, 1997; Wöhrmann, 1997). Naturally there should be further emphasis on the study of these compounds, which clearly are fundamental for the ecology of the organisms with the capability of producing them.

The meteorological regimes have a great influence on ice formation, growth and decay, and global climate warming may result in a less extensive and stable ice cover. The subsequent effects on sympagic organisms, and hence their predators, are unclear. Despite recent advances there are still great uncertainties, especially concerning physical and biological interactions as well as interactions between species, adaptive and survival mechanisms, and synchronized seasonal life cycles.

Recent literature discusses the relationship between sea ice cover and krill recruitment in the light of global warming (Loeb et al., 1997, Siegel, 2000; Brierley & Thomas, 2002). Because the ice communities are a major nutritional source for pelagic animals including fish, birds and mammals, the presence of ice and its duration is an important factor shaping the pelagic food web and for supporting a large benthic community. Hence, intensive studies of the response of krill and other sea ice organisms to changes in sea ice extent are pertinent. Additionally, increasing ozone depletion and resulting increased UV-B levels, and the biological response of endemic species, should also be considered within future research of biological consequences to global climate change.

Small-scale variations in ice morphology are compounded by rafting of ice floes and deformation, which can even within a single floe impart a tremendeous spatial heterogeneity. The under-ice topography with regard to meso-scale structures alters the interfacial pore water flux. Current velocities below fast and pack ice can reach speeds of about $30\,cm\,s^{-1}$, hence the irregular undersides of sea ice influence the spatial distribution and abundance of sympagic organisms (Dmitrenko et al., 1998; Hop et al., 2000; Krembs et al., 2000), and can explain the patchy distribution of the organisms in the ice–water interface. Further studies in a broad range of scales (from a few centimetres to large scales of hundreds of metres) on the occurrence of sympagic organisms and the under-ice structures will help to identify

preference of occupation with regard to a changing environment due to climate fluctuations.

Studies on large-scale variability within the sea ice are not possible and remain one of the biggest open questions. However, the use of scuba divers, underwater cameras, ROVs and AUVs have gained much in importance for investigating the ice–water interface. Together with more standard ice coring campaigns and echo-sound studies, these new technologies can be harnessed to develop a more integrated and synoptic view of the role of sea ice within polar ecosystems related to environmental changes. Of the highest priority is the development of multi-disciplinary research themes where ecologists, physiologists and physicists join together to address the issues raised in this chapter. Without the development of such consortia, future progress will be compromised.

References

Aarset, A.V. (1991) The ecophysiology of under-ice fauna. *Polar Research*, **10**, 309–324.

Aarset, A.V. & Aunaas, T. (1987) Physiological adaptations to low temperature and brine exposure in the circumpolar amphipod *Gammerus wilkitzkii*. *Polar Biology*, **8**, 129–133.

Aarset, A.V. & Torres, J.J. (1989) Cold resistance and metabolic responses to salinity variations in the amphipod *Eusirus antarcticus* and the krill *Euphausia superba*. *Polar Biology,* **9**, 491–497.

Andriashev, A.P. (1968) The problem of the life community associated with the Antarctic fast ice. In: *Symposium on Antarctic Oceanography*, (Ed. R.I. Currie), pp. 147–155. Scott Polar Research Institute, Cambridge.

Atkinson, A., Meyer, B., Stübing, D., Hagen, W., Schmidt, K. & Bathmann, U.V. (2002) Feeding and energy budgets of Antarctic krill *Euphausia superba* at the onset of winter – II. Juveniles and adults. *Limnology and Oceanography*, **47**, 953–966.

Atkinson, A., Ward, P., Hill, A., Brierley, A.S. & Cripps, G.C. (1999) Krill–copepod interactions at South Georgia, Antarctica, II. *Euphausia superba* as a major control on copepod abundance. *Marine Ecology Progress Series*, **176**, 63–79.

Blome, D. & Riemann, F. (1999) Antarctic sea ice nematodes, with description of *Geomonhystera glaciei* sp. nov. (Monhysteridae). *Mitteilungen aus dem Hamburgischen Zoologischen Museum und Institut*, **96**, 15–20.

Brierley, A.S., Fernandes, P.G., Brandon, M.A., Armstrong, N.W., McPhail, S.D., Stevenson, P., Pebody, M., Perrett, J., Squires, M., Bone, D.G. & Griffiths, G. (2002) Antarctic krill under sea ice: elevated abundance in a narrow band just south of ice edge. *Science*, **295**, 1890–1892.

Brierley, A.S. & Thomas, D.N. (2002) On the ecology of Southern Ocean pack ice. *Advances in Marine Biology*, **43**, 171–278.

Brierley, A.S. & Watkins, J.L. (2000) Effects of sea ice cover on the swarming behaviour of Antarctic krill, *Euphausia superba*. *Canadian Journal of Fisheries and Aquatic Sciences*, **57**, (Suppl. 3), 24–30.

Carey, A.G., Jr (1985) Marine ice fauna. In: *Sea Ice Biota*, (Ed. R.A. Horner), pp. 173–190. CRC Press, Boca Raton, Florida.

Carey, A.G., Jr (1992) The ice fauna in the shallow southwestern Beaufort Sea, Arctic Ocean. *Journal of Marine Systems*, **3**, 225–236.

Carey, A.G. & Montagna, P.A. (1982) Arctic sea ice formation assemblage: first approach to description and source of the underice meiofauna. *Marine Ecology Progress Series*, **8**, 1–8.

Cheng, C.C. & DeVries, A.L. (1991) The role of antifreeze glycopeptides and peptides in the freezing avoidance of cold-water fish. In: *Life Under Extreme Conditions. Biochemical adaptation*, (Ed. G. di Prisco), pp. 1–15. Springer-Verlag, Berlin.

Clarke, A., Doherty, N., DeVries, A.L. & Eastman, J.T. (1984) Lipid content and composition of three species of Antarctic fish in relation to buoyancy. *Polar Biology*, **3**, 77–83.

Conover, R.J, Cota, G.F., Harrison, W.G., Horne, E.P.W. & Smith, R.E.H. (1990) Ice/water interactions and their effect on biological oceanography in the Arctic Archipelago. In: *Canada's Missing Dimension: Science and History in the Canadian Arctic Islands*, (Ed. C.R. Harington), pp. 204–228. Canadian Museum of Nature, Ottowa.

Conover, R.J., Herman, A.W., Prinsenberg, S.J. & Harris, L.R. (1986) Distribution of and feeding by the copepod *Pseudocalanus* under fast ice during the Arctic spring. *Science*, **232**, 1245–1247.

Conover, R.J. & Huntley, M. (1991) Copepods in ice-covered seas – distribution, adaptations to seasonally limited food, metabolism, growth patterns and life cycle strategies in polar seas. *Journal of Marine Systems*, **2**, 1–41.

Cross, W.E. (1982) Under-ice biota at the Pond Inlet ice edge and in adjacent fast ice areas during spring. *Arctic*, **35**, 13–27.

Dahms, H.U., Bergmann, M. & Schminke, H.K. (1990) Distribution and adaptations of sea ice inhabiting Harpacticoida (Crustacea, Copepoda) of the Weddell Sea (Antarctica). *Marine Ecology*, **11**, 207–226.

Daly, K.L. (1990) Overwintering development, growth, and feeding of larval *Euphausia superba* in the Antarctic marginal ice zone. *Limnology and Oceanography*, **35**, 1564–1576.

Daly, K.L. & Macaulay, M.C. (1988) Abundance and distribution of krill in the ice edge zone of the Weddell Sea, austral spring 1983. *Deep-Sea Research*, **35**, 21–41.

Daly, K.L. & Macaulay, M.C. (1991) Influence of physical and biological mesoscale dynamics on the seasonal distribution and behavior of *Euphausia superba* in the Antarctic marginal ice zone. *Marine Ecology Progress Series*, **79**, 37–66.

Dayton, P.K., Robilliard, G.A. & DeVries, A.L. (1969) Anchor ice formation in McMurdo Sound, Antarctica, and its biological effects. *Science*, **163**, 273–274.

De la Mare, W.K. (1997) Abrupt mid-twentieth-century decline in Antarctic sea-ice extent from whaling records. *Nature*, **389**, 57–59.

DeVries, A.L. (1971) Glycoproteins as biological antifreeze agents in Antarctic fishes. *Science*, **172**, 1152–1155.

DeVries, A.L. (1982) Biological antifreeze agents in coldwater fishes. *Biological Comparative Biochemistry and Physiology, A – Physiology*, **73**, 627–640.

DeVries, A.L. (1997) The role of antifreeze proteins in survival of Antarctic fishes in freezing environemnts. In: *Antarctic Communities. Species, Structure and Survival*, (Eds B. Battaglia, J. Valencia & D.W.H. Walton), pp. 202–208. Cambridge University Press, Cambridge.

Dieckmann, G.S., Arrigo, K. & Sullivan, C.W. (1992) A high resolution sampler for nutrient and chlorophyll *a* profiles of the sea ice platelet layer and underlying water column below fast ice in polar oceans: preliminary results. *Marine Ecology Progress Series*, **80**, 291–300.

Dieckmann, G.S., Rohardt, G., Hellmer, H. & Kipfstuhl, J. (1986) The occurrence of ice

platelets at 250 m near the Filchner Ice Shelf and its significance to sea ice biology. *Deep-Sea Research*, **33**, 141–148.

Dmitrenko, I., Dehn, J., Golovina, P., Kassens, H. & Zatsepin, A. (1998) Influence of sea ice on under-ice mixing under stratified conditions: potential impacts on particle distribution. *Estuarine Coastal Shelf Science*, **46**, 523–529.

Everson, I. (Ed.) (2000) *Krill. Biology, Ecology and Fisheries*. Fish and Aquatic Resources Series, Vol. 6. Blackwell Science Ltd, Oxford.

Falk-Petersen, S., Hagen, W., Kattner, G., Clarke, A. & Sargent, J. (2000) Lipids, trophic relationhips, and biodiversity in Arctic and Antarctic krill. *Canadian Journal of Fisheries and Aquatic Sciences*, **57** (Suppl. 3), 178–191.

Frazer, T.K., Quetin, L.B. & Ross, R.M. (1997) Abundance and distribution of larval krill, *Euphausis superba*, associated with annual sea ice in winter. In: *Antarctic Communities, Species, Structure and Survival*, (Eds B. Battaglia, J. Valencia & D.W.H. Walton), pp. 107–111. Cambridge University Press, Cambridge.

Friedrich, C. (1997) Ökologische Untersuchungen zur Fauna des arktischen Meereises. *Berichte zur Polarforschung*, **246**, 1–211.

Garrison, D.L. (1991) Antarctic sea ice biota. *American Zoologist*, **31**, 17–33.

Garrison, D.L., Ackley, S.F. & Buck, K.R. (1983) A physical mechanism for establishing algal populations in frazil ice. *Nature*, **306**, 363–365.

Gradinger, R. (1999) Integrated abundance and biomass of sympagic meiofauna in Arctic and Antarctic pack ice. *Polar Biology*, **22**, 169–177.

Gradinger, R. & Schnack-Schiel, S.B. (1998) Potential effect of ice formation on Antarctic pelagic copepods: salinity induced mortality of *Calanus propinquus* and *Metridia gerlachei* in comparison to sympagic acoel turbellarians. *Polar Biology*, **20**, 139–142.

Grainger, E.H. (1991) Exploitation of arctic sea ice by epibenthic copepods. *Marine Ecology Progress Series*, **77**, 119–124.

Grainger, E.H. & Hsiao, S.I.C. (1990) Trophic relationship of the sea ice meiofauna in Frosbisher Bay, Arctic Canada. *Polar Biology*, **10**, 283–292.

Gulliksen, B. & Lønne, O.J. (1989) Distribution, abundance, and ecological importance of marine sympagic fauna in the Arctic. *Rapports et Process-Verbaux des Réunions. Conseil Permanent International pour l'Exploration de la Mer*, **188**, 133–138.

Gulliksen, B. & Lønne, O.J. (1991) Sea ice macrofauna in the Antarctic and the Arctic. *Journal of Marine Systems*, **2**, 53–61.

Günther, S., George, K.H. & Gleitz, M. (1999) High sympagic metazoan abundance in platelet layers at Drescher-Inlet, Weddell Sea, Antarctica. *Polar Biology*, **22**, 82–89.

Hofman, E.E. & Lascara, C.M. (2000) Modeling the growth dynamics of Antarctic krill *Euphausia superba*. *Marine Ecology Progress Series*, **194**, 219–231.

Hop, H., Poltermann, M., Lønne, O.J., Falk-Petersen, S., Kornes R. & Budgell, W.P. (2000) Ice amphipod distribution relative to ice density and under-ice topography in the northern Barents Sea. *Polar Biology*, **23**, 357–367.

Horner, R., Ackley, S.F., Dieckmann, G.S., Gulliksen, B., Hoshiai, T., Legendre, L., Melnikov, I.A., Reeburgh, W.S., Spindler, M. & Sullivan, C.W. (1992) Ecology of sea ice biota. 1. Habitat, terminology, and methodology. *Polar Biology*, **12**, 417–427.

Hoshiai, T., Tanimura, A. & Watanaba, K. (1987) Ice algae as food of an Antarctic ice-associated copepod, *Paralabidocera antarctica* (I.C. Thompson). *Proceedings of the NIPR Symposium on Polar Biology*, **1**, 105–111.

Huntley, M.E., Nordhausen, W. & Lopez, M.D.G. (1994) Elemental composition, metabolic activity and growth of Antarctic krill *Euphausia superba* during winter. *Marine Ecology Progress Series*, **107**, 23–40.

Janssen, H.H. & Gradinger, R. (1999) Turbellaria (Archoophora: Acoela) from Antarctic sea ice endofauna – examination of their micromorphology. *Polar Biology*, **21**, 410–416.

Jarman, S., Elliott, N., Nicol, S., McMinn, A. & Newman, S. (1999) The base composition of the krill genome and its potential susceptibility to damage by UV-B. *Antarctic Science*, **11**, 23–26.

Karentz, D., McEuen, F.S., Land, M.C. & Dunlap, W.C. (1991) Survey of mycosporine-like amino acid compounds in Antarctic marine organisms: potential protection from ultraviolet exposure. *Marine Biology*, **108**, 157–166.

Kattner, G. & Hagen, W. (1995) Polar herbivorous copepods – different pathways in lipid biosynthesis. *ICES Journal of Marine Science*, **51**, 329–335.

Krembs, C., Gradinger, R. & Spindler, M. (2000) Implications of brine channel geometry and surface area for the interaction of sympagic organisms in Arctic sea ice. *Journal of Experimental Marine Biology and Ecology*, **243**, 55–80.

Krembs, C., Tuschling, K. & von Juterzenka, K. (2001) The topography of the ice water interface – its influence on the colonisation of sea ice by algae. *Polar Biology*, **25**, 106–117.

Kurbjeweit, F., Gradinger, R. & Weissenberger, J. (1993) The life cycle of *Stephos longipes* – an example for cryopelagic coupling in the Weddell Sea (Antarctica). *Marine Ecology Progress Series*, **98**, 255–262.

Loeb, V., Siegel, V., Holm-Hansen, O., Hewitt, R., Fraser, W., Tivelpiece, W. & Trivelpiece, S. (1997) Effects of sea-ice extent and krill or salp dominance on the Antarctic food web. *Nature*, **387**, 897–900.

Marschall, P. (1988) The overwintering strategy of Antarctic krill under the pack ice of the Weddell Sea. *Polar Biology*, **9**, 129–135.

Melnikov, I.A. & Spiridonov, V.A. (1996) Antarctic krill under perennial sea ice in the western Weddell Sea. *Antarctic Science*, **8**, 323–329.

Menshenina, L.L. & Melnikov, I.A. (1995) Under-ice zooplankton of the western Weddell Sea. *Proceedings of the NIPR Symposium on Polar Biology*, **8**, 126–138.

Meyer, B., Atkinson, A., Stübing, D., Oettl, B., Hagen, W. & Bathmann, U. (2002) Feeding and energy budgets of Antarctic krill *Euphausia superba* at the onset of winter – I. Furcilia III larvae. *Limnology and Oceanography*, **47**, 943–952.

Mock, T. & Kroon, B.M.A. (2002a) Photosynthetic energy conversion under extreme conditions. I. Important role of lipids as structural modulators and energy sink under N-limited growth in Antarctic sea ice diatoms. *Phytochemistry*, **61**, 41–51.

Mock, T. & Kroon, B.M.A. (2002b) Photosynthetic energy conversion under extreme conditions. II. The significance of lipids at low temperature and low irradiances in Antarctic sea ice diatoms. *Phytochemistry*, **61**, 53–60.

Nicol, S. (2000) Understanding krill growth and aging: the contribution of experimental studies. *Canadian Journal of Fisheries and Aquatic Sciences*, **57** (Suppl. 3), 168–177.

O'Brien, D.P. (1987) Direct observations of the behaviour of *Euphausia superba* and *Euphausia crystallorophias* (Crustacea: Euphausiacea) under pack ice during the Antarctic spring. *Journal of Crustacean Biology*, **7**, 437–448.

Poltermann, M. (1997) Biologische und ökologische Untersuchungen zur kryopelagischen Amphipodenfauna des arktischen Meereises. *Berichte zur Polarforschung*, **225**, 1–170.

Quetin, L.B. & Ross, R.M. (1991) Behavioral and physiological characteristics of the Antarctic krill, *Euphausia superba*. *American Zoologist*, **31**, 49–63.

Quetin, L.B., Ross, R.M., Frazer, T.K. & Haberman, K.L. (1996) Factors affecting distribution and abundance of zooplankton, with an emphasis on Antarctic krill, *Euphausia superba*. *Antarctic Research Series*, **70**, 357–371.

Rakusa-Suszczewski, S. (1972) The biology of *Paramoera walkeri* Stebbing (Amphipoda) and the Antarctic sub-fast ice community. *Polish Archives of Hydrobiology*, **19**, 11–36.

Richardson, M.G. & Whitaker, T.M. (1979) An Antarctic fast-ice food chain: observations on the interaction on the amphipod *Pontogeneia antarctica* Chevreux with ice-associated micro-algae. *British Antarctic Survey*, **47**, 107–115.

Riemann, F. & Sime-Ngando, T. (1997) Note on sea-ice nematodes (Monhysteroidea) from Resolute Passage, Canadian High Arctic. *Polar Biology*, **18**, 70–75.

Ross, R.M., Quetin, L.B. & Lascara, C. (1996) Distribution of Antarctic krill and dominant zooplankton west of the Antarctic Peninsula. In: *Foundations for Ecological Research West of the Antarctic Peninsula*, (Eds R.M. Ross, E.E. Hofmann & L.B. Quetin), American Geophysical Union, Washington, D.C. *Antarctic Research Series*, **70**, 199–217.

Runge, J.A. & Ingram, R.G. (1988) Underice grazing by planktonic, calanoid copepods in relation to a bloom of ice microalgae in southeastern Hudson Bay. *Limnology and Oceanography*, **33**, 280–286.

Sargent, J.R., Gatten, R.R. & Henderson, R.J. (1981) Lipid biochemistry of zooplankton from high latitudes. *Océanis*, **7**, 623–632.

Schnack-Schiel, S.B., Dieckmann, G.S., Gradinger, R., Melnikov, I.A., Spindler, M. & Thomas, D.N. (2001a) Meiofauna in sea ice of the Weddell Sea (Antarctica). *Polar Biology*, **24**, 724–728.

Schnack-Schiel, S.B. & Hagen, W. (1995) Life cycle strategies of *Calanoides acutus*, *Calanus propinquus* and *Metridia gerlachei* (Copepoda: Calanoida) in the eastern Weddell Sea, Antarctica. *ICES Journal of Marine Science*, **51**, 541–548.

Schnack-Schiel, S.B., Thomas, D.N., Dahms, H.U., Haas, C. & Mizdalski, E. (1998) Copepods in Antarctic Sea ice. In: *Antarctic Sea Ice Biological Processes, Interactions and Variability*, (Eds M.P. Lizotte & K. Arrigo), American Geophysical Union, Washington, D.C. *Antarctic Research Series*, **73**, 173–182.

Schnack-Schiel, S.B., Thomas, D., Dieckmann, G.S., Eiken, H., Gradinger, R., Spindler, M., Weissenberger, J., Mizdalski, E. & Beyer, K. (1995) Life cycle strategy of the Antarctic calanoid copepod *Stephos longipes*. *Progress in Oceanography*, **36**, 45–75.

Schnack-Schiel, S.B., Thomas, D.N., Haas, C., Dieckmann, G.S. & Alheit, R. (2001b) On the occurrence of the copepods *Stephos longipes* (Calanoida) and *Drescheriella glacialis* (Harpacticoida) in summer sea ice in the Weddell Sea. *Antarctic Science*, **13**, 150–157.

Scott, C.L., Falk-Petersen, S., Sargent, J.R., Hop, H., Lønne, O. J. & Poltermann, M. (1999) Lipid and trophic interactions of ice fauna and pelagic zooplankton in the marginal zone of the Barents Sea. *Polar Biology*, **21**, 65–70.

Siegel, V. (2000) Krill (Euphausicea) life history and aspects of population dynamics. *Canadian Journal of Fisheries and Aquatic Sciences*, **57** (Suppl. 3), 130–150.

Siegel, V. & Loeb, V. (1995) Recruitment of Antarctic krill *Euphausia superba* and possible causes for its variability. *Marine Ecology Progress Series*, **123**, 45–56.

Siferd, T.D., Welch, H.E., Bergmann, M.A. & Curtis, M.F. (1997) Seasonal distribution of sympagic amphipods near Chesterfield Inlet, N.W.T., Canada. *Polar Biology*, **18**, 16–32.

Swadling, K.M., Gibson, J.A.E., Ritz, D.A. & Nichols, P.D. (1997) Horizontal patchiness in sympagic organisms of the Antarctic fast ice. *Antarctic Science*, **9**, 399–406.

Swadling, K.M., McPhee, A.D. & McMinn, A. (2001) Spatial distribution of copepods in fast ice of eastern Antarctica. *Polar Bioscience*, **13**, 55–65.

Swadling, K.M., Nichols, P.D., Gibson, J.A.E. & Ritz, D.A. (2000) The role of lipid in the life cycles of ice-dependent and ice-independent populations of the copepod *Paralabidocera antarctica*. *Marine Ecology Progress Series*, **208**, 171–182.

Tanimura, A., Hoshiai, T. & Fukuchi, M. (1996) The life cycle strategy of the ice-associated copepod *Paralabidocera antarctica* (Calanoida, Copepoda), at Syowa Station, Antarctica. *Antarctic Science*, **8**, 257–266.

Tanimura, A., Hoshiai, T. & Fukuchi, M. (2002) Change in habitat of the sympagic copepod *Paralabidocera antarctica* from fast ice to seawater. *Polar Biology*, **25**, 667–671.

Thomas, D.N., Lara, R.J., Haas, C., Schnack-Schiel, S.B., Dieckmann, G.S., Kattner, G. Nöthig, E.-M., & Mizdalski, E. (1998) Biological soup within decaying summer sea ice in the Amundsen Sea, Antarctica. In: *Antarctic Sea Ice Biological Processes, Interactions and Variability*, (Eds M.P. Lizotte & K. Arrigo), American Geophysical Union, Washington, D.C. *Antarctic Research Series*, **73**, 161–171.

Werner, I. (1997) Grazing of Arctic under-ice amphipods on sea-ice algae. *Marine Ecology Progress Series*, **160**, 93–99.

Wöhrmann, A.P.A. (1997) Freezing resistance in Antarctic fish. In: *Antarctic Communities. Species, Structure and Survival*, (Eds B. Battaglia, J. Valencia & D.W.H. Walton), pp. 209–216. Cambridge University Press, Cambridge.

Chapter 8

Sea Ice: A Critical Habitat for Polar Marine Mammals and Birds

David G. Ainley, Cynthia T. Tynan and Ian Stirling

8.1 Introduction

Marine birds and mammals, which we will refer to collectively as 'top trophics' (members of the top trophic level in marine food webs), relate to sea ice in two ways. They either have evolved ways to exploit the opportunities its presence affords (often increased through specialized access to food), or they find it merely a barrier that must recede or break into open leads and floes before they can move into an area. In a bit of irony, the resident populations of prey grow large, or otherwise benefit, from the presence of ice during the period of the predators' forced absence. Modern, industrial humans are among the organisms that find sea ice a hindrance; sea ice, particularly before the era of motorized icebreakers, was a major deterrent to human exploration of polar regions. Sea ice certainly dissuaded the pre-eminent explorer James Cooke, and others before, from discovering 'Terra Incognita'. On the other hand, in his journal, *Voyage of Discovery and Research in the Southern and Antarctic Regions during the Years 1839–43*, James Clarke Ross, upon his first encounter of Antarctic sea ice, writes of the specialized type of organism:

> 'At 6 P.M. a fine breeze sprang up from the eastward, and we carried a press of sail all night, passing a great many bergs, and much loose ice in long narrow streams, as we advanced to the southward. A beautiful white petrel was seen in the evening, giving notice of our approach to a large body of ice, although we were not at the time aware that these birds never wander far from the main pack.'

Though Cooke and others must have observed a similar association of the petrel with sea ice, it was Ross, the sailor-scientist, who first made note of it and repeated his observations, including those of other species (certain seals and penguins), several times in his journals. To this day, the snow petrel *(Pagodroma nivea*) is mentioned in the *Antarctic Pilot* to warn mariners of the immediate presence of ice in the fog-enshrouded seas that usually exist at the large-scale sea ice edge. The snow petrel is highly adapted for existence in ice-covered waters and is one of those

species classified as an obligate associate of sea ice. We now know that ice-obligate whales, seals and birds exist in both polar regions (see below; Table 8.1).

The unique nature of the Antarctic sea ice avifauna has been especially well studied and offers insights into the nature of what being a 'sea ice obligate species' entails among the top trophics. An analysis of seabird communities in the South

Table 8.1 A list of polar marine mammals and birds whose presence is characteristic of sea ice covered waters. Those marked with an asterisk (*) are obligate associates never found far from sea ice; those with a plus (+) are not of the latter, but have evolved specific morphological, physiological or behavioural adaptations to exploit sea ice habitat. The remainder are found often in the open ice pack, but ice is largely a barrier to them.

Mammals		
Antarctic	* Crabeater seal	*Lobodon carcinophagus*
	* Leopard seal	*Hydrurga leptonyx*
	Weddell seal	*Leptonychotes weddellii*
	* Ross seal	*Ommatophoca rossii*
	Antarctic fur seal	*Arctocephalus gazella*
	+ Minke whale	*Balaenoptera acutorostrata*
	Killer whale	*Orcinus orca*
	Sperm whale	*Physeter macrocephalus*
Arctic	* Ringed seal	*Phoca hispida*
	+Harp seal	*Phoca groenlandica*
	+Hooded seal	*Cystophora cristata*
	* Bearded seal	*Erignathus barbatus*
	+Walrus	*Odobenus rosmarus*
	* Polar bear	*Ursus maritimus*
	* Bowhead whale	*Balaena mysticetus*
	+Minke whale	*Balaenoptera acutorostrata*
	Grey whale	*Eschrichtius robustus*
	* Narwhal	*Monodon monoceros*
	+Beluga	*Delphinapterus leucas*
	Killer whale	*Orcinus orca*
Birds		
Antarctic	* Emperor penguin	*Aptenodytes forsteri*
	* Adélie penguin	*Pygoscelis adeliae*
	Southern giant fulmar	*Macronectes giganteus*
	Antarctic fulmar	*Fulmarus glacialoides*
	* Snow petrel	*Pagodroma nivea*
	+Antarctic petrel	*Thalassoica antarctica*
	Blue petrel	*Halobaena caerulea*
	Wilson's storm-petrel	*Oceanites oceanicus*
	+South polar skua	*Catharacta maccormicki*
Arctic	Northern fulmar	*Fulmarus glacialis*
	* Ivory gull	*Pagophila eburnea*
	* Ross's gull	*Rhodostethia rosea*
	Eider spp. (4)	*Somateria* spp.
	Oldsquaw duck	*Clangula hyemalis*
	+Thick-billed murre	*Uria lomvia*
	+Black guillemot	*Cepphus grylle*
	Dovekie	*Alle alle*

Pacific, based on many thousands of kilometres of surveys crisscrossing the entire basin, found the most distinctive of all communities to be the one that associated with the Antarctic pack ice. It was composed of five species (those marked by an asterisk or a plus in Table 8.1; Ribic & Ainley, 1988/89). In contrast, composition among lower-latitude species communities included much overlap, with community composition much less defined. Following that study was another that investigated the shift in bird communities as the extent of Antarctic sea ice waxed and waned seasonally (Ainley et al., 1994). The pack ice community remained robust year round, whereas most species in the open-water community departed high latitudes when winter arrived.

Apparently, the lack of sunlight reduced productivity and food availability in open waters, and along with the ice and the cold temperatures, forced open-water species to migrate north for the winter. These species, while able to exploit Antarctic waters during summer after the sea ice retreated, did not possess the adaptations to exploit opportunities in the pack ice during winter (or summer). Obligate pack ice species did not then stray into the seasonally vacated open waters; apparently, the pack ice offered sufficient foraging opportunities to satisfy their needs. Indeed, body mass of these birds reached its heaviest of the entire year during winter. The contrast was further demonstrated by a smaller-scale 'natural experiment', when during winter the rapid passing of weather fronts along the large-scale ice edge changed the wind direction from southerlies (very cold, off continent) to northerlies (off warmer waters; Ainley et al., 1993). Under cold, southerly conditions, seas froze northward hundreds of kilometres 'overnight'; but with the passing of the front and a switch in wind-direction a few days later, the new sea ice melted and retreated leaving the same wide band free of ice. In accord, what remained of the open-water avifauna flip-flopped with the pack ice avifauna within this zone of dynamic ice cover with the passing of each front.

A somewhat analogous pattern is demonstrated each year among large baleen whales both in the Antarctic and the Arctic (Brown & Lockyer, 1984). These are open-water creatures that can forage under ice only as far in as their breath-holding abilities allow. It has been well known since the commercial whaling days, that the great whales would follow the seasonal retreat of the pack ice. As the ice disappeared, new prey concentrations would become available, providing a continual replenishment of feeding opportunities. However, all but the minke whale in the Antarctic and the bowhead whale, narwhal and beluga in the Arctic vacate the polar region before the autumn advance of sea ice. Prior to freeze-up each year, the whaling ships (the lucky ones) departed as well.

In this chapter, we explore the adaptations that allow warm-blooded, air-breathing vertebrates to remain in ice-covered waters throughout the year.

Polynyas

Before proceeding further, however, we must first explore the subject of areas of predictable or persistent open water within the regional sea ice cover. These areas,

called polynyas, are very important to all top trophics, but especially those that are not ice-obligate species. As will become clear below, top trophics are dependent upon polynyas within the sea ice zone. The quest to access these ice-free waters that drives many of these species' life-history patterns. Hypothetically, in the 'purest' definition of the word, a polynya exists only during that time of the year when sea water should be actively freezing. In some areas, especially along headlands and fast ice edges, such as in coastal Antarctica or the North Water of northern Baffin Bay, strong, near-continual winds sweep new ice clear, along with the heat expelled from continually freezing surface water, creating what is known as a 'latent heat' polynya. Similarly, along coastal areas such as in much of the Arctic Basin or Hudson Bay, offshore winds alternate with onshore winds that alternately create open leads parallel to the shoreline or cause them to close up.

In other areas, warmer sub-surface waters are brought to the surface, usually a function of currents rising over ridges and rising shelf topography. The result is that surface waters remain above the freezing point. These are 'sensible heat' polynyas. However, even after air temperatures become warm in the late spring and surface waters are no longer cool enough to freeze, predictable open-water areas still occur within the sea ice covered region. Often these areas are the same as those present during winter as 'true' polynyas. In the larger sense of the word, then, these areas too qualify as polynyas or temporal extensions thereof.

Recurring polynyas are those that remain open throughout the winter, or open at the same time each spring, at the same location and time every year. While any polynya may be used opportunistically by top trophics at any time of year, recurring polynyas are of the greatest biological importance because overwintering or migrating species can depend on being able to breathe and feed while there.

In the Antarctic, the importance of polynyas to top trophics is not well appreciated. While physicists have launched major investigations of Antarctic polynyas, this is not the case among biologists. There are many latent-heat polynyas, generated along the coast by fierce katabatic winds. Most of the Antarctic coast is far enough south (well below the Antarctic Circle) that almost all of these polynyas are in total darkness from late autumn to early spring. For that reason, they are of little interest to birds and mammals, most of which need daylight to locate prey. Only the distribution of (winter-breeding) emperor penguin nesting colonies is affected by them, as they provide access to open water (Massom et al., 1998; Fig. 8.1). On the other hand, these polynyas continue to persist as open areas in the ice pack well into the spring (beyond the freezing period) and then affect the location of Adélie penguin colonies as well (Ainley, 2002; Fig. 8.1).

Ecologically, the situation is different in the Arctic. There, the existence of polynyas, many of which occur well to the south of the Arctic Circle (and in sunlight), is the major feature that affects life-history patterns of top trophics (Brown & Nettleship, 1981; Stirling, 1997). The distribution of most bird and mammal colonies in the Arctic, and in turn the villages (especially prehistoric ones) of native peoples, is strongly related to the presence of polynyas (Schledermann, 1980; Fig. 8.2). Major physical–biological investigations have taken place to deduce the processes that

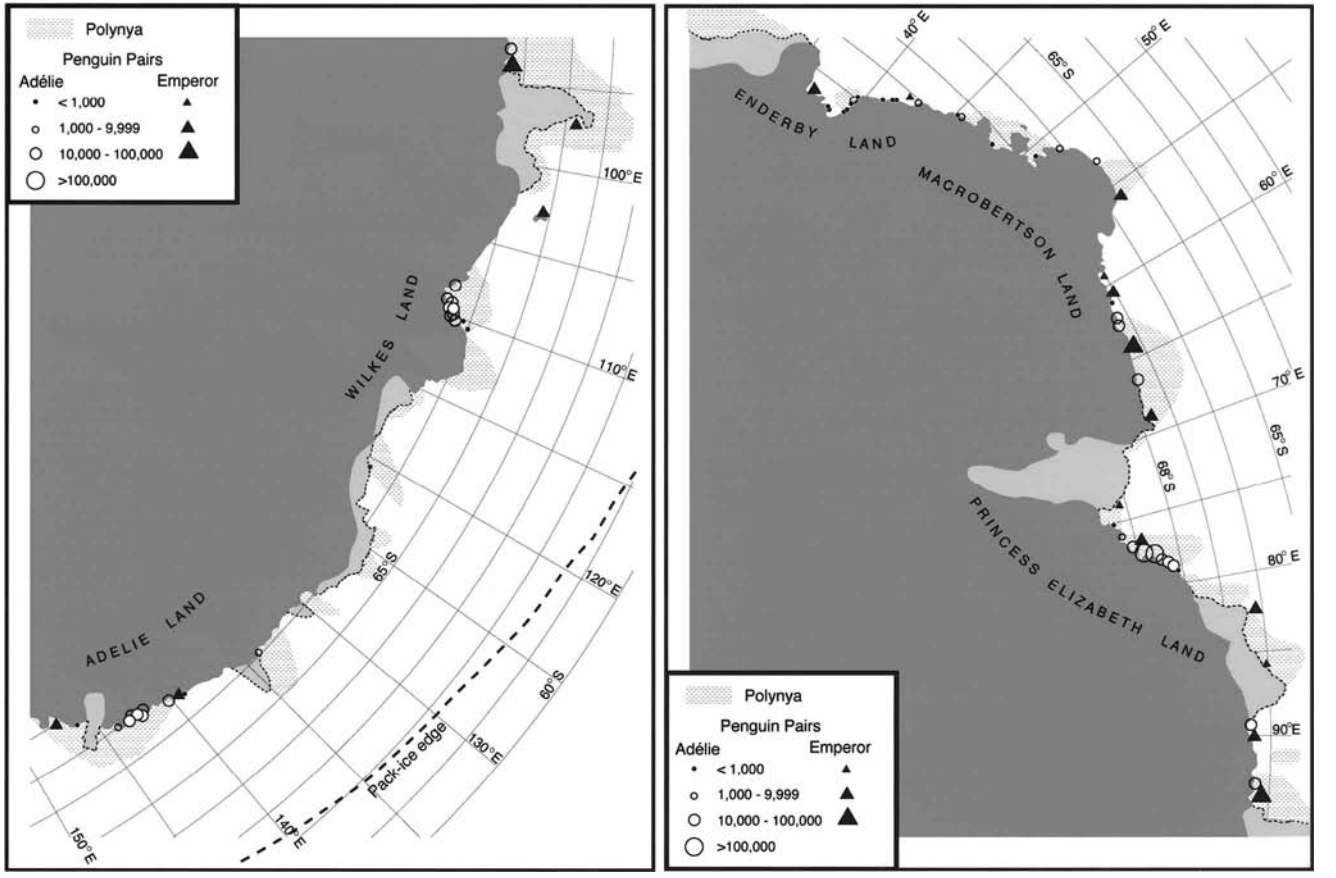

Fig. 8.1 Association of emperor and Adélie penguin nesting colonies with coastal polynyas: east Antarctica: (a) 95°E to 150°E; (b) 25°E to 95°E. (Figure redrawn from Ainley (2002) where data sources are also identified.

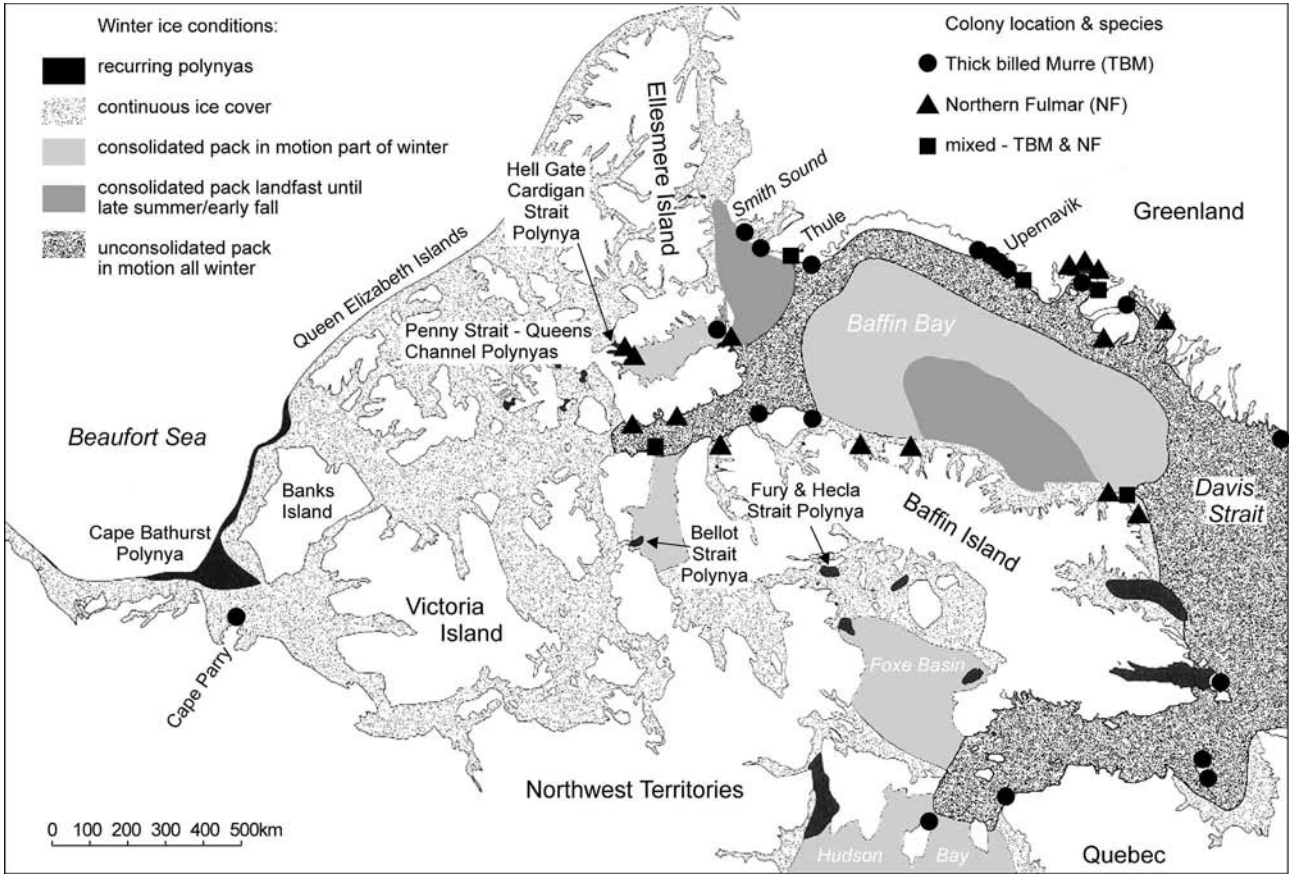

Fig. 8.2 Distribution of seabird colonies in correspondence to polynyas in the Canadian Arctic. From Brown & Nettleship (1981).

enhance their value, both in bringing access to open water and in stimulating biological productivity. The North Water of Baffin Bay provides valuable winter habitat for belugas, bowhead whales, bearded seals and walruses (Stirling, 1997; Richard et al., 1998b). Studies of other polynyas, such as the Northeast Water Polynya (Falk et al., 1997), the Cape Bathhurst Polynya (Harwood & Stirling, 1992), the major polynyas south of the Chukchi Peninsula, St. Lawrence Island and St. Matthew Island in the Bering Sea (Niebauer et al., 1999; Petersen et al., 1999), and the polynyas of the Belcher Islands in southeast Hudson Bay (Gilchrist & Robertson, 2000), all testify to the biological importance of these persistent open-water areas to overwintering mammals and birds.

Unlike the Antarctic, where the large-scale ice edge, well to the north of the continent and the Antarctic Circle, first experiences the onset of increased spring production, in the Arctic production gets a fast start at polynyas. It is all a matter of sunlight and open water. Polynyas are so important to top trophics in the Arctic that large die-offs occur when, in rare cases, a usually predictable polynya freezes for longer than several days (Stirling et al., 1981). These major mortalities of adults can alter population growth of affected species for decades. On the other hand, the hunting success of polar bears and humans increases as the amount of open water decreases (thus, confining prey) making the hunted seals more vulnerable to predation.

8.2 Habitat preferences and adaptations in the sea ice zone

Antarctic

A major requirement for several marine mammal and bird species is a platform for reproduction, and sea ice does very well in providing this. Included are the pack ice seals (crabeater, leopard, Ross and Weddell; Table 8.1) and the emperor penguin. Almost all middle- or high-latitude top trophic species time their reproductive cycles so that young become independent of parents when food availability is highest in late summer and early autumn, thus providing the best conditions for them to learn foraging techniques well enough so that they can survive the winter. This means that pups must be born, or eggs laid, in very early spring or even in winter. Seals, having very small flippers (in itself, an adaptation to retard heat loss in cold water), are far less agile than the large-flippered fur seals and sea lions (Plate 8.1). Although it is not impossible for them, they tend not to haul out on steep, rocky terrain or move very far inland. The same is true of the emperor penguin, which is very clumsy on land compared to its smaller relatives such as the Adélie penguin. In middle and lower latitudes, seals breed more on beaches (easily accessed); fur seals and sea lions breed on both beaches and rocky headlands. Beaches exist only for a very short time each year in the Antarctic (and always in the autumn). In the spring, the time when young are produced and mating occurs, the only accessible breeding

habitat for many top trophics is sea ice, because at that time beaches are layered by ice floes pushed into high ridges (5–7 m, or even higher) by winter winds. In the case of Antarctic seals, pups are born on the surface of the fast ice or stable floes where they can be nursed until weaned at and the same time avoid predators. Most seals mate in the water except for crabeater seals, which appear to mate on the surface of the floes, possibly to reduce the risk of predation by leopard seals and killer whales (Siniff et al., 1979). In the case of the emperor penguin, the best, and the only, habitat used for breeding is fast ice.

Later in the year, ice, as a platform, again comes into play in the annual cycle of Antarctic mammals and birds because they renew their pelage and feathers once per year. For the birds, the insulating properties of feathers are critical for survival in cold weather. For seals, it is the blubber layer beneath the coarse coat of hair and skin that keeps them warm. However, rather than replacing fur or feathers gradually, as some related lower-latitude species do, these animals complete their moult within a few weeks. Polar top trophics do this by laying down huge stores of fat on which they live while coats are being replaced quickly at considerable energetic cost. The abundant food of the pack ice region allows them to do this. During the moult, penguins remain on large ice floes, as do the flighted birds. The latter (snow and antarctic petrels), given that food is so abundant, become practically flightless, having dropped most of their wing feathers almost all at once during the moult. They spend most of their time sitting on icebergs or large ice floes. The seals, on the other hand, spend longer periods of the day hauled out during the moult, but most continue to feed at night, albeit for shorter periods than normal. A possible exception is the Ross seal, which appears to moult quickly and may, like elephant seals on islands, remain hauled out until moult is complete. At that time of year (February–March), all of these moulting birds as well as the pack ice seals (see below) are concentrated in just six areas where sea ice remains year round (Comiso, Chapter 4). Only the flighted birds have access, for roosting and moulting, to the many tabular icebergs that occur where food is abundant. Many icebergs also occur where food is not abundant, but the birds are not interested in these.

The other aspect of sea ice that is important to Antarctic top-trophic species is the rich under-ice community of fish and invertebrates that become prey, if these predators have the ability to exploit it (Ainley et al., 1991; Hopkins et al., 1993). The obligate species are able to do so. Emperor and Adélie penguins can hold their breath much longer than comparably sized, related species that occur in open waters (Ainley, 2002; Plate 8.2). This allows them to swim for appreciable distances under ice floes to forage. The availability of prey in ice-covered waters is often a function of the under-floe surface area. Thus, the more under-ice habitat that can be accessed, the better chance they have of finding a meal. Obviously, large floes, if the predator can get far enough away from the edge, offer the best pickings. This is especially true during winter when the only growing phytoplankton (food of the prey) is contained within the ice on the underside of floes (Ainley et al., 1991; Arrigo, Chapter 5; Lizotte, Chapter 6). The 'epontic' prey of the top trophics,

mainly euphausiids (krill), graze the phytoplankton in this under-ice habitat (Schnack-Schiel, Chapter 7; Leventer, Chapter 10). The predators either eat the euphausiids or the organisms (fish) in turn preying on them.

The two obligate ice penguins, emperor and Adélie, thus associate with sea ice for several differing reasons. It is not often clear but, presumably, they can exploit open water habitats as well as any other penguin species. Ultimately, their association comes down to what might be analogous to the question of why do songbirds associate with forests? Simply put, it is just that they evolved in association with that habitat. If the forests are cut down, the songbirds disappear; if the sea ice disappears so do these two penguin species (see Section 8.3 below). To summarize the above discussion, the emperor requires stable fast ice for breeding, and both species require reliable ice floes for moulting. Both species feed on epontic organisms to a great extent; both, however, can also dive deeply (especially the emperor) to exploit prey further down in the water column.

In the case of snow petrels, they have perfected what has become known as 'ambush feeding' (Ainley et al., 1994). Their entirely white plumage allows them to sit at the edge of floes or on floe bits waiting for an unsuspecting fish to venture out from the edge. When that happens, the snow petrel dives in to grab it. It can haul out very large fish which are too large to be carried away and, because of the concealing nature of white plumage, can usually consume the prey without gaining the notice of skuas, which steal prey from other birds (kleptoparasites). The antarctic petrel, on the other hand, which is boldly coloured black and white, is the only high-latitude bird that feeds by pursuit plunging. They fly quickly and along the edges of rapidly expanding leads, dive into the water and pursue prey, without missing a beat, by swimming using their wings for propulsion. The feeding strategies of these two main flighted species, thus, are dramatically different, but effectively exploit the opportunities that pack ice offer.

Unlike penguins (and the flighted Antarctic birds), Antarctic seals rely on a thick blubber layer to provide the insulation needed to conserve heat (Plate 8.1). Seals, of course, which can dive deeper and longer than most birds (the emperor penguin, which can dive to 300–500 m, is an exception), are less constrained by sea ice in their foraging within the pack ice zone compared to most polar birds. On the other hand, except for the Weddell seal, pack ice seals (crabeater, leopard, Ross) tend to avoid areas of consolidated pack ice where freeze-ups (of leads) are more frequent and therefore problematic (Laws, 1984; Ribic et al., 1991).

The Weddell seal is highly adapted to annual fast ice during summer and pack ice habitats during winter (Laws, 1984; Plate 8.1). There they search for fish, particularly the antarctic toothfish, *Dissostichus mawsoni*, and the antarctic silverfish, *Pleuragramma antarcticum* (Plötz et al., 2001). By breeding in fast ice areas, the problem facing Weddell seals is the maintenance of breathing holes. This they accomplish using their teeth to abrade the new ice that forms around their breathing holes, which they maintain in tidal or shear cracks in the ice. Older Weddell seals exhibit worn teeth from abrading the sea ice, and breakage of teeth appears to be a

cause of mortality (Stirling, 1969). These seals concentrate where tidal cracks and leads occur, predictably adjacent to islands and headlands. Interestingly, one group of Weddell seals that occur in the southernmost reaches of McMurdo Sound, Ross Sea, have been so isolated by extensive, uncracked, persistent sea ice between them and the main population for so long, that they have become genetically distinct (Gelatt, 2001). Seemingly, this population must have established itself during a period when fast ice in the Sound was less extensive. The combination of their relatively sedentary nature and fidelity to breeding sites has contributed to the genetic separation of Weddell seals in the southern Ross Sea from other Antarctic populations (Davis et al., 2000).

Weddell seals use both coastal fast ice and pack ice habitats, although the importance of the latter to adults and pups (especially during winter) has only recently been studied (Testa, 1994; Stewart et al., 2000). The Weddell seals in McMurdo Sound, are the most southern breeding mammal in the world and rely on the annual fast ice for breeding. Pups leave the breeding colonies at 6 weeks old, and young seals are rarely seen again for the next 4–6 years. Young seals, tracked with satellite telemetry, left McMurdo Sound in January and headed to the pack ice or open water polynyas of the Ross Sea during winter (Stewart et al., 2000). Foraging success may be enhanced at polynyas (see above). Weddell seals have evolved or learned specific behavioural tactics to help them hunt for small nototheniid fish (e.g. *P. antarcticum*) and larger antarctic toothfish (Davis et al., 1999), both of which occur mainly in waters overlying the continental shelf (and therefore areas overlain extensively by sea ice). Foraging tactics under the ice may include silhouetting their prey against the under-ice surface, perhaps helping to hide the predator, and attacking from below. Weddell seals have also been observed to force fish from ice crevices by expelling a blast of air through their muzzle or by prodding the ice with their muzzle (Davis et al., 1999).

Crabeater seals (perhaps the most numerous pinniped in the world, along with ringed seal in the Arctic; see below) and leopard seals, are predominantly species of deep pack ice through most of the year, although sub-adults also haul out on coastal fast ice, and occasionally land, during summer. During winter they occur in the divergent ice of the peripheral sea ice zone, and in the deep pack during summer are associated with ice cover of 60–70% and evenly distributed ice floes (Ribic et al., 1991). As crabeater seals feed almost exclusively on krill, linkages between sea ice dynamics and krill life history and distribution would be expected to impact their foraging ecology. As the krill occur beneath ice floes to a great extent, the crabeater seal is not known as a particularly deep-diving species. The leopard seal, another species of the looser pack ice, has the most catholic of diets among the ice seals. They feed heavily on krill, but also take significant numbers of penguins and crabeater seals (pups) as well (Siniff & Bengtson, 1977). The Ross seal in summer prefers heavier pack ice than these above two species because they appear to remain hauled out for an extended period, possibly the whole time, while moulting and thus require stable floes that will not disintegrate before they are finished. Their

predominant prey is squid (Laws, 1984). For the rest of the year, they appear to use fast ice only for periodic resting (similar to the use of islands by elephant seals) between extended periods at sea to feed.

The pack ice seals, as noted above, depend on ice as a floating substrate for resting, breeding and weaning pups. In the Weddell Sea, seasonal reductions in ice cover (Comiso, Chapter 4) lead to increases in ice seal densities, due to the fidelity of ice seals to the pack ice despite seasonal and annual changes in its distribution (Bester & Odendaal, 2000). During El Niño in 1998, the virtual absence of pack ice in the eastern Weddell Sea led to very high densities of pack ice seals hauled out on the available ice. Whether or not a reduction in pack ice, with subsequent increase in seal density, affects the foraging efficiency of the ice seals is not known. During conditions of reduced pack ice, seals spending more time swimming in transit between the ice haul outs and productive foraging grounds would be expected to expend more energy than during conditions where pack ice is located over sufficiently dense prey.

During the austral winter, some southern elephant seals (*Mirounga leonina*) occur in close association with Antarctic sea ice. For example, adult female elephant seals from King George Island fitted with satellite transmitters revealed that the seals ranged in the sea ice zone of coastal shelf waters along the Antarctic Peninsula (Bornemann et al., 2000). During winter, some of the female elephant seals with satellite radios spent several months in heavy pack ice. The availability of the Antarctic silverfish may explain why elephant seals are attracted to the pack ice to forage. In contrast to the adults, juvenile elephant seals from King George Island appear to avoid the sea ice and range in deeper open water (Bornemann et al., 2000).

The only cetacean that occurs regularly deep into the pack ice of the Southern Ocean is the minke whale. Some portion of the minke whale population is known to inhabit the Antarctic pack ice zone year round. This, the smallest of the baleen whales, has a very long, narrow and hard rostrum. The whales use their rostrum to break through new ice in order to breathe. When the ice begins to freeze in late autumn, seals and penguins may use the whales' breathing holes to aid in their own escape to areas of sparser ice cover. Thus, the community of pagophilic top trophics in the Southern Ocean, in some respects, is tightly interwoven, in part facilitated by the minke whale. Minke whales are associated with small floes, pancake and new ice (Ribic et al., 1991). They feed primarily on Antarctic krill (*Euphausia superba*) in most areas; however, the ice, or crystal, krill (*E. crystallorophias*) appears to be an important prey in waters overlying the Ross Sea shelf (and other shelves). Food availability near the ice edge appears to significantly affect minke whales (Ichii et al., 1998). Extensive sea ice conditions in the Ross Sea in 1994/95 covered the typically krill-rich slope region during summer, restricting the availability of this habitat to minke whales. This was reflected in the poor body fat condition of the whales (Ichii et al., 1998). It is unknown how warming trends in the Ross Sea area since the 1960s (Taylor & Wilson, 1990) have affected the biomass and distribution of their euphausiid prey.

Of the toothed whales (Odontocetes), the killer whale and sperm whale are most closely associated with sea ice and, at the large scale, usually occur near its outer edges. Killer whales stalk seal, penguin or cetacean prey in the pack ice habitat. They also feed extensively on the very large antarctic toothfish that is abundant in bays and sounds under the fast ice. Sperm whales observed near the ice edge are probably feeding on mesopelagic squid associated with shoaled Circumpolar Deep Water (Tynan, 1997). During summer, the distribution of migratory large baleen whales reflects the circumpolar position of the Southern Boundary of the Antarctic Circumpolar Current; as summer progresses with the southward retreat of the ice and concurrent evolution of the productive marginal ice-edge zone, these whales move closer to the continent (Tynan, 1998). Linkages between sea ice dynamics and the southernmost extent and depth of warm Upper Circumpolar Deep Water are expected to affect the productivity of the Antarctic ecosystem and the related food web.

Cetaceans appear to avoid occurring in the company of killer whales by remaining where sea ice is extensive, if possible. The behaviour of bowhead whales, belugas and narwhals in the Arctic (see below), and minke whales in the Antarctic, may be strongly influenced by the fear of killer whales. Whether sea ice serves to shelter the cetaceans from killer whales more by visual versus acoustic reduction of detection, is not known.

Arctic

Ross's and ivory gulls are as highly adapted to life in the Arctic sea ice zone as is their analogue, the snow petrel, in the Antarctic. Neither of these species are found where there is no sea ice for long. In fact, they are rarely found far from drifting sea ice at any time of the year. They are white or near-white in colour, an adaptation (as long as their background is white) by which they avoid the notice of predators and kleptoparasites. In addition, white coloration allows them to approach their prey more closely. Like the snow petrel, ivory gulls nest in ice-free terrain, which often means the tops of nunataks (mountains projecting through an ice sheet; Haney & MacDonald, 1995). Not only do they find in those localities the ice-free terrain in or on which to nest early in the spring, but the expanse of ice surrounding their colonies protects them from predators (skuas – Antarctic; foxes and polar bears – Arctic). Ross's gulls often nest on islands within lakes and, in that regard, are less associated with sea ice.

Top trophics throughout the Arctic rely greatly on arctic cod (*Boreogadus saida*), a small fish that feeds on epontic crustaceans that, in turn, graze the ice algae on the underside of ice floes (Schnack-Schiel, Chapter 7). The ivory and Ross's gulls forage at the surface, near to floe edges, often looking for prey (fish and zooplankton) washed onto floes (Haney & MacDonald, 1995). The black guillemot and thick-billed murre, on the other hand, are strong sub-surface divers that forage in this under-ice habitat. The cod and some of the larger crustaceans are their usual target

(Bradstreet, 1980). The guillemot is an almost all-black species, and the murre is dark brown on its upper side. Their coloration certainly is cryptic to prey that are looking down from the ice into the murky depths from which this predator approaches.

Among the Arctic ice seals, the ringed seal may be among the best barometers of ice conditions. This species, like its southern ecological counterpart the Weddell seal, depends on stable annual ice, sufficient snow accumulation for subnivean lairs, and proximity of productive feeding areas to their breeding habitat (Smith & Stirling, 1975; Hammill & Smith, 1989). It is especially associated with coastal, or between-island, fast ice but also occurs in offshore areas having large stable annual ice floes such as Baffin Bay and the Barents Sea (Finley et al., 1983; Wiig et al., 1999). Sufficient sea ice deformation is needed to facilitate formation of a snowdrift under which ringed seals maintain breathing holes and excavate haul-out lairs. Ringed seals use the heavy claws on their foreflippers to maintain two to four breathing holes in ice up to 2 m or more thick (Plate 8.3).

During spring, ringed seals give birth to their pups inside their subnivean lairs. The pups are born with a white coat of lanugo (soft, first coat) to make them less visible should they be exposed on the ice before they are able to escape predators by entering the water. Ringed seals mate in the water after the pups are weaned, and haul out on the ice beside a breathing hole or crack to moult. The timing of ice formation, and therefore of pupping and moulting, varies with latitude. Although in most Arctic regions, ringed seals typically rely on subnivean lairs for pupping, in the Okhotsk Sea, pups are born on the ice without any shelter of snow (Gjertz & Lydersen, 1983). In the Canadian Arctic, ringed seals show a preference for annual fast ice with greater than 75% ice cover over water 50–175 m deep (Kingsley et al., 1985), and ice deformation of less than 40% pressure ridging of the total ice cover (Frost et al., 1988). Ringed seals dive near or under the ice in search of arctic cod, other pelagic schooling fish, pelagic amphipods of the genus *Parathemisto* and amphipods associated with the benthos or under-surface of the sea ice (Finley et al., 1983; Welch et al., 1992).

Ice seals serve as barometers of ice conditions, not only by their abundance, but also by the alteration in ice conditions that they generate. The holes made by ice seals allow for rapid drainage of surface water, such as meltpond water, creating white circular areas that can be viewed by remote sensing (Digby, 1984). The breathing holes of seals can become further enlarged by the flow of melt water, which often forms a vortex (Holt & Digby, 1985). Processes that redistribute or change the prevalence of surface melt water are of critical importance for the ice energy and mass balance as it affects ice albedo and heat fluxes through the ice cover (Eicken et al., 2002). Therefore, in regions of the Arctic where first-year ice has few non-biogenic flaws or perturbations, the drainage of melt water through seal holes may be especially important. Drainage of large melt ponds should increase albedo and consequently help to conserve the ice. Further, the fresh water that drains through the seal holes may form new ice at the freshwater–seawater interface

under the ice. In this way the seals contribute to positive feedback loops that promote ice maintenance. No studies, however, have considered the links between ice seals and ocean–ice–atmosphere processes.

Complex links between climate change and the extent, structure and associated productivity of sea ice could all impact on ringed seals (Tynan & DeMaster, 1997; see below). Severity of ice conditions have been related to reduced ovulation rates and reduced body condition of ringed seals (Stirling et al., 1977; Harwood et al., 2000). For example, heavy sea ice conditions in the Beaufort Sea during the winter of 1973–74 coincided with the subsequent decline of ringed seals in 1974 and 1975 (Stirling et al., 1977; Stirling & Lunn, 1997). In Prince Albert Sound, Northwest Territories, Canada, severe ice conditions in 1974 appear to have also lead to a reduction in the prey available to seals (Harwood et al., 2000). In contrast, the earlier clearance of ice during spring 1998 provided greater availability of prey to all ages of ringed seals. Despite the apparent availability of prey, the early disruption of fast ice had a significant negative effect on the growth, condition and survival of pups still dependent on their mothers. With earlier spring warming and early break-up of the sea ice, many pups were apparently separated from their mothers, had shorter lactation, and were prematurely forced to enter the water for extended periods resulting in slower growth and higher mortality (Smith & Harwood, 2001). Early collapse of lairs from rain or warm temperatures can also expose pups to high levels of predation by polar bears and arctic foxes (Stirling & Derocher, 1993).

Bearded seals have a circumpolar distribution in the open drift ice and tend to avoid regions of continuous, thick land-fast ice (Burns, 1981). They can, however, maintain breathing holes in relatively thin ice. Bearded seals rely on drift ice over relatively shallow regions (< 100 m depth) where they feed on benthic prey (Kingsley et al., 1985). Soon after birth the pups enter the water as capable swimmers (Burns, 1981). In the northern Barents Sea, the distribution and movements of bearded seals tend to track the seasonal advance and retreat of the sea ice cover, with high densities of mother–pup pairs occurring near the ice edge in late April to early May (Wiig & Isaksen, 1995). In order to stay near suitable feeding areas, mother–pup pairs in Kongsfjorden, Svalbard, appear to move away from offshore drifting pack ice and back into the head of the fjord during May (Hammill et al., 1994). There at the flaw zone, at the edge of the fast ice, they may find more sheltered conditions with suitable ice for hauling out.

Another ice seal, the hooded seal, is a migratory, pelagic species (Bowen et al., 1987). Pups are born during March on heavy ice floes close to the ice edge in three regions of the North Atlantic: near Jan Mayen Island, off northeastern Newfoundland and in the Davis Strait. After only 4 days of lactation, pups are weaned abruptly and are ready to leave the ice (Bowen et al., 1987). Adults migrate to pack ice off southern Greenland to moult during June and July (Sergeant, 1976).

In spring, harp seals (*Phoca groenlandica*) migrate from pelagic feeding areas in the High Arctic to give birth in vast herds further south. There they seek regions of extensive drifting pack ice that is not adjacent to land, using floes further in from the

ice edge than those used by hooded seals (Lydersen & Kovacs, 1999). Pups are weaned at 12 days of age, having not yet entered the water in most cases. Hooded seals have a broad diet and forage on capelin and the amphipod *Parathemisto libellula* close to the ice edge in the Barents Sea.

The walruses comprise three currently recognized sub-species (i.e. the Atlantic walrus *Odobenus rosmarus rosmarus*, the Laptev walrus *O. r. laptevi*, and the Pacific walrus *O. r. divergens*), all of which associate with drift ice upon which they rest. Polynyas allow some groups to overwinter and breed in winter at high latitude (Sjare & Stirling, 1996). Their long tusks, for which they are renowned, serve as convenient ice axes for hauling out onto the ice floes; hence the derivation of one of their nick-names, the 'ice-walker'. They are also capable of using their heads to break through young ice up to 20 cm thick (Fay, 1982). After break-up, if ice is not available, they will haul out on land (Fay, 1981). As a highly social and gregarious species, they haul out together in large numbers, lying closely packed together. During the summer moulting period, they reside on either ice or land. Their prey consists mainly of mollusks and, therefore, they must find haul-outs near shallow regions (< 80 m) having high benthic production. In the Bering and Chukchi Seas, walruses may spend more than 85% of their time feeding (Fay, 1982). Near Svalbard, walruses feed primarily on the bivalve *Mya truncata* and the gastropod whelk *Buccinum* sp. (Gjertz & Wiig, 1992).

Walruses that haul out on drifting pack ice may be passively carried to new benthic feeding grounds. Without drift ice, walruses lose this convenient connection between motile haul outs and new benthic foraging grounds. When confronted with heavy consolidated ice, the walruses must rely on polynyas and the restricted benthic foraging grounds near them (Sjare & Stirling, 1996). Some walruses winter in the southern parts of Svalbard, as well as within the winter pack ice (Wiig et al., 1996), possibly due to the abundance of open leads within the Barents Sea ice during winter (Vinje & Kvambekk, 1991). Males in northeastern Greenland disperse in autumn and winter in the pack ice along Fram Strait and northeastern Greenland. Sea ice conditions can affect more than foraging success. Studies in the Canadian High Arctic suggest that mating systems and breeding behaviour of walruses are also strongly influenced by variability in sea ice habitat (Sjare & Stirling, 1996).

Polar bears are confined to seasonally ice-covered areas of the Arctic and sub-Arctic where they search for prey: ringed, bearded, harp, hood and harbour seals; walruses, belugas and occasional narwhals. The dynamics of sea ice can affect their access to these prey species; without ice the bears often are unable to forage. Polar bears typically rely on fast ice to search for ringed seals (especially pups). In some regions, such as the Barents Sea, they also hunt for ringed seals, as well as bearded and harp seals, along lead systems or ridged ice on larger floes of drifting pack ice (Wiig et al., 1999). Tracking of polar bears, with satellite radio collars, has shown that bears are more active and range further in active pack ice than in consolidated pack ice (Ferguson et al., 2001). Productivity, and consequently seal

availability, may be higher (albeit less predictable) in active ice than in consolidated pack.

Among the whales, belugas, narwhals and bowhead whales, as well as minke whales, are capable of breaking new ice with their backs (minke whales their rostrum; see above) in order to make breathing holes. All of these whales, with the exception of the minke, lack a dorsal fin, an adaptation thought to derive from the need to break sea ice with their back. In the case of the minke, its dorsal fin is very small and is located far along toward the tail. These cetaceans, however, are mostly found in the leads and open-water areas at the periphery of the pack ice zone. Their presence in the sea ice zone during winter is confined to persistent polynyas and shore leads.

Belugas, also called white whales (or belukhas in Alaska), engage in diverse migratory patterns in the Arctic, often travelling far into the permanent pack ice (Richard et al., 2001b). For example, the Beaufort Sea stock of belugas winters in the Bering Sea and migrates to summering areas in the Beaufort Sea and Amundsen Gulf. Belugas off northern Alaska during summer select slope and basin regions of moderate-to-heavy ice; during autumn, belugas occur over the slope in all ice conditions (Moore et al., 2000). Perhaps most remarkable, was the discovery that belugas summering along the north coast of Alaska, move great distances well offshore, in deep (> 3000 m) water and beneath areas where there is almost complete ice cover, to reach their spring feeding areas (Suydam et al., 2001). The whales were able to cover between 59 and 79 km per day through waters having an ice cover of greater than 90%. Belugas overwintering in the Bering Sea are thought to disperse in the seasonal ice, though no data exist (Harwood et al., 1996).

For many populations of belugas, such as the Cook Inlet and the Beaufort Sea belugas, their winter distribution, movements and habitats are poorly known. For other populations, such as those that summer in the central Canadian Arctic, seasonal migratory patterns have been established. Thousands of belugas that summer around Somerset Island later migrate eastward along the southern coast of Devon Island and eventually winter primarily in the North Water and, to a lesser extent, off West Greenland (Doidge & Finley, 1993; Richard et al., 1998a; Richard et al., 2001a). Belugas may select a migratory route that relates to the availability of their prey, such as arctic cod. They are capable of deep (> 300 m) dives during which they are thought to pursue benthic prey (Martin & Smith, 1999).

A system of predictably recurring leads and polynyas, such as the North Water, can provide valuable winter habitat (see Fig. 8.2). For most of the winter, the thickness of the pack ice surrounding the North Water probably prevents the belugas from leaving the region (Heide-Jørgensen et al., 1998); however, belugas may be far more frequent denizens of the thick pack ice than was previously thought. It is unknown how climate-induced changes in extent and thickness of sea ice might affect the foraging success, migratory patterns and consequently the population structure of belugas (Tynan & DeMaster, 1997).

Unlike belugas, narwhals appear to rely little on the North Water during winter. Instead, narwhals occur throughout the pack ice in the southern Baffin Bay and the southern Davis Strait down to 68°N (Dietz et al., 2001). Although this species may utilize leads or polynyas during winter, no clear areas of concentration have yet been found. Factors that affect the distribution and density of their prey (arctic cod, Greenland halibut and squid) would likely affect their migratory patterns and selected wintering grounds as well. During the autumn, narwhals move from their coastal summer habitat and head towards deeper water. Some individuals visit deep fjords, while others move to the edge of the continental shelf and slope in Baffin Bay. Here, over steep complex undersea terrain, narwhals may be focusing on deep-water cephalopod prey (Dietz et al., 2001). In November, narwhals from both Canada and Greenland converge in the northern part of the Davis Strait, an area where the shelf drops off abruptly and the water is 1000–1500 m deep. During winter, this area is completely covered with pack ice except for shifting cracks and leads. Narwhals remain and make some of the deepest dives ever recorded for a mammal (M.P. Heide-Jørgensen, pers. comm.).

The bowhead and minke whales (the latter discussed above: Antarctic) are the only baleen whales truly adapted to Arctic sea ice covered regions. Morphological adaptations of the bowhead include an elevated blowhole or rostrum for pushing through the ice to breathe (Fig. 8.3). Its migration is shorter than that of many other baleen whale species and is closely linked to climate-driven conditions of sea ice. Heavy ice or a prolonged ice season can delay the arrival of bowheads on their

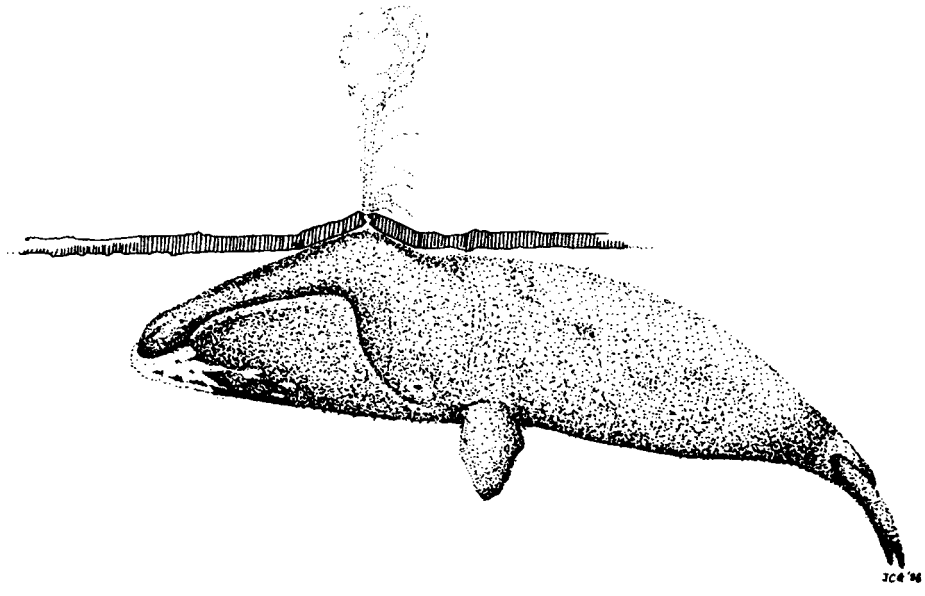

Fig. 8.3 Bowhead whale pushing upward through new ice in order to breathe. From George et al. (1989).

summer foraging grounds in the Arctic. Bowhead whales migrate northward through systems of leads during spring in order to forage on concentrations of Arctic copepods (e.g. *Calanus* sp.) or euphausiids during summer. Links between *Calanus* production and sea ice conditions are likely to have a major impact on bowhead whale foraging (Finley, 2001). For the bowhead population wintering in the eastern Canadian Arctic, their range includes Labrador, Davis Strait, and Hudson Strait; during summer, these whales occur in Baffin Bay, Foxe Basin, and west into Lancaster Sound and inlets of the Northwest Passage (Finley, 2001). Bowhead whales tend to remain farther south during seasons of heavy ice conditions. In winter they occur within the margin of the pack ice and in polynyas between 60° and 70°N. The shelter provided by the pack ice may enable bowheads to endure winter storms at high latitude, as well as provide protection from killer whales (Payne, 1995). During summer, bowhead whales off northern Alaska appear to select moderate ice cover over the continental slope (Moore et al., 2000); during autumn, bowheads select inner shelf waters during light and moderate ice conditions, but occur in deeper slope habitat in heavy ice conditions (Moore et al., 2000).

Changes in the thickness of ice and availability of leads affect the migratory paths of Arctic cetaceans. Although bowhead whales are able to break through sea ice (18 cm maximum thickness) in order to breathe (George et al., 1989), thicker and continuous multi-year ice can be a deterrent. By pushing up against the ice with their heads, in the area of the blowholes, they fracture the ice and generate a hummock through which to breathe (Fig. 8.3). It has been hypothesized that bowhead whales use sound to acoustically determine the thickness of ice in their migratory path, thereby avoiding regions where the ice is too thick for them to fracture. Despite these abilities, entrapments of bowheads and other Arctic cetacean species occur (Stirling et al., 1981). The possible importance of bowhead ice-breaking to air–sea heat exchange (e.g. George et al., 1989 observed 50–100 hummocks per km^2), sea ice dynamics and Arctic ecology, has not been examined.

Grey whales, as with other baleen whales, migrate to open waters of the northern Bering and Chukchi Seas to forage during summer, but unlike other whales, they feed on benthic infauna (especially ampelicid amphipods; Grebmeier & Barry, 1991). The seasonal extent of the sea ice therefore affects the length of time these whales can spend on preferred summer foraging grounds. In addition, complex linkages between the biophysical coupling of sea ice, ice-associated production, and carbon flux to the benthos, would be expected to impact the benthic organisms upon which grey whales depend for food. It is through such complex interactions that ultimately the effects of Arctic and sub-arctic atmospheric pressure patterns on regional weather and sea ice conditions could impact on the condition of grey whales and other benthic foragers, such as bearded seals and walruses.

8.3 The changing scene: global warming and implications for pagophilic species

Observations and predictions of climate change, as they relate to sea ice and the potential effects on Arctic marine mammals, have received recent consideration (Stirling & Derocher, 1993; Tynan & DeMaster, 1997; Stirling et al., 1999). Changes in the thickness and concentration of sea ice, as well as variability in the seasonal and spatial extent of ice cover, all have ecological consequences for mammals and seabirds. Such changes may produce species-specific alterations in demography, range and population size. For example, the loss of ice at the southern edge of the range of some species may reduce population size (e.g. polar bears in Hudson Bay), while the divergence of ice may broaden the northern boundary of other species' ranges (e.g. bearded seals; see Krajick, 2001), at least over the short term.

The loss of ice suitable for resting, moulting and breeding seals has a direct and immediate effect. Less easy to observe and evaluate are ecosystem changes in productivity, species composition and community structure that relate to changes in sea ice extent, volume and thickness. On the Bering Sea shelf, the duration and extent of the seasonal sea ice has important consequences for the timing and magnitude of the spring ice-edge bloom of phytoplankton, and consequently, the ensuing cascade of spring and summer productivity of middle and upper trophic levels. Similarly, in the Barents Sea, where more than 15 species of whales and seals forage, a high proportion of the plankton biomass is found near the ice edge and oceanic Polar Front (Sakshaug et al., 1994). In the high Arctic and Barents Sea, alteration of sea ice extent and structure is expected to affect arctic cod, a pivotal prey for many top trophics (see above) and one that preys on ice amphipods (such as *Parathemisto libellula*). Factors that affect the productivity and availability of ice-associated amphipods could therefore cascade up the Arctic food web to seabirds, cetaceans, ice seals and polar bears.

In western Hudson Bay a significant positive relationship exists between the time of sea ice break-up and the condition of adult polar bears (e.g. the earlier the break-up, the poorer is the condition of the bears; Stirling et al., 1999). This trend is in accord with rising spring temperatures for the period 1950 to 1990 and has been continuing since. It has been suggested that this region, which includes the southern edge of the bears' range, may show the earliest and largest impacts of global warming on polar bears (Tynan & DeMaster, 1997). Between 1981 and 1998, polar bears in this region have experienced a 15% decline in the average weight and number of cubs. As the sea ice in western Hudson Bay now breaks up, on average, 2 weeks earlier than it did 20 years ago, bears are forced to head for land by mid-July or earlier, a time when they are normally hunting seal pups on the ice (Stirling et al., 1999). Conversely, particularly heavy ice conditions, such as in the winters of 1973–74 and 1984–85 in the eastern Beaufort Sea, coincided with a decline in ringed seal pupping rate and consequently in polar bear numbers as well (Stirling & Lunn, 1997). Therefore, there appears to be an optimal range of sea ice conditions that

foster polar bear well being. Too little ice and the polar bears are unable to forage successfully on ice seals for long enough; too much winter and spring ice and the food web sustaining ice seals may be reduced as well as access to the seals themselves.

While consolidated pack ice has lower interannual spatial and seasonal variability, and is also associated with less productivity, divergent sea ice has higher interannual variability and greater productivity. Due to the immediate effect of ringed seal pupping rate on polar bear reproduction and cub survival, the polar bear is an excellent indicator species for changes in sea ice conditions and changes in the marine ecosystem generally (Stirling & Lunn, 1997).

The recent retreat of Arctic sea ice has had a dual effect on such avian species as black guillemot and others (e.g. horned puffin *Fratercula corniculata*, a species that frequents ice-free polar waters; Krajik, 2001, reporting data from G.J. Divoky). Initially the retreat encouraged northward extensions of range as the ice-free period lengthened sufficiently to include the long nesting period of these species. In particular the black guillemot then exploited the epontic prey in the under-ice habitat that was easily accessible nearby. Subsequently, however, continued warming has caused the sea ice to retreat so far away from limited suitable nesting habitats that it no longer is in range of the foraging birds, which must feed their chicks often enough that growth and development are ensured. As a result, reproductive success has declined and populations have begun to decline. Similarly, populations of ivory gulls are also declining as their sea ice foraging habitat has disappeared and moved farther away from nesting sites.

The effects of interannual and decadal shifts in atmospheric pressure patterns on sea ice are also reflected in top trophic levels of both northern and southern polar ecosystems. The Arctic Oscillation (AO) appears to have altered ocean circulation, ice drift and air temperatures in the Arctic during the early 1990s (Morison et al., 2000). The effects of atmospheric pressure systems and coupled with ocean response can be far reaching, such as:

- The significant correlation between the Southern Oscillation Index (SOI) and ice in the Bering Sea (Niebauer et al., 1999).
- The significant negative correlation between the El Niño Southern Oscillation (ENSO) and sea ice conditions in the Baffin Bay–Labrador Sea region (Wang et al., 1994).
- The link between monthly ENSO fluctuations and western Antarctic Peninsula air temperature and sea ice extent (Smith et al., 1996).

A number of correlations between marine mammal condition and the effects of large-scale atmospheric forcing on sea ice have been observed, but the mechanisms at the ecosystem level are often not well understood. During El Niño, the pupping rate of Weddell seals in McMurdo Sound (Ross Sea) is lower (Testa et al., 1991), as is the pup weaning mass of southern elephant seals at King George Island

(Bellingshausen Sea; Vergani et al., 2001) compared to non-ENSO years. Why these patterns exist is not known.

The Antarctic Circumpolar Wave (ACW) represents a system of coupled anomalies, including sea ice extent, pressure and wind, which propagate eastward around the periphery of the sea ice zone with a periodicity of 4–5 years (White & Peterson, 1996). The discovery of the ACW prompted a search for linkages between Antarctic biological time series and the ACW. Two seal species of the outer Antarctic pack ice (crabeater, leopard) exhibit quasi-cyclic 4–5-year patterns in their biology (Testa et al., 1991). These are in accord with ENSO, by which the ACW may be driven (Peterson & White, 1998). However, no formal test of the direct link between these seals' biology and the ACW itself has been undertaken. The effects of changes in sea ice extent on the productivity or availability of prey, and consequently on the condition of mammals and seabirds, are less well understood (Fraser et al., 1992). However, it is known that salps (a gelatinous organism that occurs in surface waters), which are a food of limited value to top trophic species, appear to dominate Antarctic pack ice communities during years of minimal ice concentration (Nicol & Allison, 1997). Conversely, krill, which is a key prey species for top trophics, exhibits high reproductive output during conditions of high winter sea ice concentration (Siegel & Loeb, 1995). Furthermore, winter sea ice also provides a source of food (e.g. ice algae) and under-ice refuge for krill (Schnack-Schiel, Chapter 7). Therefore, it might be expected that mammals and birds that inhabit the northern portion of the sea ice zone should benefit from years of higher winter ice concentration.

The two ice-obligate penguin species in the Australian–New Zealand sector of Antarctica (emperor and Adélie) have shown opposite population trajectories since the mid-1950s. The fast ice breeding emperor penguin population at Pointe Géologie declined during the 1970s (Barbraud & Weimerskirch, 2001) while the pack ice frequenting Adélie penguin on Ross Island increased in number through the same period (Wilson et al., 2001). The emperor penguin trends indicate increased mortality of males, which must recover from their winter time fasts that extend for 2 months while incubating eggs. Their nesting depends on stable fast ice and then access to food through the presence of polynyas nearby. How changes in sea ice may have affected them is not clear. The Adélie penguin, on the other hand, appears to be favoured by decreased sea ice extent during winter, at least initially. This allows the naïve juveniles an easier effort to forage effectively in the rich waters south of the Southern Boundary of the Antarctic Circumpolar Current (ACC). Extensive sea ice shifts them north of that boundary to unproductive waters. This pattern is evident on an interannual scale as the position of the outer sea ice boundary varies in accord with the SOI (and perhaps the ACW). Unfortunately, the sea ice record before 1974, when the first sea ice sensing satellite was launched, is non-existent. As a proxy for ice conditions during previous decades, however, numbers of penguins indicate that sea ice was more extensive during the 1950s and 1960s.

When winter ice consolidates, covering and restricting access to summer feeding

grounds in the Arctic, polynyas and leads associated with rich pelagic and benthic communities sustain populations of top trophics as noted above. However, the present ability of general circulation models to simulate changes in the size and productivity of these recurring, regional features is rather limited. The same is true for the Antarctic. Changes in the timing, size and subsequent ocean productivity in and adjacent to polynyas would have profound effects on polar marine birds and mammals.

In the future, researchers will be keeping a close eye on the extension and retreat of sea ice coupled to changes in weather and longer-term climate signals. In the meantime, compiling more information on the possible links between sea ice and the top trophics is a compelling area of research. Long-term monitoring of links between top trophics and ice-associated productivity and ecosystem structure is of vital importance. Without such monitoring, it is doubtful that meaningful assessments and predictions of climate-induced impacts on polar marine ecosystems will be achieved. Diverse and healthy polar marine ecosystems should be part of our world heritage.

Acknowledgements

We wish to thank C. Lydersen, J. George, and D. Nettleship for use of their graphics, which were originally published elsewhere. In part, DGA's time to prepare this chapter was funded by NSF-OPP grant 9814882. The Canadian Wildlife Service and Polar Continental Shelf Project have supported the long-term Arctic research of IS.

References

Ainley, D.G. (2002) *The Adélie Penguin: Bellwether of Climate Change*. Columbia University Press, New York.

Ainley, D.G., Fraser, W.R., Smith, W.O., Hopkins, T.L. & Torres, J.J. (1991) The structure of upper level pelagic food webs in the Antarctic: effect of phytoplankton distribution. *Journal of Marine Systems*, **2**, 111–122.

Ainley, D.G., Ribic, C.A. & Fraser, W.R. (1994) Ecological structure among migrant and resident seabirds of the Scotia–Weddell Confluence region. *Journal of Animal Ecology*, **63**, 347–364.

Ainley, D.G., Ribic, C.A. & Spear, L.B. (1993) Species-habitat relationships among Antarctic seabirds: a function of physical of biological factors. *Condor*, **95**, 806–816.

Barbraud, C. & Weimerskirch, H. (2001) Emperor penguins and climate change. *Nature*, **411**, 183–186.

Bester, M.N. & Odendaal, P.N. (2000) Abundance and distribution of Antarctic pack ice seals in the Weddell Sea. In: *Antarctic Ecosystems: Models for Wider Ecological Understanding*, (Eds W. Davison, C. Howard-Williams & P. Broady), pp. 51–55. The Caxton Press, Christchurch, New Zealand.

Bornemann, H., Kreyscher, M., Ramdohr, S., Martin, T., Carlini, A., Sellmann, L. & Plötz, J. (2000) Southern elephant seal movements and Antarctic sea ice. *Antarctic Science*, **12**, 3–15.

Bowen, W.D., Myers, R.A. & Hay, K. (1987) Abundance estimation of a dispersed, dynamic population: hooded seals (*Cystophora cristata*) in the Northwest Atlantic. *Canadian Journal of Fisheries and Aquatic Science*, **44**, 282–295.

Bradstreet, M.S.W (1980) Thick-billed murres and black guillemots in the Barrow Strait areas, NWT, during spring: diets and food availability along ice edges. *Canadian Journal of Zoology*, **58**, 2120–2140.

Brown, R.G.B. & Nettleship, D.N. (1981) The biological significance of polynyas to Arctic colonial seabirds. In: *Polynyas in the Canadian Arctic*, (Eds I. Stirling & H. Cleator), pp. 59–66. *Canadian Wildlife Service Occasional Paper*, **45**, Ottawa.

Brown, S.G. & Lockyer, C.H. (1984) Whales. In: *Antarctic Ecology*, Vol. 2, (Ed. R.M. Laws), pp. 717–781. Academic Press, London.

Burns, J.J. (1981) Bearded seal *Erignathus barbatus* Erxleben, 1777. In: *Handbook of Marine Mammals*, Vol. 2, (Eds S.H. Ridgway & R.J. Harrison), pp. 145–170. Academic Press, London.

Davis, C.S., Stirling, I. & Strobeck, C. (2000) Genetic diversity of Antarctic pack ice seals in relation to life history characteristics. In: *Antarctic Ecosystems: Models for Wider Ecological Understanding*, (Eds W. Davison, C. Howard-Williams & P. Broady), pp. 56–62. The Caxton Press, Christchurch, New Zealand.

Davis, R.W., Fuiman, L.A., Williams, T.M., Collier, S.O., Hagey, W.P., Kanatous, S.B., Kohin, S. & Horning, M. (1999) Hunting behavior of a marine mammal beneath the Antarctic fast ice. *Science*, **283**, 993–996.

Dietz, R., Heide-Jørgensen, M.P., Richard, P.R. & Acquarone, M. (2001) Summer and fall movements of narwhals (*Monodon monoceros*) from northeastern Baffin Island towards northern Davis Strait. *Arctic*, **54**, 244–261.

Digby, S.A. (1984) Remote sensing of drained ice areas around the breathing holes of ice-inhabiting seals. *Canadian Journal of Zoology*, **62**, 1011–1014.

Doidge, D.W. & Finley, K.J. (1993) Status of the Baffin Bay population of beluga, *Delphinapterus leucas*. *The Canadian Field Naturalist*, **107**, 533–546.

Eicken, H., Krouse, H.R., Kadko, D. & Perovich, D.K. (2002) Tracer studies of pathways and rates of meltwater transport through Arctic summer sea ice. *Journal of Geophysical Research* (in press).

Falk, K., Hjort, C., Andreasen, C., Christensen, K.D., Elander, M., Ericson, M., Kampp, K., Kristensen, R.M., Møbjerg, N., Møller, S. & Weslawski, J.M. (1997) Seabirds utilizing the Northeast Water polynya. *Journal of Marine Systems*, **10**, 47–65.

Fay, F.H. (1981) Walrus. In: *Handbook of Marine Mammals*, Vol. 1, (Eds S.H. Ridgeway & R.J. Harrison), pp. 1–23. Academic Press, London.

Fay, F.H. (1982) Ecology and biology of the Pacific walrus, *Odobenus rosmarus divergens* Illiger. *North American Fauna*, **74**, 1–279.

Ferguson, S.H., Taylor, M.K., Born, E.W., Rosing-Asvid, A. & Messier, F. (2001) Activity and movement patterns of polar bears inhabiting consolidated versus active pack ice. *Arctic*, **54**, 49–54.

Finley, K.J. (2001) Natural history and conservation of the Greenland whale, or bowhead, in the Northwest Atlantic. *Arctic*, **54**, 55–76.

Finley, K.J., Miller, G.W., Davis, R.A. & Koski, W.R. (1983) A distinctive large breeding population of ringed seals (*Phoca hispida*) inhabiting the Baffin Bay pack ice. *Arctic*, **36**, 162–173.

Fraser, W.R., Trivelpiece, W.Z., Ainley, D.G. & Trivelpiece, S.G. (1992) Increases in Antarctic penguin populations: reduced competition with whales or a loss of sea ice due to environmental warming? *Polar Biology*, **11**, 525–531.

Frost, K.J., Lowry, L.F., Gilbert, J.R. & Burns, J.J. (1988) *Ringed seal monitoring: relationships of distribution and abundance to habitat attributes and industrial activities*. Alaska Outer Continental Shelf Environmental Assessment Program, US Minerals Management Service, Department of the Interior, NOAA Project RU No. 667. National Oceanic and Atmospheric Administration, Anchorage, Alaska.

Gelatt, T.S. (2001) *Male reproductive success, relatedness, and the mating system of Weddell seals in McMurdo Sound, Antarctica*. PhD dissertation, University of Minnesota.

George, J.C., Clark, C., Carroll, G.M. & Ellison, W.T. (1989) Observations on the ice-breaking and ice navigation behavior of migrating bowhead whales (*Balaena mysticetus*) near Point Barrow, Alaska, spring 1985. *Arctic*, **42**, 24–30.

Gilchrist, H.G. & Robertson, G.J. (2000) Observations of marine birds and mammals wintering at polynyas and ice edges in the Belcher Islands, Nunavut, Canada. *Arctic*, **53**, 61–68.

Gjertz, I. & Lydersen, C. (1983) *Phoca hispida* pupping in the Svalbard area. *Fauna*, **36**, 65–67.

Gjertz, I. & Wiig, Ø. (1992) Feeding of walrus *Odobenus rosmarus* in Svalbard. *Polar Record*, **28**, 57–59.

Grebmeier, J.M. & Barry, J.P. (1991) The influence of oceanographic processes on pelagic–benthic coupling in polar regions: a benthic perspective. *Journal of Marine Systems*, **2**, 495–518.

Hammill, M.O., Kovacs, K.M. & Lydersen, C. (1994) Local movements by nursing bearded seal (*Erignathus barbatus*) pups in Kongsfjorden, Svalbard. *Polar Biology*, **14**, 569–570.

Hammill, M.O. & Smith, T.G. (1989) Factors affecting the distribution and abundance of ringed seal structures in Barrow Strait, Northwest Territories. *Canadian Journal of Zoology*, **67**, 2212–2219.

Haney, J.C. & MacDonald, S.D. (1995) Ivory gull (*Pagophila eburnea*). In: *The Birds of North America, No. 175*, (Eds A. Poole & F. Gill), 24pp. The Academy of Natural Sciences, Philadelphia, and The American Ornithologists' Union, Washington, D.C.

Harwood, L.A., Innes, S., Norton, P. & Kingsley, M.C.S. (1996) Distribution and abundance of beluga whales in the Mackenzie estuary, southeast Beaufort Sea, and west Amundsen Gulf during late July 1992. *Canadian Journal of Fisheries and Aquatic Science*, **53**, 2262–2273.

Harwood, L.A., Smith, T.G. & Melling, H. (2000) Variation in reproduction and body condition of the ringed seal (*Phoca hispida*) in Western Prince Albert Sound, NT, Canada, as assessed through a harvest-based sampling program. *Arctic*, **53**, 422–431.

Harwood, L.A. & Stirling, I. (1992) Distribution of ringed seals in the southeastern Beaufort Sea during late summer. *Canadian Journal of Zoology*, **70**, 891–900.

Heide-Jørgensen, M.P., Richard, P.R. & Rosing-Asvid, A. (1998) Dive patterns of belugas (*Delphinapterus leucas*) in waters near Eastern Devon Island. *Arctic*, **51**, 17–26.

Holt, B. & Digby, S.A. (1985) Processes and imagery of first-year fast sea ice during the melt season. *Journal of Geophysical Research*, **90**, 5045–5062.

Hopkins, T.L., Ainley, D.G., Torres, J.J. & Landcraft, T.M. (1993) Trophic structure in open waters of the marginal ice zone in the Scotia–Weddell confluence region during spring (1983). *Polar Biology*, **13**, 389–397.

Ichii, T., Shinohara, N., Fujise, Y., Nishiwaki, S. & Matsuoka, K. (1998) Interannual changes in body fat condition index of minke whales in the Antarctic. *Marine Ecology Progress Series*, **175**, 1–12.

Kingsley, M.C.S., Stirling, I. & Calvert, W. (1985) The distribution and abundance of seals in the Canadian High Arctic, 1980–1982. *Canadian Journal of Fisheries and Aquatic Science*, **42**, 1189–1210.

Krajick, K. (2001) Arctic life, on thin ice. *Science*, **291**, 424–425.

Laws, R.M. (1984) Seals. In: *Antarctic Ecology*, Vol. 2, (Ed. R.M. Laws), pp. 621–715. Academic Press, London.

Lydersen, C. & Kovacs, K.M. (1999) Behaviour and energetics of ice-breeding, North Atlantic phocid seals during the lactation period. *Marine Ecology Progress Series*, **187**, 265–281.

Martin, A.R. & Smith, T.G. (1999) Strategy and capability of wild belugas *Delphinapterus leucas* during deep, benthic diving. *Canadian Journal of Zoology*, **77**, 1783–1793.

Massom, R.A., Harris, P.T., Michael, K.J. & Potter, M.J. (1998) The distribution and formative processes of latent-heat polynyas in East Antarctica. *Annals of Glaciology*, **27**, 420–426.

Moore, S.E., DeMaster, D.P. & Dayton, P.K. (2000) Cetacean habitat selection in the Alaskan Arctic during summer and autumn. *Arctic*, **53**, 432–447.

Morison, J., Aagaard, K. & Steele, M. (2000) Recent environmental changes in the Arctic: a review. *Arctic*, **53**, 359–371.

Nicol, S. & Allison, I. (1997) The frozen skin of the Southern Ocean. *American Scientist*, **85**, 426–439.

Niebauer, H.J., Bond, N.A., Yakunin, L.P. & Plotnikov, V.V. (1999) An update on the climatology and sea ice of the Bering Sea. In: *Dynamics of the Bering Sea: A Summary of Physical, Chemical and Biological Characteristics and a Synopsis of Research on the Bering Sea*, (Eds T.R. Loughlin & K. Ohtani), pp. 29–59. North Pacific Marine Science Organization (PICES), University of Alaska Sea Grant, Fairbanks, Alaska.

Payne, R.S. (1995) *Among Whales*. Scribner, New York.

Petersen, M.R., Larned, W.W. & Douglas, D.C. (1999) At-sea distribution of spectacled eiders: a 120-year-old mystery solved. *The Auk*, **116**, 1009–1020.

Peterson, R.G. & White, W.B. (1998) Slow teleconnections linking the Antarctic Circumpolar Oceanic Wave with the tropical El Niño-Southern Oscillation. *Journal of Geophysical Research*, **103**, 24573–24583.

Plötz, J., Bornemann, H., Knust, R., Schröder, A. & Bester, M. (2001) Foraging behaviour of Weddell seals, and its ecological implications. *Polar Biology*, **24**, 901–909.

Ribic, C.A. & Ainley, D.G. (1988/89) Constancy of seabird species assemblages: an exploratory look. *Biological Oceanography*, **6**, 175–202.

Ribic, C.A., Ainley, D.G. & Fraser, W.R. (1991) Habitat selection by marine mammals in the marginal ice zone. *Antarctic Science*, **3**, 181–186.

Richard, P.R., Heide-Jørgensen, M.P. & St. Aubin, D. (1998a) Fall movements of belugas (*Delphinapterus leucas*) with satellite-linked transmitters in Lancaster Sound, Jones Sound, and Northern Baffin Bay. *Arctic*, **51**, 5–16.

Richard, P.R., Heide-Jørgensen, M.P., Orr, J.R., Dietz, R. & Smith, T.G. (2001a) Summer and autumn movements and habitat use by belugas in the Canadian High Arctic and adjacent areas. *Arctic*, **54**, 207–222.

Richard, P.R., Martin, A.R. & Orr, J.R. (2001b) Summer and autumn movements of belugas of the eastern Beaufort Sea stock. *Arctic*, **54**, 223–226.

Richard, P.R., Orr, J.R., Dietz, R. & Dueck, L. (1998b) Sightings of belugas and other marine mammals in the North Water, late March 1993. *Arctic*, **51**, 1–4.

Sakshaug, E., Bjørge, A., Gulliksen, B., Loeng, H. & Mehlum, F. (1994) Structure, biomass distribution, and energetics of the pelagic ecosystem in the Barents Sea: a synopsis. *Polar Biology*, **14**, 405–411.

Schledermann, P. (1980) Polynyas and prehistoric settlement patterns. *Arctic*, **33**, 292–302.

Sergeant, D.E. (1976) Research on hooded seals *Cystophora cristata* Erxleben in 1976. *ICNAF Research Document* 76/126, Ser. No. 4012. International Commission for the NorthWest Atlantic Fisheries, Canada.

Siegel, V. & Loeb, V. (1995) Recruitment of Antarctic krill *Euphausia superba* and possible causes for its variability. *Marine Ecology Progress Series*, **123**, 45–56.

Siniff, D.B. & Bengtson, J.L. (1977) Observations and hypotheses concerning interactions among crabeater seals, leopard seals, and killer whales. *Journal of Mammalogy*, **58**, 414–416.

Siniff, D.B., Stirling, I., Bengtson, J.L. & Reichle, R.A. (1979) Social and reproductive behavior of crabeater seals (*Lobodon carcinophagus*) during the austral spring. *Canadian Journal of Zoology*, **57**, 2243–2255.

Sjare, B. & Stirling, I. (1996) The breeding behavior of Atlantic walruses, *Odobenus rosmarus rosmarus*, in the Canadian High Arctic. *Canadian Journal of Zoology*, **74**, 897–911.

Smith, R.C., Stammerjohn, S.E. & Baker, K.S. (1996) Surface air temperature variations in the western Antarctic Peninsula region. *Antarctic Research Series*, **70**, 105–121.

Smith, T.G. & Harwood, L.A. (2001) Observations of neonate ringed seals, *Phoca hispida*, after early break-up of the sea ice in Prince Albert Sound, Northwest Territories, Canada, spring 1998. *Polar Biology*, **24**, 215–219.

Smith, T.G. & Stirling, I. (1975) The breeding habitat of the ringed seal (*Phoca hispida*): the birth lair and associated structures. *Canadian Journal of Zoology*, **53**, 1297–1305.

Stewart, B.S., Yochem, P.K., Gelatt, T.S. & Siniff, D.B. (2000) First-year movements of Weddell seal pups in the Western Ross Sea, Antarctica. In: *Antarctic Ecosystems: Models for Wider Ecological Understanding*, (Eds W. Davison, C. Howard-Williams & P. Broady), pp. 71–76. The Caxton Press, Christchurch, New Zealand.

Stirling, I. (1969) Tooth wear as a mortality factor in the Weddell seal (*Leptonychotes weddellii)*. *Journal of Mammalogy*, **50**, 559–565.

Stirling, I. (1997) The importance of polynyas, ice edges, and leads to marine mammals and birds. *Journal of Marine Systems*, **10**, 9–21.

Stirling, I., Archibald, W.R. & DeMaster, D. (1977) Distribution and abundance of seals in the eastern Beaufort Sea. *Journal of the Fisheries Research Board of Canada*, **34**, 976–988.

Stirling, I., Cleator, H. & Smith, T.G. (1981) Marine mammals. In: *Polynyas in the Canadian Arctic*, (Eds I. Stirling & H. Cleator), pp. 45–58. *Canadian Wildlife Service Occasional Paper*, **45**, Ottawa.

Stirling, I. & Derocher, A.E. (1993) Possible impacts of climatic warming on polar bears. *Arctic*, **46**, 240–245.

Stirling, I. & Lunn, N.J. (1997) Environmental fluctuations in arctic marine ecosystems as reflected by variability in reproduction of polar bears and ringed seals. In: *Ecology of Arctic Environments*, (Eds S.J. Woodin & M. Marquiss), pp. 167–181. Blackwell Science, Oxford.

Stirling, I., Lunn, N.J. & Iacozza, J. (1999) Long-term trends in the population ecology of polar bears in western Hudson Bay in relation to climatic change. *Arctic*, **52**, 294–306.

Suydam, R.S., Lowry, L.F., Frost, K.J., O'Corry-Crowe, G.M. & Pikok, D., Jr (2001) Satellite tracking of eastern Chukchi Sea beluga whales into the Arctic Ocean. *Arctic*, **54**, 237–243.

Taylor, R.H. & Wilson, P.R. (1990) Recent increase and southern expansion of Adélie penguin populations in the Ross Sea, Antarctica, related to climate warming. *New Zealand Journal of Zoology*, **14**, 25–29.

Testa, J.W. (1994) Over-winter movements and diving behavior of female Weddell seals (*Leptonychotes weddellii*) in the southwestern Ross Sea, Antarctica. *Canadian Journal of Zoology*, **72**, 1700–1710.

Testa, J.W., Oehlert, G., Ainley, D.G., Bengtson, J.L., Siniff, D.B., Laws, R.M. & Rounsevell, D. (1991) Temporal variability in Antarctic marine ecosystems: periodic fluctuations in the phocid seals. *Canadian Journal of Fisheries and Aquatic Science*, **48**, 631–639.

Tynan, C.T. (1997) Cetacean distributions and oceanographic features near the Kerguelen Plateau. *Geophysical Research Letters*, **24**, 2793–2796.

Tynan, C.T. (1998) Ecological importance of the Southern Boundary of the Antarctic Circumpolar Current. *Nature*, **392**, 708–710.

Tynan, C.T. & DeMaster, D.P. (1997) Observations and predictions of Arctic climatic change: potential effects on marine mammals. *Arctic*, **50**, 308–322.

Vergani, D.F., Stanganelli, Z.B. & Bilenca, D. (2001) Weaning mass variation of southern elephant seals at King George Island and its possible relationships with 'El Niño' and 'La Niña' events. *Antarctic Science*, **13**, 37–40.

Vinje, T. & Kvambekk, Å.S. (1991) Barents Sea drift ice characteristics. *Polar Research*, **10**, 59–68.

Wang, J., Mysak, L.A. & Ingram, R.G. (1994) Interannual variability of sea-ice cover in Hudson Bay, Baffin Bay and the Labrador Sea. *Atmosphere–Ocean*, **32**, 421–447.

Welch, H.E., Bergmann, M.A., Siferd, T.D., Martin, K.A., Curtis, M.F., Crawford, R.E., Conover, R.J. & Hop, H. (1992) Energy flow through the marine ecosystem of the Lancaster Sound region, arctic Canada. *Arctic*, **45**, 343–357.

White, W.B. & Peterson, R.G. (1996) An Antarctic circumpolar wave in surface pressure, wind, temperature, and sea-ice extent. *Nature*, **380**, 699–702.

Wiig, Ø., Derocher, A.E. & Belikov, S.E. (1999) Ringed seal (*Phoca hispida*) breeding in the drifting pack ice of the Barents Sea. *Marine Mammal Science*, **15**, 595–598.

Wiig, Ø., Gjertz, I. & Griffiths, D. (1996) Migration of walruses (*Odobenus rosmarus*) in the Svalbard and Franz Josef Land area. *Journal of Zoology (London)*, **238**, 769–784.

Wiig, Ø. & Isaksen, K. (1995) Seasonal distribution of harbour seals, bearded seals, white whales and polar bears in the Barents Sea. *Norsk Polarinstitutt Meddelelser*, **136**, 47–59.

Wilson, P.R., Ainley, D.G., Nur, N., Jacobs, S.S., Barton, K.J., Ballard, G. & Comiso, J.C. (2001) Adélie penguin population change in the Pacific sector of Antarctica: relation to sea-ice extent and the Antarctic Circumpolar Current. *Marine Ecology Progress Series*, **213**, 301–309.

Chapter 9

Biogeochemistry of Sea Ice

David N. Thomas and Stathis Papadimitriou

9.1 Introduction

The study of the chemistry of the oceans has been at the forefront of oceanographic endeavours ever since the first expeditions took their first water samples. During the past 50 years, there have been dramatic advances in the suite of analytical tools available for measuring dissolved constituents down to trace levels. Marine chemists have readily adopted these tools, although often considerable effort has had to be expended in adapting methodologies to the very pertinent problem of working in a highly saline matrix.

In the past 25 years the rapid advances in our knowledge of the chemistry of the marine environment have been paralleled by equally dramatic advances in our appreciation of the dominant biological processes of the open oceans and coastal waters. Among the most far-reaching developments has been our increased understanding of the smallest organisms, such as viruses, bacteria, micro-algae and protozoans, and the complex interactions within this microbial network. It has been the harnessing of state-of-the-art analytical methodologies, including flow cytometry and molecular techniques, that has enabled the biologists to unravel the complex growth patterns and interactions at the microscopic level.

Organisms are greatly influenced by the chemistry of the medium surrounding them and have tolerance limits towards individual chemical constituents within which they are physiologically viable, and within which growth and reproduction can take place. For some organisms, these limits will be wide, while others will exhibit a very narrow tolerance of changes in the chemical environment to which they are exposed. However, it is also clear that the biology of the oceans, in particular the microbiology, is driving much of the chemistry measured by the chemists. This realization has led to an ever increasingly closer union between biologists and chemists in their study of the oceans, the dynamics of biology and elemental flow between the living and non-living reservoirs.

The basis of much of the life in the oceans is the harvest of energy from sunlight and the fixation of carbon into biomass by phototrophic organisms through photosynthesis or primary production (Arrigo, Chapter 5). Just as the grasslands in terrestrial systems, the aquatic primary producers, predominantly the phyto-

plankton, are the food for grazing organisms. Primary production can only take place in that part of the water column in which light penetrates, and therefore is generally restricted to the top 50 m of the ocean (euphotic zone). The fate of the biology from the upper ocean is ultimately that it is recycled through microbial transformations, or that it sinks to the sediments below. Only a very small fraction of the primary production in the euphotic zone eventually becomes incorporated into the sediments, and an even smaller amount escapes recycling by benthic organisms within the upper sediment layers and is buried into the sediments. This buried organic matter that originates in the upper ocean is nevertheless sufficient to provide the geologists with the tools by which they can reconstruct detailed descriptions of changes in environmental constraints over time.

The dominant abiotic conditions prevailing at the time the organisms grow result in particular biochemical signatures being developed within those organisms. On the other hand particular abiotic conditions may instead select for particular species or groups of species within each organism grouping. Preservation of these organisms and their biochemical signatures within the sediments is a large study area for both geologists and geochemists alike, but the fact that these characteristics are ultimately tied with metabolism has resulted in 'biogeochemistry' becoming a leading field of research over the past decade or so. The term ideally describes the multidisciplinary approach that is needed to fully understand the complexity of the chemistry and biology in the oceans, and the implications for the geological record.

We have been studying the biology of sea ice since the mid-19th century, and in earnest in the past 50 years (Dieckmann & Hellmer, Chapter 1). The complexity of the sea ice microbial network, although not fully appreciated, is well studied (Lizotte, Chapter 6), as are the implications for the wider ecosystem dynamics (Arrigo, Chapter 5; Schnack-Schiel, Chapter 7; Ainley et al., Chapter 8). The chemical environment has only really been studied in terms that are pertinent to the biogeochemical processes within the ice since the early 1980s, and in any comprehensive way since the 1990s (Thomas & Dieckmann, 2002a). Despite the apparent lag behind other disciplines interested in sea ice, the biogeochemistry of sea ice is a rapidly growing research area, unifying biologists, chemists and geologists with a common goal. Naturally their research is underpinned by, and cannot advance without, the complementary research of the physicists: ultimately it is the unique physical structure and processes that determine the chemistry and biology of the sea ice matrix.

9.2 Sea ice chemistry

Abiotic modification of seawater chemistry during freezing

Eicken (Chapter 2) has described in detail the phase relationships within sea ice and the relationships between freezing, temperature and the major salts that are dissolved within sea water. The major chemical transformation within sea ice is the

dramatic change in the ionic composition and ionic strength of the solution expelled from the ice crystal matrix. This results in brine inclusions in sea ice with higher than average seawater (~ 35 g salt kg^{-1}) salinity. The physical concentration of major and minor dissolved species in the brine pockets of sea ice has direct bearing on thermodynamic equilibria. Salinity and temperature exert control on the thermodynamic parameters that describe the solubility of gases (e.g. CO_2 and O_2) and mineral salts (including carbonate minerals), as well as the speciation in solution of the dissolved weak acids and bases, such as carbonic acid, which buffer sea water and influence its pH. The relationship between these parameters is well established in the temperature range of 0 to 45°C and in the salinity range of 0 to 45 (Garcia & Gordon, 1992; Millero, 1995), while a wide range of experimental and field data exists for hypersaline solutions (salinity >45) at 25°C, or higher, from seawater evaporation systems (Lazar et al., 1983; Sherwood et al., 1991; Lazar & Erez, 1992; Barkan et al., 2001; Millero et al., 2002).

Studies in hypersaline solutions derived from the evaporation of sea water at 25°C (Lazar et al., 1983) have shown an abiotic drop in pH with increasing ionic strength. Further, existing thermodynamic relationships indicate that the solubility of gases in sea water at equilibrium with air increases as temperature drops, while the increase in salinity has the opposite effect, i.e. decreased gas solubility. In the absence of biology, the combined effect on gas solubility during sea ice conditions will depend on the relative change of temperature and salinity. For example, a comparatively large salinity increase will lead to a net decrease in gas solubility. Superimposed on the thermodynamic trend will be the physical concentration of dissolved gases as a result of expulsion of solution from the forming ice matrix, leading to increased concentration of dissolved gas relative to that at thermodynamic equilibrium of the brine with air (i.e. supersaturation). Consequent on the concentration of dissolved gases above air saturation during freezing is the nucleation of gas bubbles and their entrapment within the ice matrix, as has been demonstrated in experimental low ionic strength media (Killawee et al., 1998). The degassing of natural solutions during freezing and the composition of gas in bubbles trapped in ice is an area of intense interest because of its direct implications for measurements of past climatic parameters in ice cores.

To date there have been very few studies to measure the total gas content and gas composition of sea ice. Tison et al. (2002) review what is currently known about major gas inclusions found in sea ice in the absence of biological transformation. Existing measurements range from 2 to 25 ml of total (gaseous + dissolved) gas per kilogram of ice, and its composition tends to reflect origin from sea water saturated with air. However, there is significant variability in this data, especially considering the concentrations of O_2 and CO_2. A considerable amount of gas will be incorporated into sea ice as bubbles during ice formation especially in turbulent water conditions (Killawee et al., 1998; Mock et al., 2002; Tison et al., 2002). Additionally, the decrease in gas solubility with increasing salinity results in degassing of sea ice as it gets colder and older, with accumulation of total gas within the brine, subsequent

migration into gas bubbles (degassing) and ultimate release of the gaseous component to the atmosphere above or in the underlying water (Mock et al., 2002). The relationship between salinity and O_2 (and presumably other gases) found in the work of Mock et al. (2002) and Glud et al. (2002) indicates that O_2 responds similarly to solutes in sea water that are conservatively expelled in relation to temperature and salinity changes within the ice matrix. To date relevant measurements, made in artificial sea ice for O_2, indicate that brine released from sea ice tends to be supersaturated with O_2, whereas melting ice is undersaturated. Glud et al. (2002) speculate that the O_2 depletion in thawing ice can be so low that favourable conditions for anaerobic bacteria to grow may develop, with anoxic processes, such as sulphate reduction and denitrification, possibly occurring within the ice matrix. Petri & Imhoff (2001) report anoxygenic phototrophic purple sulphur bacteria from horizons in the inner parts of ice cores from the Baltic Sea, a good indication that oxygen deficient or anoxic zones are present within the ice. It is an intriguing concept that anaerobic processes may be taking place within the top metre or so over many millions of square kilometres of ocean.

Similarly to dissolved gases, thermodynamic constraints on mineral solubility coupled with the physical concentration of their ionic species in the expelled solution can lead to precipitation of minerals during freezing of sea water. The state of saturation of a solution with respect to a mineral $[A_xB_y]$ is commonly described by the dimensionless saturation index, Ω (after Berner, 1980):

$$\Omega = \frac{\mathrm{ICP}}{K_c}, \qquad \text{(Equation 9.1)}$$

where $\mathrm{ICP} = [A]^x\,[B]^y$, the actual ion concentration product (KP) in the given solution, and K_c = the equilibrium ion concentration product, i.e. the ICP of the solution at thermodynamic equilibrium with the mineral phase, which is a function of the salinity and temperature (as well as pressure) of the solution (Millero, 1995). Once K_c is exceeded by the ICP of the solution ($\Omega >> 1$), crystals will begin to nucleate, and the ions will precipitate out of solution as an authigenic mineral phase. A suite of mineral phases is predicted to precipitate at the low temperatures encountered during sea ice conditions (see Eicken, Chapter 2), with carbonate minerals, such as calcite and aragonite, precipitating at -1.8°C, sodium sulphate at -8.2°C, calcium sulphate at -10°C and sodium chloride at -22°C (Eicken, Chapter 2). While carbonate mineral precipitation has been documented in ice derived from low ionic strength media (Killawee et al., 1998, and references therein), there is little conclusive evidence for the precipitation of these, or other, salts in natural sea ice (Anderson & Jones, 1985; Gleitz, 1995; Günther et al., 1999; Anderson, 2001). At this stage, extrapolation of known occurrences of authigenic cryogenic mineral precipitates does not appear to extend to sea ice conditions, possibly due to the climatic history to which the sea ice is exposed and, also, as a result of the extent of biological activity within sea ice. Further investigation into

this aspect of the physical chemistry of sea ice is clearly required to document the absence of mineral authigenesis despite favourable thermodynamic conditions in sea ice, and, if it occurs as shown in other glacial systems (Killawee et al., 1998), to examine the fate of the precipitates as sea ice ages.

Available observations of gas content and composition, and mineral precipitation within sea ice have often deviated from predictions based on theoretical solubility constants. This discrepancy may be because sea ice rarely forms and grows under constant abiotic forces but is rather a historical record of a large number of diverse climatic conditions. To complicate matters further, there is also an overriding dissolved gas signature in the ice due to the biological production and/or consumption of gases such as O_2 and CO_2 (see below). This is because most of the available field observations are spot measurements taken during, or directly after, periods of high biological activity within the sea ice. Lastly, in many sea ice settings, there can be conditions conducive to solute exchange between the ice matrix and the sea water and, hence, to divergence of the sea ice chemistry from theoretical predictions.

As described by Eicken (1992; Chapter 2), throughout a single ice floe the ice is characterized by large temporal and spatial gradients of brine channel volume, temperature and salinity. These gradients in the major physical–chemical parameters are reflected in corresponding gradients in the chemical composition of the sea ice, which can lead to diffusive migration of dissolved species and their exchange with sea water. At the margins of ice floes, or in under-ice accumulations of platelet ice, there is the possibility for sea water exchange and, therefore, replenishment of biologically important dissolved gases and inorganic nutrients. Also, in young sea ice, or in warm and/or rotten porous ice, the interior of ice floes is only rarely isolated from the influence of sea water exchange. In these cases, the exchange of solutes between sea ice and sea water will be limited by the constraints of ion diffusion across diffusive boundary layers similar to those commonly described at the sediment–water interface and only recently studied at the sea–ice interface (O_2 micro-sensor studies; Rysgaard et al., 2001; Mock et al., 2002). It is only in older consolidated sea ice, especially at low ambient temperatures, that brine channel systems become isolated and can be regarded as closed chemical environments. This compromises issues such as categorization and chemical classification for various ice types or ice ages (Weeks & Ackley, 1982; Meese, 1989; Dieckmann et al., 1991).

9.3 The influence of biological processes on the dissolved gases of sea ice

Several researchers have looked at the effects on sea ice chemistry of the high standing stocks of sea ice algae and the correspondingly high rates of photosynthesis (O_2-producing, CO_2-consuming) and associated high rates of heterotrophic respiration (O_2-consuming, CO_2-producing). It is important to note that algae both photosynthesize and respire, while heterotrophic bacteria and grazers (including

protozoans and metazoans) only respire. The vast standing stocks of algae and, at times, of bacteria and grazers, have the potential for completely altering the gaseous composition predicted under abiotic conditions. The limited existing data on dissolved gases in sea ice brine and platelet ice systems show that where high primary production and concomitant accumulation of large algal standing stocks have occurred, the brine is characterized by substantial reductions in total dissolved inorganic carbon (ΣCO_2) and exhaustion of dissolved CO_2, highly alkaline pH, with values up to 10, and O_2 supersaturation (Gleitz et al., 1995; Gleitz et al., 1996a; Günther et al., 1999; Thomas et al., 2001b). Such depletion in ΣCO_2 and dissolved CO_2, and accumulation of O_2, all indicate that photosynthetic activity by the algae can be in excess of the net respiration by all of the organisms within the ice. Naturally such a relationship can only hold true at times of the year when significant photosynthesis and growth of the algal component of the ice microbial network is taking place. If heavy grazing activity occurs, or there is mass mortality of the algae with an increasing growth in bacterial metabolism, this trend will not be maintained but, in fact, will be reversed. Likewise in winter, or in thick ice where light conditions for photosynthesis are poor, it is plausible to speculate that the biological assemblages will tend towards being net heterotrophic and the scenario postulated by Gleitz et al. (1995) will not hold. However, to date this can only remain a speculation since the relevant data do not exist. The measurements made to date have only been conducted in spring or summer ice, where active algal growth was clearly taking place. There is a clear need for similar measurements to be made at times of the year when the dominant biological processes turn from being net phototrophic to net heterotrophic.

The possibility that sea ice algae switch from photoautotrophy to heterotrophy as a means for winter survival has been postulated in the past (Palmisano & Sullivan, 1985; Rivkin & Putt, 1987). Zaslavskaia et al. (2001) have shown that all the necessary activities for glucose metabolism exist in certain diatom cells, and the potential to transform from obligate photoautotrophy to full heterotrophy can be achieved. Whether a switch to heterotrophy by sea ice algae is possible *in situ* is still open to much speculation. However, if a switch in algal metabolism occurs, especially by large standing crops often found in sea ice, the O_2 and ΣCO_2 balance within the sea ice will be altered significantly in winter.

Sea ice and high oxygen concentrations

Low CO_2 conditions, although rare, can occur in sea water after periods of dense phytoplankton blooms. In contrast, situations where there is supersaturation with O_2 (hyperoxia) are seldom found in marine systems (Raven et al., 1994). Although in itself O_2 is not toxic, potentially harmful reactive oxygen species such as hydrogen peroxide and hydroxyl radicals may accumulate at very high levels of O_2 (Vincent & Roy, 1983; Raven, 1991; Prézelin et al., 1998). Toxic photochemical products are also produced by the interaction of UV-B radiation, O_2 and certain organic

molecules. Little is known about how sea ice organisms cope with oxidative stress, but isolated sea ice diatoms have been shown to have high activities of protective antioxidative enzymes, such as catalase, glutathione peroxidase and glutathione reductase (Schriek, 2000). As discussed elsewhere by Lizotte (Chapter 5) and below, there can be a large production of dimethylsulphoniopropionate (DMSP) and its derivative dimethyl sulphide (DMS) in sea ice. Sunda et al. (2002) have shown that various breakdown products of DMSP readily scavenge hydroxyl radicals and other reactive oxygen species. Thus the high concentrations of DMSP/DMS within the sea ice may therefore serve as an antioxidant system, which Sunda et al. (2002) speculate may be regulated by the enzymatic cleavage of DMSP.

Oxygen is also a competitive inhibitor of the enzymatic CO_2 carboxylation by ribulose bisphosphate carboxylase/oxygenase (RUBISCO), the key enzyme in photosynthetic carbon assimilation by algae (Arrigo, Chapter 5). To suppress the oxygenase activity of the enzyme, many algal species have carbon-concentrating mechanisms (CCM), thereby ensuring that there is a high supply of dissolved inorganic carbon in the form of HCO_3^- at the RUBISCO site within the cell. Although a CCM has been observed in some sea ice diatoms, it is not found in all algae and, hence, will be an important feature for those species exposed to low external CO_2 concentrations, possibly providing a competitive advantage over those species without such mechanism (Gleitz et al., 1996b; Mitchel & Beardell, 1996).

Photosynthetic quotient

A measure of carbon metabolism and photosynthetic performance within a biological assemblage is the photosynthetic quotient, PQ (PQ = moles O_2 produced/moles of CO_2 fixed). Photosynthetic organisms growing under nutrient replete conditions tend to exhibit PQs between 1.0 and 1.4. The relative proportions of O_2 and CO_2 found within a closed sea ice matrix will therefore provide a record of the dominant carbon metabolism. In the few studies that have examined both O_2 and ΣCO_2 concentrations in sea ice, the calculated PQs tend to fall within a range of 1.2 to 1.4, therefore well within the 'typical range' (Gleitz et al., 1995; Günther et al., 1999; Glud et al., 2002). This demonstrates that generally in sea ice photosynthetic activity and carbon assimilation are the driving forces in determining the dissolved gas composition within the ice. These measurements have been made over a wide range of ice types and biological standing stocks but are biased towards periods of significant algal growth. As with most of the parameters discussed in this chapter, there is an obvious lack of data from times of the year when switches in metabolism from net photoautrophy to heterotrophy may significantly alter such chemical signatures.

Stable carbon isotopes and restricted gas exchange in sea ice

Another method, which has been used to trace metabolic processes, is the measurement of stable carbon isotopes, ^{12}C and ^{13}C, at their natural abundance level.

Photosynthetic carbon assimilation results in discrimination against ^{13}C, with the largest biological isotope effect occurring at the RUBISCO site within the cell (Burkhardt et al., 1999). As a result, the produced biomass becomes enriched in ^{12}C and the remaining ΣCO_2 pool becomes relatively enriched in ^{13}C. This is reflected in their stable isotope ratio, which is commonly reported on a per mil basis in the δ notation relative to the international standard Vienna Pee Dee Belemnite (VPDB) as $\delta^{13}C = 1000\,[(R/R_{VPDB}) - 1]$, with $R = {}^{13}C/{}^{12}C$, negative values indicating ^{12}C enrichment and positive values indicating ^{13}C enrichment. The isotope effect attributable to RUBISCO is *ca.* $-27‰$ in photosynthetic algae (Burkhardt et al., 1999). In other words, the RUBISCO effect alone will result in a $\delta^{13}C$ of the photosynthetically produced organic carbon (hereafter, $\delta^{13}C_{POC}$) that is more enriched in ^{12}C (i.e. isotopically lighter) than the CO_2 available for assimilation by an equivalent amount. This can be observed during growth in CO_2-replete conditions. However, the overall (net) biological isotope fractionation during photosynthesis and, hence, the final $\delta^{13}C_{POC}$ are a complex function of a number of factors, such as the dissolved CO_2 concentration, the type of carboxylating enzyme, passive and/or active dissolved inorganic carbon transport into the cell, growth rate, cell size and cell geometry (Dehairs et al., 1997; Burkhardt et al., 1999). The above factors conspire to reduce the RUBISCO isotope effect during photosynthesis close to 0‰, with the $\delta^{13}C_{POC}$ essentially reflecting the isotopic composition of the source (CO_2). This can occur in CO_2-limiting conditions, such as those imposed by high growth rates and, hence, high CO_2 demand, with the $\delta^{13}C_{POC}$ being isotopically less enriched in ^{12}C than predicted from the RUBISCO effect alone. By comparison, the isotope effect during biological respiration is minimal, with the CO_2 produced during this process having the same stable isotope ratio as that of the bulk organic carbon respired.

The restricted CO_2 exchange with the external sea water combined with high rates of algal growth results in depletion of ΣCO_2 concentration in sea ice. This is likely to be compounded by the initial expulsion of CO_2 during the consolidation of the ice as discussed above. Existing measurements indicate coupling of elemental depletion with isotopic enrichment in ^{13}C of the ΣCO_2 pool in sea ice, indicative of the photosynthetic isotope effect (Gleitz et al., 1996a; Gibson et al., 1999; Thomas et al., 2001a; Kennedy et al., 2002). In general, values of open ocean particulate organic carbon ($\delta^{13}C_{POC}$) from polar latitudes range from $-21‰$ to $-30‰$ (see Kennedy et al., 2002). In contrast, $\delta^{13}C_{POC}$ values up to $-8‰$ have been measured in samples from sea ice habitats, consistent with the hypothesis that these samples represent algal populations that grew in a CO_2-limiting environment (Fischer, 1991; Rau et al., 1991; Dunbar & Leventer, 1992; McMinn et al., 1999; Thomas et al., 2001b; Kennedy et al., 2002). Several of these studies concluded that high algal biomass with the most ^{13}C-enriched values occurred in the sea ice habitats with maximal degree of limitation of CO_2 exchange with the external sea water. However, the work of Kennedy et al. (2002) has shown that this relationship does not necessary apply, especially because some of the highest algal standing stocks in sea ice are associated with

mainly semi-enclosed rather than closed systems, such that replenishment of nutrients, in particular dissolved inorganic carbon and nitrate, is possible. Due to methodological problems in sampling brine, there have been only very few measurements of the stable carbon isotopic composition of total dissolved inorganic carbon ($\delta^{13}C_{DIC}$) from sea ice. In the most comprehensive study to date in which these measurements have been made, Kennedy et al. (2002) showed that variations in $\delta^{13}C_{DIC}$ were commensurate with the changes predicted from nitrate deficits caused by algal growth. However, these measurements were only made on samples from surface ponds and gap waters from freeboard layers. This means that the link between inorganic carbon limitation and increased values of $\delta^{13}C_{POC}$ is far from being satisfactorily addressed at the present time. The implications of the stable carbon isotope signature of sea ice diatoms and the enrichment of ^{13}C in sediments as a proxy for past CO_2 concentrations in surface waters and sea ice distribution is discussed by Leventer (Chapter 10) and Armand & Leventer (Chapter 11).

The pH of sea ice

The changes in carbon chemistry can result in significant changes in the pH of the sea ice brines, or trapped interstitial waters in platelet systems or rotten ice. Once again, the number of studies citing pH in sea ice is rather limited and is based on spring and summer measurements. The collection of undisturbed sea ice brine samples, as well as complications in measuring stable pH values at the elevated salinity of concentrated brine solutions, both hinder the collection of realistic pH values from sea ice. In general, there is a decrease in pH with increasing ionic strength (Lazar et al., 1983; Gleitz et al., 1995), which in turn would tend to an increase in the solubility of calcium carbonate, and may be a possible explanation why the predicted calcium carbonate precipitation is not frequently observed when ice forms. However, this trend is clearly masked by the effects of photosynthetic activity within the ice, and instead of a lowering of pH, the reports are generally of elevated pH in closed sea ice systems or within dense standing stocks of sea ice organisms. The observed pH increase in colonized sea ice habitats results from the depletion of dissolved inorganic carbon as a result of photosynthetic carbon assimilation.

9.4 Sampling for the dissolved and gaseous component in ice

One of the greatest difficulties in the measurement of dissolved gases and realistic pH values within sea ice, especially of brines, is the collection of undisturbed samples. Total gas content of the ice is relatively easy to sample, since the total gas can be trapped from disrupted whole pieces of ice (Tison et al., 2002). However, the *in situ* chemistry of brines and different phases of ice is not so straightforward. To date, most of chemical analyses in the sea ice are performed on bulk melted ice core

sections and brines collected by centrifugation or by drainage collection into 'sack holes' cored into the ice. In the latter, the ice is partially cored to leave a core hole in the ice. When this is done carefully and only cored to a depth to ensure that sea water from below does not enter the hole, brine drains from the surrounding ice into the hole and can be collected.

Clearly there are significant problems with each of these sampling strategies when looking at the gas content of the ice. Sack holes do not fill immediately, and in cold ice where brine volumes are small, it can take considerable time to collect enough solution for analyses. Therefore, during the accumulation of the brine, there is scope for changes in the brine chemistry by equilibration with the atmosphere. The brines collected in sack holes are also collected from an undefined area of the surrounding ice, probably representing a mixture of localized brine pockets. This, of course, can be viewed as being positive for the estimation of more generic descriptions of ice chemistry; however, the uncertainty of the origin of the collected solution from within the ice is a downfall of the method. Further, sack hole brine collection is hardly useful in very cold ice, since only minimal brine drainage will occur. In addition, it is rather unsuitable for sampling warm porous ice because of the increased possibility for contamination with brines and/or sea water from large distances from the sack hole.

The centrifugation of ice cores at *in situ* temperatures has been a valuable addition to the methodologies for sampling sea ice brines (Weissenberger et al., 1992; Krembs et al., 2000, 2001a,b). Typically the ice core is placed on the porous grid of a centrifuge bucket and the brine drained during centrifugation is collected underneath the grid. When care is taken, and long enough centrifugation times are used, the percentage brine recovery can be high. However, the more efficient centrifugation times, the longer the time for gas equilibration in the collecting brines.

Sampling melted sea ice samples

The slow melting of ice core sections at low temperatures is by far the method employed most often to routinely measure the chemical and biological components of sea ice cores. Since the organisms pass from a highly saline brine to generally low salinity melted ice solution, there are losses of fragile organisms due to osmotic shocks during the melting process (Garrison & Buck, 1986). Considering the internal cellular pools within these organisms of the main nutrients and chemicals routinely measured by sea ice biogeochemists, the input of dissolved chemicals into the sample from cell disruption is often insignificant relative to the concentrations usually measured within sea ice (Thomas et al., 1998). It is only in the very highest biological standing stocks measured in sea ice that such artifacts will become a problem. It must be stressed that such sample treatment is inappropriate for the measurement of gases and pH. A modification of this method consists of melting the core in large volumes of filtered sea water, thereby combatting the osmotic changes,

or in dialysis tubing. This method maintains better the full spectrum of the biological assemblage but does not confer any advantage to the measurement of the dissolved chemical constituents.

Microelectrodes and sea ice

Microelectrode technologies are amongst the most sophisticated analytical tools to have been developed in aquatic sciences in the past 20 years. They have revolutionized the study of small-scale nutrient, gas, light and pH gradients in aquatic biofilms and sediments, as well as across diffusion boundary layers. It was only natural that effort be taken to utilize microelectrodes for the study of sea ice biogeochemical processes. This technology can generate highly pertinent measurements for describing the photosynthetic and respiratory dynamics in bottom ice communities, which are common features in both the Antarctic and the Arctic (McMinn & Ashworth, 1998; McMinn et al., 2000; Trenerry et al., 2001). To date only oxygen electrodes have been employed in sea ice studies, although it cannot be long until other electrodes are also used in conjunction with high-resolution irradiance sensors. Most of the successful microelectrode studies in sea ice environments offered unparalleled insight into oxygen exchange at the ice–water interface through millimetre-scale micro-profiles (McMinn & Ashworth, 1998; Kühl et al., 2001; Rysgaard et al., 2001). However, the semi-solid sea ice matrix significantly restricts the use of these probes to the ice–water interface and porous ice, typically at best in the bottommost few centimetres of ice floes, where ice crystals are still loose, and electrode tips are not so easily damaged. Although such measurements are highly informative for the bottom ice communities, these assemblages are dominated by dissolved gas and inorganic nutrient regimes where exchange with the surrounding sea water is possible. They are not at all representative of those biological assemblages growing in the interior of ice floes and surface gap layers where exchange is limited to some degree or another.

Despite the rapid advances in micro-sensor technology in recent years, the robust methodologies for measuring *in situ* gas fluxes in the interior of the ice have remained illusive, which is frustrating since it is within closed or semi-enclosed parts of the ice that the greatest changes to sea ice chemistry will take place. The microelectrode studies to date in sea ice have relied on deployment methodologies that are not well suited to the long term (weeks, months) under extreme field conditions. This is because the electrodes are fragile and inflexible, a major problem in a dynamic ice matrix. Oxygen microelectrodes also consume oxygen, a methodological hindrance when measuring the O_2 dynamics in confined spaces. Finally, microelectrodes also measure the partial pressure of O_2 and so changes in temperature and salinity affect the sensor signal even when O_2 concentrations themselves remain constant (Glud et al., 2002). Recent developments in micro-optode design have allowed the freezing of optode arrays into ice as it forms (Mock et al., 2002). These optical-fibre-based sensors proved robust enough to withstand

being frozen into the ice, can be temperature and salinity compensated for, and do not consume O_2. Therefore, they overcome many of the methodological constraints imposed by the 'traditional' microelectrodes. Microscopic analysis of the optode tips in the ice showed that they remained in brine pockets within the ice, and were able to record realistic changes in dissolved O_2 over several weeks of deployment in a growing ice sheet. Mock et al. (in press) have used these fibre optodes for measuring the O_2 gradients within bottom, and skeletal layer, ice algal assemblages in laboratory grown sea ice. As further optical sensors are developed, it can be envisioned that these will be the 'next step' in elucidating dissolved gas dynamics in the sea ice matrix.

9.5 Dimethyl sulphide in sea ice

Dimethyl sulphide production in sea ice

The same kind of diffusion limitation that results in the build up of O_2 in ice will apply to other dissolved gases produced by sea ice organisms. One of the few to be studied in any detail is dimethyl sulphide (DMS), which is derived from dimethylsulphoniopropionate (DMSP). The concentration of DMSP within sea ice organisms can be orders of magnitude higher than those measured in the open ocean water and sea water underlying ice (Kirst et al., 1991; DiTullio et al., 1998). Light, temperature and nutrient supply all influence the production of DMSP (Malin & Kirst, 1997). Hefu & Kirst (1997) showed that ultraviolet (UV) radiation significantly reduced the production of DMSP by *Phaeocystis antarctica*, a common algal species in surface ice assemblages. In sea ice, however, salinity is the dominant factor influencing DMSP production by the ice algae, with DMSP being synthesized and accumulating internally in the cells in hypersaline conditions. DMSP is broken down to release DMS and acrylic acid into the surrounding medium when ambient salinity decreases. Furthermore, DMSP is also broken down to release DMS in alkaline conditions, such that the shifts of pH up to ~ 10 that have been measured in sea ice brine (Gleitz et al., 1995) may enhance this reaction within the sea ice habitat. Lastly, DMSP is broken down to DMS and acrylic acid through the action of the enzyme DMSP-lyase and, also, from grazing by protozoans and metazoans, as well as viral infection. An increase in the conversion rate of DMSP to DMS and acrylic acid was observed to accompany its reduced production rate by UV radiation (Hefu & Kirst, 1997).

Distribution of dimethyl sulphoniopropionate in sea ice and fate of dimethyl sulphide

To date, observations indicate great variation in the distribution of DMSP in sea ice, largely reflecting the variability in species composition of the local assemblages of

organisms. However, the small-scale spatial heterogeneity of the physical factors that influence the production of DMSP by ice algae, namely light, salinity and temperature, are also responsible for the observed variability in the DMSP distribution within sea ice.

In remote ocean regions, DMS accounts for most of the non-sea salt sulphate in the atmosphere, and its chemistry in the atmosphere is closely linked to the production of aerosol particles that serve as cloud condensation nuclei as part of a complex system of localized and global climate control (Malin & Kirst, 1997). Brine channel morphology, which determines the extent of grazing activity within the ice (Krembs et al., 2000), will determine the degree of grazing-induced release of DMS under sea ice conditions. It is certain, however, that the greatest release of DMS from sea ice regions is associated with melting ice and the corresponding reduction in ambient salinity, when cells containing hypersalinity-induced high concentrations of DMSP are released into the sea water. Periods of ice ablation are also times when elevated grazing activity in ice edge waters will increase the release of DMS into surface waters and therefore into the atmosphere.

Other volatile gases associated with sea ice

DMS is not the only volatile gas to be emitted from marine algae that may be incorporated into sea ice with consequences for atmospheric chemistry. Reactive halogen species significantly contribute to the destruction of ozone in the polar stratosphere, as well as the underlying troposphere. The origins of the increased halogen concentrations, and the spatial and temporal extents of their influence, remain unclear. However, tropospheric air enrichment of reactive bromine species closely associated with sea ice has been observed (Wagner & Platt, 1998). It has been speculated that short-term high concentrations of BrO in the troposphere are due to autocatalytic bromine release from sea salts in sea ice rather than due to degradation of unstable organic compounds containing halogens.

Both Arctic and Antarctic sea ice algae also produce significant quantities of a suite of brominated hydrocarbons including bromoform, dibromomethane, bromochloromethanes and methyl bromide, all of which may be converted photochemically into active forms of bromine (Sturges et al., 1992, 1993). The levels of production evidently have important implications for the chemistry of the polar oceans and may be of similar orders of magnitude to the influence of anthropogenic and macrophyte sources on a global scale (Sturges et al., 1992).

9.6 Nitrogen, phosphorus and silicate

Dynamics of dissolved inorganic macro-nutrients within sea ice

By far the greatest attention to the chemistry of sea ice has been given to the dynamics of inorganic nutrients such as nitrate, nitrite, ammonium, phosphate and

silicate. In abiotic systems, as ice forms and consolidates, the concentration of these inorganic nutrients will change in a conservative manner, i.e. in proportion to the salinity change. For example, in bulk ice, their concentration will decrease linearly with decreasing bulk salinity of the ice, while their concentration will increase proportionally to salinity when measured directly in brine pockets. However, in reality such straightforward scenarios are rarely encountered. Major ions such as sodium, potassium, magnesium, chloride, sulphate and calcium from different types and ages of ice generally follow closely to theoretical dilution lines predicted from salinity changes taking place in ice (Meese, 1989). However, when nitrate, phosphate, silicate, nitrite and ammonium are compared with theoretical dilution lines, there is often significant deviation from this trend (Meese, 1989; Dieckmann et al., 1991; Thomas et al, 1998; Arrigo et al., 2003). As with dissolved gases discussed above, these deviations are clearly associated with the biological activity occurring within the ice, which introduces a high degree of spatial heterogeneity. Several workers have tried to categorize ice age and/or type by the concentration of these nutrients, only to be confounded by the large-scale variability within and between ice cores (Meese, 1989; Dieckmann, 1992). Depletion and even complete exhaustion of these nutrients are recorded, as would be expected due to desalination of the ice and uptake by organisms. However, in many cases these nutrients are present far in excess of what would be predicted from simple conservative behaviour during freezing of sea water. Specifically, they often exhibit concentrations more akin to those found in heterotrophic environments, such as in sediment pore waters, where these nutrients are liberated into solution by the heterotrophic oxidation of organic matter during respiration.

Nutrients and water exchange

One of the key factors influencing the nutrient dynamics of sea ice is the degree to which there is possible exchange with the surrounding sea water. In biological assemblages at the periphery of ice floes, especially bottom ice assemblages, nutrient depletion is only seldom reported as being a growth-limiting factor, because exchange with the underlying water is readily possible. Small-scale differences in the topography of the ice–water interface were shown to be conducive to an increased fluid and, hence, nutrient exchange across irregular undersides of sea ice floes (Krembs et al., 2001b). The small-scale exchange rates in bottom ice skeletal layers were measured to be 100 times those for pore water exchange in sandy sediments and more than enough to satisfy algal nutrient demands (Krembs et al., 2001b). The transient nature of such small topographical features is evidently one of the key features in determining not only the variability of nutrient and gas fluxes across the ice–water interface, but also the localized variability in the accumulation (abundance) of organisms that depend on nutrient supply to grow. It must be noted that exchange processes decrease away from the ice–water interface and further into

the ice. Even after distances of 5–10 cm from the ice–water interface, there can be significant nutrient depletion and limitation of algal growth (McMinn et al., 1999).

Macro-nutrient exhaustion in sea ice

Nutrient exhaustion has only rarely been reported in assemblages within platelet ice underlying more consolidated ice (Dieckmann et al., 1992; Arrigo et al., 1995), because replenishment of nutrients is possible even in dense aggregates of platelets that can extend tens of metres under the ice (Thomas et al., 2001a). Similarly, in porous summer sea ice and surface layers such as the gap, infiltration and freeboard layers (Ackley & Sullivan, 1994; Fritsen et al., 1998, 2001; Haas et al., 2001), the high algal standing stocks often recorded will be supported to a large degree by replenishment of nutrients from the surrounding sea water by exchange processes (Garrison & Buck, 1991; Fritsen et al., 1994; Thomas et al., 1998; Kennedy et al., 2002). Surface gap, freeboard and infiltration layers are often not continuous throughout a floe. In some regions in the ice, such layers can be cut off from nutrient re-supply, resulting in overall nutrient depletion locally (Fritsen et al., 2001), even within a few centimetres from that part of the floe which exchanges fully with the surrounding sea water. Zones of highest productivity within ice floes are clearly governed by the degree of re-supply of nutrients (Syvertsen & Kristiansen, 1993; Gleitz et al., 1996a; Kennedy et al., 2002).

One aspect of sea ice nutrient loading that has not been studied in any detail is the prospect for atmospheric deposition of nutrients into surface ice layers. This is likely to be a very significant source of inorganic nutrients to ice-covered regions. Atmospheric precipitation has been considered to control the dynamics of the nutrients in surface sea ice in the Baltic Sea (Kaartokallio, 2001). A significant number of nutrients, such as nitrate, ammonium and sulphate, are well known for being deposited and stored in snow. Naturally, as snow is transformed and incorporated into the gross structure of ice floes (Eicken et al., 1994; Haas et al., 2001; Massom et al., 2001), there will be input of the stored nutrients into the potentially nutrient-depleted surfaces of ice floes.

Biological effect on macro-nutrient dynamics

In contrast to situations where significant biological standing crops are supported by continuous exchange of inorganic nutrients between sea ice and the surrounding sea water (open systems), several comprehensive studies have shown that nitrate-based primary production within closed or semi-enclosed sea ice habitats proceeds in general stoichiometric balance, with nitrate, phosphate and silicate decreasing with decreasing ΣCO_2 and increasing O_2 (Gleitz et al., 1995; Günther et al., 1999; Fritsen et al., 2001; Kennedy et al., 2002). However, as is discussed below, sea ice assemblages are not universally nitrate-based due to high accumulation of ammonium within the sea ice matrix. Even after nitrate exhaustion, photosynthetic activity

continues, with synthesis and accumulation of low nitrogen compounds (e.g. lipids, carbohydrates). In these cases, the resulting rise in pH and depletion of ΣCO_2 are much greater than can be accounted for by including inorganic nitrogen pools in the stoichiometric mass balance (Gleitz et al., 1996a, b; Günther et al., 1999; Kennedy et al., 2002).

Lipids in sea ice organisms

One of the biochemical observations most commonly reported for nutrient-limited sea ice algae is the production of conspicuous lipid droplets within the cells (Nichols et al., 1989; Priscu et al., 1990a; Gleitz et al., 1996a) and changes in lipid class abundances (Nichols et al., 1989; Fahl & Kattner, 1993; McMinn et al., 1999; Mock & Gradinger, 2000). Nutrient limitation coupled with low temperature and low light has been shown to influence significantly the fatty acid composition of the cell membrane responses in sea ice diatoms (Mock & Kroon, 2002a, b). During periods of nitrogen limitation, protein biosynthesis is affected, and the loss of bilayer-stabilizing proteins and pigments could disrupt chloroplast membranes and, consequently, photosynthesis. In sea ice diatoms, loss of membrane protein caused by nutrient limitation can be compensated for by the production of bilayer-forming fatty acids, such as digalactosyldiaglycerol and phosphatidylglycerol (Mock & Kroon 2002b). These processes have important consequences for the quality of sea ice assemblages as a food source for grazing protozoans and metazoans, as well as for the chemotaxonomy and organic geochemistry of algal assemblages and associated sediments (Nichols et al., 1989). In particular, the use of lipid composition as biomarkers for identifying the source of organic matter in sediments will be influenced greatly by the changes induced within the nutrient depleted (or limited) sea ice system (Volkman et al., 1998).

Elevated concentrations of macro-nutrients in sea ice

The most striking feature of the sea ice nutrient studies to date is not the potential for nutrient depletion but quite the opposite, namely the elevated nutrient concentrations recorded in many instances, which are far in excess of anything that can be argued from a physical–chemical stand point. In particular, high ammonium values up to $\sim 200\,\mu M$ and phosphate values up to $\sim 70\,\mu M$ (Arrigo et al., 2002) have been recorded in sea ice. These are associated with nitrate values up to $\sim 300\,\mu M$ and silicate values up to $\sim 320\,\mu M$. These unusually high concentrations are frequently found in association with dense, evidently actively growing, standing stocks of algae and, on occasions, high concentrations of bacteria. This feature is not restricted to sea ice from high latitude regions but is also a characteristic of Baltic sea ice (Mock et al., 1997; Kaartokallio, 2001). Such high nutrient concentrations, equivalent to nutrient regeneration rates of $35\,\mu mol\,l^{-1}\,d^{-1}$ for phosphate and in excess of $31\,\mu mol\,l^{-1}\,d^{-1}$ for ammonium, were considered to be due to high rates of

(heterotrophic) bacterial metabolism and/or excretion by metazoan grazers (Arrigo et al., 1995; Grossmann et al., 1996), which can reach high population abundance in these ammonia- and phosphate-rich systems (Schnack-Schiel, Chapter 7). Several diatom species also release ammonium at high rates under conditions of excess cellular energy (Lomas & Glibert, 2000). Further, algal mortality and cell lysis, amplified by inefficient metazoan grazing within high algal standing stock, can liberate considerable dissolved organic matter and inorganic nutrients (Günther et al., 1999). However, it seems unlikely that the extraordinarily high concentrations of phosphate and ammonium can be explained by the release of internal pools alone. The most probable explanation is that the large nutrient reserves result from a combination of factors such as cell lysis coupled with significant nitrogen and phosphorus remineralization processes. Nitrite levels are generally low in sea ice, although in some studies elevated concentrations of this nutrient have been reported (Thomas et al., 1995; Gradinger & Ikävalko, 1998; Kaartokallio, 2001). Active denitrifying bacteria have been reported in sea ice, although only on a few occasions (Kaartokallio, 2001). This is probably not a reflection of their distribution but rather a lack of relevant measurements. However, for denitrification to take place, oxygen levels must be low, since oxygen inhibits the activity of denitrifying enzymes. Low oxygen zones will occur in sea ice due to the degassing of ice as discussed above. It is possible that anoxic conditions may prevail, and there are a very few reports of a hydrogen sulphide smell in ice (G.S. Dieckmann, pers. comm.) However, most of the measurements in sea ice that support active biological communities indicate that O_2 concentration is often well in excess for denitrification to occur. On the other hand, the measured O_2 concentration would support high activity of nitrification, e. g. the stepwise oxidation of ammonia to nitrite and nitrate. The activity of nitrifying bacteria in O_2-replete conditions would produce the large concentrations of nitrate that are frequently measured at the same time as high levels of ammonium. Ammonium oxidizing bacteria have been found in sea ice assemblages (Priscu et al., 1990b). The activity of nitrifiers will be enhanced by attachment to surfaces, such as ice crystals, polysaccharide gels, or organisms, since ammonium and nitrite oxidizing activity in other marine systems is induced by attachment.

Whatever the processes responsible for ammonium and phosphate accumulation within sea ice, the production of these nutrients is clearly greater than the apparent capacity for utilization within these systems. The accumulation of such high concentrations also indicates that exchange with the surrounding water must be low, otherwise the high concentrations would be diluted by the relatively less nutrient-loaded sea water. However, the systems in which high concentrations develop cannot be fully closed off from external exchange, because algal biomass could never reach levels higher than the starting concentrations of oxygen, carbon, nitrogen and phosphorus permit without some exchange with sea water. The fact that these levels are so often grossly exceeded indicates that in these cases biomass increase has been supported by both external exchange of nutrients, as well as

nutrient release and regeneration processes within the system (Arrigo et al., 1995; Thomas et al., 1998; Arrigo et al., 2002; Kennedy et al., 2002).

Nitrate and ammonium affinity at low temperature

Marine algae and bacteria have a lower affinity for substrates such as inorganic nutrients and/or organic compounds at low temperatures below their optimum growth temperature (reviewed by Nedwell, 1999; Pomeroy & Wiebe, 2001). In order for the organisms to grow, it is vital that the necessary substrates and nutrients are present in high enough concentrations to counterbalance the reduced affinity. The high levels of ammonium, phosphorus and dissolved organic matter (see below) in sea ice will fulfill such temperature-affected metabolic constraints. Similarly, and in slight contrast to this line of thought, low substrate affinity has also been proposed as the reason that available substrates are not exploited despite the high concentrations in the ice (Pomeroy & Wiebe, 2001). Although not working with sea ice isolates, Reay et al. (1999) measured a consistent decrease in the specific affinity of micro-organisms from polar regions for nitrate with decreasing temperatures. Priscu & Sullivan (1998) also showed that it is nitrate transport into the cell that is the limiting factor at low temperature, since the enzymatic nitrate reduction is more efficient at low temperature than the transport of nitrate into the cell. This is not the case for ammonium, for which the specific affinity is evidently temperature independent (Reay et al., 1999). The differences are attributable to the fact that active uptake processes, as is the case for nitrate, are more influenced by the changes in membrane structure that occur at low temperatures than passive uptake processes that are involved in ammonia transport into the cells. These differences in nitrogen uptake processes therefore have profound effects on which source of inorganic nitrogen is used by photosynthetic organisms at low temperatures.

The first stage in the reduction of nitrate into a form that can be used for cellular metabolism involves the enzyme nitrate reductase (NR) that converts nitrate to nitrite. Priscu & Sullivan (1998) show that extra nitrate did not increase protein-specific NR activity in sea ice algae and that NR activity was significantly suppressed at ammonium concentrations below 1 mM. Ammonium inhibition of nitrate assimilation is well reported for marine phytoplankton (Thompson et al., 1989; Flynn, 1991). Further, there is an increase in the proportion of ammonia (NH_3) compared to ammonium (NH_4^+) at high (alkaline) pH, which can diffuse directly into cells (Flynn, 1991; Raven et al., 1992; Reay et al., 1999). The high levels of ammonium frequently measured in sea ice will inhibit nitrate assimilation by algae, while the elevated ambient pH often measured in sea ice brine will be favourable to ammonium assimilation. In other words, sea ice may be one of the few marine environments where ammonium-dominated nitrogen metabolism prevails (cf. Raven et al., 1992).

In diatoms, the dominant algal group within sea ice systems, intracellular concentrations of nitrate can be stored, whereas ammonium is generally not stored.

The transport of ammonium into the cell is inactivated if the intracellular levels of ammonium are excessive (Flynn, 1991). In contrast, flagellates can store high amounts of ammonium within their cells (Lomas & Glibert, 2000). Possibly differences in nitrogen assimilation patterns within sea ice assemblages play a role in determining the species composition of photosynthesizing organisms within the sea ice. Studies of seasonal shifts in the primary nitrogen uptake (Kristiansen et al., 1992, 1998) reported nitrate to be the main nitrogen source for infiltration algae in spring, whereas ammonium became a much more important nitrogen source during summer.

Silicate in sea ice

Silicate concentration and its turnover within sea ice are fundamental to the dominance of diatoms in sea ice habitats. Silicate availability controls the species composition, while nitrogen supply determines maximum standing stock of diatoms within the ice (Günther & Dieckmann, 1999, 2001). Although silicate is certainly often depleted within the ice compared with surface water concentrations, it is rarely exhausted, even in association with high-standing stocks of diatoms. Active uptake of silicate from the external medium (silicification) is governed by the many factors that control diatom growth, such as temperature, light and other inorganic nutrient demands. Cell size affects the amount of silica needed, but factors such as low temperature can also induce the production of thicker frustules. Limiting levels of trace metals also induce increased silicification in some diatom species. Diatoms grown in silicate-limited conditions have less silicified frustules and structures such as spines may be reduced (Martin-Jézéquel et al., 2000).

Key to the dynamics of the silicate pool is the dissolution of diatom frustules that leads to enrichment of this nutrient within sea ice. The dissolution of diatom frustules is hastened by bacterial activity, which facilitates the degradation of the protective organic layer of the frustules (Bidle & Azam, 1999). Impurities in the diatom frustule and its surface area are all factors that combine to make species-specific differences in frustule dissolution, which is also significantly altered by temperature, salinity and pH (Barker et al., 1994; Martin-Jézéquel et al., 2000; Greenwood et al., 2001). Grazing activity may increase dissolution rates by damaging the protective coatings of the frustules but mostly by fragmenting the frustules, thereby increasing exposed surface areas. However, the packaging of diatoms into membrane-bound faecal pellets, as is commonly found in sea ice (Buck et al., 1990; Thomas et al., 2001b), will effectively reduce frustule dissolution by considerably reducing the surface area. A highly significant factor influencing the dissolution of frustules in the sea ice system is pH. Shifts in pH to highly alkaline values in highly productive sea ice assemblages (Gleitz & Thomas, 1993; Gleitz et al., 1995, 1996a, b) will significantly enhance the dissolution rate of frustules. This increased dissolution may be counterbalanced by retardation of dissolution rates at low temperatures

(Martin-Jézéquel et al., 2000) coupled with a decreased affinity of the diatoms for silicate at low temperature (Stapleford & Smith, 1996).

9.7 Dissolved organic matter

Central to the concept of a closely coupled microbial network is that there is a significant pool of dissolved organic matter (DOM) within sea ice. This pool of diverse organic compounds is operationally defined as the organic matter that will pass through a 0.2 μm filter. In practice, glass fibre filters (GF/F) are routinely used, with operational pore sizes closer to 0.7 μm. In marine systems, DOM is derived from the death and lysis of organisms ranging from bacteria through to whales. It is also derived by excretion of organic material and as a result of inefficient feeding by grazing organisms. In the sea ice microbial network, algae are sinks for dissolved inorganic nutrients, as discussed above, whereas the heterotrophic protozoans and metazoans excrete dissolved compounds (Lizotte, Chapter 6). Heterotrophic bacteria utilize organic matter for their growth and cell maintainance (respiration) as well as inorganic nutrients. Bacteria can compete with algae for nutrients depending on the elemental composition of the organic substrate available to grow on. However, heterotrophic bacteria also release nutrients in order to maintain a steady state elemental composition. The degree of nutrient 'regeneration' depends largely on the composition of the organic matter source to which the bacteria are exposed.

Most of the work to date in marine systems has focused on the dynamics of dissolved organic carbon (DOC) and dissolved organic nitrogen (DON), and to a lesser extent dissolved organic phosphorus (DOP). For a comprehensive coverage of the latest developments in marine DOM research see Hansell & Carlson (2002). This organic pool is a diverse mixture of compounds ranging in size from simple monomers through to large biopolymers, such as carbohydrates, amino acids, proteins and complex humic substances of undefined and highly changeable structure. Some of this material will be readily broken down and utilized by bacteria (biologically labile), whereas some of the other components of the DOM pool will only slowly be broken down by bacterial activity (biologically refractory).

Dissolved organic matter in sea ice

Despite the obvious importance of DOM to the sea ice system, it is only in recent years that studies have actually been made to investigate this pool of organic compounds within the ice. This was spurred on by the realization that the production and transformation of DOM would be central to any biogeochemical cycling within the ice and that large amounts of DOM were needed to mediate the observed ecology of algae, bacteria and protozoans within the ice (Gleitz et al., 1996a; Grossmann et al., 1996; Günther et al., 1999).

In recent years there has been a concerted effort to measure the DOC and, to a

lesser extent, the DON content within sea ice in both the Antarctic (Thomas et al., 1998; Herborg et al., 2001; Thomas et al., 2001a, b; Carlson & Hansell, in press) and the Arctic (Thomas et al., 1995; Smith et al., 1997; Amon et al., 2001; Krembs et al., in press). Giannelli et al. (2001) have shown that, in artificial abiotic ice, the DOM incorporated from the water column into a growing ice matrix behaves conservatively during sea ice formation, following the dynamics of inorganic salts and dissolved gases. Similar exclusion of DOM and coloured dissolved organic matter (CDOM) have been reported from freshwater lake ice from Canadian lakes and rivers (Belzile et al., 2002). These researchers found that only low molecular weight molecules were retained in the ice.

Despite the loss of DOM from the ice due to brine expulsion, many field investigations confirm that generally there is significant accumulation of DOM within the ice, with DOC concentrations up to 450-fold greater than that of surface waters (Thomas et al., 2001b; Carlson & Hansell, in press). These are frequently associated with the highest standing stocks of organisms in the ice, albeit not always. There are many instances of a poor correlation between chlorophyll or particulate material and DOM, while, on occasions, high DOM concentrations are found where no living ice organisms are present, suggesting that it could be a remnant of past biological activity (Thomas et al., 2001a).

The high accumulation of DOM in the ice indicates that there is an uncoupling of the DOM production and consumption processes. Pomeroy & Wiebe (2001) review this phenomenon and conclude that the reduced substrate affinity of bacteria (as discussed above for nutrient uptake) at low temperatures may be responsible for the uncoupling, resulting in poor exploitation of the high concentrations of available organic substrates in the ice.

DOM derived from sea ice either on ice melt, or through exchange between ice and sea water, has also been considered to be an important source of organic matter for stimulating increased microbial activity just below the ice in waters at the ice–water interface (Kähler et al., 1997; Krembs & Engel, 2001). Due to massive dilution effects, it is likely that these effects will only be pertinent in waters very close to the ice, or where stabilized melt water lenses or features persist for some time (cf. Krembs & Engel, 2001). However, in the diffuse skeletal layer this source of organic material will certainly result in increased bacterial activity, in particular in regions of the ice bottom surface where topography induces the build-up of particulate material (Krembs et al., 2001b). It has also been proposed that 'bio-active agents', such as organic ligands or trace metals associated with (i.e. complexed by) the DOM pool, may play a role in 'conditioning' surface water layers for phytoplankton growth (Brandini & Baumann, 1997; Apollonio et al., 2002).

Characteristics of sea ice dissolved organic matter

Arrigo et al. (1995) showed that amino acids and sugars accumulated in platelet layers, although the reported concentrations were at sub-mM level, which is very

low compared with the levels of DOC and DON reported above. The work of Herborg et al. (2001) indicates that up to 99% of the DOC pool can be composed of carbohydrates, with the majority of this being mono- rather than poly-carbohydrates. Amon et al. (2001) showed that DOM from Arctic ice samples was characterized by high neutral sugar and amino acids, with a dominance of glucose and glutamic acid, which pointed to fresh DOM presumed to be produced by ice algae.

In contrast, Calace et al. (2001) found a large accumulation of DOM in Antarctic sea ice and refered to the ice acting as 'an organic matter tank'. In particular, these authors found high levels of humic substances in the ice and propose that active humification of DOM derived from the sea ice algae can occur within the ice. They identified there to be high contents of proteinaceous and carbohydrate material, especially the latter, within samples taken from the ice. Humic substances have largely undefined chemical structure but are generally thought to be biologically refractory. The accumulation of DOM in sea ice, and the apparent under-utilization of this resource by the heterotrophic bacteria in many of the ice samples studied to date, may be partially explained by its refractory nature.

Dissolved organic carbon and dissolved organic nitrogen in sea ice

There have only been three published studies that have measured both the DOC and the DON components of the same sample. Again this limited data set points to sea ice DOM being highly carbon enriched, with variable C/N ratios as low as 3 but more commonly as high as 50 (Thomas et al., 2001a, b). Similarly, high DOC/DON ratios in Arctic sea ice (Thomas et al., 1995) were attributed to an uncoupling of the carbon and nitrogen metabolism, such that a nitrogen-rich pool of amino acids was hydrolysed and was utilized faster than carbon-rich polysaccharide pools. Guglielmo et al. (2000) also have shown a preferential turnover of nitrogen enriched organic matter, estimating potential utilization of the entire protein pool within 3 hours in the sea ice system studied, whereas it could take up to 102 hours for the complete utilization of the carbohydrate pool.

Photochemical reactions and dissolved organic matter

There is great potential for photochemical reactions (Mopper et al., 1991; Kieber & Mopper, 1996) to take place within sea ice floes. These photochemical processes have the potential to change the chemical characteristics and biological lability of the DOM pool, and therefore its biogeochemical properties. Working with Antarctic diatom-derived DOM, Thomas & Lara (1995) indicated that this pool is resistant to photodegradation, although photochemical effects are dependent on the nature of the DOM before exposure to UV radiation (Tranvik & Kokalj, 1998). Obernosterer et al. (1999) have shown that freshly released labile DOM might be rendered more biologically refractory by photochemical reactions, whereas the

bioavailability of refractory DOM can be actually enhanced upon exposure to solar radiation. Little work has been conducted on the effects of UV radiation on sea ice DOM. Belzile et al. (2000) showed a strong absorption of UV radiation in Arctic sea ice by DOM and concluded that significant photochemical reactions could occur. Sea ice is an effective barrier to UV radiation and, thus, photochemical modification of the DOM pool is likely to be important near the ice surface. In their work with freshwater ice, Belzile et al. (2002) have demonstrated that as CDOM is excluded from the ice, there is a decrease in CDOM absorption of light and correspondingly higher transmission of UV wavelengths. Surface ice can be the site of the most dynamic biogeochemical processes, and, hence, the photochemical transformations may play a major role in determining the availability of DOM to the bacterial component of the sea ice microbial network.

Exopolymeric substances and the dissolved organic matter pool in sea ice

Many aquatic organisms excrete large amounts of exopolymeric substances (EPS), mainly polysaccharides. These range in diversity from capsules secreted by bacteria and algae to surround the cells through to loose mucus or slimes. Diatoms are well-known producers of EPS and are likely the major contributor to EPS loading in the sea ice. However, EPS in aquatic systems are produced when algae and bacteria are associated with surfaces and particles, and especially in biofilms. In algal blooms, especially those of diatoms, large amounts of EPS are formed during both the exponential growth phase and during the subsequent stationary phase (Decho, 1990, 2000; Passow, in press). Formation of EPS by algae and bacteria is reportedly stimulated by changes in temperature, salinity, inorganic nutrients, as well as quantity and quality of irradiance. Therefore, high levels of EPS production would be expected to occur within the sea ice matrix.

Exopolymeric substances and biofilms in the ice?

Very high concentrations of EPS were found in winter Arctic sea ice, which were closely correlated with DOC concentration and bacterial cell density but not with nutrient or chlorophyll distribution (Krembs et al., in press). By means of non-invasive microscope techniques, it was demonstrated that diatoms in the ice are often within EPS-filled pockets or channels (Krembs et al., in press). It has been suggested that the matrix of EPS may anchor the cells to ice crystals, changing diffusive properties of salts in forming ice, so that localized defects in ice may be formed that evolve into mucus-filled pockets (Krembs et al., in press). The consequences for bacterial–algal interactions, as well as the effects of such matrices for hindering efficient feeding by algal and bacterial grazers, will be profound. The production of EPS, coupled with the narrow channel space, might well be another reason for the apparent breakdown of the classic microbial loop in the sea ice matrix

and the subsequent accumulation of DOM. Our conceptual thinking of nutrient and gas exchange within the brine channel system will need to be significantly altered, and may well also have to change. The general concepts already developed from biofilm studies in aquatic microbiology, and the effect of EPS on the permeability and solute transport in other porous media such as rocks, soils, sediments and aquifers, may become highly pertinent to sea ice studies in the future (Meyer-Reil, 1994; Decho, 2000).

Sea ice and transparent exopolymer particles

In the past 15 years there has been increasing interest by marine microbiologists in a particular type of EPS, namely the transparent exopolymer particles (TEP). These are transparent particulate gels, consisting of acid polysaccarides, which are visualized when stained with alcian blue (reviewed by Passow, in press). They range in size from sub-μm to hundreds of μm and are highly changeable in shape because of their gelatinous consistency. It is important to note that although these particles are exopolymers, not all EPS are, or can form, TEP. TEP are formed from the coagulation and continuous aggregation of dissolved polysaccharide fibrillar (a few nanometres in diameter) precursors in the DOM pool. TEP also form when mucus pieces detach from organisms or cell surfaces. The importance of TEP in marine systems is profound, especially in the formation of microhabitats. One of the better-studied aspects is the attachment of bacteria to TEP surfaces, with significant consequences for elemental biogeochemical cycling. It is not so much the fact that bacteria can utilize TEP (some TEP are resistant to bacterial degradation), but rather that increased concentrations of bacteria, in microhabitats, on the surfaces of TEP can increase the rates of bacteria-mediated biogeochemical processes.

Sea ice as a habitat offers conditions favourable to significant TEP formation through large diatom and bacterial production of DOM and, in particular, EPS within a confined space. Krembs & Engel (2001) and Meiners et al. (in press) have measured high concentrations of TEP in interior ice, as well as in the bottom layers of Arctic ice floes. In both of these works, the authors link TEP with the production of EPS by sea ice diatoms. It is proposed that at least some of the larger particles measured may be fragments of biofilms coating the surfaces of brine channel walls. It is highly pertinent that future sea ice studies concentrate on defining what type of physicochemical system is encountered by the organisms recruited in sea ice. We have up to now considered the sea ice matrix to be a labyrinthine system of brine filled channels and pores, containing attached and free organisms. We may have to rethink this perspective and rather consider biofilms on the surfaces of pores and channels, and viscous gel-filled spaces, in which organisms are embedded as opposed to simply being suspended within a liquid brine. Additionally, the presence of high EPS and TEP within the ice will alter the viscosity of brine and also the properties with regard to diffusive transport of ions and gases.

9.8 Arctic river inputs

The Southern Ocean is largely cut off from terrestrial influence, except for limited aerial deposition. In contrast, the Arctic Basin is characterized by a high input of fresh water – almost 10% of global river discharge – from many large river systems, such as the Ob', Lena, Yenisey, MacKenzie and Yukon (Anderson, 2001; Holmes et al., 2001; Anderson, 2002). This translates into high riverine discharge of suspended solids, DOM and dissolved nutrients, e.g. ammonium, nitrate, silicate and phosphate (Kattner et al., 1999; Holmes et al., 2001; Anderson, 2002). In addition, these rivers also convey pollutants, such as PCBs, heavy metals and biological contaminants that will be absent from the Southern Ocean. As a result of such large amounts of freshwater input, much of the surface waters of the Kara, Laptev, East Siberian and Beaufort Seas exhibit low salinities. Arctic ice formed in coastal areas can be heavily laden with sediments, which are then transported large distances in the moving ice fields carried by transpolar currents (see Haas, Chapter 3). Even allochthonous material, such as tree trunks and soil turfs, becomes encased in Arctic ice floes, eventually being released many thousands of kilometres from the place it was initially caught up in the ice.

Lara et al. (1998), Kattner et al. (1999) and Lobbes et al. (2000) measured the organic matter at the mouths of these rivers and have concluded that much of the DOM is soil-derived material with a high degree of degradation. The DOC and DON inputs are very large, up to 1000 μM and 30 μM, respectively, but much of this organic material will be biologically refractory and, therefore, available to be transported long distances through transarctic drift. The chemical composition of the particulate and dissolved lignin phenols, which are exclusively of terrestrial origin, in river discharge waters of twelve Russian rivers is significantly correlated with the proportion of tundra and taiga in the drainage areas. The contribution of lignin to overall carbon flux from Russian rivers is only 0.3% of total carbon export but is a useful tracer for organic matter fluxes from tundra and taiga regions (Lobbes et al., 2000). Anderson (2002) gives a more comprehensive discussion of the processes controlling DOC in the Arctic Ocean.

Although the dynamics of freshwater input into the Arctic significantly influence large-scale sea ice formation processes, it is unclear how the higher organic matter and nutrient loading influence the biogeochemical processes in the ice. Little is known about the biogeochemical processes in ice subjected to large river discharge, especially the influence of coastal discharges during ice formation, the effects of river plumes under the ice and/or seasonal flooding of ice sheets with DOM and nutrient-rich waters. In general, it can be conceived that Arctic sea ice has a far greater potential for carbon loading than ice in the Antarctic. Of course, the Arctic Ocean is not the only ice-covered region that is influenced by significant freshwater inputs. The Baltic Sea is also a semi-enclosed water body, with large river discharges, and many of the biogeochemical processes occurring in the ice formed in

weakly saline Arctic coastal waters will be pertinent to ice formed in the low salinity waters of the Baltic.

9.9 Future perspectives

The study of sea ice biogeochemistry has largely evolved from the study of sea ice ecology and in particular the extensive investigations devoted to the understanding of photosynthesis within the ice (Arrigo, Chapter 5). A major focus of the ecological studies was sea ice microbial dynamics (Lizotte, Chapter 6), with sea ice algal growth being central to these studies. Because of these research roots, the progress in our understanding has largely been led by a desire to understand the biology of sea ice. It is only in recent years that the chemical processes dominant within sea ice have been considered in 'their own right'.

Ice tank facilities

In reviewing the subject, it is evident that our understanding of 'geochemical' processes within sea ice remains limited. One of the main reasons for this is that studies of abiotic sea ice are limited and can only take place in facilities that allow the formation of realistic sea ice in laboratory conditions. This is not a trivial task and involves considerable logistical costs and difficulties. Recently, the adaptation of large-scale ice tank facilities such as those at the Hamburg Ship Model Basin in Hamburg, Germany (www.hsva.de) have gone far to address this issue (Eicken et al., 1998; Haas et al., 1999; Giannelli et al., 2001; Tison et al., 2002). As our experience with such facilities grows, much will be learnt about the fundamental changes in sea ice chemistry, which are often masked by the effects of biology in sea ice sampled in the field. There has also been some success in introducing biology into these 'artificial' sea ice systems (Weissenberger, 1998; Krembs et al., 2001a; Mock et al., 2002) to produce experiments in which the biology can be investigated under controlled abiotic conditions. Similar large-scale mesocosms will make it much easier for biogeochemists in the future to unravel the complexity of biological and chemical processes taking place in the ice.

Variability and the problem of scale

It is likely that microelectrodes/optodes will be more often deployed during studies to measure nutrient and gas fluxes in sea ice, especially at the ice–water interface. Such technology gives highly defined measurements on scales (micrometre) that are relative to the biology living within the sea ice brine channel systems. These are important findings, of course, but present problems in scaling up the findings to consider processes on the scale of tens of metres. The sea ice habitat is notoriously patchy, and the variability of both chemical and biological parameters is a problem

that vexes the establishment of general paradigms being formed within sea ice biogeochemistry. More and more sophisticated technology is being developed to examine micro-scale processes within sea ice (see also Junge et al., 2001; Krembs et al., in press). It is important that future studies that use such techniques also employ resources and time to find ways of extrapolating small-scale dynamic events to larger, and arguably, ecologically more important scales.

The biochemical characterization of the DOM pools within sea ice is a major requirement for our understanding of the biogeochemistry of sea ice. To date, we know very little about what actually makes up the DOM and how biologically labile this material is. In addition, there is much need to characterize the enzyme and bacterial activities that control the turnover of this material. In particular, the biochemical basis of reduced substrate affinity of sea ice organisms needs to be further linked to measurements of organic and inorganic nutrient pools within the ice (Pomeroy & Wiebe, 2001). For these studies to be successful there is a pressing need for the study of sea ice biogeochemistry to move forward and harness biochemical and molecular techniques that are now routinely used for the study of biogeochemistry of comparable marine systems such as sediments and biofilms.

Time-series measurements

Of paramount need is the opportunity to study the changes in biogeochemistry within growing ice sheets with dynamic biological assemblages, where succession of species and organism type develops in step with changes in the physicochemical characteristics of the ice. Time-series type of measurements is one of the main positive aspects of mesocosm or abiotic ice tank experiments. The only way that such measurements will happen in natural sea ice systems will be logistically difficult long-term field campaigns, either from land-based stations and/or drift experiments with research ships. Most of the biogeochemical measurements we have to date come from 'spot samples' of sea ice. It is impossible to separate the 'historical' chemical signature of developing ice from the present composition of the biological assemblage in the sample. The adoption of stable isotope methodologies can go part of the way to divulging such historical processes during the evolution of a piece of ice, but far more will be learnt from actually being able to follow these processes as they take place.

Acknowledgements

Many colleagues have contributed to our, still scant, knowledge of biogeochemistry of sea ice. These are too numerous to mention here; however, it seems fitting that we acknowledge Markus Gleitz who initiated the new impetus in the biogeochemical study of sea ice. David Thomas is grateful to the Hanse Institute for Advanced

Study, the NERC, the British Council, the Royal Society and the European Union for funding opportunities to continue sea ice work.

References

Ackley, S.F. & Sullivan, C.W. (1994) Physical controls on the development and characteristics of Antarctic sea ice biological communities – a review and synthesis. *Deep-Sea Research*, **41**, 1583–1604.

Amon, R.M.W., Fitznar, H.P. & Benner, R. (2001) Linkages among the bioreactivity, chemical composition, and diagenetic state of marine dissolved organic matter. *Limnology and Oceanography*, **46**, 287–297.

Anderson, L.G. (2001) Chemical oceanography in polar oceans. In: *Physics of Ice-covered Seas*, Vol. 2, (Ed. M. Leppäranta), pp. 787–810. Helsinki University Press, Helsinki, Finland.

Anderson, L.G. (2002) DOC in the Arctic Ocean. In: *Biogeochemistry of Marine Dissolved Organic Matter*, (Eds D.A. Hansell & C.A. Carlson), pp. 665–683. Academic Press, San Diego.

Anderson, L.G. & Jones, E.P. (1985) Measurements of total alkalinity, calcium, and sulfate in natural sea ice. *Journal of Geophysical Research*, **90**, 9194–9198.

Apollonio, S., Pennigton, M. & Cota, G.F. (2002) Stimulation of phytoplankton photosynthesis by bottom-ice extracts in the Arctic. *Polar Biology*, **25**, 350–354.

Arrigo, K.R., Dieckmann, G.S., Gosselin, M., Robinson, D.H., Fritsen, C.H. & Sullivan, C.W. (1995) High resolution study of the platelet ice ecosystem in McMurdo Sound, Antarctica – biomass, nutrient, and production profiles within a dense microalgal bloom. *Marine Ecology Progress Series*, **127**, 255–268.

Arrigo, K.R., Robinson, D.H., Dunbar, R.B., Leventer, A.R. & Lizotte, M.P. (2003) Physical control of chlorophyll *a*, POC, and TPN distributions in the pack ice of the Ross Sea, Antarctica. *Journal of Geophysical Research*.

Barkan, E., Luz, B. & Lazar, B. (2001) Dynamics of the carbon dioxide system in the Dead Sea. *Geochimica et Cosmochimica Acta*, **65**, 355–368.

Barker, P., Fontes, J.-C., Gasse, F. & Druart, J.-C. (1994) Experimental dissolution of diatom silica in concentrated salt solutions and implications for paleoenvironmental reconstruction. *Limnology and Oceanography*, **39**, 99–110.

Belzile, C., Gibson, J.A.E. & Vincent, W.F. (2002) Colored dissolved organic matter and dissolved organic carbon exclusion from lake ice: implications for irradiance transmission and carbon cycling. *Limnology and Oceanography*, **47**, 1283–1293.

Belzile, C., Johannessen, S.C., Gosselin, M., Demers, S. & Miller, W.L. (2000) Ultraviolet attenuation by dissolved and particulate constituents of first-year ice during late spring in an Arctic polynya. *Limnology and Oceanography*, **46**, 1265–1273.

Berner, R.A. (1980) *Early Diagenesis: A Theoretical Approach*. Princeton University Press, Princeton, New Jersey.

Bidle, K.D. & Azam, F. (1999) Accelerated dissolution of diatom silica by marine bacterial assemblages. *Nature*, **397**, 508–512.

Brandini, F.P. & Baumann, M.E.M. (1997) The potential role of melted 'brown ice' as sources of chelators and ammonia to the surface waters of the Weddell Sea, Antarctica. *Proceedings of the NIPR Symposium on Polar Biology*, **10**, 1–13.

Buck, K.R., Bolt, P.A. & Garrison, D.L. (1990) Phagotrophy and fecal pellet production by an athecate dinoflagellate in Antarctic sea ice. *Marine Ecology Progress Series*, **60**, 75–84.

Burkhardt, S., Riebesell, U. & Zondervan, I. (1999) Effects of growth rate, CO_2 limitation and cell size on the stable carbon isotope fractionation in marine phytoplankon. *Geochimica et Cosmochimica Acta*, **63**, 3729–3741.

Calace, N., Castrovinci, D., Maresca, V., Petronio, B.M., Pietroletti, M. & Scardala, S. (2001) Aquatic humic substances in pack ice–seawater–sediment system. *International Journal of Environmental Analytical Chemistry*, **79**, 315–329.

Carlson, C.A. & Hansell, D.A. (in press) The contribution of DOM to the biogeochemistry of the Ross Sea. In: *Biogeochemical Cycles in the Ross Sea*, (Eds G. DiTullio & R. Dunbar), American Geophysical Union, Washington, D.C. *Antarctic Research Series*.

Decho, A.W. (1990) Microbial exopolymer secretions in ocean environments – their roles in food webs and marine processes. *Oceanography and Marine Biology An Annual Review*, **28**, 73–153.

Decho, A.W. (2000) Microbial biofilms in intertidal systems: an overview. *Continental Shelf Research*, **20**, 1257–1273.

Dehairs, F., Kopczynska, E., Nielsen, P., Lancelot, C., Bakker, D.C.E., Koeve, W. & Goeyens, L. (1997) Partial derivative C-13 of Southern Ocean suspended organic matter during spring and early summer: regional and temporal variability. *Deep-Sea Research*, **44**, 129–142.

Dieckmann, G.S., Arrigo, K. & Sullivan, C.W. (1992) A high resolution sampler for nutrient and chlorophyll *a* profiles of the sea ice platelet layer and underlying water column below fast ice in Polar oceans: preliminary results. *Marine Ecology Progress Series*, **80**, 291–300.

Dieckmann, G.S., Lange, M.A., Ackley, S.F. & Jennings, J.C., Jr (1991) The nutrient status in sea ice of the Weddell Sea during winter: effects of sea ice texture and algae. *Polar Biol*ogy, **11**, 449–456.

DiTullio, G., Garrison, D.L. & Mathot, S. (1998) Dimethylsulfoniopropionate in sea ice algae from the Ross Sea polynya. In: *Antarctic Sea Ice Biological Processes, Interactions and Variability*, (Eds M.P. Lizotte & K.R. Arrigo), American Geophysical Union, Washington, D.C. *Antarctic Research Series*, **73**, 139–146.

Dunbar, R.B. & Leventer, A. (1992) Seasonal variation in carbon isotopic composition of Antarctic sea ice and open water plankton communities. *Antarctic Journal of the United States*, **27**, 79–81.

Eicken, H. (1992) The role of sea ice in structuring Antarctic ecosystems. *Polar Biology*, **12**, 3–13.

Eicken, H., Lange, M.A., Hubbertan, H.-W. & Wadhams, P. (1994) Characteristics and distribution patterns of snow and meteoric ice in the Weddell Sea and their contribution to the mass balance of sea ice. *Annales Geophysicae*, **12**, 80–93.

Eicken, H., Weissenberger, J., Cottier, F., Evers, K.-V., Kuosa, H., Hall, R. et al. (1998) Ice tank studies of physical and biological sea ice processes. In: *Ice in Surface Waters*, *Proceedings of the 14th International Symposium on Ice*, (Ed. H.T. Shen), pp. 363–370. Potsdam, New York.

Fahl, K. & Kattner, G. (1993) Lipid content and fatty acid composition of algal communities in sea ice and water from the Weddell Sea (Antarctica). *Polar Biology*, **13**, 405–409.

Fischer, G. (1991) Stable carbon isotope ratios of plankton carbon and sinking organic matter from the Atlantic sector of the Southern Ocean. *Marine Chemistry*, **35**, 581–596.

Flynn, K.J. (1991) Algal carbon–nitrogen metabolism: a biochemical basis for modelling the interactions between nitrate and ammonium uptake. *Journal of Plankton Research*, **13**, 373–382.

Fritsen, C.H., Ackley, S.F., Kremer, J.N. & Sullivan, C.W. (1998) Flood–freeze cycles and microalgal dynamics in Antarctic pack ice. In: *Antarctic Sea Ice Biological Processes, Interactions and Variability*, (Eds M.P. Lizotte & K.R. Arrigo), American Geophysical Union, Washington, D.C. *Antarctic Research Series*, **73**, 1–21.

Fritsen, C.H., Coale, S.L., Neenan, D.R., Gibson, A.H. & Garrison, D.L. (2001) Biomass, production and microhabitat characteristics near the freeboard of ice floes in the Ross Sea, Antarctica, during the austral summer. *Annals of Glaciology*, **33**, 280–286.

Fritsen, C.H., Lytle, V.I., Ackley, S.F. & Sullivan, C.W. (1994) Autumn bloom of Antarctic pack-ice algae. *Science*, **266**, 782–784.

Garcia, H.E. & Gordon, L.I. (1992) Oxygen solubility in seawater: better fitting equations. *Limnology and Oceanography*, **37**, 1307–1312.

Garrison, D.L. & Buck, K.R. (1986) Organism losses during ice melting: a serious bias in sea ice community studies. *Polar Biology*, **6**, 237–239.

Garrison, D.L. & Buck, K.R. (1991) Surface-layer sea ice assemblages in Antarctic pack ice during the austral spring: environmental conditions, primary production and community structure. *Marine Ecology Progress Series*, **75**, 161–172.

Giannelli, V., Thomas, D.N., Haas, C., Kattner, G., Kennedy, H.A. & Dieckmann, G.S. (2001) Behaviour of dissolved organic matter and inorganic nutrients during experimental sea ice formation. *Annals of Glaciol*ogy, **33**, 317–321.

Gibson, J.A.E., Trull, T., Nichols, P.D., Summons, R.E. & McMinn, A. (1999) Sedimentation of C-13 rich organic matter from Antarctic sea ice algae: a potential indicator of past sea ice extent. *Geology*, **27**, 331–334.

Gleitz, M., Grossmann, S., Scharek, R. & Smetacek, V. (1996a) Ecology of diatom and bacterial assemblages in water associated with melting summer sea ice in the Weddell Sea, Antarctica. *Antarctic Science*, **8**, 135–146.

Gleitz, M., Kukert, H., Riebesell, U. & Dieckmann, G.S. (1996b) Carbon acquisition and growth of Antarctic sea ice diatoms in closed bottle incubations. *Marine Ecology Progress Series*, **135**, 169–177.

Gleitz, M., Rutgers van der Loeff, M., Thomas, D.N., Dieckmann, G.S. & Millero, F.J. (1995) Comparison of summer and winter inorganic carbon, oxygen and nutrient concentrations in Antarctic sea ice brine. *Marine Chemistry*, **51**, 81–91.

Gleitz, M. & Thomas, D.N. (1993) Variation in phytoplankton standing stock, chemical composition and physiology during sea ice formation in the southeastern Weddell Sea, Antarctica. *Journal of Experimental Marine Biology and Ecology*, **173**, 211–230.

Glud, R.N., Rysgaard, S. & Kühl, M. (2002) A laboratory study in O_2 dynamics and photosynthesis in ice algal communities: quantification by microsensors, O_2 exchange rates, ^{14}C incubations and a PAM fluorometer. *Aquatic Microbial Ecology*, **27**, 301–311.

Gradinger, R. & Ikävalko, J. (1998) Organisms incorporation into newly forming Arctic sea ice in the Greenland Sea. *Journal of Plankton Research*, **20**, 871–886.

Greenwood, J.E., Truesdale, V.W. & Rendell, A.R. (2001) Biogenic silica dissolution in seawater – in vitro chemical kinetics. *Progress in Oceanography*, **48**, 1–23.

Grossmann, S., Lochte, K. & Scharek, R. (1996) Algal and bacterial processes in platelet ice during late austral summer. *Polar Biology*, **16**, 623–633.

Guglielmo, L., Carrada, G.C., Catalano, G., Dell'Anno, A., Fabiano, F., Lazzara, L., Mangoni, O., Pusceddu, A. & Saggiomo, V. (2000) Structural and functional properties of sympagic communities in the annual sea ice at Terra Nova Bay (Ross Sea, Antarctica). *Polar Biology*, **23**, 137–146.

Günther, S. & Dieckmann, G.S. (1999) Seasonal development of algal biomass in snow-covered fast ice and the underlying platelet layer in the Weddell Sea, Antarctica. *Antarctic Science*, **11**, 305–315.

Günther, S. & Dieckmann, G.S. (2001) Vertical zonation and community transition of sea-ice diatoms in fast ice and platelet layer, Weddell Sea, Antarctica. *Annals of Glaciology*, **33**, 287–296.

Günther, S., Gleitz, M. & Dieckmann, G.S. (1999) Biogeochemistry of Antarctic sea ice: a case study on platelet ice at Drescher Inlet, Weddell Sea. *Marine Ecology Progress Series*, **177**, 1–13.

Haas, C., Cottier, F., Smedsrud, L.H., Thomas, D.N., Buschmann, U., Dethleff, D., Gerland, S., Giannelli, V., Hoelemann, J., Tison, J.-L. & Wadhams, P. (1999) Multidisciplinary ice tank study shedding new light on sea ice growth processes. *EOS, Transactions of the American Geophysical Union*, **80**, 507–513.

Haas, C., Thomas, D.N. & Bareiss, J. (2001) Surface properties and processes of perennial Antarctic sea ice in summer. *Journal of Glaciology*, **47**, 613–625.

Hansell, D.A. & Carlson, C.A. (Eds) (2002) *Biogeochemistry of Marine Dissolved Organic Matter*. Academic Press, San Diego.

Hefu, Y. & Kirst, G.O. (1997) Effect of UV-radiation on DMSP content and DMS formation of *Phaeocystis antarctica*. *Polar Biology*, **18**, 402–409.

Herborg, L.-M., Thomas, D.N., Kennedy, H., Haas, C. & Dieckmann, G.S. (2001) Dissolved carbohydrates in Antarctic sea ice. *Antarctic Science*, **13**, 119–125.

Holmes, R.M., Peterson, B.J., Zhulidov, A.V., Gordeev, V.V., Makkaveev, P.N., Stunzhas, P.A., Kosmenko, L.S., Köhler, G.H. & Shiklomanov, A.I. (2001) Nutrient chemistry of the Ob' and Yenisey Rivers, Siberia: results from June 2000 expedition and evaluation of long-term data sets. *Marine Chemistry*, **75**, 219–227.

Junge, K., Krembs, C., Deming, J., Stierle, A. & Eicken, H. (2001) A microscopic approach to investigate bacteria under in situ conditions in sea ice samples. *Annals of Glaciology*, **33**, 304–310.

Kaartokallio, H. (2001) Evidence for active microbial nitrogen transformations in sea ice (Gulf of Bothnia, Baltic Sea) in midwinter. *Polar Biology*, **24**, 21–28.

Kähler, P., Bjørnsen, P.K., Lochte, K. & Antia, A. (1997) Dissolved organic matter and its utilisation by bacteria during spring in the Southern Ocean. *Deep-Sea Research*, **44**, 341–353.

Kattner, G., Lobbes, J.M., Fitzner, H.P., Engbrodt, R., Nöthig, E.-M. & Lara, R.J. (1999) Tracing dissolved organic substances and nutrients from the Lena river through Laptev Sea (Arctic). *Marine Chemistry*, **65**, 25–39.

Kennedy, H., Thomas, D.N., Kattner, G., Haas, C. & Dieckmann, G.S. (2002) Particulate organic carbon in Antarctic summer sea ice: concentration and stable carbon isotopic composition. *Marine Ecology Progress Series*, **238**, 1–13.

Kieber, D.J. & Mopper, K. (1996) Photochemistry of Antarctic waters during the 1994 austral summer. *Antarctic Journal of the United States*, **30**, 150–151.

Killawee, J.A., Fairchild, I.J., Tison, J.-L., Janssens, L. & Lorrain, R. (1998) Segregation of

solutes and gases in experimental freezing of dilute solutions: implications for natural glacial systems. *Geochimica et Cosmochimica Acta*, **62**, 3637–3655.

Kirst, G.O., Thiel, C., Wolff, H., Nothangel, J., Wanzek, M. & Ulmke, R. (1991) Dimethylsulfoniopropionate (DMSP) in ice-algae and its possible biological role. *Marine Chemistry* **35**, 381–388.

Krembs, C., Eicken, H., Junge, K. & Deming, J.W. (in press) High concentrations of exopolymeric substances in Arctic winter sea ice: implications for the Polar ocean carbon cycle and cryoprotection of diatoms. *Deep-Sea Research*.

Krembs, C. & Engel, A. (2001). Abundance and variability of microorganisms and transparent exopolymer particles across the ice–water interface of melting first-year sea ice in the Laptev Sea (Arctic). *Marine Biology*, **138**, 173–185.

Krembs, C., Gradinger, R., & Spindler, M. (2000) Implications of brine channel geometry and surface area for the interaction of sympagic organisms in Arctic sea ice. *Journal of Experimental Marine Biology and Ecology*, **243**, 55–80.

Krembs, C., Mock, T. & Gradinger, R. (2001a). A mesocosm study of physical–biological interactions in artificial sea ice: effects of brine channel surface evolution and brine movement on algal biomass. *Polar Biology*, **24**, 356–364.

Krembs, C., Tuschling, K. & von Juterzenka, K. (2001b) The topography of the ice water interface – its influence on the colonisation of sea ice by algae. *Polar Biology*, **25**, 106–117.

Kristiansen, S., Farbrot, T., Kuosa, H., Myklestad, S. & Quillfeldt, C.H. (1998) Nitrogen uptake in the infiltration community, an ice algal community in Antarctic pack-ice. *Polar Biology*, **19**, 307–315.

Kristiansen, S., Syvertsen, E.E. & Farbrot, T. (1992) Nitrogen uptake in the Weddell Sea during late winter and spring. *Polar Biology*, **12**, 245–251.

Kühl, M., Glud, R.N., Borum, J., Roberts, R. & Rysgaard, S. (2001) Photosynthetic performance of surface-associated algae below sea ice as measured with a pulse-amplitude-modulated (PAM) fluorometer and O_2 microsensors. *Marine Ecology Progress Series*, **223**, 1–14.

Lara, R.J., Rachold, V. Kattner, G., Hubberten, H.W., Guggenberger, G., Skoog, A. & Thomas, D.N. (1998) Dissolved organic matter and nutrients in the Lena River, Siberian Arctic: characteristics and distribution. *Marine Chemistry*, **59**, 301–309.

Lazar, B. & Erez, J. (1992) Carbon geochemistry of marine-derived brines: I. ^{13}C depletion due to intense photosynthesis. *Geochimica et Cosmochimica Acta*, **56**, 335–345.

Lazar, B., Starinsky, A., Katz, A. & Sass, E. (1983) The carbonate system in hypersaline solutions: alkalinity and $CaCO_3$ solubility of evaporated seawater. *Limnology and Oceanography*, **28**, 978–986.

Lobbes, J.M., Fitzner, H.P. & Kattner, G. (2000) Biogeochemical characteristics of dissolved and particulate organic matter in Russian rivers entering the Arctic Ocean. *Geochimica et Cosmochimica Acta*, **64**, 2973–2983.

Lomas, M.W. & Glibert, P.M. (2000) Comparisons of nitrate uptake storage and reduction in marine diatoms and flagellates. *Journal of Phycology*, **36**, 903–913.

McMinn, A. & Ashworth, C. (1998) The use of oxygen microelectrodes to determine the net production by an Antarctic sea ice algal community. *Antarctic Science*, **10**, 39–44.

McMinn, A., Ashworth, C. & Ryan, K.G. (2000) *In situ* net primary productivity of an Antarctic fast ice bottom algal community. *Aquatic Microbial Ecology*, **21**, 177–185.

McMinn, A., Skerratt, J., Trull, T., Ashworth, C. & Lizotte, M. (1999) Nutrient stress

gradient in the bottom 5 cm of fast ice, McMurdo Sound, Antarctica. *Polar Biology*, **21**, 220–227.

Malin, G. & Kirst, G.O. (1997) Algal production of dimethyl sulfide and its atmospheric role. *Journal of Phycology*, **33**, 889–896.

Martin-Jézéquel, V., Hildebrand, M. & Brezinski, M.A. (2000) Silicon metabolism in diatoms: implications for growth. *Journal of Phycology*, **36**, 821–840.

Massom, R.A., Eicken, H., Haas, C., Jeffries, M.O., Drinkwater, M.R., Sturm, M., Worby, A.P., Wu, X.R., Lytle, V.I., Ushio, S., Morris, K., Reid, P.A., Warren, S.G. & Allison I. (2001) Snow on Antarctic Sea ice. *Reviews of Geophysics*, **39**, 413–445.

Meese, D.A. (1989) The chemical and structural properties of sea ice in the southern Beaufort Sea. *CRREL Report*, **89-25**, 1–97.

Meiners K., Gradinger, R., Fehling, J., Civitarese, G. & Spindler, M. (in press) Vertical distribution of transparent exopolymer particles (TEP) in sea ice of the Fram Strait (Arctic) during autumn. *Marine Ecology Progress Series*.

Meyer-Reil, L.-A. (1994) Microbial life in sedimentary biofilms – the challenge to microbial ecologists. *Marine Ecology Progress Series*, **112**, 303–311.

Millero, F. J., Huang, F. & Laferiere, A.L. (2002) Solubility of oxygen in the major sea salts as a function of concentration and temperature. *Marine Chemistry*, **78**, 217–230.

Millero, F. J. (1995) Thermodynamics of the carbon dioxide system in the ocean. *Geochimica et Cosmochimica Acta*, **59**, 661–677.

Mitchell, C. & Beardall, J. (1996) Inorganic carbon uptake by an Antarctic sea-ice diatom, *Nitzschia frigida*. *Polar Biology*, **16**, 95–99.

Mock, T., Dieckmann, G.S., Haas, C., Krell, A., Tison, J.-L., Belem, A.L., Papadimitriou, S. & Thomas, D.N. (2002) Micro-optodes in sea ice: a new approach to investigate oxygen dynamics during sea ice formation. *Aquatic Microbial Ecology*, **29**, 297–306.

Mock, T. & Gradinger, R. (2000) Changes in photosynthetic carbon allocation in algal assemblages of Arctic sea ice with decreasing nutrient concentrations and irradiance. *Marine Ecology Progress Series*, **202**, 1–11.

Mock, T. & Kroon, B.M.A. (2002a) Photosynthetic energy conversion under extreme conditions. I. Important role of lipids as structural modulators and energy sink under N-limited growth in Antarctic sea ice diatoms. *Phytochemistry*, **61**, 41–51.

Mock, T. & Kroon, B.M.A. (2002b) Photosynthetic energy conversion under extreme conditions. II. The significance of lipids at low temperature and low irradiances in Antarctic sea ice diatoms. *Phytochemistry*, **61**, 53–60.

Mock, T., Kruse, M. & Dieckmann, G.S. (in press) A new microcosm to investigate oxygen dynamics at the sea-ice water interface. *Aquatic Microbial Ecology*.

Mock, T., Meiners, K.M. & Giesenhagen, H.C. (1997) Bacteria in sea ice and underlying brackish water at 54°26′50″N (Baltic Sea, Kiel Bight). *Marine Ecology Progress Series*, **158**, 23–40.

Mopper, K., Zhou, X., Kieber, R.J., Kieber, D. J., Sikorski, R.J. & Jones, R.D. (1991) Photochemical degradation of dissolved organic carbon and its impact on the oceanic carbon cycle. *Nature*, **353**, 60–62.

Nedwell, D.B. (1999) Effect of low temperature on microbial growth: lowered affinity for substrates limits growth at low temperature. *FEMS Microbiology Ecology*, **30**, 101–111.

Nichols, P.D., Palmisano, A.C., Rayner, M.S., Smith, G.A. & White, D.C. (1989) Changes in

the lipid composition of Antarctic sea ice diatom communities during a spring bloom: an indication of community physiological status. *Antarctic Science*, **1**, 133–140.

Obernosterer, I., Reitner, B. & Herndl, G.J. (1999) Contrasting effects of solar radiation on dissolved organic matter and its bioavailability to marine bacterioplankton. *Limnology and Oceanography*, **44**, 1645–1654.

Palmisano, A.C. & Sullivan, C.W. (1985) Growth, metabolism, and dark survival in sea ice microalgae. In: *Sea Ice Biota*, (Ed. R.A. Horner), pp. 131–146. CRC Press, Boca Raton, Florida.

Passow, U. (in press) Transparent exopolymer particles (TEP) in aquatic environments. *Progress in Oceanography*.

Petri, R. & Imhoff, J.F. (2001) Genetic analysis of sea-ice bacterial communities of the Western Baltic Sea using an improved double gradient method. *Polar Biology*, **24**, 252–257.

Pomeroy, L.R. & Wiebe, W.J. (2001) Temperature and substrates as interactive limiting factors for marine heterotrophic bacteria. *Aquatic Microbial Ecology*, **23**, 187–204.

Prézelin, B., Moline, M.A. & Matlick, H.A. (1998) ICECOLORS '93: Spectral UV radiation effects on Antarctic frazil ice algae. In: *Antarctic Sea Ice Biological Processes, Interactions and Variability*, (Eds M.P. Lizotte & K.R. Arrigo), American Geophysical Union, Washington, D.C. *Antarctic Research Series*, **73**, 45–83.

Priscu, J.C., Downes, M.T., Priscu, L.R., Palmisano, A.C. & Sullivan, C.W. (1990b) Dynamics of ammonium oxidizer activity and nitrous oxide (N_2O) within and beneath Antarctic sea ice. *Marine Ecology Progress Series*, **62**, 37–46.

Priscu, J.C., Priscu, L.R., Palmisano, A.C. & Sullivan, C.W. (1990a) Estimation of neutral lipid levels in Antarctic sea ice microalgae by nile red fluorescence. *Antarctic Science*, **2**, 149–155.

Priscu, J.C. & Sullivan, C.W. (1998) Nitrogen metabolism in Antarctic fastice microalgal assemblages. In: *Antarctic Sea Ice Biological Processes, Interactions and Variability*, (Eds M.P. Lizotte & K.R. Arrigo). American Geophysical Union, Washington, D.C. *Antarctic Research Series*, **73**, 147–160.

Rau, G.H., Sullivan, C.W. & Gordon, L. (1991) $\delta^{13}C$ and $\delta^{15}N$ variations in Weddell Sea particulate organic matter. *Marine Chemistry*, **35**, 355–369.

Raven, J.A. (1991) Plant responses to high O_2 concentrations: relevance to previous high O_2 episodes. *Palaeogeography, Palaeoclimatology, Paleaoecology*, **97**, 19–38.

Raven, J.A., Johnston, A.M., Parsons, R. & Kübler, J. (1994) The influence of natural and experimental high O_2 concentrations on O_2-evolving phototrophs. *Biological Review*, **69**, 61–94.

Raven, J.A., Wollenweber, B. & Handley, L.L. (1992) A comparison of ammonium and nitrate as nitrogen sources for photolithotrophs. *New Phytologist*, **121**, 19–32.

Reay, D.S., Nedwell, D.B., Priddle, J. & Ellis-Evans, J.C. (1999) Temperature dependence of inorganic nitrogen uptake: reduced affinity for nitrate at suboptimal temperatures in both algae and bacteria. *Applied and Environmental Microbiology*, **65**, 2577–2584.

Rivkin, R.B. & Putt, M. (1987) Heterotrophy and photoheterotrophy in Antarctic microalgae: light-dependent incorporation of amino acids and glucose. *Journal of Phycology*, **23**, 442–452.

Rysgaard, S., Kühl, M., Glud, R.N. & Hansen, J.W. (2001) Biomass, production and horizontal patchiness of sea ice algae in a high-Arctic fjord (Young Sound, NE Greenland). *Marine Ecology Progress Series*, **223**, 15–26.

Schriek, R. (2000) Effects of light and temperature on the enzymatic antioxidative defense systems in the Antarctic ice diatom *Entomoneis kufferathii* Manguin. *Reports on Polar Research*, **349**, 1–130.

Sherwood, J.E., Stagnitti, F., Kokkinn, M.J. & Williams, W.D. (1991) Dissolved oxygen concentration in hypersaline waters. *Limnology and Oceanography*, **36**, 235–250.

Smith, R.E.H., Gosselin, M., Kudoh, S., Robineau, B. & Taguchi, S. (1997) DOC and its relationship to algae in bottom ice communities. *Journal of Marine Systems*, **11**, 71–80.

Stapleford, L.S. & Smith, R.E.H. (1996) The interactive effects of temperature and silicon limitation on the psychrophilic ice diatom *Pseudonitszchia seriata*. *Polar Biology*, **16**, 589–594.

Sturges, W.T., Cota, G.F. & Buckley, P.T. (1992) Bromoform emission from Arctic ice algae. *Nature*, **358**, 660–662.

Sturges, W.T., Sullivan, C.W., Schnell, R.C., Heidt, L.E. & Pollock, W.H. (1993) Bromoalkene production by Antarctic ice algae. *Tellus*, **45**, 120–126.

Sunda, W., Kieber, D.J., Kiene, R.P. & Hunstman, S. (2002) An antioxidant function for DMSP and DMS in marine algae. *Nature*, **418**, 317–320.

Syvertsen, E.E. & Kristiansen, S. (1993) Ice algae during EPOS leg 1: assemblages, biomass, origin and nutrients. *Polar Biology*, **13**, 61–65.

Thomas, D.N. & Dieckmann, G.S. (2002a) Antarctic sea ice – a habitat for extremophiles. *Science*, **295**, 641–644.

Thomas, D.N. & Dieckmann, G.S. (2002b) Biogeochemistry of Antarctic sea ice. *Oceanography and Marine Biology: an Annual Review*, **40**, 143–169.

Thomas, D.N., Engbrodt, R., Giannelli, V., Kattner, G., Kennedy, H., Haas, C. & Dieckmann, G.S. (2001a) Dissolved organic matter in Antarctic sea ice. *Annals of Glaciology*, **33**, 297–303.

Thomas, D.N., Kennedy, H., Kattner, G., Gerdes, D., Gough, C. & Dieckmann, G.S. (2001b) Biogeochemistry of platelet ice: its influence on particle flux under fast ice in the Weddell Sea, Antarctica. *Polar Biology*, **24**, 486–496.

Thomas, D.N. & Lara, R.J. (1995) Photodegradation of algal derived dissolved organic carbon. *Marine Ecology Progress Series*, **116**, 309–310.

Thomas, D.N., Lara, R.J., Eicken, H., Kattner, G. & Skoog, A. (1995) Dissolved organic matter in Arctic multi-year sea ice during winter: major components and relationship to ice characteristics. *Polar Biology*, **15**, 477–483.

Thomas, D.N., Lara, R.J., Haas, C., Schnack-Schiel, S.B., Dieckmann, G.S., Kattner, G. Nöthig, E.-M., & Mizdalski, E. (1998) Biological soup within decaying summer sea ice in the Amundsen Sea, Antarctica. In: *Antarctic Sea Ice Biological Processes, Interactions and Variability*. (Eds M.P. Lizotte & K.R. Arrigo), American Geophysical Union, Washington, D.C. *Antarctic Research Series*, **73**, 161–171.

Thompson, P.A., Levasseur, M.E. & Harrison, P.J. (1989) Light-limited growth on ammonium vs. nitrate: what is the advantage for marine phytoplankton. *Limnology and Oceanography*, **34**, 1014–1024.

Tison, J.-L., Haas, C., Gowing, M.M., Sleewaegen, S. & Bernard, A. (2002) Tank study of physico-chemical controls on gas content and composition during growth of young sea ice. *Journal of Glaciology*, **48**, 177–191.

Tranvik, L. & Kokalj, S. (1998) Decreased biodegradability of algal DOC due to interactive effects of UV radiation and humic matter. *Aquatic Microbial Ecology*, **14**, 301–307.

Trenerry, L.J., McMinn, A. & Ryan, K.G. (2001) *In situ* oxygen microelectrode measurements of bottom-ice algal production in McMurdo Sound, Antarctica. *Polar Biology*, **25**, 72–80.

Vincent, W.F. & Roy, S. (1993) Solar ultraviolet-B radiation and aquatic primary production: damage, protection and recovery. *Environment Review*, **1**, 1–12.

Volkman, J.K., Barrett, S.M., Blackburn, S.I., Mansour, M.P., Sikes, E.L. & Gelin, F. (1998) Microalgal biomakers: a review of recent research developments. *Organic Geochemistry*, **29**, 1163–1179.

Wagner, T. & Platt, U. (1998) Satellite mapping of enhanced BrO concentrations in the troposphere. *Nature*, **395**, 486–490.

Weeks, W.F. & Ackley, S.F. (1982) The growth, structure and properties of sea ice. *CRREL Monograph*, **82** (1), 1–130.

Weissenberger, J. (1998) Arctic sea ice biota: design and evaluation of a mesocosm experiment. *Polar Biology*, **19**, 151–159.

Weissenberger, J., Dieckmann, G.S., Gradinger, R. & Spindler, M. (1992) Sea ice: a cast technique to examine and analyse brine pockets and channel structure. *Limnology and Oceanography*, **37**, 179–183.

Zaslavskaia, L.A., Lippmeier, J.C., Shih, C., Ehrhardt, D., Grossman, A.R. & Apt, K.E. (2001) Trophic conversion of an obligate phototrophic organism through metabolic engineering. *Science*, **292**, 2073–2075.

Chapter 10

Particulate Flux from Sea Ice in Polar Waters

Amy Leventer

10.1 Introduction

Annually, sea ice extent in polar regions fluctuates greatly, with northern hemisphere sea ice ranging from a minimum of $8.4 \times 10^6\,km^2$ in August to a maximum of $15 \times 10^6\,km^2$ in March, and southern sea ice retreating and advancing from 4×10^6 to $20 \times 10^6\,km^2$ between February and September of each year (Squire, 1990; Comiso, Chapter 4). During retreat, melting sea ice can have a tremendous impact on local and regional physical, chemical and biological oceanographic processes. Low salinity melt water floats on top of higher density sea water forming a relatively stable surface layer (Smith & Nelson, 1986; Nelson et al., 1987; Mitchell & Holm-Hansen, 1991), unless disturbed by strong winds (Lancelot et al., 1991a). Nutrients, inorganic and organic particulates, including sea ice algae, contained within the ice, are released to the upper water column, with consequences for all levels of the biological system.

Phytoplankton blooms are commonly associated with the retreating sea ice edge where stable surface layers persist (El-Sayed, 1971; Alexander & Niebauer, 1981; Sakshaug & Holm-Hansen, 1984; Smith & Nelson, 1985; Niebauer & Alexander, 1985; Smith & Nelson, 1986; Nelson et al., 1987; Sullivan et al., 1988; Sakshaug & Skjoldal, 1989; Comiso et al., 1990; Lancelot et al., 1991a, b; Bianchi et al., 1992; Comiso et al., 1993; Schloss & Estrada, 1994). These blooms are thought to be responsible for a considerable proportion of polar productivity. For example, Smith & Nelson (1986) estimated that approximately 50% of annual primary production in the Southern Ocean is associated with the marginal ice zone blooms, while the Legendre et al. (1992) estimate is slightly greater, at about 60%. Clearly these blooms have an impact on successively higher levels of the food web (McRoy et al., 1972; Ainley & Jacobs, 1981; Bradstreet & Cross, 1982; Stretch et al., 1988; Bedo et al., 1990; Runge et al., 1991; Lancelot et al., 1993a, b). Even when ice edge blooms do not occur (Sakshaug, 1989; Lancelot et al., 1991a, b; Veth et al., 1992; Lancelot et al., 1993; Scharek et al., 1994; Boyd et al., 1995), flux of material out of the disin-

tegrating ice can be a food source for pelagic grazers and plays an important role in linking the surface and deep ocean.

This chapter summarizes the current state of understanding of flux from the sea ice, including data from both the Arctic and the Antarctic. First, the general characteristics of particle flux, in terms of composition, total mass and chemical signature, and the mechanisms of settling, are considered. Following this general review, three major questions are addressed. First, the role of sea ice flux in controlling the taxonomic composition and quality/quantity of primary productivity in the marginal ice zone is considered, by assessing the likelihood that algal cells released from the sea ice *seed* ice edge communities. Second, the importance of organic carbon released from the sea ice in supporting the pelagic community is evaluated. This is addressed by considering the role of sea ice algae as a food source for pelagic consumers both in the winter and during the late spring to summer. Many researchers have documented active grazing at the under-surface of the ice; a process that likely sustains overwintering pelagic consumers. In addition, the annual release of a large mass of organic particulates to the water column as the annual ice breaks up is very important as a seasonal food source for planktonic grazers. Finally, the role of sea ice flux in determining the structure of the open water food web is reviewed. In particular, the relationship between the sea ice flux and the development of a diatom-based versus microbially based food network (Smetacek et al., 1990) in the upper water column is examined.

10.2 General characteristics of particle flux

Other papers in this book address the general characteristics and distribution of particulates contained within sea ice (Arrigo, Chapter 5; Lizotte, Chapter 6; Schnack-Schiel, Chapter 7), so this will not be reviewed here. With regard to particle flux, the important thing to consider is that when the ice breaks up each late spring/summer, these constituents, which include variable concentrations of biogenic carbonates and silicates, particulate organic matter and lithogenic debris, are released to the underlying water column, where they play a role in ecosystem processes, both in the water column and at the sea floor. The timing and rate at which particles are released is a function of both their distribution within the ice and the rate at which the ice disintegrates (Leventer et al., 1987). For example, if particles are concentrated in the lower portion of the ice, as is common in Antarctic fast ice and Arctic multi-year ice floes, and that ice breaks up via melting from below, particle flux from the ice may be at a maximum as the ice begins to thin, prior to complete ice breakout (Leventer et al., 1987). If, on the other hand, particles are distributed throughout the ice column, as is more commonly the case in pack ice, particle flux may be distributed over a longer time span, though significant flux may be noted as ice retreat takes place (Fischer et al., 1988).

Honjo (1990) presents an excellent summary of particle flux in polar seas,

including a discussion of the history of particle flux experiments in these waters, an overall characterization and comparison of flux in the southern versus northern polar ocean, and a general description of the mechanisms of settling. Though his article is not focused exclusively on flux from the sea ice, many of his points are very relevant to this discussion and are reviewed below.

Particle flux experiments

The most comprehensive information on flux from the sea ice has been derived from studies that are based primarily on sediment trap deployments (Figs 10.1, 10.2). The primary advantages of sediment trap studies are their ability to collect sub-ice information that is difficult to gain access to any other way, and second, that they can provide long-term and continuous data sets, as opposed to the snapshot view provided by an individual research cruise. These particle interceptor traps may be deployed through the sea ice, where they monitor flux during the later winter

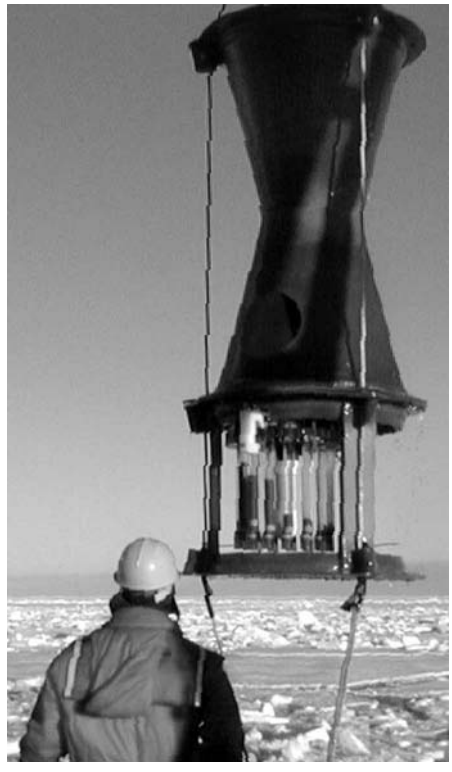

Fig.10.1 Sediment trap recovery in the Ross Sea. Note the carousel of collection tubes at the base of the sediment trap. These collection tubes rotate into place on a pre-set schedule.

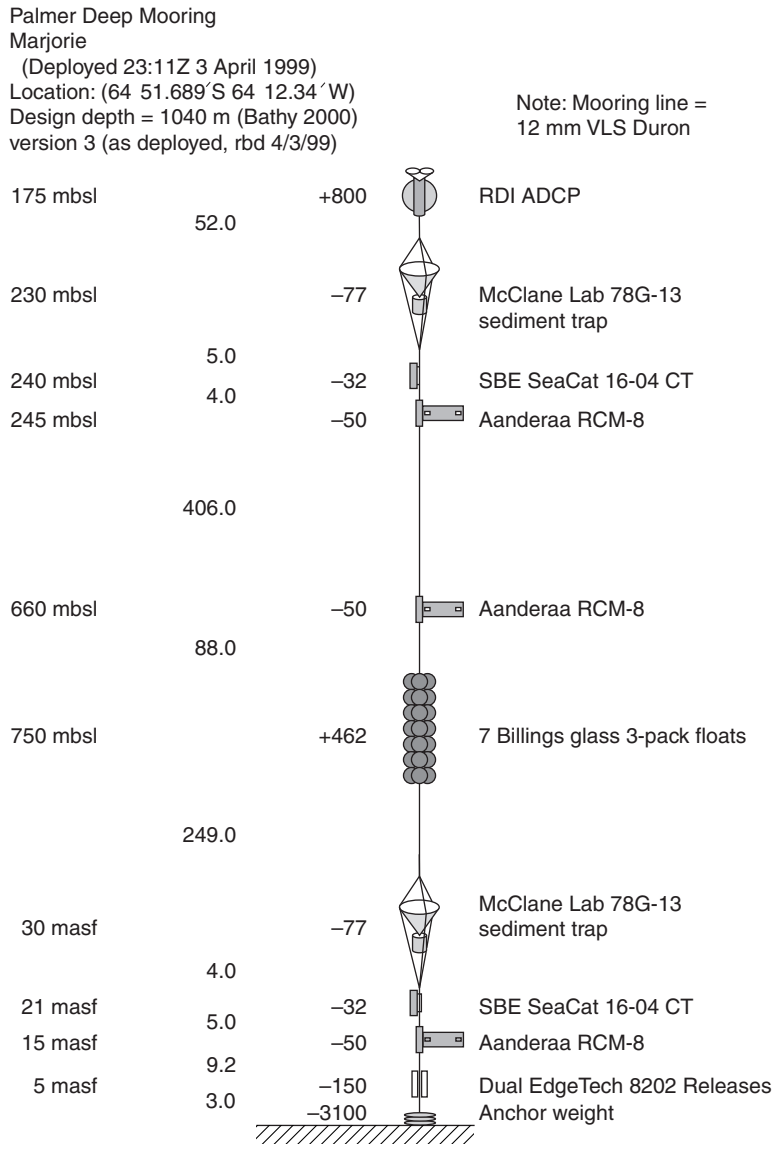

Fig. 10.2 A schematic describing a typical mooring deployment. Along the mooring line are two sediment traps, as well as several other instruments, including an Acoustic Doppler Current Profiler (ADCP), current meters (Aanderaa RCM-8), and conductivity–temperature recorders (SBE SeaCat 16-04 CT). Flotation to keep the mooring tightly upright is placed at the top of the mooring and along the mooring line. From left to right, vertical columns indicate the estimated metres below sea level (mbsl) of each instrument, the length of line between instruments and the flotation characteristics of each instrument.

through early summer, prior to ice breakout (Carey, 1987; Leventer & Dunbar, 1987; Tremblay et al., 1989; McMinn, 1996; Sakoh et al., 1997; Thomas et al., 2001). The sediment traps are suspended on a line anchored to the overlying sea ice. Traps can be sampled manually, as frequently as necessary, through a hole in the ice, or can be equipped with collection cups that rotate at pre-set intervals. Many of these studies are designed to focus on specific connections between the sea ice and the underlying water column and sea floor. These are discussed in more detail later in this chapter. Investigations range from studies of the role of ice algae in seeding open water blooms (as McMinn, 1996), the source of organic matter enriched in ^{13}C (Thomas et al., 2001), and the importance of ice algae as a food source for pelagic zooplankton (Michel et al., 1996).

For longer-term and/or year-round information, moored arrays with automatically rotating collection cups (Fig. 10.1) can allow for comparison of flux between ice-covered and ice-free conditions (Hebbeln & Wefer, 1991; Hebbeln, 2000; also see review in Honjo (1990) and Table 10.1). These sediment traps are anchored in place via a mooring line stretched between a bottom weight at the sea floor and buoyancy floats above. Top floats are usually placed deep enough below the sea surface such that drifting icebergs with deep drafts will not catch on the floats and destroy the mooring. The mooring is typically attached to the bottom anchor with an acoustic release, so that the mooring can float free to the surface for recovery, once the acoustic release is opened. A typical mooring design is illustrated in Fig. 10.2.

In the Arctic, systematic deployment of sediment traps has focused on the Nordic Seas, including the Greenland, Norwegian and Barents Seas (data summarized by Honjo, 1990; Table 10.1). In the Antarctic, many major research programmes have had a strong sediment trap component:

- Antarctic Peninsula region (Wefer et al., 1982; Dunbar, 1984; Gersonde, 1986; Gersonde & Wefer, 1987; RACER [Research on Antarctic Coastal Ecosystem Rates] – Karl et al., 1991; Leventer, 1991; Palmer LTER [Palmer Long Term Ecological Research] – Ross et al., 1996).
- Weddell Sea (Fischer et al., 1988; Wefer et al., 1990).
- Ross Sea (DeMaster et al., 1992; Dunbar & Leventer, 1987; Dunbar et al., 1987, 1988; Leventer & Dunbar, 1996; Dunbar et al., 1998; Langone et al., 2000); ROAVERRS [Research on Ocean–Atmosphere Variability and Ecosystem Response in the Ross Sea], and SOJGOFS [Southern Ocean Joint Global Ocean Flux Study] (Collier et al., 2000; Honjo et al., 2000).

Table 10.1 lists some of the major sediment trap studies that are discussed in this chapter. Both sub-ice deployments and year-round moorings are listed. The year-round trap studies were selected based on their specific reference to seasonal changes in sea ice distribution and its influence on particle flux.

Table 10.1 Selected references on sediment traps deployed in polar seas, discussed in this chapter. Comments: 1 = sub-ice deployment; 2 = moored array with year-round data.

Reference/Year	Location	Dates	Comments
Arctic			
Bathmann et al., 1990	Norwegian Sea	6/86–10/87	2
Berner & Wefer, 1990	Fram Strait	8/84–8/85; 7/87–6/88	2
Berner & Wefer, 1994	Fram Strait, Norwegian Sea	Summary paper	2
Carey, 1987	Beaufort Sea	4/80–6/80	1
Hebbeln, 2000	Fram Strait	7/87–6/90	2
Hebbeln & Wefer, 1991	Fram Strait	7/88–6/89	2
Kohly, 1998	Greenland–Norwegian Sea	6/91–7/92	2
Michel et al., 1996	Canadian Arctic	4/92–6/92	1
Ramseier et al., 1999	Greenland Sea	8/85–8/96	2
Tremblay et al., 1989	Hudson Bay	4/86–5/86	1
Antarctic			
Abelmann & Gersonde, 1991	Antarctic Peninsula, Weddell Sea	1983–1990 summary data	2
Accornero et al., 1999	Ross Sea	1/95–1/96	2
Collier et al., 2000	Ross Sea	11/96–1/98	2
DeMaster et al., 1992	Ross Sea	1/90–2/91	2
Dunbar et al., 1987	Ross Sea	12/84–12/84; 10/86–2/87	1
Dunbar et al., 1998	Ross Sea	1/90–2/92	2
Fischer et al., 1988	Weddell Sea	1/85–3/86	2
Gersonde, 1986	Antarctic Peninsula	12/83–11/84	2
Gersonde & Wefer, 1987	Antarctic Peninsula, Weddell Sea	3/83–12/83	2
Honjo et al., 2000	Western Pacific sector of Southern Ocean	11/96–1/98	2
Langone et al., 2000	Ross Sea	12/94–1/96	2
Leventer & Dunbar, 1987	Ross Sea	10/84–12/84	1
McMinn, 1996	Ellis Fjord, East Antarctica	11/92–12/92	1
Wefer & Fischer, 1991	Atlantic sector of Southern Ocean	1983	2
Wefer et al., 1990	Antarctic Peninsula, Weddell Sea	12/83–11/87	2

Major differences between particle fluxes in the Arctic versus the Antarctic

One key characteristic distinguishing Arctic and Antarctic sea ice is that Arctic ice is predominantly multi-year as contrasted to the more common single-year ice in Antarctica (Dieckmann & Hellmer, Chapter 1). Consequently, a high percentage of particles contained in Southern Ocean sea ice are released into the water column each spring, as the ice melts. In the Arctic, on the other hand, though particle flux from the ice can be seasonal in nature, there is a greater likelihood that particles will be retained in the ice for multiple years, to be released as the multi-year ice decays.

In addition, as described by Pfirman et al. (1989b), while in new ice, lithogenic particles are likely to be distributed evenly through the ice column (a consequence of particles carried with frazil ice during the formation of sea ice), as ice ages and goes through seasonal melt and freeze cycles, the particles will become concentrated at the surface of the ice floes. Then, individual events, such as the draining of a melt pond on the ice surface, waves washing over the ice, or the overturning of an ice floe, can result in the delivery of a large mass of sediment to the sea floor.

The general composition of particulates in sea ice also varies greatly from the Arctic to the Antarctic. In particular, despite regional variability, both lithogenic and carbonate material are usually more abundant in Arctic sea ice than in Antarctic sea ice. Honjo (1990) describes how the multi-year sea ice that crosses the Arctic from the Siberian side out through the Fram Strait via the Transpolar Drift, is very 'dirty' and contains abundant lithogenic particles, much of which might be wind-blown silt and sand carried from places like Northern Greenland and Svalbard, where exposed rock is subject to strong winds. Pfirman et al. (1989a) also describe, for example, how the surface of approximately half the sea ice encountered on a 1986 cruise to the Arctic (84°–86°N), was covered with fine-grained particulate material, mostly lithogenic in origin. This is not to suggest that terrigenous debris is equally distributed over all Arctic sea ice; in particular, ice in regions south of 84°N that are not influenced by the Transpolar Drift, has much lower surface concentrations of debris (Pfirman et al., 1989b).

Much of the Arctic sea ice initially forms in the broad and very shallow continental shelves that rim the Arctic, where the ice is able to incorporate fine-grained material (Pfirman et al., 1990). Sediment is incorporated into the sea ice primarily during the autumn, through frazil ice formation and entrainment of fine-grained sediment from the shallow sea floor (Reimnitz et al., 1993; Eicken et al., 1997). Anchor ice formation may also lift sediment from the sea floor where it will eventually become incorporated into the ice pack. Consequently, lithogenic material entrained in sea ice can comprise a significant portion of the sediment budget in specific regions of the Arctic. For example, Reimnitz et al. (1993), in the Beaufort Sea, estimate a deposition rate of material from the ice of $\sim$2 cm/1000 years, a considerable fraction of the entire sediment budget in a region with an estimated sediment accumulation rate of only 2–3 cm/1000 years. Berner & Wefer (1994) summarize particle flux data from the Fram Strait and the Greenland–Norwegian Sea that demonstrate lithogenic fluxes that range between 54 and 78%, and between 23 and 50%, respectively, of the total mass flux each year.

Sediment trap data support these visual observations of a sea ice surface often characterized by high concentrations of lithogenic material that falls to the sea floor as the ice retreats. Data presented from the Fram Strait, between Greenland and Svalbard (Honjo, 1990; Hebbeln & Wefer, 1991), illustrate the early spring flux of sand-sized rock fragments as the overlying sea ice melts. Prior to ice break-out, flux of particles is minimal. However, as melting occurred along the edges of the ice, maximum sedimentation was observed over the sediment trap sites (Hebbeln &

Wefer, 1991). The timing of maximum lithogenic sediment flux can vary regionally however. For example, high winter-time lithogenic flux was described by Hebbeln (2000) in sediment traps from the eastern Fram Strait. This was attributed to the southward movement of drifting ice over the trap site, where it came in contact with waters warm enough to melt the ice and release the entrained lithogenic particles.

In contrast, lithogenic debris comprises only a small fraction of the particulate matter in Antarctic sea ice, for two primary reasons. First, most of the Antarctic continental shelf is remarkably deep, with an average shelf depth of 500 metres (Johnson et al., 1982). Given these water depths, entrainment of lithogenic material from the sea floor via frazil ice formation and/or anchor ice formation, does not occur on any significant scale. Second, the Antarctic continent is 98% covered by ice, so only a limited amount of debris is available to be wind blown. Although aeolian-derived material is visible on the sea ice surface in some areas of the Antarctic (Barrett et al., 1983; MacPherson, 1987), the distribution must be extremely limited, given the very small area of bare rock that is exposed. This is not true in the Arctic, an ocean surrounded by continental rock, much of which is exposed to weathering and can be wind blown onto the sea ice, where it will later melt out and settle to the sea floor.

General characteristics of flux – annual particle flux data

Making generalizations about particle flux can be difficult, given the many differences among particle trap experiments, including different kinds of sediment traps with different trapping efficiencies, different water depths at which traps are placed, different post-collection sample treatment, and temporal differences as related to natural interannual variability. However, significant points can be made with regard to total mass flux in the Arctic and Antarctic.

Several studies in the Arctic have been designed to address differences in particle flux as a function of varying ice cover, from ice free to mainly ice covered. Berner & Wefer (1994) present a comprehensive summary of work comparing sediment data from three distinct regions of the Fram Strait which they define as *polar*, *Arctic-Atlantic*, and *ice-margin* types. Their *polar* setting is characterized by long-term and heavy ice cover, as observed in areas bathed by Polar Surface Water. As a consequence of the lengthy duration of ice cover and cold waters, total flux is low. Biogenic production is inhibited and lithogenic flux from sea ice is limited by the small amount of ice melting that takes place. Total flux is seasonal and determined by the timing of primary production and subsequent biogenic flux. On the other end of the spectrum is the *Arctic-Atlantic* type setting, where seasonal ice cover is restricted and both biogenic and lithogenic fluxes are high. Primary production is higher in the Atlantic waters, and as in the *polar* setting, a seasonal pattern for phytoplankton flux is observed. Lithogenic flux occurs when sea ice drifts southward and comes in contact with warm Atlantic waters, melting the ice and releasing large amounts of lithogenic material; a process that can take place even in the winter

(Hebbeln, 2000), resulting in a more aseasonal pattern. In both these settings, lithogenic flux makes up more than 60% of the total flux, highlighting the importance of lithogenic flux in the Arctic. In the '*ice-margin*' setting, both total and lithogenic fluxes are moderate, and are a function of movement of the ice edge. Hebbeln & Wefer (1991) describe how in this setting, increases in both biogenic and lithogenic flux can be detected as the ice margin moves over sediment traps. Total mass flux ranges from $< 8\,g\,m^{-2}\,yr^{-1}$ in the *polar* setting, to $\sim 36.5\,g\,m^{-2}\,yr^{-1}$ in the *ice-margin* setting, to $\ll 36.5\,g/m^{-2}\,yr^{-1}$ in the *Arctic-Atlantic* setting (Berner & Wefer, 1994).

As a comparison to the Fram Strait, where ice cover clearly exerts a strong control on flux, Berner & Wefer (1994) also present a summary of sediment trap data from the Norwegian Sea, from sites that lie outside the average winter ice margin. The data document a total mass flux between ~ 15 and $30\,g\,m^{-2}\,yr^{-1}$; ~ 20–30% of the flux is lithogenic. In general, flux is seasonal, with higher fluxes in the spring and summer, and lower fluxes as primary productivity decreases in the autumn and winter.

Kohly (1998) presents a similar comparison between the Greenland Sea, with variable ice cover, and the ice-free Norwegian Sea. Kohly's (1998) diatom flux data show that biosiliceous flux occurs as a single large pulse in the Greenland Sea, during the period of open water, with extremely low flux recorded under the ice. In the Norwegian Sea, biogenic flux occurs during both summer and autumn blooms, each characterized by different diatom species. Total downward diatom flux in the Greenland Sea exceeds that in the Norwegian Sea (at 500 m water depth), but this large difference in flux is not translated into the sedimentary record, a consequence of the thinner and more easily dissolved diatom frustules in the Greenland Sea, and perhaps their slower settling rate. Ramseier et al. (1999) also use sediment trap data from the Greenland Sea to evaluate the effect of sea ice on particle flux. By comparing flux data with satellite imagery of ice cover, they quantitatively define a Biological Marginal Ice Zone that is the site of maximum flux of biogenic particles.

Sediment trap studies in the Southern Ocean report both highly seasonal variability in flux, as well as very large regional differences in total flux (Table 10.2). In addition, it is important to note that a large proportion of the total mass flux, which is primarily biogenic and not lithogenic, is not sourced directly from the sea ice, but is related to seasonal open water phytoplankton blooms. Winter-time downward fluxes are almost universally low. For example, negligible flux was recorded in traps from the Weddell Sea between July 1984 and January 1985 (Fischer et al., 1988). Measurable, but extremely low, fluxes were similarly observed during the winter-time in the Bransfield Strait (Wefer et al., 1990) and the Ross Sea (Dunbar et al., 1998; Accornero et al., 1999; Collier et al., 2000; Honjo et al., 2000; Langone et al., 2000). In general, flux does not begin to increase until ice retreat has taken place, and there can be a fairly significant time delay between ice retreat and peak flux. Fischer et al. (1988) note a 10-week delay, for example, in the northern Weddell Sea in the spring of 1985, and Dunbar et al. (1998) note that peak particle flux occurred

Table 10.2 Selected total mass flux data from Antarctica, based on sediment trap samples. * = average based on carbon and silicon flux data

Reference/Year	Location	Total mass flux ($g\,m^{-2}\,yr^{-1}$)
Fischer et al., 1988	Bransfield Strait	107.7
Wefer et al., 1990	Bransfield Strait	60
Fischer et al., 1988	Weddell Sea	0.37
Honjo et al., 2000	Western Pacific sector, ~63°S, 170°W	80.6
Honjo et al., 2000	Western Pacific sector, ~66°S, 170°W	27.6
Accornero et al., 1999	Ross Sea	6.18
Collier et al., 2000	Ross Sea	17.26–87.6
Dunbar et al., 1998	Ross Sea	35*
Langone et al., 2000	Ross Sea	3.93–30.0

between 2 and 12 weeks after the ice had retreated from sites in the Ross Sea. They attributed this delay to intense wind mixing of the upper water column following ice break-out, and point out that earlier blooms can form if winds are less energetic (Dunbar et al., 1998).

Peak flux is concentrated over a very short time period, and is associated with ice-free as opposed to ice-covered conditions. For example, in the Bransfield Strait, more than 95% total of the annual flux was recorded over a 1–2 month period (Wefer et al., 1990). Abelmann & Gersonde (1991) similarly recorded biosiliceous flux as distinct pulses of 2–9 weeks' duration, during the period of open water in the northern Antarctic Peninsula and Weddell Sea. In the Ross Sea, Accornero et al. (1999) measured 93% of total flux between December 1995 and March 1996, and Langone et al. (2000) measured 99% of the annual flux in only 3 months. Given that particle flux in the Antarctic is largely biogenic in origin, seasonal variability is driven by factors that control primary production, including light and nutrient availability. Regionally, total mass flux is extremely variable, with lowest values recorded in the Weddell Sea and values several times higher in all other areas studied (Table 10.2).

General characteristics of flux – particle chemistry

The chemical composition of material incorporated into the ice is significant for several reasons; two of these are addressed here. First, several authors (Martin, 1990; Sedwick & DiTullio, 1997; Collier et al., 2000; Edwards, 2002) have speculated on the role of iron released from sea ice as it melts (the iron may be contained in the overlying snow cover) in driving high primary productivity along the ice-receding ice edge. Sedwick & DiTullio (1997) for example, conducted iron-enrichment

bottle-incubation experiments in the Ross Sea. The experiments were completed first under conditions of melting sea ice and later in ice-free conditions. Their results showed a significant increase in iron concentrations in the presence of melting sea ice and a subsequent increase in algal biomass. The authors suggest that the seasonal release of iron from melting sea ice may be a factor responsible for the occurrence of algal blooms in the marginal ice zone. Similarly, Collier et al. (2000) observed that opal fluxes in their Ross Sea sediment traps were associated with iron export pulses. They state, 'While uncertainties about specific processes that introduce Fe to the Ross Sea ecosystem remain, our observations suggest a connection between opal export, availability of Fe, and the presence of ice. Peak fluxes of opal and iron, as well as fractionated Fe/Al values are associated with partial ice cover.' They suggest that a possible source for the iron is via aeolian material blown onto sea ice and/or its snow cover.

At a greater distance from any continental source, Lescher et al. (1997), working in the Atlantic region of the Antarctic, did not find sea ice to be a source of iron. Extremely low lithogenic fluxes captured by sediment traps deployed in the western Pacific sector of Antarctica (Honjo et al., 2000), suggest the same, that melting sea ice does not supply iron that in turn initiates phytoplankton blooms. In fact, Honjo et al. (2000) suggest that ultimately the strong stratification that results from ice melt may eventually limit production, by preventing upward mixing of iron. The difference between these two findings, the Ross Sea versus the open ocean, may be a function of proximity to a source for wind-blown debris.

While many authors have discussed the critical importance of a relatively fresh meltwater lens in stratifying the water column adjacent to the retreating ice edge, and the role of this physical stratification in driving large phytoplankton blooms (El-Sayed, 1971; Alexander & Niebauer, 1981; Sakshaug & Holm-Hansen, 1984; Niebauer & Alexander, 1985; Smith & Nelson, 1985, 1986; Nelson et al., 1987; Sullivan et al., 1988; Sakshaug & Skjoldal, 1989; Comiso et al., 1990; Lancelot et al., 1991a, b; Bianchi et al., 1992; Schloss & Estrada, 1994), the potential role of released micronutrients, such as iron, cannot be ignored. Clearly the question of iron concentrations in sea ice and its role in driving ice edge blooms deserves additional study. Within this context, regional differences must be considered as well, with continental shelf versus deep-sea sites perhaps quite different from one another based on differences in the sediment load of the sea ice and overlying snow.

Second, the distinctive chemistry of biogenic material released from the sea ice may be a tool that can be used to trace the extent of sea ice over time. While the reconstruction of the history of sea ice extent is addressed in Chapter 11 (Armand & Leventer), the isotopic characteristics of particulate organic carbon in the sea ice is briefly reviewed here. Several researchers have shown an enrichment in the ^{13}C of particulate organic carbon from the sea ice (Fischer, 1991; Rau et al., 1991; Rogers & Dunbar, 1993; Rogers, 1995; Gibson et al., 1999; Villinski et al., 2000; Kennedy et al., 2002). The degree of enrichment varies, from $-8‰$ measured in fast ice from McMurdo Sound, Antarctica (Rogers & Dunbar, 1993) and Prydz Bay, Antarctica

(Gibson et al., 1999), to −11‰ in pack ice from the Bellingshausen, Amundsen and Ross Seas (Rogers, 1995), to −18‰ in Antarctic pack ice (Fischer, 1991; Rau et al., 1991). Wada et al. (1987) suggested that this enrichment was a function of high algal growth rates and depletion of dissolved carbon dioxide in the sea ice environment, which can be restricted from rapid exchange with sea water (Kennedy et al. 2002; Thomas & Papadimitriou, Chapter 9). Contrary data are presented by Thomas et al. (2001), who did not observe a significant carbon isotopic enrichment in organic material contained in sea ice from the Weddell Sea. However, they suggest that their data, which are based on measurements of the isotopic composition of sediment trap material, much of which was derived from faecal pellets, may be biased toward organic material that originated at the outer edges of the platelet layer where conditions are much less restricted, hence the lack of carbon isotopic enrichment. Although more work needs to be done, the potential for tracking sea ice through time as a function of carbon isotopic enrichment in sediments, remains a strong possibility (Gleitz et al. 1995; Gibson et al., 1999; Villinski et al., 2000).

Mechanisms of settling

Biogenic particles released from the sea ice may settle as individual particles, via faecal pellets produced by a variety of pelagic grazers, or as millimetre-sized aggregates, termed 'marine snow'. Repackaging as either pellets or marine snow will greatly increase settling rates (Alldredge & Silver, 1988), increasing the likelihood that biogenic material will reach the sea floor. Honjo (1990) suggests that the formation of amorphous aggregates may be relatively more important in terms of increasing downward flux rates in the Arctic, while pellet production may play a more important role in the Southern Ocean, in particular, in the southern Atlantic sector where dense krill concentrations are often observed. Particles that remain suspended in the upper water column are more likely to be available to serve as a seed population or as food for pelagic grazers.

Grazing by many species of zooplankton and subsequent pellet production has been reported in a number of studies, though a specific link to grazing of material released from the ice is not always apparent. Dunbar et al. (1998) note that faecal pellets and particle aggregates account for 4–70% of mass flux during peak summer events in the Ross Sea, with most of the pellets attributed to grazers other than krill. Von Bodungen (1986) observed the production of large, string-shaped krill pellets, averaging 160 μm in diameter and between 300 and 1200 μm in length, in the Bransfield Strait, and calculated that 45% of the primary productivity in late November to early December 1983 was lost via grazing. The field area was completely ice free during this time period, hence it is not clear if krill pellet production had a specific and significant impact on algae released from the ice. Similarly, Cadée (1992) discusses the significance of grazing by krill swarms in the downward flux of carbon during ice retreat in the Scotia–Weddell Sea. He suggests that while krill faecal pellets may be directly responsible for the flux of carbon to the sea floor,

some of those pellets will be degraded and/or repackaged before reaching the bottom (von Bodungen et al., 1987; Cadée et al., 1992; Gonzalez, 1992).

Scharek et al. (1994), speculate that krill grazing has a significant impact on ice algae, based on observational data of dense concentrations of krill scraping away at algae on the surface of disintegrating ice floes, during a 1986 cruise in the pack ice covered Weddell Sea. Also, Stretch et al. (1988) and Daly (1990) have observed krill, *Euphausia superba*, feeding on algal cells on the under-surface of sea ice in several areas of the Southern Ocean, including the Weddell and Scotia Seas, and waters off the Antarctic Peninsula. More direct data are reported from the Antarctic by Thomas et al. (2001) who noted that faecal pellets in traps underneath fast ice in the Weddell Sea were composed of diatoms from the platelet ice. However, these authors propose that protozoans were the major producers of the pellets rather than larger metazoan grazers. In the Arctic, many studies demonstrate the presence of ingested ice algae, based on microscopy and the presence of degraded pigments, in zooplankton faecal pellets (Conover et al., 1986; Carey, 1987; Tremblay et al., 1989; Michel et al., 1996).

Similarly, the formation of 'marine snow' has been observed by many researchers (Honjo et al., 1984; Asper & Smith, 1999). Most relevant to this review is the paper by Riebesell et al. (1991), who observed that when algae are released from the ice, they tended to form aggregates at a much higher rate than other algae; within the first 2 hours after release from melted ice, aggregates were observed. They suggest that many species of ice algae are 'inherently sticky', producing an extracellular polysaccharide mucilage that permits attachment to the ice substrate (Palmisano & Sullivan, 1985; Thomas & Papadimitriou, Chapter 9) and also increases their aggregation, even within the brine pockets of the ice (Riebesell et al., 1991). Although sinking rates were different for interior ice and infiltration ice assemblages, both groups settled at a rate of between about 200 and 600 m d^{-1}. Aggregation rates appear to be species specific, with flagellates and the small pennate diatom, *Fragilariopsis cylindrus*, much less common in aggregates. Riebesell et al. (1991) also noted that cells that were metabolically more active and growing tended to remain unaggregated, and thus were more likely to remain suspended. Ice algae that were metabolically less active aggregated to a greater degree, and were thus more likely to flux quickly to deeper waters. This variability in 'stickiness' may play an important role in determining which species of ice algae are most likely to seed a planktonic algal community following ice break-out. For example, the data from Riebesell et al. (1991) may help explain why *F. cylindrus*, a species commonly found in the sea ice and not very 'sticky', is also so successful in exploiting the marginal ice zone (Leventer, 1998).

10.3 Seeding of open water phytoplankton populations by sea ice algae

The question of whether open water and ice edge blooms in polar regions are 'seeded' by algae released from the melting sea ice has been addressed by many

researchers (for example, Horner, 1976; Ackley et al., 1979; Alexander, 1980; Schandelmeier & Alexander, 1981; Garrison et al., 1983; Smith & Nelson, 1986; Wilson et al., 1986; Garrison et al., 1987, 1993). Whether or not these sea ice algae function as a seed population depends on many factors, including the speed at which the particles settle through the water column, the presence of pelagic consumers and the viability of the cells once released from the sea ice.

Critically, if the sea ice algae settle rapidly (Mathot et al., 1991; Riebesell et al., 1991; Michel et al., 1997) or are quickly grazed by pelagic zooplankton and incorporated into rapidly settling pellets (Lancelot et al., 1993b; Scharek et al., 1994; Michel et al., 1996), then the released algal cells never have the chance to serve as an inoculum for an open water phytoplankton bloom. Several studies document situations when seeding did not take place. Mathot et al. (1991), for example, observed the development of a flagellate community following the release of a diatom-dominated sea ice community in the Weddell Sea during the period November 1988 to January 1989 (EPOS II – European Polarstern Study). They suggested that either rapid settling and/or grazing of the diatoms may have been responsible for the shift in the assemblage of primary producers. As previously discussed, Riebesell et al. (1991), working on samples from EPOS 2, conducted experimental work that demonstrated the tendency of some species of sea ice diatoms to form aggregates, with settling rates three orders of magnitude higher than non-aggregated cells. They proposed that rapid settling of these aggregates may be responsible for the lack of seeding observed in this study.

Michel et al. (1997) noted that algae released from annual sea ice in Saroma-Ko Lagoon, in the Sea of Okhotsk, rapidly settled to the sea floor, where the organic particulates were an important source of food for benthic organisms. Given rapid transit out of the water column, no seeding was observed. In addition, a pelagic microbial food network, rather than a diatom-based food web, developed in the water column following ice melt since the sea ice diatoms quickly reached the sea floor and were eaten. It is important to point out that the authors note that water depths in this region are very shallow (average 14.5 metres) so processes occurring here may not be directly applicable to the deeper water areas that are characteristic of a large proportion of the ice-covered areas in both the Arctic and the Antarctic.

Michel et al. (1997) suggest that rapid settling and benthic consumption of sedimented ice algae, as observed in the Sea of Okhotsk, may play a similar ecological role to zooplankton grazing at the polar ice edge, in terms of community development within the water column. Specifically, Michel et al. (1997) are referring to the study by Lancelot et al. (1993b), who describe the development of a nanophytoplankton bloom in the northwestern Weddell Sea, when high grazing pressure quickly removed sea ice diatoms from the upper water column. Michel et al. (1996), working in the Canadian Arctic, also note that algae may remain suspended in the upper water column, but are then eaten by grazers. The removal of released sea ice diatoms from the system by either rapid settling or grazing, and its effect on the structure of the heterotrophic community, is discussed in more detail later in this chapter.

Under conditions where algae released from the sea ice remain in suspension in the upper water column and are not eaten quickly, the possibility of seeding exists. Garrison et al. (1987) outline several criteria that must be met to make a convincing argument for the importance of seeding. First, they note that if the sea ice community serves as the seed for open water populations, then the sea ice algal and planktonic algal assemblages must be taxonomically similar to one another. Numerous studies from both the Arctic and the Antarctic, including those of Schandelmeier & Alexander (1981), Krebs (1983), Garrison & Buck (1985), Smith & Nelson (1985, 1986), Garrison et al. (1987), Garrison & Buck (1989), Wefer et al., (1990), Kang & Fryxell (1992) and Michel et al. (1993), have demonstrated that this is the case. Haecky et al. (1998) make the excellent point that the taxonomic composition of spring blooms in the Baltic Sea differs depending on whether the winter was ice free or ice covered, an observation that supports the role of seeding by sea ice algae. Garrison (1991; Tables 1 and 2) presents an extremely thorough species list of algae (and other micro-organisms) observed in all types of Antarctic sea ice. Many, though not all, of these species are also important components of the plankton, such as *Fragilariopsis curta* and *F. cylindrus* (Leventer & Dunbar, 1987; Wefer et al., 1990; Kang & Fryxell, 1992).

It is important to note that not all studies demonstrate a remarkable similarity between sea ice and water column algal assemblages, although a connection between the two ecosystems is still evident. In these cases, ice edge blooms may be more strongly influenced by the introduction of phytoplankton from other water masses. For example, Bianchi et al. (1992) note that the dominant species in an ice edge bloom in the Weddell Sea (EPOS I) were *Thalassiosira gravida* and *Chaetoceros neglectum*, neither common in the nearby sea ice. They speculate that these species may have been advected from the Bransfield Strait area. However, small *Nitzschia* were also common in the marginal ice zone; presumably these species could have been seeded from melting ice, since species like *F. cylindrus* are extremely common in annual ice. Saito & Taniguchi (1978) also note a mixed sea ice algal/pelagic diatom community in the northern Bering and Chukchi Seas during and after ice melt, reinforcing the finding that even if seeding by ice algae occurs, algae advected from other areas may be of equal or greater importance.

Second, the planktonic species must be incorporated into the sea ice as it forms in the autumn and winter (Garrison et al., 1987). Many studies have addressed the concentration of algae from the plankton into newly forming sea ice (Bunt, 1968; Bunt & Lee, 1970; Garrison et al., 1983, 1986; Ackley et al., 1987; Watanabe & Satoh, 1987; Garrison et al., 1989; Lange et al., 1989; Grossmann & Gleitz, 1993; Gleitz et al., 1994) and the viability of algal cells incorporated into the ice (Gleitz & Thomas, 1992, 1993). Garrison et al. (1989) performed laboratory experiments that demonstrate the ability of ascending ice crystals to scavenge algal cells from the water, though natural concentration exceeds what they were able to reproduce in the lab. They suggest that this may be due to several factors, including the limited temporal and spatial nature of their experiments, as well as the possibility of other

processes, such as Langmuir circulation, that could act in concert to increase the concentration of algal cells in aggregates of frazil ice. In addition, observations such as those made by Gleitz & Thomas (1993), that the concentration of algae in newly formed ice can be 1.5 to 2.5 times greater than their concentration in open water, support the hypothesis that plankton are incorporated into newly forming sea ice.

Smetacek et al. (1992) present another scenario for incorporation of diatoms into sea ice and later seeding of an open water population. They describe a centric algal assemblage, dominated by *Thalassiosira antarctica*, in the Weddell Sea, that was associated with thick platelet ice. They proposed that the ice platelets along with the summer algal bloom cells were incorporated into the seasonal ice cover, and subsequently transported west with the Weddell Sea Gyre. A spring bloom of *T. antarctica* observed in the western Antarctic Peninsula the following spring (von Bodungen, 1986) may have resulted as this advected ice released its incorporated algae to the water column.

Third, the timing of the release of algae in the spring should closely precede the development of the open water bloom (Garrison et al., 1987). As described earlier in this chapter, phytoplankton blooms commonly are associated with the retreating sea ice edge where stable surface layers persist (El-Sayed, 1971; Alexander & Niebauer, 1981; Sakshaug and Holm-Hansen, 1984; Niebauer & Alexander, 1985; Smith & Nelson, 1985, 1986; Nelson et al., 1987; Sullivan et al., 1988; Sakshaug & Skjoldal, 1989; Comiso et al., 1990; Lancelot et al., 1991a, b; Bianchi et al., 1992; Schloss & Estrada, 1994), thus providing a temporal link between the two systems.

Finally, cells released from the ice must be able to survive and grow in open water (Garrison et al., 1987). As stated previously, not all diatom species common in the sea ice are well adapted to life in open water. This topic has been reviewed by Leventer (1998) and is summarized briefly here. Several of the larger diatom species common in congelation ice (a primary component of fast ice), such as *Entomoneis kjellmanii* and *Pleurosigma* sp., for example, do not compete successfully in the ice edge zone, so despite their abundance in sea ice, they do not end up contributing to the phytoplankton community. Several factors may contribute to the inability of some species to survive in an open water setting. First, many of the larger pennate forms found in congelation ice are 'benthic' and may need to remain within or attached to a substrate to survive. Those species with a raphe, such as *Pleuosigma* sp., *Pinnularia quadratarea* and *Navicula glaciei*, may have a competitive advantage within the sea ice, where they are able to move and maintain their position within a favourable environment. This advantage would be lost in the open water environment. Second, many species of ice algae are physiologically 'shade-adapted' (Grossi, 1985; Palmisano & Sullivan, 1985; Grossi et al., 1987; Rivkin & Putt, 1987; Arrigo, Chapter 5), so they may not fare well under the high irradiances of the marginal ice zone. Finally, as Riebesell et al. (1991) have shown, many species of ice algae have a tendency to form sticky aggregates and sink rapidly, taking them quickly out of the photic zone. These factors may help explain why the taxonomic composition of fast ice communities (mostly congelation ice) differs from that characteristic of the

water column, as observed by several studies (Bunt & Wood, 1963; Krebs, 1983; Palmisano & Sullivan, 1983).

Two species in particular, *Fragilariopsis curta* and *F. cylindrus*, are extremely common in both the sea ice and ice edge communities (Garrison & Buck, 1985; Smith & Nelson, 1985; Fryxell, 1986; Fryxell et al., 1987; Garrison et al., 1987; Leventer & Dunbar, 1987; Fryxell et al., 1988, 1989; Garrison & Buck, 1989; Kang & Fryxell, 1991, 1992; Bianchi et al., 1992). Leventer (1998) suggests that these species may succeed not only in the sea ice but also can dominate ice edge blooms, because of their high growth rate and low sinking rate. For example, in Sommer's (1989) work, *F. cylindrus* has the highest growth rate of those species studied. Both species are relatively small (*F. cylindrus* is typically $< 10\,\mu m$ in length, while *F. curta* is slightly longer, averaging $28\,\mu m$ in a Ross Sea ice edge bloom – Wilson et al., 1986) and often occur on only short chains (*F. cylindrus* most commonly as doublets – Kang & Fryxell, 1992; *F. curta* from a 1990 ice edge bloom in the Ross Sea, also most commonly as doublets). Consequently, their settling rates are likely to be low (Smayda, 1970). Their size advantage, coupled to *F. cylindrus*'s tendency not to form aggregates (Riebesell et al., 1991), may give these species a competitive advantage in exploiting the stable upper water column associated with melting sea ice.

Experimental work by Kuosa et al. (1992) documents the process of seeding. In their study, the authors added crushed sea ice to seawater aquaria, to evaluate potential seeding of open water by sea ice microbes. Addition of sea ice with high chlorophyll concentrations resulted in rapid growth of algae in the aquaria, though growth was not immediate (average 6 days later). The genus *Nitzschia* dominated the phytoplankton, in particular, the small *Nitzschia* species. *Fragilariopsis cylindrus*, known to be an important component of sea ice and ice edge blooms, was the dominant contributor to the assemblage in the aquaria, while larger forms of *Nitzschia* failed to flourish.

It is important to note that not all studies demonstrate the viability of sea ice algae, including small forms of *Nitzschia*, when released from the sea ice. For example, McMinn's (1996) work in Ellis Fjord showed a negligible contribution of seeding, most likely because a high percentage (often $> 80\%$) of the *F. cylindrus* cells released from the sea ice were dead. In conclusion, although most data support the hypothesis that algal cells released from the sea ice can serve as a seed population for the ice edge community, not all species are equally adept at life in both ecosystems, nor do all cells have an equal opportunity to act as an inoculum.

10.4 Food for the pelagic community

In Chapter 7, Schnack-Schiel reviews the macrobiology of sea ice. This section builds upon that introduction and focuses on flux of organic carbon from the sea ice, in the form of algal material, as an important source of food for the pelagic grazing

community. It is important to note that the availability of this food source is not limited to the time of ice break-up in the spring, but is also important prior to ice break-up. Data from both the Arctic and the Antarctic suggest that grazing of sea ice algae is an important component of the overwintering strategies of marine zooplankton, such as amphipods, copepods and euphausids (Marschall, 1988). For example, Stretch et al. (1988) and Daly (1990) have observed krill, *Euphausia superba*, feeding on algal cells on the under-surface of sea ice in several areas of the Southern Ocean, including the Weddell and Scotia Seas, and waters off the Antarctic Peninsula.

Bradstreet & Cross (1982) observed sea ice algae (mostly pennate diatoms from the genera *Nitzschia* and *Navicula*) in the gut contents of several species of both amphipods and copepods recovered from under fast ice off Baffin Island, prior to ice melt. The importance of this observation is that under-ice grazing may be a significant source of nutrition to zooplankton over the winter (see also Bedo et al., 1990; Conover & Huntley, 1991). Conover et al. (1986) presented data concerning the Arctic copepod, *Pseudocalanus* sp., and noted opportunistic feeding occurs near the ice–water interface, based on the high phaeophorbide concentration in faecal pellets. They are unsure if the copepods are grazing directly on the algae at the bottom of the ice or from material close to the ice–water interface fluxing out of the ice.

Runge et al. (1991) noted a strong link between the timing and magnitude of the ice algal bloom and copepod life cycles. In their south-eastern Hudson Bay study, copepod feeding occurred both at the ice–water interface and later continued (and increased) at the time of ice melt, when large quantities of sea ice algae were released into the ocean. They confirmed grazing on sea ice algae by the concentration of phaeopigments in their guts, which increased following night-time migration upward to the ice–water interface. Runge & Ingram (1988, 1991) also observed fragmented ice diatoms in copepod guts and noted that increased egg production of dominant copepod species occurred following ice melt. In addition, Runge & Ingram (1988), observed a ten-fold increase in the concentration of phaeopigments in copepod digestive tracts once the interfacial bloom began.

Once sea ice algae are released from the ice, their value as a food source is at least partially dependent on whether the algae are maintained in the upper water column or sink rapidly to deeper waters and the sea floor. Tremblay et al. (1989), working in the south-eastern Hudson Bay in the Canadian Arctic, observed the retention of sea ice algae in suspension following their flux out of melting sea ice, with generally $<2\%$ lost directly to the benthos during the period of study. Moderate levels of grazing were also noted, based on the flux of phaeopigments and the occurrence of faecal pellets. Michel et al. (1996), also assessing the role of ice algal production as a carbon source for zooplankton in the Canadian Arctic, had similar findings. The sea ice communities were monitored via ice cores, Niskin bottles and sediment traps. They conclude first, that zooplankton actively graze on ice algae prior to their release into the water column, based on the high proportion of phaeopigments in

both suspended and sinking material at a time prior to the presence of algal cells in the water. Second, they conclude that a large proportion (>65%) of algal material released from the sea ice remains in suspension long enough to serve as a food source for grazers, despite the fact that senescent cells generally sink out of suspension more rapidly than live ones (Smayda, 1970). They speculate on both biological and physical mechanisms that may be responsible for the continued suspension of algal material, including the physiological state of the cells and the presence of a strong pycnocline. Regardless of the mechanism, Michel et al. (1996) demonstrate that the continued suspension of carbon released from the sea ice supplies food for zooplankton. Subsequent faecal pellet production by these herbivores is the primary means through which the algal material eventually is exported to the sea floor (Michel et al., 1996).

In the Antarctic, the life history of the krill, *Euphausia superba*, is clearly tied to the marginal ice zone (Daly & Macaulay, 1991; Schnack-Schiel, Chapter 7). In addition to an overwintering strategy linked to feeding off ice algae scraped from the underside of annual ice (Stretch et al., 1988; Daly, 1990), numerous studies document krill grazing on ice algae at the ice edge (Stretch et al., 1988; Hamner et al., 1989; Daly, 1990; Siegel et al., 1990; Daly & Macaulay, 1991). Although less data are available on other pelagic grazers in the Southern Ocean, several species of copepods appear to have life cycles that are also tied to the sea ice (Conover & Huntley, 1991; Schnack-Schiel, Chapter 7).

10.5 Community structure in the marginal ice zone as related to sea ice flux

The role of sedimenting ice algae in structuring the community in the marginal ice zone has been discussed indirectly in previous sections. This larger scale picture connecting the pieces of the ecosystem together is the most critical for continued and future study over the next decade. The links between the downward flux of sea ice algae and the open water ecosystem can be divided broadly into three major categories. First, whether the overall composition of the assemblage at the ice edge is diatom based or microbially based is at least partly a function of the fate of the sea ice algae. Lancelot et al. (1993b) propose two scenarios that may partially explain whether diatoms or nanoflagellates dominate the ice edge community. In the Weddell Sea, where large populations of krill overwinter, grazing of sea ice diatoms over the winter by krill might result in limiting the amount of seeding that takes place as the ice retreats; consequently nanoflagellates may dominate the ice edge bloom, resulting in a microbial food web, with correspondingly low phytoplankton concentrations. Where overwintering krill are more sparse, as in the Ross Sea, seeding of the ice edge bloom by algae released from the sea ice may be more common, resulting in high concentrations of phytoplankton, either diatoms or perhaps *Phaeocystis*, that may eventually be grazed by copepods.

Grazing by pelagic zooplankton as the ice retreats is at least as important in limiting the degree of seeding by ice algae. As discussed earlier, if algae released from the ice settle quickly to the sea floor, either as aggregates or in faecal pellets, their role in seeding an open water community may be minimized. For example, during EPOS II, in the north-western Weddell Sea, while the ice assemblages were heterogeneous but dominated by diatoms, the water column was dominated by autotrophic flagellates, always $<15\%$ diatoms (Mathot et al., 1991). Although seeding by sea ice diatoms may have occurred, the taxonomic differences between the sea ice and ice edge communities do suggest the possibility that grazing and/or rapid settling removed the diatoms from the upper water column, possibly a case of size selection at work, since krill appear to feed more effectively on larger particles (Meyer and El-Sayed, 1983; Segawa et al., 1983; Boyd et al., 1984). Although the relative importance of grazing, at any time of year, by krill, copepods or micro-protozoans (Burkill et al., 1995), pellet formation and the formation of rapidly settling aggregates, in the establishment of an ice edge community dominated by either diatoms or nanoflagellates remains to be determined, it is likely that all contribute to the composition of the community found in the marginal ice zone.

As discussed earlier, flux of organic material from the sea ice, both during the winter and as the ice retreats, provides food for pelagic grazers and has been shown to be an important source of carbon, even during the long periods of darkness when photosynthesis is at a minimum. Runge et al. (1991) explore this link in more detail by presenting a strong case for the critical significance of ice algal production in helping define both zooplankton life cycle strategies and larval fish recruitment in Hudson Bay. For example, under-ice grazing by the copepods *Calanus* sp. and *Pseudocalanus* sp. appears to be related to the timing and magnitude of copepod egg production, and to the growth and development of copepodite stages. In turn, the appearance of fish larvae as the ice breaks out appears to be timed to be coincident with the life cycle of the copepods.

Finally, in the most general sense, the role of flux from the sea ice, and the consequent ice edge bloom that may result, must be considered in terms of the upper portion of the polar ecosystem, a topic that has been addressed by many researchers (Ainley & Jacobs, 1981; Fraser & Ainley, 1986; Sakshaug & Skjoldal, 1989). While this paper has focused on the downward flux of particles from the sea ice, and the role that flux plays in lower levels of the food web, clearly, the processes described have a tremendous impact on higher trophic levels, including seabirds, penguins, seals and whales.

10.6 Conclusions

'Particle transport ... controls the transfer of carbon from surface to deep waters, nutrient regeneration, delivery of food to benthic communities, and preservation of sediment records of climate change' (Dunbar et al., 1998). In both the Arctic and the

Antarctic, where seasonal ice cover is an integral component of the ecosystem, particle flux from the sea ice clearly plays an important role. Not only does downward transport of material impact oceanic carbon and silica cycles, flux of materials plays a key role in structuring and shaping the polar ecosystem. As described in this chapter, algae released from the ice can provide a seed community for ice edge and open water blooms, and are a source of food for pelagic grazers. The fate of sedimenting particles also influences community structure of the food web and whether it is diatom or microbially based.

Given the critical role of sediment flux as the connection between different layers of the ocean, particle flux studies in seasonally ice-covered waters are a key ingredient to advancing our understanding of polar oceanic processes. These studies should continue their focus in two directions. First, in order to evaluate the direct impact of particles released from the sea ice on the underlying biological community, there should be an emphasis on more sediment trap studies that sample both the ice and the water column through the period of ice retreat.

Since all ecosystems experience a great deal of interannual variability, continued long-term monitoring of particle flux via moored instruments is necessary. As illustrated in Table 10.1, most studies are just a few years in length, though in selected areas nearly decadal data sets exist. These longer records, with specific reference to the relationship between sea ice and particle flux, will be instrumental in providing the type of information necessary to understand the implications of global change on the polar ecosystem.

References

Abelmann, A. & Gersonde, R. (1991) Biosiliceous particle flux in the Southern Ocean. *Marine Chemistry*, **35**, 503–536.

Accornero, A., Bergamasco, A., Monaco, A. & Tucci, S. (1999) Particle fluxes at the edge of the Ross Ice Shelf: the role of physical forcing. In: *Oceanography of the Ross Sea, Antartica*, (Eds G. Spezie & G.M.R. Guiseppe), pp. 177–195. Springer, Italy.

Ackley, S.F., Buck, K.R. & Taguchi, S. (1979) Standing crop of algae in the sea ice of the Weddell Sea region. *Deep-Sea Research*, **26**, 269–281.

Ackley, S.F., Dieckmann, G. & Shen, H. (1987) Algal and foram incorporation into new sea ice. *EOS, Transactions of the American Geophysical Union*, **68**, 1736.

Ainley, D.G. & Jacobs, S.S. (1981) Sea-bird affinities for ocean and ice boundaries in the Antarctic. *Deep-Sea Research*, **28**, 1173–1185.

Alexander, V. (1980) Interrelationships between the seasonal sea ice and biological regimes. *Cold Regions Science and Technology Reports*, **2**, 157–178.

Alexander, V. & Niebauer, H.J. (1981) Oceanography of the Bering Sea ice-edge zone in spring, *Limnology and Oceanography*, **26**, 1111–1125.

Alldredge, A.L. & Silver, M.W. (1988) Characteristics, dynamics, and significance of marine snow. *Progress in Oceanogr*aphy, **20**, 41–82.

Asper, V.L. & Smith, W.O., Jr. (1999) Particle fluxes during austral spring and summer in the southern Ross Sea, Antarctica. *Journal of Geophysical Research*, **104**, 5345–5359.

Barrett, P.J., Pyne, A.R. & Ward, B.L. (1983) Modern sedimentation in McMurdo Sound, Antarctica. In: *Antarctic Earth Sciences*, (Eds R.L. Oliver, P.R. James & J.B. Jago), pp. 550–554. Australian Academy of Science, Canberra, Australia.

Bathmann, U.V., Peinert, R., Noji, T.T. & von Bodungen, B. (1990) Pelagic origin and fate of sedimenting particles in the Norwegian Sea. *Progress in Oceanography*, **24**, 117–125.

Bedo, A.W., Head, E.J.H., Conover, R.J., Horne, E.P.W. & Harris, L.R. (1990) Physiological adaptation of an under-ice population of *Pseudocalanus* in Barrow strait (NWT) to increasing food supply in the spring. *Polar Biology*, **10**, 561–570.

Berner, H. & Wefer, G. (1990) Physiographic and biologic factors controlling surface sediment distribution in the Fram Strait, In: *Proceedings of the 1988 NATO Advanced Research Workshop on Geological History of the Polar Oceans; Arctic versus Antarctic. NATO ASI Series C: Mathematical and Physical Sciences*, **308**, 317–335.

Berner, H. & Wefer, G. (1994) Clay-mineral flux in the Fram Strait and Norwegian Sea. *Marine Geology*, **116**, 327–345.

Bianchi, F., Boldrin, A., Cioce, F., Dieckmann, G., Kuosa, H., Larsson, A.-M., Nöthig, E.-M., Sehlstedt, P.-I., Socal, G. & Syvertsen, E.E. (1992) Phytoplankton distribution in relation to sea ice, hydrography and nutrients in the northwestern Weddell Sea in early spring 1988 during EPOS. *Polar Biology*, **12**, 225–235.

von Bodungen, B. (1986) Phytoplankton growth and krill grazing during spring in the Bransfied Strait, Antarctica – implications from sediment trap collections. *Polar Biology*, **6**, 153–160.

von Bodungen, B., Fischer, G., Nöthig, E.M. & Wefer, G. (1987) Sedimentation of krill faeces during spring development of phytoplankton in Bransfield Strait, Antarctica. *Mitteilungen des Geologisch-Paläontologischen Instituts der Universität Hamburg (Sonderband)*, **62**, 243–257.

Boyd, C.M., Heyraud, M. & Boyd, C.N. (1984) Feeding of the Antarctic krill *Euphausia superba*. *Journal of Crustacean Biology*, **4**, 123–141.

Boyd, P.W., Robinson, C., Savidge, G. & Williams, P.J.le B. (1995) Water column and sea-ice primary production during Austral spring in the Bellingshausen Sea. *Deep-Sea Research*, **42**, 1177–1200.

Bradstreet, M.S.W. & Cross, W.E. (1982) Trophic relationships at high Arctic ice edges. *Arctic*, **35**, 1–12.

Bunt, J.S. (1968) Microalgae of the Antarctic pack ice zone. In: *Symposium on Antarctic Oceanography*, (Ed. R.I. Currie), pp. 198–218. W. Heffer & Sons, Cambridge.

Bunt, J.S. & Lee, C.C. (1970) Seasonal primary production in Antarctic sea ice at McMurdo Sound in 1967. *Journal of Marine Research*, **28**, 304–320.

Bunt, J.S. & Wood, E.J.F. (1963) Microalgae and Antarctic sea-ice. *Nature*, **199**, 1254–1255.

Burkill, P.H., Edwards, E.S. & Sleigh, M.A. (1995) Microzoooplankton and their role in controlling phytoplankton growth in the marginal ice zone of the Bellingshausen Sea. *Deep-Sea Research*, **45**, 1277–1290.

Cadée, G.C. (1992) Organic carbon in the upper layer and its sedimentation during the ice-retreat period in the Scotia-Weddell Sea, 1988. *Polar Biology*, **12**, 253–259.

Cadée, G.C., Gonzalez, H. & Schnack-Schiel, S. (1992) Diet affects sinking rate of krill faecal strings. *Polar Biology*, **12**, 75–80.

Carey, A.G., Jr (1987) Particle flux beneath fast ice in the shallow southwestern Beaufort Sea, Arctic Ocean. *Marine Ecology Progress Series*, **40**, 247–257.

Collier, R., Dymond, J., Honjo, S., Mangonini, S., Francois, R. & Dunban, R. (2000) The vertical flux of biogenic lithogenic material in the Ross Sea: moored sediment trap observations 1996–1998. *Deep-Sea Research*, **47**, 3491–3520.

Comiso, J.C., McClain, C.R., Sulllivan, C.W., Ryan, J.P. & Leonard, C.L. (1993) Coastal zone color scanner pigment concentrations in the Southern Ocean and relationships to geophysical surface features. *Journal of Geophysical Research*, **98**, 2419–2451.

Comiso, J.C., Maynard, N.G., Smith, W.O., Jr & Sulllivan, C.W. (1990) Satellite ocean color studies of Antarctic ice edges in summer/autumn. *Journal of Geophysical Research*, **95**, 9481–9496.

Conover, R.J., Herman, A.W., Prinsenberg, S.J. & Harris, L.R. (1986) Distribution and feeding by the copepod *Pseudocalanus* under fast ice during the Arctic spring. *Science*, **232**, 1245–1247.

Conover, R.J. & Huntley, M. (1991) Copepods in ice-covered seas – distribution, adaptations to seasonally limited food, metabolism, growth patterns and life cycle strategies in polar seas. *Journal of Marine Systems*, **2**, 1–41.

Daly, K.L. (1990) Overwintering development, growth and feeding of larval *Euphausia superba* in the Antarctic marginal ice zone. *Limnology and Oceanography*, **35**, 1564–1576.

Daly, K.L. & Macaulay, M.C. (1991) Influence of physical and biological mesoscale dynamics on the seasonal distribution and behavior of *Euphausia superba* in the Antarctic marginal ice zone. *Marine Ecology Progress Series*, **79**, 37–66.

DeMaster, D.J., Dunbar, R.B., Gordon, L.I., Leventer, A.R., Morrison, J.M., Nelson, D.M., Nittrouer, C.A. & Smith, W.O., Jr (1992) Cycling and accumulation of biogenic silica and organic matter in high-latitude environments: the Ross Sea. *Oceanography*, **5**, 146–153.

Dunbar, R.B. (1984) Sediment trap experiments on the Antarctic continental margin. *Antarctic Journal of the United States*, **19**, 70–71.

Dunbar, R.B. & Leventer, A. (1987) Sediment fluxes beneath fast ice: October, 1986 through February, 1987. *Antarctic Journal of the United States*, **22**, 112–114.

Dunbar, R.B., Leventer, A.R. & Mucciarone, D.A. (1998) Biogenic sediment fluxes in the Ross Sea, Antarctica: atmospheric and sea ice forcing. *Journal of Geophysical Research*, **103**, 30741–30760.

Dunbar, R.B., Leventer, A.R. & Stockton, W.L. (1987) Biogenic sedimentation in McMurdo Sound, Antarctica. *Marine Geology*, **85**, 155–179.

Edwards, R. (2002) The iron content of seasonal sea-ice: a biologically-significant source of iron to the Southern Ocean? Abstract from *2002 Ocean Sciences Meeting, Honolulu, Hawaii, 11–15 February 2002*. American Geophysical Union, Washington, D.C.

Eicken, H., Reimnitz, E., Alexandrov, V., Martin, T., Kasser, H. & Vichoff, T. (1997) Sea-ice processes in the Laptev Sea and their importance for sediment export. *Continental Shelf Research*, **17**, 205–233.

El-Sayed, S. (1971) Observations on phytoplankton bloom in the Weddell Sea. In: *Biology of the Antarctic Seas*, Vol. IV, (Eds G.A. Llano & J.E. Wallen), American Geophysical Union, Washington, D.C. *Antarctic Research Series*, **17**, 310–312.

Fischer, G. (1991) Stable carbon isotope ratios of plankton carbon and sinking organic matter from the Atlantic sector of the Southern Ocean. *Marine Chemistry*, **35**, 581–596.

Fischer, G., Futterer, D., Gersonde, R., Honjo, S., Ostermann, D. & Wefer, G. (1988) Seasonal variability of particle flux in the Weddell Sea and its relation to sea ice cover. *Nature*, **335**, 426–428.

Fraser, W.R. & Ainley, D.G. (1986) Ice edges and seabird occurrence in Antarctica. *BioScience*, **36**, 258–263.

Fryxell, G.A. (1986) Microalgae at the ice edge in the northern Weddell Sea. *Antarctic Journal of the United States*, **21**, 166–168.

Fryxell, G.A., Kang, S.-H. & Ashworth, T.K. (1989) AMERIEZ 1988 and ODP Leg 119: Antarctic summer and winter stage indicators. *Antarctic Journal of the United States*, **24**, 156–157.

Fryxell, G.A., Kang, S.-H. & Reap, M.E. (1987) AMERIZ 1986: Phytoplankton at the Weddell Sea ice edge. *Antarctic Journal of the United States*, **22**, 173–175.

Fryxell, G.A., Reap, M.E. & Kang, S.-H. (1988) Antarctic phytoplankton dominants, life stages, and indicators. *Antarctic Journal of the United States*, **23**, 129–131.

Garrison, D.L. (1991) Antarctic sea ice biota. *American Zoologist*, **31**, 17–33.

Garrison, D.L., Ackley, S.F. & Buck, K.R. (1983) A physical mechanism for establishing algal populations in frazil ice. *Nature*, **306**, 363–365.

Garrison, D.L. & Buck, K.R. (1985) Sea-ice algal communities in the Weddell Sea: species composition in ice and plankton assemblages. In: *Marine Biology of Polar Regions and Effects of Stress on Marine Organisms*, (Eds J.S. Gray & M.E. Christiansen), pp. 103–122. John Wiley and Sons, New York.

Garrison, D.L. & Buck, K.R. (1989) The biota of Antarctic pack ice in the Weddell Sea and Antarctic Peninsula regions. *Polar Biology*, **10**, 211–219.

Garrison, D.L., Buck, K.R. & Fryxell, G.A. (1987) Algal assemblages in Antarctic pack ice and in ice-edge plankton. *Journal of Phycology*, **23**, 564–572.

Garrison, D.L., Buck, K.R. & Gowing, M.M. (1993) Winter plankton assemblage in the ice edge zone of the Weddell and Scotia Seas: composition, biomass and spatial distributions. *Deep-Sea Research*, **40**, 311–338.

Garrison, D.L., Close, A.R., & Reimnitz, E. (1989) Algae concentrated by frazil ice: evidence from laboratory experiments and field measurements. *Antarctic Science*, **1**, 313–316.

Garrison, D.L., Sullivan, C.W. & Ackley, S.F. (1986) Sea ice microbial communities in Antarctica. *BioScience*, **36**, 243–250.

Gersonde, R. (1986) Biogenic siliceous particle flux in Antarctic waters and its palaeoecological significance. *South African Journal of Science*, **82**, 500–501.

Gersonde, R. & Wefer, G. (1987) Sedimentation of biogenic siliceous particles in Antarctic waters from the Atlantic sector. *Marine Micropaleontology*, **11**, 311–332.

Gibson, J.A.E., Trull, T., Nichols, P.D., Summons, R.E. & McMinn, A. (1999) Sedimentation of ^{13}C-rich organic matter from Antarctic sea-ice algae; a potential indicator of past sea-ice extent. *Geology*, **27**(4), 331–334.

Gleitz, M., Bathmann, U.V. & Lochte, K. (1994) Build-up and decline of summer phytoplankton biomass in the eastern Weddell Sea, Antarctica. *Polar Biology*, **14**, 413–422.

Gleitz, M., Rutgers van der Loeff, M., Thomas, D.N., Dieckmann, G.S. & Millero, F.J. (1995) Comparison of summer and winter inorganic carbon, oxygen and nutrient concentrations in Antarctic sea ice brine. *Marine Chemistry*, **51**, 81–91.

Gleitz, M. & Thomas, D.N. (1992) Physiological responses of a small Antarctic diatom (*Chaetoceros* sp.) to simulated environmental constraints associated with sea-ice formation. *Marine Ecology Progress Series*, **88**, 271–278.

Gleitz, M. & Thomas, D.N. (1993) Variation in phytoplankton standing stock, chemical

composition and physiology during sea-ice formation in the southeastern Weddell Sea, Antarctica. *Journal of Experimental Marine Biology and Ecology*, **173**, 211–230.

Gonzalez, H.E. (1992) Distribution and abundance of minipellets around the Antarctic peninsula. Implications for protistan feeding behaviour. *Marine Ecology Progress Series*, **90**, 223–236.

Grossi, S.M. (1985) *Response of a Sea-Ice Microalgal Community to a Gradient in Under-Ice Irradiance*. PhD dissertation, University of Southern California, Los Angeles.

Grossi, S.M., Kottmeier, S.T., Moe, R.L., Taylor, G.T. & Sullivan, C.W. (1987) Sea ice microbial communities. VI. Growth and primary production in bottom ice under graded snow cover. *Marine Ecology Progress Series*, **35**, 153–164.

Grossmann, S. & Gleitz, M. (1993) Microbial responses to experimental sea-ice formation: implications for the establishment of Antarctic sea-ice communities. *Journal of Experimental Marine Biology and Ecology*, **173**, 273–289.

Haecky, P., Jonsson, S. & Andersson, A. (1998) Influence of sea ice on the composition of the spring phytoplankton bloom in the northern Baltic Sea. *Polar Biology*, **20**, 1–8.

Hamner, W.M., Hamner, P.P., Obst, B.S. & Carleton, J.H. (1989) Field observations on the ontogeny of schooling *Euphausia superba* furciliae and its relationship to ice in Antarctic waters. *Limnology and Oceanography*, **34**, 451–456.

Hebbeln, D. (2000) Flux of ice-rafted detritus from sea-ice in the Fram Strait. *Deep-Sea Research*, **47**, 1773–1790.

Hebbeln, D. & Wefer, G. (1991) Effects of ice coverage and ice-rafted material on sedimentation in the Fram Strait. *Nature*, **350**, 409–411.

Honjo, S. (1990) Particle fluxes and modern sedimentation in the polar oceans. In: *Polar Oceanography, Part B, Chemistry, Biology, and Geology*, (Ed. W.O. Smith, Jr), pp. 687–739. Academic Press, San Diego, California.

Honjo, S., Doherty, K.W., Agrawal, Y.C. & Asper, V.L. (1984) Direct optical assessment of large amorphous aggregates (marine snow) in the deep ocean. *Deep-Sea Research*, **31**, 67–76.

Honjo, S. Francois, R., Manginini, S., Dymond, J. & Collier, R. (2000) Particle fluxes to the interior of the Southern Ocean in the western Pacific sector along 170°W. *Deep-Sea Research*, **47**, 3521–3548.

Horner, R. (1976) Sea ice organisms. *Oceanography Marine Biology, An Annual Review*, **14**, 167–182.

Johnson, G.L., Vanney, J.R. & Hayes, D. (1982) The Antarctic continental shelf – a review paper. In: *Antarctic Geoscience*, (Ed. C. Craddock), pp. 995-1002. University of Wisconsin Press, Madison, Wisconsin.

Kang, S.-H. & Fryxell, G.A. (1991) Most abundant diatom species in water column assemblages from ice ODP Leg 119 drill sites in Prydz Bay, Antarctica: distributional patterns. In: *Proceedings of the Ocean Drilling Program Scientific Reports*, (Eds J. Barron & B. Larsen), pp. 645–666. ODP, College Station, Texas.

Kang, S.-H. & Fryxell, G.A. (1992) *Fragilariopsis cylindrus* (Grunow) Krieger: the most abundant diatom in water column assemblages of Antarctic marginal ice edge zones. *Polar Biology*, **12**, 609–627.

Karl, D.M., Tilbrook, B.D. & Tien, G. (1991) Seasonal coupling of organic matter production and particle flux in the western Bransfield Strait, Antarctica. *Deep-Sea Research*, **38**, 1097–1126.

Kennedy, H., Thomas, D.N., Kattner, G., Haas, C. & Dieckmann, G.S. (2002) Particulate organic carbon in Antarctic summer sea ice: concentration and stable carbon isotopic composition. *Marine Ecology Progress Series*, **238**, 1–13.

Kohly, A. (1998) Diatom flux and species composition in the Greenland Sea and the Norwegian Sea in 1991-1992. *Marine Geology*, **145**, 293–312.

Krebs, W.N. (1983) Ecology of neritic marine diatoms, Arthur Harbor, Antarctica. *Micropaleontology*, **29**, 267–297.

Kuosa, H., Norrman, B., Kivi, K. & Brandini, F. (1992) Effects of Antarctic sea ice biota on seeding as studied in aquarium experiments. *Polar Biology*, **12**, 333–339.

Lancelot, C., Billen, G., Veth, C., Mathot, S. & Becquevort, S. (1991a) Modelling carbon cycling through phytoplankton and microbes in the Scotia–Weddell Sea area during sea ice retreat. *Marine Chemistry*, **35**, 305–324.

Lancelot, C., Mathot, S., Veth, C. & de Baar, H.W.J. (1993a) Factors controlling phytoplankton ice-edge blooms in the marginal ice-zone of the north western Weddell Sea during sea ice retreat 1988: field observations and mathematical modeling. *Polar Biology*, **13**, 377–387.

Lancelot, C., Mathot, S., Becquevort, S., Dandois, J.-M. & Billin, G. (1993b) Carbon and nitrogen cycling through the microbial network of the marginal ice zone of the Southern Ocean with particular emphasis on the north-western Weddell Sea. In: *Belgium Scientific Research Programme on the Antarctic Scientific Results of Phase Two (10/1998–05/1992). Vol. 1. Plankton Ecology and Marine Biogeochemistry* (Ed. S. Caschettu), pp. 1–110. Belgium Science Policy Office, Brussels.

Lancelot, C., Veth, C. & Mathot, S. (1991b) Modelling ice-edge phytoplankton bloom in the Scotia–Weddell Sea sector of the Southern Ocean during spring 1988. *Journal of Marine Systems*, **2**, 333–346.

Lange, M.A., Ackley, S.F., Wadhams, P., Dieckmann, G.S. & Eicken, H. (1989) Development of sea ice in the Weddell Sea. *Annals of Glaciology*, **12**, 92–96.

Langone, L., Frignani, M., Ravaioli, M. & Bianchi, C. (2000) Particle fluxes and biogeochemcal processes in an area influenced by seasonal retreat of the ice margin (Northwestern Ross Sea, Antarctica). *Journal of Marine Systems*, **27**, 221–234.

Legendre, L., Ackley, S.F., Dieckmann, G.S., Gulliksen, B., Horner, R., Hoshiai, T., Melnikov, I.A., Reeburgh, W.S., Spindler, M. & Sullivan, C.W. (1992) Ecology of sea ice biota: 2. Global significance. *Polar Biology*, **12**, 429–444.

Lescher, B.M., de Barr, H.J.W., de Jung, J.T.M., Veth, C. & Dehairs, F. (1997) The distribution of Fe in the Antarctic Circumpolar Current. *Deep-Sea Research*, **44**, 143–187.

Leventer, A. (1991) Sediment trap diatom assemblages from the northern Antarctic Peninsula region. *Deep-Sea Research*, **38**, 1127–1143.

Leventer, A. (1998) The fate of Antarctic 'sea ice diatoms' and their use as paleoenvironmental indicators. In: *Antarctic Sea Ice: Biological Processes, Interactions and Variability*, (Eds M.P. Lizotte & K.R. Arrigo), American Geophysical Union, Washington, D.C. *Antarctic Research Series*, **73**, 121–137.

Leventer, A. & Dunbar, R.B. (1987) Diatom flux in McMurdo Sound, Antarctica. *Marine Micropaleontology*, **12**, 49–64.

Leventer, A. & Dunbar, R.B. (1996) Factors influencing the distribution of diatoms and other algae in the Ross Sea. *Journal of Geophysical Research*, **101**, 18489–18500.

Leventer, A., Dunbar, R.B., Allen, M.R. & Wayper, R.Y. (1987) Ice thickness in McMurdo Sound, Antarctica. *Antarctic Journal of the United States*, **22**, 94–96.

McMinn, A. (1996) Preliminary investigation on the contribution of fast-ice algae to the spring phytoplankton bloom in Ellis Fjord, eastern Antarctica. *Polar Biology*, **16**, 301–307.

MacPherson, A.J. (1987) *The MacKay Glacier/Granite Harbor system (Ross Dependency, Antarctica) – a study in nearshore glacial marine sedimentation*. PhD Dissertation, Victoria University, New Zealand.

McRoy, P.C., Goering, J.J. & Shiles, W.E. (1972) Studies of primary production in the eastern Bering Sea. In: *Biological Oceanography of the Northern North Pacific Ocean*, (Ed. A.Y. Takenouti), pp. 199–216. Idemitsu Shoten, Tokyo, Japan.

Marschall, H.P. (1988) The overwintering strategy of Antarctic krill under the pack ice of the Weddell Sea. *Polar Biology*, **9**, 129–135.

Martin, J.H. (1990) Glacial-interglacial CO_2 change: the iron hypothesis. *Paleoceanography*, **5**, 1–13.

Mathot, S., Becquevort, S. & Lancelot, C. (1991) Microbial communities from the sea ice and adjacent water column at the time of ice melting in the northwestern part of the Weddell Sea. In: *Proceedings of the Pro Mare Symposium on Polar Marine Ecology, Trondheim, 12–16 May 1990*, (Eds. E. Sakshaug, C.C.E. Hopkins & N.A. Oritsland), Norwegian Polar Institute, Tromsø, Norway. *Polar Research*, **10**, 267–275.

Meyer, M.A. & El-Sayed, S. (1983) Grazing of *Euphausia superba* Dana on natural phytoplankton populations. *Polar Biology*, **1**, 193–203.

Michel, C., Legendre, L., Ingram, R.G., Gosselin, M. & Levasseur, M. (1996) Carbon budget of sea-ice algae in spring: evidence of a significant transfer to zooplankton grazers. *Journal of Geophysical Research*, **101**, 18345–18360.

Michel, C., Legendre, L. & Taguchi, S. (1997) Coexistence of microalgal sedimentation and water column recycling in a seasonally ice-covered ecosystem (Saroma-ko Lagoon, Sea Okhotsk, Japan). *Journal of Marine Systems*, **11**, 133–148.

Michel, C., Legendre, L., Therriault, J.-C., Demers, S. & Vandevelde, T. (1993) Springtime coupling between ice algal and phytoplankton assemblages in southeastern Hudson Bay, Canadian Arctic. *Polar Biology*, **13**, 441–449.

Mitchell, B.G. & Holm-Hansen, O. (1991) Observations and modeling of the phytoplankton crop in relationship to mixing depth. *Deep-Sea Research*, **38**, 981–1008.

Nelson, D.M., Smith, W.O., Gordon, L.I. & Huber, B.Q. (1987) Spring distribution of density, nutrients and phytoplankton biomass in the ice-edge zone of the Weddell-Scotia Sea. *Journal of Geophysical Research*, **92**, 7181–7190.

Niebauer, H.J. & Alexander, V. (1985) Oceanographic frontal structuring and biological production at an ice edge. *Continental Shelf Research*, **4**, 367–388.

Palmisano, A.C. & Sullivan, C.W. (1983) Sea ice microbial communities (SIMCO). I. Distribution, abundance, and primary production of ice microalgae in McMurdo Sound, Antarctica in 1980. *Polar Biology*, **2**, 171–177.

Palmisano, A.C. & Sullivan, C.W. (1985) Physiological response of micro-algae in the ice platelet to low light conditions. In: *Antarctic Nutrient Cycles and Food Webs*, (Eds W.R. Siegfried, P.R. Condy & R.M. Laws), pp. 84–88. Springer-Verlag, Berlin.

Pfirman, S., Gascard, J.-C., Wollenburg, I., Mudie, P. & Abelmann, A. (1989a) Particle-laden Eurasian Arctic sea ice: observations from July and August 1987. *Polar Research*, **7**, 59–66.

Pfirman, S., Lange, M., Wollenburg, I. & Schlosser, P. (1990) Sea ice characteristics and the role of sediment inclusions in deep-sea deposition: Arctic–Antarctic comparisons. In: *Geological History of the Polar Oceans: Arctic versus Antarctic*, (Eds U. Bleil & J. Thiede), NATO ASI Series C, Vol. 308, pp. 187–211. Kluwer Academic Publishers, Dordrecht.

Pfirman, S., Wollenburg, I., Thiede, J. & Lange, M. (1989b) Lithogenic sedimentation in Arctic pack ice: potential Aeolian flux and contribution to deep sea sediments. In: *Paleoclimatology and Paleometeorology: Modern and Past Patterns of Global Atmospheric Transport*, (Eds M. Sarnthein & M. Leinen), pp. 463–493. Kluwer, Dordrecht.

Ramseier, R.O., Garrity, C., Bauerfeind, E. & Peinert, R. (1999) Sea-ice impact on long-term particle flux in the Greenland Sea's Odden-Nordbukto region, 1985–1996. *Journal of Geophysical Research*, **104**, 5329–5343.

Rau, G.H., Sullivan, C.W. & Gordon, L. (1991) $\delta^{13}C$ and $\delta^{15}N$ variations in Weddell Sea particulate organic matter. *Marine Chemistry*, **35**, 355–369.

Reimnitz, E., Bornes, P.W. & Weber, W.S. (1993) Particulate matter in pack ice of the Beaufort Gyre. *Journal of Glaciology*, **39**, 131, 186–198.

Riebesell, U., Schloss, I. & Smetakek, V. (1991) Aggregation of algae released from melting sea ice: implications for seeding and sedimentation. *Polar Biology*, **11**, 239–248.

Rivkin, R.B. & Putt, M. (1987) Photosynthesis and cell division by Antarctic microalgae: comparison of benthic, planktonic and ice algae. *Journal of Phycology*, **23**, 223–229.

Rogers, J.C. (1995) *$^{13}C/^{12}C$ ratios in surface water and sea ice organic matter: variability and contributions to the sediments of the Ross Sea, Antarctic*. M.S. Thesis, Rice University, Houston, Texas.

Rogers, J.C. & Dunbar, R.B. (1993) Carbon isotopic composition of particulate organic carbon in Ross Sea surface waters during austral summer. *Antarctic Journal of the United States*, **28**, 81–83.

Ross, R.M., Hofmann, E.E. & Quetin, L.B. (Eds) (1996) *Foundations for Ecological Research West of the Antarctic Peninsula*, American Geophysical Union, Washington, D.C. *Antarctic Research Series*, **70**, 1–448.

Runge, J.A. & Ingram, R.G. (1988) Underice grazing by planktonic, calanoid copepods in relation to a bloom of ice microalgae in southeastern Hudson Bay. *Limnology and Oceanography*, **33**, 280–286.

Runge, J.A. & Ingram, R.G. (1991) Under-ice feeding and diel migration by the planktonic copepods *Calanus glacialis* and *Pseudocalanus minutus* in relation to the ice algal production cycle in southeastern Hudson Bay, Canada. *Marine Biology*, **108**, 217–225.

Runge, J.A., Therriault, J.-C., Legendre, L., Ingram, R.G. & Demers, S. (1991) Coupling between ice microalgae productivity and the pelagic, metazoan food web in southeastern Hudson Bay: a synthesis of results. In: *Proceedings of the Pro Mare Symposium on Polar Marine Ecology, Trondheim, 12–16 May 1990*, (Eds E. Sakshaug, C.C.E. Hopkins, & N.A. Oritsland). *Polar Research*, **10**, 325–328.

Saito, K. & Taniguchi, A. (1978) Phytoplankton communities in the Bering Sea and adjacent seas. 2. Spring and summer communities in seasonally ice-covered areas. *Astarte*, **11**, 27–35.

Sakoh, H., Matsuda, O., Michel, C., Legendre, L., Rajendran, N. & Yamamoto, T. (1997) Temporal variation of chlorophyll-like pigment composition in sinking particles during the ice-covered season in Saroma-ko Lagoon. *Journal of Marine Systems*, **11**, 123–131.

Sakshaug, E. (1989) The physiological ecology of polar phytoplankton. In: *Proceedings of the 6th Conference of the Comite Artique International*, (Eds W.R. Rey & V. Alexander), pp. 61–89. Leiden, E.J. Brill.

Sakshaug, E. & Holm-Hansen, O. (1984) Factors governing pelagic production in polar oceans. In: *Marine Phytoplankton and Productivity, Lecture Notes Coastal and Estuarine Studies*, Vol. 8, (Eds O. Holm-Hansen, L. Bolis & R. Gilles), pp. 1–18. Springer, Heidelberg.

Sakshaug, E. & Skjoldal, H.R. (1989) Life at the ice edge. *Ambio*, **18**, 60–67.

Schandelmeier, L. & Alexander, V. (1981) An analysis of the influence of ice on spring phytoplankton population structure in the southeastern Bering Sea. *Limnology and Oceanography*, **26**, 935–943.

Scharek, R., Smetacek, V., Fahrbach, E., Gordon, L.I., Rohardt, G. & Moore, S. (1994) The transition from winter to early spring in the eastern Weddell Sea, Antarctica: plankton biomass and composition in relation to hydrography and nutrients. *Deep-Sea Research*, **41**, 1231–1250.

Schloss, I. & Estrada, M. (1994) Phytoplankton composition in the Weddell–Scotia Confluence area during austral spring in relation to hydrography. *Polar Biology*, **14**, 77–90.

Sedwick, P.N. & DiTullio, G.R. (1997) Regulation of algal blooms in Antarctic shelf waters by the release of iron from melting sea ice. *Geophysical Research Letters*, **24**, 2515–2518.

Segawa, S., Kato, M. & Murano, M. (1983) Growth, moult and filtering rate of krill in laboratory conditions. *Memoires of the National Institute Polar Research, Special Issue*, **27**, 93–103.

Siegel, V., Bergstron, B., Stromberg, J.O. & Schalk, P.H. (1990) Distribution, size frequencies and maturity stages of krill, *Euphausia superba*, in relation to sea-ice in the northern Weddell Sea. *Polar Biology*, **10**, 549–557.

Smayda, T.J. (1970) The suspension and sinking of phytoplankton in the sea. *Oceanography and Marine Biology, An Annual Rev*iew, **8**, 353–414.

Smetacek, V., Scharek, R., Gordon, L.I., Eicken, H., Fahrbach, E., Rohardt, G. & Moore, S. (1992) Early spring phytoplankton blooms in ice platelet layers of the southern Weddell Sea. *Deep-Sea Research*, **39**, 153–168.

Smetacek, V., Scharek, R. & Nöthig, E.-M. (1990) Seasonal and regional variation in the pelagial and its relationship to the life history of krill. In: *Antarctic Ecosystems. Ecological Change and Conservation*, (Eds K.R. Kerry & G. Hempel), pp. 103-114. Springer-Verlag, Berlin.

Smith, W.O. & Nelson, D. (1985) Phytoplankton bloom produced by a receding ice edge in the Ross Sea: spatial coherence with the density field. *Science*, **227**, 163–166.

Smith, W.O. & Nelson, D. (1986) Importance of ice edge phytoplankton production in the Southern Ocean. *BioScience*, **36**, 251–257.

Sommer, U. (1989) Maximal growth rates of Antarctic phytoplankton: only weak dependence on cell size. *Limnology and Oceanography*, **34**, 1109–1112.

Squire, V.A. (1990) Sea ice: its formation, distribution and properties. In: *Polar Marine Diatoms*, (Eds L.K. Medlin & J. Priddle), pp. 3–8. British Antarctic Survey, Cambridge.

Stretch, J.J., Hamner, P.P., Hamner, W.M., Michel, W.C., Cook, J. & Sullivan, C.W. (1988) Foraging behavior of Antarctic krill *Euphausia superba* on sea ice microalgae. *Marine Ecology Progress Series*, **44**, 131–139.

Sullivan, C.W., McClain, C.R., Comiso, J.C. & Smith, W.O., Jr (1988) Phytoplankton standing crops within an Antarctic ice edge assessed by satellite remote sensing. *Journal of Geophysical Research*, **93**, 12487–12498.

Thomas, D.N., Kennedy, H., Kattner, G., Gerdes, D., Gough, C. & Dieckmann, G.S. (2001) Biogeochemistry of platelet ice: its influence on particle flux under fast ice in the Weddell Sea, Antarctica. *Polar Biology*, **24**, 486–496.

Tremblay, C., Runge, J.A. & Legendre, L. (1989) Grazing and sedimentation of ice algae

during and immediately after a bloom at the ice–water interface. *Marine Ecology Progress Series*, **56**, 291–300.

Veth, C., Lancelot, C. & Ober, S. (1992) On processes determining the vertical stability of surface waters in the marginal ice zone of the north-western Weddell Sea and their relationship with phytoplankton bloom development. *Polar Biology*, **12**, 237–243.

Villinski, J.C., Dunbar, R.B. & Mucciarone, D.M. (2000) Carbon 13/carbon 12 ratios of sedimentary organic matter from the Ross Sea, Antarctica: a record of phytoplankton bloom dynamics. *Journal of Geophysical Research*, **105**, 14163–14172.

Wada, E., Terazaki, M., Kabaya, Y. & Nemoto, T. (1987) ^{15}N and ^{13}C abundances in the Antarctic Ocean with emphasis on the biogeochemical structure of the food web. *Deep-Sea Research*, **34**, 829–841.

Watanabe, K. & Satoh, H. (1987) Seasonal variations of ice algal standing crop near Syowa Station, East Antarctica 1983/84. *Bulletin of the Plankton Society of Japan*, **34**, 143–164.

Wefer, G. & Fischer, G. (1991) Annual primary production and export flux in the Southern Ocean from sediment trap data. *Marine Chemistry*, **35**, 597–613.

Wefer, G., Fischer, G., Futterer, D.K., Gersonde, R., Honjo, S. & Ostermann, D. (1990) Particle sedimentation and productivity in Antarctic waters of the Atlantic sector. In: *Geological History of the Polar Oceans: Arctic versus Antarctic*, (Eds U. Bleil & J. Thiede), pp. 363–379. Kluwer, Dordrecht, The Netherlands.

Wefer, G., Suess, E., Balzer, W., Liebezeit, G., Muller, P.J., Ungerer, C.A. & Zenk, W. (1982) Fluxes of biogenic components from sediment trap deployment in circumpolar waters of the Drake Passage. *Nature*, **299**, 145–147.

Wilson, D.L., Smith, W.O., Jr & Nelson, D.M. (1986) Phytoplankton bloom dynamics of the western Ross Sea ice edge – I. Primary productivity and species-specific production. *Deep-Sea Research*, **33**, 1375–1387.

Chapter 11

Palaeo Sea Ice Distribution – Reconstruction and Palaeoclimatic Significance

Leanne K. Armand and Amy Leventer

11.1 Introduction

Since the 1970s, oceanographers have worked towards reconstructing past oceanographic conditions. One of the most significant studies of its time, the CLIMAP (Climate, Long-Range Investigation, Mapping and Prediction) project, had the goal of reconstructing earth's climate at specific time-slices of the past, such as the Last Glacial Maximum (LGM) 21 000 years ago (CLIMAP Project Members, 1976, 1981). The field of palaeoceanographic research has subsequently thrived, employing increasingly sophisticated methods, more highly resolved records, and a wider suite of proxies. Reconstruction of past sea-surface temperatures and salinities, the position of oceanographic boundaries, palaeoproductivity and palaeo sea ice distribution has become a standard field of research. Specific interest in reconstructing sea ice distribution through time rests upon the role sea ice plays in climate, oceanographic and ecological systems.

Sea ice plays a key role in moderating the exchange of both heat and gas, as carbon dioxide, between the atmosphere and ocean in polar latitudes (Maykut, 1978). By virtue of its high albedo (Grenfell, 1983; Eicken, Chapter 2; Hass, Chapter 3), it also impacts climate, since the reflectivity of sea ice greatly exceeds that of open water. In this way, decreased sea ice extent may have a positive feedback effect on climate change, through the greater absorption of heat by exposed sea water. The location of the ice edge has been shown to influence regional weather patterns in polar regions (Gloersen et al., 1989; Comiso, Chapter 4). Second, the formation of sea ice and consequent brine rejection affects oceanic circulation through the formation of dense water masses (Gordon, 1978; Killworth, 1983; Broecker et al., 1998; Rintoul, 1998; Dieckmann & Hellmer, Chapter 1). This vertical convection of the polar oceans has important consequences on the ventilation of deep waters. Conversely, sea ice melt produces a low salinity meltwater layer that stratifies the upper water column and decreases vertical circulation. Third, polar regions are globally

significant sites of primary productivity, located in the sea ice, open water and in regions of sea ice melt known as marginal ice zones (Smith & Sakshaug, 1990; Arrigo, Chapter 5). Changes in the overall levels and nature of production that govern the transfer of organic material to the sea floor may have significantly influenced global carbon and silica budgets through time (Kumar et al., 1995; Leventer, Chapter 10). These changes are most likely to have included varying proportions of overall production in each of these different settings: the sea ice, ice edge and open ocean.

Palaeoceanographic reconstructions that include estimates of palaeo sea ice extent are, therefore, of great interest to researchers ranging from global climate and ocean circulation modellers to palaeoclimatologists. These reconstructions are particularly significant today as most models of global warming predict that polar regions will warm more rapidly than most of the globe (Budd & Wu, 1998; Warner & Budd, 1998; Matear & Hirst, 1999; Bi et al., 2001), with profound consequences for the sea ice regime. Significantly, sea ice thickness and extent in the Arctic appears to be decreasing (Johannessen et al., 1995; Wadhams, 1995; Rothrock et al., 1999; Vinnikov et al., 1999; Serreze et al., 2000; Wadhams & Davis, 2000; Haas, Chapter 3; Comiso, Chapter 4), though not all researchers have confidence in the trends given the large amount of interannual variability in sea ice (McLaren et al., 1992; Parkinson, 2000). However, this finding of decreased sea ice thickness also reflects instrumental data that cover only several decades. Whether changes in Antarctic sea ice extent are occurring due to global warming are also inconclusive, observed trends relying entirely on the number of years of satellite data used (Watkins & Simmonds, 2000; Comsio & Steffan, 2001; Zwally et al., 2002; Comiso, Chapter 4). Palaeo sea ice distribution data allow scientists to develop a better and very necessary understanding of the relationship between climate change and sea ice, within the context of a longer-term perspective.

The objective of this chapter is to review the methods for reconstructing past sea ice distribution and its seasonal variability based on microfossil assemblage distribution, and geochemical and sedimentological tracers (e.g. ice rafted debris) that have been established for polar regions. In addition, palaeo sea ice reconstruction on time-slices, such as the LGM, and in time-series during the Quaternary will be reviewed.

In general, in both the northern and southern high latitudes, the primary method through which sea ice cover is reconstructed is by using the microscopic remains of marine organisms in marine sediments. For example, the CLIMAP project inferred palaeo sea ice cover by tracking the relative distribution of biosiliceous versus clay-rich sediments, assuming that permanent sea ice cover would inhibit light penetration and the ability of siliceous-tested diatoms to photosynthesize and grow (CLIMAP Project Managers, 1976, 1981). This approach has continued to the present, with diatom data from the Arctic (for example, the northernmost Pacific – Sancetta, 1983; the Nordic Seas – Koç et al., 1993, and Baffin Island – Williams, 1990) and in the circum-Antarctic (Burckle, 1984; Armand, 1997; Burckle &

Mortlock, 1998; Crosta et al., 1998a, b; Armand, 2000; Gersonde & Zielinski 2000). Although diatom assemblage data have been most useful in the Antarctic, in the Arctic (including the northern North Atlantic and Pacific), quantitative analysis of dinocyst assemblages has been a more powerful tool (Rochon et al., 1998, 1999; de Vernal et al., 2000, 2001). Given the large differences in the utility of types of palaeo sea ice proxies that are useful in the northern versus southern polar regions, the Arctic and the Antarctica are reviewed separately.

11.2 Antarctic

Methods for reconstructing past sea ice distribution and seasonal variability

Unlike the Arctic, the Antarctic is uniquely surrounded by ocean and is, thus, subjected to asymmetric and zonally defined atmospheric and oceanographic climatic forcing. Both atmospheric and oceanic systems circulate by bringing warmth from the tropics to the polar regions. The transfer of this heat along with insolation variability in response to changes in the orbital rotations of the earth around the sun, affect the cover and extent of annual sea ice from the Antarctic coast into the Southern Ocean. In turn the cover of sea ice feeds back upon the climate system by reducing heat transfer between the ocean and the atmosphere through its high reflectivity (albedo). We know from modern satellite observations that sea ice extent, thickness and duration undergo considerable variation from year to year (Haas, Chapter 3; Comiso, Chapter 4). Pre-satellite data, predominately reports from whaling records, also indicate that the sea ice edge was located further northward in the past (Parkinson, 1990; De la Mare, 1997; Vaughan, 2000). Yet, of all the climate variables studied that are fundamental to our understanding of climate change in the southern hemisphere, and the earth, sea ice is the least well documented and modelled. Primarily, this has been due to the lack of historical knowledge and importance placed on the Antarctic sea ice regime (Watkins & Simmonds, 2000). Since satellite sea ice records have only been available for the past 30 years, it is upon these annually combined records that reconstruction of the Holocene and Quaternary periods must rely.

Estimates of sea ice in the Southern Ocean have evolved from sedimentological and micropalaeontological studies in the 1970s and are now almost uniquely linked to the study of fossil diatom remains. The focus onto these single-celled microscopic organisms as indicators of sea ice conditions is a product of their abundance in the fossil record, and therefore the sediments surrounding Antarctica. More importantly, their relationship with the sea ice environment upon which many individual species are associated, is key to this emphasis (Horner, 1985; Armand, 1997; Zielinski & Gersonde, 1997; Crosta et al., 1998a; Arrigo, Chapter 5; Lizotte, Chapter 6; Leventer, Chapter 10). In the following sub-sections we describe the approaches

undertaken to document past sea ice cover before examining the results of these methods under time-slice scenarios.

Sedimentological tracers

Lithological changes in the sediments surrounding Antarctica provided the first evidence of the effects of overlying sea ice cover on the sea floor (Lisitzin, 1972). The belt of diatomaceous ooze that surrounds Antarctica (Burckle, 1984) is dominant between 50 and 60°S, and extends both south- and north-ward of the modern maximum winter sea ice edge (Plate 11.1). The earliest sea ice estimates combined biological and lithogical evidence, such that summer sea ice extent was determined by mapping core locations with siliceous clay and silt overlain by Holocene diatomaceous ooze, and winter sea ice extent was delineated by a mid-way point between a faunally identified Polar Front and the summer sea ice boundary (CLIMAP Project Managers, 1976; Hays et al., 1976).

The southern lithological boundary has still yet to be conclusively related to an observed physical boundary. In contrast to the CLIMAP compilations, the boundary has been identified as representing three various entities: the winter sea ice edge in the South Atlantic (DeFelice, 1979; DeFelice & Wise, 1981); a region experiencing greater than 35% annual sea ice cover (Crowley & Parkinson, 1988); or linked with pack ice cover in late spring (i.e. >65% concentration in November, Burckle et al., 1982). It would appear that sea ice cover might not be the only determinant of the southern lithological boundary. A simple overlay of the southern limit of the Upper Circumpolar Deep Water boundary (Orsi et al., 1995; Plate 11.1) suggests that oceanographic and linked primary productivity responses in regions external to the Ross and Weddell Seas may have some bearing on the positioning of the southern lithological boundary.

Hays (1978) believed that estimating maximum winter sea ice extent was best obtained by looking for records of sea ice transported volcanic ejecta in the sediments. He was less concise in describing methods of estimating winter sea ice extent in later work, citing a mixture of ice-rafted debris (IRD) distribution, lithological and sediment rate changes (Cooke & Hays, 1982). There is some evidence that correlations between IRD and abundance of the diatom *Eucampia antarctica* were used for winter sea ice estimates as well as stratigraphic control for glacial periods (Cooke et al., 1977; Burckle, 1984; Burckle & Burak, 1988). This continues today (Bianchi & Gersonde, 2002) even though *Eucampia* abundance is considered unrepresentative of sea ice extent (Fryxell & Prasad, 1990; Armand, 1997; Zielinski & Gersonde, 1997), and also diachronous for stratigraphic control in cores south of the Polar Front (Burckle & Abrams, 1986). The northern lithological silica boundary appears unlikely to be linked directly to sea ice cover. This boundary most likely indicates the summer position of the Sub-Antarctic Front (SAF), having been tied to diatom thermal tolerances and subsequent low primary productivity north of this oceanographic feature (Burckle, 1983; Burckle & Cirilli, 1987). Silica and iron

availability (Sedwick et al., 1997; Clementson et al., 1998; Takeda, 1998) are among other factors that are likely to define the northern lithological boundary. The relationship between the northern lithological boundary and the Sub-tropical Front is evident when viewed against the oceanographic frontal positions of Orsi et al. (1995; Plate 11.1).

IRD abundances were a successful tool in providing additional evidence for sea ice cover in the early stages of this research field. A resurgence of the IRD abundance method has taken place in recent times with two methods of analysis being adopted. The first of these is x-ray analysis of core material and counts of IRD particles greater than 2 mm in size being counted in 1 cm intervals (Grobe, 1987; Kunz-Pirrung et al., 2002). The second method relies on counting particles remaining in sieved fractions such as from $>150\,\mu m$ to 2 mm (Hodell et al., 2001). Both methods purport to represent IRD contribution from melting icebergs. Results from these methods must be interpreted with reference to known iceberg pathways or against sea-surface temperature estimates that may reflect the survivability of ice features.

Microfossil assemblage distribution

Studies of diatom associations with respect to sea ice cover, primarily developed by DeFelice and Burckle in the early 1980s, have since evolved into a major research effort to define past sea ice conditions. Almost all the methods employed today rely on the biogeographic distributions of diatoms and, therefore, their relationships to the sea ice environment to reconstruct Antarctic sea ice. Several methods have been developed in tandem with individual data sets to determine sea ice conditions in the Southern Ocean.

For winter and summer sea ice extents, specific sea ice indicator diatom abundance patterns are employed (Gersonde & Zielinski, 2000; Bianchi & Gersonde, 2002). Sea ice duration, as a month per year coverage estimate, enlists an applied statistical method (i.e. Modern Analogue Technique (MAT): Crosta et al., 1998a, b; Hodell et al., 2001). Another applied statistical method is used to estimate sea ice concentrations (Armand, 1997, 2000; L.K. Armand, S. Barry, W. Howard, J.-J. Pichon, X. Crosta & L.D. Labeyrie, in preparation). The methods are briefly described below.

The summer sea ice edge proxy relies on the combined abundance data of *Fragilariopsis curta* and *F. cylindrus*. Both, well-documented, diatoms exist in sea ice and sea ice melt environments (reviewed in Armand, 1997; Zielinski & Gersonde, 1997). The abundance of these species in moderate to well-preserved core records were ground-truthed by Gersonde & Zielinski (2000) so that combined relative abundances in excess of 3% were considered representative of the averaged maximum extent of winter sea ice in the Weddell Sea. In the same manner, the summer sea ice edge was considered to be defined by relative abundances of *F. oblique-costata* greater than 3%. Application of this proxy is based on the understanding

that the thickly silicified *F. obliquecostata* is apparent in conditions with markedly low sedimentation rates (Gersonde & Zielinski, 2000). Recent ground-truthing of the summer sea ice extent method indicates that the proxy is unique to the Weddell Sea and perhaps should only be applied in this region (L.K. Armand, S. Barry, W. Howard, J.-J. Pichon, X. Crosta & L.D. Labeyrie, in preparation).

Annual sea ice cover and maximum sea ice extents (summer and winter) are determined from application of the MAT to take into account species abundances and their individual relationships to sea ice cover. The basis of this approach is to avoid single representation of the sea ice condition by one or two species, and to use all diatom data available (i.e. generally species with more than 2% relative abundance) to elucidate subtle variations through statistical analysis (Crosta et al., 1998a, b). The MAT compares the diatom assemblage data down-core to a subset of modern core-top analogues within a larger Southern Ocean data set by calculating a dissimilarity coefficient between the down-core sample and the core-top analogue (Prell, 1985; Crosta et al., 1998a). The sea ice estimates provided by MAT are weighted averages of the core-top analogues and each estimate is reported with a standard error of the estimate. The main disadvantages of this method are the need for an extensive distribution of core-top samples for the analogue situations, and problems associated with the dissolution and winnowing in diatom preservation relative to modern and past conditions.

Finally, sea ice concentration (the amount of sea ice cover versus open ocean) estimates are produced by advanced statistical methods (Armand, 1997; L.K. Armand, S. Barry, W. Howard, J.-J. Pichon, X. Crosta & L.D. Labeyrie, in preparation). Here, log transformed and factor analysed diatom counts are modelled against presence and abundance of sea ice via a Generalized Additive Model (GAM – Hastie & Tibshirani, 1990). This allows for non-linear responses between the factors and the mean response. As the data is pseudo-binomial the means are logistically regressed. Backward elimination techniques are applied to select variables (factors and quadratic terms) for each bootstrapped estimation model that provides the sea ice condition estimates (i.e. monthly concentrations and annual sea ice cover). Errors are also provided for each estimate produced.

Within each of the proxy models described above it is also worth noting that two sources of modern sea ice conditions are employed. For the specific sea ice diatom proxies and the MAT method, the authors have sourced the Naval Oceanography Command Detachment (1985) data maps. Under the sea ice concentration method of Armand (1997; L.K. Armand, S. Barry, W. Howard, J.-J. Pichon, X. Crosta & L.D. Labeyrie, in preparation) reference to the Schweitzer (1995) compilation of 13.25 years of satellite sea ice is made. These two sea ice database sources were developed differently. In the 1970s and 1980s, the Navy maps were based mainly on visible and infrared data primarily from AVHRR (Advanced Very High Resolution Radiometer – Comiso, Chapter 4) and so the ice edge was determined quantitatively. In contrast, Schweitzer's compilation is based entirely on passive microwave data and allows for the user to apply the 15% sea ice concentration edge, routinely

enforced by sea ice researchers to take into account weather effects (Gloersen & Cavalieri, 1986; Cavalieri et al., 1995; Comiso, Chapter 4). Thus, biases between the sea ice databases are expected, not only because of the difference in technique, but also because the ice edge is not defined the same way (J.C. Comiso, pers. comm.). This has implications for the way sea ice estimates may vary between the different methodologies presented.

Other tracers

Other notable means of elucidating Antarctic sea ice extents or concentration data have been attempted by Bromwich (1984) and Burckle & Mortlock (1998). Bromwich (1984, pers. comm.) used correlations between stable isotope changes in early Antarctic ice core records, modern snow $\delta^{18}O$ observations and sea ice reappraisals of Burckle et al. (1982), to define the summer and winter sea ice extent. The method requires fresh evaluation in light of advances in ice core recovery and interpretation. Burckle & Mortlock (1998) hypothesized the percentage of biogenic opal in surface sediments could be used to estimate annual sea ice cover as a percentage over a site. They based this approach on the role sea ice plays in manipulating surface water productivity and export in regions partly covered by annual sea ice.

Time-slice palaeo sea ice reconstructions

Holocene (0–10 ka BP)

Satellite sea ice coverage has been available for a little over 30 years now and thus we have a reasonable indication of sea ice extent and variability in the most recent past (Comiso, Chapter 4). Pre-satellite records of sea ice that cover the past 100 years continue to be teased from whaling records (Parkinson, 1990; De la Mare, 1997), penguin population records (Barbraud & Weimerskirch, 2001; Wilson et al., 2001) and methane sulphonic acid (MSA) records from ice cores (M. Curran, T. Van Ommen, V. Morgan, K. Phillips & A. Palmer, in preparation). Most of the pre-satellite records imply that sea ice conditions, as we know them now, were significantly more expansive prior to recent documentation. Yet, upon searching for the most recent of potential sea ice expansions, the Little Ice Age (maximum cold conditions $\sim$180 years BP), historical records in the Antarctic, unlike the Arctic, were lacking and inconclusive (Parkinson, 1990).

De la Mare's (1997) summer sea ice extent determined from whaling ship records suggest a 25% decrease between the mid-1950s and early 1970s. The use of whaling records alone, with lack of reference to historically reported sea ice edge data, was questioned by Vaughan (2000), opening the discussion of whether or not summer sea ice extent had indeed extended so far northward. Covering roughly the same period of time as the De la Mare study, penguin population changes in the Ross Sea

region are presented as a proxy for winter sea ice extent (Wilson et al., 2001). In this study, smaller penguin population numbers were found to be highly correlated to the northward ice extent 5 years earlier, the offset between the parameters being related to the 3–7-year sub-adult survival to breeding capability. The penguin population study suggests sea ice extent was greater in the winter seasons from the 1950s to the early 1970s, whereas in the overlapping satellite record era penguin populations increased relative to a decrease in winter sea ice extent. Wilson et al.'s (2001) work also identified relationships with sea ice concentrations and the Southern Ocean Oscillation Index relevant to penguin life history. Both factors may provide future sources of physical settings in the Antarctic region over the last few centuries. Other recent penguin studies covering the past 50 years expose links between decreased adult survival and diminished annual sea ice extent, and in an opposed sense decreased hatching success with increased winter sea ice extension (Barbraud & Weimerskirch, 2001). It is obvious that the link between sea ice cover and higher predator success is an area where future assessment can play a role in deciphering and potentially ground-truthing the historical regional sea ice and climate conditions in the Antarctic.

One way of confirming the high correlations, historical records and satellite data, is by looking into high-resolution ice core records. A new continuous MSA record from the Law Dome ice core currently provides an insight into maximum winter sea ice extent since the 1840s (M. Curran, T. Van Ommen, V. Morgan, K. Phillips & A. Palmer, in preparation). MSA is the biogenic sulphur compound produced, via atmospheric oxidation, from marine algae occurring in the surface ocean waters. MSA data from the Law Dome ice core show a significant positive relationship with remotely sensed September sea ice extent records since 1973. A drop in MSA levels is observed in the Law Dome ice core since the 1950s and, thus, in the region 80–140°E the September sea ice extent is thought to have decreased by approximately 22%. The data suggest that years with greater sea ice extent (in September) produce more MSA (in summer) as a result of the increased ice-covered ocean area which 'captures' a greater area for the summer biological activity (M. Curran, T. Van Ommen, V. Morgan, K. Phillips & A. Palmer, in preparation). It is anticipated that the MSA record from the Law Dome will stretch back 90 000 years (M. Curran, pers. comm.). Additional studies of varying MSA concentrations in the Holocene are reported from the Taylor Dome (Steig et al., 1998). Steig and colleagues noted a relationship between the elevation of MSA in the ice core and an increase in the abundance of the sea ice related diatom *F. curta* in sediment cores from the western Ross Sea around 6000 years BP.

A recent report of sea ice extensions during the early Holocene and into the mid-Holocene period comes from a core studied in the South Atlantic near Bouvet Island (Hodell et al., 2001). MAT estimates of sea ice extent combined with IRD concentrations suggest sea ice free conditions prevailed between 10 000 years BP and 5000 years BP. After 5000 years BP a dramatic advance of sea ice, a decrease of sea-surface temperatures and an increase in IRD was recorded in line with previous

southern hemisphere records of glacial conditions at this time. Other sea ice proxy records from the South Atlantic covering the Holocene period (equivalent to Marine Isotope Stage (MIS) 1) were presented by Gersonde & Zielinski (2000). They observed sea ice indicator species from cores covering the Sea Ice Zone (SIZ) to the Sub-Antarctic Zone, which support, across their west–east transect, predominately sea ice free conditions during the early Holocene and other warm intervals of MIS 1. Over their north–south transect MIS 1 variations are best observed from a high-resolution core at the current, maximum winter, sea ice boundary near Bouvet Island. This core record reveals an early Holocene warm event and a re-established winter sea ice expansion similar to that present during the mid-Holocene, potentially the same Neoglacial cold phase reported in Hodell et al. (2001).

Early Holocene warmth and decreased sea ice cover is also recorded in the Palmer Deep, Antarctic Peninsula (Leventer et al., 2002), as noted by both increased abundance of the sub-polar form of *E. antarctica*. The mid-Holocene Climatic Optimum observed in Antarctic sediments elsewhere (Shevenell et al., 1996; Taylor et al., 1997; Cunningham et al., 1999; Harris et al., 2001; Leventer et al., 2002; Sjunneskog & Taylor, 2002; Taylor & Sjunneskog, 2002) may be manifest in the decrease of winter sea ice indicator diatoms and increased organic carbon content of many of the cores studied. Recovery of winter sea ice diatom indicator abundances from the warming event to modern abundances and sea ice conditions complete the observations undertaken (Gersonde & Zielinski, 2000). Cores located within the current SIZ reveal less co-ordinated patterns of sea ice coverage from the proxies over the Holocene period, in part a reflection of the low sedimentation recovery during this period.

In the south-east Indian Ocean of the Southern Ocean a core along the 56°S meridian and within the modern Permanently Open Ocean Zone recounts some variability in maximum sea ice cover during the Holocene (MIS 1 – Armand, 1997, 2000; M. Curran, T. Van Ommen, V. Morgan, K. Phillips & A. Palmer, in preparation). Early Holocene sea ice extent at this site was estimated at nearly 4 m yr^{-1} cover with a maximum of 30% September sea ice concentration. Sea ice is thought to have decreased through the mid-Holocene with a subsequent rebound to 2 m yr^{-1} and $\sim$25% September sea ice concentration and then later a decrease to modern conditions of no sea ice cover (i.e. less than 15% = no sea ice cover, Plate 11.2).

Fast ice estimations within Antarctic fjords are evaluated by various indices (McMinn, 1993, 2000). Such fast ice estimations are linked to continental ice sheet advance and retreat, and are currently limited to events within the past 3000 years.

Quaternary (10–1800 ka BP) and Last Glacial Maximum (18-21 ka BP)

Quaternary studies of sea ice cover in the Antarctic are focused at two levels. First, as continuous records of sea ice extent and percentage cover and second, as time-slice events, specifically the Last Glacial Maximum (LGM) in MIS 2. We

concentrate on the LGM records first and then move on to the other records reported over the remainder of the Quaternary period.

The CLIMAP Project Members (1976; 1981) undertook the first major combined effort to describe global conditions of the LGM on earth. Winter sea ice extent was estimated to have migrated northward to the approximate position of the modern Polar Front. Summer sea ice was also projected significantly northward. This latter interpretation was challenged and found to represent spring sea ice conditions when viewed with respect to the modern sea ice cycle (Burckle & Cirilli, 1987). In more recent assessments of the CLIMAP diatom data (Crosta et al., 1998b) and in other studies (Bromwich, 1984; Armand, 1997; Gersonde & Zielinski, 2000) CLIMAP's northward summer sea ice extent was considered overestimated. Current hypotheses suggest summer sea ice extent in the LGM is similar to today's (Bromwich, 1984; Crosta et al., 1998b) or that summer sea ice extent in the South Atlantic was somewhere between the modern maximum winter sea ice extent and the modern maximum summer sea ice extent (Gersonde & Zielinski, 2000). Today, controversy over the actual summer extent of Antarctic sea ice remains since no high-resolution sediment records south of the winter sea ice edge are available to document summer sea ice variability over the Quaternary and Holocene periods.

Winter sea ice extent has now been covered by several studies and the results of the studies are summarized in Plate 11.2. All of the studies have concentrated on variations in the siliceous record in locations between the CLIMAP winter extent boundary and within the modern winter sea ice edge, with the exception of Burckle & Mortlock (1998) who included a sample near the Antarctic continental shelf. Synthesizing the results of the published/in-press records post-CLIMAP is difficult since each of the studies employs varying methodology and databases to derive their sea ice estimates.

In the South Atlantic region the findings of Gersonde & Zielinski (2000) allowed spatial reconstruction of the LGM between 30°W and 0°. By way of their winter sea ice indicator abundance pattern, a slightly reduced winter sea ice edge extent, in the order of 3° latitude, was observed with respect to findings of CLIMAP (1976) and Crosta et al. (1998a; Plate 11.2). The reduced biogenic sedimentation rate and the presence of *F. obliquecostata* in core sediments under and northward by 3° of the modern winter sea ice extent suggested to Gersonde & Zielinski (2000) a predominately sea ice-covered summer sea ice extent in this part of the South Atlantic. Conclusions from Burckle & Mortlock's (1998) biogenic opal content regression with annual percentage of sea ice cover, indicated similar sites in the South Atlantic experienced more extensive sea ice conditions during the LGM than today. Their most northern site in the South Atlantic, with 25–45% annual sea ice cover, is supportive of the Gersonde & Zielinski (2000) slightly less extensive sea ice edge for this sector during the LGM. These findings are consistent with an independent analysis of the modern mean Polar Front location and subsequent position of the modern sea ice edge by Moore et al. (2000). Moore and colleagues suggested the CLIMAP winter sea ice edge was overestimated in some regions and that the

modern bathymetrically tied Polar Front position marked the maximum extent of seasonal sea ice cover ($\pm 1^{\circ}$latitude) and the seasonal sea ice zone around the Southern Ocean during the LGM. At the most southern South Atlantic core site of Burckle & Mortlock (1998), near the modern, maximum winter sea ice edge, 50–70% annual sea ice cover (i.e. 6–8 m yr^{-1}) was estimated for the LGM. This finding does not support Gersonde & Zielinski's (2000) suggestion of predominately sea ice covered (i.e. summer cover) conditions at this latitude at the LGM. A more thorough comparison between the two methods, and their results, is required to substantiate the expression of summer sea ice conditions at the LGM in the South Atlantic.

On the other side of the Southern Ocean, in the south-east Indian Ocean sector, a single study has captured the LGM sea ice signal. Armand (1997) utilized regression techniques to determine sea ice concentration and duration (month/year) data from diatom assemblages. This work has evolved into a non-linear regression technique as described by L.K. Armand, S. Barry, W. Howard, J.-J. Pichon, X. Crosta & L.D. Labeyrie (in preparation). Crosta and colleagues (submitted) also estimate sea ice duration (m yr^{-1}) using the MAT from a core in the same region. In both cores winter sea ice indicator species are present occasionally at >3% abundance levels, whereas the summer sea ice indicator species is not observed. The LGM September sea ice concentration results of Armand (1997; L.K. Armand, S. Barry, W. Howard, J.-J. Pichon, X. Crosta & L.D. Labeyrie, in preparation) are presented in Plate 11.2. Over MIS 2 the highest sea ice concentration estimates are ~65% (with large 95% confidence intervals) indicative of consolidated sea ice cover as observed in pack ice. Armand's study is in agreement with the northward LGM winter sea ice expression of CLIMAP (1976) and Crosta et al. (1998a).

Beyond the LGM time-slice, estimated Quaternary sea ice conditions are few and far between, the most continuous series of sea ice conditions to date being provided by the study of Gersonde & Zielinski (2000) in the South Atlantic. Their appraisal of sea ice edge extents continue back to MIS 10 although their interpretation of sea ice advance and retreat through time are limited back to MIS 5.5. Marine Isotope Stage 6 (~128 ka) would appear, based on the *Fragilariopsis* indices in their cores PS1772-8, PS1649-2 and PS1768-8, to have experienced similar sea ice advance as suggested in both MIS 4 and MIS 2 for the South Atlantic region. New research on seven cores in the Atlantic and western Indian Ocean specifically target sea ice conditions in early MIS 5 and late MIS 6 (Bianchi & Gersonde, 2002). Here their observations also suggest sea ice advance conditions in the late MIS 6 not unlike that of the LGM. Bianchi & Gersonde (2002) conclude that as the reduced sedimentation rate and occurrence of *F. obliquecostata* at 3% abundance levels imply an expansion of summer sea ice cover, that sea ice seasonality was reduced during late MIS 6. Another notable finding in the Bianchi & Gersonde study is the difference in sea ice responses: locations under the influence of the Weddell Gyre indicated a strong extension of sea ice, against those to the east of the gyre in the south-west Indian

Ocean which experienced more stable and less northward extension under the same timeframe.

The MIS 11 warm period is another time-slice event that has received sea ice estimation attention as a result of its analogue to modern and future climate conditions. A South Atlantic study by Kunz-Pirrung et al. (2002) covering MIS 12 to MIS 10 (450–340 ka) using the *Fragilariopsis* abundance indicators of Gersonde & Zielinski (2000), suggests variations in seasonal sea ice cover in the glacial MIS 12 and MIS 10 periods. Sea ice free conditions during the warm MIS 11 (containing the Mid Brunhes Event at 400 ka) are derived from decreases in the abundance of sea ice taxa, increases in open-ocean species, decreases in IRD content and $\sim 2^{\circ}$C warmer than modern sea-surface temperature estimates. Seasonal sea ice cover during both MIS 10 and MIS 12 extended out to the Polar Front not dissimilar to reconstructions in other more recent glacial periods.

The longest record of sea ice estimation was provided by Kaczmarska et al. (1993) employing knowledge of chain formation ratios in the polar and sub-polar varieties of *E. antarctica*. A ratio of intercalary to terminal valves was used to define the northern limit of winter sea ice. The study was located on the Kerguelen Plateau at ODP Leg 119 Site 745B (59°S, 85°E) and projected back to 800 ka, revealing that the first northward expansion of sea ice over the Kerguelen site was around 500 ka. This response is similar to that recorded by Kunz-Pirrung et al. (2002), but would require common proxies to evaluate these surficial similarities. A decrease in the *Eucampia* ratio, as an indicator of increasing winter sea ice cover, continued until 100 000 ka at which point the index remains near or below present day ratio levels observed in surface water plankton distributions. Kaczmarska et al. (1993) also reported the first observation of diatom-derived sea ice cover responsive to oscillations in the earth's obliquity. Although the *Eucampia* ratio held much promise, it has not been employed in sea ice estimation studies, simply due to the fact that the ratio has not been ground-truthed with respect to the distribution of *Eucampia* varieties in the surface sediments around Antarctica (Armand, 2000; Gersonde & Zielinski, 2000).

Palaeo sea ice modelling

Palaeo-modelling of climate conditions in the past, most notably the Last Glacial Maximum (LGM), has been brought about primarily to simulate a climate regime different to the present in the hope of assessing the reliability of General Circulation Models (GCM) for predicting future climate. Initial palaeo-modelling of the LGM within GCM or combined Atmospheric-GCMs (AGCM) was concerned with the role of different boundary conditions, in particular sea-surface temperature (SST) and ice sheet reconstructions in an effort to obtain cooling in the tropical regions as evidenced by coral records (e.g. Ramstein & Joussaume, 1995; Webb et al., 1997). The transport of heat and energy through the oceans and radiative forcings replaced the CLIMAP SST boundary condition in the evolution of GCMs so that simulations

of SST and associated sea ice conditions could be developed (Hewitt & Mitchell, 1997; Webb et al., 1997). Such studies were able to identify the importance of sea ice cover, corresponding albedo effects and sea ice thickness feedbacks within the climate system. In the Hewitt & Mitchell (1997) study near-surface air temperature changes were found to increase the thickness of sea ice cover by ~ 1 m in the Southern Ocean along with a northern extension of the sea ice extent in winter. However, of more notable interest is their conclusion that sea ice extent was not observed to have extended as far as the CLIMAP projection, a topic raised by Moore et al. (2000) and most micropalaeontological-based studies since (see earlier).

Coupled ocean–atmosphere GCMs have tried to elucidate the role of oceanic circulation redistribution, insolation forcings and changes in CO_2 release and uptake to ascertain the cause of oceanic cooling. Some studies maintain oceanic circulation changes were significant factors (Ganopolski et al., 1998), whereas others have asserted changes in the CO_2 uptake and release were more important (Weaver et al., 1998). In both studies sea ice extents were determined for the LGM condition. Weaver et al. (1998) note that their maximum winter sea ice condition was reduced with respect to the Ganopolski et al. (1998) reconstruction.

In Plate 11.3 we show the modelled winter and summer LGM outcomes of Weaver et al. (1998) and Ganopolski et al. (1998) against the palaeontological reconstructions of Crosta et al. (1998a, b) and the modern maximum seasonal sea ice extents of Schweitzer (1995). The LGM winter modelled extents of Ganopolski et al. (1998) are generally in tune with palaeontological evidence in the South Atlantic and South Indian Ocean sectors, whereas in the Pacific sector the Weaver et al. (1998) output has a closer fit to the Crosta et al. (1998a) data. In the region south of Australia and New Zealand neither models approach the palaeontological reconstruction. Under the LGM summer condition, the Ganopolski et al. (1998) model delimits an extended northward sea ice boundary similar to the modern winter sea ice extent. As mentioned earlier, current palaeontological-based hypotheses suggest summer sea ice extent in the LGM was either similar to today's summer extent (Bromwich, 1984; Crosta et al., 1998b) or that the extent was between the modern maximum winter sea ice extent and the modern maximum summer sea ice extent (eg. the South Atlantic, Gersonde & Zielinski, 2000). The Weaver et al. (1998) summer reconstruction appears unrelated to current sea ice observations and does not corroborate with current palaeontological interpretations.

With additional studies the sensitivity of sea ice cover upon GCM outputs has become a sticking point in the feedback to oceanic cooling and variability of oceanic overturning via shifts in deep water formation and expansion of bottom water coverage (Ganopolski et al., 1998; Fieg & Gerdes, 2001). Other hypothetical models of multiple steady states of glacial conditions suggest a shift in the Antarctic freshwater balance near the Polar Front as an important modulator of thermohaline circulation over glacial and interglacial periods (Keeling & Stephens, 2001a, b). However, even in their study the importance of ice-albedo feedback to the growth

of sea ice and southern hemisphere cooling is disclosed as an unknown key to determining oceanic and climate variability. Keeling & Stephens (2001a, b) also suggested that the extended sea ice cover in glacial conditions trapped large amounts of CO_2, which would aid in lowering the atmospheric concentration of CO_2 in the atmosphere during the LGM. Their hypothesis gave no room for sea ice seasonality as shown in micropalaeontological reconstructions (see earlier) and was further found to be lacking reference to the potential outgassing of CO_2 by leads and other deformations in the ice pack brought about by increased winds in the LGM (Morales Maqueda & Rahmstorf, 2002).

Modellers applying AGCMs to the southern hemisphere are more cautious towards extrapolating the use of short-term modern relationships between atmospheric parameters and sea ice cover to previous geological periods (Godfred-Spenning & Simmonds, 1996; Simmonds, 1996; Watkins & Simmonds, 2000). Watkins & Simmonds (1995) suggest that increased sea ice cover and more permanent sea ice would depress air temperature variability seasonally, influence the pressure systems, and consequently decrease the genesis of storms. A recent LGM AGCM (Wyrwoll et al., 2000), based essentially on southern hemisphere storm track proxies, concluded that the enhanced 'cold-pole effect' (strengthened meridional temperature gradient) of the Antarctic and its increased sea ice skirt, provided adequate forcing for poleward movement of the winter westerlies, most notably in the Indian Ocean–Australian sector. Furthermore, winter precipitation over the Australian sector sea ice margin was reduced. Unrelated studies from the Vostok ^{10}Be record have also suggested a reduction of evaporation, and consequently precipitation, in glacial periods (Yiou et al., 1985). Modelling studies continue to support the ideas of increased albedo, and increased thermal gradient between the equator and the poles during the LGM (Gildor & Tziperman, 2000, 2001).

More recent GCMs endeavour to incorporate ice physics and dynamics within the models (Holland et al., 2001; Weaver et al., 2001) yet both related studies imply their reconstructions of modern sea ice conditions and movements are less than satisfactory in the southern hemisphere. Interestingly though, the study of Holland et al. (2001) suggests that competing responses from melting sea ice (i.e. upward heat flux and evaporation making a cold, more saline and denser ocean surface, or increased freshwater flux decreases surface water density) occur as a result of sea ice loss in increasing CO_2 models. The two competing effects on ocean density thus determine Antarctic deep-water formation. GCMs have now moved on to increased CO_2 scenarios. These continue to link major climate change effects with the loss of polar sea ice cover (Hudson & Hewitson, 2001).

The most notable long-term (past 160 ka), sea ice extent GCM-derived prediction was provided by Budd & Rayner (1993). Their predictions of latitudinal maximum and minimum sea ice extents, and thus the magnitude of the seasonal cycle of Antarctic sea ice, show great changes over time in tune with projections of the northern hemisphere continental ice and snow line. They observed that the magnitude of the Antarctic sea ice seasonal cycle varies primarily with changes in the

earth's perihelion (20 ka) and eccentricity (100 ka) cycles, a feature recently re-identified by Gildor & Tziperman (2000, 2001).

When looking to the future of palaeo Antarctic sea ice estimation and modelling, continued concentration on regional sectors for the evaluation of sea ice change or a climate signal is warranted. Parkinson (1992) suggested the Ross Sea and East Antarctic sector would be reasonable choices because of their consistent ice coverage and minimal variability during the winter season. When extending our knowledge of sea ice conditions to the atmospheric features that companion them, Simmonds (1996) argues strongly that there are dangers in further extrapolating estimated sea ice variations back in time to the position of storm tracks. Such caution stems from the current studies on cyclonic processes and sea ice extent which are complex, involve other factors such as heat flux and air temperature and are, thus, limited in interpretation (Simmonds & Wu, 1993; Jones & Simmonds, 1994; Watkins & Simmonds, 1995). However, Simmonds (1996) mentions that connections in sea ice 'concentrations' and synoptic features may in the future elucidate atmospheric relationships and provide past cyclonic structure. Beyond this need for caution we still require models to incorporate palaeo sea ice data (both extent and concentrations) as boundary conditions to help assess the atmospheric forcings and responses that we may only currently glimpse or appreciate in extreme instances in the modern instrumental/satellite record.

11.3 Arctic

Methods for reconstructing past sea ice distribution and seasonal variability

As with records of Antarctic sea ice, historical data on sea ice extent in the Arctic are temporally limited, hence our need to rely on proxy indicators of sea ice extent in order to gain a long-term perspective on changes in the distribution of ice over time. General concern over the 'state of sea ice' in the Arctic has been highlighted by recent reports of decreases in both ice extent (Gloersen & Campbell, 1991; Chapman & Walsh, 1993; Johannessen et al., 1995; Bjorgo et al., 1997; McPhee et al., 1998; Johannessen et al., 1999; Vinnikov et al., 1999) and ice thickness (Rothrock et al., 1999; Haas, Chapter 3) over the past several decades, decreases that have raised an alarm over the possible impact of human-induced climate change. For example, Johannessen et al. (1999) note a reduction in ice extent of $\sim$3% per decade since 1978; Vinnikov et al. (1999) also observe a significant decrease over the past 46 years. Data on sea ice thickness measured from US nuclear submarine missions in 1958 and 1976, and supplemented by more recent data in 1993, 1996 and 1997 from the Scientific Ice Expeditions (SCICEX), demonstrate a mean decrease in ice thickness of 1.3 m, from 3.1 m to 1.8 m, over less than 50 years (Rothrock et al., 1999). In addition to concern over changes in total areal extent of sea ice, and in ice

thickness, the timing of spring ice melt is also a concern, as discussed by Stabeno & Overland (2001), who note the impact of the ice edge zone on primary and secondary productivity in the Bering Sea and point out the role of sea ice as a platform for walrus, polar bears and northern natives.

Satellite-derived records of sea ice extent, however, go back only to the early 1970s, with continuous microwave-derived satellite records from the Nimbus-7 Scanning Multichannel Microwave Radiometer (SMMR) and from the Special Sensor Microwave/Imagers (SSM/I) (Comiso, Chapter 4). Due to this relatively short time-scale, the relationship of changes in sea ice extent and thickness to natural cycles, such as the North Atlantic and Arctic Oscillations, versus anthropogenically induced warming, are not completely clear (Johannessen et al., 1999; Rothrock et al., 1999). Modelling work by Vinnikov et al. (1999) suggests that the observed changes over the past century are larger than would be expected as a consequence of natural climate variability alone. In addition, a decrease in sea ice extent is not observed universally in the Arctic (Parkinson, 1995). Given these uncertainties, it is clear that longer, detailed records of sea ice extent, thickness and dynamics in the Arctic, are necessary, with proxy records as the most likely source of information.

Similar to work in the Antarctic, estimates of sea ice in the high northern latitudes were first put forward by CLIMAP (1976, 1981), but since have been revised dramatically by more extensive work using sedimentological, geochemical and micropalaeontological tracers of sea ice. While a variety of microfossil groups have provided data on palaeo sea ice distribution, including diatoms, coccolithophorids and foraminifera, dinoflagellate cyst assemblages have been utilized most successfully in these studies, due to their diversity and abundance in sediments from both the Arctic and sub-Arctic seas. As with our presentation of data from the Antarctic, we first describe the approaches undertaken when documenting past sea ice cover and then examine the results of these methods under time-slice scenarios.

Ice core data

Physical and geochemical properties of glacial ice in the Arctic have been related to sea ice cover, though it seems that their full potential remains to be utilized. Koerner (1977), for example, found a positive relationship between melt layers in glacial ice of the Devon Island Ice Cap and maximum open water in the nearby Queen Elizabeth Islands region. This relationship is driven by warmer summers that produce both surface melting on the ice cap that subsequently refreezes as a melt layer, and less summer sea ice. Consequently, the number and thickness of melt layers in glacial ice holds potential as a palaeo sea ice proxy.

The concentration of sea salts in glacial ice may also provide a record of sea ice cover, through the transport and deposition of marine aerosols from open water to glacial ice. However, this relationship is only applicable in situations in which aerosol transport is more a function of the area of open water, though other factors

may also be important. In the case of the Greenland Ice Core, strength of polar atmospheric circulation has a stronger control on the concentration of sea salts in the glacial ice, so even when sea ice concentration increases, increased strength of atmospheric transport can result in a greater amount of sea salt being deposited in the glacial ice (Mayewski et al., 1994; O'Brien et al., 1995). However, in the Penny Ice Cap, on Baffin Island, Grumet et al. (2001) demonstrated the existence of an inverse relationship between spring sea ice extent in Baffin Bay and the concentration of sea salt in the glacial ice.

Sedimentological tracers: ice-rafted debris including driftwood

Both sea ice and icebergs carry lithogenic material that is released as the ice melts (ice-rafted debris – IRD) and is consequently fluxed to the sea floor (Leventer, Chapter 10). While icebergs are able to transport material of all sizes (Clark and Hanson, 1983; Dowdeswell & Dowdeswell, 1989), more than 90% of the lithogenic material carried by sea ice is clay to silt-sized particles (Pfirman et al., 1989; Wollenburg, 1993). For this reason, particles $>500\,\mu m$ that are randomly distributed at the sea floor are generally considered to be iceberg rafted. A large body of literature exists concerning changes in the volume and source of iceberg-rafted material over time (Heinrich, 1988; Bischof, 1990; Bond et al., 1992; Hebbeln & Wefer, 1997; Ruddiman, 1977, 1997; Hebbeln et al., 1998). Distinction of sea ice versus iceberg-rafted material, however, is not always clear, even though in some settings this material can dominate mass flux (Hebbeln, 2000). Difficulty in tracking the exact source of fine-grained lithogenic particles, which can be ice rafted by either icebergs or sea ice, has resulted in few studies that utilize fine-grained IRD as a proxy for sea ice extent. An exception is work by Bond et al. (1997) who demonstrate that the concentration of volcanic glass ($>100\,\mu m$) erupted onto drifting ice, from either Iceland or Jan Mayen, can be used as a tracer for drifting sea ice through the Holocene. Their rationale for this distinction is the probable absence of Icelandic tidewater glaciers during the middle to late Holocene and the large size of the grains, ruling out both iceberg rafting and aeolian transport.

Larger objects, such as wood also are transported by drifting ice. River bank erosion in North America and Eurasia results in the delivery of wood to the Arctic that is then transported, with moving sea ice, via surface currents such as the Transpolar Drift and Beaufort Gyre (Dyke et al., 1997; Tremblay et al., 1997). After several years of drift as part of the moving pack ice, the wood can be stranded on the distant coastlines of the Canadian Arctic, Iceland, Greenland and Svalbard. Although not directly supplying information on the distribution of sea ice over time, radiocarbon dating of stranded wood has been used to identify changes in sea ice drift patterns over time that are then related to changes in atmospheric circulation patterns (Dyke et al., 1997; Tremblay et al., 1997).

Geochemical tracers: clay minerals and biomarkers

As with the work on driftwood, clay mineral studies of particles transported by sea ice do not provide direct data on sea ice distribution through time, but provide information on both the source of the sediments and the transport path of the sea ice. For example, Dethleff et al. (2000) have traced different branches of the Transpolar Drift originating in the Laptev Sea, based on the transport of specific clay minerals with the sea ice. In this study, the incorporated sediment is delivered to the ocean via rivers, and is then frozen into the sea ice. Pfirman et al. (1997), interested in the role of sea ice in distributing both contaminants and sediments in the Arctic, have developed a method to backtrack ice motion in the Eurasian Arctic, based on historical drift data. To verify their trajectories, they link clay mineralogical data of the sediment carried within the sea ice to sea floor sediments in the suspected sources.

Geochemical work using photosynthetic biomarker pigments (Rosell-Melé & Koç, 1997) and C_{37} alkenones (Rosell-Melé, 1998; Rosell-Melé et al., 1998) has been used to address the question of variable sea ice cover in the Nordic seas since the last glacial. In both cases, the principle guiding the use of these proxies is the association of the chemistry with photosynthetic organisms. Consequently, their presence in marine sediment cores suggests the lack of permanent ice cover. More specifically, Rosell-Melé & Koç (1997) measured the concentration of chlorins and porphyrins, diagenetic products of the photosynthetic pigment chlorophyll, in sediment cores from the Nordic seas, in order to assess whether these seas were permanently ice covered during the LGM, as indicated by the CLIMAP (1976, 1981) project. The presence of these compounds during the end of the last glacial and the Younger Dryas shows that seasonally ice-free conditions must have existed at those times. The C_{37} alkenones are associated with the coccolithophorid *Emiliani huxleyi*, a photosynthetic organism common in waters that are ice-free for at least part of the year. As with the chlorins and porphyrins, the presence of C_{37} alkenones indicates the lack of permanent ice cover in the Nordic seas during the Younger Dryas (Rosell-Melé et al., 1998).

Microfossil assemblage distribution: calcareous microfossils

Calcareous microfossils, such as coccolithophorids and planktonic foraminifera, have been used to track sea ice cover over time in the high northern latitudes, with the caveat that there is greater dissolution of calcium carbonate as water temperature decreases and reduced species diversity as latitude increases. For example, only a single species of planktonic foraminifera, *Neogloboquadrina pachyderma*, is common in the polar setting. Coccolithophorid diversity is slightly higher, although dominated by two species, *Emiliani huxleyi* and *Coccolithus pelagicus* (Braarud, 1979; Samtleben & Schroder, 1992; Baumann et al., 2000). The productivity and downward flux of coccoliths is greatly decreased in polar waters with seasonal ice

cover (Eide, 1990). In addition, since planktonic foraminifera can live deeper in the water column, their distribution is not as directly linked to the presence or absence of sea ice as that of the phytoplanktonic coccolithophorids.

That said, work with both microfossil groups has provided useful information on the variability of permanent sea ice cover in the Arctic and sub-Arctic seas. As with the biomarker methods, simply the presence of coccoliths in marine sediments suggests seasonally ice-free conditions, since the algae need enough light to photosynthesize. For example, Rahman & de Vernal (1994) used the presence versus absence of calcareous nannofossils to trace the history of sea ice in the Labrador Sea over the past 31 000 years. Hebbeln & Wefer (1997) do the same for the Fram Strait, though their data go back farther in time, to oxygen isotope stage 5 at 128 ka. This concept is expanded upon by Hebbeln et al. (1998) in their review of the 200 000-year record of palaeoceanographic conditions in the North Atlantic.

Large-scale work with planktonic foraminifera is in progress through the use of a modern analogue technique with a similarity index, SIMMAX, which is being used to develop maps of sea-surface temperatures that can be used to infer palaeo sea ice extent (Pflaumann et al., 1996). One of the principal advantages of this statistical method, over previously used techniques such as the MAT alone, or the CLIMAP transfer function method (Imbrie & Kipp, 1971), is the ability to estimate very low sea-surface temperatures (-1.4°C for caloric winter and 0.4°C for caloric summer; Pflaumann et al., 1996). This ability is critical for work in the higher latitudes, where these sea-surface temperature estimates will be used to reconstruct sea ice distribution.

Microfossil assemblage distribution: diatoms

Based on their abundance and diversity in the sea ice, water column and sediments, and the associations of certain species with specific habitats, diatoms have proven to be excellent palaeo sea ice proxies in the Southern Ocean, as presented earlier in this chapter. However, their use in the northern high latitudes is more limited, primarily as a result of the more lightly silicified and more easily dissolved frustules found in the nutrient-poor Arctic (Machado, 1993; Kohly, 1998). As a result, although diatoms are relatively diverse and abundant in Arctic surface waters, their distribution in surface sediments is patchy enough that a circum-Arctic database is unlikely to be developed. However, in specific regions – the Bering Sea and Sea of Okhotsk (Sancetta, 1979, 1981, 1982, 1983), the Greenland, Iceland and Norwegian Seas (Koç Karpuz & Schrader, 1990; Koç et al., 1993), the Labrador Sea (De Sève, 1999), Baffin Bay, Frobisher Bay and the Davis Strait (Williams, 1990), and the Laptev Sea (Bauch & Polyakova, 2000) – diatoms are abundant enough in sediments that their records have provided important palaeoceanographic insights. Note that with the exception of the Laptev Sea, these sites are all outside the enclosed Arctic Ocean.

In the northern Pacific, including both the Bering Sea and the Sea of Okhotsk,

diatoms are common in surface sediments (Jousé, 1962) and have been worked on extensively by Sancetta (1979, 1981, 1982, 1983). Sancetta (1981) presents quantitative diatom data, from 200 surface sediment samples from this region, that link distinct diatom assemblages to specific oceanographic conditions, including an assemblage from the Bering Sea associated with 'shelf waters covered by sea ice for six months of the year, with productivity occurring in very early spring at the margin of the melting ice'. This sea ice assemblage is dominated by *Thalassiosira nordenskioldii* and species of *Nitzschia* such as *Nitzschia grunowii* (now *Fragilariopsis grunowii*) and *Nitzschia cylindrus* (now *Fragilariopsis cylindrus*), which are commonly associated with sea ice (Gran, 1904; Horner & Alexander, 1972). Notably, *F. cylindrus* holds a similar ecological position in the Southern Ocean.

Sancetta (1983) applies this understanding of the modern distribution of diatoms in the northern Pacific, to five sediment cores from the North Pacific and Bering Sea that span the past 40 000 years. The most obvious change in assemblage downcore is the increased abundance of the two sea ice species, *F. grunowii* and *F. cylindrus*, during the last glacial, indicating increased sea ice cover at that time, in the Bering Sea. These species are rarely found in the two North Pacific cores she studied, even during the last glacial, which indicates that sea ice expansion did not extend that far south. Additionally, the diatom data show that the prolonged sea ice cover characteristic of the Sea of Okhotsk today, was more widespread during the last glacial. This is based on the greater distribution of diatom species associated with sea ice melt and cool, low salinity surface water layers.

Koç et al. (1993) reconstruct the palaeoceanographic history of the Greenland, Iceland and Norwegian Seas over the past 14 000 years based on diatom assemblage work initially developed by Koç Kapuz (1990). Like Sancetta's (1983) work in the high latitude Pacific, Koç et al. note the association of species as *Nitzschia cylindrica* (now *Fragilariopsis cylindrus*), *F. grunowii* and *Thalassiosira hyalina*, with sea ice, and use this information to track sea ice distribution over time. More simply, they also trace the ice margin through the first occurrence of diatoms in the nine sediment cores they analysed.

Similarly, De Sève (1999) used Q-mode factor analysis on 66 surface sediment samples from the Labrador Sea to develop transfer functions relating assemblage information to August and February sea-surface temperatures and salinities. De Sève's (1999) Factor 2 dominated by *T. gravida* is associated with cold Arctic surface waters 'indicative of heavy and prolonged ice coverage (p. 255)'. Factor 6, dominated by *N. frigida*, is her sea ice assemblage. Based on the results of her factor analysis, it is likely that down-core reconstruction of sea ice distribution over time is possible for the Labrador Sea.

Slightly to the north in the Baffin Bay–Davis Strait region, Williams (1986, 1990, 1993) used diatom abundance data to look at both the recent and deglacial/Holocene history of the area. Using CABFAC factor analysis, Williams was able to distinguish several assemblages associated with sea ice. Her Baffin Current assemblage, dominated by *T. gravida*, is associated with prolonged and heavy ice

cover, as was found by De Sève (1999). Her summer pack ice assemblage has high concentrations of *Actinocyclus curvatulus* and *Thalassiosira trifulta*, and a third assemblage is associated with fast ice (*Porosira glacialis*). In her down-core work, Willliams (1990, 1993) notes that initial ice break-up at the end of the glacial is generally indicated by the appearance of *T. gravida*. In addition, *N. grunowii* (*F. grunowii*) and *N. cylindra* (*F. cylindrus*), not *P. glacialis*, are used to track sea ice extent through the Holocene.

Finally, in the Arctic Ocean, data on diatom assemblages are presented by Polyakova (1989 – Barents Sea, White Sea, Kara Sea, East Siberian Sea, Chukchi Sea and the Canadian Arctic), Polyakova et al. (1992 – Barents Sea) and Bauch & Polyakova (2000 – Laptev Sea). As was found with the previous studies, *F. grunowii* and *F. cylindrus* (and *Fossula arctica*) are used as indicators of sea ice.

Clearly, as in the Southern Ocean, specific diatoms can be, and are, used to trace the distribution of sea ice over time. However, for large portions of the central and marginal Arctic Ocean, diatom abundances are so low, and preservation so poor, that other proxies must be utilized.

Microfossil assemblage distribution: dinoflagellate cysts

In the high northern latitudes, dinoflagellate cysts have proven to be the most powerful proxy recorder of palaeo sea ice, with reconstructions using best analogue techniques capable of estimating past sea ice cover with an error of prediction of $\pm$ 1.5 months/year (de Vernal et al., 2001). Their utility of these cysts, which form as a normal part of the dinoflagellate life cycle, is the result of several factors. As with other micro-organisms living within the photic zone such as diatoms and coccolithophorids, dinoflagellate distribution is sensitive to changes within the upper water column, including fluctuations in sea-surface temperature and salinity, and of course, sea ice cover. Annual sea ice cover restricts the amount of light available for photosynthesis, thus forcing a disruption of metabolic activities. In the case of the dinoflagellates, this interruption influences the life stage of the dinoflagellate.

Dinoflagellate populations are relatively diverse ($\sim$30 dinocyst species and 10 distinctive morphotypes have been recorded in Arctic surface samples – Rochon et al., 1999; de Vernal et al., 2001) and widespread in the Arctic, with changes in assemblage composition directly a function of changes in surface water conditions (Table 11.1). This is ideal for transfer function analyses, since the resolution of transfer functions increases as both species diversity and the range of ecological niches represented increases (Mudie et al., 2001). Species commonly found in regions with extensive sea ice cover include *Brigantedinium* spp. and *Operculodinium centrocarpum*, both of which tolerate a broad range of environmental conditions, and others such as *Islandinium minutum*, which is more specifically adapted to colder and ice-covered conditions (de Vernal & Hillaire-Marcel, 2000; Head et al., 2001). In contrast, the extremely low diversity exhibited by planktonic foraminiferal populations (essentially only left-coiling *N. pachyderma*) and the coccolithophorids (primarily *E. huxleyi* and

Table 11.1 List of dinocyst studies relevant to palaeo sea ice reconstruction.

Reference/year	Region	Time period
Boessenkool et al., 2001	South-east Greenland Margin	Modern
Grøsfjeld et al., 1999	Western Norway fjords	Late glacial – Holocene
Head et al., 2001	Arctic/Kara and Laptev Seas	Modern
Kunz-Pirrung, 2001	Arctic/Laptev Sea	Modern
Kunz-Pirrung et al., 2001	Arctic/Laptev Sea	Late Holocene
Levac & de Vernal, 1997	Labrador Coast	Postglacial
Levac et al., 2001	Baffin Bay	Postglacial
Matthiessen & Knies, 2001	Barents Sea	Oxygen Isotope Stage 5
Mudie, 1992	Circum-Arctic	Neogene and Quaternary
Mudie & Rochon, 2001	Canadian Arctic	Modern
Mudie et al., 2001	Arctic and high latitude circum-Arctic basins	Introduction to special volume
Peyron & de Vernal, 2001	Arctic and sub-Arctic seas	Modern and 25 000 year records
Radi et al., 2001	Bering and Chukchi Seas	Modern
Rochon & de Vernal, 1994	Labrador Sea	Modern and Holocene
Rochon et al., 1998	North Sea	Late glacial – deglacial
Rochon et al., 1999	North Atlantic	Modern
de Vernal & Hillaire-Marcel, 2000	North-west N. Atlantic	Last Glacial Maximum versus modern
de Vernal et al., 1993a	Gulf of St Lawrence	Late glacial – Holocene
de Vernal et al., 1993b	North Atlantic	Modern
de Vernal et al., 1997	North Atlantic	Modern
de Vernal et al., 2000	North Atlantic	Last Glacial Maximum
de Vernal et al., 2001	North Atlantic, Arctic, sub-Arctic Seas compilation	Modern
Voronina et al., 2001	Barents Sea	Holocene

C. pelagicus) in the Arctic, makes it difficult to track changes in sea ice cover by examining variability in the microfossil assemblage. Moreover, dinoflagellates and dinocysts are euryhaline, existing in environments with salinities ranging from estuarine to normal marine, while planktonic foraminifera are stenohaline, living under only normal marine salinities. In addition, while dominantly photosynthetic, many dinoflagellates are capable of heterotrophic behaviour. This, in combination with their ability to encyst, results in their ability to survive even under very harsh environmental conditions (Mudie et al., 2001; de Vernal et al., 2001).

Finally, many of the dinocysts are composed of dinosporin, a complex and refractory organic compound that is very resistant to dissolution (de Vernal et al., 2001; Zonneveld et al., 2001). Even when siliceous and calcareous microfossils have dissolved, dinocysts are commonly well preserved. Consequently, the records of dinocysts are much more continuous, in both glacial and interglacial sediments (de Vernal & Mudie, 1989), than those of other microfossil groups (Thiede et al., 1989).

Mudie et al. (2001) presents an excellent summary of the progress made in the use of statistical assessments of dinocyst assemblages to reconstruct sea ice cover. Quantitative studies completed by Mudie & Short (1985) and Mudie (1992) were

among the first to use Q-mode factor analysis to develop dinocyst-based transfer functions for sea-surface temperature and sea surface, but not sea ice cover. These studies were based on the eastern Canadian continental margin, using less than 100 samples. Later work by Rochon et al. (1999) and de Vernal & Hillarie-Marcel (2000) increased the geographical coverage to include the northern North Atlantic, Gulf of St Lawrence, Hudson Bay and Barents Sea. This larger data set, of almost 400 core tops, was analysed with a Best Analogue Technique (BAT). The primary advantage of this technique over the Imbrie-Kipp Q-mode factor analysis is in its logarithmic transformation of abundance data that allocates greater significance than otherwise, to sparsely represented taxa, which do have an ecological significance. One of the most significant problems, however, with these analyses, was the occurrence of non-analogue situations in the palaeo record. In order to address this issue, de Vernal et al. (2001) increased the database to include almost 700 samples that cover a wider range of environmental variability. In addition, Peyron & de Vernal (2001) apply another statistical approach to calibrate dinocyst assemblages and specific environmental parameters, Artificial Neuron Networks (ANN). The advantage of ANN is that it does not assume a unimodal response by taxa to an environmental parameter. Their results show that ANN can be used successfully, and are in good agreement with the results of the BAT work. In summary, over the past two decades, researchers have seen a progression over time that has increased the number of sample sites and the total range of ecological variability, and have worked with these data using increasingly sophisticated statistical methods. Work still must be done to deal with the problems of non-analogue situations and those related to reconstruction of environmental variables, like sea ice cover, that exhibit a large amount of interannual and/or interdecadal variability.

Mudie et al. (2001) and de Vernal et al. (2001) list several avenues for continued research, in order to improve the accuracy and resolution of dinocyst assemblage-based reconstructions of sea ice cover. Continued work on dinocyst taxonomy is critical. In addition, a better understanding of the ecological framework for each taxon is important. This includes more work on the species distribution and dynamics of Arctic dinoflagellate and dinocyst populations, which can be accomplished through a combination of water column and sediment trap work. The link between dinoflagellates and their cysts needs to be addressed more completely, with incubation studies to confirm taxonomic relationships and the environmental controls on encystment and germination.

Time-slice palaeo sea ice reconstructions

Last Glacial Maximum (~16–20 ka in ^{14}C years)

One of the key questions leading the effort to reconstruct sea ice extent in the high northern latitudes has been that of ice extent during the LGM. Based primarily on the sparse distribution of coccoliths in LGM sediments and data from planktonic foraminiferal transfer functions, CLIMAP (1976, 1981) proposed extensive sea ice

cover in the northern North Atlantic. This interpretation was further supported by the work of several scientists, including for example, Gard (1987) and Gard & Backman (1990) in Nordic Seas, Rahman & de Vernal (1994) in the Labrador Sea that described very sparse LGM coccolith assemblages, and foraminiferal studies by Kellogg (1976).

However, since the initial CLIMAP reconstruction, evidence for at least seasonally ice-free waters in the Nordic Seas during the LGM has accumulated (Henrich et al., 1989; Hebbeln et al., 1994; Johannessen et al., 1994; Wagner & Henrich, 1994; Sarnthein et al., 1995; Weinelt et al., 1996; Rosell-Melé, 1997). In addition, evidence points to the growth of the Barents Sea Ice Sheet during the last Ice Age, about 22 ka (Elverhoi et al., 1993). The moisture source for ice growth is problematic, if, as suggested by CLIMAP, the Nordic Seas were permanently ice covered at that time (Hebbeln et al., 1994). Given conflicting lines of evidence, the need to further investigate sea ice extent during the LGM became clear.

Several lines of evidence have been pursued aggressively, including dinocyst work (de Vernal & Hillaire-Marcel, 2000; de Vernal et al., 2000), oxygen-isotope based studies (Sarnthein et al., 1995), and multi-proxy work (Hebbeln et al., 1994; Hebbeln & Wefer, 1997; Hebbeln et al., 1998). For example, de Vernal & Hillaire-Marcel (2000) and de Vernal et al. (2000) have shown that permanent sea ice in the North Atlantic, though much more extensive than today, was as much as 10° further north than indicated by the CLIMAP study. In addition, dinocyst and planktonic foraminiferal isotope data suggest that surface waters were strongly stratified during the LGM (de Vernal & Hillaire-Marcel, 2000), which must have slowed down North Atlantic circulation and reduced heat transport to both the Arctic and western Europe. de Vernal & Hillaire-Marcel (2000) speculate that one of the consequences of this stratification was expansion of winter sea ice extent off of eastern North America.

Hebbeln et al. (1994) and Hebbeln & Wefer (1997) suggest seasonally ice-free conditions in the Nordic Seas between 27–22.5 ka and 19.5–14.5 ka, based on increased abundances of both coccoliths and planktonic foraminifera, in cores from the Fram Strait. These ice-free periods are termed 'Nordway events'. Hebbeln et al. (1998) summarize the current state of knowledge concerning palaeo sea ice extent in the North Atlantic by stating,

> 'During the last fifteen years the CLIMAP palaeoceanographic view of the glacial Polar North Atlantic as an almost permanently isolated sea covered by heavy sea ice throughout the year has shifted to a much more dynamic view of the environmental conditions. A meridional current system similar to the present-day conditions secured the exchange of water, ice and heat between the Polar North Atlantic and the Atlantic and Arctic Oceans. Although affected by variations in strength and intensity this meridional current pattern resulted in an almost permanent presence of at least some seasonally ice-free areas, with all the consequences for e.g. marine life and deep water formation.'

Holocene (0–10 ka BP).

Great interest in Holocene climate, in general, springs from the relationship between well-documented human activities and climate over the past 10 000 years. For example, as summarized by Grove (1988), relatively recent climatic events, such as the Little Ice Age, a cool climatic interval that lasted from around the mid-1300s to the mid-1800s, had a strong impact on European societies of the time. Cooler temperatures and increased Nordic Sea ice extent at that time are thought to have been a factor in the disappearance of Viking colonies in Greenland (Grove, 2001). Given the strong impact of sea ice extent on human activities in the area, some of the longest suites of historical data documenting sea ice are from here. In particular, data from Iceland extend back to the earliest days of Iceland's colonization, during the 9th century. These data have been collated by Thoroddsen (1916/17), updated by Koch (1945), and re-evaluated more recently by Sigtryggsson (1972) and Ogilvie (1981, 1983). The data can be used to supplement the relatively short instrumental data set, derived from satellites, that goes back only to the early 1970s (Comiso, Chapter 4). Other methods, through which the instrumental data set can be supplemented, include fishing and ships' logs (Bergthorsson, 1969 and Catchpole, 1992, respectively) and biological data on the distribution of different species of seals, as indicated by the distribution of bones in archaeological sites (Woollett, 1999).

Regional differences in sea ice behaviour, and the need for more quantitative data, have led to research efforts to acquire more information on Arctic sea ice extent through the Holocene. Based on a statistically significant relationship between sea salt concentration in glacial ice from the Penny Ice Cap (Baffin Island) and Baffin Bay spring sea ice extent (90-year data set), Grumet et al. (2001) reconstruct ice distribution over the past 700 years. Their data do show increased sea ice during the Little Ice Age. Their data also demonstrate links between sea ice extent and the North Atlantic Oscillation, reinforcing that the behaviour of these oceanic and atmospheric systems are closely coupled and need to be studied in parallel. However, the Grumet et al. (2001) data set, while intriguing, is still relatively short; longer records of a similar type are much needed.

To date, multi-proxy and micropalaeontological analysis of marine sediment cores have provided longer records detailing Holocene sea ice extent. For example, multi-proxy work by Bond et al. (1997) in the North Atlantic demonstrate $\sim$1500-year cyclicity in North Atlantic circulation throughout the Holocene, that can be tied to oceanographic cycles of the same frequency during the last glacial (Bond & Lotti, 1995) and to changes in atmospheric circulation recorded in the Greenland Ice Core (O'Brien et al., 1995). Bond et al. (1997) suggest the alternation of two modes of oceanographic circulation. Maximum IRD input and cooler sea-surface temperatures occur during periods characterized by southward advection of waters originating from north of Iceland that includes drifting sea ice carrying volcanic glass erupted onto the sea ice. Giraudeau et al. (2000) presents a 12 000-year,

coccolith-based study of a core from south of Iceland. Both long-term trends and higher frequency instabilities are noted. Millennial-scale variability in the accumulation of *E. huxleyi* is in phase with associated IRD peaks described by Bond et al. (1997) that have been linked to changes in the advection of cooler, icy waters from the north. Jennings et al. (2002) also find links to the millennial scale cycles of Bond et al. (1997) in their multi-proxy data set from the East Greenland margin.

Diatom data document changes in sea ice cover over the past 10 000 years, though the data are qualitative and geographically discontinuous (Williams, 1990; Koç et al., 1993; Bauch & Polyakova, 2000). For example, Williams (1990) links reduced diatom abundance in cores from Baffin Bay to reduced diatom productivity at times when sea ice extent was more severe than today. She links increased sea ice cover to the presence of low salinity melt water, as this would freeze more easily than surface waters of normal salinity. The timing of these events is dependent upon location. Koç et al., (1993) notes that the eastern Nordic Seas were ice-free by 13.4 ka (oldest part of record), with decreasing ice extent through the mid-Holocene, followed by cooling and increased ice extent until today. Finally, Bauch & Polyakova (2000), working in the Laptev Sea on a relatively short record (> 3000 years), find that more severe pack ice marks the earliest part of their record.

Dinocyst assemblage data similarly have been used to examine changes in sea ice cover through the Holocene in the Labrador Sea (Rochon & de Vernal, 1994; Levac & de Vernal, 1997), Baffin Bay (Levac et al., 2001), and the Barents Sea (Voronina et al., 2001). In each of these studies the data demonstrate non-uniform sea ice cover through the Holocene, with generally warmer conditions with less sea ice cover characteristic of the mid-Holocene, followed by a cooling trend to modern conditions. In addition to this general trend, several studies document short-lived cold pulses with heavy sea ice cover, particularly during the past 3000 years (Levac et al., 2001; Voronina et al., 2001).

11.4 Conclusion

Palaeo sea ice estimates commenced in both the southern and northern polar regions primarily as a result of sea-surface temperature estimates under CLIMAP. As such the development of sea ice proxies and statistical modelling remains in its infancy, with Arctic researchers taking an active lead in advancing sea ice estimation through grouped dinocyst databases and advanced, yet comparable, estimation models. Antarctic sea ice estimation, developed primarily on circumpolar diatom distributions, has stalled and remains divided by two databases and multiple, yet-to-be compared, proxies. Even the source data for modern sea ice extent and concentrations remain non-standardized and dated. The lack of consensus remains one of the greatest impediments to advancing Antarctic sea ice estimation through geological time. There is some hope that these obstacles will be addressed in the near future with plans for the 'new CLIMAP' project (Multiproxy Approach for the

Reconstruction of the Glacial Ocean surface – MARGO). The result of this programme will finally provide a best-approach method and single database for future Antarctic work.

Antarctic sea ice variation over the Quaternary is best recorded from the South Atlantic sector, and lightly covered in the south Indian Ocean. As with most palaeo-records, palaeo sea ice in the south Pacific sector is barely studied and mostly hypothetical. Arctic sea ice knowledge for the Holocene and the LGM are now well documented and highly advanced, pulling on evidence from many microfossil and lithological sources. Extension of the record to longer-term variation over the Arctic region is within reach and should allow for sea ice boundary conditions over time to be incorporated into GCMs, providing the spatial coverage required by the GCM is attended to.

The relationship between climate and sea ice is a complex and progressive research area. With the advance of palaeo sea ice records, and elucidation of the forcings upon the sea ice long-term variability (e.g. atmosphere, heat flux and isolation), this key climate modulator will eventually be understood. Our understanding of past boundary conditions will be insightful when married to results from modern-day physical interaction studies between the ice, ocean and atmosphere. The study of sea ice and atmospheric phenomena will elucidate probable trends in both hemispheres and to global weather. Global atmospheric responses with respect to Antarctic sea ice variability have been noted in the past and continue to make headway (e.g. Peng & Wang, 1989; Simmonds & Jacka, 1995; Yuan & Martinson, 2000; Gloersen & White, 2001). So although sea ice characteristics can now be reasonably modelled in GCMs of the present, there are no current models that have used recent (i.e. non-CLIMAP) palaeontologically determined sea ice conditions to simulate the past climate. This is a challenge for both sea ice estimators and modellers in the future.

Acknowledgements

This chapter would not have been possible without the financial assistance provided by the Australian Cooperative Research Centre for the Antarctic and Southern Ocean Environment at the University of Tasmania, Hobart, and the Department of Geology, Colgate University, Hamilton, NY, USA. David Thomas is expressly thanked for his patience and invitation to contribute to this publication. International colleagues are thanked for supplying in press and unpublished data contained in this chapter.

References

Armand, L.K. (1997) The use of diatom transfer functions in estimating sea-surface temperature and sea ice in cores from the southeast Indian Ocean. PhD thesis, Australian National University, Canberra.

Armand, L.K. (2000) An ocean of ice – advances in the estimation of past sea ice in the Southern Ocean. *GSA Today*, **10**, 1–7.

Barbraud, C. & Weimerskirch, H. (2001) Emperor penguins and climate change. *Nature*, **411**, 183–186.

Bauch, H.A. & Polyakova, Y.I. (2000) Late Holocene variations in Arctic shelf hydrology and sea ice regime: evidence from north of the Lena Delta. *International Journal of Earth Sciences*, **89**, 569–577.

Baumann, K.-H., Andruleit, H.A. & Samtleben, C. (2000) Coccolithophores in the Nordic Seas: comparison of living communities with surface sediment assemblages. *Deep-Sea Research*, **47**, 1743–1772.

Bergthorsson, P. (1969) An estimate of drift ice and temperature in Iceland in 1000 years. *Joekull*, **19**, 94–101.

Bi, D., Budd, W.F., Hirst, A.C. & Wu, X. (2001) Collapse and reorganisation of the Southern Ocean overturning under the global warming in a coupled model. *Geophysical Reserch Letters*, **28**, 3927–3930.

Bianchi, C. & Gersonde, R. (2002) The Southern Ocean surface between Marine Isotope Stages 6 and 5d: shape and timing of climate change. *Palaeogeography, Palaeoclimatology, Palaeoecology*, **187**, 151–177.

Bischof, J. (1990) Dropstones in the Norwegian–Greenland Sea – indications of late Quaternary circulation patterns? *Geological History of the Polar Oceans: Arctic versus Antarctic*, (Eds U. Bleil & J. Thiede), NATO ASI Series C, Vol. 308, pp. 499–518. Kluwer Academic Publishers, Dordrecht.

Bjørgo, E., Johannessen, O.M. & Miles, M.W. (1997) Analysis of merged SMMR-SSMI time series of Arctic and Antarctic sea ice parameters 1978–1995. *Geophysical Research Letters*, **24**, 413–416.

Boessenkool, K.P., Van Gelder, M.-J., Brinkhuis, H. & Troelstra, S.R. (2001) Distribution of organic-walled dinoflagellate cysts in surface sediments from transects across the Polar Front offshore southeast Greenland. *Journal of Quaternary Science*, **16**, 661–666.

Bond, G., Heinrich, H., Broecker, W.S., Labeyrie, L., McManus, L., Andrews, J., Huon, S., Jantschik, R., Clasen, S., Simet, C., Tedesco, K., Klas, M., Bonani, G. & Ivy, S. (1992) Evidence for massive discharge of icebergs into the North Atlantic ocean during the last glacial period. *Nature*, **360**, 245–249.

Bond, G., Showers, W., Cheseby, M., Lotti, R., Almasi, P., deMenocal, P., Priore, P., Cullen, H., Hajdas, I. & Bonani, G. (1997) A pervasive millennial-scale cycle in North Atlantic Holocene and glacial climates. *Science*, **278**, 1257–1266.

Bond, G.C. & Lotti, R. (1995) Iceberg discharges into the North Atlantic on millennial time scales during the last glaciation. *Science*, **267**, 1005–1010.

Braarud, T. (1979) The temperature range of the non-motile stage of *Coccolithus pelagicus* in the North Atlantic region. *British Phycological Journal*, **14**, 349–352.

Broecker, W.S., Peacock, S.L., Walker, S., Weiss, R., Fahrbach, E., Schroder, M., Mikolajewicz, U., Heinze, C., Key, R., Peng, T.-H. & Rubin, S. (1998) How much deep water is formed in the Southern Ocean. *Journal of Geophysical Research*, **103**, 15833–15843.

Bromwich, D.H. (1984) A reconstruction of the coastal Antarctic climate and summer sea-ice position at 18 ka BP (Abstract). *Annals of Glaciology*, **5**, 201.

Budd, W.F. & Rayner, P. (1993) Modelling ice sheet and climate changes through the ice

ages. In: *Ice in the Climate System*, (Ed. W.R. Peltier), NATO ASI Series, Vol. 12., pp. 291–319. Springer-Verlag, Berlin.

Budd, W.F. & Wu, X. (1998) Modelling long term global and Antarctic changes resulting from increased greenhouse gases. In: Coupled Climate Modelling: *Proceedings of the Tenth Annual BMRC Modelling Workshop, 12–13 October 1998, Melbourne, Victoria*, pp. 71–74. Bureau of Meteorology Research Centre, Melbourne.

Burckle, L.H. (1983) Diatom dissolution patterns sediments of the Southern Ocean. *Journal of the Geological Society of America*, **15**, 536–537.

Burckle, L.H. (1984) Diatom distribution and palaeoceanographic reconstruction in the Southern Ocean – present and last glacial maximum. *Marine Micropalaeontology*, **9**, 241–261.

Burckle, L.H. & Abrams, N. (1986) Biotic response to two late Neogene intervals of global climatic change: evidence from the deep-sea record. *South African Journal of Science*, **82**, 69.

Burckle, L.H. & Burak, R.W. (1988) Fluctuations in late Quaternary diatom abundances: stratigraphic and paleoclimatic implications from subantarctic deep sea cores. *Palaeogeography, Palaeoclimatology, Palaeoecology*, **67**, 147–156.

Burckle, L.H. & Cirilli, J. (1987) Origin of diatom ooze belt in the Southern Ocean: implications for late Quaternary paleoceanography. *Micropaleontology*, **33**, 82–86.

Burckle, L.H. & Mortlock, R. (1998) Sea ice extent in the Southern Ocean during the Last Glacial Maximum: another approach to the problem. *Annals of Glaciology*, **27**, 302–304.

Burckle, L.H., Robinson, D. & Cooke, D. (1982) Reappraisal of sea ice distribution in the Atlantic and Pacific sectors of the Southern Ocean at 18,000 yr BP. *Nature*, **299**, 435–437.

Catchpole, A.J.W. (1992) Hudson Bay Company Ships log-books as sources of sea ice data 1751–1870. In: *Climate Since AD 1500*, (Eds R.S. Bradley & P.D. Jones), pp. 17–39. Routledge, London.

Cavalieri, D.J., St Germain, K.M. & Swift, C.T. (1995) Reduction of weather effects in the calculation of sea ice concentration with the DMSP SSM/I. *Journal of Glaciology*, **41**, 455–464.

Chapman, W.L. & Walsh, J.E. (1993) Recent variations of sea ice and air temperature in high latitudes. *Bulletin of the American Meteorological Society*, **74**, 33–47.

Clark, D.L. & Hanson, A. (1983) Central Arctic Ocean sediment texture: a key to ice transport mechanisms. In: *Glacial-Marine sedimentation*, (Ed. B.F. Molnia), pp. 301–330. Plenum, New York.

Clementson, L.A., Parslow, J.S., Griffiths, F.B., Lyne, V.D., Mackey, D.J., Harris, G.P., McKenzie, D.C., Bonham, P.I., Rathbone, C.A. & Rintoul, S. (1998) Controls on phytoplankton production in the Australiasian sector of the subtropical convergence. *Deep-Sea Research*, **45**, 1627–1661.

CLIMAP Project Members (1976) The surface of the Ice-Age Earth. *Science*, **191**, 1131–1137.

CLIMAP Project Members (1981) *Seasonal reconstructions of the Earth's surface at the last glacial maximum*. Geological Society of America: Map and Chart Series MC-36.

Comiso, J.C. & Steffen, K. (2001) Studies of Antarctic sea ice concentrations from satellite data and their applications. *Journal of Geophysical Research*, **106**, 31361–31385.

Cooke, D.W., Burckle, L.H. & Hays, J.D. (1977) Winter sea ice cover during the late Pleistocene in the Antarctic Ocean. *EOS, Transactions of the American Geophysical Union*, **58**, 416.

Cooke, D.W. & Hays, J.D. (1982) Estimates of Antarctic Ocean seasonal sea ice cover during Glacial intervals. In: *Antarctic Geoscience*, (Ed. C. Craddock), Series B, No. 4, pp. 1017–1025. International Union of Geological Sciences, The University of Wisconsin Press, Wisconsin.

Crosta, X., Pichon, J.-J. & Burckle, L.H. (1998a) Application of modern analog technique to marine Antarctic diatoms: reconstruction of maximum sea ice extent at the Last Glacial Maximum. *Palaeoceanography*, **13**, 286–297.

Crosta, X., Pichon, J.-J. & Burckle, L.H. (1998b) Reappraisal of Antarctic seasonal sea ice at the Last Glacial Maximum. *Geophysical Research Letters*, **25**, 2703–2706.

Crosta, X., Sturm, A., Armand, L. & Pichon, J.-J. (submitted) Late Quaternary sea ice history in the Indian sector of the Southern Ocean as recorded by diatom assemblages. *Marine Micropaleontology*.

Crowley, T.J. & Parkinson, C.L. (1988) Late Pleistocene variations in Antarctic sea ice I: effect of orbital insolation changes. *Climate Dynamics*, **3**, 85–91.

Cunningham, W.L., Leventer, A., Andrews, J.T., Jennings, A.E. & Litch, K.J. (1999) Late Pleistocene–Holocene marine conditions in the Ross Sea, Antarctica: evidence from the diatom record. *The Holocene*, **9**, 129–139.

De la Mare, W.K. (1997) Abrupt mid-twentieth-century decline in Antarctic sea ice extent from whaling records. *Nature*, **389**, 57–60.

De Sève, M.A. (1999) Transfer function between surface diatom assemblages and sea-surface temperature and salinity of the Labrador Sea. *Marine Micropalaeontology*, **36**, 249–267.

DeFelice, D.R. (1979) Relative diatom abundance as tool for monitoring winter sea ice fluctuations in southeast Atlantic. *Antarctic Journal of the United States*, **14**, 105–106.

DeFelice, D.R. & Wise, S.W.J. (1981) Surface lithofacies, biofacies and diatom diversity patterns as models for delineation of climatic change in the southeast Atlantic Ocean. *Marine Micropalaeontolgy*, **6**, 29–70.

Dethleff, D., Rachold, V., Tintelnot, M. & Antonow, M. (2000) Sea ice transport of riverine particles from the Laptev Sea to Fram Strait based on clay mineral studies. *International Journal of Earth Sciences*, **89**, 496–502.

Dowdeswell, J.A. & Dowdeswell, E.K. (1989) Debris in icebergs and rates of glacimarine sedimentation: observations from Spitsbergen and a simple model. *Journal of Geology*, **97**, 221–231.

Dyke, A.S., England, J., Reimnitz, E. & Jette, H. (1997) Changes in driftwood delivery to the Canadian Arctic archipelago: the hypothesis of postglacial oscillations of the transpolar drift. *Arctic*, **50**, 1–16.

Eide, L.K. (1990) Distribution of coccoliths in surface sediments in the Norwegian–Greenland Sea. *Marine Micropalaeontology*, **16**, 65–75.

Elverhoi, A., Russwurm, L., Fjeldskaar, W., Solheim, A. & Nyland-Berg, M. (1993) The Barents Sea ice sheet – a model of its growth and decay during the last ice maximum. *Quaternary Science Reviews*, **12**, 863–873.

Fieg, K. & Gerdes, R. (2001) Sensitivity of the thermohaline circulation to modern and glacial surface boundary conditions. *Journal of Geophysical Research*, **106**, 6853–6867.

Fryxell, G.A. & Prasad, A.K.S.K. (1990) *Eucampia antarctica* var. *recta* (Mangin) stat. nov. (Biddulphiaceae, Bacillariophyceae): life stages at the Weddell Sea ice edge. *Phycologia*, **29**, 27–38.

Ganopolski, A., Rahmstorf, S., Petoukhov, V. & Claussen, M. (1998) Simulation of modern

and glacial climates with a coupled global model of intermediate complexity. *Nature*, **391**, 351–356.

Gard, G. (1987) Late Quaternary nannofossil biostratigraphy and sedimentation patterns: Fram Strait, Arctic. *Palaeoceanography*, **2**, 519–529.

Gard, G. & Backman, J. (1990) Synthesis of Arctic and sub-Arctic coccolith biochronology and history of North Atlantic Drift water influx during the last 500,000 years. In: *Geological History of the Polar Oceans: Arctic versus Antarctic*, (Eds. U. Bleil & J. Thiede), NATO ASI Series C, Vol. 308, pp. 417–438. Kluwer Academic Publishers, Dordrecht.

Gersonde, R. & Zielinski, U. (2000) The reconstruction of late Quaternary Antarctic sea-ice distribution – the use of diatoms as a proxy for sea-ice. *Palaeogeography, Palaeoclimatology, Palaeoecology*, **162**, 263–286.

Gildor, H. & Tziperman, E. (2000) Sea-ice as the glacial cycles' climate switch: role of seasonal and orbital forcing. *Palaeoceanography*, **15**, 605–615.

Gildor, H. & Tziperman, E. (2001) A sea-ice climate switch mechanism for the 100-kyr glacial cycles. *Journal of Geophysical Research*, **106**, 9117–9133.

Giraudeau, J., Cremer, M., Manthe, S., Labeyrie, L. & Bond, G. (2000) Coccolith evidence for instabilities in surface circulation south of Iceland during Holocene times. *Earth and Planetary Science Letters*, **179**, 257–268.

Gloersen, P. & Campbell, W.J. (1991) Recent variations in Arctic and Antarctic sea ice covers. *Nature*, **352**, 33–36.

Gloersen, P. & Cavalieri, D.J. (1986) Reduction of weather effects in the calculation of sea ice concentration from microwave radiances. *Journal of Geophysical Research*, **91**, 3913–3919.

Gloersen, P. & White, W.B. (2001) Reestablishing the circumpolar wave in sea ice around Antarctica from one winter to the next. *Journal of Geophysical Research*, **106**, 4391–4395.

Gloersen, P.E., Mollo-Christensen, & Hubanks, P. (1989) Observations of Arctic polar lows with the Nimbus 7 Scanning Multichannel Microwave Radiometer. In: *Polar and Arctic Lows*, (Eds P.F. Twitchell, E.A. Rasmussen & K.L. Davidson), pp. 359–371. A. Deepak, Hampton, Virginia.

Godfred-Spenning, C.R. & Simmonds, I. (1996) An analysis of Antarctic sea ice and extratropical cyclone associations. *International Journal of Climatology*, **16**, 1315–1332.

Gordon, A.L. (1978) Deep Antarctic convection west of Maud Rise. *Journal of Physical Oceanography*, **8**, 600–612.

Gran, H.H. (1904) Diatomaceae from the ice-floes and plankton of the Arctic Ocean. In: *The Norwegian North Polar Expedition 1893–1896*, Vol. 4, (Ed. F. Nansen), pp. 1–74. Longmans, London.

Grenfell, T.C. (1983) A theoretical model of the optical properties of sea ice in the visible and near infrared. *Journal of Geophysical Research*, **88**, 9723–9735.

Grobe, H. (1987) A simple method for the determination of ice-rafted debris in sediment cores. *Polarforschung*, **57**, 123–126.

Grøsfield, K., Larsen, E., Sejrup, H.P., de Vernal, A., Flatebø, T., Vestbø, M., Haflidason, H. & Aarseth, I. (1999) Dinoflagellate cysts reflecting surface-water conditions in Voldafjorden, western Norway during the last 11,300 years. *Boreas*, **28**, 403–415.

Grove, J.M. (1988) *The Little Ice Age*. Routledge, London.

Grove, J.M. (2001) The initiation of the 'Little Ice Age' in regions round the North Atlantic. *Climatic Change*, **48**, 53–82.

Grumet, N.S., Wake, C.P., Mayewski, P.A., Zielinski, G.A., Whitlow, S.I., Koerner, R.M.,

Fisher, D.A. & Woolett, J.M. (2001) Variability of sea-ice extent in Baffin Bay over the last millennium. *Climatic Change*, **49**, 129–145.

Harris, P.T., Brancolini, G., Armand, L., Busetti, M., Beaman, R.J., Giorgetti, G., Presti, M. & Trincardi, F. (2001) Continental shelf drift deposits indicate non-steady state Antarctic bottom water production in the Holocene. *Marine Geology*, **179**, 1–8.

Hastie, T. & Tibshirani, R. (1990) *Generalized Additive Models*. Chapman and Hall, London.

Hays, J.D. (1978) A review of the Late Quaternary climatic history of Antarctic Seas. In: *Antarctic Glacial History and World Palaeoenvironments: Proceedings of the 10th INQUA*, (Ed. B. van Zinderen), pp. 57–71. Balkema, Rotterdam.

Hays, J.D., Lozano, J.A., Shackleton, N. & Irving, G. (1976) Reconstruction of the Atlantic and western Indian Ocean sectors of the 18,000 B.P. Antarctic Ocean. *Geological Society of America, Memoir*, **145**, 337–372.

Head, M.J., Harland, R. & Matthiessen, J. (2001) Cold marine indicators of the late Quaternary: the new dinoflagellate cyst genus *Islandinium* and related morphotypes. *Journal of Quaternary Science*, **16**, 621–636.

Hebbeln, D. (2000) Flux of ice-rafted detritus from sea ice in the Fram Strait. *Deep-Sea Research*, **47**, 1773–1790.

Hebbeln, D., Dokken, T., Andersen, E.S., Hald, M. & Elverhoi, A. (1994) Moisture supply for northern ice-sheet growth during the last glacial maximum. *Nature*, **370**, 357–360.

Hebbeln, D., Henrich, R. & Baumann, K.-H. (1998) Palaeoceanography of the last interglacial/glacial cycle in the polar North Atlantic. *Quaternary Science Reviews*, **17**, 125–153.

Hebbeln, D. & Wefer, G. (1997) Late Quaternary palaeoceanography in the Fram Strait. *Palaeoceanography*, **12**, 65–78.

Heinrich, H. (1988) Origin and consequences of cyclic ice-rafting in the northeast Atlantic Ocean during the past 130,000 years. *Quaternary Research*, **29**, 142–152.

Henrich, R., Kassens, H., Vogelsang, E. & Thiede, J. (1989) Sedimentary facies of glacial–interglacial cycles in the Norwegian Sea during the last 350 ka. *Marine Geology*, **86**, 283–319.

Hewitt, C.D. & Mitchell, J.F.B. (1997) Radiative forcing and response of a GCM to ice age boundary conditions: cloud feedback and climate sensitivity. *Climate Dynamics*, **13**, 821–834.

Hodell, D.A., Kanfoush, S.L., Shemesh, A., Crosta, X., Charles, C.D. & Guilderson, T.P. (2001) Abrupt cooling of Antarctic surface waters and sea ice expansion in the South Atlantic Sector of the Southern Ocean at 5000 cal yr B.P. *Quaternary Research*, **56**, 191–198.

Holland, M.M., Bitz, C.M. & Weaver, A.J. (2001) The influence of sea ice physics on simulations of climate change. *Journal of Geophysical Research*, **106**, 19639–19655.

Horner, R.A. (Ed.) (1985) *Sea Ice Biota.* CRC Press, Boca Raton, Florida.

Horner, R.A. & Alexander, V. (1972) Algal populations in Arctic sea ice: an investigation of heterotrophy. *Limnology and Oceanography*, **17**, 454–458.

Hudson, D.A. & Hewitson, B.C. (2001) The atmospheric response to a reduction in summer Antarctic sea-ice extent. *Climate Research*, **16**, 79–99.

Imbrie, J. & Kipp, N.G. (1971) A new micropalaeontological method for quantitative palaeoclimatology; application to a late Pleistocene Caribbean core. In: *The Late Cenozoic Glacial Ages*, (Ed. K.K. Turekian), pp. 71–147. Yale University Press, New Haven.

Jennings, A.E., Andrews, J.T., Knudsen, K.L., Hald, M. & Hansen, C.V. (2002) A mid-Holocene shift in Arctic sea-ice variability on the East Greenland Shelf. *Holocene*, **12**, 49–58.

Johannessen, O.M., Miles, M. & Bjorgo, E. (1995) The Arctic shrinking sea ice. *Nature*, **376**, 126–127.

Johannessen, O.M., Shalina, E.V. & Miles, M.W. (1999) Satellite evidence for an Arctic sea ice cover in transformation. *Science*, **286**, 1937–1939.

Johannessen, T., Jansen, E., Flatoy, A. & Ravelo, A.C. (1994) The relationship between surface water masses, oceanographic fronts and palaeoclimatic proxies in surface of the Greenland, Iceland, Norwegian Seas. In: *Carbon Cycling in the Glacial Ocean: Constraints on the Oceans's Role in Global Change*, (Eds R. Zahn, T.F. Pedersen, M.A. Kaminski & L. Labeyrie), pp. 61–85. Springer, Berlin.

Jones, D.A. & Simmonds, I. (1994) A climatology of Southern Hemisphere anticyclones. *Climate Dynamics*, **10**, 333–348.

Jousé, A.P. (1962) *Stratigraphicheskiye I Palaeogeographicheskiye Issledovaniya v Severo-Zapadnoy Chasti Tikhogo Okeana*. Akademia Nauk S.S.S.R.

Kaczmarska, I., Barbrick, N.E., Ehrman, J.M. & Cant, G.P. (1993) *Eucampia* Index as an indicator of the Late Pleistocene oscillations of the winter sea ice extent at the ODP Leg 119 Site 745B at the Kerguelen Plateau. *Hydrobiologia*, **269/270**, 103–112.

Keeling, R.F. & Stephens, B.B. (2001a) Antarctic sea ice and the control of Pleistocene climate instability. *Palaeoceanography*, **16**, 112–131.

Keeling, R.F. & Stephens, B.B. (2001b) Correction to 'Antarctic sea ice and the control of Pleistocene climate instability'. *Palaeoceanography*, **16**, 330–334.

Kellogg, T.B. (1976) Late Quaternary climatic changes: evidence from deep-sea cores of Norwegian and Greenland Seas. *Geological Society of America Memoir*, **145**, 77–110.

Killworth, P.D. (1983) Deep convection in the world ocean. *Geophysics and Space Physics*, **21**, 1–26.

Koç, N., Jansen, E. & Haflidason, H. (1993) Palaeoceanographic reconstructions of surface ocean conditions in the Greenland, Iceland and Norwegian seas through the last 14 ka based on diatoms. *Quaternary Science Reviews*, **12**, 115–140.

Koç Karpuz, N. & Schrader, H. (1990) Surface sediment diatom distribution and Holocene palaeotemperature variations in the Greenland, Iceland and Norwegian Sea. *Palaeoceanography*, **5**, 557–580.

Koch, L. (1945) The east Greenland ice. *Meddelelser om Grønland*, **130**, 1–374.

Koerner, R.M. (1977) Devon Island ice cap: core stratigraphy and palaeoclimate. *Science*, **196**, 15–18.

Kohly, A. (1998) Diatom flux and species composition in the Greenland Sea and the Norwegian Sea in 1991–1992. *Marine Geology*, **145**, 293–312.

Kumar, N., Anderson, R.F., Mortlock, R.A., Froelich, P.N., Kubik, P., Dittrich-Hannen, B. & Suter, M. (1995) Increased biological productivity and export production in the glacial Southern Ocean. *Nature*, **378**, 675–680.

Kunz-Pirrung, M. (2001) Dinoflagellate cyst assemblages in surface sediments of the Laptev Sea region (Arctic Ocean) and their relationship to hydrographic conditions. *Journal of Quaternary Science*, **16**, 637–649.

Kunz-Pirrung, M., Gersonde, R. & Hodell, D.A. (2002) Mid-Bruhnes century scale diatom sea surface temperature and sea ice records from the Atlantic sector of the Southern Ocean (ODP Leg 177, sites 1093, 1094 and core PS2089-2). *Palaeogeography, Palaeoclimatology, Palaeoecology*, **182**, 305–328.

Kunz-Pirrung, M., Matthiessen, J. & de Vernal, A. (2001) Late Holocene dinoflagellate cysts

as indicators for short-term climate variability in the Eastern Laptev Sea (Arctic Ocean). *Journal of Quaternary Science*, **16**, 711–716.

Levac, E. & de Vernal, A. (1997) Postglacial changes of terrestrial and marine environments along the Labrador coast: palynological evidence from cores 91-045-005 and 91-045-006, Cartwright Saddle. *Canadian Journal of Earth Sciences*, **34**, 1358–1365.

Levac, E., de Vernal, A. & Blake, W., Jr (2001) Sea-surface conditions in northernmost Baffin Bay during the Holocene: palynological evidence. *Journal of Quaternary Science*, **16**, 353–363.

Leventer, A., Domack, E., Barkoukis, A., McAndrews, B. & Murray, J. (2002) Laminations from the Palmer Deep: a diatom-based interpretation. *Palaeoceanography*, **17**, 1–15, DOI: 10.1029/2001PA000624.

Lisitzin, A.P. (1972) *Sedimentation in the World Ocean.* Special Publication No. 17. Society of Economic Palaeontologists and Mineralogists, Tulsa, Oklahoma.

McGovern, T.H. (1991) Climate, correlation, and causation in Norse Greenland. *Arctic Anthropology*, **28**, 77–100.

Machado, E. (1993) Production, sedimentation and dissolution of biogenic silica in the northern North Atlantic. PhD dissertation, University of Kiel, Germany.

McLaren, A.S., Wittmann, W., Walsh, J.E., Bourke, R.H. & Weaver, R.L. (1992) Variability in sea ice thickness over the North Pole from 1977 to 1990. *Nature*, **358**, 224–226.

McMinn, A. (1993) Determination of past Antarctic fast-ice cover by analysis of sea-ice diatoms. In: *Program and Abstracts of the Inter-INQUA: The Quaternary of the Australian Region*, (Ed. P. DeDeckker), Special Publication of the Australian Quaternary Association, pp. 59. Australian Quaternary Association, Canberra.

McMinn, A. (2000) Late Holocene increase in sea ice extent in fjords of the Vestfold Hills, eastern Antarctica. *Antarctic Science*, **12**, 80–88.

McPhee, M.G., Stanton, T.P., Morison, J.H. & Martinson, D.G. (1998) Freshening the upper ocean in Arctic: is perennial sea ice disappearing? *Geophysical Research Letters*, **25**, 1729–1732.

Matear, R. & Hirst, A.C. (1999) Climate change feedback on the future oceanic CO_2 uptake. *Tellus*, **51**, 722–733.

Matthiessen, J. & Knies, J. (2001) Dinoflagellate cyst evidence for warm interglacial conditions at the northern Barents Sea margin during marine oxygen isotope stage 5. *Journal of Quaternary Science*, **16**, 727–737.

Mayewski, P.A., Meeker, L.D., Whitlow, S.I., Twickler, M.S., Morrison, M.C., Bloomfield, P., Bond, G.C., Alley, R.B., Gow, A.J., Grootes, P.M., Meese, D.A., Ram, D.A., Taylor, K.C. & Wumkes, W. (1994) Changes in atmospheric circulation and ocean ice cover over the North Atlantic during the last 41,000 years. *Science*, **263**, 1747–1751.

Maykut, G.A. (1978) Energy exchange over young sea ice in the central Arctic. *Journal of Geophysical Research*, **83**, 3646–3658.

Moore, J.K., Abbott, M.R., Richman, J.G. & Nelson, D.M. (2000) The Southern Ocean at the last glacial maximum: a strong sink for atmospheric carbon dioxide. *Global Biogeochemical Cycles*, **14**, 455–475.

Morales Maqueda, M.A. & Rahmstorf, S. (2002) Did Antarctic sea ice expansion cause glacial CO_2 decline? *Geophysical Research Letters*, **29**, 1011, DOI: 10.1029/2001GL13240.

Mudie, P.J. (1992) Circum-Arctic Quaternary and Neogene marine palynofloras: palaeoecology and statistical analysis. In: *Neogene and Quaternary Dinoflagellate Cysts and*

Acritarchs, (Eds M.J. Head & J.H. Wrenn), pp. 347–390. American Association of Stratigraphic Palynologists Foundation, Dallas, Texas.

Mudie, P.J., Harland, R., Matthiessen, J. & de Vernal, A. (2001) Marine dinoflagellate cysts and high latitude Quaternary palaeoenvironmental reconstructions: an introduction. *Journal of Quaternary Science*, **16**, 595–602.

Mudie, P.J. & Rochon, A. (2001) Distribution of dinoflagellate cysts in the Canadian Arctic marine region. *Journal of Quaternary Science*, **16**, 603–620.

Mudie, P.J. & Short, S.K. (1985) Marine palynology of Baffin Bay. In: *Quaternary Environments*, (Ed. J.T. Andrews), pp. 263–308. Allen & Unwin, Boston.

Naval Oceanography Command Detachment (1985) *Sea Ice Climatic Atlas.* NSTL MS 39529-500, NAVAIR 50-1C-540, ADA-168716. Commander, Naval Ocaenography Command, 1: Antarctic, Asheville.

O'Brien, S., Mayewski, P.A., Meeker, L.D., Meese, D.A., Twickler, M.S. & Whitlow, S.I. (1995) Holocene climate as reconstructed from a Greenland ice core. *Science*, **270**, 1962–1964.

Ogilvie, A.E.J. (1981) Climate and society in Iceland from the medieval period to the late eighteenth century. PhD thesis, University of East Anglia, Norwich, UK.

Ogilvie, A.E.J. (1983) The past climate and sea ice record from Iceland, 1, Data to AD 1780. *Climate Change*, **6**, 131–152.

Orsi, A.H., Whitworth, T., III & Nowlin, W.D. (1995) On the meridional extent and fronts of the Antarctic Circumpolar Current. *Deep-Sea Research*, **42**, 641–673.

Parkinson, C.L. (1990) Search for the Little Ice Age in Southern Ocean sea ice records. *Annals of Glaciology*, **14**, 221–225.

Parkinson, C.L. (1992) Interannual variability of monthly Southern Ocean sea ice distributions. *Journal of Geophysical Research*, **97**, 5349–5363.

Parkinson, C.L. (1995) Recent sea ice advances in Baffin Bay/Davis Strait and retreats in the Bellingshausen Sea. *Annals of Glaciology*, **21**, 348–352.

Parkinson, C.L. (2000) Variability of Arctic sea ice: the view from Space, an 18-year record. *Arctic*, **53**, 341–358.

Peng, G.-B. & Wang, P.K. (1989) Influence of the Antarctic sea-ice on the north-west Pacific subtropical high and its background of ocean–atmospheric circulation. *Chinese Science Bulletin*, **34**, 1464–1465.

Peyron, O. & de Vernal, A. (2001) Application of artificial neural networks (ANN) to high-latitude dinocyst assemblages for the reconstruction of past sea-surface conditions in Arctic and sub-Arctic seas. *Journal of Quaternary Science*, **16**, 699–709.

Pfirman, S.L., Colony, R., Nürnberg, D., Eicken, H. & Rigor, I. (1997) Reconstructing the origin and trajectory of drifting Arctic sea ice. *Journal of Geophysical Research*, **102**, 12575–12586.

Pfirman, S.L., Wollenburg, I., Thiede, J. & Lange, M.A. (1989) Lithogenic sediment on Arctic pack ice: potential aeolian flux and contributions to deep sea sediments. In: *Palaeoclimatology and Palaeometeorology: Modern and Past Pattern of Global Atmospheric Transport*, (Eds M. Sarnthein & M. Leinen), pp. 463–493. Kluwer, Dordrecht.

Pflaumann, U., Duprat, J., Pujol, C. & Labeyrie, L.D. (1996) SIMMAX: a modern analog technique to deduce Atlantic sea surface temperatures from planktonic foraminifera in deep-sea sediments. *Palaeoceanography*, **11**, 15–35.

Polyakova, E. (1989) Diatoms in Arctic shallow seas and sediments. In: *The Arctic Sea*, (Ed. Y. Herman), pp. 481–496. Van Nostrand Reinhold, New York.

Polyakova, Y., Pavlidis, Y.A. & Levin, A.A. (1992) Factors governing diatom fossil distributions in the surface layer of bottom sediments on the Barents Sea Shelf. *Oceanology*, **32**, 112–119.

Prell, W.L. (1985) The stability of low-latitude sea-surface temperatures: an evaluation of the CLIMAP reconstructions with emphasis on the positive SST anomalies. *US Department of Energy Technical Report. DOE/ER/60167.* US Department of Energy, Office of Energy Research, Washington, D.C.

Radi, T., de Vernal, A. & Peyron, O. (2001) Relationships between dinoflagellate cyst assemblages in surface sediment and hydrographic conditions in the Bering and Chukchi seas. *Journal of Quaternary Science*, **16**, 667–680.

Rahman, A. & de Vernal, A. (1994) Surface oceanographic changes in the eastern Labrador Sea: nannofossil record of the last 31,000 years. *Marine Geology*, **121**, 247–263.

Ramstein, G. & Joussaume, S. (1995) Sensitivity experiments to sea surface temperatures, sea ice extent and ice-sheet reconstruction, for the Last Glacial Maximum. *Annals of Glaciology*, **21**, 343–347.

Rintoul, S.R. (1998) On the origin and influence of Adélie Land bottom water. In: *Ocean, Ice, and Atmosphere: Interactions at the Antarctic Continental Margin*, (Eds S.S. Jacobs and R. Weiss), American Geophysical Union, Washington, D.C. *Antarctic Research Series*, **75**, pp. 151–171.

Rochon, A. & de Vernal, A. (1994) Palynomorph distribution in recent sediments from the Labrador Sea. *Canadian Journal of Earth Sciences*, **31**, 115–127.

Rochon, A., de Vernal, A., Sejrup, H.-P. & Haflidason, H. (1998) Palynological evidence of climatic and oceanographic changes in the North Sea during the last deglaciation. *Quaternary Research*, **49**, 197–207.

Rochon, A., de Vernal, A., Turon, J.L., Matthiessen, J. & Head, M.J. (1999) Distribution of recent dinoflagellate cysts in surface sediments from the North Atlantic Ocean and adjacent seas in relation to sea-surface parameters. *American Association of Stratigraphic Palynologists, Contribution Series*, **35**, 1–152.

Rosell-Melé, A. (1997) Appraisal of CLIMAP temperature reconstruction in the NE Atlantic using alkenone proxies. *EOS, Transactions of the American Geophysical Union*, **78**, F28.

Rosell-Melé, A. (1998) Interhemispheric appraisal of the value of alkenone indices as temperature and salinity proxies in high-latitude locations. *Palaeoceanography*, **13**, 694–703.

Rosell-Melé, A. & Koç, N. (1997) Palaeoclimatic significance of the stratigraphic occurrence of photosynthetic biomarker pigments in the Nordic seas. *Geology*, **25**, 49–52.

Rosell-Melé, A., Weinelt, M., Sarnthein, M., Koç, N. & Jansen, E. (1998) Variability of the Arctic front during the last climatic cycle: application of a novel molecular proxy. *Terra Nova*, **10**, 86–89.

Rothrock, D.A., Yu, Y. & Maykut, G.A. (1999) Thinning of the Arctic sea-ice cover. *Geophysical Research Letters*, **26**, 3469–3472.

Ruddiman, W.F. (1977) Late Quaternary deposition of ice rafted sand in the subpolar North Atlantic (lat. 40°N to 65°N). *Bulletin of the Geological Society of America*, **88**, 1813–1827.

Ruddiman, W.F. (1997) North Atlantic ice rafting: a major change at 75,000 years before present. *Science*, **196**, 1208–1211.

Samtleben, C. & Schroder, A. (1992) Living coccolithophore communities in the Norwegian–Greenland Sea and their record in sediment. *Marine Micropalaeontology*, **19**, 333–354.

Sancetta, C. (1979) Oceanography of the North Pacific during the last 18,000 years: evidence from fossil diatoms. *Marine Micropalaeontology*, **4**, 103–123.

Sancetta, C. (1981) Oceanographic and ecologic significance of diatoms in surface sediments of the Bering and Okhotsk seas. *Deep-Sea Research*, **28**, 789–817.

Sancetta, C. (1982) Distribution of diatom species in surface sediments of the Bering and Okhotsk Seas. *Marine Micropalaeontology*, **28**, 221–257.

Sancetta, C. (1983) Effect of Pleistocene glaciation upon oceanographic characteristics of the North Pacific Ocean and Bering Sea. *Deep-Sea Research*, **30**, 851–869.

Sarnthein, M., Jansen, E., Weinelt, M., Arnold, M., Duplessy, J.C., Erlenkeuser, H., Flatoy, A., Johannessen, G., Johannessen, T., Jung, S., Koç, N., Labeyrie, L., Maslin, M., Pflaumann, U. & Schulz, H. (1995) Variations in Atlantic surface ocean palaeoceanography, 50–80°N: a time-slice record of the last 30,000 years. *Palaeoceanography*, **10**, 1063–1094.

Schweitzer, P.N. (1995) *Monthly averaged polar sea ice concentration*. US Geological Survey Digital Data Series: Virginia. CD, Ed. 1. DDS-27.

Sedwick, P.N., Edwards, P.R., Mackey, D.J., Griffiths, F.B. & Parslow, J.S. (1997) Iron and manganese in surface waters of the Australian subantarctic region. *Deep-Sea Research*, **44**, 1239–1253.

Serreze, M.C., Walsh, J., Chapin, F., Osterkamp, T., Dyurgerov, M., Romanovsky, V., Oechel, W., Morison, J., Zhang, T. & Barry, R. (2000) Observational evidence of recent change in the northern high-latitude environment. *Climate Change*, **46**, 159–207.

Shevenell, A.E., Domack, E.W. & Kernan, G.M. (1996) Record of Holocene palaeoclimate change along the Antarctic Peninsula: evidence from glacial marine sediments, Lallemand Fjord. *Papers and Proceedings of the Royal Society of Tasmania*, **130**, 55–64.

Sigtryggsson, H. (1972) An outline of sea ice conditions in the vicinity of Iceland. *Joekull*, **22**, 1–11.

Simmonds, I. (1996) Climatic role of the Southern Hemisphere extratropical cyclones and their relationship with sea ice. *Papers and Proceedings of the Royal Society of Tasmania*, **130**, 95–100.

Simmonds, I. & Jacka, T.H. (1995) Relationships between the interannual variability of Antarctic sea ice and the Southern Oscillation. *Journal of Climate*, **8**, 637–647.

Simmonds, I. & Wu, X. (1993) Cyclone response to changes in winter southern hemisphere sea-ice concentration. *Quaternary Journal of the Royal Meteorological Society*, **119**, 1121–1148.

Sjunneskog, C. & Taylor, F. (2002) Postglacial marine diatom record of the Palmer Deep, Antarctic Peninsula (ODP Leg 178, Site 1098). I: total diatom abundance. *Palaeoceanography*, **17**, DOI: 10.1029/2000PA000563.

Smith, W.O., Jr & Sakshaug, E. (1990) Polar phytoplankton. In: *Polar Oceanography*, *Part B Chemistry, Biology, and Geology*, (Ed. W.O. Smith, Jr), pp. 477–525. Academic Press, San Diego, California.

Stabeno, P.J. & Overland, J.E. (2001) Bering Seashifts toward an earlier spring transition. *EOS, Transactions of the American Geophysical Union*, **82**, 317.

Steig, E.J., Hart, C.P., White, J.W.C., Cunningham, W.L., Davis, M.D. & Saltzman, E.S. (1998) Changes in climate, ocean and ice sheet conditions in the Ross embayment, Antarctica, at 6 ka. *Annals of Glaciology*, **27**, 305–310.

Takeda, S. (1998) Influence of iron availability on nutrient consumption ratio of diatoms in oceanic waters. *Nature*, **393**, 774–777.

Taylor, F., McMinn, A. & Franklin, D. (1997) Distribution of diatoms in surface sediments of Prydz Bay, Antarctica. *Marine Micropalaeontology*, **32**, 209–229.

Taylor, F. & Sjunneskog, C. (2002) Postglacial marine diatom record of the Palmer Deep, Antarctic Peninsula (ODP Leg 178, Site 1098) 2. Diatom assemblages. *Palaeoceanography*, **17**, DOI: 10.1029/2000PA000564.

Thiede, J., Eldholm, O. & Taylor, E. (1989) Variability of Cenozoic Norwegian–Greenland Sea palaeoceanography and Northern Hemisphere palaeoclimate; synthesis of palaeoenvironmental studies of ODP Leg 104, Voring Plateau, Norwegian continental margin. *Proceedings of the Ocean Drilling Program, Scientific Results*, **104**, 1067–1118.

Thoroddsen, Th. (1916/17) Árferdi á Íslandi í thúsund ár, 432 pp., Hid Íslenska Fraedafjelag í Kaupmannahöfn, S.L. Møller, Copenhagen, 1916 (pt. 1) and 1917 (pt. 2) (in Icelandic).

Tremblay, L.-B., Mysak, L.A. & Dyke, A.S. (1997) Evidence from driftwood records for century-to-millenial scale variations of the high latitude atmospheric circulation during the Holocene. *Geophysical Research Letters*, **24**, 2027–2030.

Vaughan, S. (2000) Can Antarctic sea ice extent be determined from whaling records? *Polar Record*, **36**, 345–347.

de Vernal, A., Guiot, J. & Turon, J.-L. (1993a) Late and postglacial palaeoenvironments of the Gulf of St. Lawrence: marine and terrestrial palynological evidence. *Géographie physique et Quaternaire*, **47**, 167–180.

de Vernal, A., Henry, M., Matthiessen, J., Mudie, P.J., Rochon, A., Boessenkool, K.P., Eynaud, F., Grøsfield, K., Guiot, J., Hamel, D., Harland, R., Head, M.J., Kunz-Pirrung, M., Levac, E., Loucheur, V., Peyron, O., Pospelova, V., Radi, T., Turon, J.-L. & Voronina, E. (2001) Dinoflagellate cyst assemblages as tracers of sea-surface conditions in the northern North Atlantic, Arctic and sub-Arctic seas: the new 'n = 677' data base and its application for quantitative palaeoceanographic reconstruction. *Journal of Quaternary Science*, **16**, 681–698.

de Vernal, A. & Hillaire-Marcel, C. (2000) Sea ice cover, sea-surface salinity and halothermocline structure of the northwest North Atlantic: modern versus full glacial conditions. *Quaternary Science Reviews*, **19**, 65–85.

de Vernal, A., Hillaire-Marcel, C., Turon, J.-L. & Matthiessen, J. (2000) Reconstruction of sea-surface temperature, salinity, and sea ice cover in the northern North Atlantic during the last glacial maximum based on dinocyst assemblages. *Canadian Journal of Earth Sciences*, **37**, 725–750.

de Vernal, A. & Mudie, P.J. (1989) Late Pliocene to Holocene palynostratigraphy at ODP Site 645, Baffin Bay. *Proceedings of the Ocean Drilling Program*, **105**, 401–422.

de Vernal, A., Rochon, A., Turon, J.-L. & Matthiessen, J. (1997) Organic-walled dinoflagellate cysts: palynological tracers of sea-surface conditions in middle to high latitude marine environments. *GEOBIOS*, **30**, 905–920.

de Vernal, A., Turon, J.-L. & Guiot, J. (1993b) Dinoflagellate cyst distribution in high-latitude marine environments and quantitative reconstruction of sea-surface salinity, temperature, and seasonality. *Canadian Journal of Earth Sciences*, **31**, 48–62.

Vinnikov, K.Y., Robock, A., Stouffer, R.J., Walsh, J.E., Parkinson, C.L., Cavalieri, D.J., Mitchell, J.F.B., Garrett, D. & Zakharov, V.F. (1999) Global warming and northern hemisphere sea ice extent. *Science*, **286**, 1934–1937.

Voronina, E., Polyak, L., de Vernal, A. & Peyron, O. (2001) Holocene variations of sea-surface conditions in the southeastern Barents Sea, reconstructed from dinoflagellate cyst assemblages. *Journal of Quaternary Science*, **16**, 717–726.

Wadhams, P. (1995) Arctic sea ice extent and thickness. *Philosophical Transactions – Royal Society of London*, **A352(1699)**, 301–319.

Wadhams, P. & Davis, N.R. (2000) Further evidence of ice thinning in the Arctic Ocean. *Geophysical Research Letters*, **27**, 3973–3975.

Wagner, T. & Henrich, R. (1994) Organo- and lithofacies of TOC-lean glacial/interglacial deposits in the Norwegian–Greenland Sea: sedimentary and diagenetic responses to palaeoceanographic and palaeoclimatic changes. *Marine Geology*, **120**, 335–364.

Warner, R.C. & Budd, W.F. (1998) Modelling the long-term response of the Antarctic ice sheet to global warming. *Annals of Glaciology*, **27**, 161–168.

Watkins, A.B. & Simmonds, I. (1995) Sensitivity of numerical prognoses to Antarctic sea ice distribution. *Journal of Geophysical Research*, **100**, 22681–22696.

Watkins, A.B. & Simmonds, I. (2000) Current trends in Antarctic sea ice: the 1990s impact on a short climatology. *Journal of Climate*, **13**, 4441–4451.

Weaver, A.J., Eby, M., Fanning, A.F. & Wiebe, E.C. (1998) Simulated influence of carbon dioxide, orbital forcing and ice sheets on the climate of the Last Glacial Maximum. *Nature*, **394**, 847–853.

Weaver, A.J., Eby, M., Wiebe, E.C., Bitz, C.M., Duffy, P.B., Ewen, T.L., Fanning, A.F., Holland, M.M., MacFadyen, A., Matthews, H.D., Meissner, K.J., Saenko, O., Schmittner, A., Wang, H. & Yoshimori, M. (2001) The UVic Earth System Climate Model: model description, climatology, and applications to past, present and future climates. *Atmosphere-Ocean*, **39**, 361–428.

Webb, R.S., Rind, D.H., Lehman, S.J., Healy, R.J. & Sigman, D. (1997) Influence of ocean heat transport on the climate of the Last Glacial Maximum. *Nature*, **385**, 695–699.

Weinelt, M., Sarnthein, M., Pflaumann, U., Schulz, H., Jung, S. & Erlenkeuser, H. (1996) Ice-free Nordic seas during the last glacial maximum? Potential sites of deepwater formation. *Palaeoclimates*, **1**, 283–309.

Williams, K.M. (1986) Recent arctic marine diatom assemblages from bottom sediments in Baffin Bay and Davis Strait. *Marine Micropalaeontology*, **10**, 327–341.

Williams, K.M. (1990) Late Quaternary palaeoceanography of the western Baffin Bay region: evidence from fossil diatoms. *Canadian Journal of Earth Sciences*, **27**, 1487–1494.

Williams, K.M. (1993) Ice sheet and ocean interactions, margin of the East Greenland Ice Sheet (14 ka to present): diatom evidence. *Palaeoceanography*, **8**, 69–83.

Wilson, P.R., Ainley, D.G., Nur, N., Jacobs, S.S., Barton, K.J., Ballard, G. & Comiso, J.C. (2001) Adélie penguin population change in the Pacific sector of Antarctica: relation to sea-ice extent and the Antarctic Circumpolar Current. *Marine Ecology Progress Series*, **213**, 301–309.

Wollenburg, I. (1993) Sedimenttransport durch das arktische Meereis: Die rezente lithogene und biogene Materialfracht. *Berichte zur Polarforschung*, **127**, 1–159.

Woollett, J. (1999) Living in the narrows: subsistence economy and culture change in Labrador Inuit society during the contact period. *World Archaeology*, **30**, 370–387.

Wyrwoll, K.-H., Dong, B. & Valdes, P. (2000) On the position of the southern hemisphere westerlies at the Last Glacial Maximum: an outline of AGCM simuation results and evaluation of their implications. *Quaternary Science Reviews*, **19**, 881–898.

Yiou, F., Raisbeck, G.M., Bourles, D., Lorius, C. & Barkov, N.I. (1985) ^{10}Be in ice at Vostok Antarctica during the last climatic cycle. *Nature*, **316**, 616–617.

Yuan, X. & Martinson, D.G. (2000) Antarctic sea ice extent variability and its global connectivity. *Journal of Climate*, **13**, 1697–1717.

Zielinski, U. & Gersonde, R. (1997) Diatom distribution in Southern Ocean surface sediments (Atlantic sector): implications for palaeoenvironmental reconstructions. *Palaeogeography, Palaeoclimatology, Palaeoecology*, **129**, 213–250.

Zonneveld, K.A.F., Versteegh, G.J.M. & de Lange, G.J. (2001) Palaeoproductivity and postdepositional aerobic organic mater decay reflected by dinoflagellate cyst assemblages of the Eastern Mediterranean S1 sapropel. *Marine Geology*, **172**, 181–195.

Zwally, H.J., Comiso, J.C., Parkinson, C.L., Cavalieri, D.J. & Gloersen, P. (2002) Variability of Antarctic sea ice 1979–1998. *Journal of Geophysical Research*, **107**, 1029–1047, DOI: 10.1029/2000JC000733.

Glossary

Abiotic: Not living, non-biological, usually describing factors in an ecosystem such as atmospheric gases, inorganic salts, mineral soil particles and water. This expression is also used to describe the chemical and physical factors, such as temperature, salinity and humidity, which influence organisms.

Ablation: The sum of processes through which an ice cover is losing mass, either to the air (evaporation, erosion and resuspension of snow) or the water (surface melt and run-off, bottom melt).

Accessory pigment: Photosynthetic pigment that traps light energy and channels it to chlorophyll *a*, the primary pigment, which initiates the reactions of photosynthesis. Accessory pigments include the carotenoids, phycobiliproteins, and chlorophylls *b*, *c* and *d*.

Acoel: Lack of a coelom (body cavity).

Aeolian: Processes including the erosion, transport and deposition of material by wind.

Aerobic: Aerobic micro-organisms (aerobes) are those that require oxygen for growth; obligate aerobes cannot survive in the absence of oxygen. The opposite are anaerobic organisms, which do not require oxygen for growth; obligate anaerobes cannot survive in the presence of oxygen.

Albedo: The fraction of the incident shortwave radiation (at wavelengths between 0.4 and 1.5 μm) that is reflected from a surface (i.e. the ratio between the upwelling and downwelling shortwave radiation at a reference level above a given surface).

Algae: General term for eukaryotic, chlorophyll-containing, oxygen-producing photosynthetic organisms that are not plants.

Amphipods: A member of an order of crustaceans, Amphipoda, with over 4600 species. They are generally flattened laterally and look hunch-backed, sometimes even swimming on their sides.

Anaerobic: See **aerobic**.

Antarctic Circumpolar Wave (ACW): A propagating wave observed to cause disruptions at the sea ice margin and moves around the Antarctic with a period of approximately 8 years and a wave number of 2.

Antifreeze proteins (AFP) and antifreeze glycoproteins (AFGP): Proteins

produced by an organism in order to prevent freezing of its tissues or body fluids when subjected to sub-zero environmental temperatures. Many animals living in cold climates adopt a strategy of preventing ice formation in their tissues when subject to freezing conditions. One way of achieving this is to accumulate solutes in their blood, thereby raising the osmotic concentration and so depressing the supercooling point.

Archaea: Prokaryotic organisms belonging to the third major domain of life (the other two are the eubacteria and the eukaryota), with most known species associated with extreme environments.

Authigenic: Applied to materials (minerals, etc.) that formed in the rock of which they are a part during, or soon after, its deposition.

Autotrophic: The ability to utilize inorganic carbon (usually CO_2) as the sole source for carbon for organic synthesis, based on energy from light (photoautotrophic) or from oxidation of inorganic compounds (chemoautotrophic).

Avifauna: All the bird species that occur in a region.

Baleen whale: Large cetacean, whose mouth is lined with bristles which are used to strain food from sea water (the larger species are referred to as 'great whales,' but the latter also includes sperm whales which have teeth).

Benthic: Refers to the sea floor, or waters in contact with the sea floor; see also **mesopelagic**.

Benthos: In freshwater and marine ecosystems, the collection of organisms attached to, or resting on, the bottom sediments (epifaunal), and those which bore or burrow into the sediments (infaunal).

Biogenic: Applied to material, processes, or activities, of living or once-living organisms.

Biogeochemistry: Science concerned with the effects of living things on subsurface geology; or with the distribution and fixation of chemical elements in the biosphere.

Biomass: The total mass of all the organisms of a given type and/or in a given area. May be expressed in terms of wet weight, dry weight, carbon, chlorophyll, etc.

Biosiliceous sediment: Siliceous sediment derived from living organisms.

Bottom water: Water mass at the deepest part of the water column in the ocean.

Carnivore: An animal that feeds largely or exclusively on other animals. The term is used most frequently for members of the order Carnivora, which includes flesh-eating mammals such as dogs, cats, bears and seals.

Chemosynthesis: The use of the energy contained in reduced inorganic compounds to synthesize organic material from carbon dioxide and water.

Chemotaxis: The movement of a cell or a micro-organism in response to an external chemical stimulus.

Chlorophyll: A group of green pigments in photosynthetic organisms involved in harvesting light by absorption, excitation and transfer of energy.

Ciliates: Protozoans, up to 0.15 mm long, which swim actively, engulfing small food particles via mouth and gullet.

Convection: Movement of a fluid resulting from density instabilities. In sea water, this is usually driven by surface cooling or by increased surface salinity due to evaporation or brine rejection.

Copepodids (copepodite stages): Larval stage of copepods.

Copepods: A small aquatic crustacean of the class Copepoda, without a carapace and with paddle-like feet. Many are minute but they form a major component of marine plankton.

Cryopelagic: Environment including sea ice and the underlying water.

Cryosphere: Frozen water, in the form of snow, floating ice, sub-surface permafrost, glaciers and ice sheets, that constitutes a component of the earth's surface and near-surface layers, interacting with the oceans, atmosphere and crust.

Denitrification: A chemical process in which nitrates in the soil or water are reduced to molecular nitrogen, which is released into the atmosphere. This process is effected by denitrifying bacteria, which use nitrates as a source of energy for other chemical reactions in a manner similar to respiration in other organisms.

Detritivores: An animal that feeds on detritus. Detritivores play an important role in the breakdown of organic matter from decomposing animals and plants.

Detritus: Dead particulate organic material.

Diatom: (Bacillariophyceae), unicellular algae with a cell wall of amorphous silica. Adapted to a wide range of pelagic and benthic marine habitats.

Dimethyl sulphide (DMS): A volatile sulphur compound produced by marine phytoplankton and transferred to the atmosphere. Following oxidation to sulphate particles, DMS affects the radiative properties of the atmosphere by reflecting solar radiation and by affecting the concentration of cloud condensation nuclei (CCN). It is the main natural source of sulphate aerosol and the major route by which sulphur is recycled from the ocean to the continents. The production of dimethylsulphoniopropionate (DMSP, the precursor of DMS) in the ocean is strongly dependant on the phytoplankton species.

Dimethylsulphoniopropionate (DMSP): See **dimethyl sulphide (DMS).**

Dinoflagellate: A single-celled micro-organism capable of limited propulsion through use of whip-like flagella.

Dispersal: Moving from an area of birth or growth to another area.

Draft: The depth of the ice underside below the water level.

Ectotherms: All animals except birds and mammals which exhibit poikilothermy, the passive variation in the internal body temperature of an animal, which depends on the temperature of the environment.

Emissivity: The ratio of the radiation emitted by a surface to the radiation emitted by a blackbody at the same temperature.

ENSO (El Niño Southern Oscillation) cycle: Refers to the coherent, large-scale fluctuation of ocean temperatures, rainfall, atmospheric circulation, vertical motion and air pressure across the tropical Pacific.

Enthalpy of freezing or melting: The amount of energy that has to be supplied to,

or removed from, a system in order for it to undergo a phase change from liquid to solid or vice versa (often also referred to as latent heat of freezing or melting). For pure ice, this amounts to 334 J g^{-1}, i.e. approximately 80 times the amount of heat required to warm a gram of water by 1 K.

Epiphyte: An organism living on the surface of a plant; also used to describe bacteria and other micro-organisms living on the surface of photoautotrophic microbes.

Epontic organism: Organism that exists closely associated with sea ice, usually within the interstitial spaces between ice crystals or within brine channels in sea ice.

Eukaryotes: Organisms with a cellular nucleus and typically having DNA arranged in multiple chromosomes.

Euphausiids: Relatively large (10–70 mm) shrimp-like, holoplanktonic crustaceans of the phylum Arthropoda.

Euphotic zone: The topmost layer of a lake or sea in which there is sufficient light for net primary production. The depth varies, depending on such factors as turbidity, supply of nutrients in the water, tidal turbulence, and temperature. For example, high nutrient levels will encourage a greater biomass of phytoplankton near the surface, which causes shading and consequent reduction in depth of the euphotic zone. It typically ranges from < 1 m to about 30 m in lakes and coastal waters, and rarely reaches depths of more than 200 m in the open ocean.

Euryhaline: Able to tolerate a wide range of salinities.

Eutectic: When two liquids are mixed, the mixture typically freezes at a lower temperature than either pure substance. That composition which has the lowest melting point is called the eutectic from the Greek for 'easily melted'.

Extremophile: A micro-organism that thrives under extreme environmental conditions of temperature, pH, or salinity.

Fast ice: Permanent, often multi-year, ice covering oceanic/fjord water which is literally stuck 'fast' to the continent or to some other fixed objects such islands, grounded icebergs, and peninsulas.

Fatty acid: An organic acid with a long straight hydrocarbon chain and an even number of carbon atoms. Fatty acids are the fundamental constituents of many important lipids, including triglycerides. Some fatty acids can be synthesized by the body; others, the essential fatty acids, must be obtained from the diet.

First year ice: Sea ice of not more than one winter's growth, developing from young ice and having a thickness > 30 cm and usually with snow cover.

Flooded ice: Sea ice with liquid water at the snow–ice interface caused by negative freeboard due to snow loading.

Fluorescence: Emission of light of a certain wavelength when activated by light of another, lower wavelength.

Foraminifer: A protozoan of the mainly marine order Foraminifera, having a

perforated shell through which amoeba-like pseudopodia emerge. The shells eventually drop to the sea bed to form calcareous ooze, and fossil deposits of foraminifers form the main constituent of chalk.

Frazil ice: Fine spicules or plates of ice suspended in water during ice formation.

Freeboard: The height of the ice surface above the water level.

Freezing point: Temperature at which a small seed ice crystal is formed in an antifreeze solution, i.e. the temperature of additional freezing because ice is already present.

Frustule: Silica cell wall of a diatom, generally two per cell.

Gastropods: (Gastropoda) snails of the phylum Mollusca.

Global Circulation Model (GCM): A computer-based model that calculates and predicts what climate patterns will look like in a number of years. The GCM programs look at several equations at once. They take into account conservation of mass, energy, and momentum in a grid box system. The model focuses on each grid box and the transfer of energy between grid boxes. Once calculated you can determine a number of climate patterns, from ocean and wind currents to patterns in precipitation and evaporation rates that could affect lake levels and agricultural levels.

Glycolipid: Organic molecule containing both a sugar and a fat component.

Grazing: The consumption of plants by herbivores which include protozoans and zooplankton.

Grease ice: A soupy thin layer of ice at the water surface formed from the accumulation of frazil ice.

Herbivore: An animal that feeds on plants.

Heterotrophic: The ability to obtain carbon for organic synthesis by metabolizing organic materials.

Holocene: The last ten thousand years (ka) of post-glacial deposition.

Holoplankton: Planktonic organisms that spend their entire lives in the water column, i.e. have a completely pelagic life cycle.

Hyperosmotic: The organism's total osmotic concentration is higher than that of the environment.

Hypersaline: More saline than sea water.

Hyposaline: Less saline than sea water.

Hyposmotic: The organism's total osmotic concentration is less than that of the environment.

Ice-albedo feedback: Due to the substantial contrast in albedo between the open and ice/snow-covered ocean, the former absorbs more than 90% of the incoming solar radiation whereas the latter typically absorbs less than 30%. Hence, changes in the extent or albedo of the oceans' sea ice cover triggered, e.g. by the effects of anthropogenic atmospheric warming, can lead to an amplification of such perturbations, since a reduction in ice extent provides more solar heat to the ocean which in turn helps reduce the ice cover even further (and vice versa in the case of cooling).

Ice area: The actual area (extent) covered by ice and is the sum of the product of the ice concentration and the area of each data element in the ice-covered ocean.

Ice concentration: The percentage of ice-covered surfaces within the satellite footprint or grid. Often expressed out of ten, i.e. a scale from 1/10 to 10/10.

Ice edge: The demarcation between ice-free ocean (or sea) and ice-covered ocean (or sea) and is usually set at 15% ice concentration when using satellite microwave data. Definition depends on scale. At smallest scale, refers to the edge of fast ice (where it meets open water) in bays. At the largest scale this refers to where the pack ice meets the open sea.

Ice extent: The sum of the area of all data elements which has at least 15% sea ice concentration.

Ice floe: A discrete section of sea ice that varies in area from a few square metres to the area of a small town.

Ice-obligate species: An organism that is always found in the presence of sea ice, and which inhabits only those areas where sea ice is a major feature for most of the year.

Ice-rafted debris (IRD): Sediment transported to the deep sea by the melting of floating icebergs.

Infauna: Refers to organisms that live in the mud and ooze of the ocean floor. See also **benthos**.

Infrared radiation: Electromagnetic radiation whose wavelength lies in the range from 0.75 μm to 1000 μm. Thermal infrared radiation lies in the range from 9 to 14 μm

Interannual: Refers to the year-to-year variation in an environmental property, such as wind strength or sea ice cover.

Interstitial fauna: Animals that live in the space between adjacent particles in a substrate (sea ice or sediment).

Inuit: A member of the Eskimo peoples inhabiting northernmost North America from northern Alaska to eastern Canada and Greenland.

Iso-osmotic: The organism's total osmotic concentration is the same as that of the environment.

Katabatic wind: A wind (or component thereof) directed down the slope of an incline and caused by greater air density near the slope than at the same levels some distance horizontally from the slope.

Kleptoparasite: A species that steals food from other species.

Krill: Norwegian word meaning whale food, and usually referring to schooling crustaceans of the family Euphausiacea. Often specifically *Euphausia superba* of the Antarctic Ocean.

Lead: A linear feature of open water that occurs in the ice pack between ice floes caused by ice break-up (see **ice floe**), and may be covered by new ice.

Lithogenic sediment: Sediment derived from the weathering of rocks (see **terrigenous sediment**).

Lithology: A term applied to sediments, referring to their general characteristics or variation in composition and texture.

Lorica: Protective covering that surrounds an algal cell.

Lysis: Rupturing of a cell and loss of cell contents.

Marginal ice zone: A geographical zone at the ice edge where ice floes are relatively loose and influenced by waves.

Meiofauna: Small animals that live between particles. See **interstitial fauna**.

Melting point: There should be no difference between the freezing and melting temperatures at equilibrium. In a solution containing molecular antifreeze, however, the crystal may not increase in size until the solution is cooled. The extent of cooling prior to crystal growth depends on, for example, type and concentration of antifreeze. If, subsequent to freezing, the temperature of a solution is increased, melting of the ice does not occur at the freezing point but only at a higher temperature.

Meroplankton: Planktonic organisms that spend only part of their life cycle in the water column, e.g. eggs and larvae of benthic species.

Mesopelagic: Refers to species that rarely, if ever, ascend to surface waters, but which do not occur either at the sea floor.

Metazoans: Multicellular animals. cf. **protozoans**.

Microstructure: A term commonly used in the study of snow and ice (and other geophysical or geological disciplines) to describe the size, shape, and spatial arrangement of component phases in a particular medium. In the case of sea ice, this would include in particular the size, shape and distribution of brine and gas inclusions, as well as that of individual ice crystals harbouring such inclusions. While usage of this term and the related term of 'texture' varies widely in different fields, microstructure is typically limited to the scale of individual grains or small groups of grains, whereas texture describes features that relate to the larger-scale patterns of grain arrangement and orientation.

Microwave radiation: Electromagnetic radiation with wavelength ranging from 0.3 cm to 30 cm corresponding to frequencies from 1 to 100 GHz.

Mixotrophic: The ability to obtain carbon for organic synthesis from both inorganic sources (autotrophy) and organic materials (heterotrophy).

Multi-year ice: Sea ice that has survived at least one summer melt period.

Mycosporine-like amino acid (MAA): A molecule that absorbs strongly in the UV range. Many organisms produce this molecule for use as a 'sunscreen'.

Mysids: Shrimp-like crustaceans of the phylum Arthropoda.

Nauplii: Early development stage in many crustaceans such as copepods and euphausiids.

Nematodes: (Nematoda) small cylindrical roundworms of the phylum Aschelminthes.

Neritic: Pertaining to shallow waters.

New ice: A general term for newly formed ice, which includes frazil ice, grease ice, shuga, and nilas.

Nitrification: A chemical process in which nitrogen (mostly in the form of ammonia) in plant and animal wastes, and dead remains, are oxidized at first to nitrites and then to nitrates. These reactions are effected mainly by the nitrifying bacteria *Nitrosomonas* and *Nitrobacter*, respectively. See **denitrification**.

Omnivore: An animal that eats both animal and vegetable matter.

Osmo-conformers: Allows the concentrations of the extracellular fluids to vary in parallel with ambient salinity, at least over a certain range of salinity.

Osmolyte: Dissolved ion or organic material within a cell that helps maintain an osmotic pressure within the cell equal to that outside the cell, thus avoiding cell lysis (too much internal pressure) or shrinkage (too little internal pressure).

Oxygen microelectrode: A small metallic (often platinum) probe capable of measuring dissolved oxygen concentrations in small volumes.

Pack ice: All sea ice except that which is attached to terrestrial ice.

Pagophilic: A technical term meaning 'ice-loving', for example pagophilic seals are those which use ice for some period of their life cycle. This can be free-floating pack ice or fast ice.

Pancakes: Predominantly circular pieces of ice from about 3 cm to 3 m in diameter, less than 10 cm in thickness and with raised edges.

Pelagic: Describing organisms that swim or drift in a sea or a lake, as distinct from those that live on the bottom (see **benthos**). Pelagic organisms are divided into plankton and nekton.

Phaeophorbide: Specific breakdown product of chlorophyll.

Phaeopigments: Degradation products of chlorophyll.

Phagotrophic: The ability to consume particles to obtain organic materials.

Phase: In the context of thermodynamics, a phase describes a microscopically homogeneous part of a system, with distinct boundaries separating it from other phases in the same system. In sea ice, these typically include the ice, liquid brine, gas inclusions (both in ice and brine) and salt precipitates or other mineral inclusions. A phase diagram delineates the limits of stability of different phases within a system, such as the complete absence of ice in a system composed of pure water at temperatures above 0°C.

Phospholipids: A group of lipids that consist of a phosphate group and one or more fatty acids. They are major components of cell membranes in plants and animals.

Photoacclimation: The ability of algae to respond relatively quickly to changes in light conditions. Photoacclimation responses can include changes in chloroplast configuration, pigment concentration and composition.

Photorespiration: A metabolic pathway that occurs in plants in the presence of light, in which ribulose bisphosphate carboxylase/oxygenase (RUBISCO), the enzyme involved in carbon dioxide fixation with ribulose bisphosphate, accepts oxygen, in place of carbon dioxide, resulting in the formation of a two-carbon compound, glycolate, which is subsequently metabolized to carbon dioxide. Unlike respiration, there is no production of adenosine triphosphate (ATP).

Photosynthesis: The process by which the energy of sunlight is used by green plants and some unicellular organisms to synthesize carbohydrates from carbon dioxide and water.

Photosynthetically available radiation (PAR): Radiation at wavelengths between 400 and 700 nm (visible light) which are absorbed by algae for the process of photosynthesis.

Phytoplankton: The photosynthesizing organisms of plankton (see below), consisting chiefly of microscopic algae, such as diatoms and dinoflagellates. Near the surface of the sea there may be many millions of such organisms per cubic metre.

Pisces: (Fish) aquatic vertebrates of the phylum Chordata.

Plankton: Pelagic organisms (mostly microscopic) that drift or float passively with the current in a sea or lake. Plankton includes many microscopic organisms, such as algae, protozoans, various animal larvae, and some worms. It forms an important food source for many other members of the aquatic community and is divided into **zooplankton** and **phytoplankton**.

Platelet ice: Leaf or disc-like ice crystals either free floating or fixed under sea ice, usually fast ice.

Polychaetes: (Polychaeta) marine segmented worms of the phylum Annelida. Some are planktonic, but most are benthic, many with meroplanktonic larvae.

Polynya: Non-linear opening enclosed by ice that may be formed as a latent heat (or coastal) polynya, formed near coastal areas or islands by wind displacement, or a sensible heat (or deep ocean) polynya formed by the upwelling of warm water.

Polysaccharide: Any of a group of carbohydrates comprising long chains of monosaccharide (simple sugar) molecules.

Polyunsaturated fatty acids (PUFA): Fatty acids with two or more double bonds. Organic acids consisting of carbon chains with a carboxyl group at the end. The nutritionally important fatty acids have an even number of carbon atoms, commonly between twelve and twenty-two.

Pressure ridge: An elongated ridge or wall of broken ice forced up by ice pressure between two ice floes.

Primary production: The photosynthetic carbon fixation per unit area, per unit of time.

Prokaryotes: Organisms lacking a cellular nucleus and typically having DNA in a single molecule.

Protist: General term for eukaryotic microbes (algae and protozoa). Also used more specifically to refer to species in Protista in a five-kingdom taxonomy (with Monera, Fungi, Planta, and Animalia) – but this diverse group is commonly divided into several major groups at this level.

Protozoans: (Protozoa) microscopic unicellular organisms.

Psychrophilic: Describing an organism that lives and grows optimally at relatively low temperatures, usually below 15°C, and cannot grow above 20°C. Psychrophiles, which consist mainly of bacteria, algae, fungi and protozoans, are restricted to permanently cold climates.

Psychrotolerant: Organisms live and grow best at higher temperatures (20–40°C), but are able to tolerate cold conditions.

Pycnocline: A zone characterized by a large change in density over a short vertical depth.

Q_{10}: Change in physiological rate normalized to a 10°C change in temperature.

Quantum yield of photosynthesis (ϕ_p): The amount of carbon fixed per unit of light absorbed.

Quaternary: The latest period of time in the stratigraphic column representing the last 2 million years.

Remineralize: Transforming organic materials into inorganic forms, such as organic carbon to CO_2.

Remote sensing: The gathering and recording of information concerning the earth's surface by techniques that do not involve actual contact with the object or area under study. These techniques include photography (e.g. aerial photography), multispectral imagery, infrared imagery, and radar. Remote sensing is generally carried out from aircraft and, increasingly, satellites.

Rheology: Study of deformation and flow of materials.

Ridge keel: The bottom section of a pressure ridge protruding below the level ice underside. Typically, ridge keels are three to five time thicker than ridge sails.

Ridge sail: The top section of a pressure ridge rising above the level ice surface.

Rotifer: A protozoan belonging to the phylum Rotifera (about 2000 species), also called wheel animalcule, found mainly in fresh water. Rotifers vary in shape from spherical to worm-like and range between 0.1 and 0.5 mm in length.

RUBISCO (Ribulose bisphosphate carboxylase/oxygenase): The enzyme that mediates the carboxylation of ribulose bisphosphate in the first stage of the dark reaction of photosynthesis.

Salps: Barrel-shaped planktonic tunicates of the phylum Chordata.

SAR: Synthetic Aperture Radar.

Scintillation counting: Here it refers to the technique used to measure the uptake by phytoplankton of radionuclides such as ^{14}C-labelled bicarbonate.

Sea ice concentration: The fraction of open water within sea ice cover, e.g. 0–15% = open ocean; 100% = total ice cover.

Sea ice extent: The edge of the sea ice. Generally, defined by the 15% concentration expression from satellite data, due to resolution problems between the ice edge and weather effects on the sensitivity of brightness temperatures used to derive sea ice concentration.

Shuga: Spongy ice lumps, several centimetres wide, formed from a wind-driven accumulation of grease ice or slush.

Slush: A viscous mixture of snow and water.

Snow-ice interface: The ice surface before the first snow fall.

Solute segregation: Ice does not incorporate most common sea salt ions and other impurities into its crystal lattice, hence these solutes are concentrated ahead of a freeze-front in a salt water system in a process referred to as segregation. The

amount of solutes excluded from newly forming ice layers depends on the rate of ice growth, the type of solute and other factors, which can be subsumed through the definition of an effective segregation coefficient that describes the ratio of impurities in the ice relative to that in the parent water mass at the time of ice formation.

Species diversity index: Derived from combining the number of species with the number of individuals per species.

Stoichiometry: The ratios in which the reactants in a chemical reaction combine to form the products. For example, two moles of hydrogen react with one mole of oxygen, giving two moles of water. The stoichiometric equation summarizes this as $2H_2 + O_2 \rightarrow 2H_2O$. In stoichiometric compounds, the elements are present in simple whole number ratios: for example, the ratio is one to one in hydrogen chloride, HCl. In contrast, iron sulphide, Fe_xS, is a non-stoichiometric compound, x taking a range of values slightly less than one.

Strand community: An ice algal community that extends vertically into the upper water column from an ice floe. They can reach a metre or more in length and are generally restricted to Arctic regions.

Stratigraphy: The sequence of layers and units that constitute a sea ice cover. Typically, the stratigraphy is derived from thick and thin sections produced from ice cores drilled through the entire thickness of a floe. The stratigraphy is also crucial in establishing the growth history and evolution of an ice cover.

Succession: In ecology, replacement of one community by another.

Supercooling: The degree to which the actual temperature of a water body has been lowered to below its freezing point without the formation of ice. In the open ocean, with numerous biogenic and inorganic particulates aiding in the process of nucleation and ice formation, supercooling is typically less than 0.1 K. However, pure water in the absence of impurities and other potential sites for ice nucleation and growth, can be supercooled to more than 30 K below its freezing point.

Sympagic: Organisms living with sea ice.

Teleosts: (Teleostei) fish with bony skeletons.

Terrigenous sediment: Sediment derived from the weathering of rocks (see **lithogenic sediment**).

Texture: Typically describes the spatial arrangement and orientation of (sea ice) grains at a scale somewhat larger than that relevant for the microstructure (see **microstructure**).

Thermal hysteresis: (Antifreeze activity) refers to the fact that the temperature at which an ice crystal grows in a solution containing the antifreeze is lower than the temperature at which the crystal is observed to melt.

Thermodynamics: The science of the relations between heat and other (mechanical, electrical, etc.) forms of energy, and, by extension, of the relationships and interconvertibility of all forms of energy.

Thermohaline: The combined impact of temperature and salinity on seawater

density. In the polar oceans this is dominated typically by the impact of salinity, in particular in such areas where the loss of highly saline brine from growing sea ice can substantially increase seawater density and induce convective overturning and amplify thermohaline mixing.

Thylakoid membrane: The membranes within a chloroplast that contain the photosynthetic apparatus.

Triacylglycerol: An ester of glycerol (propane-1,2,3-triol) in which all three hydroxyl groups are esterified with a **fatty acid**. Triglycerides are the major constituent of fats and oils and provide a concentrated food energy store in living organisms.

Trophic: Used to describe feeding relationships, such as levels in a food chain.

Turbellarians: (Turbellaria) oval to elongated unsegmented flatworms of the phylum Platyhelminthes.

ULS: Upward looking sonar.

Visible radiation: Electromagnetic radiation with wavelength ranging approximately from 4000 to 7700 angstroms and is capable of causing sensation to vision.

Wax ester: Organic compounds produced by the reaction of an alcohol with an acid, with the elimination of water.

Xenobiotic: Substances foreign to the body.

Young ice: Ice in the transition stage between nilas and first-year ice, 10–30 cm in thickness.

Zooplankton: Animals of the plankton. See **plankton**.

Index

Page numbers in italic refer to figures, those in bold refer to tables.

abiotic conditions, 268, 271, 280, 287
abiotic modification, seawater chemistry, 268–71
absorption coefficients, 157
Acartia longiremis (copepod), 213, 216
ACC (Antarctic Circumpolar Current), 8, 251, 260
acclimation, algae, 144–5
Acoustic Doppler Current Profiler (ADCP), *306*
acrylic acid, 199, 203, 278
Actinocyclus curvatulus (diatom), 353
ACW *see* Antarctic Circumpolar Wave (ACW)
Adam of Bremmen, 3
adaptation, 233
  biochemical, 14, 219–21
  birds, 246–7
  low light, 144
  low-temperature, 195–8
  mammals, 246–57
  micro-organisms, 195–9
  physiological, 14
  salinity acclimation, 198–9
  sea birds, 251
  whales, 256
ADCP (Acoustic Doppler Current Profiler), *306*
Advanced Very High Resolution Radiometer (AVHRR), 114–15, 132, 338
advection, ice, 87
Adélie Land, 161
AFGPs (antifreeze glycoproteins), 220–21, 233
AFPs (antifreeze proteins), 220–21
AGCMs (Atmospheric Global Circulation Models), 344, 345, 346
aggregates, 314, 316, 322
aircraft, surveys, 97–100, 109
Alaska, 91, 103, 104, 255
  whales, 257
albedo, 28, 32, 65–7, 126, 333, 345
  changes, 346
  definition, 65
  factors affecting, 72
  parameterization schemes, 74
  reduction, 89, 106
  sea ice *vs*. lake ice, 25, 26, 37
  snow, 30
alcian blue, 290
Alfred Wegener Institute, 89, *99*
algae, 14, 48, 74
  acclimation, 144–5
  ammonium uptake, 194
  autotrophic, 201–202
  carbon assimilation, 273
  carbon isotopic composition, 145
  β-carboxylation, 145
  colonization, 200
  concentrations, 282
  distribution, 159
  dynamics, 157–9
  effects on sea ice chemistry, 271–2
  excretion, 289
  flux, 321–2
  as food source, 251, 304, 314–15
  gases, 279
  grazing, 320, 321
  habitats, 143, 148–9
  heterotrophic uptake, 195
  heterotrophy, 272
  incorporation, 199–200
  lipids, 282
  mortality, 283
  nitrate assimilation inhibition, 284
  nutrients, 280
  photoautotrophy, 272
  photosynthesis, 144, 193, 194, 195, 271–2
  physiology, 192–3
  phytoplankton seeding, 207, 304, 307, 315–19, 323
  pigment concentration, 191
  pigmented, 184, 205
  pioneer communities, 205
  primary production, 143–83
  production rates, **162–6**
  salinity acclimation, 198
  species diversity, 204, 317
  standing stocks, **162–6**
  studies, 267
  substrate affinity, 284
  see also diatoms
algal absorption coefficient (a*), 151–2
algal biomass accumulation, 149, 202–203, 313
  estimates, 167–70
  in situ measurements, 161–7
algal blooms, 203, 204, 217, 289, 321
  occurrence, 313
  see also phytoplankton blooms algal cells, 317–18, 321
  concentrations, 200–201
algal growth, 157, 160
  rates, 161, 314, 319
Algidasphaeridium minutum (dinoflagellate), 353
algorithms, 113, 116, 137
  mixing, 115
alkaline phosphatase, 197
alkenones, 350
ambush feeding, 248

amino acids, 233, 286
  accumulation, 287–8
  hydrolysis, 288
ammonia, 283
  accumulation, 194
  cellular diffusion, 284
  oxidation, 283
ammonium, 279, 280, 291
  accumulation, 281
  cellular diffusion, 284
  cellular transport, 285
  concentrations, 195, 218, 282, 283, 284
  dissociation, 194
  ions, 38
  low-temperature affinity, 284–5
  in snow, 281
  uptake, 194, 196
amoebae, 187, 188
amphipods, 12, 168, 211, 214
  abundance, 232
  adaptation, 219, 220
  feeding, 221, 222, 320
  as food source, 252, 254
  gammeriid, 216, 219, 222, 223, 224
  and global climate change, 258
  life cycles, 224
Amundsen, Roald, 49
Amundsen Gulf, 255
Amundsen Sea, 116, 126, 131, 134, 138
  carbon enrichment, 314
  copepods, 224
  sea ice primary production, 173–5
  sea ice thickness, 92
α-amylase, 196–7
Anderson model, 35, *36*
ANN (Artificial Neuron Networks), 355
anoxic processes, 270, 283
Antarctic
  algal biomass, 161–7, 169
  and Arctic compared, 10–13
  biota, 49
  birds, **241**, 242, 260
  chlorophyll abundance, 161
  climate, 335
  diatoms, 187
  early studies, 3, 4–5
  fish, 217
  food webs, *222*
  global climate change, 2
  habitats, 246–51
  heat flux, 29–30
  ice cover variability, 112–14, 116, 124–6, 133–8, **171–2**
  ice formation, 27
  ice temperature profiles, 56
  mammals, **241**, 260–61
  metazoans, 211, 212, 219–21, 224–7, 232
  microfossil distribution, 337–9
  palaeo sea ice distribution, 335–47
  particle flux, 304, 308–310, 311–12, 313–14
  photosynthetic rates, 168
  polynyas, 243, 246
  salinity studies, 52
  sea ice growth, 35, 117, 146
  sea ice melting, 33
  sea ice primary production, 169–76
  sea ice thickness, 92–3, 97
  snow cover, 30
  snow thickness, 90
  whales, 242
Antarctic Bottom Water, 7
Antarctic Circle, 243
  crossings, 5
Antarctic Circumpolar Current (ACC), 8, 251, 260
Antarctic Circumpolar Wave (ACW), 9, 124–5, 126, 133, 137, 138
  and global climate change, 260
Antarctic Peninsula, 92, 131, 134, 138, 173, 174
  climate, 259, 341
  diatoms, 318
  krill, 230, 315, 320
  particle flux, 307, 312
  seals, 250
Antarctic Treaty, 92, 95
antifreeze glycopeptides, 221
antifreeze glycoproteins (AFGPs), 220–21, 233
antifreeze proteins (AFPs), 220–21
antioxidation, 273
ANZFLUX study, 31
AO (Arctic Oscillation), 104, 134, 259, 348
Apherusa glacialis (amphipod), 216, 220, 222
  life cycle, 224
appendicularians, 216
aragonite, 270
Archaea, 15, 184, 187, 188
  pioneer communities, 205
  species diversity, 204, 206
archaeological sites, 357
Arctic, 1
  algal biomass, 161–7, 169
  and Antarctic compared, 10–13
  birds, **241**
  diatoms, 187
  early studies, 3–4
  fast ice, 51–2
  fish, 217
  habitats, 251–7
  heat flux, 29
  ice cover variability, 32, 112, 113, 116, 119–24, 137–8
  ice drift, 87
  ice thickness variability, 102–106
  mammals, **241**, 258–60
  melt water, 54
  metazoans, 211, 212–13, 219–21, 224, 227, 232
  microfossil distribution, 350–55
  palaeo sea ice distribution, 347–58
  particle flux, 304, 308–11
  photosynthetic rates, 168
  polynyas, 243–6
  river inputs, 291–2
  salinity evolution, 49–50
  sea ice growth, 35–6, 146
  sea ice melting, 33
  sea ice primary production, 169–70
  snow cover, 30–31
  surface melt ponds, 32
  whales, 242
  see also Canadian Arctic
Arctic Basin, 116, 133, 203, 291
  polynyas, 243
Arctic Circle, 243
Arctic Ocean, 2, 3, 8, 9, 291, 356
  albedo, 72
  diatoms, 353
  ice cover variability, 128–9, 133, 138
  ice formation, 27
  ice thickness distribution, 89–91
  ice thickness variability, 102–106
Arctic Oscillation (AO), 104, 134, 259, 348
Arctogadus glacialis (fish), 217, 221, 223
Argentine Basin, 8
Aristotle, 4
Artificial Neuron Networks (ANN), 355

astrobiological issues, sea ice, 13–15
Atlantic Ocean, 8, 10, 116, 122, 356
  ice thickness, 90
atmosphere, 134, 279, 333
  pressure systems, 259–60
  sea-ice effects, 5–9
Atmospheric Global Circulation Models (AGCM), 344, 345, 346
Australia, 260, 345, 346
authigenesis, minerals, 271
authigenic cryogenic minerals, 270–71
autocorrelation function, 63
Autonomous Underwater Vehicles (AUVs), 94–5, 109, 219, 234
Autosub Project (UK), 109, 227
autotrophs, 187–8, 201–202
autotrophy, net, 194
AUVs (Autonomous Underwater Vehicles), 94–5, 109, 219, 234
AVHRR (Advanced Very High Resolution Radiometer), 114–15, 132, 338

bacteria, 13, 14, 146, 193
  ammonium uptake, 194
  anaerobic, 270
  anoxygenic, 270
  chemo-autotrophy, 188
  concentrations, 201, 282
  denitrifying, 283
  enzymes, 15
  excretion, 289
  growth rates, 196
  habitats, 232
  heterotrophy, 189, 286
  incorporation, 201
  non-photosynthetic, 184
  parasitism, 189, 195
  photosynthetic, 184, 185
  pioneer communities, 205
  respiration, 271–2, 286
  species diversity, 204, 206
  studies, 17, 267
  substrate affinity, 284
  see also cyanobacteria
bacteria–algae interactions, 289
Baffin Bay, 122, 124, 129, 132, 259, 349
  diatoms, 351, 352–3, 358
  dinoflagellate cysts, 358
  habitats, 246, 252
  polynyas, 243
  sea salt concentration, 357
  whales, 256, 257
Baffin Island, 227, 320, 349, 357
Baltic Sea, 1, 3, 270, 281
  phytoplankton blooms, 317
  river inputs, 291–2
Barents Sea, 8, 91, 122, 129, 132
  amphipods, 216
  diatoms, 353
  dinoflagellate cysts, 355, 358
  habitats, 252
  Ice Sheet, 356
  particle flux, 307
  rotifers, 212
  seals, 253, 254
  walruses, 254
Barrow (Alaska), 25, *36*, *41*, *57*
BAT (Best Analogue Technique), 355
beaches, 246–7
Beaufort Gyre, 91, 92, 104, 349
Beaufort Sea, 91, 104, 124, 132, 133
  ice thickness variability, 107
  particle flux, 309
  salinity, 291
  seals, 253, 258
  whales, 255
Beer–Lambert law, 156
Beer's law, 64–5
Belcher Islands, 246
Bellingshausen Sea, 116, 126, 131, 134, 138, 260
  carbon enrichment, 314
  copepods, 224
  sea ice primary production, 173–5
  sea ice thickness, 92
belugas, 242, 246, 251, 254
  habitats, 255
bentho-pelagic coupling, 211
Bering Sea, 122–3, 124, 129, 132, 133, 137
  atmospheric effects, 259
  diatoms, 317, 351–2
  plankton biomass, 258
  polynyas, 246
  walruses, 254
  whales, 255, 257
Bering, Vitus, 3
Best Analogue Technique (BAT), 355
bicarbonate, ^{14}C radio-labelled, 150, 153, 154, 169
bio-active agents, 287
biochemical adaptation, 219–21
biofilms, 289–90, 293
biogeochemistry
  field of study, 268
  future research, 292–3
  issues, 292–3
  sea ice, 267–302
  time-series measurements, 293
Biological Marginal Ice Zone, 311
biological processes, effects on dissolved gases, 271–5
biology
  sea ice, 3, 74, 268, 292
  see also macrobiology; microbiology
biomarkers, 282, 350
  for biomass, 191–2
biomass
  autotrophic, 202
  biomarkers, 191–2
  determination, 191
  die-off, 194, 205
  estimation, 193
  formation, 267
  and global climate change, 258
  heterotrophic, 202
  increase, 283–4
  and metazoans, *213*
  micro-organisms, 189
  see also algal biomass accumulation
biopolymers, 286
biota, 49, 176–7, 185
biotechnology
  ice organisms, 14–15
  natural products, 14–15
biovolume-to-carbon conversion factors, 191
birds, 240–66
  adaptation, 246–7
  and global climate change, 2, 258–61
  habitats, 246–57
  insulation, 247
  species diversity, 12
  see also penguins; sea birds
bivalves, 254
blue-green algae *see* cyanobacteria
Bodde, Ivarr, 3
Bootstrap Algorithm, 113, 115
Boreogadus saida (fish), 12, 217, 220, 221
  feeding grounds, 223
  as food source, 251
bottom water, formation, 7–8
Bouguer–Lambert law, 64–5
Bouvet Island, 340, 341

brackish ice, growth, 46
Bransfield Strait, 311, 312, 314, 317
breeding grounds, 246–7, 248
  seals, 249, 250, 252, 253–4, 258, 259–60
Bremerhaven Regional Ice–Ocean Simulations (BRIOS), 89
Brigantedinium spp. (dinoflagellates), 353
brine
  density, 43, 44–5, 160
  flux, 155
  gases in, 269–70, 272
  mass fraction, 40
  pH, 275
  relative volume fraction, 42, 43, 55
  salinity, 43, 160
  sampling, 275
  see also salt
brine channels, 56–7, 213, 214, 218, 290
  metazoans, 223
brine drainage, 50, 56–7, 200
brine expulsion, 53, 54
brine inclusions, 70, 72, 269
  effects on albedo, 66
brine rejection, 6, 112
BRIOS (Bremerhaven Regional Ice–Ocean Simulations), 89
brittle failure, 68, 69
bromine compounds, 279
bromochloromethanes, 279
bromoform, 279
Buccinum spp. (whelk), 254
buoys, 107

CABFAC factor analysis, 352–3
Calanoides acutus (copepod), 219
Calanus spp. (copepods), 257, 322
Calanus glacialis (copepod), 213, 216, 219, 221
Calanus hyperboreus (copepod), 216, 219
calcareous microfossils, 350–51, 354
calcite, precipitation, 204, 270
calcium carbonate, 275, 350
calcium ions, 38, 280
calcium sulphate, 270
cameras, underwater, 234
Canada, 101, 133, 253, 256, 355
  lakes, 287
Canada Basin, 91, 104
Canadian Archipelago, 91, 103, 116, 124, 129
  ice cover variability, 132, 133
Canadian Arctic, *245*, 255, 257, 316, 320, 349
  diatoms, 353
Canadian Coast, 104
Canadian High Arctic, 216, 254
Cape Ann, 114
Cape Bathhurst Polynya, 246
carbohydrates, 282, 286, 288
carbon, 193, 320, 321, 334
  biogenic, 172
  dissolved inorganic, 275
  flux, 314–15, 322, 323
  organic, 304, 319
  particulate organic, 191, 313–14
  photosynthetic assimilation, 273, 274, 275
  see also dissolved organic carbon (DOC)
carbonate(s), 269
  abundance, 309
  buffering, 193
  concentrations, 304
  precipitation, 270
carbon-concentrating mechanisms (CCMs), 273
carbon dioxide, 193, 204, 271, 333, 345
  carboxylation, 273
  concentrations, 269, 346
  depletion, 282
  dissolved, 271–2, 314
  exchange, 274–5
  solubility, 269
carbon fixation, 143, 196
  estimation, 169
  mechanisms, 144–5, 267
carbonic acid, 269
carbon isotopes, 232, 314, 350
  stable, 273–5
carbon isotopic composition, 145
β-carboxylation, 145
carboxylation, 273, 274
β-carotene, 144, 145
Caspian Sea, 1, 3
catalase, 273
catalytic processes, 74
CCMs (carbon-concentrating mechanisms), 273
CDOM (coloured dissolved organic matter), 287, 289
cell membranes, 282
  structure, 284
cells
  aggregation rates, 315
  ammonium transport, 285
  carbon transport, 274
  counting methods, 190–91
  freeze tolerance, 197
  lysis, 193, 195, 283
  metabolism, 284
  microstructure, 191
  nitrate transport, 284
  see also algal cells
cetaceans *see* whales
Chaetoceros neglectum (diatom), 317
chaetognaths, 216
chemical environment, organisms, 267
chemistry
  physical, 37–44
  sea ice, 17, 74, 268–71
  seawater, 268–71
  see also biogeochemistry
chemo-autotrophy, 188
chemoheterotrophs, 189
chemotaxis, 201
chloride, 22
chloride ions, 38, 280
chlorins, 350
chlorophyll, 144, 145, 149, 150–51, 157
  abundance, 158, 161, 169
  accumulation, 167, 168, 169
  concentrations, 160, 319
  fluorescence, 190, 192, 193
  pigments, 350
chlorophyll–carbon ratios, 191–2
chlorophytes, 188
chloroplasts
  membranes, 282
  thylakoid membranes, 144, 197
choanoflagellates, 187, 188
chrysophytes, 188
Chukchi Peninsula, 246
Chukchi Sea, 91, 133, 317
  diatoms, 353
  walruses, 254
  whales, 257
chytrids, 188
ciliates, 12, 187, 188, 202
  food webs, *222*
^{14}C incorporation, *in situ,* 153–4, 169
Circumantarctic Current, 91
Circumpolar Deep Water, 251
cirripedes, 217
citrate synthase, 197
clay minerals, 334, 350

CLIMAP *see* Climate, Long-Range Investigation, Mapping and Prediction (CLIMAP)
climate
  Antarctic, 335
  and melting, 88–9
  models, 72–3
  patterns, 333
  sea-ice effects, 1, 253
  see also global climate change; global warming
Climate, Long-Range Investigation, Mapping and Prediction (CLIMAP), 334, 336, 342–3, 345, 348, 350
  future research, 358–9
  goals, 333
  reconstructions, 355–6
  sea-surface temperature estimates, 358
  transfer function method, 351
Climatic Optimum, 341
climax communities, 204, 205–206
coccolithophorids, microfossils, 348, 350–51, 353–4, 356, 357–8
Coccolithus pelagicus (coccolithophorid), 350, 353–4
cod, 12, 217, 255, 256, 258
cold-active enzymes
  applications, 14–15
  catalysis, 15
  production, 14
colonization, micro-organisms, 199–201
colonization (human), 357
coloured dissolved organic matter (CDOM), 287, 289
community structure
  food webs, 323
  marginal ice zones, 321–2
congelation ice, 28, 154, 161, 168, 199
  diatoms, 318
  formation, 27
  growth, 48–9, 154–5
  taxonomic composition, 318–19
contaminants, 350
  biological, 291
continental shelves, 6–7
convection, mechanisms, 8
convergence, ice, 88, 90
Cook Inlet, 255
Cook, James, 5, 240
copepods, 12, 168, 211, 223, 228
  abundance, *215*, 232
  adaptation, 219–20
  calanoid, 212, 213, 216, 221, 224–6, 232
  cyclopoid, 212–13, 227
  egg production, 320
  as food source, 257
  food webs, *222*
  grazing, 320, 321, 322
  harpacticoid, 212, 213, 214, 216, 218, 226–7
  life cycles, 224–7, 321, 322
  occurrence, 216
  spatial variability, 213–14
  species diversity, 217–18
cores (ice) *see* ice cores
Coriolis force, 88, 92
Coriolis vector, 74
Cosmonaut Sea, 114
crack propagation, 70, 71
crustaceans, 223
  as food source, 251–2
  species diversity, 12, 217–18
  see also copepods; euphausiids
cryoplagic organisms, 232
CryoSat (satellite), 15, 101, 102, 109
crypsis, 189
Ctenocalanus citer (copepod), 212, 216
cyanobacteria
  autotrophy, 188
  early studies, 184
  habitats, 187
Cyclopina gracilis (copepod), 212
Cyclopina schneideri (copepod), 212
  life cycle, 227

DAACs (Distributed Active Archive Centers), 16
databases, sea ice, 338–9
data interpretation, issues, 113, 116
Davis Strait, 253, 256, 257
  diatoms, 351, 352–3
decomposers, 193, 200
deep water, formation, 7–8
deformation
  ice, 88, 97
  ice floes, 70–71, 233
  sea ice, 33, 69–70, 92
degree-day models, 34
dendritic growth, 46
denitrification, 194, 270
density, 159, 160
  brine, 43, 44–5
  measurement, 94
  pure ice, 43
desalination, mechanisms, 53–4
desaturases, 197
deuterium isotopes, 31
Devon Island, 255
  Ice Cap, 348
diatomaceous ooze, 336
diatoms, 5, 12, 48, 146
  abundance, 184, 358
  acclimation, 144
  aggregation rates, 315
  antioxidants, 273
  autotrophy, 188
  carbon–chlorophyll ratios, 169
  dissolved organic matter, 288–9
  enzyme production, 14
  excretion, 289, 290
  in faecal pellets, 315
  flux, 311
  as food source, 320, 321
  food webs, 202, *222*, 304, 316
  glucose metabolism, 272
  habitats, 232
  in ice cover studies, 334–5
  incorporation, 318
  light absorption, 144, 145
  lipids, 282
  in marginal ice zones, 321, 322
  microfossils, 335, 337–8, 348, 351–3
  nitrate reductase, 195
  nitrate storage, 284–5
  nitrogen uptake, 194–5
  nutrition, 193
  pioneer communities, 204–205, 316
  silicate uptake, 285
  species diversity, 317
  stable carbon isotope studies, 275
  studies, 17
  taxonomy, 186–7
  see also frustules
diatoxanthin, 145
dibromomethane, 279
dielectric constant, 61
dielectric loss factor, 61, *62*
dielectric properties, 31, 60–64
diffusion, Fick's law of, 152–3
digalactosyldiaglycerol, 282
dimethyl sulphide (DMS), 198–9, 203, 273
  abundance, 279

in sea ice, 278–9
dimethylsulphoniopropionate (DMSP), 198–9, 203, 273
distribution, 278–9
production, 278
dimethylsulphoniopropionate-lyase, 278
dimethylsulphoxide (DMSO), 197
dinoflagellates, 188, 202
cysts, 335, 348, 353–5, 356, 358
life cycles, 353
dinosporin, 354
dissolved gases
biological effects, 271–5, 314
sampling, 275–8
dissolved organic carbon (DOC), 286, 288, 291
concentrations, 289
measurement, 286–7
dissolved organic matter (DOM), *186*, 286–90, 291
accumulation, 193, 203, 290
characteristics, 287–8
concentrations, 194, 284
decomposition, 195
future research, 293
and photochemical reactions, 288–9
production, 195, 286
in succession, 204
dissolved organic nitrogen (DON), 286, 288, 291
measurement, 287
dissolved organic phosphorus (DOP), 286
Dissostichus mawsoni (fish), 217, 221, 248
Distributed Active Archive Centers (DAACs), 16
divergence, ice, 87, 90
DMS *see* dimethyl sulphide (DMS)
DMSO (dimethylsulphoxide), 197
DMSP *see* dimethylsulphoniopropionate (DMSP)
DNA, 230–31
damage, 145
DOC (dissolved organic carbon), 286, 288
DOM *see* dissolved organic matter (DOM)
DON *see* dissolved organic nitrogen (DON)
DOP (dissolved organic phosphorus), 286
Drescheriella glacialis (copepod), 212, 216, 218
life cycle, 224, 226–7
swimming ability, 232
Drescher Inlet, 217
driftwood, 349
Drygalski, Erich von, 5
d'Urville, Dumont, 5

East Antarctic, 347
East Greenland, 358
East Greenland Current, 91
East Siberian Islands, 107
East Siberian Sea, 91, 103, 104, 107
diatoms, 353
salinity, 291
ecology
micro-organisms, 199–206
polar, 143
sea ice, 16, 31
ecosystems, 323
ecotones, 205
eddy currents, 95, 96, 97
electrical conductivity, 95–6
electromagnetic induction (EMI) sounding, 83–5, 93, 95–100, *108*
airborne, 16, 97–100, 109
instrumentation, 96
ship-based, 97, *98*, 100
electromagnetic waves
penetration depth, 61–2
propagation, 60–61
electron microscopy, 191
Ellis Fjord, 319
El Niño Southern Oscillation (ENSO), 9, 126, 134, 138
effects on seals, 259–60
and sea ice, 250
Emiliani huxleyi (coccolithophorid), 350, 353–4, 358
EMI sounding *see* electromagnetic induction (EMI) sounding
emissivity, 63
energy fluxes, 10
ENSO *see* El Niño Southern Oscillation (ENSO)
Entomoneis kjellmanii (diatom), 318
ENVISAT (satellite), 101
enzymes, 144–5
antioxidative, 273
carboxylating, 274
extracellular, 193, 195, 196–7
intracellular, 195, 197
nitrate reduction, 284
reaction rates, 196
salt-tolerant, 198
studies, 196–7
see also cold-active enzymes
epifluorescent microscopy, 190, 192
epiphytes, 189
EPOS (European Polarstern Study), 316, 317, 322
EPS *see* exopolymeric substances (EPS)
equilibrium ion concentration product, 270
ERS-1 (satellite), 101
ERS-2 (satellite), 101
Eubacteria, 187
Eucampia antarctica (diatom), 336, 341, 344
euglenophytes, 188
eukaryotes, 15, 189
Euphausia crystallorophias (euphausiid), 216, 250
feeding grounds, 221–2
Euphausia superba (euphausiid), 12, 216, 219, 220, 227–9
climate effects, 230–31
feeding grounds, 221, 315, 320
feeding strategies, 228–9
as food source, 250
life cycle, 321
euphausiids, 211, 216, 221, 247
abundance, 232
as food source, 257
food webs, *222*
grazing, 320
see also krill
Eurasia, 349
Eurasian Arctic, 350
Europa (moon), 13–14, 76
Europe, 357
satellites, 101
European Polarstern Study (EPOS), 316, 317, 322
Eusirus antarcticus (amphipod), 219, 220
excretion, 218, 286, 289
faecal pellets, 285, 314–15, 316, 320, 321, 322
grazers, 283, 314–15
exopolymeric substances (EPS), 289–90
transparent, 290
extinction coefficient, 61
extraterrestrial life, 13–14

extraterrestrial systems, sea ice as proxy for, 13–14, 76
extremophiles, 15

faecal pellets, 285, 314–15, 316, 320, 321, 322
fast ice *see* land-fast ice
fatty acids, 220, 282
feeding grounds, 260–61, 315
  sea ice, 221–3
Fick's law, 152–3
fish, 217, 220, 237, 248
  antifreeze glycoproteins, 221, 233
  feeding grounds, 222–3
  as food source, 248, 249, 251, 252, 255, 256
  and global climate change, 258
  larval, 322
  species diversity, 12
FISH (fluorescent *in situ* hybridization), 192
fjords, 253, 341
flagellates, 202, 285
  aggregation rates, 315
  food webs, *222*
  habitats, 232
  in marginal ice zones, 321, 322
  pioneer communities, 316
  see also dinoflagellates
Flexibacter–Bacteroides–Cytophaga groups, 187, 189
flow cytometry, 191, 267
fluorescence, chlorophyll, 190, 192, 193
fluorescent *in situ* hybridization (FISH), 192
fluorescent pigments, 190–91
fluorine ions, 38
flushing
  rates, 204
  sea water, 194
food sources
  algae, 251, 304, 314–15
  amphipods, 252, 254
  copepods, 257
  crustaceans, 251–2
  diatoms, 320
  fish, 248, 249, 251, 252, 255, 256
  for grazers, 282, 289, 319–21
  krill, 249, 260
  for pelagic animals, 304, 307, 319–21, 322
  penguins, 249, 251
  phytoplankton, 247–8, 267–8
  seals, 251, 258–9
food webs, 12, 258, 303–304, 316, 322
  Antarctic, *222*
  community structure, 323
  metazoans, 221–3
  micro-organisms, *186*, 201–203, 321
  structural differences, 169
  top trophics, 247–8
  whales, 251, 257
foraminifera, 12, 187, 188
  food webs, *222*
  microfossils, 348, 350–51, 353, 354, 356
Fossula arctica (diatom), 353
Foxe Basin, 257
Fragilariopsis curta (diatom), 12, 317, 319
  abundance, 337, 340
Fragilariopsis cylindrus (diatom), 12, 315, 317, 319, 352, 353
  abundance, 337
Fragilariopsis grunowii (diatom), 352, 353
Fragilariopsis obliquecostata (diatom), 337–8, 342, 343, 344
Fram Strait, 8, 90, 91, 95, 351
  foraminifera, 356
  ice thickness variability, 107
  particle flux, 309, 310, 311
  walruses, 254
Franklin, Sir John, 4
Fratercula corniculata (puffin), 259
frazil ice, 31, 48–9, 168, 199
  algal cells, 318
  crystal structure, 38
  formation, 27, 28, 114, 146, 223
  particle flux, 309, 310
freezing
  and ions, 38
  sea water, 1, 26–7, 159, 268–71
freezing point, sea ice, 60
fresh water, 291–2, 346
Frobisher Bay, diatoms, 351
Frobisher, Martin, 3
frustules
  dissolution, 285–6, 311, 351
  studies, 186
fucoxanthin, 144, 145
fungi, 188, 193

GAC (Global Area Coverage), 114
β-galactosidase, 197
GAM (Generalized Additive Model), 338
Gammarus oceanicus (amphipod), 219
Gammarus wilkitzkii (amphipod), 216, 219, 220, 223
  feeding, 222
  life cycle, 224
Ganymede (moon), 13
gases
  exchange, 333
  production, 74
  and salinity, 269–70
  sampling, 275–8
  in sea ice, 269–70, 271, 283
  solubility, 269
  volatile, 279
  see also carbon dioxide; dissolved gases; nitrogen; oxygen
gas fluxes, 292
  measurement, 277
gastropods, 254
gas vacuolate bacteria, 201
GCMs (Global Circulation Models), 15, 66, 74, 344–6, 359
Generalized Additive Model (GAM), 338
geochemical modelling, 44
geochemical tracers, 334, 350
Geonics EM-31 (electromagnetic sounder), 96, 97
Germany, 292
GF/Fs (glass fibre filters), 286
glacial ice, 348
glaciers, 117, 349
glass fibre filters (GF/Fs), 286
Global Area Coverage (GAC), 114
Global Circulation Models (GCMs), 15, 66, 74, 344–6, 359
global climate change, 1–2, 72, 233, 279
  and ice cover variability, 258–9, 347–8
  and pagophilic species, 258–61
  and sea ice, 15–16, 230–31
  studies, 2–3
global sea ice cover *see* ice cover variability
global warming, 15, 126, 233, 258
  and climate change, 1–2
  impacts, 82

models, 334
glucose, 288
metabolism, 272
glutamic acid, 288
glutathione peroxidase, 273
glutathione reductase, 273
glycolate, 195
glycolipids, 144
glycoproteins, 197
antifreeze, 220–21, 233
Gothus, Olaus Magnus, 3
grain size, 70
granular ice, 27, 48–9
gravity drainage, 53–4
grazers, 193, 200, 203, 216, 232
diet, 220
and dimethyl sulphide release, 279
excretion, 283, 314–15, 316
feeding grounds, 221
food sources, 282, 289, 319–21
habitats, 168
pelagic, 304, 314, 322, 323
respiration, 271–2
grease ice, 114, 146
Great Northern Expedition, 3
Great Salinity Anomaly, 8
greenhouse warming, 113
Greenland, 3, 91, 117, 253, 349
diatoms, 351, 352
Northern, 309
Vikings, 357
walruses, 254
whales, 256
Greenland Ice Core, 349, 357
Greenland–Scotland Ridge, 8
Greenland Sea, 8, 122, 129, 132
amphipods, 216
particle flux, 307, 309, 311
rotifers, 212
guanine–cytosine base pairs, 230
guillemots, 251–2, 259
Gulf of St Lawrence, 124, 129, 355
gulls, habitats, 251–2
gut flora, 189
gyres, 91, 92, 170, 318, 343–4

habitats, 48, 168–9
algae, 143, 148–9
metazoans, 211
micro-organisms, 143, 146, 184, 232
platelet ice, 217–18
preferences, 246–57
sea ice, 146–9
sub-ice, 214–17
top trophics, 240–66
Halectinosoma spp. (copepods), 213
halogens, 279
Hamburg Ship Model Basin (Germany), *47*, *52*, 292
Harpacticus spp. (copepods), 213
heat budgets
sea ice, 28–30, 34
and snow cover, 30
heat exchange, 333
heat flux, 10, 31–2, 33, 45, 54
conductive, 28–30, 35
and melting, 88–9
and sea ice growth, 86, 90–91
heat transfer, convective, 56–7
heavy metals, 291
helicopter EM (HEM), 97–100, 109
helicopters, surveys, 97–100
heliozoans, 188
HEM (helicopter EM), 97–100, 109
herbivores, 168, 199, 222
heterotrophic uptake, 195
heterotrophs, 188, 194, 200–201, 205
feeding, 232
food webs, 202, 203
heterotrophy
algae, 272
bacterial, 189, 286
net, 194
High Arctic, 253, 258
high-performance liquid chromatography (HPLC), 192
high salinity shelf water, 6–7
Holocene
diatomaceous ooze, 336
palaeo sea ice distribution, 335, 339–41, 349, 353, 357–8
Hooker, Joseph, 5
HPLC (high-performance liquid chromatography), 192
Hudson Bay, 10, 122, 124, 129, 355
copepods, 320
polar bears, 258
polynyas, 243, 246
primary production, 322
Hudson Strait, 257
humans, 243, 246, 348
colonization, 357
hydrocarbons, brominated, 279
hydrogen isotopes, 31
hydrogen peroxide, 272
hydrogen sulphide, 283
hydrohalite, precipitation, 39–40
hydroxyl radicals, 272, 273
hyperosmosis, 220
hyperosmotic regulation, 220
hyperoxia, 272
hypersaline solutions, 269

ice
advection, 87
age, 90, 280
brackish, 46
convergence, 88, 90
deformation, 88, 97
divergence, 87, 90
glacial, 348
granular, 27, 48–9
grease, 114, 146
morphology, 233
multi-year, 205
pancake, 27, 114, 146, 250
types of, 66, 280
see also congelation ice; frazil ice; lake ice; land-fast ice; melted sea ice; pack ice; platelet ice; pure ice; sea ice; snow ice
Ice Age, 356
ice augers, 150
icebergs, 337, 349
ice-breakers, 2, 240
ice concentration, 115
fields, 106
ice cores, 190, 218, 280
palaeo distribution studies, 340–41, 348–9
sampling, 276–7
ice cover variability, 32, 176, 250
annual, 303
Antarctic, 112–14, 116, 124–6, 133–7, **171–2**
Arctic, 112, 113, 116, 119–24, 137–8
and climate, 335
data interpretation issues, 113, 116
determination, 337–8
and global climate change, 258–9, 347–8
global trends, 126–32
large-scale, 113
monitoring, 82–3
regional trends, 126–32
satellite studies, 113–16, 134, 137, 334, 339, 348
seasonal, 342
spatial, 116–26

and surface temperature, 113–14, 132–7
temperature trends, 132–7
temporal, 116–26, 146
see also palaeo sea ice distribution
ice crystals, 269, 283, 289, 317
formation, 26–7
ice extent *see* ice cover variability
ice floes, 291
algae, 315
deformation, 70–71, 233
evolution, 50, 82
habitats, 146–8, 247, 252
melting, 33
metazoans, 214
nutrients, 281
particle flux, 304, 309
physical–chemical parameters, 271
rafting, 233
studies, 93, 114
thickness, 28, 35, 83–6, 131
ice freeboard, 100, 101, 148, 160, 218
ice growth/salt-flux model, 54
ice Ih
crystal structure, 37–8
use of term, 37
Iceland, 3, 349
coccolithophorids, 357–8
colonization, 357
diatoms, 351, 352
ice-obligate species, 241–2, 243, 247, 260
ice-rafted debris (IRD), 336, 344, 349, 357–8
abundances, 337, 340–41
IceSat (satellite), 102
Ice Shelf Water (ISW), 7
ice strength, macroscopic, 67–71
ice tank facilities, 292
ice thickness, 15, 28
and coverage, 82–3
decrease, 334
determination, 35, 96
simulations, 33
and snow cover, 30–31
see also thickness distribution
ice thickness fields, 104–105, *106*
ice thickness variability, 160, 257
decadal, 102–106
interannual, 106–109, 334
mechanisms, 155
ice velocity fields, 104, *105*
ice volume, 82–3
ice–water interface, 50–51, 205
bacteria, 13
boundary conditions, 40
copepods, 320
dissolved organic matter, 287
ionic diffusion, 271
metazoans, **217**
nutrient exchange, 280–81
perturbations, 45–6
planar *vs.* lamellar, 44–8
studies, 16, 292
ICP (ion concentration product), 270
ikaite, precipitation, 39
imaging, 114–16
microwave, 160
satellite, 311
sensors, 100–101
incorporation
metazoans, 223
micro-organisms, 199–201
Indian Ocean, 10, 116, 126, 131, 176, 346
copepods, 224
ice cover variability, 341, 343, 344, 359
infrared data, 114, 115
insulation
seals, 248
top trophics, 248
INTERICE, *46*, *52*
Inuit, 1
invertebrates, 223, 247
ectothermic, 219
ion concentration product (ICP), 270
ions
concentrations, 270
diffusion, 271
dilution, 280
and freezing, 38
in sea water, 38
IRD *see* ice-rafted debris (IRD)
Ireland, 3
iron, 336–7
concentrations, 313
and particle flux, 312–13
ISW (Ice Shelf Water), 7

Jan Mayen, 253, 349
Japan, Sea of, 10
Jupiter (planet), 13, 76

Kara Gate, 97
Kara Sea, 91, 97, *98*, 122, 129, 132
diatoms, 353
salinity, 291
Kerguelen Plateau, 344
keystone species, 230
kinetoplastids, 188
King George Island, 250, 259–60
Kongsfjorden, 253
krill, 143, 227–9, 248
abundance, 232
adaptation, 219, 220
climate effects, 230–31
distribution, 12, 13, 227, *228*
faecal pellets, 314–15
as food source, 249, 260
food webs, *222*
grazing, 315, 321, 322
life cycles, 321
recruitment, *231*, 233
studies, 16
see also euphausiids

Labrador, 257
Labrador Sea, 8, 124, 129, 259, 351, 356
diatoms, 351, 352
dinoflagellate cysts, 358
β-lactamase, 197
lake ice
albedo, 25, 26, 37
deformation, 69–70
growth, 45, 46
radiative transfer, 64
vs. sea ice, 25–6
Lancaster Sound, 257
land-fast ice, 51–2, *147*, 148, 153, 154, 159
algal biomass, 167
carbon enrichment, 313
diatoms, 353
habitats, 169, 252, 253
palaeo distributions, 341
photosynthetic rates, 168
sampling, 218
taxonomic composition, 318–19
Landsat, Thematic Mapper, 114
Langmuir circulation, 318
Laptev Sea, 91–2, 107, 108, 350, 358
diatoms, 351
rotifers, 212
salinity, 291
laser altimeters, 97, 102
Last Glacial Maximum (LGM), 333, 341–3, 346, 350, 359
modelling, 344, 345
palaeo sea ice distribution, 334, 355–6
latent heat, conductive removal, 155
latent heat of fusion, 58–60

latent heat polynyas, 6, 112–13
latitude, effects on sea ice growth, 90–91
Law Dome, 340
Lazarev Sea, 219
leads, 256
  imaging, 101, 115
LGM *see* Last Glacial Maximum (LGM)
life cycles, 1, 223–9, 321, 322, 353
ligands, organic, 287
light-harvesting efficiency, 144
light limitation, 157, 158
light microscopy, 190–91
light scattering, 64–5, 73
lignin phenols, 291
lipase, 197
lipid membranes, 220
lipids, 145
  in sea ice organisms, 282
  see also phospholipids
liquid films, 72
liquid inclusions, 25
lithogenic particles, 304, 309–11, 349
Little Ice Age, 339, 357
lysis, 193, 195, 198, 283, 286

MAAs *see* mycosporine-like amino acids (MAAs)
McMurdo Sound, 148, 154, 159, 161, 223
  carbon enrichment, 313
  seals, 249, 259
macrobiology
  future research, 233–4
  sea ice, 211–39
macro-nutrients
  biological effects, 281–2
  dissolved, 279–80
  elevated concentrations, 282–4
  exhaustion, 281
  and water exchange, 280–81
magnesium ions, 38, 280
magnetic resonance imaging (MRI), 40, *41*
Makarov, Admiral, 4
Malmgren, Finn, 4, 49–50
mammals, 240–66
  adaptation, 246–57
  and global climate change, 2, 258–61
  habitats, 246–57
  insulation, 247
  see also polar bears; seals; walruses; whales
maps, 338–9
Mare Concretum, 3
marginal ice zones, 334
  community structure, 321–2
MARGO (Multiproxy Approach for the Reconstruction of the Glacial Ocean), 358–9
Marine Isotope Stages (MISs), 341–4
marine snow, 314, 315
Mars (planet), 13
MAT (Modern Analogue Technique), 337, 338, 343, 351
Maud Rise, 7
Maxwell's equations, 60
Melosira arctica (diatom), 12
melted sea ice
  effects, 303, 333, 346
  sampling, 276–7
melting
  mechanisms, 88–9
  sea ice, 1, 31–3
    salinity profiles, 49–50
melting point, sea ice, 60
melt ponds, 72, 89, 107
  cyanobacteria, 187
  drainage, 252
  surface, 32
melt water, 303, 313
  production, 54
meltwater flushing, 54
meltwater plumes, 7
membrane fluidity, 197
membrane phospholipids, 14, 220
Mesodinium rubrum (ciliate), 188
metabolism, 288
  cellular, 284
  glucose, 272
meta pancakes, 27
metazoans, 12, 194, 282, 283
  adaptation, 211, 219–21, 233
  and biomass, *213*
  dominant species, **212**
  excretion, 218, 286
  feeding grounds, 221–3
  future research, 233–4
  grazing, 278
  habitats, 211
  in ice–water interface, **217**
  incorporation, 223
  in platelet ice, 217–18
  sampling, 218–19
  sea ice community, 212–13
    sampling, 218
  spatial variability, 213–14, 233–4
  species diversity, 212–13
  species richness, 211
  sub-ice community, 214–17
meteorological data, 134
methane sulphonic acid (MSA), 339, 340
methyl bromide, 279
micro-algae *see* algae
microbes *see* micro-organisms
microbiology
  future research, 206–207
  of sea ice, 184–209
microelectrodes, 277–8, 292
  development, 16, 277
  oxygen, 152–3, 169
microfossils, 348
  calcareous, 350–51, 354
  distribution, 334, 335, 337–9, 350–55
  siliceous, 354
microheterotrophs, 158
micro-organisms, 30, 48, 74
  abundance, 189–92
  adaptation, 195–9
  biochemistry, 192–9, 267
  biomass, 189
  colonization, 199–201
  ecological roles, 187–9
  ecology, 199–206
  food webs, *186*, 201–203, 321
  habitats, 143, 146, 184, 232
  in ice cover studies, 334–5
  incorporation, 199–201
  lipids, 282
  nutrition, 193–5
  physiology, 192–9
  remineralization, 193–5
  sampling, 190
  species diversity, 184–92
  and succession, 204–206
  survival, 40
  taxonomy, **185**, 186–7
microstructure (sea ice) *see* sea ice microstructure
microwave data, 113, 114, 116, 137, 160
  active *vs.* passive, 115
  ice cover variability studies, 348
  sea ice concentration studies, 338–9
microwave frequencies, *62*, 63–4
microwave sensors, 100
Mid Brunhes Event, 344
migration, 243
  sea birds, 242
minerals
  authigenesis, 271

precipitation, 270, 271
solubility, 270
mineral salts, solubility, 269
mirabilite, precipitation, 39, 44
Mirounga leonina (seal), 250
MISs (Marine Isotope Stages), 341–4
mixotrophs, 188, 201
Modern Analogue Technique (MAT), 337, 338, 343, 351
Monhysteroidea, 212
Monod formulation, 158
moons, 76
extraterrestrial life, 13
moorings
oceanographic, 95
sediment traps, *306*, 307
moulting, 247, 252, 253, 254
MRI (magnetic resonance imaging), 40, *41*
MSA (methane sulphonic acid), 339, 340
mucus, 289, 290
Multiproxy Approach for the Reconstruction of the Glacial Ocean (MARGO), 358–9
Mya truncata (bivalve), 254
mycosporine-like amino acids (MAAs), 230
sunscreens, 145
mysids, 216, 224
Mysis polaris (mysid), 224

NADW (North Atlantic Deep Water), 8
Nansen Basin, 102
Nansen, Fridtjof, 4
NAO (North Atlantic Oscillation), 104, 107, 134, 348, 357
NAOSIM (North Atlantic Ocean Sea Ice Model), 89
narwhals, 242, 251, 254
habitats, 256
National Aeronautics and Space Administration (NASA), 16, 102
National Snow and Ice Data Center (NSIDC) (USA), 16
native peoples, 243, 348
natural products, 14–15
natural resource exploration, future trends, 13–15
Naval Oceanography Command Detachment, 338
Navicula spp. (diatoms), 320
Navicula glaciei (diatom), 318
nematodes, 12, 211, 212, 223, 224
abundance, 232
spatial variability, 214
Neoglacial phase, 341
Neogloboquadrina pachyderma (foraminifer), 12, 350, 353
Newfoundland, 253
New Siberian Islands, 91
Newtonian liquids, 68
New Zealand, 260, 345
nilas, 66, 69, 146
Nimbus-7, 348
NIPR-I sampler, 218–19
Niskin bottles, 320
nitrate, 193, 279, 280, 291
biosynthesis, 283
concentrations, 282, 283
depletion, 194
low-temperature affinity, 284–5
in snow, 281
transport, 284
uptake, 194–5, 196
nitrate reductase (NR), 195, 284
nitrite, 279, 280
accumulation, 194
biosynthesis, 284
concentrations, 283
nitrogen, 193, 279–86
uptake, 194–5
see also dissolved organic nitrogen (DON)
nitrogen compounds, 282
nitrogen isotopes, 232
Nitzschia spp. (diatoms), 317, 319, 320, 352
Nitzschia cylindrus see Fragilariopsis cylindrus (diatom)
Nitzschia frigida (diatom), 352
Nitzschia grunowii (diatom), 352, 353
NMR (nuclear magnetic resonance) spectroscopy, 16, 44, 233
Nobile, Umberto, 49
non-linear regression, 343
Nordic seas, 350, 356, 357, 358
Nordway events, 356
North America, 349, 356
North Atlantic, 8, 91, 253, 335, 355, 356
circulation, 357
North Atlantic Deep Water (NADW), 8
North Atlantic Ocean Sea Ice Model (NAOSIM), 89
North Atlantic Oscillation (NAO), 104, 107, 134, 348, 357
Northeast Passage, 49
Northeast Water Polynya, 246
North Pacific, 352
North Pole, 10, 91, 103, 107, 116
North Water (Baffin Bay), 243, 246, 255
Northwest Passage, 2, 257
Northwest Territory (Canada), 253
Norwegian Sea, 8
diatoms, 351, 352
particle flux, 307, 309, 311
NR (nitrate reductase), 195, 284
NSIDC (National Snow and Ice Data Center) (USA), 16
nuclear magnetic resonance (NMR) spectroscopy, 16, 44, 233
numerical modelling
one-dimensional, 154–9, 177
quasi three-dimensional, 159–61, 177
nutrient limitation, 157, 158, 176, 282
nutrients
concentration, 160, 161
dissolved, 291
flux, 155–6
release, 313
supply, 174, 275, 281
and water exchange, 280–81
see also macro-nutrients
nutrition, micro-organisms, 193–5

Ob′ Bay, 97
oceans, sea-ice effects, 1, 5–9
Odden ice tongue, 112, 122
Odobenus rosmarus (walrus), 254
Odobenus rosmarus divergens (walrus), 254
Odobenus rosmarus laptevi (walrus), 254
oil, exploration, 17
Oithona similis (copepod), 212, 213, 216
Okhotsk, Sea of, 1, 10, 122–3, 129, 316
diatoms, 351–2
Oncaea curvata (copepod), 212, 216
Onismus spp. (amphipods), life cycles, 224

Onismus glacialis (amphipod), 219, 220, 222
Onismus nanseni (amphipod), 222
opal
  biogenic, 339
  fluxes, 313
Operculodinium centrocarpum (dinoflagellate), 353
optical extinction coefficient, 26
optical properties, 64–7, 72, 73
optodes, 16, 277–8, 292
organic molecules, 272–3
organisms
  biotechnology applications, 14–15
  chemical environment, 267
  cryoplagic, 232
  lipids, 282
  mortality, 286
  photosynthetic, 202, 273
  see also micro-organisms
osmoconformers, 220
osmolytes, 198–9
oxygen, 271
  concentrations, 194, 269, 272–3
  dissolved, 271–2
  enzymatic inhibition, 273
  level changes, 193–4
  and salinity, 270
  solubility, 269
  supersaturation, 272
oxygen electrodes, 277
oxygen isotopes, 31, 52, 54, 339, 351
oxygen microelectrodes, 152–3, 169, 277–8
oxygen radicals, 194
ozone depletion, 231, 279
ozone holes, 145

Pacific Ocean, 10, 116, 122, 335, 345
  diatoms, 351–2
pack ice, *147*, 148, 153, 154, 159, 161
  algae, 315
  carbon enrichment, 314
  habitats, 169
  particle flux, 304
  photosynthetic rates, 168
  sampling, 218
  sea birds, 242
  seals, 260
  whales, 255
Pagodroma nivea (petrel), 240–41
pagophilic species, and global climate change, 258–61
Pagothenia borchgrevinki (fish), 12, 217, 220, 221
  feeding grounds, 223
  food, **223**
  food webs, *222*
palaeoceanography
  field of study, 333
  reconstructions, 334
palaeo sea ice
  extents, 334
  modelling, 334, 344–7
palaeo sea ice distribution, 333–72
  Antarctic, 335–47
  Arctic, 347–58
  future research, 347
  reconstructions, 335–9, 347–58
    time-slice, 339–44, 355–8
  seasonal variability, 335–9, 347–58
Palmer Deep, 341
Palmer Long Term Ecological Research, 307
pancake ice, 27, 114, 146, 250
Paralabidocera antarctica (copepod), 212, 216, 219, 221
  habitat, 232
  life cycle, 224, 226
Paramoera walkeri (amphipod), 222, 224
parasitism, bacteria, 189, 195
Parathemisto spp. (amphipods), 252
Parathemisto libellula (amphipod), 216, 223, 254, 258
PAR (photosynthetically available radiation), 145, 151
Parry, William Edward, 4
particle aggregation, 199
particle flux
  annual data, 310–12
  Antarctic *vs.* Arctic, 308–10
  Arctic-Atlantic, 310–11
  biogenic, 310, 311, 312–13, 314–15
  characteristics, 304–15
  chemistry, 312–14
  experiments, 305–308
  ice-margin, 310–11
  lithogenic, 310–11, 349
  polar, 310–11
  roles, 304, 322–3
  sea ice, 303–332
  settling mechanisms, 314–15
particulate organic carbon (POC), 191, 313–14
particulate organic matter (POM), *186*, 304
  accumulation, 193, 203
  catalysis, 193
  decomposition, 194, 195
  inputs, 202
pathogens, 203
PCBs (polychlorinated biphenyls), 10, 291
PCR (polymerase chain reaction), 192
PDFs (probability density functions), 85, *108*
pelagic animals
  food sources, 304, 307, 319–21, 322
  see also plankton
penetration depth, 61–2
penguins, 240, 322
  breeding grounds, 247, 248
  colonies, 243, *244*
  as food source, 249, 251
  foraging, 247
  and global climate change, 260
  habitats, 246, 248
  population records, 339–40
Penny Ice Cap (Baffin Island), 349, 357
PEPCase (phosphoenolpyruvate carboxylase), 144–5
PEPCKase (phosphoenolpyruvate carboxykinase), 144–5
PE response curves *see* photosynthesis–irradiance (PE) response curves
Permanently Open Ocean Zone, 341
permeability
  of free space, 61
  sea ice, 56, 75–6
permittivity, *62*
  of free space, 61
  relative, 61, 63
peroxides, 194
petrels, 240–41, 247
  feeding strategies, 248
  habitats, 251
pH, 269, 272, 284
  changes, 193–4, 204, 278, 282
  sea ice, 275

Phaeocystis spp. (prymnesiophytes), 188, 321
Phaeocystis antarctica (prymnesiophyte), 278
phaeopigments, 320–21
phagotrophs, 188
phase diagrams, sea ice, *39*, 40
phase fractions, 40–42
phase relations, 38–40
Phoca groenlandicus (seals), 253
phosphate, 193, 279, 280, 281, 291
  concentrations, 282, 283
phosphatidylglycerol, 282
phosphoenolpyruvate carboxykinase (PEPCKase), 144–5
phosphoenolpyruvate carboxylase (PEPCase), 144–5
phosphoglycerate kinase, 197
phospholipids, 197
  membrane, 14, 220
phosphorus, 193, 279–86
  concentrations, 194, 284
photoacclimation, parameters, 143–4
photoadaptation parameter, 143–4
photoautotrophy
  algae, 272
  mechanisms, 187–8
photoautotrophy–heterotrophy transition, 272
photochemical reactions, and dissolved organic matter, 288–9
photochemicals, toxic, 272–3
photorespiration, 195
photosynthesis, 147, 188, 192, 322
  algae, 193, 194, 195, 271–2
  inhibition, 145
  and primary production, 143, 267–8, 274
  rates, 198
  studies, 277, 292
  tracers, 193
photosynthesis–irradiance (PE) response curves, 143–4, 153
  primary production studies, 150–52
photosynthetically available radiation (PAR), 145, 151
photosynthetically usable radiation (PUR), 158
photosynthetic carbon assimilation, 273, 274, 275
  see also primary production
photosynthetic efficiency (α^*), 150, 151–2
photosynthetic isotope effect, 274
photosynthetic organisms, 202, 273
photosynthetic parameters, 150–51
photosynthetic quotient (PQ), 273
photosynthetic rates, 144
  estimation, 167–8
Photosystem II, 145
phytoplankton, 48, 144, 145, 148, 221
  concentrations, 321
  flux, 310
  as food source, 247–8, 267–8
  nitrate assimilation inhibition, 284
  production, 170
phytoplankton blooms, 272, 311, 313
  and primary production, 303–304
  seeding, 315–19
  taxonomic composition, 317, 318–19
  see also algal blooms
phytoplankton seeding, algae, 207, 304, 307, 315–19, 323
pigments, 282, 315, 320–21
  analysis, 191–2
  as biomarkers, 350
  fluorescent, 190–91
Pinnularia quadratarea (diatom), 318
pioneer communities, 204–205, 316
planets, 76
  albedo, 66
  extraterrestrial life, 13
plankton, 202, 223, 258
  sampling, 190
  see also phytoplankton; zooplankton
plastiquinone, 144
platelet ice, 149, 154, 199
  algal biomass, 161, 167, 168
  formation, 223
  metazoans, 217–18
Pleuragramma antarcticum (fish), 248, 249
Pleurosigma spp. (diatoms), 318
POC (particulate organic carbon), 191, 313–14
polar bears, 3, 12, 246, 348
  and global climate change, 258–9
  habitats, 254–5
  thin ice strategies, 69
Polar Front, 258, 336, 342–3, 344, 345
Polar North Atlantic, 356
Polar Surface Water, 310
pollutants, 291
pollution, 10
polychaetes, 216–17
polychlorinated biphenyls (PCBs), 10, 291
polyketide synthases, 197
polymerase chain reaction (PCR), 192
polynyas, 8, 242–6
  formation, 30, 87, 175, 243
  global climate effects, 261
  imaging, 115
  latent heat, 6, 112–13, 243
  sensible heat, 7, 243
  studies, 114–15
  top trophics, 242–6
  walruses, 254
  whales, 255, 256, 257
polysaccharides, 288, 289, 315
  gels, 283, 290
polyunsaturated fatty acids (PUFAs), 14, 15, 197, 220
POM *see* particulate organic matter (POM)
Pontogeneia antarctica (amphipod), 222, 224
pore model, 70, *71*
pores, 40–42, 44, *46*, 70
  evolution, 73
  microstructure, 75–6
pore waters, 280
Porosira glacialis (diatom), 353
porphyrins, 350
potassium ions, 38, 280
PQ (photosynthetic quotient), 273
practical salinity scale (pss), 26
prasinophytes, 188
pressure ridges, 82, 90, 91, 94, 97
primary production, 348
  distribution, 333–4, 336
  estimation, 150
  and iron release, 312–13
  mechanisms, 143–5
  and photosynthesis, 143, 267–8, 274

and phytoplankton blooms, 303–304
see also sea ice primary production
Prince Albert Sound, 253
probability density functions (PDFs), 85, *108*
probes, rRNA-targeted, 192
prokaryotes
biomass, 192
epiphytic, 189
species diversity, 187, 192, 204
protease, 197
proteins, 286
antifreeze, 220–21
biosynthesis, 282
cold-shock, 197
membrane-bound, 197
stress-induced, 197
see also glycoproteins
γ-Proteobacter group, 187, 189
protists, 146, 168, 186, 193
early studies, 184
food webs, 203
heterotrophic, 195, 201, 204, 205
identification, 187
photosynthetic, 188
species diversity, 186
taxonomy, 186–7
protozoans, 12, 267, 278, 282
excretion, 286
faecal pellets, 315
grazing, 322
habitats, 232
Prydz Bay, carbon enrichment, 313
prymnesiophytes, 188
Pseudocalanus spp. (copepods), 213, 216, 221, 320, 322
Pseudocyclopina belgicae spp. (copepods), 216
pss (practical salinity scale), 26
psychrophiles, 195–6, 197
PUFAs (polyunsaturated fatty acids), 14, 15, 197, 220
puffins, 259
pulse radar sounding, 93
pure ice
density, 43
radiative transfer, 64
PUR (photosynthetically usable radiation), 158
pycnoclines, 321

Q_{10} values, 196
Q-mode factor analysis, 352, 355
Quaternary, palaeo sea ice distribution, 334, 335, 341–4, 359
Queen Elizabeth Islands, 348
QuickSCAT, 116

RACER (Research on Antarctic Coastal Ecosystem Rates), 307
radar altimeters, 101, 116
radar backscatter coefficients, 63
radar imagery, 63
RADARSAT (satellite), 101
radar scatterometers, 100, 107
radiative transfer, 64–5, 156–7
radiocarbon dating, 349
radiometers, 100
reactive oxygen species, 272, 273
Redfield ratio, 161
remineralization, 283
micro-organisms, 193–5
remotely operated vehicles (ROVs), 219, 234
remote sensing, 2–3, 15, 16, 31, 100–102
extraterrestrial, 76
and penetration depth, 61
see also satellites
Research on Antarctic Coastal Ecosystem Rates (RACER), 307
Research on Ocean–Atmosphere Variability and Ecosystem Response in the Ross Sea (ROAVERRS), 307
research stations, 2
Resolute Passage, 161
resource limitation, 157–8
respiration, 277, 286
biological, 274
heterotrophic, 271–2
restricted gas exchange, 273–5
rheology, 88
ribulose bisphosphate carboxylase/oxygenase (RUBISCO), 144–5, 195, 273, 274
ridge formation modelling, 88
ridge sails, 101
rivers
erosion, 349
and sea ice biogeochemistry, 291–2
ROAVERRS (Research on Ocean–Atmosphere Variability and Ecosystem Response in the Ross Sea), 307
rock fragments, 309
Ross Island, 260
Ross, James Clark, 4, 5, 240
Ross Sea, 5, 116, 126, 131, 138
algal biomass, 175
carbon enrichment, 314
diatoms, 340
future research, 347
iron concentrations, 313
krill, 321
particle flux, 307, 311, 312, 314
penguins, 340
sea ice primary production, 6, 173, 175, 176, 336
seals, 249, 259
sediment traps, *305*
whales, 250
rotifers, 12, 211, 212
abundance, 232
spatial variability, 213–14
ROVs (remotely operated vehicles), 219, 234
rRNA
cloned, 187
gene sequences, 192
RUBISCO (ribulose bisphosphate carboxylase/oxygenase), 144–5, 195, 273, 274
Russia, 133, 291
sea ice research, 4
RV Polarstern, 97–9

SAF (Sub-Antarctic Front), 336, 337
St Lawrence Island, 246
St Matthew Island, 246
salinity, 39
acclimation, 198–9
and algal growth, 148
brine, 43, 160
bulk, 42
effects
on micro-organisms, 190
on thermal properties, 60
evolution, 45, 49–54, 112
and gases, 269–70
profiles, 49–50
sea ice *vs*. lake ice, 25
sea water, 161, 269
as state variable, 42–4
surface, 32, 100
units, 26
salinity-dependent growth coefficient, 158
Salpa thompsoni (tunicate), 230

salps, 260
salt
  flux, 48
  mineral, 269
  in sea ice, 269
  segregation, 50–53, 54
  transport, 45
  see also brine
sampling
  brine, 275
  dissolved gases, 275–8
  gases, 275–8
  ice cores, 276–7
  metazoans, 218–19
  micro-organisms, 190
  primary production studies, 149, 150, 153, 176–7
  sea ice, 17, 40, 42, 190, 276–7
  sediment traps, 305–308
Saroma-Ko Lagoon, 316
SAR (Synthetic Aperture Radar), 100–101, 116
satellites, 15, 16
  animal tracking studies, 254–5
  ice cover variability studies, 113–16, 134, 137, 334, 339, 348
  ice thickness surveys, 92, 107, 109
  imaging, 311
  penguin studies, 340
  radar imagery, 63
  sea ice concentration studies, 338–9
  see also remote sensing
saturated fatty acids, 197
saturation index, 270
Scanning Multichannel Microwave Radiometer (SMMR), 348
scatterometers, 116
scavenging, mechanisms, 199, 201
SCICEX (Scientific Ice Expeditions) (USA), 94, 347
Scientific Ice Expeditions (SCICEX) (USA), 94, 347
Scotia Sea
  carbon flux, 314–15
  krill, 315, 320
Scott, Robert Falcon, 5
scuba divers, 234
sea birds, 322
  adaptation, 251
  colonies, *245*
  foraging, 251–2
  and global climate change, 258, 259, 260
  migration, 242
  studies, 241–2
sea ice
  abundance, 1
  albedo, 25, 26, 37, 65–7, 72, 333
  artificial, 292
  astrobiological issues, 13–15
  biogeochemistry, 267–302
  biology, 3, 74, 268, 292
  chemistry, 17, 74, 268–71
  composition, 38
  concentration, 338–9, 343, 347
  current issues, 15–17
  databases, 338–9
  deformation, 33, 69–70, 92
  density, 159, 160
  desalination, 53–4
  draft, 159
  duration, 343
  ecology, 16, 31
  effects
    on atmosphere, 5–9
    on climate, 1
    on oceans, 1, 5–9
  extent, 6
  as feeding ground, 221–3
  formation, 7–8, 27–8
  freezing point, 60
  gases, 269–70, 271, 283
  and global climate change, 15–16, 230–31
  as habitat, 146–9
  heat budgets, 28–30, 34
  importance, 1–21
  latent heat of fusion, 58–60
  macrobiology, 211–39
  melting, 1, 31–3
    salinity profiles, 49–50
  melting point, 60
  microbiology, 184–209
  modifications, 1
  particle flux, 303–332
  permeability, 56, 75–6
  pH, 275
  phase diagrams, *39*, 40
  phase fractions, 40–42
  phase relations, 38–40
  physical chemistry, 37–44
  processes, microscopic *vs.* macroscopic, 71–3
  properties, 24
    dielectric, 31, 60–64
    optical, 64–7, 72, 73
    thermal, 55–60
  radiative transfer, 64–5
  research, 2, 3–5
    future trends, 17, 73–6
  roles, 333–4
  salinity, 39
    evolution, 49–54
  sampling, 17, 40, 42, 190, 276–7
  specific heat capacity, 58–60
  stratigraphy, 23–4
  surface energy balance, 28–30
  thermal thickness, 58
  thickness distribution, 6, 82–111
  and top trophics, 240–42
  vs. lake ice, 25–6
  see also ice cover variability; ice thickness; palaeo sea ice
sea ice exploration, 1
  historical background, 3–5
sea ice growth, 45
  and heat flux, 86, 90–91
  mechanisms, 82
  models, 34–7
  rates, 6, 29
  salinity profiles, 49
  salt segregation, 50–53
  seasonal variations, 117–19, 146
  simulations, 35, *36*
  and snow cover, 30–31
sea ice microstructure, 22–6, 69
  evolution, 40–42
  future research, 73–6
  hysteresis, 46
  models, 62–3
  and solute segregation, 44–9
sea ice models, 24, 33, 34–7
  bio-optical, 65
  dynamical, 15, 16
  dynamic–thermodynamic, 103, 104
  elastic–viscous–plastic, 16
  large-scale, 50, 66
  microstructural, 74
  thermodynamic, 9
sea ice primary production, 143–83
  estimation methods, 149–61, 167–70
  future research, 177
  in situ measurements, 161–7, 177
  large-scale modelling, 170–76
  mechanisms, 143–5
  numerical modelling, 154–61, 177
  rates, 145, 161–76

significance, 322
spatial variability, 173
temporal variability, 170–72
Sea Ice Zone (SIZ), 341
sealing, 5
sea lions, habitats, 246
seals, 3, 12, 240, 322
bones, 357
breeding, 249, 250, 252, 253–4, 258, 259–60
as climatic markers, 252
as food source, 251, 258–9
foraging, 249, 252
habitats, 246–7, 248–50, 252–4
insulation, 248
sea salt ions, 38, 50
sea-surface temperature (SST), 344–5, 358
Sea-viewing Wide Field-of-view Sensor (SeaWiFS), 16
sea water
density, 159
enclosure mechanisms, 199
flushing, 194
freezing, 1, 26–7, 159, 268–71
ions in, 38
salinity, 161, 269
seawater chemistry, abiotic modification, 268–71
seawater flooding, 30
SeaWiFS (Sea-viewing Wide Field-of-view Sensor), 16
secondary production, 348
sedimentation rates, 342
sedimentological tracers, 334, 336–7, 349
sediments
clay-rich, 334, 350
lithological changes, 336
particle flux, 309, 323
sediment traps, 305–308, 309–10, 311, 320
moorings, *306*, 307
segregation, salt, 50–53, 54
segregation coefficient, 50–52
equilibrium, 51
sensors
airborne, 97–100, 109
high-resolution irradiance, 277
imaging, 100–101
see also microelectrodes
settling mechanisms, particles, 314–15
Shackleton, Ernest Henry, 5
ship-based surveys, 97, *98*, 100, 109
shuga, 114
Siberia, 90, 107, 309
Siberian Arctic, 102
Siberian Shelf, 91
silica, 323, 334, 336–7
silicate(s), 279, 280, 281, 285–6, 291
biogenic, 193
concentrations, 282, 304
silicic acid, 193
depletion, 194
silicification, 285
silicon, 193
similarity indexes, 351
SIMMAX, 351
siphonophores, 216
SIRAL (Synthetic Interferometric Aperture Radar Altimeter), 101
SIZ (Sea Ice Zone), 341
skuas, 248
SMMR (Scanning Multichannel Microwave Radiometer), 348
snow
albedo, 30
density, 159, 160
marine, 314, 315
nutrients, 281
thermal conductivity, 58
thickness, 90
snow cover, 8, 173–4, 175–6
and sea ice growth, 30–31
snow ice
formation, 31
occurrence, 31
sodium, 220
sodium chloride, 38, 40, 221
precipitation, 270
sodium ions, 38, 280
sodium sulphate, 270
SOI (Southern Oscillation Index), 259, 340
SOJGOFS (Southern Ocean Joint Global Ocean Flux Study), 307
solute segregation, 44–9
Somerset Island, 255
sonars
submarine, 102
upward looking, 16, 93–5, 107, 109
South Atlantic, 336, 340–41, 342–4, 345, 359
Southern Indian Ocean, sea ice primary production, 176
Southern Ocean, 1, 159, *174*, 291
brine rejection, 6
copepods, 321
diatoms, 338, 351, 352, 353
frazil ice, 48
ice cover variability, 335, 341, 343
ice formation, 27
ice thickness, 28
ice thickness distribution, 89–91
krill, 230, 231, 315, 320
particle flux, 308, 311, 314
phytoplankton blooms, 303
sea ice conditions, 337
sea ice primary production, 172, 176
snow ice, 31
whales, 250
Southern Ocean Joint Global Ocean Flux Study (SOJGOFS), 307
Southern Oscillation Index (SOI), 259, 340
South Indian Ocean, 345
South Magnetic Pole, 5
South Pacific Ocean, 174, 241–2, 359
sea ice primary production, 175–6
spacing distributions, 86
Special Sensor Microwave/Imager (SSM/I), 116, 160, 348
species diversity, 12
algae, 204, 317
crustaceans, 12, 217–18
diatoms, 317
future research, 206
metazoans, 212–13
micro-organisms, 184–92
species richness, metazoans, 211
specific heat capacity, 58–60
spectral downwelling attenuation coefficient, 156
squid, 250, 251, 256
SSM/I (Special Sensor Microwave/Imager), 116, 160, 348
SST (sea-surface temperature), 344–5, 358
stable isotopes, 232, 339
carbon, 273–5
state variables, 42–3
limitations, 43–4
use of term, 42
Stephos longipes (copepod), 212, 216, 218, 219, 221
life cycle, 224–6
Stogryn model, 62

stoichiometric balance, 281–2
stony fields, 28
strain rates, 68–9
stratigraphy, sea ice, 23–4
stratosphere, 279
Sub-Antarctic Front (SAF), 336, 337
submarines
  military, 92
  surveys, 94–5, 102, *103*, 109, 347–8
substrates, low-temperature affinity, 284–5
subtilisin, 197
succession
  and micro-organisms, 204–206
  primary, 204, 205
  secondary, 204, 205
sugars, accumulation, 287–8
sulphate ions, 38, 280
sulphates, 199
  reduction, 270
  in snow, 281
sunlight, 267
supercooling, constitutional, 45, 51
surface energy balance, 28, 34
  sea ice, 28–30
surface flooding, 54, 148, 203
surface pre-melting, 73
surface temperature, and ice cover variability, 113–14, 132–7
Svalbard, 49, 253, 254, 309, 349
swimming ability, 232
Synchaeta hyperborea (rotifer), 212
Synchaeta tamara (rotifer), 212
Synthetic Aperture Radar (SAR), 100–101, 116
Synthetic Interferometric Aperture Radar Altimeter (SIRAL), 101

taigas, 291
Taimyr Peninsula, 97
taxonomy
  micro-organisms, **185**, 186–7
  phytoplankton blooms, 317, 318–19
Taylor Dome, 340
teleosts, 220
temperature
  and ice cover variability, 132–7
  Q_{10} values, 196
  sea-surface, 344–5, 358
  as state variable, 42–4
TEP (transparent exopolymer particles), 290
terrigenous debris, 309
Thalassiosira antarctica (diatom), 318
Thalassiosira gravida (diatom), 317, 352–3
Thalassiosira nordenskioldii (diatom), 352
Thalassiosira trifulta (diatom), 353
thermal conductivity, 55–6
  snow, 58
thermal diffusity, 59
thermal hysteresis agents, 220
thermal properties, 55–60
thermal thickness, 58
thermohaline circulation, 9, 27, 113, 345
thickness distribution, 6, 82–111
  change models, 86
  factors affecting, *83*
  future research, 108–109
  global, 89–92
  large-scale spatial, 88
  measurement techniques, 92–102
  processes, *87*
  statistics, 83–6
  thermodynamics, 86
  see also palaeo sea ice distribution
thylakoid membranes, chloroplasts, 144, 197
time-series measurements, 206–207, 293
Tisbe furcata (copepod), 213
  life cycle, 227
Tomopteris carpenteri (polychaete), 216–17
top trophics
  food webs, 247–8, 322
  and global climate change, 258–61
  habitats, 240–66
  insulation, 248
  and polynyas, 242–6
  use of term, 240
  see also birds; mammals
trace metals, 287
tracers, 52, 54, 145, 187, 291, 339
  geochemical, 334, 350
  for photosynthesis, 193
  sedimentological, 334, 336–7, 349
  see also biomarkers
transfer coefficients, 35
transparent exopolymer particles (TEP), 290
Transpolar Drift, *84*, 91, 107, 309, 349, 350
triacylglycerols, 219–20
triglycerides, 145, 226
triosephosphate isomerase, 197
troposphere, 134, 279
Tsurikov, V. L., 4
tundra, 291
tunicates, 230
turbellarians, 12, 211, 212, 223, 224
  abundance, *215*, 232
  food webs, *222*
  spatial variability, 213–14

Ui-te-Rangiara, 4–5
ULSs (upward looking sonars), 16, 93–5, 107, 109
ultrasonic sounding, 93
ultraviolet (UV) light, 145, 230–31, 233, 272, 278
  effects on dissolved organic matter, 289
Upper Circumpolar Deep Water, 251, 336
upward looking sonars (ULSs), 16, 93–5, 107, 109

video studies, 93
Vienna Pee Dee Belemnite (VPDB), 274
Vikings, 357
viruses, 184, 188–9, 195, 267
visible data, 114, 115
volcanic glass, 349, 357
volcanoes, 336
Vostok, 346
VPDB (Vienna Pee Dee Belemnite), 274

walruses, 348
  habitats, 246, 254
water
  enclosure mechanisms, 199
  solid–liquid interface, 13, 16
water exchange, and macro-nutrients, 280–81
wax esters, 219, 221
weather *see* climate
weathering, 310
Weddell Basin, 7
Weddell Sea
  carbon enrichment, 314
  carbon flux, 314–15
  copepods, 224, 227
  diatoms, 318, 322

flagellates, 316, 322
high salinity shelf water, 6–7
ice cover variability, 116, 119, 126, 131, 250, 337–8
ice drift, 87
ice thickness variability, 107
krill, 227, 315, 320, 321
metazoans, 217–18
pack ice, 154, 159, 161, 315
particle flux, 307, 311–12
phytoplankton blooms, 316, 317
polynyas, 7, 8, 30
sea ice primary production, 173, 175, 336
sea ice thickness, 92, 95
seals, 250
snow ice, 31
Weddell Sea Bottom Water (WSBW), 7
Weddell Sea Deep Water (WSDW), 7
Weddell Sea Gyre, 92, 318, 343–4
Western Pacific Ocean, 126, 131
West Greenland, 255
whales, 12
adaptation, 256
food webs, 251, 257, 322
habitats, 246, 250–51, 255–8
migration patterns, 242, 251, 255, 256–7
see also belugas; narwhals
whaling, 242
data, 136–7, 335, 339
White Sea, 10
diatoms, 353
Wilkes, Charles, 5
wind-blown debris, 313
winds, 243
WSBW (Weddell Sea Bottom Water), 7
WSDW (Weddell Sea Deep Water), 7

x-ray analyses, 337
xylanase, 197

Yenisey River, 97
yield stress, 68–9, 70
Younger Dryas, 350

zooplankton, 307
faecal pellets, 314, 315
grazing, 316, 320–21, 322
life cycles, 322